MAGNETIC CHARACTERISTICS OF BROKEN HILL TYPE DEPOSITS AND THEIR HOST PROVINCES.

T.L.KERR B.Sc. (Hons)
Tracey

Submitted in fulfillment
of the requirements for the degree of
Master of Economic Geology,
University of Tasmania
September 1994.

This thesis contains no material which has been accepted for a degree or diploma by the University or any other institution, except by way of background information and duly acknowledged in the Thesis, and to the best of the Candidates knowledge and belief no material previously published or written by another person except where due acknowledgement is made in the text of the Thesis.

Tracey L. Kerr

This thesis is not to be made available for loan or for copying for five years following the date this statement was signed. Following that time the thesis may be made available for loan and limited copying in accordance with the *Copyright Act 1968*.

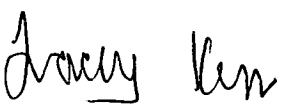

Tracey L. Kerr

ABSTRACT

In technical geological publications it has been demonstrated that Broken Hill Type deposits and their host provinces are characterised by similarities in their geological settings and ore deposit mineralogy at both local and regional scales. The purpose of this thesis was to examine magnetic characteristics of the globally most significant BHT deposits, and their host provinces, in order to develop a magnetic exploration model for BHT deposits. This involved detailed aeromagnetic interpretation of available datasets with reference to mapped geology.

Four significant BHT provinces were studied:

Broken Hill Block	- Australia
Eastern Succession, Mt Isa Block	- Australia
Bergslagen District	- Sweden
Aggenys -Gamsberg District	- South Africa

The study showed that host provinces to BHT deposits share common magnetic characteristics which reflect common geological characteristics. However, significant differences in the aeromagnetic character occur which are related to differences in volume of BHT host stratigraphy, basement stratigraphy and structural style of the host province.

BHT deposits naturally divide into two classes, based on the presence or absence of magnetic minerals within the ore. This may result from differing ore-forming environments and/or fluid chemistry. Deposits which contain magnetic minerals within the ore are commonly associated with magnetic anomalies which are amongst the strongest within the host metasedimentary /metavolcanic sequence. Deposits which do not contain magnetic minerals within the ore itself are associated with a locally anomalous signature when the immediate environs of the ore deposit are considered. The most economically signifcant deposit, Broken Hill (Australia), is of this type, although both types include large tonnage deposits.

Thermodynamic modelling was undertaken to test whether the variations of magnetic deposit signatures could be explained by variations in the environment of exhalation. The roles of boiling, cooling and seawater mixing (oxidised and reduced) as precipitation mechanisms were examined. The modelling showed that a single fluid can give rise to a spectrum of iron oxide distribution, depending on whether the dominant precipitation mechanism was boiling, cooling, mixing with oxidised sea water or mixing with reduced sea water. Precursors to metamorphosed BHT ore and gangue minerals were produced by several of these thermodynamic models.

It is concluded that the interpreter, when defining the likely spectrum of magnetic responses of a BHT deposit, must consider the likely range of environments of deposition consistent with known geology.

ACKNOWLEDGEMENTS

I am grateful to organisations around the world who freely provided essential data for this study. PASMINCO provided access to detailed aeromagnetic data over the Broken Hill deposit. The Swedish Geological Survey, in particular Mrs Kajsa Hult, provided assistance in obtaining aeromagnetic data and geological maps from the Bergslagen district.

The assistance of my supervisors was much appreciated, particularly David Cooke who provided much advice and assistance with the thermodynamic modelling section of the study.

Thanks are due to many colleagues within BHP Minerals Exploration, particularly Tom Whiting, Noel White, Ken Witherley, Steve Walters and Frank Bunting for their encouragement and technical input, and Mandy Johnson and Alasdair Cooke for their assistance in overcoming many image processing problems.

I would particularly like to thank my husband for his patience, support and technical input during the course of my degree.

Finally, I would like to thank my employer, BHP Minerals Pty Ltd, for supporting this project.

TABLE OF CONTENTS

LIST OF FIGURES

LIST OF TABLES

LIST OF APPENDICES

LIST OF PLATES

Plate 9	Regional aeromagnetic data, Soldiers Cap Group, Eastern Succession, Australia. Reduction to pole. 1:500 000 scale.
Plate 10	Regional aeromagnetic data, Soldiers Cap Group, Eastern Succession, Australia. Reduction to pole - 1st vertical derivative. 1:500 000 scale.
Plate 11	Regional aeromagnetic interpretation, Soldiers Cap Group, Eastern Succession, Australia. 1:500 000 scale.
Plate 12	Regional aeromagnetic interpretation (colour) draped on vertical derivative (intensity), Soldiers Cap Group, Eastern Succession, Australia. 1:500 000 scale.
Plate 13	Regional aeromagnetic data, Pegmont-Cannington region, Australia. Reduction to pole. 1:150 000 scale.
Plate 14	Regional aeromagnetic data, Pegmont-Cannington region, Australia. Reduction to pole - 1st vertical derivative. 1:150 000 scale.
Plate 15	Regional aeromagnetic interpretation, Pegmont-Cannington region, Australia. 1:150 000 scale.
Plate 16	Regional aeromagnetic interpretation (colour) draped on vertical derivative (intensity), Pegmont-Cannington region, Australia. 1:150 000 scale.
Plate 17	Detailed aeromagnetic data, Cannington, Australia. Reduction to pole. 1:25 000 scale.
Plate 18	Detailed aeromagnetic data, Cannington, Australia. Reduction to pole - 1st vertical derivative. 1:25 000 scale.
Plate 19	Detailed aeromagnetic interpretation, Cannington, Australia. 1:25 000 scale.
Plate 20	Detailed aeromagnetic interpretation (colour) draped on vertical derivative (intensity), Cannington, Australia. 1:25 000 scale.
Plate 21	Regional aeromagnetic data, Bergslagen, Sweden. Reduction to pole. 1:100 000 scale.
Plate 22	Regional aeromagnetic data, Bergslagen, Sweden. Reduction to pole - 1st vertical derivative. 1:100 000 scale.

Plate 23 Regional aeromagnetic interpretation, Bergslagen, Sweden. 1:100 000 scale.

Plate 24 Regional aeromagnetic interpretation (colour) draped on vertical derivative (intensity), Bergslagen, Sweden. 1:100 000 scale.

Plate 25 Regional aeromagnetic data, Aggenys-Gamsberg District, South Africa. Reduction to pole. 1:150 000 scale.

Plate 26 Regional aeromagnetic data, Aggenys-Gamsberg District, South Africa. Reduction to pole - 1st vertical derivative. 1:150 000 scale.

Plate 27 Regional aeromagnetic interpretation, Aggenys-Gamsberg District, South Africa. 1:150 000 scale.

Plate 28 Regional aeromagnetic interpretation (colour) draped on vertical derivative (intensity), Aggenys-Gamsberg District, South Africa. 1:150 000 scale.

1. INTRODUCTION

Broken Hill Type (BHT) deposits have been recognised as a special class of deposits, separate from Volcanic Hosted Massive Sulfide (VHMS) and Sediment Hosted Massive Sulfide (SHMS) deposits, by authors such as Beeson (1990), Plimer (1986) and Walters (1984, 1992). These deposits and their host provinces are similar in their tectono-stratigraphic settings and ore deposit mineralogy. The purpose of this thesis is to document and compare the magnetic characteristics of these deposits and host provinces in order to develop a magnetic exploration model for BHT deposits.

Significant BHT provinces, which formed the basis for this study, include :

Broken Hill Block	- Australia
Eastern Succession, Mt Isa Block	- Australia
Bergslagen District	- Sweden
Aggenys - Gamsberg District	- South Africa

Other examples of BHT districts may include parts of the Georgetown Block (Australia), Arunta Complex (Australia), the Eyre Peninsular (Australia) and the Boquira deposit (Bahia State, Brazil). The locations of these districts are shown in Figure 1.1

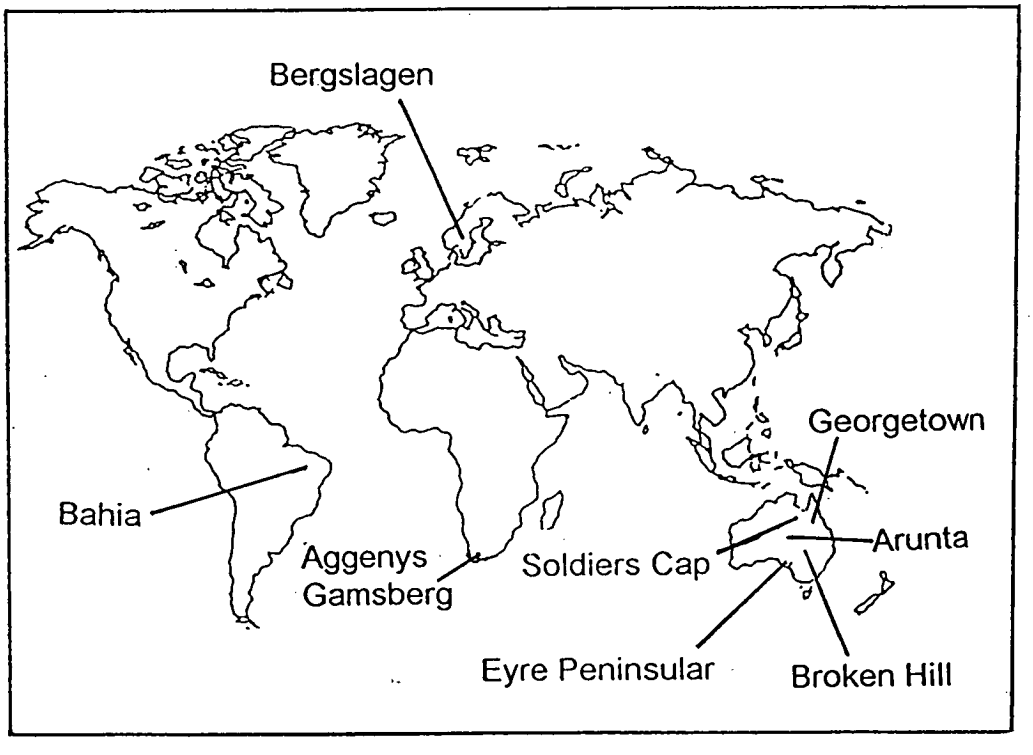

Figure 1.1 Locations of some Broken Hill Type deposits (after Beeson, 1990).

Aeromagnetic data were acquired over each of the Broken Hill, Eastern Succession, Bergslagen and Aggenys - Gamsberg Provinces. The data were interpreted at 1:100 000 scale, with reference to 1:100 000 and 1:50 000 scale geology maps. Higher resolution data permitted a more detailed study at 1:25 000 scale of the Australian BHT deposits - Broken Hill, Pegmont and Cannington.

The magnetic characteristics of BHT deposits and their host provinces, as defined by detailed interpretations of magnetic data over the four provinces, were compared and contrasted.

Thermodynamic modelling was then undertaken to test whether the variations of magnetic deposit signatures could be explained by variations in the environment of exhalation. The roles of boiling, cooling and seawater mixing (oxidised and reduced) as precipitation mechanisms were examined.

The results from the detailed magnetic study and thermodynamic modelling were then synthesised to consider the potential range of aeromagnetic signatures of BHT deposits.

2. GEOLOGICAL CHARACTERISTICS OF BHT DEPOSITS AND THEIR HOST PROVINCES

The following summary of the geological characteristics of BHT deposits and their host provinces draws largely on the work of Walters (1984, 1992) and Beeson (1990).

BHT mineralisation typically occurs in early to middle Proterozoic (1.9 - 1.6 Ma) mobile belt terrains. In this very active tectonic setting, structural and metamorphic overprints and intrusive activity complicate the interpretation of the mineralisation and its host lithologies.

The host stratigraphy is generally an oxidised sequence, which contrasts markedly with the reduced carbonaceous sequences hosting SHMS deposits (Walters, 1992). The regional stratigraphy shows a zonation from lower quartzofeldspathic/acid volcanic rock dominated sequences to upper psammopelite/pelite/greywacke dominated sequences. The lower quartzofeldspathic sequences show a strong association between distinctive basic gneisses and quartzofeldspathic gneisses which are generally accepted as representing bimodal basaltic and rhyodacitic volcanic rocks. Economic Pb-Zn-Ag mineralisation occurrences are concentrated at the transition between the lower quartzofeldspathic/acid volcanic sequence and the upper pelite/greywacke sequence. Maximum exhalite activity occurs at this transition. Carbonate/calc-silicate rocks may also be associated.

Within the host stratigraphic sequence there is a defined pattern to the distribution and variation of iron formation types, exhalites and base metal mineralisation throughout the Lower and Transitional Sequences, up to the level of significant Pb-Zn-Ag mineralisation. This pattern is summarised in Figure 2.1.

At a prospect scale, significant mineralisation is associated with increasing diversity, frequency and complexity of unusual exhalites and alterites, dominated by Si, Fe, Mn, Ca and to a lesser degree by P, F, K and carbonate enrichment (Fig. 2.2, Table 2.1). Common mineral phases associated with BHT deposits are listed in Table 2.2. Possible metamorphic precursors are discussed in section 12.4.

BHT mineralisation is characterised by high base metal/sulfur ratios, with elevated base metal concentrations in a wide variety of non-sulfide phases, e.g., gahnite, magnetite. Common ore minerals include galena and sphalerite, with minor chalcopyrite and trace silver-bearing phases including friebergite, acanthite and native silver .

Iron minerals include amphiboles, pyroxenes, olivines, garnets, chlorites, micas, magnetite, hematite, pyrite, pyrrhotite and siderite.

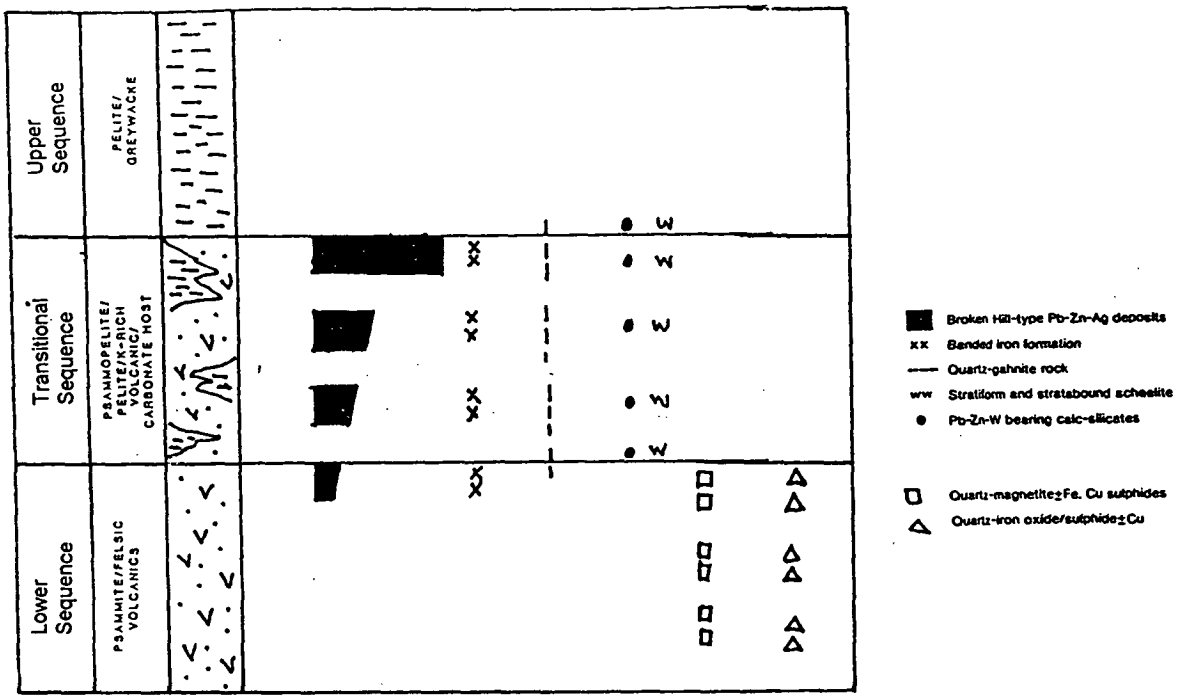

Figure 2.1 Schematic section through a BHT stratigraphic sequence (after Beeson, 1990 and Plimer, 1985).

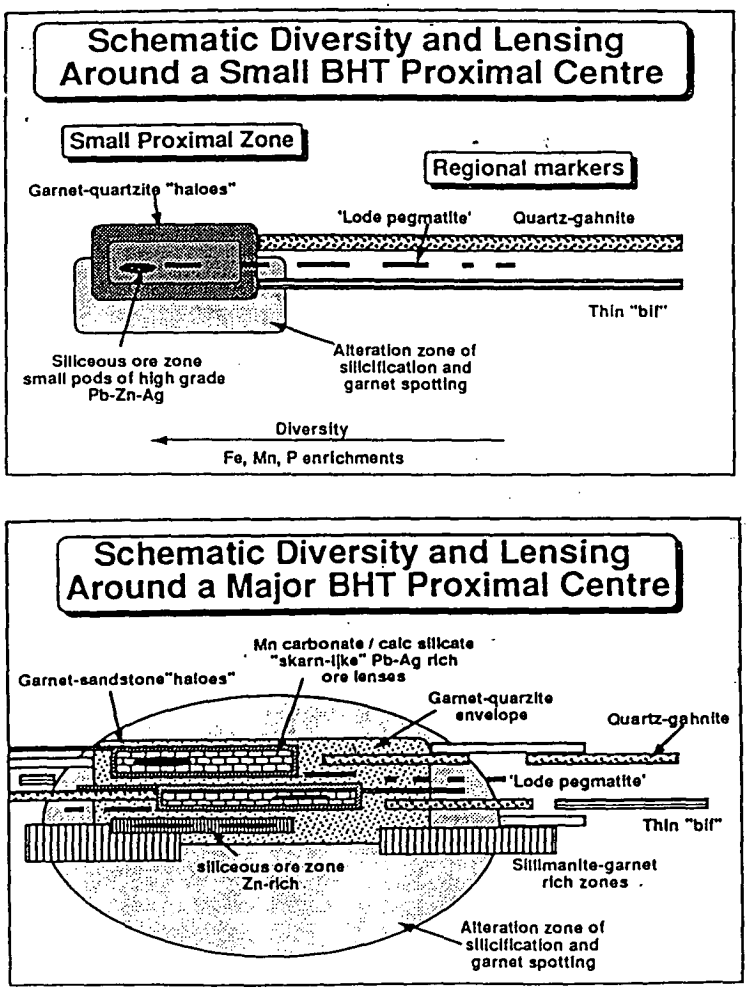

Figure 2.2 Schematic diversity and lensing around BHT proximal centres (Walters, 1992).

Type	Dominant Phases	Minor Phases
SILICEOUS	quartz (commonly blue)	spessartine, gahnite sulphides, tourmaline, magnetite, muscovite
MANGANIFEROUS	spessartine-grossular, quartz	apatite, gahnite, scheelite sulphides, arsenopyrite, biotite, sillimanite, magnetite, piedmontite
FERRUGINOUS		
Sulphide facies	pyrite, pyrrhotite, quartz	muscovite, CaFe pyroxene fayalite, rhodonite
Carbonate facies	CaMg pyroxene, quartz	sulphides, grossular-spessartine, epidote
Silicate facies	grunerite, quartz	magnetite, fayalite, almandine-spessartine, sulphides, stilpnomelane
Oxide facies		
Phosphatic	magnetite, spessartine-grossular, quartz, apatite	sulphides, fayalite, grunerite
Quartz–magnetite	quartz, magnetite	barite, apatite, sulphides, sillimanite, muscovite
ZINCIAN	gahnite, quartz	sphalerite, Pb orthoclase, spessartine-grossular, sphalerite, galena, sillimanite, apatite, tourmaline,
	muscovite, biotite, magnetite ilmenite	
BARIAN	barite or celsian/ hyalophane	sulphides, quartz, sillimanite, biotite, muscovite
CALCAREOUS	grossular, diopside, wollastonite, plagioclase, calcite, idocrase, quartz	tremolite–actinolite, fluorite, graphite, scheelite, sphalerite, epidote, clinozoisite sulphides, gahnite
BORON-RICH	quartz, tourmaline	feldspars, spessartine–almandine, feldspars, biotite, graphite, sillimanite, apatite, sulphides, gahnite, magnetite

Table 2.1 Mineralogy of principal exhalite types from the Broken Hill Block (Plimer, 1986).

Phase	Enrichment	Comments	Phase	Enrichment	Comments	Phase	Enrichment	Comments
Wollastonite	Ca		Spessartine	Mn, Fe	Garnet	Magnetite	Fe	Spinel
Grossular	Ca	Garnet end-member	Rhodonite	Mn, Ca, Fe	Similar to Wollastonite	Hedenbergite	Fe, Ca	Clinopyroxene
Fluorite	Ca, F		Bustamite	Mn, Ca, Fe	Similar to Wollastonite	Fayalite	Fe	Olivine
Epidote	Ca, Fe		Pyroxmangite	Mn, Fe	Similar to Wollastonite	Fe-chlorite	Fe	Chlorite series
Diopside	Ca, Mg, Fe	Clinopyroxene	Tephroite-knebellite	Mn, Fe	Olivine	Biotite	Fe, K	Mica
Calcite	Ca	Carbonate end-member	Rhodochrosite	Mn	Carbonate end-member	Siderite	Fe	Carbonate end-member
Tremolite	Ca, Mg, Fe	Amphibole	Mn-hedenbergite	Mn, Ca, Fe	Clinopyroxene	Grunerite	Fe	Amphibole
Apatite	Ca, P, F	Fluoro-apatite variations				Phlogopite	Fe, K, F, Mg	Mica
Plagioclase	Ca	Anorthite end-member				Actinolite	Fe, Ca	Amphibole
Vesuvianite	Ca, Mg, Fe	Similar to garnet				Hornblende group	Fe, Mg, Na, K	Amphibole
						Almandine	Fe	Garnet
						Tourmaline	Fe, Mg, F	Complex chemistry

Phase	Enrichment	Comments	Phase	Enrichment	Comments	Phase	Enrichment	Comments
Microcline	K	Feldspar	Forsterite	Mg	Olivine	Blue quartz	Si	Primary silica gel?
Orthoclase	K	Feldspar	Mg-chlorites	Mg	Chlorite series	Gahnite	Zn	Spinel
Albite	Na	Plagioclase end-member	Dolomite	Mg, Fe	Carbonate end-member	Pb-orthoclase	Pb, K	Green Feldspar
Muscovite	K	Mica	Enstatite	Mg	Orthopyroxene	Barite	Ba	
Sillimanite	Al	Includes fibrolite	Anthophyllite	Mg, Fe	Amphibole	Celsian-hyalophane	Ba, K, Na	Ba feldspar
			Gedrite	Mg, Fe	Amphibole			
			Chondrodite	Mg, F				
			Cordierite	Mg, Fe, Al				

Table 2.2 Common mineral phases in BHT systems (Walters, 1992).

3. GEOLOGY AND MINERALISATION OF THE BROKEN HILL BLOCK, AUSTRALIA.

3.1 Regional Geology

The Broken Hill Block is located in western NSW, Australia (Fig. 3.1). It is comprised of rocks of the Willyama Supergroup (Fig. 3.2). The Willyama Supergroup hosts the most significant deposit within the Broken Hill Type class. The Broken Hill deposit contains 300 MT of Pb-Zn-Ag ore grading in excess of 15% combined Pb and Zn, including 150 MT grading more than 20% combined Pb and Zn.

Stratigraphy

The Willyama Supergroup (Fig. 3.2) may be divided into three sequences:

Lower Sequence -	quartzofeldspathic gneisses and amphibolites (interpreted to be bimodal felsic/mafic volcanic rocks and volcaniclastic rocks with minor metasedimentary rocks) - **Thackaringa Group**;
Transitional Sequence -	psammitic/pelitic metasedimentary rocks and interbedded felsic and mafic gneisses - **Broken Hill Group**;
Upper Sequence-	metasediments (pelites and psammites) overlain by graphitic metasedimentary rocks - **Sundown Group** and **Paragon Group**.

A sub-cycle is seen within the Thackaringa Group, from a lower volcanic rock dominated sequence of quartzofeldspathic gneisses (Rasp Ridge, Alma Gneiss) and sodic plagioclase quartz rocks (Lady Brassey Fm., Himalaya Fm.) to an overlying transitional sequence of psammopelitic to psammitic gneisses and mafic gneisses (Cues Fm.).

Interpreted depositional environments of the Willyama Supergroup are summarised in Table 3.1.

Metamorphism

Metamorphic grade varies across the Block, increasing from upper greenschist (andalusite-muscovite) grade in the north-west to granulite (two pyroxene - hornblende) grade in the south-east. Near the deposit the metamorphic grade is upper amphibolite to granulite facies.

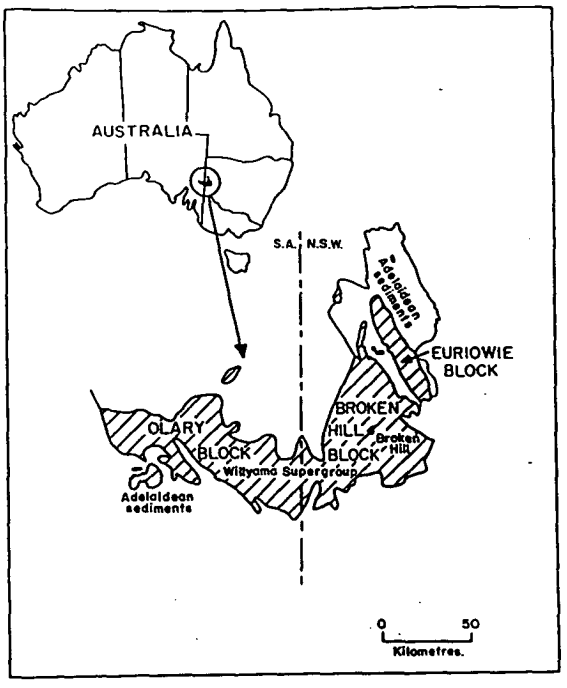

Figure 3.1 Location of the Broken Hill Block, Western NSW, Australia. (Haydon and McConachy, 1987)

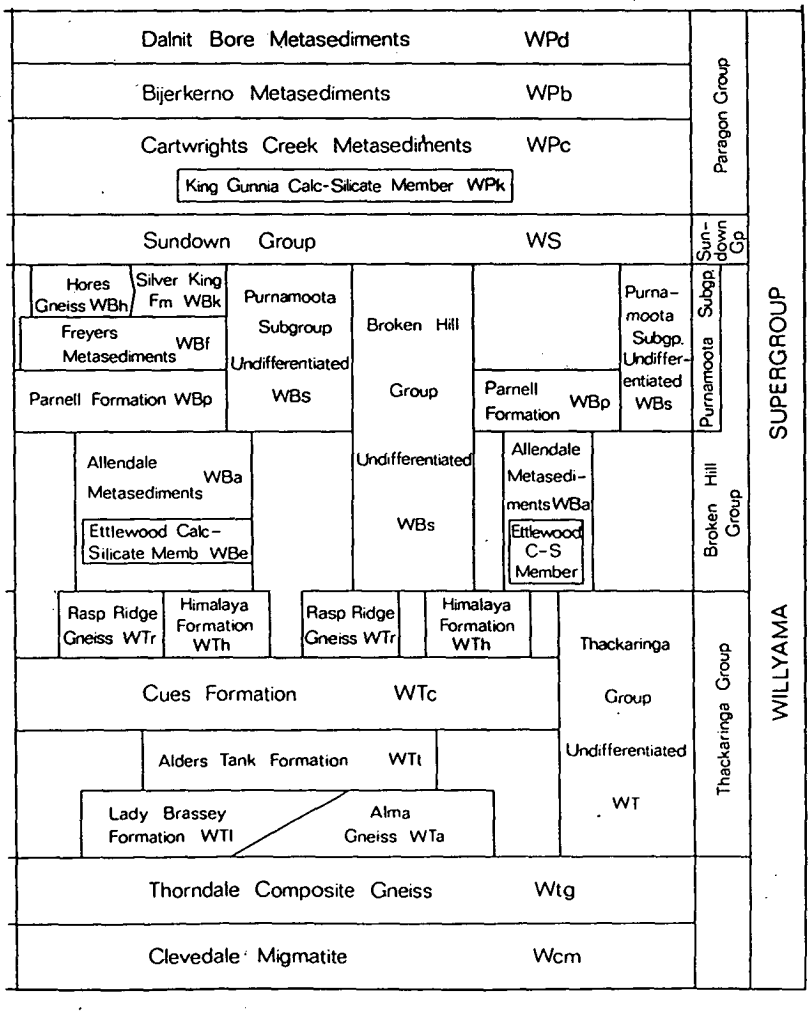

Figure 3.2 Stratigraphic subdivisions of the Broken Hill Block. (after Willis et al, 1983).

	Willis et al. (1983)	Wright, Haydon and McConachy (1987)	Stevens et al. (1988)
Paragon Group	Deepwater deposition from turbidites + suspension; extensive contourite sands.	Deepwater sediments.	Shelf muds overlain by delta front sand-silt, shallow lacustrine sands, deeper fine turbidites.
Sundown Group	Distal(?) to medial turbidites + proximal massive sands in moderate to deep fan system.	Shelf sediments overlain by deep-water sediments.	Shelf muds and silts with storm-surge sands + shallow marine sheet sands.
Broken Hill Group	Deeper shelf, turbidites, some traction current deposition/reworking. Tholeiitic-calc-alkaline rhyodacites and oceanic tholeiites.	Shelf muds and silts with storm-surge sands, shallow marine sheet sands, overlain by fluvio-deltaic arkose.	Shelf muds and silts with storm-surge sand, shallow marine sheet sands. Intercalated rhyodacitic+tholeiitic volcanics.
Thackaringa Group	Shallow marine shelf with bimodal felsic/basic volcanism, medial (to proximal) to volcanic source.	Shallow marine sediments with 3 major progradational fluviodeltaic arkose wedges.	Evaporitic lacustrine or coastal sabkha, with possible marine incursions in Cues Fmn. Acidic and basic volcanics abundant.
Thorndale Composite Gneiss	Feldspathic sands and silts (volc. derived) with thin airfall acid tuffs, thin basic tuffs + intrusives relatively shallow shelf medial to volc. source.	Shallow marine sediments.	Fluvio-deltaic and lacustrine or sabkha environment in a low relief landscape.
Clevedale Migmatite		Progradational fluvio-deltaic wedge.	
Mulculca Ednas, Redan Formations	Not specifically considered.		

Table 3.1 Interpreted depositional environments, Broken Hill Block. (Stevens et al, 1990)

Structure

Three superimposed deformational and metamorphic events have been recognised within the Broken Hill Block. The first event was the most intense and involved the development of regional isoclinal recumbent nappe-like folds (Willis *et al*, 1983). In the southern part of the Block large regions of overturned stratigraphy are evidence of this recumbent folding event (Fig. 3.3). A change from downward facing to upward facing F2 structures, or vice versa, is interpreted to indicate the axis of an F1 fold. In the northern part of the Block upright F1 folds have been identified on the basis of style and superposition of F2 and F3 (Fig. 3.3).

A second intense deformational event is present at all scales and varies from tight isoclinal folds in the southern part of the Willyama Supergroup to open warping in the north. In the south F2 folds plunge to the south-west. In the north F2 folds have sub-horizontal axes (Fig.3.4).

The third deformation event produced north-trending upright folds on a small and large scale. This folding event is accompanied by the development of a regional retrograde axial planar S3 fabric. Major retrograde shear zones are a prominent feature of the Block and have been interpreted to have been active early in D3 (Fig.3.5).

The Broken Hill deposit lies within the overturned limb of an extensive F1 recumbent fold and may have been transported tens of kilometres from its original point of deposition (Majoribanks *et al*, 1980). The ore body lies adjacent to a major F2 antiform (the Broken Hill Antiform, Fig. 3.6). The orebody is folded by a parasitic F3 fold pair developed on the steep limb of a much larger regional F3 monocline. The adjacent Globe - Vauxhall Shear Zone is considered to be one of many NE-trending D3 shear zones. It does not appear to have significant throw and is considered by Majoribanks *et al* (1980) to have been given undue significance simply because of its proximity to the ore deposit.

Mineralisation

The Broken Hill Block is extensively mineralised. There is a wide variety of styles and commodities in addition to BHT mineralisation (Fig. 3.7). Hundreds of small mineral deposits of elements such as Pb, Ag, Zn, Cu, W, Sn, Co, Ni, Pt, U, Au, Fe, Be and Bi are present.

Mineralisation occurs throughout the Wylliama Supergroup but the significant deposits are concentrated within the Thackaringa and Broken Hill Groups.

There is a gradation from coarse quartz-magnetite +/- sulfide (magnetite, hematite, pyrite, Cu, Co) mineralisation in the Thackaringa Group (Lower Sequence) to BHT (Pb, Zn, Ag, BIF) mineralisation in the upper part of the Broken Hill Group (Transitional Sequence). BHT mineralisation, in the form of

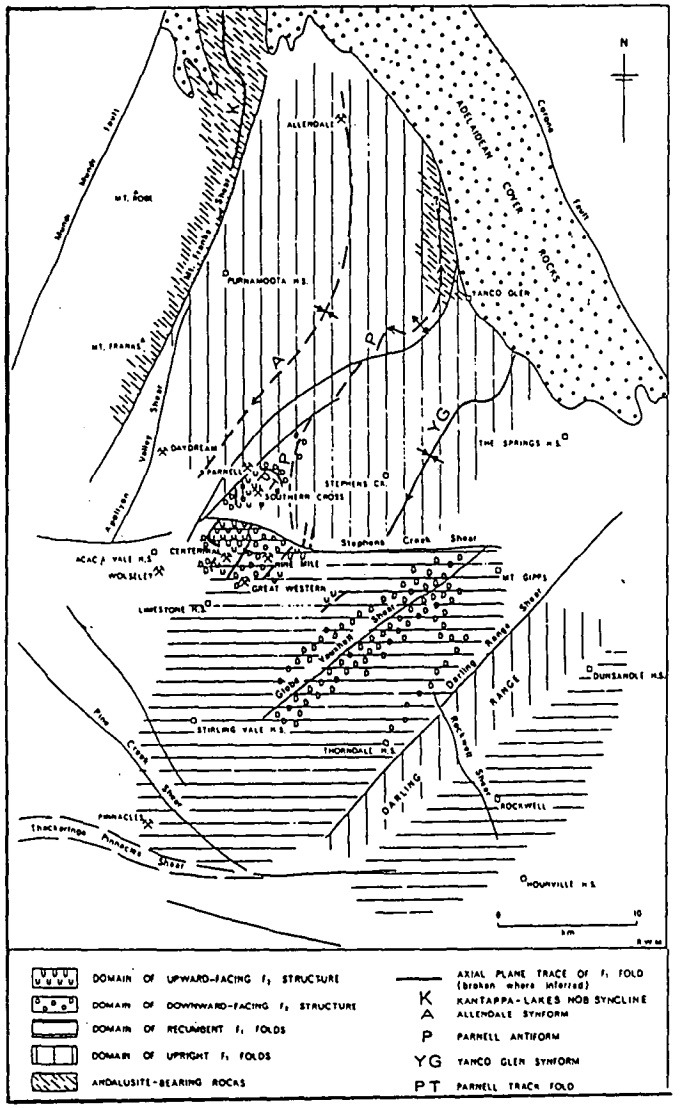

Figure 3.3 Overturned and upright F1 structural domains, Broken Hill Block.
(Majoribanks et al, 1980)

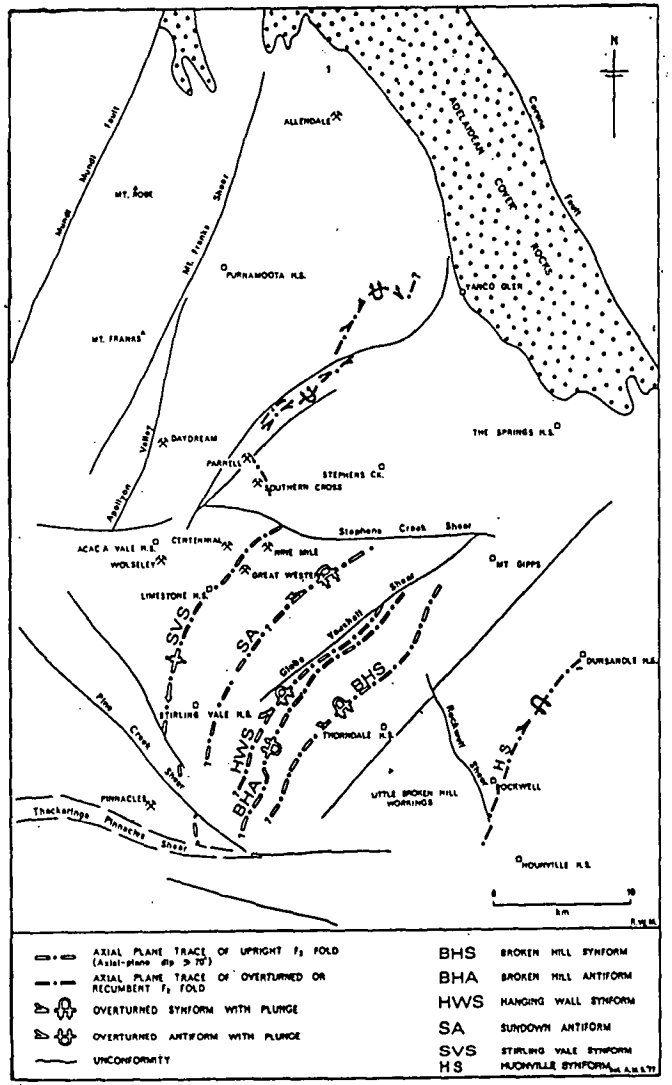

Figure 3.4 F2 structures, Broken Hill Block.
(Majoribanks et al, 1980)

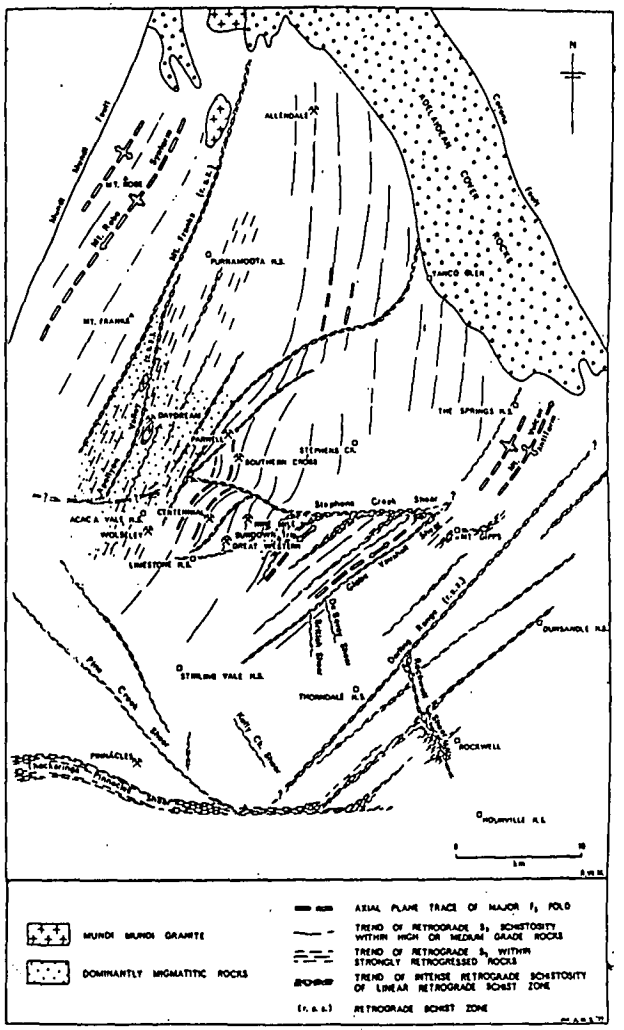

Figure 3.5 F3 structures, Broken Hill Block.
(Majoribanks et al, 1980)

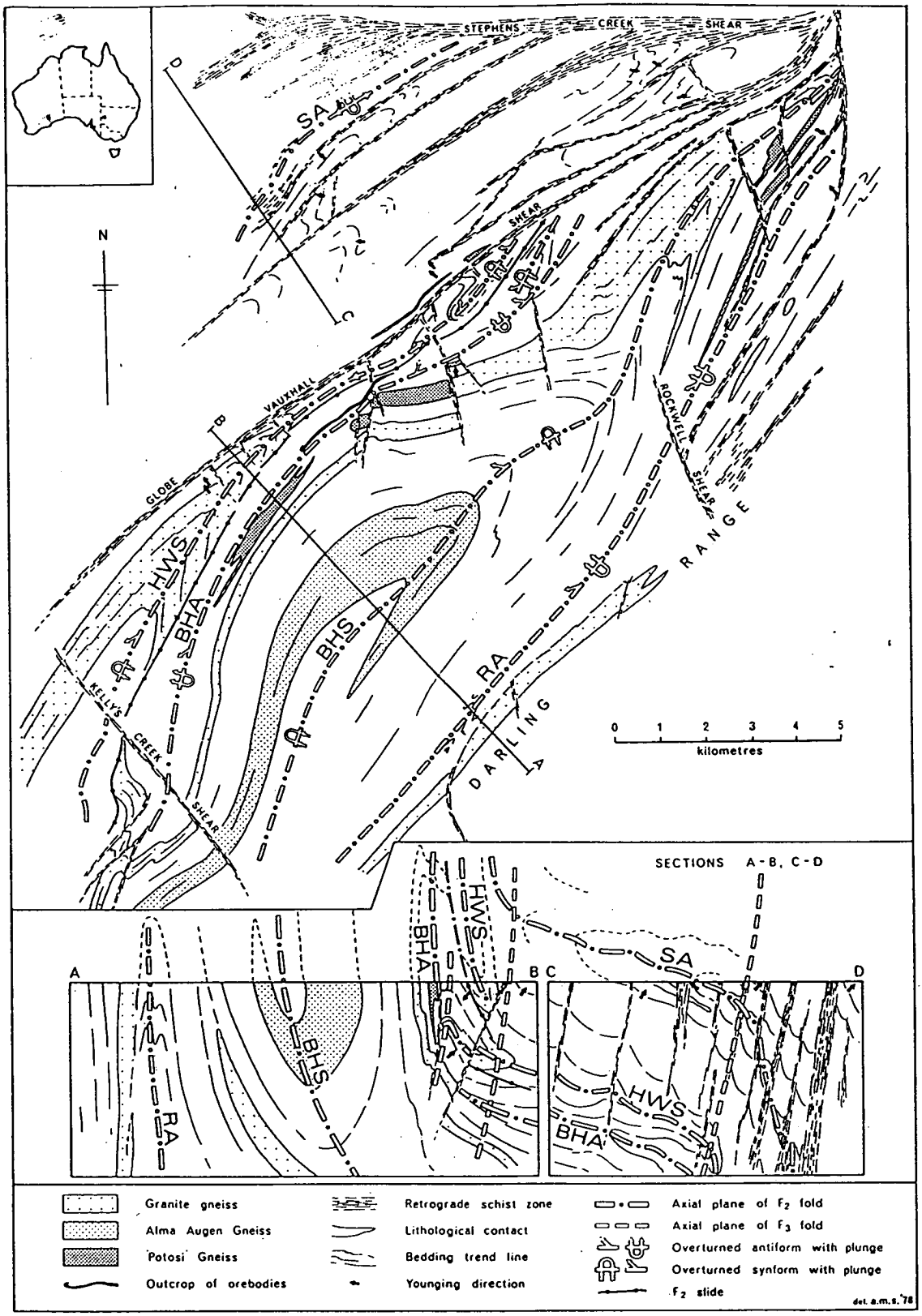

Figure 3.6 Structure in the vicinity of the Broken Hill deposit. (Laing et al, 1978)

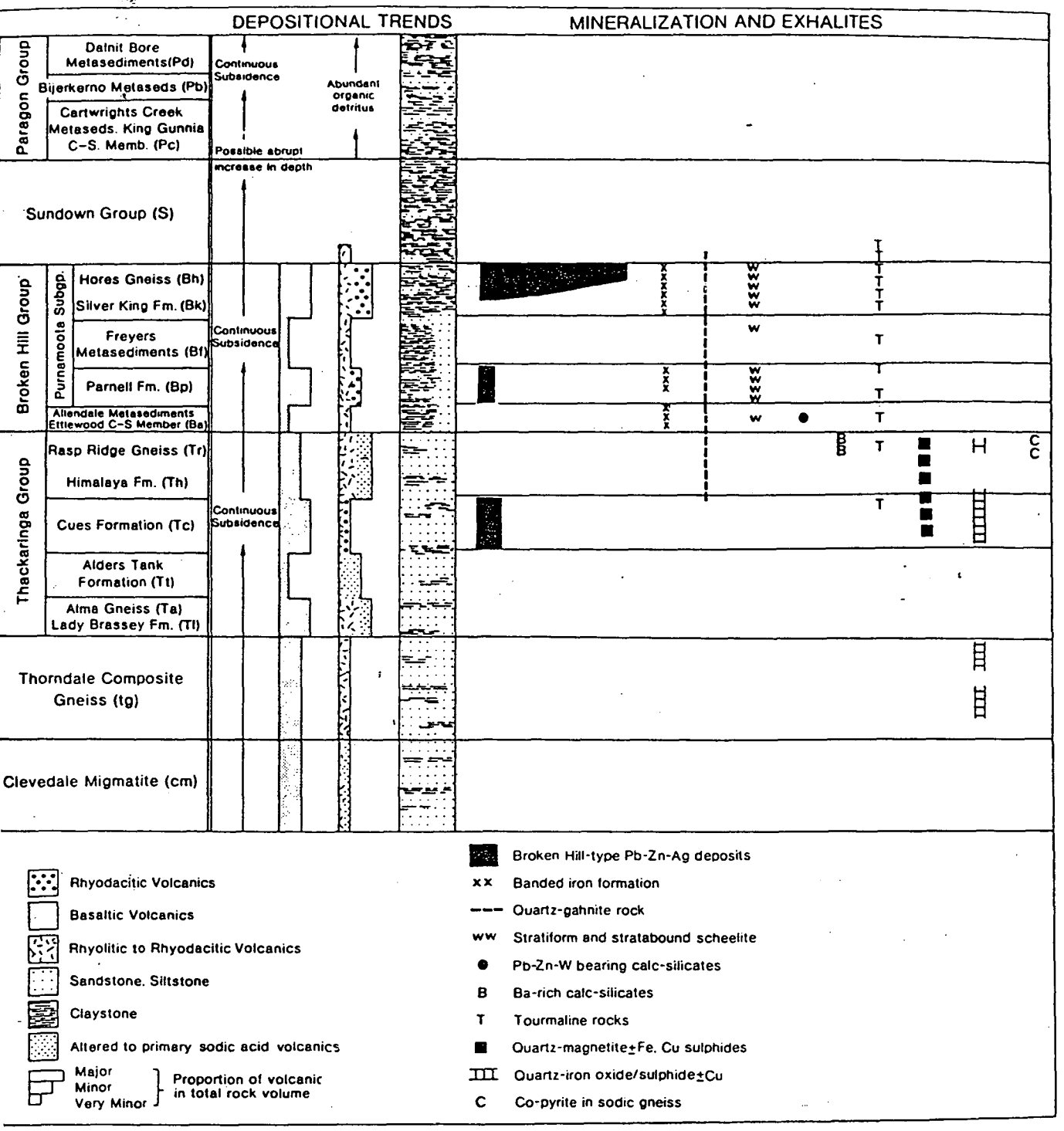

Figure 3.7 Stratigraphy of the Willyama Supergroup, with distribution of mineralisation.
(Plimer, 1985)

the Pinnacles deposit, is also found in the Cues Formation which is the Transitional Sequence within the Thackaringa Group. However some (e.g. Parr, 1994) would argue that the Pinnacles deposit may be hosted within the Broken Hill Group, rather than the Cues Formation.

There are four main styles of mineralisation present within the Willyama Supergroup:

1. stratiform
2. stratabound
3. vein - transgressive
4. intrusion related

Characteristics of stratabound, vein style and intrusion related mineralisation are summarised in Tables 3.2, 3.3 and 3.4 respectively.

Seven types of stratiform mineralisation in addition to BHT style mineralisation have been recognised. The main characteristics of each of these types are summarised in Table 3.5. BHT mineralisation is the most economically significant mineralisation style within the Broken Hill Block.

BHT deposits within the Broken Hill Block occur as stratiform disseminations or pods. Primary ore minerals are galena and Fe-rich sphalerite. Other common sulfide minerals include pyrrhotite, chalcopyrite, arsenopyrite, and loellingite. Non-sulfide gangue minerals are dominantly quartz, feldspar, gahnite and garnet. Accessory minerals include muscovite, biotite, apatite and tourmaline. Major gangue minerals present in the Broken Hill Ore deposit which are absent in smaller occurrences include rhodonite, manganhedenbergite, bustamite, roepperite, calcite, wollastonite and fluorite.

There is a very skewed tonnage-grade distribution of BHT deposits. Broken Hill is the largest, with more than 200 million tonnes of ore. The next most significant deposit is the Pinnacles deposit, with less than 1 million tonnes of ore. Most BHT occurrences are an order of magnitude smaller again.

Throughout the block BHT mineralisation is grossly conformable, although local remobilisation of ore into fold hinges has occurred. Most occurrences of mineralisation are strongly folded, as are the host rocks. Originally, however, the mineralisation would have had a very elongate tabular form. The Broken Hill ore lenses have length to width ratios of more than 8:1.

Most BHT mineralisation occurrences are hosted by pelitic to psammopelitic metasedimentary rocks. In most smaller BHT occurrences mineralisation occurs in granular quartz-gahnite rocks, although mineralisation may be hosted by garnet-rich rocks. Basic gneiss (amphibolite), Potosi Gneiss (quartz-feldspar-biotite +/- garnet gneiss with distinctive garnet spots up to 1cm, commonly

Type	Major commodities	Minor commodities	Primary ore mineralogy	Secondary ore mineralogy	Gangue mineralogy	Host rocks	Textures and layering	Main examples	Major stratigraphic setting
Silver King type: Pb, Zn, Cu, Ag, Au, W in grossly concordant quartz bodies or as disseminations in basic gneiss	Pb, Ag, Zn, Cu	Au, W	Galena, sphalerite, chalcopyrite, wolframite, arsenopyrite, loellingite, pyrrhotite, scheelite	Cerussite, chlorargyrite, malachite	Quartz, feldspar, amphibole (garnet, gahnite, tourmaline, epidote, fluorite, calcite)	Amphibolite, metasediments, pegmatite, "Potosi-type gneiss"	Generally granular with poor layering grading to vein like. Also fine to medium disseminations	Silver King, Black Prince, Jersey Lily, Yuba	Broken Hill Group; Silver King Formation, Parnell Formation
Hores type: scheelite ± wolframite in quartz-muscovite-tourmaline pegmatite or as disseminations in "BG" gneiss or flanking tourmalinites	W	As, Pb	Wolframite, scheelite, (arsenopyrite, pyrite, pyrrhotite, galena)	(Scorodite, cerussite)	Quartz, muscovite, tourmaline, feldspar, (garnet, gahnite, biotite, fluorite)	Quartz-feldspar-biotite (±garnet) gneiss, tourmalinite	Pegmatitic to vein like, some coarsely granular. Also as disseminations in gneiss	Hores, Freyers, Annandale	Broken Hill Group; Hores Gneiss, Parnell Formation
Diamond Jubilee type: copper-gold bearing quartz-pyrite-magnetite lenses in migmatite	Cu, Au		Chalcopyrite, pyrite, magnetite, haematite	Malachite, azurite	Quartz, biotite, feldspar, muscovite	Quartzo-feldspathic migmatite	Medium to coarse granular, poor layering. Also interlocking euhedral quartz masses	Diamond Jubilee	Thackaringa Group

Table 3.2 Characteristics of stratabound mineralisation, Broken Hill Block. (Barnes, 1988)

Type	Primary mineralogy	Secondary ore minerals	Dimensions	Relationship to host rocks	Textures	Main examples	Other comments
Thackaringa type: silver-lead-bearing siderite-quartz veins	Siderite, quartz, (calcite, barite), argentiferous galena, (sphalerite, chalcopyrite, pyrite, tertrahedrite, arsenopyrite, sulphosalts)	Silver halides, cerussite, bindheimite, native silver	Narrow veins or shoots and pods of ore in veins in faults. Width of veins approx. 1 cm to 1 m, generally < 0.3 m	In fault zones within retrograde schist zones (e.g. Apollyon Valley) or in areas of strong retrogression (e.g. south-east of Purnamoota)	Crustiform textures poorly to well developed. Some mild deformation textures	Thackaringa mines, Apollyon Valley mines, Umberumberka mines, Consols mine, Mayflower, Maybell, and Lubra mines	Post-date retrograde metamorphism
Copper-bearing siderite-quartz veins	Siderite, quartz, chalcopyrite	Malachite, chrysocolla, jarosite, atacamite, azurite, cuprite	As for Thackaringa type	As for Thackaringa type	As for Thackaringa type	In Mount Darling Range, Oakdale areas	Post-date retrograde metamorphism
Mount Robe type: lead-silver-zinc copper-bearing quartz-fluorite veins	Quartz, fluorite, galena, sphalerite, chalcopyrite	Cerussite, smithsonite, silver halides, anglesite	Thin, long, tabular bodies. Width up to several metres, length up to at least 1 km	Veins transgress layering in host rocks or parallel retrograde schistosity	Some ?tectonic banding, some weak crustiform textures	Mount Robe mine, Mount Elite fluorite mine	Highly "anomalous" lead isotope ratios
Lead-bearing quartz veins	Quartz, galena (chalcopyrite)	Cerussite	Width 0.3 to 2 m rarely to 10 m	As for copper-bearing quartz veins	Strong shearing in some, some weakly crustiform	Morning Star mine, Lily mine	Includes several generations of veins
Copper-bearing quartz veins, including rare gold-bearing varieties	Quartz, (chlorite, calcite, siderite, fluorite), pyrite, chalcopyrite, (galena, gold)	Malachite, azurite, chrysocolla, cuprite	Width 0.3 m to 2 m, length 5 m to 200 m. Commonly en echelon lenses	Most occur in narrow retrograde schist zones or faults. Some show no structural control	Crustiform textures with little deformation in some, severe deformation and recrystallization in others	Umberumberka East, King Gunnia mine, Lady Dorothy copper mine, Nadbuck mine, Invincible mine	Most veins parallel retrograde schistosity and are partly sheared. Most veins formed before or during retrogression
Pyrite-quartz veins (excluding laminated types)	Quartz (chlorite), pyrite	Iron oxides	As for copper-bearing quartz veins	As for copper-bearing quartz veins	As for copper-bearing quartz veins		Most field features are similar to copper-bearing quartz veins
Laminated pyritic quartz veins	Quartz, pyrite, (chalcopyrite, magnetite)	Iron oxides, sulphur	Width 0.3 to 2 m, up to several hundred metres length	Predominantly concordant to retrograde schistosity in schist host rocks	Frosty appearance caused by extensive recrystallization. Tectonic banding and mylonitic textures	Purnamoota area, Lone Star	
Gold-bearing quartz veins	Quartz, (chlorite), pyrite, (chalcopyrite), gold	Iron oxides, (malachite)	As for copper-bearing quartz veins	As for copper-bearing quartz veins	As for copper-bearing quartz veins	Golden King, Panama Hat, Mulculca	Essentially pyritic or cupriferous quartz veins with some gold

Table 3.3 Characteristics of vein mineralisation, Broken Hill Block. (Barnes, 1988)

Type	Major commodities	Main ore mineralogy	Rock type hosting mineralization	Main examples	Structural/stratigraphic setting	Other comments
Waukeroo type: tin-bearing pegmatites	Sn	Cassiterite	Pegmatite	Waukeroo tin field (Yanco Glen)	Concentrated in sediments above the Broken Hill Group (mainly Paragon Group)	Similar deposits at Bijerkerno in Euriowie Block
Mulga Springs type: ultrabasic intrusives with Pt-Cu-Ni	Platinoids, Cu, Ni, (Au)	Pyrite, pyrrhotite, chalcopyrite, pentlandite, native metals	Serpentinites, peridotites, pyroxenites	Mulga Springs, Mount Darling Creek	Largest and best mineralized bodies are localized in major retrograde schist zones	Occurs as stockworks and masses near contacts
Iron Duke type: magnetite-pyrite in, and associated with, granitic intrusives, or as pods or veins in metasediments	Fe	Magnetite, pyrite, jarosite, iron oxides	Umberumberka-type granitoids and metasediments	Iron Duke, (Umberumberka-western Lakes Creek area)	Strong clustering in the Umberumberka area	Included are magnetite-pyrite disseminations and irregular masses in granitic intrusions; breccias of magnetite ± pyrite and granitic rock, massive magnetite-pyrite "veins" and discordant bodies in metasediments and some layered magnetite-pyrite occurrences.
Bakers type: uranium-bearing granitoids and pegmatites	U, Th	Davidite, carnotite, brannerite, thorite, monazite	Pegmatites, microgranite, aplite, mica schists	Thackaringa davidite belt	Strong clustering and tendency to concentrate near Thackaringa - Broken Hill Group boundary	Includes "veins", dykes, pods, and disseminations in granitic and aplitic rock and in surrounding host rocks
Base metal in pegmatite (other than tin or tungsten bearing types)	Pb, Cu	Galena, chalcopyrite, malachite	Pegmatites of various generations		Various	Very minor occurrences, no production
Rutile-bearing pegmatite	(Ti)	Rutile	Pegmatite		Various	Very minor occurrences, no production

Table 3.4 Characteristics of mineralisation associated with intrusive rocks, Broken Hill Block.
(Barnes, 1988)

Type commodities	Major commodities	Minor commodities	Primary ore mineralogy	Secondary ore mineralogy	Gangue mineralogy	Host rocks	Textures and layering	Main examples	Major stratigraphic setting
Broken Hill type: Pb-Ag-Zn in quartz gahnite, garnet-quartz, or other related rock type	Pb, Ag, Zn	Cu, Sb, Cd, Au, Co, S	Galena, sphalerite (pyrrhotite, chalcopyrite, arsenopyrite, loellingite)	Cerussite, cerargyrite, malachite	Quartz, feldspar, gahnite, garnet; in Broken Hill Main lode, manganese silicates, calcite, fluorite	Pelitic-psammitic metasediments, basic gneiss, "Potosi-type" gneiss	Generally granular with poor to well-developed layering	Broken Hill Main lode Pinnacles, Allendale, Parnell, Southern Cross, Angus, Little Broken Hill area	Broken Hill Group, Hores Gneiss, Parnell Formation. Thackaringa Group, Cues Formation
Miscellaneous stratiform horizons related to Broken Hill type:									
Banded iron formation (bif)		Fe	Magnetite		Garnet, quartz, apatite,	Metasediments	Excellent fine layering (bif)	Broken Hill mines area	Broken Hill Group
Garnet-quartz/garnet-haematite rock		Fe, Co, Pb, Ag, Zn	Galena, sphalerite, magnetite loellingite	Cerussite	Garnet, quartz, amphibole,	Metasediments	Granular, variably poor to well-developed layering	Pinnacles area	Thackaringa Group
Quartz-fluorite rock		F	Galena, sphalerite		Fluorite, quartz, amphibole	Metasediments	Poorly layered, granular (quartz-fluorite)	Thackaringa fluorite belt	Thackaringa Group
Other related horizons									
Ettlewood type: layered calc-silicate rock with sulphides or base metals	Zn, Pb, Ag, W	Cu	Galena, sphalerite, scheelite, chalcopyrite, pyrrhotite, (molybdenite)	Malachite, cerussite	Amphibole, epidote, clinopyroxene, (quartz, plagioclase, vesuvianite, garnet, wollastonite, scapolite, calcite)	Mineralization occurs in calc-silicate rock in metasediments	Fine to medium-grained, excellent fine to medium layering	Ettlewood occurrences, Bomangaldy Hill	Ettlewood Calc-silicate Member, lower Broken Hill Group
Corruga type: irregular quartz-garnet-epidote-amphibole rock containing scheelite or base metals	W	Pb, Ag, Zn, Cu	Scheelite, galena, (sphalerite, chalcopyrite, pyrite, magnetite)	Cerussite, (malachite, azurite, chyrsocolla)	Quartz, garnet, epidote, clinozoisite, amphibole, (diopside, tourmaline, apatite, zircon, fluorite, gahnite, calcite)	Garnetiferous or pyroxene or epidote-rich basic gneiss, "Potosi-type" gneiss	Mixed fine to medium-grained layered rock and coarse granular rock; some veinlike remobilized rock	Corruga prospects, Black Hill prospect, Esmeralda, Mount Eitle area, Little Broken Hill area	Parnell Formation, Broken Hill Group
Sisters type: quartz-magnetite ± iron sulphide rock		Fe, Cu, Co	Magnetite, haematite (pyrite, pyrrhotite, chalcopyrite)	Iron oxides, malachite	Quartz, apatite, (garnet, chlorite)	Plagioclase-quartz granofels, metasediments	Granular, medium to coarse-grained, good to excellent layering	The Sisters, Razorback, Pinnacles, Sentinel	Himalaya Formation, Cues Formation, Thackaringa Group
Great Eastern type: granular quartz-iron-sulphide (± garnet) rock	Cu	Co	Pyrite, pyrrhotite, chalcopyrite, (arsenopyrite, cobaltite)	Iron oxides, malachite	Quartz, feldspar (chlorite, sillimanite, sphene gahnite)	Psammitic metasediments, composite gneiss	Granular, poor to well-developed layering	Great Eastern, Mount Darling Ranges, Eastern copper mineralization, Coultra copper mine	Cues Formation
Big Hill type: pyrite (± cobalt) in plagioclase-quartz granofels	Pyrite, Co		Pyrite	Iron oxides	Host rock, albite/ oligoclase, quartz	Plagioclase-quartz granofels	Disseminations to lenticular masses parallel to bedding in host rocks	Big Hill, Pyrite Hill, Stirling Vale	Himalaya Formation

Table 3.5 Characteristics of stratiform mineralisation, Broken Hill Block. (Barnes, 1988)

retrogressed to biotite) and leucocratic gneiss or pegmatite commonly occur within tens of metres of mineralisation. Deposits in the Parnell Formation are commonly very closely related to basic gneiss.

BHT mineralisation occurs at several stratigraphic levels but is concentrated in three formations: the Cues Fm. (Thackaringa Group), the Parnell Fm. and the Hores Gneiss (Broken Hill Group) (Fig. 3.7). Smaller concentrations of BHT mineralisation occur in the Allendale Metasediments and minor occurrences are known within the Sundown Group.

There is a gradation in the chemistry of BHT mineralisation with stratigraphic position. BHT mineralisation in the Thackaringa Group is associated with more iron-rich lithologies. BHT mineralisation at the base of the Broken Hill Group is richer in iron sulfides than occurrences in the Parnell Formation, which are commonly iron-sulfide poor. The Broken Hill ore body, which is located at the top of the Broken Hill Group, is significantly richer in Ca, Mn, P and F, not to mention Pb, Zn and Ag.

3.2 Geology of the Broken Hill Ore Deposit and its Host Stratigraphy

An excellent description of the geology of the Broken Hill ore deposit, and its host stratigraphy, is provided by Haydon and McConachy (1987). The following description largely draws on this paper.

The host stratigraphy within the mine leases is described in Figure 3.8 and Table 3.6. A plan view of the geology is shown in Figure 3.9. A cross section is shown in Figure 3.10 and a long section is presented as Figure 3.11.

The ore deposit is comprised of eight mineable lodes (Fig.3.10) which are interpreted to be stratigraphically inverted:

Stratigraphic Base	C		Zn
	B		Zn
	A	- upper	Zn
		- lower	Zn
	1	- upper Zn	
		- lower Zn	
	2		Pb
Stratigraphic Top	3		Pb

The mining grades and gangue mineralogy of the individual lodes are summarised in Table 3.7.

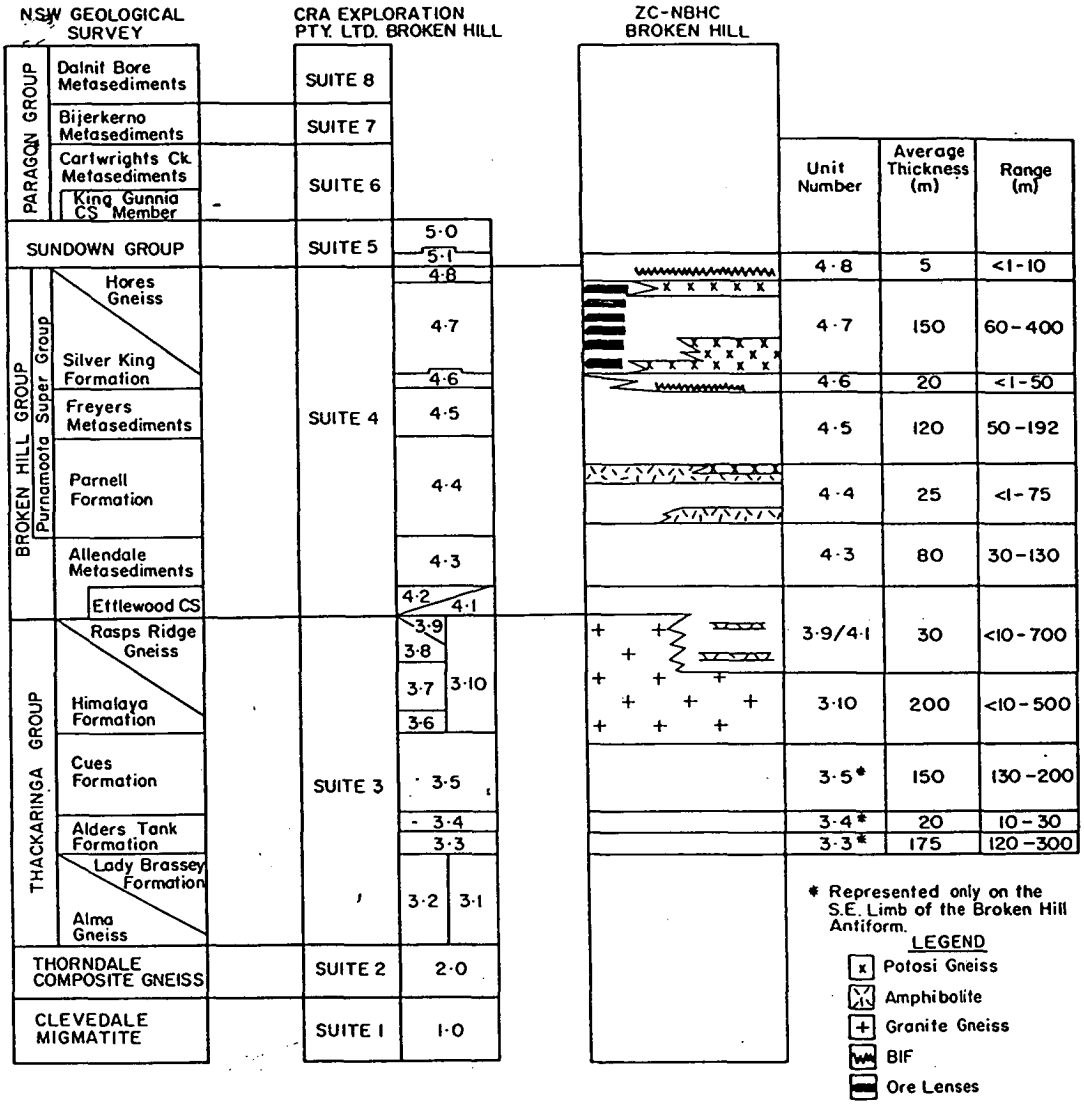

Figure 3.8 Stratigraphic subdivisions within the Broken Hill Mine Leases.
(Haydon and McConachy, 1987)

Nomenclature	Nomenclature					
Unit 5.0	Sundown Group	- well bedded pelite and psammites - common calc-silicate ellipsoids - isolated occurences of well developed thick psammites, occasionally containing abundant magnetite - minor base metal mineralisation in psammitic and quartz gahnite horizons at base			Yes	Yes
Unit 4.8	Upper Hores Gneiss	- pelite of variable thickness - abundant biotite, sillimanite, k-feldspar - local development of magnetite or BIF or thin banded garnet rich psammite	5m	<1 - 10m	Yes	No
Unit 4.7	Mid Hores Gneiss	- comples association of Potosi gneiss, moderate to poorly bedded psammopelites, pelites - local development of quartz rich psammites and lodes - basal Potosi gneiss and upper Potosi gneiss unit - basal Potosi gneiss unit is laterally equivalent to spotted psammopelite (garnet-feldspar-sillimanite) - contains sulfide ore bodies and lode rocks - garnet quartzites, garnet sandstones, blue quartz-gahnite, lode pegmatite, calc-silicates	150m	60 - 400m	No	Yes
Unit 4.6	Lower Hores Gneiss	- laterally persistent pelite - abundant biotite, sillimanite, k-feldspar - local development of magnetite - at base BIF (less than 1m thick) or fine banded gametiferous psammite	20m	<1 - 50m	Yes	No
Unit 4.5	Freyers Metasediments	- pelites, psammites, psammopelites (thin bedded at base, thick bedded at top local graded bedding - most obvious change upwards is the appearance of thick massive blue quartz rich psammites interbedded with thick pelites - minor disseminated sphalerite/galena/pyrrhotite/chalcopyrite in upper psammites	120m	50 - 190m	No	Yes
Unit 4.4	Parnell Formation	- single basal mafic hornblende rich amphibolite which grades upward into felsic and gametiferous variants and Pototsi Gneiss (gradation over 5 - 15m) - Potosi gneiss may be capped by thin amphibolite - thin bands/pods of quartz rich lode with minor galena/sphalerite/pyrrhotite/chalcopyrite within metasediments overlying basal amphibolite - unit 4.4 may be absent (in southern leases) or comprised of three amphibolites	25m	<1 - 75m	Yes	Yes
Unit 4.3	Allendale Metased.	- well bedded psammopelites, pelites and thin psammites with fine grained garnets	80m	30 - 130m	No	No
Unit 4.2	Ettlewood Calc-Silicate	- not present within the mine leases				
Unit 3.10	Rasp Ridge Gneiss Himalaya Formation	- Granitic Gneiss with thin uppermost unit of aplitic granite gneiss, feldpsathic psammite and interbedded psammopelite at top	200m	<10 - 500	No	No
Unit 3.9/4.1	Rasp Ridge Gneiss Himalaya Formation Allendale Metased.	- Pelitic to psammopelitic gneiss with coarse garnets, thin feldspar segregation layers, thin plagioclase rich psammites - Contains thin amphibolites with local development of broad zones of disseminated Po	30m	<10 - 700	Yes	No

Table 3.6 Stratigraphy within the Broken Hill Mine Leases

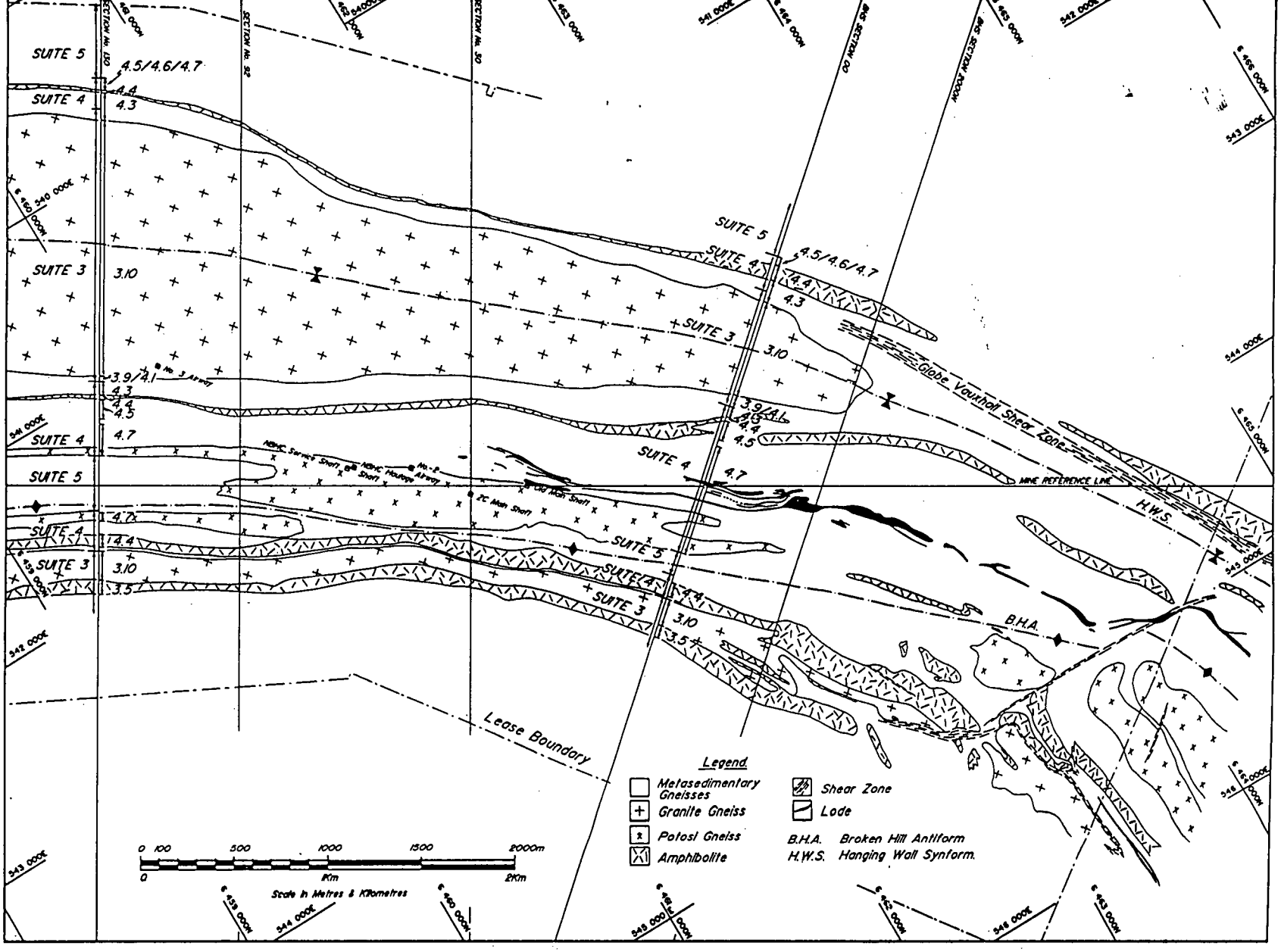

Figure 3.9 Geological plan within the Broken Hill mine leases.
(Haydon and McConachy, 1987)

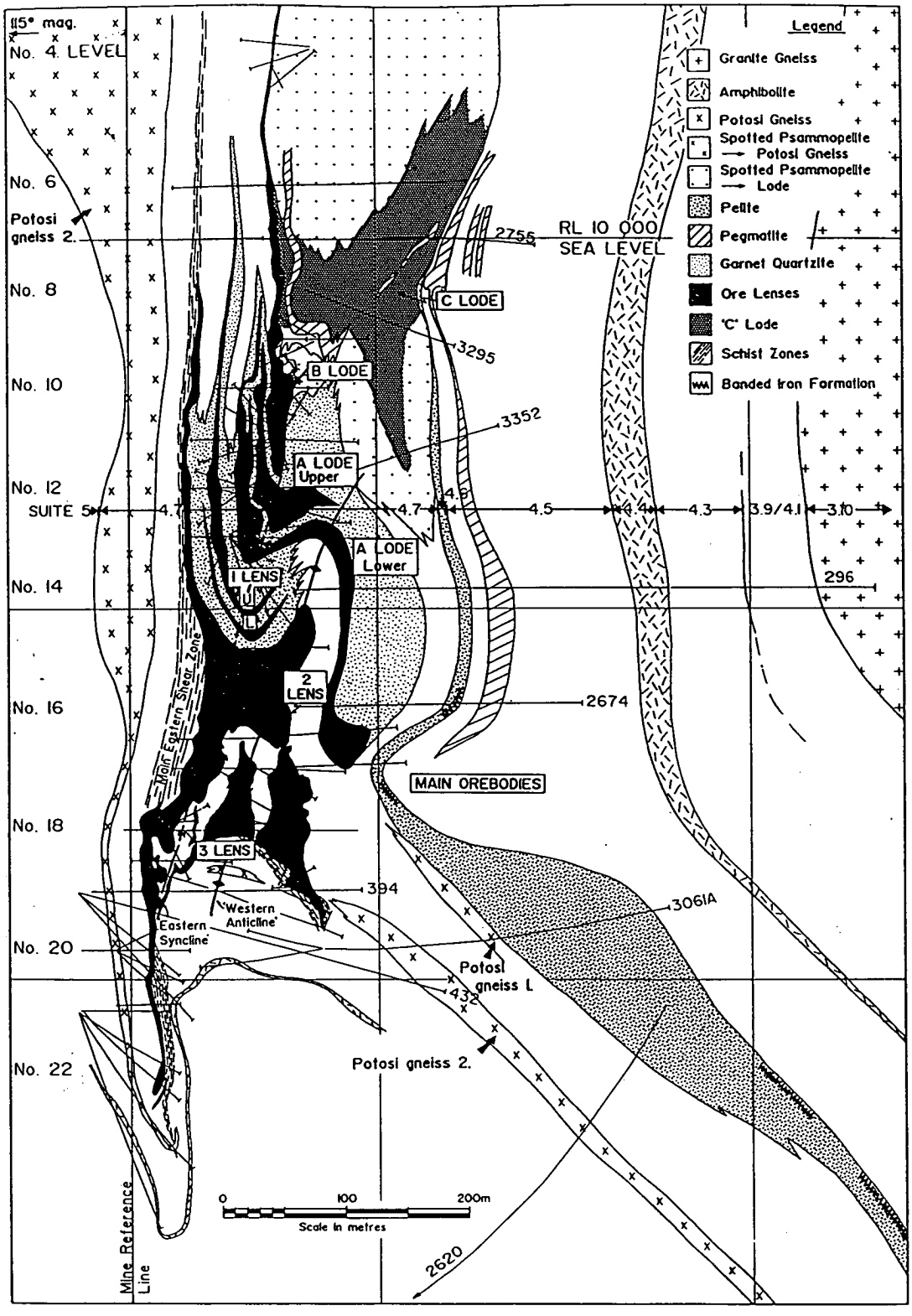

Figure 3.10 Cross section of the Broken Hill ore deposit (Section 30 - see Figure 3.9 for location)

(Haydon and McConachy, 1987)

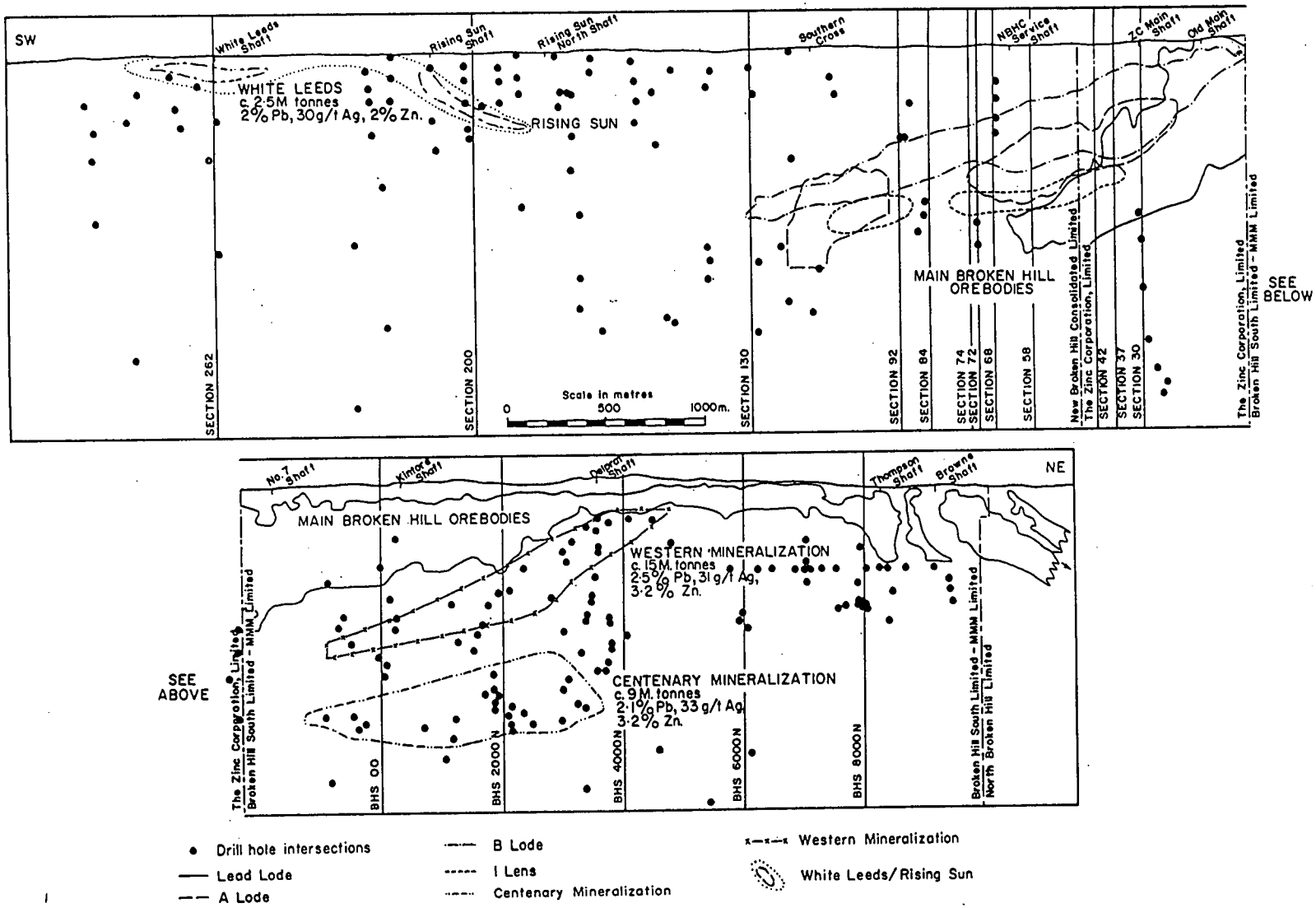

Figure 3.11 Longsection of the Broken Hill ore deposit, showing spatial relationship of the main lodes and minor mineralisation.
(Haydon and McConachy, 1987)

Orebody	Gangue	Pb (%)	Ag (g)	Zn (%)
No. 3 lens (south-western end)	*Quartz, fluorite,* rhodonite, garnet	7.8	169	11.9
No. 2 lens	*Calcite, rhodonite,* bustamite, "manganhedenbergite," knebelite, quartz, garnet, fluorite, apatite	16.4	118	12.4
No. 1 lens	*Quartz, calcite,* wollastonite, bustamite, "manganhedenbergite," epidote	9.6	53	22.4
A lode	*Rhodonite, "manganhedenbergite," quartz,* garnet, calcite, cummingtonite, dannemorite, wollastonite	4.3	31	10.4
B lode	*Quartz,* "manganhedenbergite," garnet, apatite, gahnite, damourite, rhodonite, calcite	4.3	33	12.4
C lode	*Quartz, garnet, biotite,* gahnite, "manganhedenbergite," clinozoisite, feldspar	3.2	34	6.4[1]

Table 3.7 Gangue mineralogy and ore grades of the Broken Hill (Australia) ore lenses.
(Haydon and McConachy, 1987)

The lodes are developed in an *en echelon* stack, with zinc lodes at the south end and lead lodes at the north end. The C lode is comprised of spotted psammopelite and blue-quartz rich lode rocks containing pods and zones of disseminated sulfide. There is a major change in rock type from C to B lodes , with B lode being hosted by garnet quartzites (10 varieties are recognised!). Lateral equivalents to B lode include blue-quartz rich rocks and finer grained psammites.

A lode and B lode are separated by garnet quartzite, and to a lesser degree lode pegmatite. The lateral equivalent to A lode is garnet quartzite. Garnet quartzite also separates the upper and lower A lodes. Cummingtonite and grunerite are characteristic of the garnet quartzites of A lode.

The upper and lower No. 1 lenses are once again enveloped by garnet quartzite. Small occurrences of pyrrhotite rich lode rocks occur toward the southern end. Garnet sandstone is developed along the southern and western margins.

No. 2 and No. 3 lenses are the lead lodes. They are the largest and most extensive. They remain physically separate over their entire 7 kilometre length. Lateral equivalents are garnet quartzites, blue quartz-gahnite lode rocks, garnet sandstone and metasedimentary rocks containing sulfides and green feldspar. Up-dip equivalents are obscured by a shear but appear to be similar lithologies to the lateral equivalents, with pyrrhotite, trace galena, sphalerite and chalcopyrite.

The No. 2 and No. 3 lodes converge at the southern end before terminating. Further south of the termination, a layer of blue quartz rich psammopelite with minor galena. sphalerite and chalcopyrite is interpreted to be laterally equivalent. More distally, psammites are lateral equivalents.

Enveloping the western downdip termination of the No.2 lens, near the NBHC service shaft (Fig. 3.10, 3.11), is a selvage of pyrrhotite associated with zones containing Fe-Ti oxides (magnetite, hematite, ilmenite, rutile) and gahnite. Close to the termination zone parts of the No 2 lens have abundant jacobsite ($MnFe_2O_4$).

3.3 Other Mineralisation Within the Line of Lode

Within the mine leases there are three other significant occurrences of mineralisation within the lode horizon. These occurrences are the White Leeds, Western and Centenary mineralisation. The relationship of these occurrences to the Main Lodes is shown in Figure 3.11.

White Leeds mineralisation is comprised of 2.5 MT grading 2% Pb, 2% Zn and 30 g/t Ag. Mineralisation is hosted by bands of blue quartz lode rock and psammites within quartz-biotite schist and retrogressed psammopelites.

Western mineralisation consists of 15 MT grading 2% Pb, 3% Zn and 30g/t Ag. Mineralisation occurs as bands and stringers of sulfide within garnet quartzite. The mineralisation is terminated down dip by the Globe Vauxhall Shear Zone.

The Centenary mineralisation, 9 MT grading 2% Pb, 3% Zn and 30 g/t Ag, occurs in lodes dominated by blue quartz-garnet and calc-silicate gangue, in addition to garnet quartzites. The calc-silicate gangue is comprised of quartz, garnet, epidote, clinozoisite, hornblende, hedenbergite, calcite and rhodonite, similar to the composition of calc-silicates in A lode.

Haydon and McConachy (1987) produced a schematic reconstruction of the ore deposit environment, showing stratigraphic and lithological relationships near the Main Lode, White Leeds, Western and Centenary Mineralisation (Fig. 3.12).

3. 4 Geology of the Pinnacles Deposit.

The Pinnacles deposit, located approximately 14 km south-west of the main lode, is the second most significant example of BHT mineralisation within the Broken Hill Block. Despite this it is more than two orders of magnitudes smaller than the Broken Hill deposit. 0.2 MT has been extracted at a grade of 6-11% Pb, 2.5% Zn and 300-500g/t Ag in the main stratabound Pb lode, and 1% Pb, 10-15% Zn and 30 g/t Ag in the Zn lodes (Parr, 1994). Remaining ore reserves are estimated to be between 0.2 and 0.6 MT.

The Pinnacles deposit has been mapped as being hosted by the Cues Formation within the Thackaringa Group, but this interpretation has been questioned by Parr (1994) who suggested that it may be stratigraphically equivalent to the Broken Hill ore deposit.

A geological plan showing the Pinnacles deposit relative to the adjacent Middle and South Pinnacles is presented as Figure 3.13. The Pinnacles deposit is dominated by sulfide rich rocks, in contrast to the quartz-magnetite rocks associated with the Middle and South Pinnacles.

The Pinnacles deposit is comprised of a series of stacked lodes. The major lode is a Pb lode, with Zn lodes stratigraphically above and below. There is a general vertical zonation from Zn-rich at the stratigraphic base to Pb-rich at the stratigraphic top, with a second Zn-rich event superimposed (Parr, 1994). The ores are hosted by a dominantly pelitic sequence, with interbedded psammopelites, garnetites (>80% garnet), garnet-quartz rocks and quartz-gahnite rocks (Parr, 1994).

The Pb lode is comprised of galena with minor sphalerite, pyrite, pyrrhotite, arsenopyrite and chalcopyrite. Other gangue minerals include almandine garnet, quartz, calcite, biotite, pyroxene and retrograde hornblende.

The Pinnacles Pb lode differs from the Broken Hill Pb lode in that the Broken Hill Pb ore is typically a galena-rhodonite assemblage, with high Ca and Mn contents, while the Pinnacles Pb lode is relatively Fe rich and Mn-Ca poor.

Two Zn lodes occur in the footwall to the Pb lode, and one occurs in the hanging wall. The Zn lodes are comprised of sphalerite, quartz, garnet, gahnite and biotite. The sphalerite is Fe rich and has a similar composition to the sphalerite at Broken Hill.

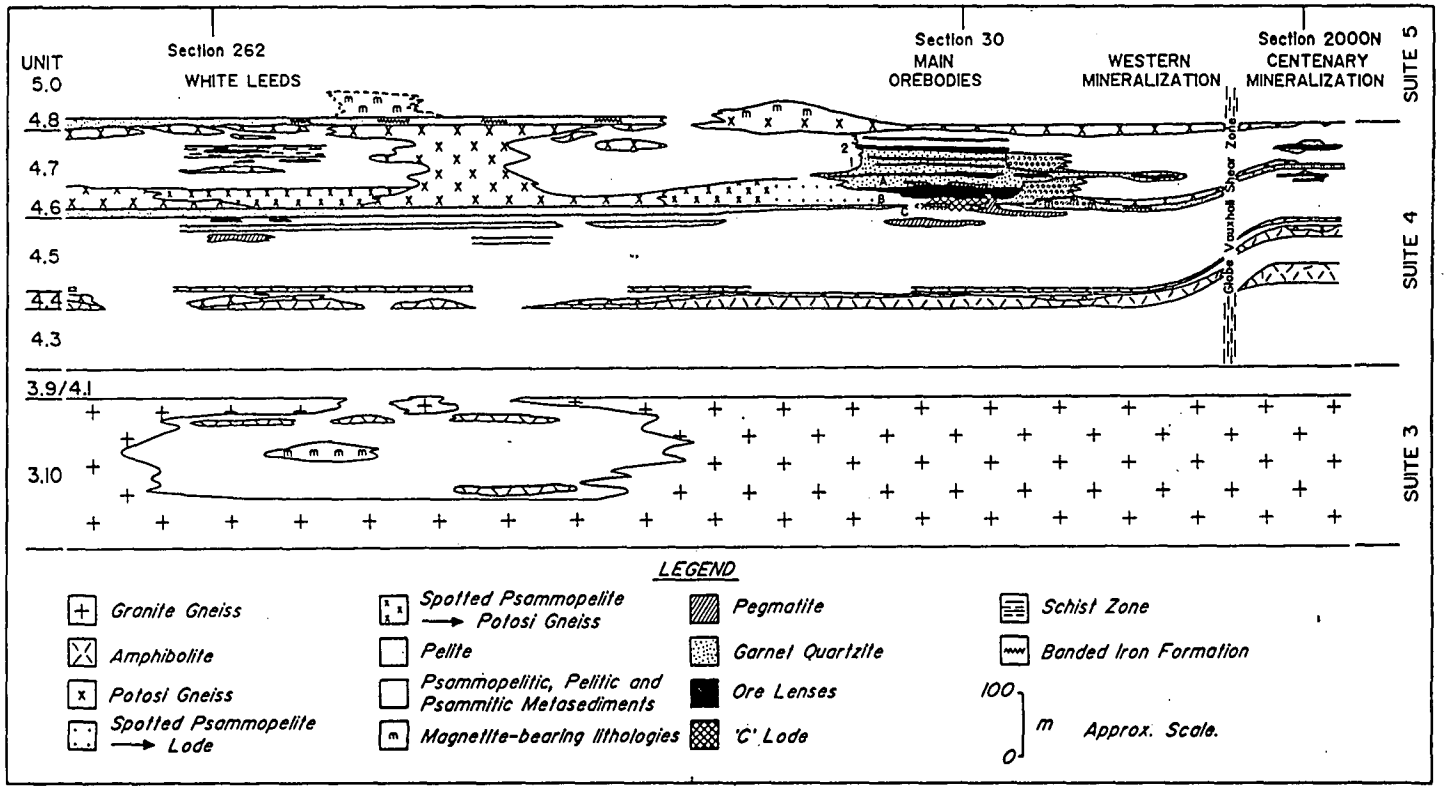

Figure 3.12 Schematic reconstruction of the Broken Hill ore setting
(Haydon and McConachy, 1987)

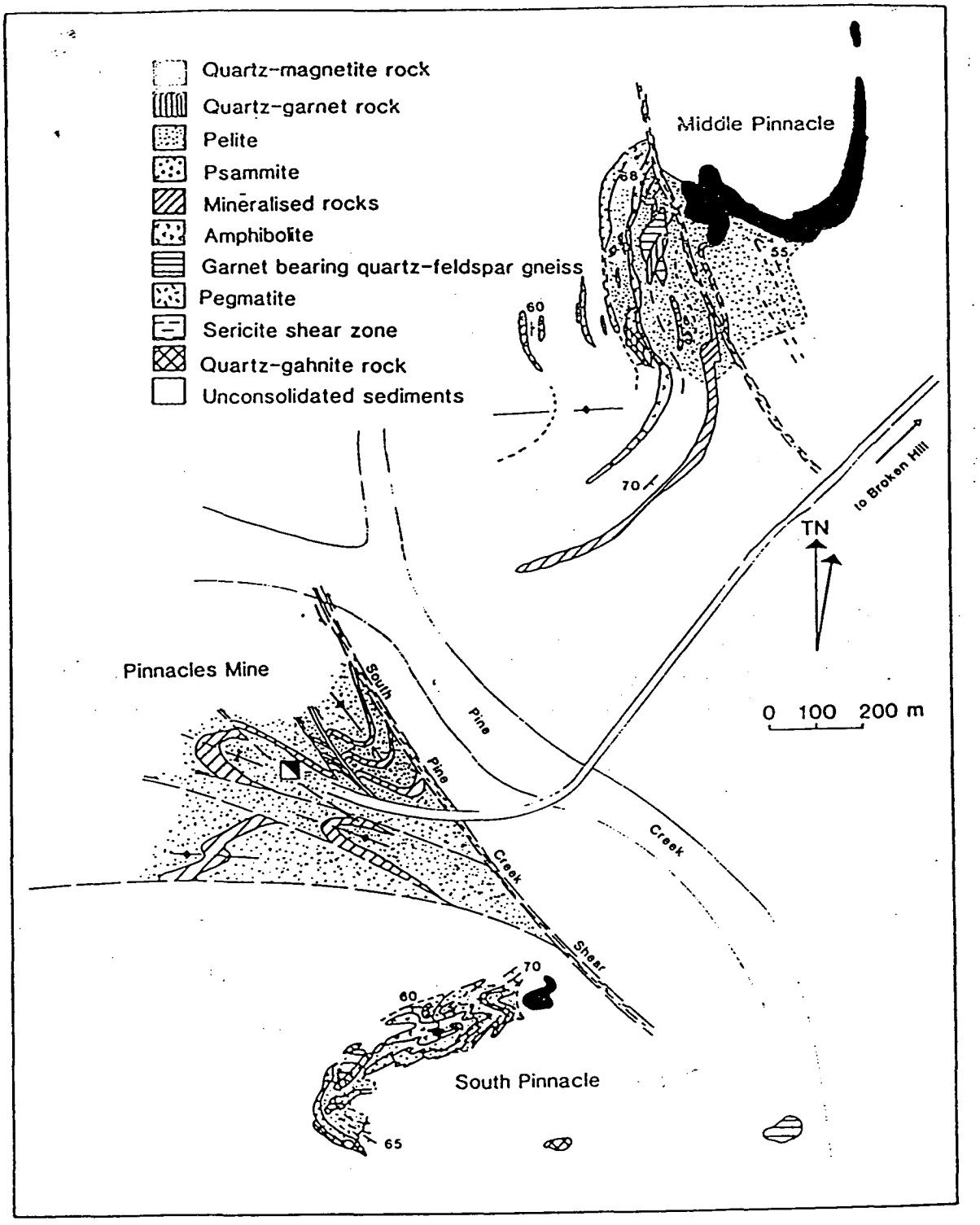

Figure 3.13 Geological plan of the Pinnacles deposit, Broken Hill Block (Parr, 1994)

The main differences between the Pinnacles and Broken Hill ore bodies may be summarised as follows (after Parr, 1994) :

- High Fe:Mn ratio, low Ca at Pinnacles,
- abundance of Fe-oxide rocks associated with Pinnacles,
- lack of substantial volumes of Potosi Gneiss at Pinnacles.

Garnets intimately associated with Pinnacles ore are almandine (Fe-rich) rather than spessartine (Mn-rich). Gangue minerals at Broken Hill commonly include Mn silicates such as rhodonite and bustamite whereas ferroan gahnite and biotite are more common at Pinnacles.

Pyrite is common at Pinnacles. Pyrrhotite, whilst minor, is the dominant iron sulfide species at Broken Hill. Quartz magnetite rocks are common in the vicinity of Pinnacles, but Fe-oxide facies are rare at Broken Hill. Where present at Broken Hill Fe-oxides occur as BIF rather than quartz magnetite. There is no quartz-magnetite rock recorded within the Broken Hill Group.

Fluorite and apatite are abundant at Broken Hill whereas only apatite is common at Pinnacles. The lack of fluorite at Pinnacles, together with isotopic evidence, suggests that the Broken Hill deposit may have tapped a deeper, more primitive hydrothermal source. This may also explain the large difference in the size of the deposits

Parr concludes that these differences may be explained by lateral facies variations from a shallower water environment at Pinnacles to a deeper water environment at Broken Hill, rather than invoking a different stratigraphic setting.

An alternate view point would be that the Pinnacles deposit is hosted by Cues Formation in the Thackaringa Group and that the differences between the two deposits do not reflect lateral facies variations, but significant temporal variations. The Thackaringa Group is noted for the prevalence of Fe-oxide exhalites, and is inferred to be a shallower water, more oxidised sequence than the Broken Hill Group. It is also possible that hydrothermal systems operating at that time may have been less evolved.

4. MAGNETIC CHARACTERISTICS OF STRATIGRAPHY AND BHT MINERALISATION OF THE BROKEN HILL BLOCK, AUSTRALIA.

4.1 Regional Magnetic Characteristics

Images of aeromagnetic data over the Broken Hill Block are presented in Figures 4.1 and 4.2, and Plates 1 and 2. The regional aeromagnetic data set is comprised of two surveys. The survey specifications and locations are shown in Figure 4.3

Within the aeromagnetic image three distinct zones can quickly be recognised. To the south-east an extremely contorted magnetic zone is the most obvious feature. To the north-west another zone of irregular, strongly magnetic stratigraphy is evident. These two sequences are interpreted to be gneissic granulite facies basement to the BHT regional stratigraphic sequence.

The south-eastern sequence is comprised of the Redan Gneiss, Ednas Gneiss and Mulculca Formation of the Broken Hill Block.

The north-western sequence in this image is entirely under cover but is interpreted to be the Composite Gneiss Suite of the Olary Block, which is thought to be equivalent to the Redan Gneiss of the Broken Hill Block. This region may also contain units of the Quartzofeldspathic Suite of the Olary Block, a strongly magnetic sequence equivalent to the Thackaringa Group within the Broken Hill Block.

Between these two zones a band of stratigraphy with a relatively non-magnetic background is evident. Within this relatively non-magnetic background numerous narrow, linear, sub-parallel magnetic units occur. This band of stratigraphy shows magnetic characteristics consistent with metavolcanic and metasedimentary rocks within a strongly deformed mobile belt tectonic setting. It is comprised of the Lower, Transitional and Upper Sequences of the BHT regional host stratigraphy.

The Lower Sequence corresponds to the Thackaringa Group, which is comprised of quartzofeldspathic gneisses and amphibolites. These lithologies are interpreted to represent bimodal felsic/mafic volcanic and volcaniclastic rocks with minor metasedimentary rocks.

The Transitional Sequence is represented by the Broken Hill Group, a sequence of psammitic/pelitic metasedimentary rocks and interbedded felsic and mafic gneisses.

The Upper Sequence is comprised of metasedimentary rocks (pelites and psammites) of the Sundown Group, overlain by graphitic metasedimentary rocks of the Paragon Group.

Tucker (1983) summarised the magnetic characteristics of the stratigraphy of the Broken Hill Block (Fig. 4.4), based on exploration data from CRAE. This figure gives an indication of the stratigraphic distribution of magnetic units and the range of magnetic susceptibilities.

Figure 4.1 Regional Aeromagnetic Data, Broken Hill, Australia.
Reduction To Pole

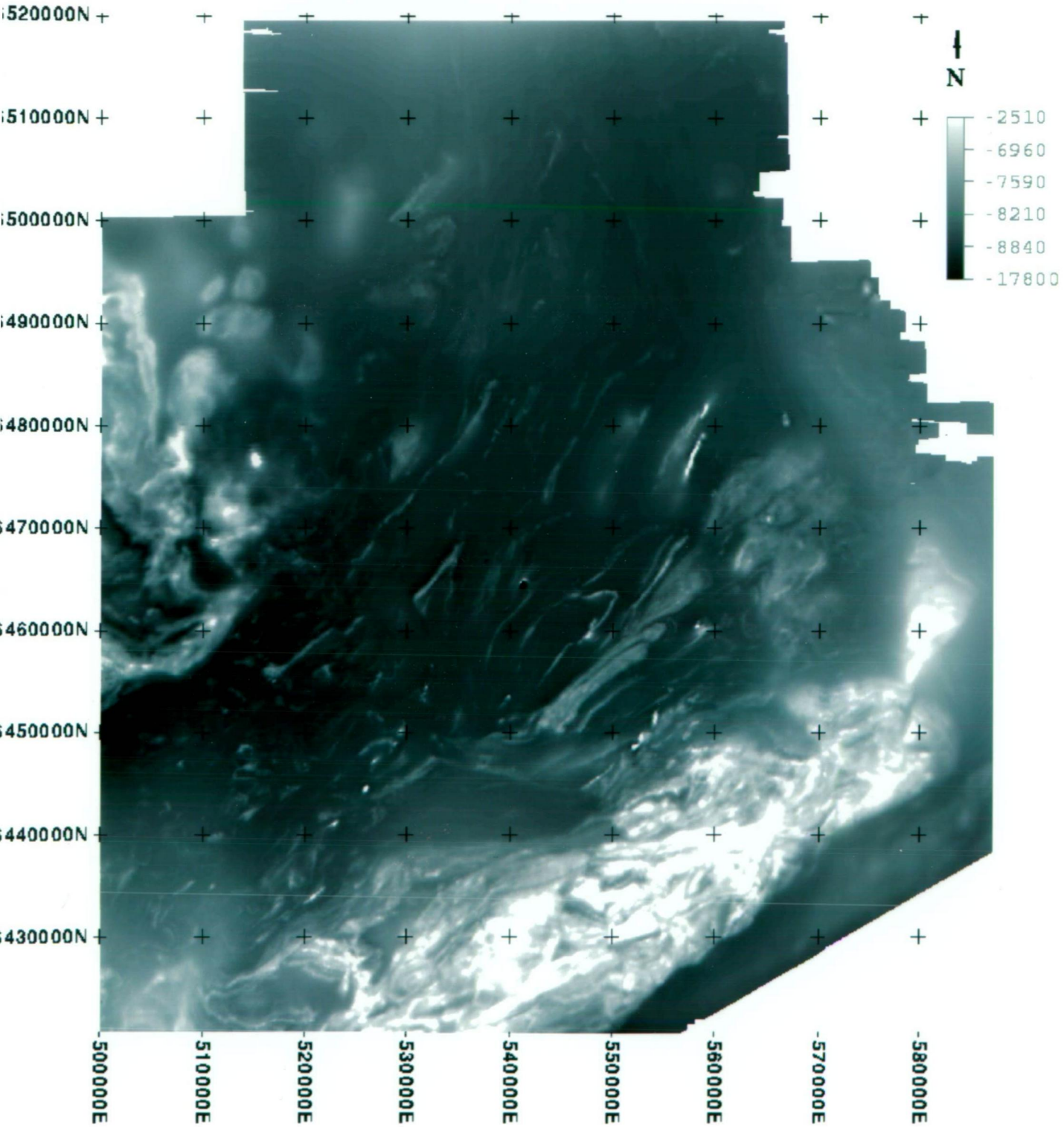

Figure 4.2 Regional Aeromagnetic Data, Broken Hill, Australia.
Reduction To Pole – 1st Vertical Derivative

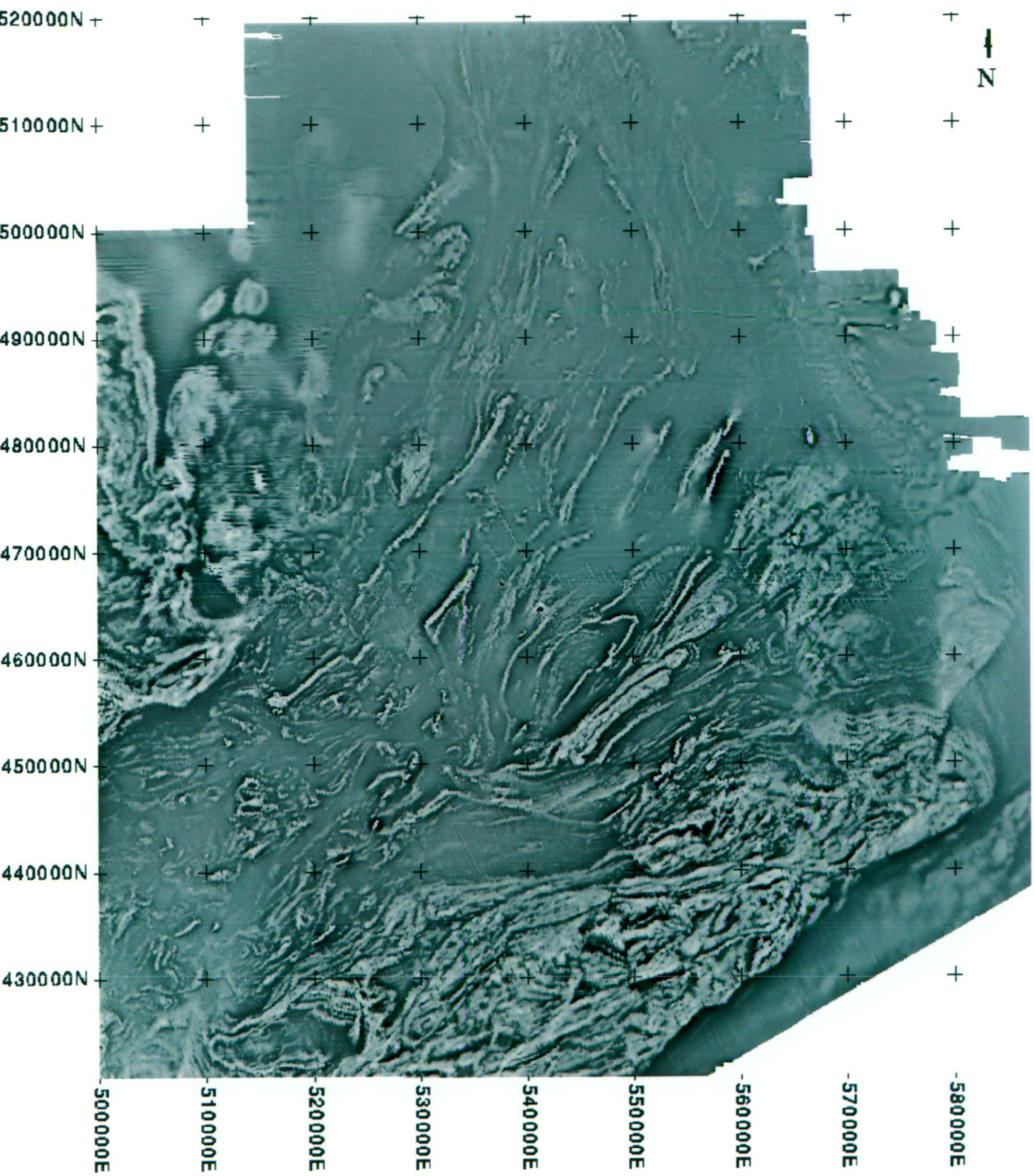

Figure 4.3 Regional aeromagnetic survey locations and specifications, Broken Hill, Australia.

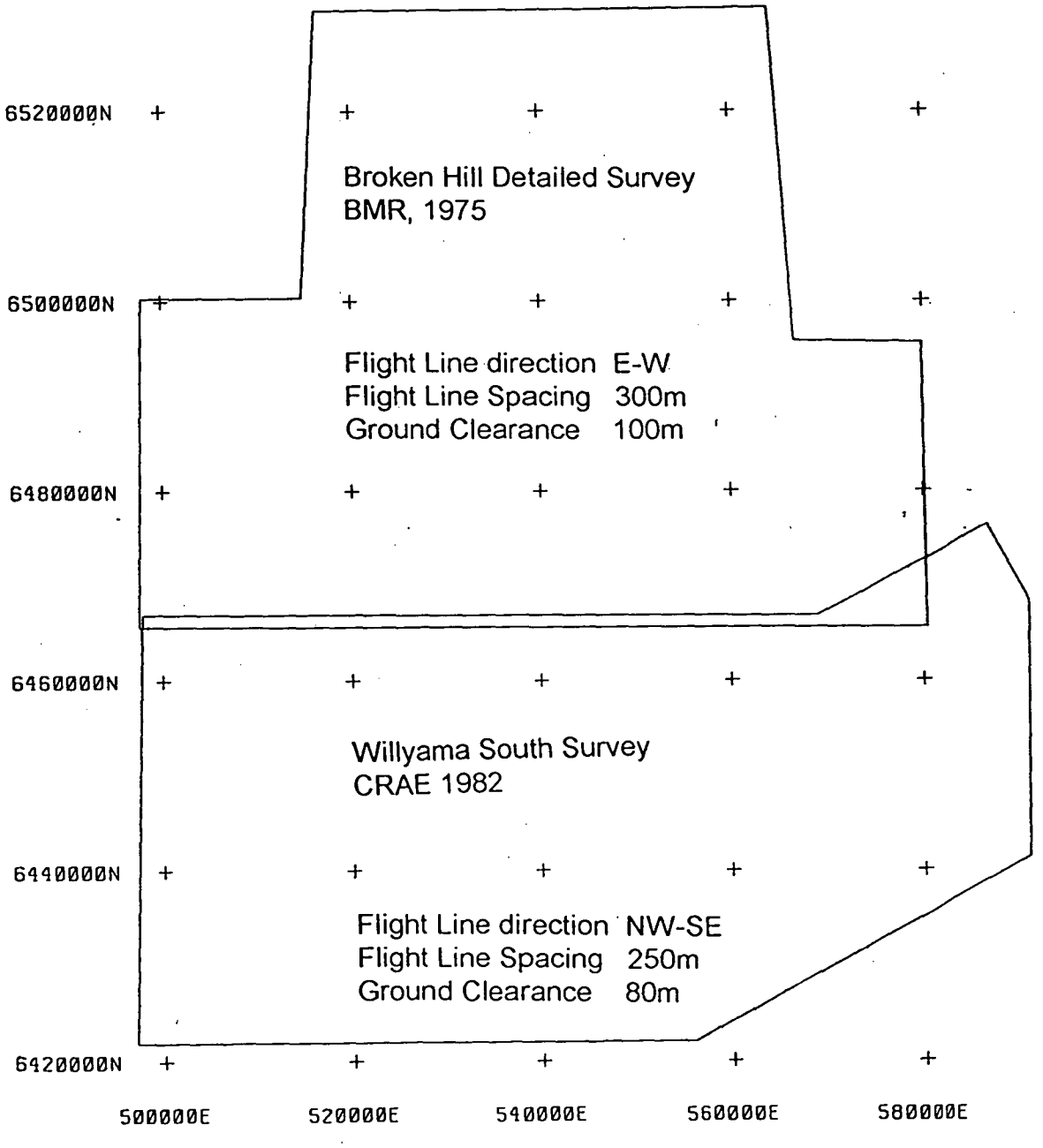

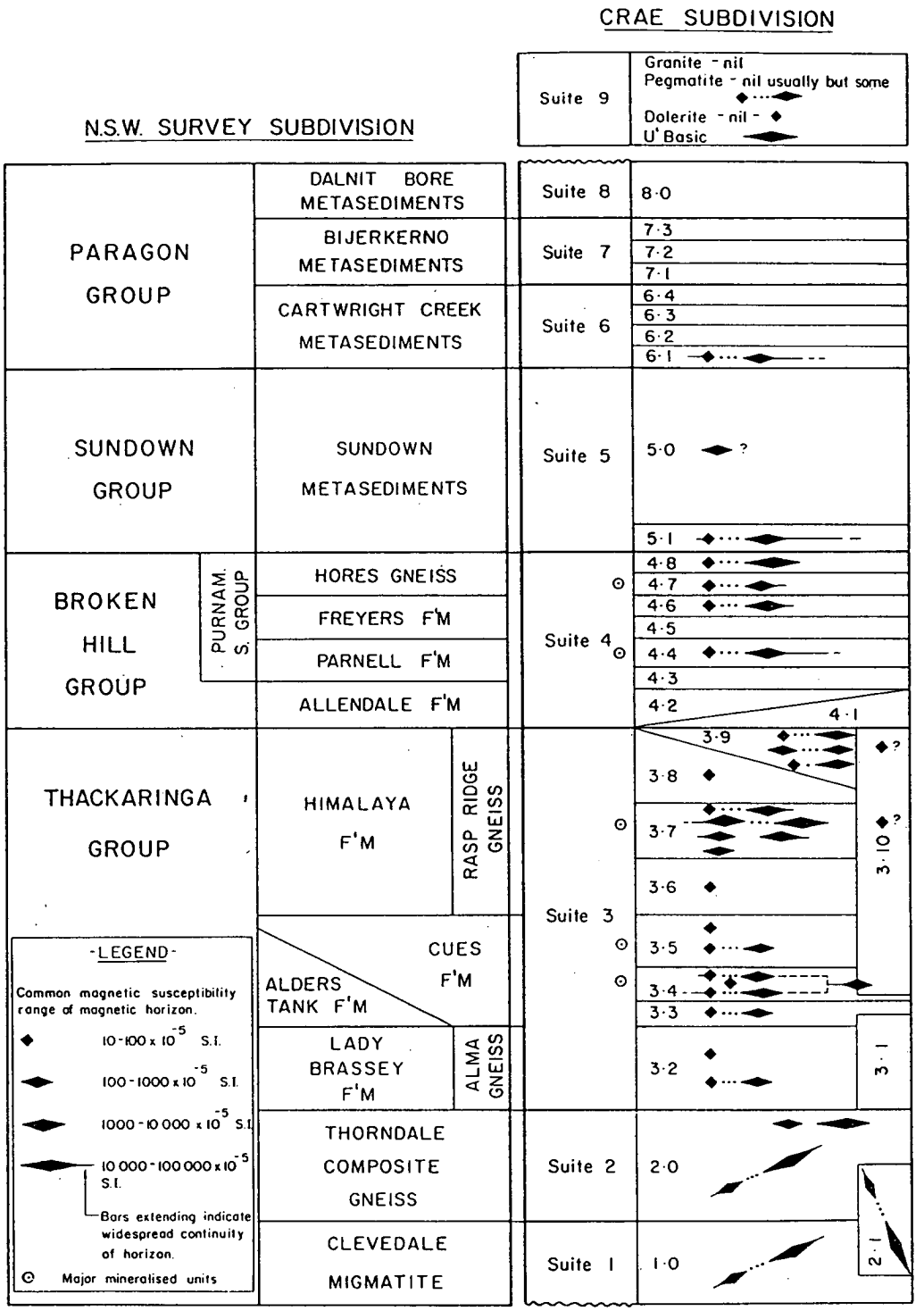

Figure 4.4 Stratigraphic distribution of magnetic lithologies, Broken Hill, Australia.
(Tucker, 1983)

An aeromagnetic interpretation of the regional data set is presented in Figure 4.5 and Plate 3. An image of the interpretation draped over a vertical derivative of the aeromagnetic data is presented as Figure 4.6 and Plate 4.

Basement Sequences

The Basement has been subdivided into four categories, based on magnetic character. All of the Basement sequences display an irregular, contorted magnetic texture, reflecting strongly deformed granulite facies gneisses.

Very strongly magnetic basement (> 2000 nT) corresponds to the Redan Gneiss and Ednas Gneiss. These are largely comprised of albite-hornblende-quartz rock, sodic-plagioclase-quartz-magnetite rock and quartz-albite-magnetite gneiss.

Areas mapped as strongly magnetic basement (1000 to 2000 nT) largely correspond to Mulculca Formation, with lesser Redan Gneiss and Ednas Gneiss. Mulculca Formation is dominantly metasedimentary composite gneiss, with sodic plagioclase-quartz-magnetite rock and quartz-albite gneiss.

Moderately magnetic basement (1000 - 1500 nT) corresponds to the Clevedale Migmatite and the Thorndale Composite Gneiss. These two units have been included in the Basement Sequence for the purpose of this interpretation, but they may actually be the basal units of the Lower Sequence. The Clevedale Migmatite consists of migmatite to quartzofeldspathic composite gneiss with minor basic gneiss. The Thorndale Composite Gneiss is a metasedimentary quartz-feldspar-biotite-sillimanite $\pm$ garnet $\pm$ cordierite composite gneiss, consisting of interlayered beds of psammite and psammopelite with rare quartz-magnetite and quartz-iron oxide/sulfide rocks.

Relatively non-magnetic basement corresponds to the units of the Thorndale Composite Gneiss.

Lower Sequence

The Lower Sequence corresponds to the Thackaringa Group. It has been subdivided into three units based on magnetic character.

Strongly magnetic (1000 to 1500 nT) Lower Sequence largely corresponds to the Lady Brassey Formation. This unit is comprised of poorly bedded sodic-plagioclase rocks within psammitic to pelitic metasedimentary composite gneisses. It contains substantial basic gneiss and is described as magnetite rich (Willis, 1989).

Moderately magnetic (500 to 1000 nT) Lower Sequence is dominantly Himalaya Formation, with lesser Lady Brassey Formation, Cues Formation and Rasp Ridge Gneiss. Himalaya Formation contains extensive bodies of saccharoidal sodic plagioclase - quartz $\pm$ K feldspar $\pm$ biotite rocks within metasedimentary composite gneiss and basic gneiss. The formation contains 0.5 to 10m thick units of thinly bedded quartz magnetite rock within the sodic plagioclase rock.

Figure 4.6 Regional Aeromagnetic Interpretation (Colour)
Draped On Vertical Derivative (Intensity)
Broken Hill, Australia.

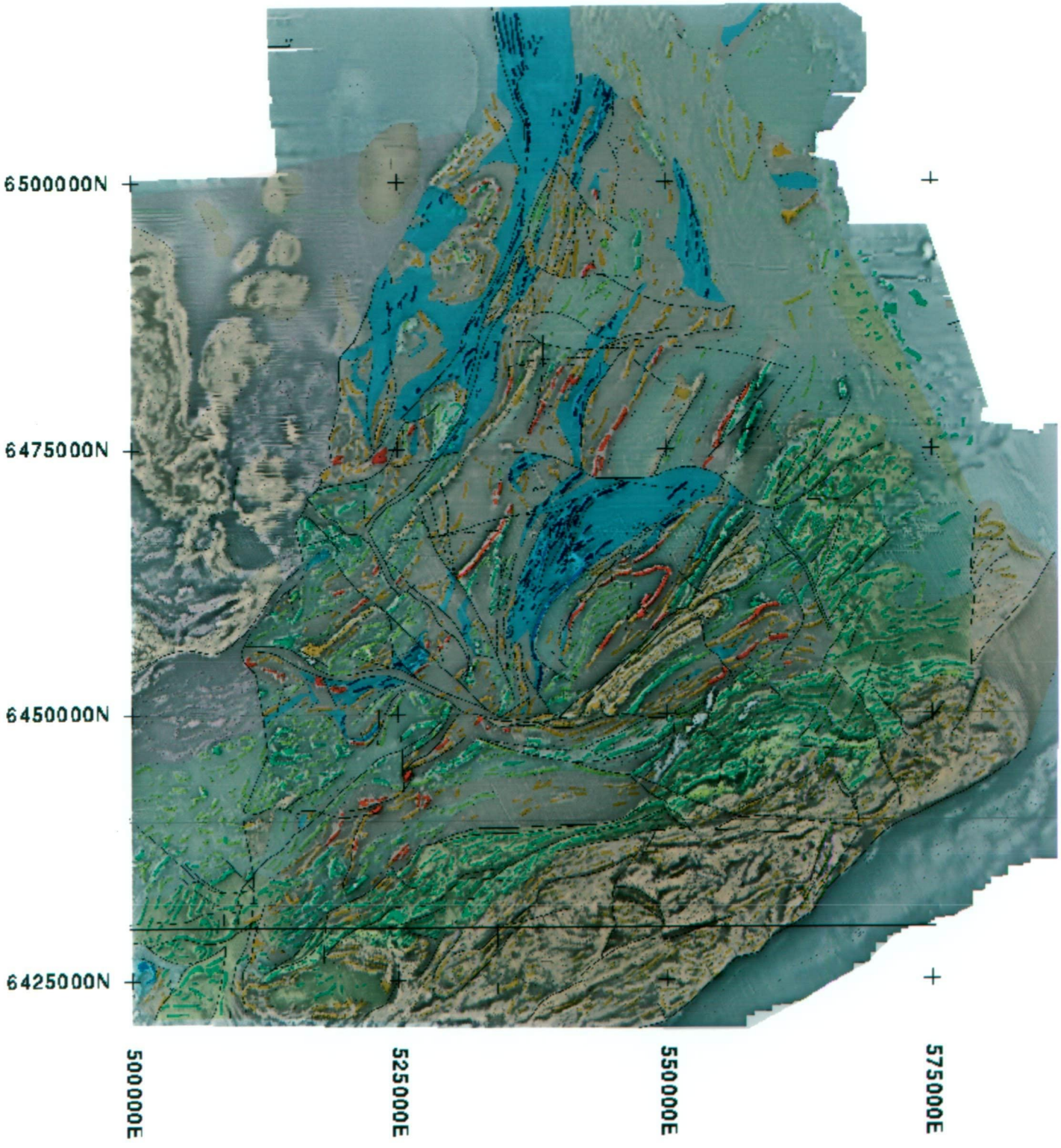

Relatively non-magnetic Lower Sequence is largely comprised of Cues Formation, followed by Alma Gneiss and Rasp Ridge Gneiss. Cues Formation is comprised of psammopeltic to psammitic composite gneisses or metasedimentary rocks with intercalated basic gneiss. The Cues Formation contains stratiform horizons of granular garnet-quartz ± magnetite rocks, quartz-iron oxide/sulfide rocks and quartz magnetite rocks. The Alma Gneiss is typically a quartz-feldspar-biotite ± garnet gneiss with augen shaped feldspar megacrysts. Rasp Ridge Gneiss is largely comprised of quartz-K feldspar-plagioclase-biotite "granite gneiss".

Magnetic units within the relatively non-magnetic Lower Sequence include magnetic amphibolite, granular garnet-quartz + magnetite rocks, quartz-iron oxide/sulfide rocks and quartz magnetite rocks, particularly within the Cues Formation.

Transitional Sequence

The Transitional Sequence corresponds to the Broken Hill Group. The Broken Hill Group is comprised of metasedimentary rocks and interbedded quartzo-feldspathic and basic gneisses.

The basal unit is the Allendale Metasediments, a sequence of metasedimentary rocks and metasedimentary composite gneiss. Basic gneiss, quartz gahnite rock and quartz iron sulfide rock are described (Willis, 1989). Calc-silicate nodules are abundant, with the Ettlewood Calc-silicate member occurring toward the base.

The Parnell Formation contains extensive units of basic gneiss, garnetiferous quartzofeldpathic gneiss (Potosi Gneiss - interpreted to be rhyodactic metavolcanics on the basis of volcanic textures observed in lower grade metamorphic equivalents) and exhalites intercalated with metasedimentary rocks. Broken Hill Type mineralisation is associated with the exhalites, which include quartz gahnite and BIF.

Freyers Metasediments is comprised of psammitic to pelitic metasedimentary rocks, with rare basic gneiss and quartz gahnite rock.

Hores Gneiss is the host to the Broken Hill ore deposit, and numerous other small showings of BHT mineralisation. It is largely comprised of the garnetiferous quarztofeldspathic gneiss, Potosi Gneiss.

The Transitional Sequence has not been subdivided in the aeromagnetic interpretation. It is comprised of a flat, uniform, relatively non-magnetic host sequence containing narrow linear magnetic anomalies. The linear magnetic units are generally sub-parallel and trend east-north-east in the south, swinging more north-easterly to northerly in the north.

It has been proposed by other authors (e.g. Isles, 1983) that the frequency and strike extent of magnetic units within the Transitional Sequence increases toward the Broken Hill deposit. This has been interpreted to indicate that much of the iron is of hydrothermal origin, with iron content increasing as the hydrothermal vent which sourced the Broken Hill deposit is approached.

The Transitional Sequence is relatively indistinguishable from much of the relatively non-magnetic stratigraphy within the Lower Sequence. In the southern half of the survey the relatively non-magnetic background of the Lower Sequence generally contains a greater frequency of linear magnetic units than the Transitional Sequence, although this is not always the case.

The Transitional Sequence is easily distinguished from the moderately and strongly magnetic stratigraphy of the Lower Sequence.

Magnetic units within the Transitional Sequence may occur within any of the formations. Strongly magnetic units are more common in the Parnell Formation and Allendale Metasediments.

In the regional aeromagnetic data the Hores Gneiss, host to the Broken Hill ore deposit, is commonly not evident, even as a weakly magnetic unit. However in more detailed aeromagnetic surveys the unit can be traced reasonably continuously.

Magnetic units within the Transitional Sequence may include magnetic amphibolite, BIF and magnetite in metasediments. The calc-silicate bodies known as the Ettlewood Calc-silicates also contain magnetite.

Upper Sequence

The Upper Sequence is comprised of metasedimentary rocks and graphitic metasedimentary rocks of the Sundown and Paragon Groups, respectively. The Upper Sequence is relatively non-magnetic, with few intercalated magnetic units. A notable exception is a moderately magnetic unit toward the base of the Upper Sequence which forms a prominent extensive marker horizon. This magnetic unit attains amplitudes of up to 500 nT in the vicinity of the Broken Hill ore deposit. It is caused by magnetite in a metasedimentary rock unit.

Another magnetic unit corresponds to the King Gunnia Calc-Silicate member within the Paragon Sequence.

Mineralisation

A number of deposit locations are shown in Plate 4.5. Each of the Broken Hill Type deposits shown has had historical production of more than $10 000 (1967 $ equivalent, from Barnes, 1986). As previously mentioned, the Broken Hill deposit is by far the most significant with more than 200 million tons of ore. The next most significant deposit, Pinnacles, is more than two orders of magnitude smaller with only 1 million tonnes of ore. The other BHT deposits are an order of magnitude smaller again.

Of the quartz-magnetite associated deposits of the Thackaringa Group only the Iron Blow has produced more than $10 000 (1967 $) of ore. This deposit is approximately an order of magnitude smaller than Pinnacles.

The aeromagnetic image shows that the quartz-magnetite deposits of the Thackaringa group are all intimately associated with very strong magnetic anomalies:

Sisters -	1400 nT
Razorback -	5000 nT
North Pinnacles -	800 nT
Middle Pinnacles -	2500 nT

BHT occurrences are notable for their lack of a direct magnetic response. Only the Consolidated and Imperial deposits and parts of the Broken Hill deposit are associated with magnetic stratigraphy, and the strength of the magnetic response is modest compared to the quartz-magnetite-associated mineralisation.

4.2 Deposit Scale Magnetic Characteristics - Broken Hill Ore Deposit.

Detailed aeromagnetic data were obtained over the Broken Hill Mine Leases from PASMINCO. This data set is comprised of two surveys, the Northern Leases survey and the Enterprise survey. Survey specifications and locations are presented in Figure 4.7.

Images of the aeromagnetic data are presented in Figures 4.8 and 4.9, and Plates 5 and 6. An interpretation of the aeromagnetic survey is presented in Figure 4.10 and Plate 7. An image of the interpretation draped on a vertical derivative of the aeromagnetic data is presented in Figure 4.11 and Plate 8.

Stratigraphic Interpretation

The interpretation is based on detailed surface geological plans published by Haydon and McConachy (1987), the 1: 100 000 scale Broken Hill Stratigraphy map published by the NSW Geological Survey (NSWGS) and 1:25 000 scale outcrop geology maps, also published by the NSWGS.

This interpretation shows a significant departure from the published stratigraphic interpretation of the NSWGS. In Figure 4.8 a magnetic unit has been highlighted. This unit defines a broad regional fold. On the west side of the fold the magnetic unit is mapped as occurring within the Parnell Formation of the Broken Hill Group. Detailed examination of both the 1:25 000 scale maps and Haydon and McConachy's detailed geology of the mine leases has established that the magnetic unit is definitely within the Parnell Formation on the western side of the fold. The Parnell Formation is mapped here as being comprised dominantly of amphibolite, with lesser psammite-psammopelite.

On the eastern side of the fold the magnetic unit is mapped as occurring within the Thackaringa Group. Close inspection of the 1:25 000 scale geology maps draped on the magnetic data shows that, near the magnetic unit, areas mapped as Thackaringa Group are poorly outcropping. The outcrop geology is mapped as amphibolite and psammite-psammopelite, with some sillimanite-magnetite units. This

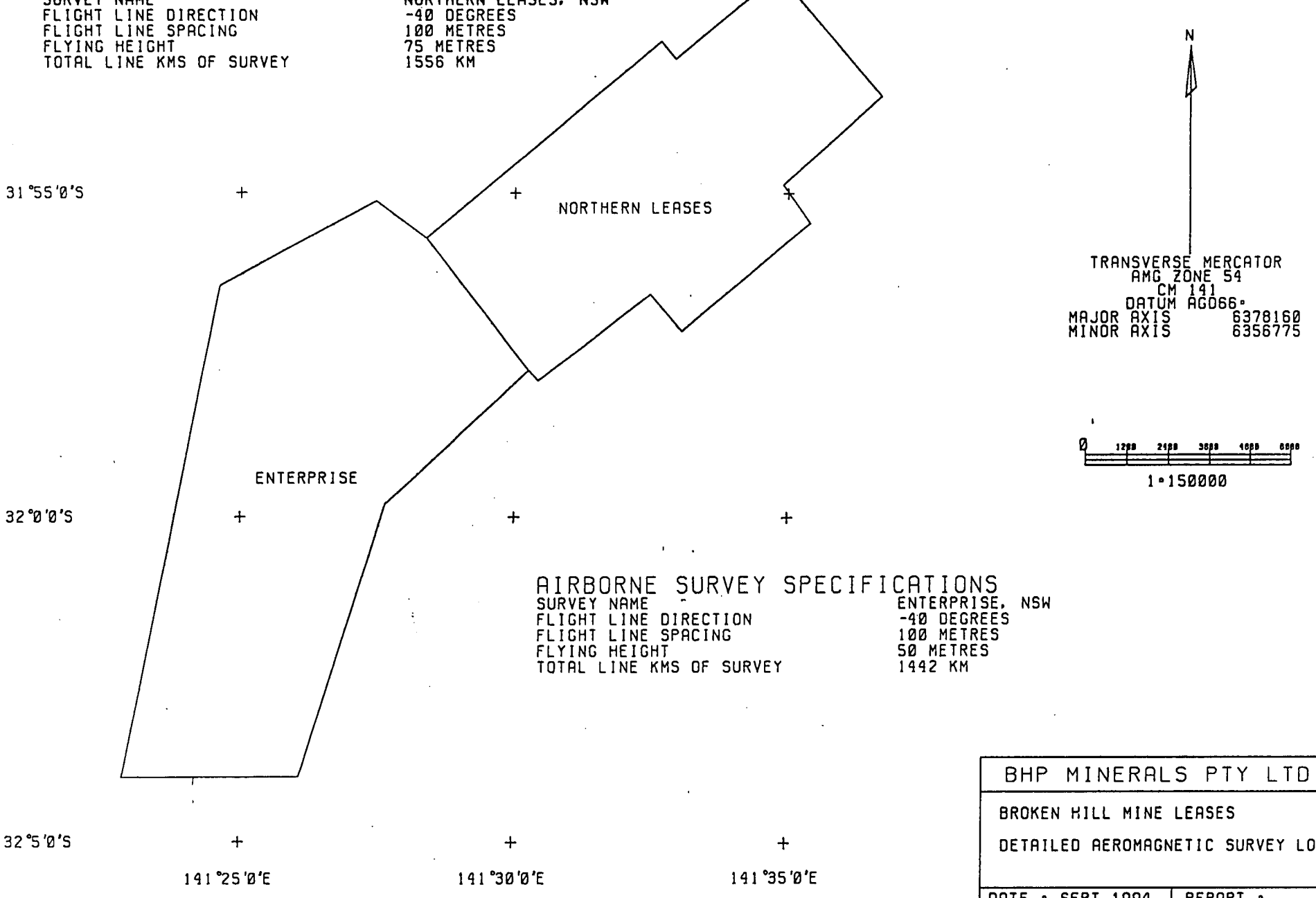

Figure 4.7 Detailed aeromagnetic survey locations and specifications, Broken Hill mine leases, Australia.

Figure 4.8 Detailed Aeromagnetic Data, Broken Hill, NSW, Australia.
Reduction To Pole

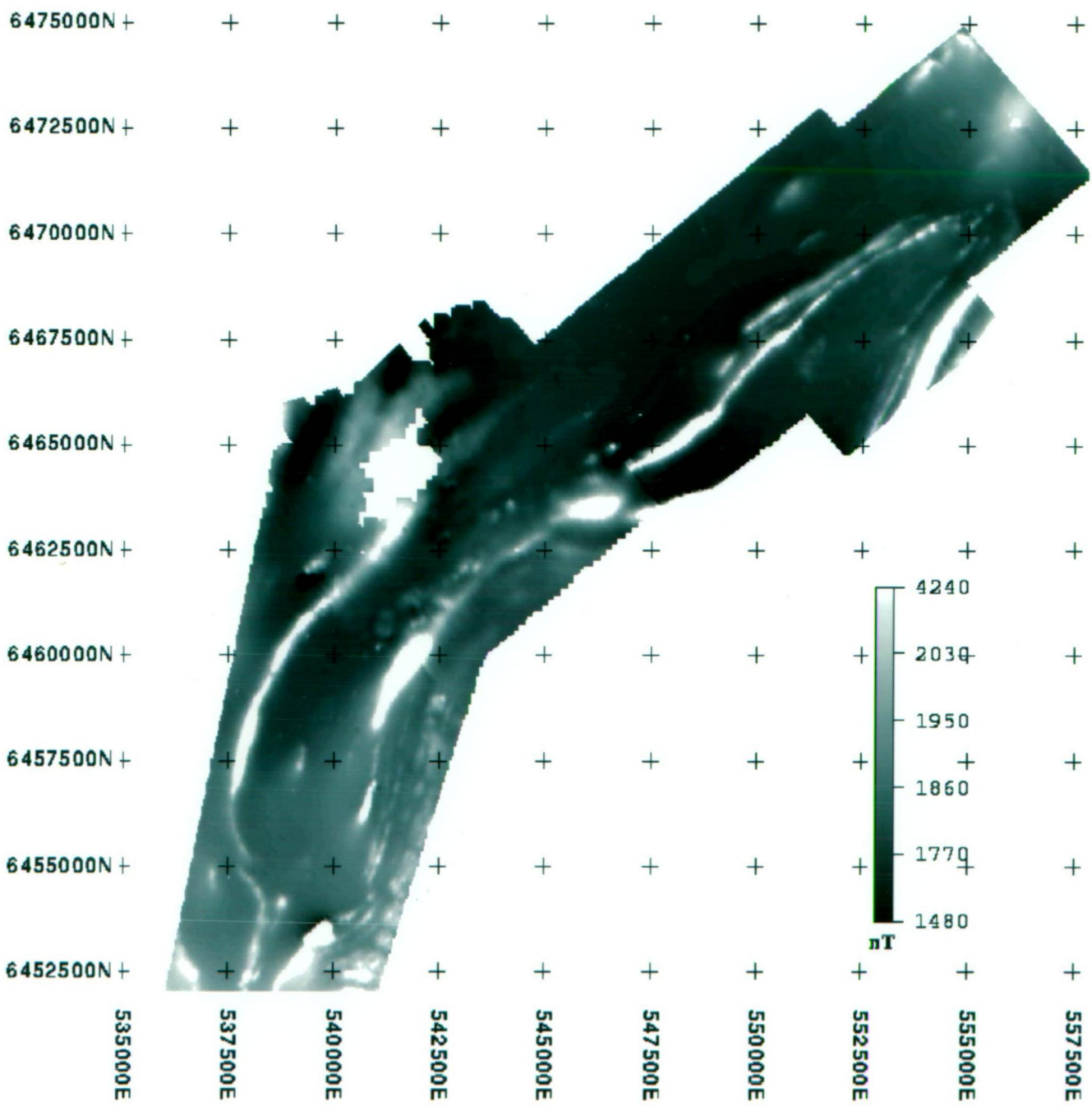

Figure 4.9 Aeromagnetic Data Stitch, Broken Hill, NSW, Australia.
Reduction To Pole – 1st Vertical Derivative

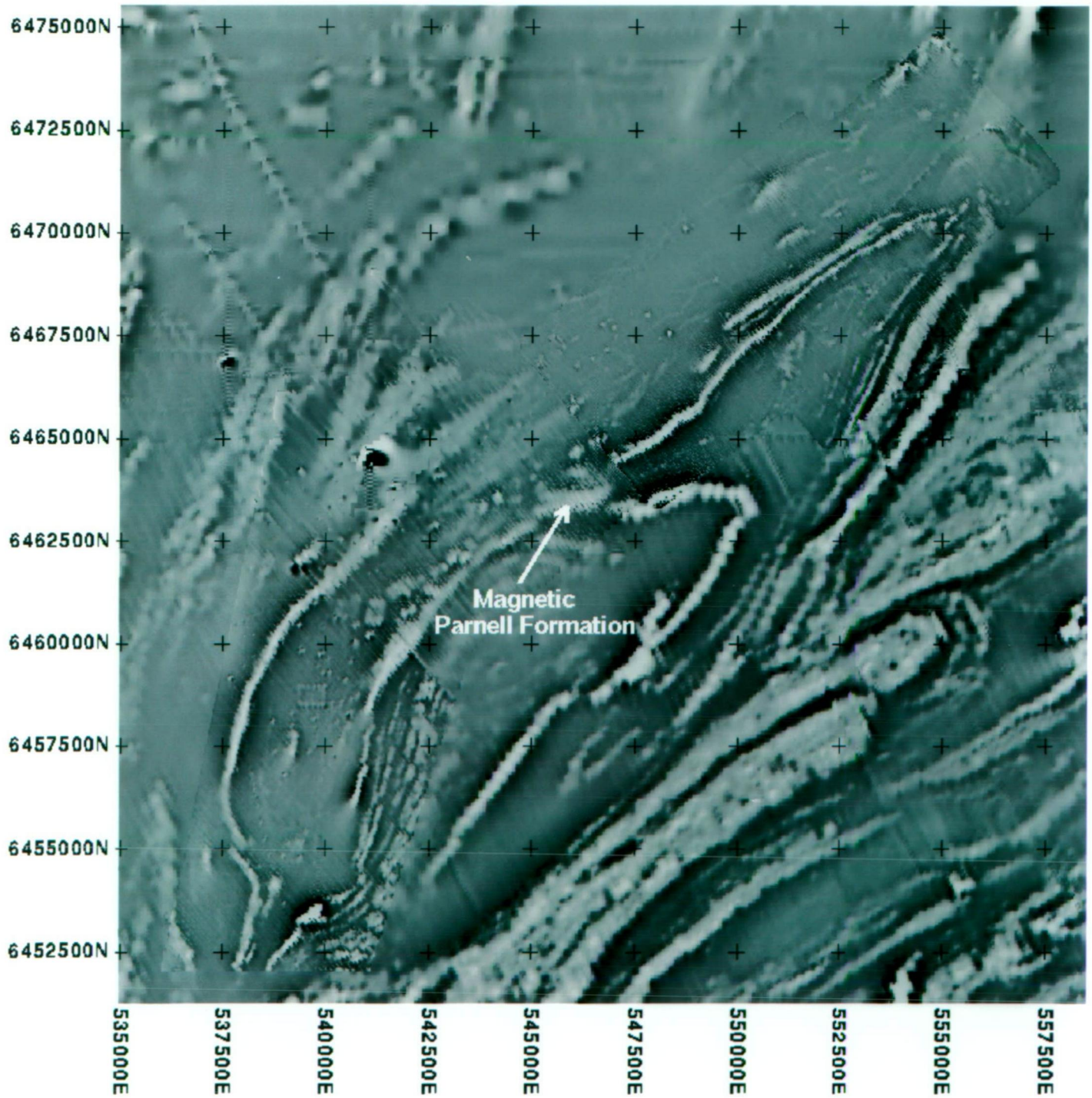

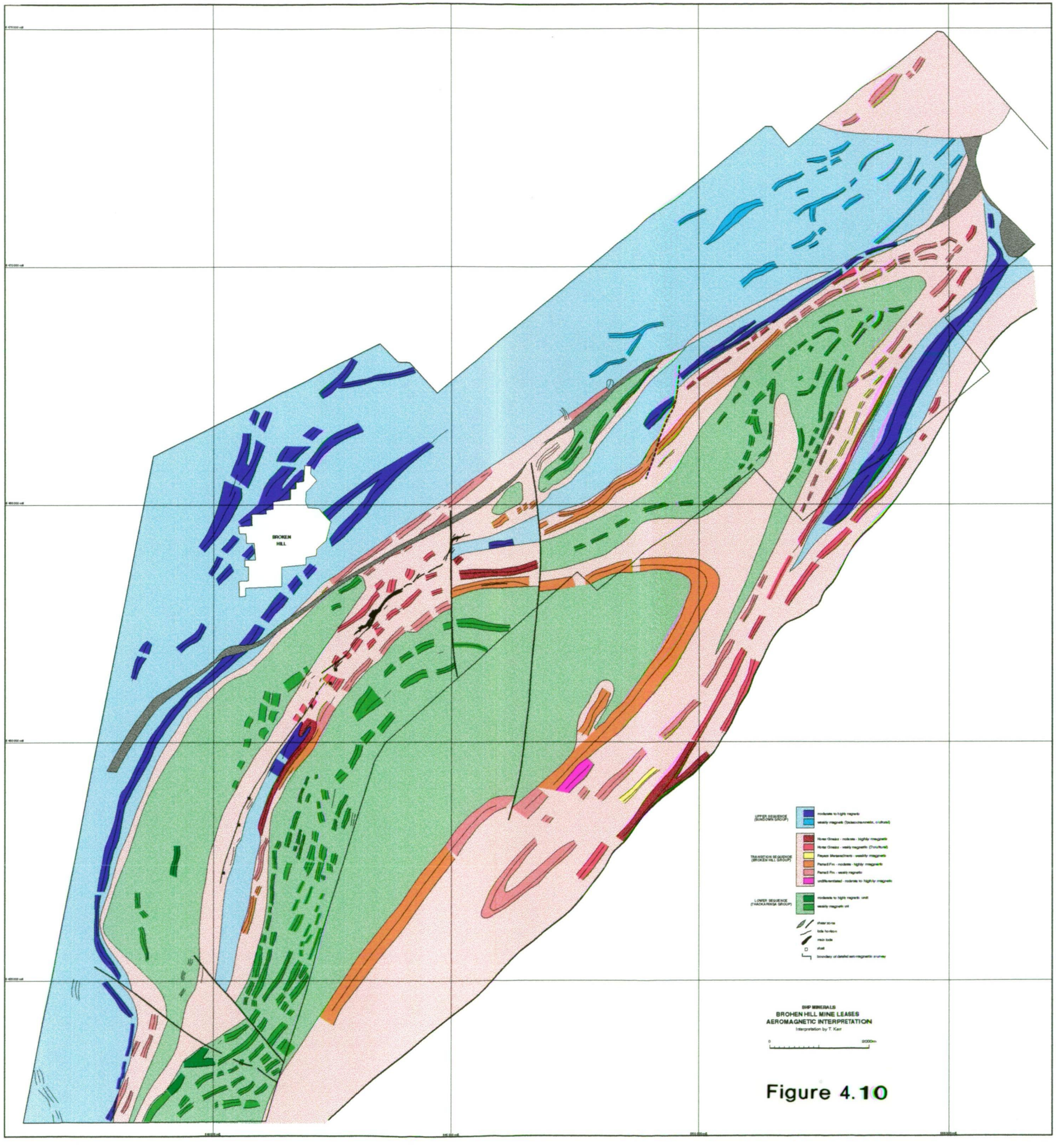
BROKEN HILL
UPPER SEQUENCE (SUNDOWN GROUP)
moderate to highly magnetic
weakly magnetic (Volcaniclastic, cruhuta)
TRANSITION SEQUENCE (BROKEN HILL GROUP)
Horse Creaks - moderate - highly magnetic
Horse Creaks - weakly magnetic (Thorlkuna)
Paysen Metasediment - weakly magnetic
Parnell Fm - moderate - highly magnetic
Parnell Fm - weakly magnetic
undifferentiated - moderate to highly magnetic
LOWER SEQUENCE (THACKARINGA GROUP)
moderate to highly magnetic unit
weakly magnetic unit
shear zone
lode horizon
main lode
shaft
boundary of detailed aeromagnetic survey
BHP MINERALS
BROKEN HILL MINE LEASES
AEROMAGNETIC INTERPRETATION
Interpretation by T. Kerr
0
2000m

Figure 4.10

Figure 4.11 Detailed Aeromagnetic Interpretation (Colour)
Draped On Vertical Derivative (Intensity)
Broken Hill Mine Leases, Australia.

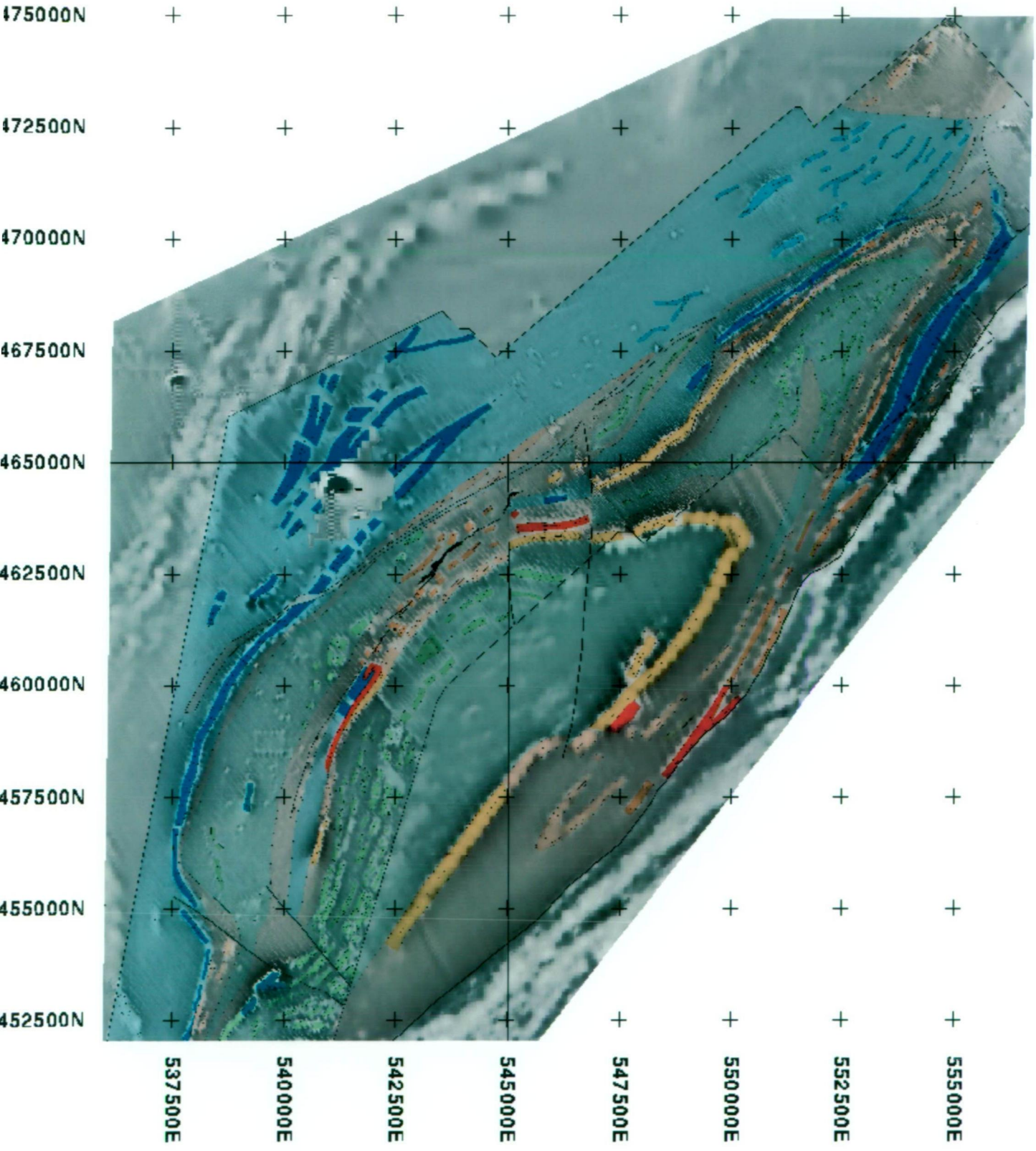

outcrop geology is very similar to that mapped as Parnell Formation on the west side of the fold. Hence in the aeromagnetic interpretation, regions previously mapped as the Thackaringa Group have been reassigned to the Broken Hill Group.

Magnetic Characteristics of the Broken Hill Ore Deposit

The ore deposit does not have a direct magnetic response. No magnetite has been described within the deposit itself. Pyrrhotite occurs as an envelope to the C lode but it is of the non-magnetic variety. Numerous short strike length magnetic anomalies visible near the deposit in Figures 4.8 and 4.9 may reflect local magnetite development, but are most likely cultural features.

It is proposed, however, the deposit and its immediate surrounds display a distinctive magnetic signature which may be applied to exploration.

Oppy (1992) looked at lateral variations in magnetic character within the lode horizon itself. Despite the lack of a magnetic response from the Main Lode, he stated that the spatial relationship between magnetite and the ore bodies could potentially be used as an exploration target.

He described results from a major magnetic susceptibility logging program within the mine. These indicate that the Potosi gneiss structurally immediately below the ore bodies is weakly to non-magnetic, but becomes more strongly magnetic distally. Pelitic intervals occur between the Potosi Gneiss and the ore bodies. Below the ore bodies the pelite is also weakly to non-magnetic, but once again becomes more strongly magnetic distally. Oppy also described variations in pegmatitic segregations within the pelite. Below the deposit the pegmatites contain green feldspar (Pb substitution within the lattice), while distally they contain orange feldspar (Fe substitution within the lattice). Oppy (1992) concluded that "with increasing proximity to the ore bodies there is a change from iron oxides and silicates to base metal sulfides and silicates in some of the metasediments". The aeromagnetic data provide further evidence for this lateral variation. Near the southern termination of the main lode, moderate magnetic anomalies (< 300 nT) are associated with the lode horizon.

In developing a magnetic exploration model an important feature to consider is the variation in magnetic character of the footwall and hanging wall stratigraphy. A strongly magnetic unit occurs in the footwall stratigraphy within the Parnell Formation. As the Main Lode is approached, the magnetic response within the Parnell Formation increases, achieving a maximum immediately below the margins of the deposit. The magnetic intensity of the Parnell Formation then decreases markedly below the ore deposit itself.

This variation in magnetic character may be reflecting the effects of hydrothermal activity within the footwall. The strongly magnetic signature of the Parnell Formation may be due to a previous exhalative event from the same hydrothermal vent which sourced the Broken Hill deposit. The later hydrothermal event which produced the

Broken Hill ore deposit may have resulted in magnetite destruction within the strongly magnetic Parnell Formation.

The magnetic signature described in the Parnell Formation which is associated with the Broken Hill ore deposit is repeated on the eastern side of a regional fold (Figure 4.8). This repeated magnetic signature is an obvious exploration target and occurs within interpreted Parnell Formation, previously mapped as Thackaringa Group.

Within the hanging wall stratigraphy the magnetic unit within the Sundown Group is regionally most strongly magnetic in the hanging wall of the deposit. This increase in magnetic intensity may be due to increased detrital magnetite content from exhalites associated with the Broken Hill deposit or increased metamorphic grade. Alternatively the magnetite may sourced from later pulse of hydrothermal activity from the same vent which sourced the Broken Hill ore deposit.

Ground Magnetic Profile Over the Broken Hill Ore Deposit

Tucker (1983) published a ground magnetic profile over the Broken Hill ore deposit (Figure 4.12). The position of the traverse is shown in Figure 3.9. The ground magnetic profile agrees well with the aeromagnetic data.

There is no significant ground magnetic anomaly directly associated with the ore itself. The strongest magnetic anomalies on the traverse are approximately 400 nT. They are associated with the base of the Upper Sequence (Suite 5) and with the Hores Gneiss (Unit 4.7) within the Transitional Sequence. At this point the magnetic response of the Parnell Formation is relatively low within the interpreted footwall alteration zone.

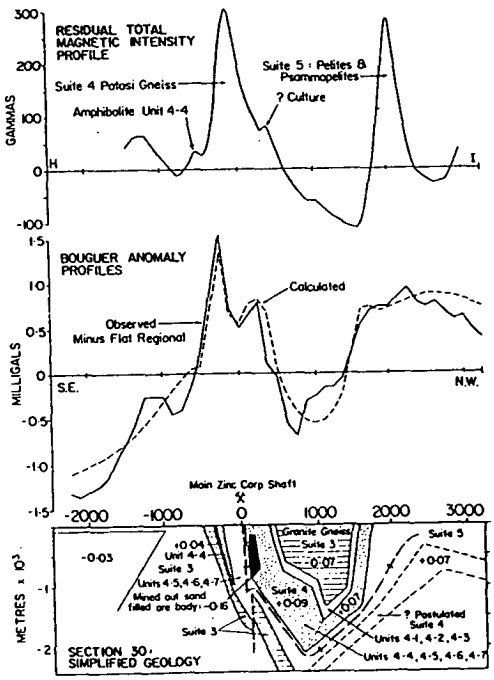

Figure 4.12 Ground magnetic profile, Broken Hill ore deposit, Australia. (Tucker, 1983)

5. GEOLOGY AND MINERALISATION OF THE EASTERN SUCCESSION, MT ISA BLOCK, QLD, AUSTRALIA

The Eastern Succession of the Mt Isa Block hosts the Cannington and Pegmont deposits, in addition to a number of smaller BHT occurrences. Cannington was discovered in 1990 as a result of drill testing anomalies from an aeromagnetic survey. It occurs beneath approximately 40m of Cretaceous and younger cover. Current published reserves are 45.3 million tonnes grading 11.1 % Pb, 3.4% Zn and 500 g/t Ag.

5.1 Regional Geology (after Walters, 1994)

Stratigraphy

The Eastern Succession is one of three lithotectonic domains defined within the Mt Isa Block (Fig. 5.1). These three domains contain Early to Mid Proterozoic sedimentary rocks, volcanic rocks and intrusives which have been deformed and metamorphosed. The stratigraphy has been interpreted in terms of a basement sequence, deformed and metamorphosed during the Barramundi Orogeny (1900 - 1870 Ma), and a series of three cover sequences representing ensialic rifting events (Blake and Stewart, 1992).

Extensional basin sedimentation at the end of Cover Sequence 3 was terminated by the compressional event known as the Isan Orogeny (1620 - 1520 Ma). This orogeny involved N-S compression and the development of thrusting and nappe tectonics (D1). This event was followed by east-west compression and the development of north-south trending upright folds (D2). Peak metamorphism occurred during D2, dated at 1550 Ma. A period of significant granite intrusion followed, with the unusual strongly fractionated Naraku and Williams Batholiths emplaced in the Eastern Succession at around 1500 Ma. A later phase of north-south and northeast-southwest strike-slip faulting, in particular the Quilalar and Pilgrim Fault Zones, divided the inlier into the three domains evident today (Figure 5.1).

The Quilalar and Pilgrim Faults have lateral displacements of the order of tens of kilometres and hence correlation of stratigraphy, structure and metamorphism across these faults is problematical. Blake and Stewart (1992) published a description of the stratigraphy and relationships between the three domains which is currently the most widely accepted (Figure 5.2) one.

The Eastern Succession is comprised of two zones (Figures 5.1, 5.2) divided by the Cloncurry Fault Zone (Cloncurry Overthrust of Blake and Stewart, 1992). West of the fault zone the stratigraphy is comprised of pre-1870 Ma basement (the Double Crossing Metamorphics) and Cover Sequences 2 and 3.

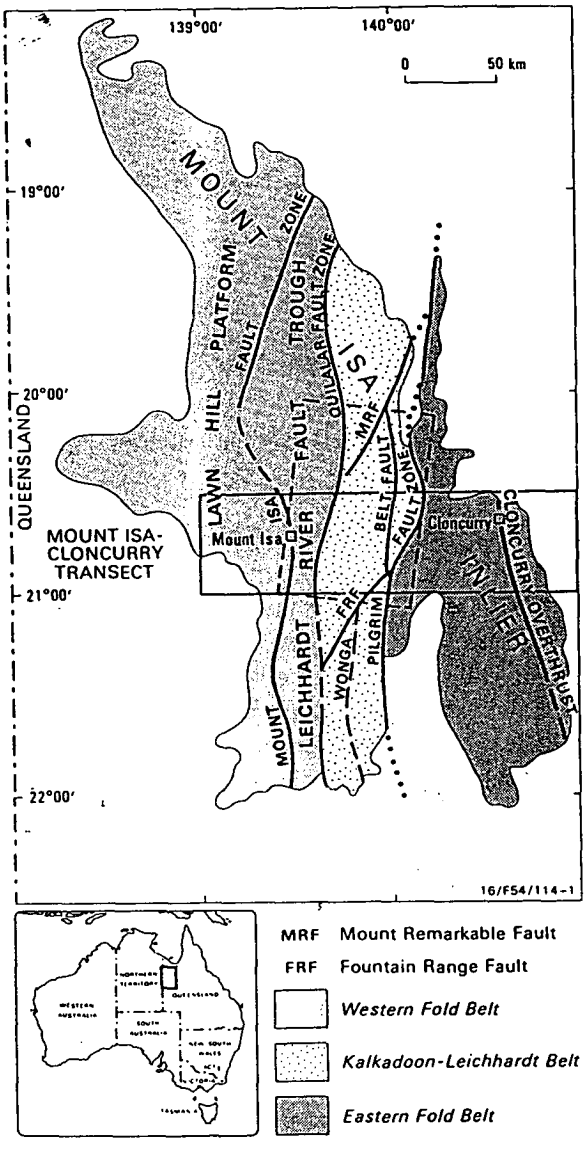

Figure 5.1 Tectonic domains within the Mt Isa Block. (Blake and Stewart, 1992)

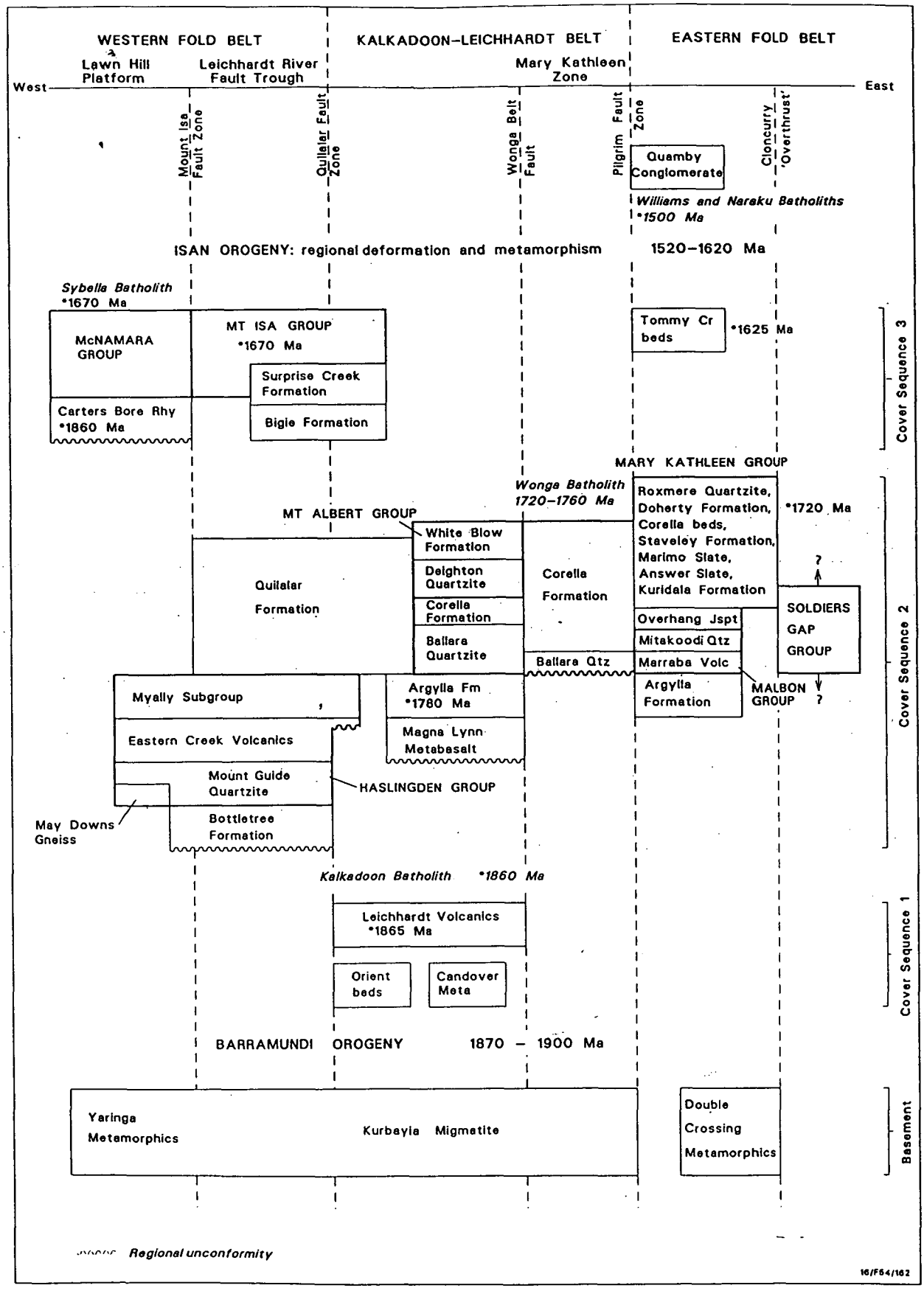

Figure 5.2 Stratigraphic relationships within the Mt Isa Block. (Blake and Stewart, 1992)

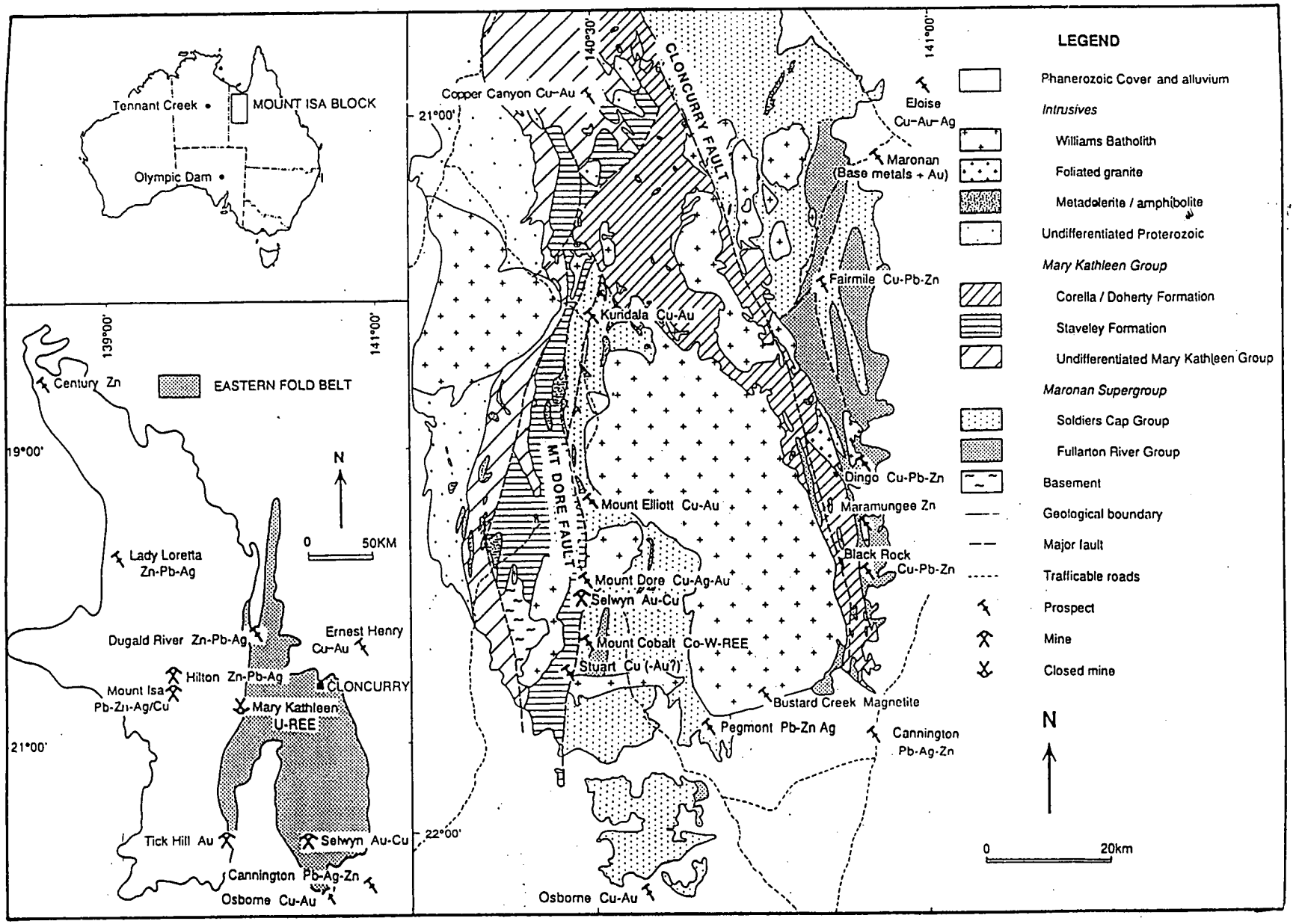

Figure 5.3 Geology of the Eastern Succession south of Cloncurry (Williams and Blake, 1994).

UNIT			BRIEF LITHOLOGICAL DESCRIPTION	INTERPRETED PARENT LITHOLOGY	INTERPRETED DEPOSITIONAL ENVIRONMENT	APPROXIMATE THICKNESS	METAMORPHIC GRADE	RIFT PACKAGE	
MARONAN SUPERGROUP	SOLDIERS CAP GROUP	TOOLE CK VOLCANICS	Amphibolites, carbonaceous slates, blue quartzites, laminated scapolitic siltstones.	Subaqueous mafic volcanics and relate dolerite dykes. Fine grained clastic sediments and minor evaporitic deposits.	Maturing clastic sedimentation, deposited by suspension or diffuse turbidity currents in an environment of indeterminate water depth.	2000 m	BIO-CHL; STAUR CHLD; CHLD; AND-CORD	2 - 3	ONE CYCLE RIFT
		MOUNT NORNA QUARTZITE	Thickly-bedded feldspathic psammites, quartzites, poorly-bedded pelites, and amphibolite. Minor marble, calc-silicates and BIFs.	Medium-grained turbidite sands and muds, with distal exhalative BIF and carbonates. Possible mafic intrusives.	Moderate to low energy, submarine fan-related sedimentation. Chemogenic sedimentation associated with medial-distal fan regime. Precipitation of Fe, Pb, Zn, Ag.	2000 m		2	
		LLEWELLYN CK FORMATION	Medium to thickly-bedded quartz-mica psammites, subordinate psammopelites and minor pelites. Locally abundant graded bedding, scour-and-fill structures, load casting and some ripple cross-lamination. Partial to complete Bouma sequences are common.	Medium to coarse-grained, medial to distal turbidites, with minor shallow water sands.	Turbidite deposition in a shelf to deep basin environment.	2000 m		2	
	FULLARTON RIVER GROUP	NEW HOPE ARKOSE	Thickly-bedded, quartzofeldspathic psammites, and minor biotite-rich psammopelites and pelites.	Coarse-grained volcaniclastic and quartzose sediments, with minor silts and muds.	Shallow to moderate water depth, shelf-shore sedimentation.	1500 m?	SILLIMANITE-MUSCOVITE	1	
		OLEN IDOL SCHIST	Description as for New Hope Arkose. In addition, it has quartzofeldspathic segregations and late pegmatite swarms.	Facies equivalents of the New Hope Arkose, but at a higher metamorphic grade.	Shallow to moderate water depth, shelf-shore sedimentation. Facies equivalent of the New Hope Arkose.	1500 m?		1	
		GANDRY DAM GNEISS	Upper part: Thinly-bedded to massive, homogeneous quartz + feldspar + biotite + muscovite + sillimanite + garnet pelitic to psammopelitic schists, with calc-silicate breccia horizons, BIF, gahnite-bearing quartzite, leucogneiss, granite gneiss and amphibolite. Abundant quartzo-feldspathic segregations. Lower part: Poorly-bedded quartz + feldspar + biotite + sillimanite psammopelitic schists, with interbedded feldspathic psammites and blue quartzites. Some garnet-bearing amphibolites, thin BIFs and massive sillimanite rocks.	Thick sequence of poorly-sorted volcaniclastic and epiclastic material, with some mafic volcanics, chemogenic BIF and carbonate. Poorly-bedded sequence of sands and silts, with volcaniclastic horizons, and possible mafic and felsic volcanics. Minor chemogenic BIF and facies equivalents.	Medial fan deposition in moderate water depth. Intermittent volcanism and exhalation of metalliferous fluids (Fe, Pb, Zn, Ag). Shallow to moderate water depth, dominated by traction current sedimentation. Intermittent phases of mafic and felsic volcanism, and exhalation of metalliferous fluids (Fe, Pb, Zn, Ag).	>4000 m?	SILLIMANITE-K-FELDSPAR	1	

Metamorphic grade indicated is the highest attained for each unit. Abbreviations: and = andalusite; bio = biotite; chl = chlorite; chld = chloritoid; cord = cordierite; staur = staurolite. For a more detailed consideration of the Maronan Supergroup, the reader is referred to Newbery et al. (in preparation).

Table 5.1 Lithostratigraphy of the proposed Maronan Supergroup. (Beardsmore et al, 1988)

East of the Cloncurry Fault Zone the Soldiers Cap Group, host to the Cannington and Pegmont BHT deposits and numerous smaller BHT showings, is developed. The relationship of the Soldiers Cap Group to other sequences in the Mt Isa Group is still not fully defined, as shown in Figure 5.2. The Soldiers Cap Group is juxtaposed against the remainder of the Mt Isa Block across the Cloncurry Fault Zone, which has been interpreted as a major terrane boundary (Laing, 1993).

The Soldiers Cap Group was initially defined in the Cloncurry area. Three Formations were recognised:

Toole Creek Formation - basic volcanic rocks with minor interbedded shales, quartzites and calc-silicate rocks,

Mount Norna Quartzite - thin cross-bedded quartzofeldspathic arenites and quartzites interbedded with siltstones,

Llewellyn Creek Formation - planar bedded pelites of turbiditic affinity.

Banded iron formations (BIF's) occur at restricted intervals throughout the stratigraphy and are associated with numerous BHT showings, particularly within the Mount Norna Quarztite (Walters, 1994).

Metamorphic grade in the outcropping type area is greenschist facies, but metamorphic grade increases to the south and east, undercover, reaching upper amphibolite facies at Cannington. Metamorphic grade then decreases to the west from Cannington to Pegmont, before rapidly decreasing further west of Pegmont.

South of the type area the higher grade metamorphic rocks of the Soldiers Cap were mapped as undifferentiated Soldiers Cap Group in the published geology maps (Blake *et al*, 1983; Blake, Jaques and Donchak, 1983). Beardsmore *et al.* (1988) attempted to extend the lithostratigraphy further south, resulting in the definition of the Gandry Dam Gneiss, Glen Idol Schist and New Hope Arkose, which were assigned to a new sequence, the Fullarton River Group (Figure 5.3).

Beardsmore *et al.* (1988) considered the Fullarton River Group to underly the Soldiers Cap Group and assigned the Soldiers Cap Group and the Fullarton River Group to a proposed Maronan Supergroup (Table 5.1). However the chief difference between the Soldiers Cap and Fullarton River Groups appears to be metamorphic grade and other authors consider the Fullarton River Group to be simply the higher metamorphic equivalent of the Soldiers Cap Group (Walters, 1994).

The stratigraphic interpretation is also complicated in the area between Cannington and Pegmont. The Kuridala Formation of the Mary Kathleen Group and the Soldiers Cap Group are generally separated by the Williams Batholith and the Doherty Metasomatic Zone. The contact between the two formations should occur near the Pegmont deposit, a region of poor outcrop. Although the host sequence to Pegmont is of lower metamorphic grade than the host to Cannington, the similar host lithologies and metallogenic characteristics have led authors to infer that Pegmont lies within the

Soldiers Cap Group (Walters, 1994). However further west of Pegmont the metamorphic grade decreases markedly and the mineralisation style changes to Cu-Au systems within the Kuridala and Mt Stavely Formations, suggesting a major terrane boundary (Walters, 1994).

The outcropping Soldiers Cap Group is poorly understood in terms of lithostratigraphy. Aeromagnetic data confirm that higher grade equivalents extend far to the east under cover. From aeromagnetic data it is also clear that many units within the Soldiers Cap Group do not outcrop. Hence it is difficult to classify the sequence in terms of Lower, Transitional and Upper Sequences according to the BHT model outlined in Section 2. Nevertheless, the Soldiers Cap Group fits many of the characteristics of the regional BHT model:

- Mid Proterozoic mobile belt setting,
- stratigraphic change from basal quartzo-feldspathic gneisses to upper meta-greywackes and meta-shales,
- predominance of oxidised lithologies within the sequence,
- high metamorphic grade,
- regional occurrences of BHT style mineralisation (Dingo, Black Rock, Cowie, Fairmile, Maronan, Altia, Pegmont, Cannington),
- close association of BIF with mineralisation,
- complex and varied nature of exhalites and alterites associated with BHT mineralisation,
- host stratigraphic package of clastic rocks (turbidites).

Structure

The Soldiers Cap Group is interpreted to be allochthonous to the Mt Isa Block (Walters, 1994). It is thought to have docked near the Cloncurry Fault Zone before the intrusion of the 1500 Ma Williams and Narraku batholiths. Hence, the Group may have quite a different structural history to the remainder of the Mt Isa Block. It is considered to have more similarities with the structural history of the Tommy Creek Block, a fault bounded slice of upper amphibolite grade metamorphic rocks, which has been interpreted as a thrust klipper separated from the Soldiers Cap Group by erosion (Walters, 1994). The structural style of the Tommy Creek Block is summarised in Figures 5.4 and 5.5. For more details refer to Hill *et al.*, 1992.

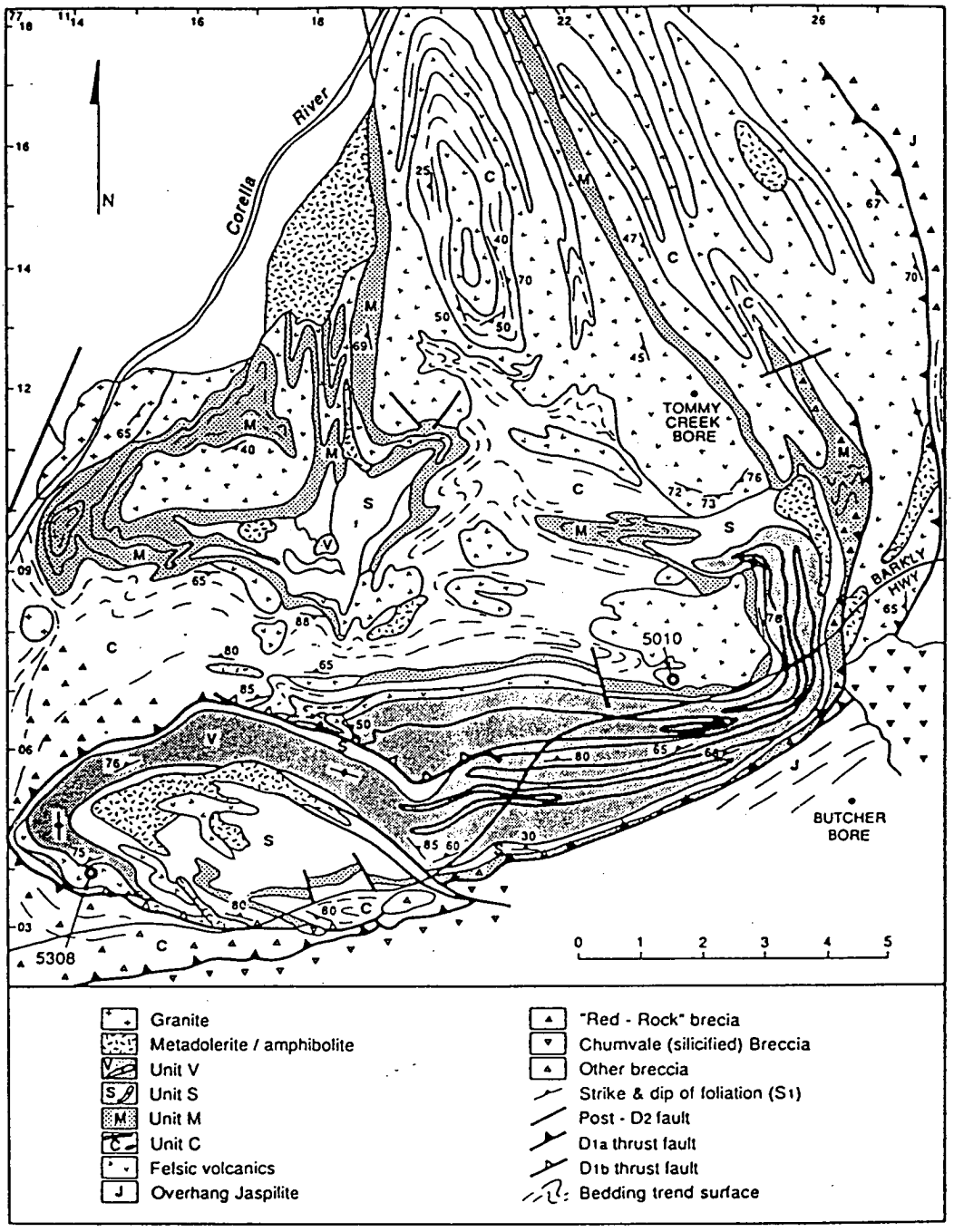

Figure 5.4 Geology of the Tommy Creek Block
(Hill, et al, 1993)

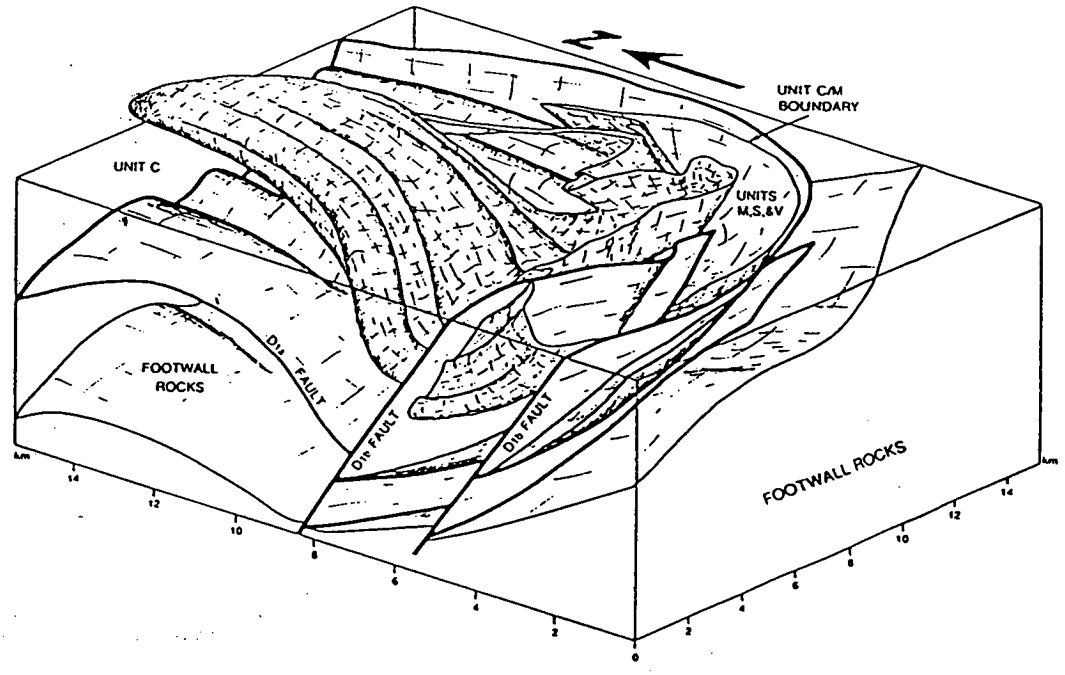

a) Schematic block diagram of the interpreted structure of the Tommy Creek Block.

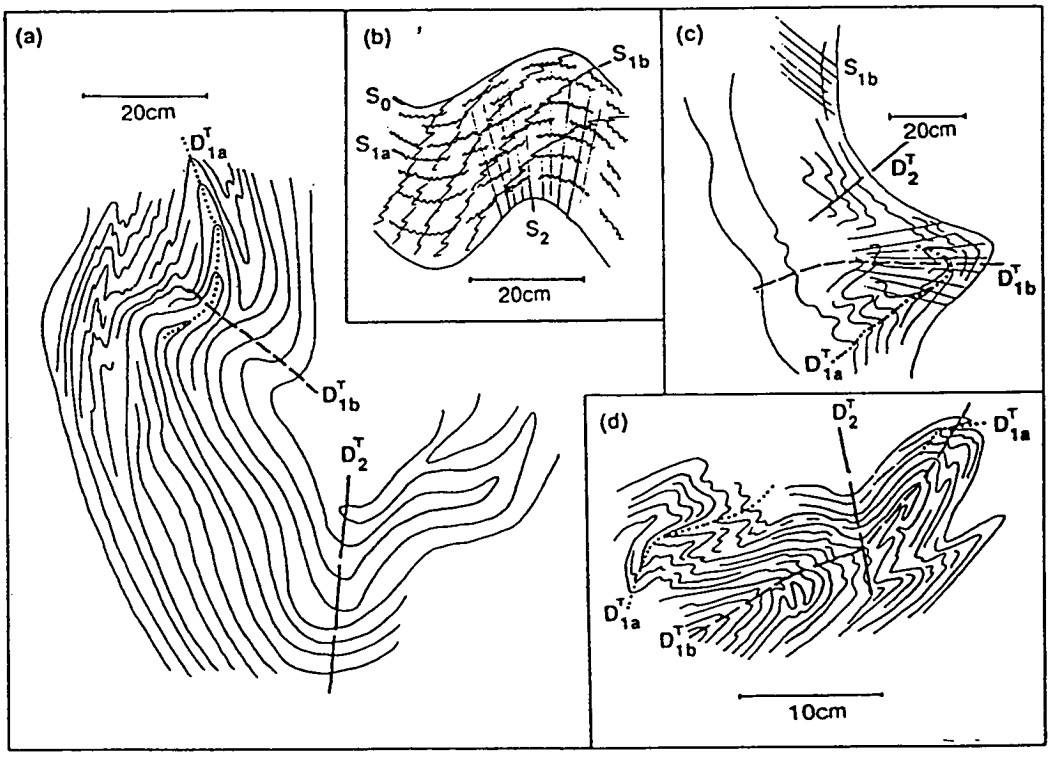

b) Field sketches of fold interference patterns, Tommy Creek Block.

Figure 5.5 Structure of the Tommy Creek Block (Hill et al., 1992)

Mineralisation

The Soldiers Cap Group hosts the Cannington and Pegmont BHT deposits. In addition to the Cannington and Pegmont deposits numerous other small BHT occurrences are known. These include Cowie, Dingo, Fairmile, Maronan, Black Rock and Altia (Figure 5.3). At Fairmile stratiform Pb-Cu-Zn mineralisation is hosted by BIF associated with garnetiferous quartzite, amphibolite and calc-silicate. At Dingo stratiform Cu-Pb-Zn-Ag mineralisation, associated with pyrrhotite and magnetite gangue and quartz gahnite rock, is hosted by BIF and garnetiferous quartzite. Black Rock is a Pb-Zn-Cu prospect with mineralogy similar to Pegmont, hosted by BIF with proximal garnet quartzite and quartz gahnite rock. Cowie is a Pb-Zn prospect hosted by one metre thick BIF (2.5 km strike length) with ore and gangue minerals also similar to Pegmont.

5.2 Geology of the Cannington Deposit.

The Cannington deposit is currently undergoing feasibility studies. If it proceeds it will be the second largest economic BHT deposit in the world, after Broken Hill, Australia. Current reserves are 45 Mt grading 11.9% Pb, 4.8% Zn and 520 g/t Ag (Roche, 1994).

The regional stratigraphic setting is problematical due to the lack of outcrop. The deposit occurs beneath 20 to 40m of Cretaceous and younger sediments. It is hosted by migmatitic and banded quartzofeldspathic gneisses which are regionally unremarkable. They are thought to correlate with rocks mapped as the Gandry Dam Gneiss near the Cowie prospect. No significant carbonate or calc-silicate units have been intersected. Minor occurrences of amphibolite are widespread, but have been interpreted to be intrusive because of their limited thickness and extent (Walters, 1994).

The deposit is enveloped by an extensive zone of quartz-K feldspar-biotite-sillimanite-garnet schist and psammite, which extends up to 200m from the deposit. It has been interpreted as a primary alteration halo (Walters, 1994).

Four phases of deformation have been identified. The most significant events in terms of the geometry of the deposit are D2, which resulted in tight isoclinal folding of the deposit, and D4 which involved late brittle fracturing and faulting.

A representative cross section through the deposit is shown in Figure 5.6. The ore zone is subdivided into five lodes and 10 mineralisation types. Characteristics of the the lodes and mineralisation types are summarised in Table 5.2 All of the mineralisation types except Glenholme can be classified as Pb or Zn dominant and mafic or siliceous (Table 5.2).

The deposit has been strongly overprinted by metasomatism, with siliceous alteration centred on the Brolga fault zone. Within the siliceous alteration zone magnetite is notably absent (Figure 5.6). A schematic genetic model of the deposit, showing chemical zonations prior to metasomatic overprinting, is presented as Figure 5.7.

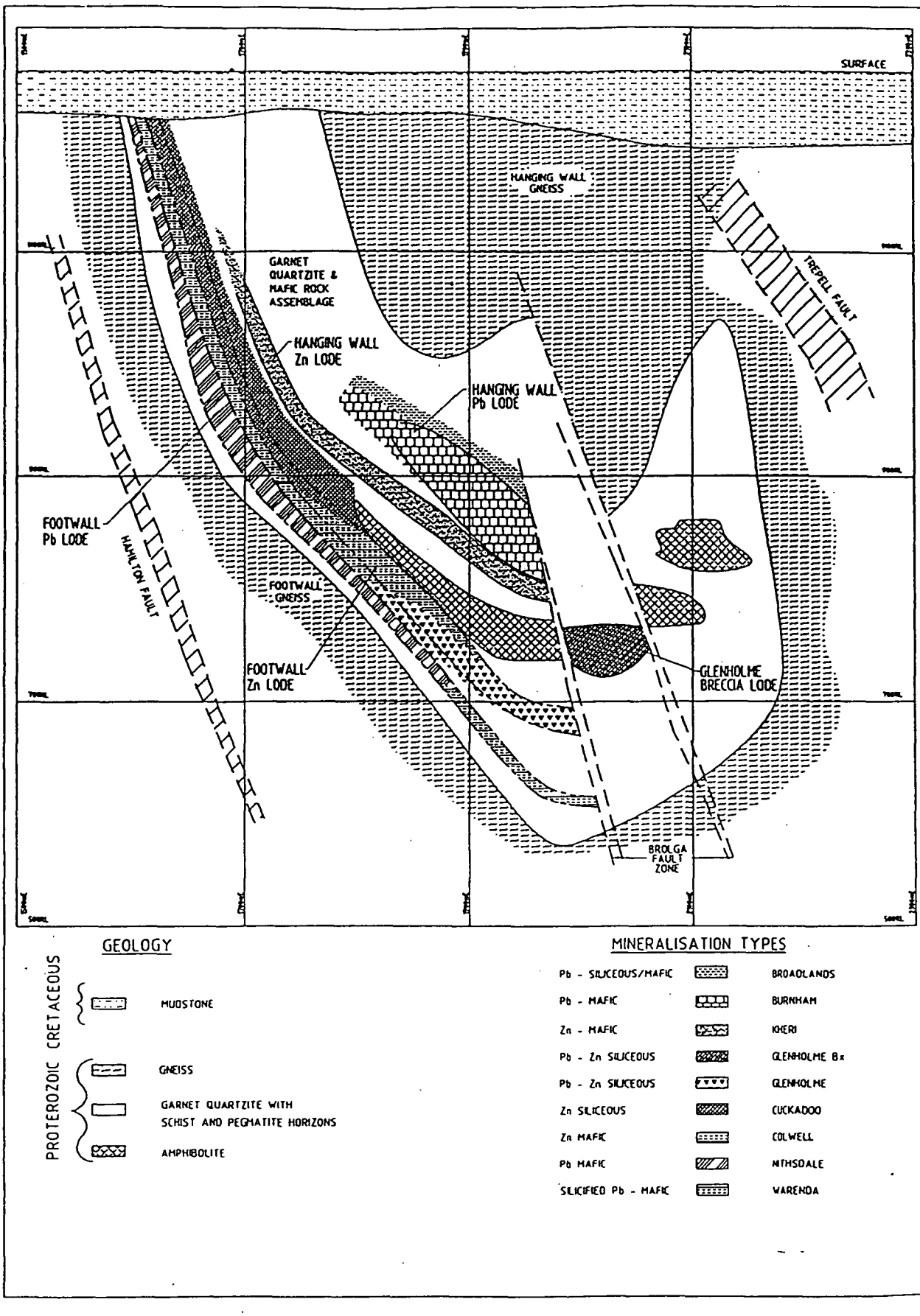

Figure 5.6 Representative Cross-section, Cannington Southern Zone (Roche, 1994)

LODE HORIZON	MINERALISATION	STYLE	PB/ZN	GRADE*	GANGUE
Hangingwall Pb	Broadlands	siliceous-mafic	Pb	M - L	Quartz-pyroxmangite-garnet
Hangingwall Pb	Burnham	mafic	Pb	H	magnetite-fluorite-pyroxmangite-pyroxene-quartz
Hangingwall Zn	Kheri	mafic	Zn	L	pyroxene-quartz-magnetite-fluorite
Hangingwall Zn	Kheri-Colwell	mafic	Zn	L	magnetite-fluorite-pyroxene-quartz
Footwall Zn	Colwell	mafic	Zn	L - M	magnetite-fluorite-pyroxene-quartz
Footwall Zn	Cuckadoo	siliceous	Zn	M	quartz (chlorite-garnet)
Footwall Zn	Glenholme	siliceous	Pb/Zn	H	quartz (carbonate)
Footwall Pb	Nithsdale	mafic	Pb	M	magnetite-fluorite-pyroxmangite-pyroxene-quartz
Footwall Pb	Warrenda	mafic	Pb	L	Quartz-pyroxmangite-garnet
Brolga Fault	Glenholme	siliceous	Pb/Zn	H	quartz (carbonate)

*L - low, M - medium, H - high

Table 5.2 Summary of Cannington Southern Zone mineralisation types (after Roche, 1994).

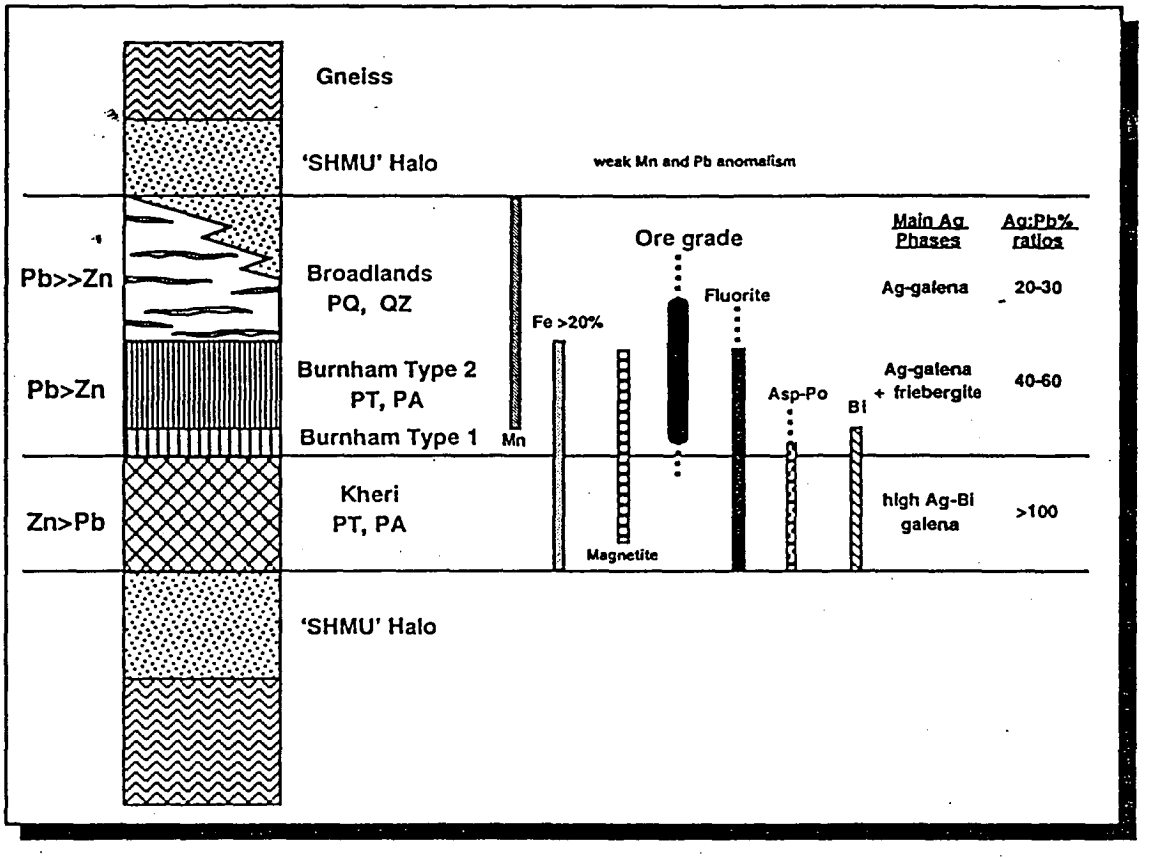

Figure 5.7 Schematic reconstruction, Cannington Southern Zone. (Walters, 1994)

5.3 Geology of the Pegmont Deposit

The Pegmont deposit contains oxide reserves of 3.5 MT grading 6.4% Pb, 2.33% Zn, 8 ppm Ag and sulfide reserves of 6.6 MT grading 8.35% Pb, 3.67% Zn, 11.5 ppm Ag. Mineralisation is closely associated with BIF and garnet quartzite. Previously the deposit was thought to be hosted by Kuridala Formation although some (William and Blake, 1994), including this author, would now place it within the Soldiers Cap Group.

The host stratigraphy to the Pegmont deposit is summarised in Table 5.4. A plan view of the geology of the immediate ore environment is presented as Figure 5.8. Metamorphic grade is upper amphibolite facies. The mineralised horizon is 4 to 6m thick and is surrounded by garnetiferous schist and arkose. Sulfide minerals include galena, sphalerite, pyrite, minor pyrrhotite, and trace chalcopyrite. Gangue minerals include magnetite, gahnite, garnet, apatite, finely disseminated and rarely flaky graphite (0.5 to 2%), fayalite, hornblende, quartz and pyroxene.

The deposit is interpreted to have accumulated as a sub-circular basin or mound, with thickest and highest grade mineralisation in the centre (Stanton and Vaughan, 1979). This is illustrated in Figure 5.9. Mineralogical variations across the mound or basin are summarised in Table 5.4 and Figure 5.10. The deposit shows a metal zonation from proximal Pb > Zn through intermediate Zn > Pb to distal Zn > Cu. The thickest mineralisation is intimately associated with magnetite and fayalite. Intermediate mineralisation is associated with hornblende-pyroxene rocks and pyrite-pyrrhotite, and garnet and pyrrhotite dominate at the margins. Whole rock chemistry also shows zonation:

Central unit	- higher Fe, Mn, Pb, Zn - lower Ca, Al, Cu
Intermediate Unit	- lower Fe, Mn, Pb and Zn - higher Ca, Al, Cu
Margin	- lower in Pb, Zn, Ca - higher Al, Cu, Fe, Mn

Stanton and Vaughan interpret this zonation as indicating a primary, proximal composition of Pb and Zn sulfides and low silica Fe-Mn precursors to magnetite, fayalite and grunerite. In the intermediate zone more Al-Si rich Fe-Mn silicates were precipitated as precursors to clinopyroxene, garnet and hornblende. On the margins even more Si-Al rich silicates precipitated as precursors to quartz, biotite and garnet.

They suggest that the presence of proximal magnetite at Pegmont, and its absence at Broken Hill, may be attributed to excess Fe at Pegmont, such that Fe remained, after silica and sulfur were consumed, to form ferric-ferrous oxides. On the margins pyrite and pyrrhotite formed due to excess sulfide after Pb-Zn sulfide precipitation.

100 m:	hanging wall metaarkose, schist, pegmatite
1-10 m:	metaakose grading into schist; both with garnet
4-6 m:	Pb-Zn mineralized horizon
1-8 m:	garnet-schist grading to garnet-metaarkose
0-1 m:	low grade Pb-Zn footwall mineralized horizon
1-5 m:	garnet-schist to garnet-metaarkose, quartzite
100-200 m:	biotite-muscovite-schist, metaarkose, micaceous quartzite, pegmatite
1-20 m:	banded amphibolite, several hundred metres schist, footwall metaarkose, occasional amphibolite, frequent pegmatite

Table 5.3 Pegmont host stratigraphy. (Locsei, 1977)

Central holes		Intermediate holes		Edge hole
PD1	PD18	PD19	PD20	PD31
High grade mineralization; galena > sphalerite	High grade mineralization; galena > sphalerite	Slightly weaker mineralization; galena > sphalerite	Much weaker mineralization; sphalerite > galena	Very weakly mineralized; minor sphalerite and chalcopyrite
Magnetite	Magnetite	Magnetite	Magnetite pyrite minor pyrrhotite	Pyrrhotite minor pyrite
Quartz absent	Quartz absent	Quartz absent	Quartz present	Quartz abundant
Abundant fayalite	Abundant fayalite	Some fayalite	Fayalite absent	Fayalite absent
Subordinate clinopyroxene green hornblende grunerite	Subordinate clinopyroxene green hornblende grunerite	Green hornblende and clinopyroxene more abundant; grunerite subordinate	Green hornblende and clinopyroxene dominant; green hornblende > clinopyroxene	Trace green hornblende
Subordinate garnet present	Subordinate garnet present	Subordinate garnet present	Garnet becoming dominant	Garnet dominant
~7% apatite	~7% apatite	~7% apatite	~7% apatite	~7% apatite
Minor biotite	Minor biotite	Minor biotite	Minor biotite	Abundant biotite

Table 5.4 Mineralogical variations from the centre of Pegmont mound/basin to the edge. (Stanton and vaughan, 1979)

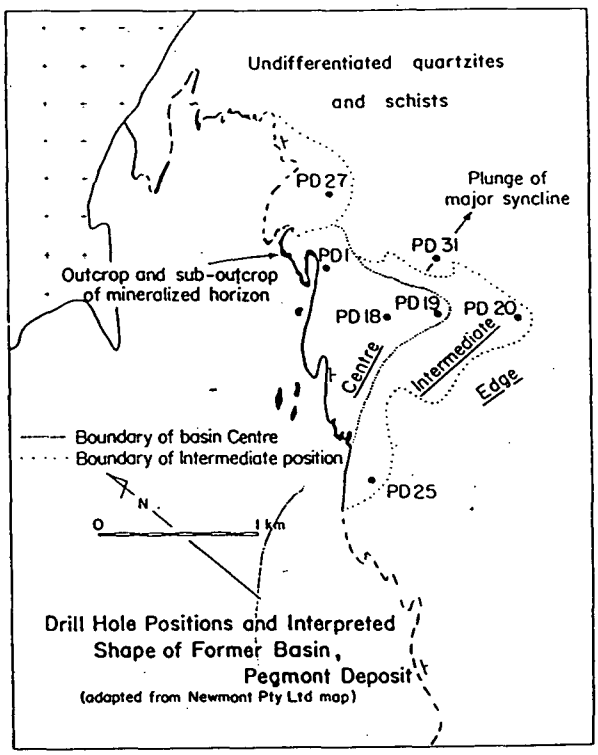

Figure 5.9 Simplified geological map of the Pegmont area, showing the interpreted sub-basin.
(Stanton and Vaughan, 1979)

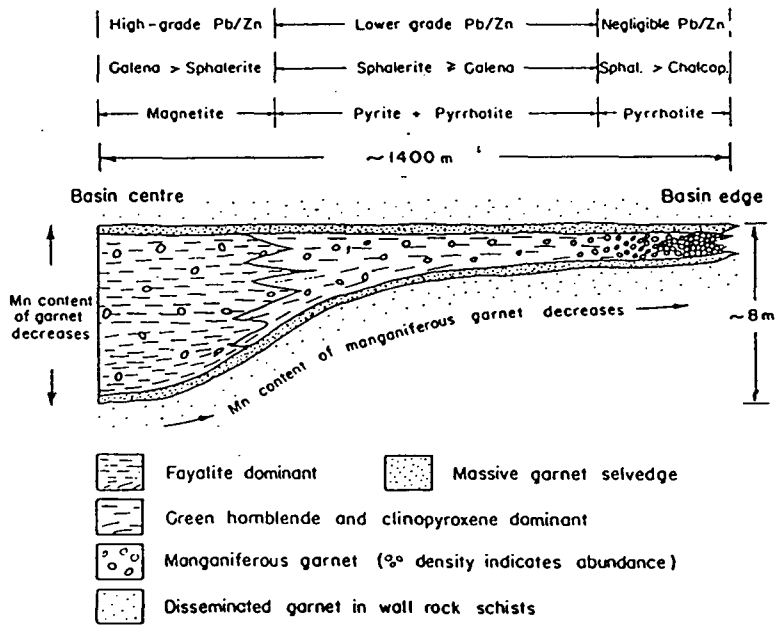

Figure 5.10 Mineralogical zonation across the Pegmont basin (?mound).
(Stanton and Vaughan, 1979)

6. MAGNETIC CHARACTERISTICS OF STRATIGRAPHY AND BHT MINERALISATION OF THE EASTERN SUCCESSION, MT ISA BLOCK, AUSTRALIA.

6.1 Regional Aeromagnetic Characteristics of the Soldiers Cap Group

The Soldiers Cap Group hosts the BHT mineralisation of the Eastern Succession. Much of this sequence occurs under cover and hence it is difficult to reconcile the sequence with the regional stratigraphic BHT model. Aeromagnetic data are heavily relied upon for regional geological interpretation and targeting of exploration programs.

A regional aeromagnetic image covering the Soldiers Cap Group and adjoining formations is presented as Figures 6.1 and 6.2, and Plates 9 and 10. This image incorporates numerous separate surveys. Their specifications and locations are shown in Figure 6.3. An interpretation of the regional aeromagnetic data is presented in Figure 6.4 and Plate 11. The interpretation is draped on the regional aeromagnetic data in Figure 6.5 and Plate 12.

In the outcropping type area of the Soldiers Cap Group, the Llewellyn Creek Formation, Mt Norna Quartzite and Toole Creek Volcanics can be distinguished readily in the magnetic data. The Llewellyn Creek Formation contains a prominent magnetic unit near the contact with the overlying Mt Norna Quartzite. This magnetic unit is comprised of amphibolite. The Mt Norna Quartzite is characterised by linear, laterally continuous magnetic marker horizons reflecting BIF and amphibolite units within the sequence. The overlying Toole Creek Formation shows zones of weak irregular magnetic response corresponding to mafic volcanic rocks and thin weakly magnetic linear horizons within the pelitic sequence, probably reflecting subtle variations in magnetite content within metasedimentary units.

Further south, as metamorphic grade increases, the outcropping Soldiers Cap Group is undifferentiated in published mapping. The sequence contains numerous magnetic units, but they are of shorter strike length and are less clearly confined to particular stratigraphic levels. It is more difficult to define a magnetic lithostratigraphy. A number of the magnetic units may be related to magnetite in shear zones and magnetic amphibolites in addition to magnetite in metasedimenty rocks.

Near the Pegmont and Cannington deposits the Soldiers Cap Group shows markedly different magnetic characteristics. Linear extensive magnetic units are now completely absent and the magnetic character is generally flat and uniform, with magnetic units being rare.

West of Pegmont there is an abrupt change in magnetic character across an interpreted terrane boundary into the Mt Stavely-Kuridala Formations. This terrane boundary is inferred by some authors (e.g. Walters, 1994) to represent an allochthonous boundary between the Soldiers Cap Group and the remainder of the Eastern Succession.

Figure 6.1 Regional Aeromagnetic Data
Soldiers Cap Group, Eastern Succession
Reduction To Pole

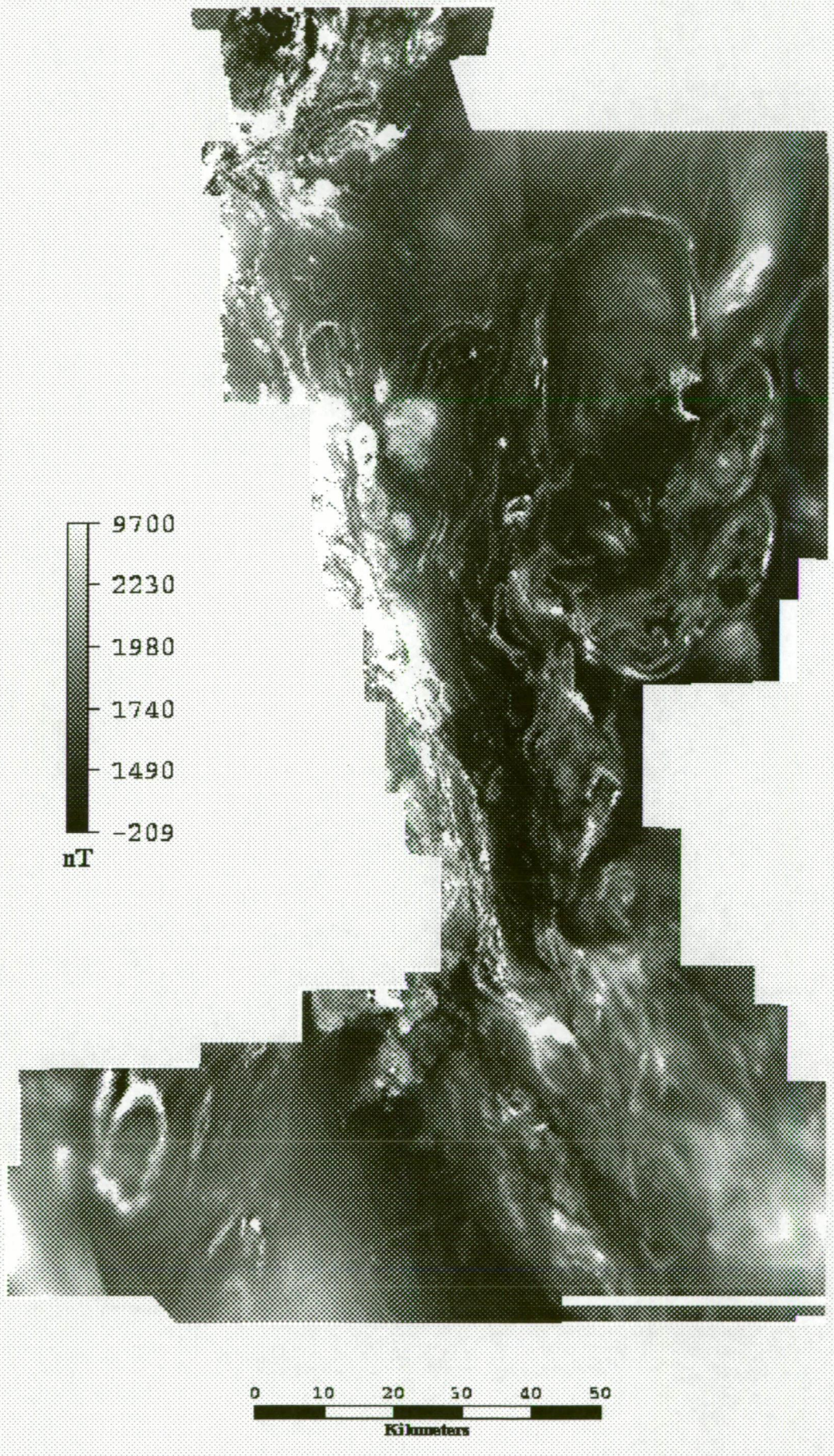

Figure 6.2 Regional Aeromagnetic Data
Soldiers cap Group, Eastern Succession
Reduction To Pole - 1st Vertical Derivative.

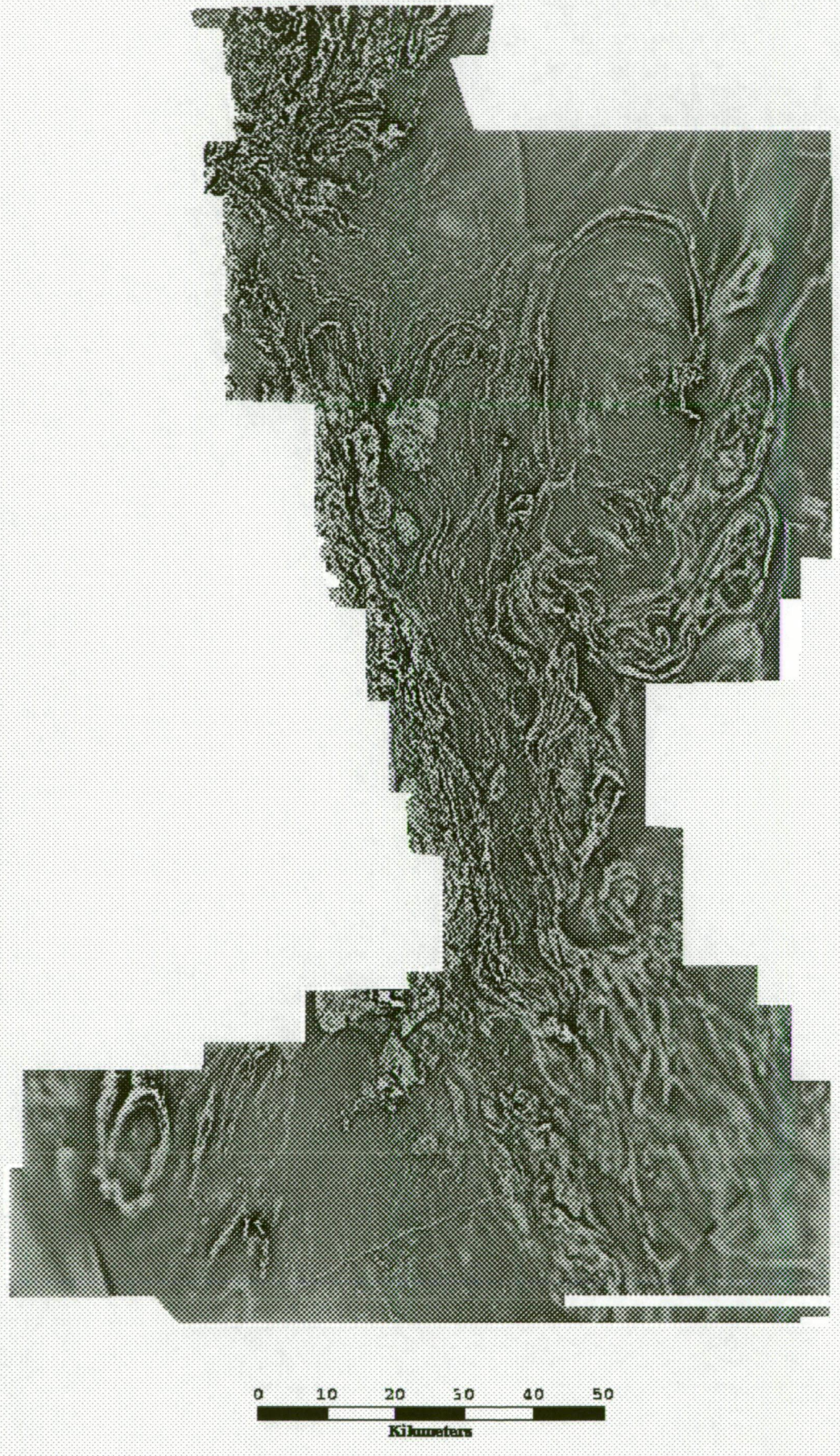

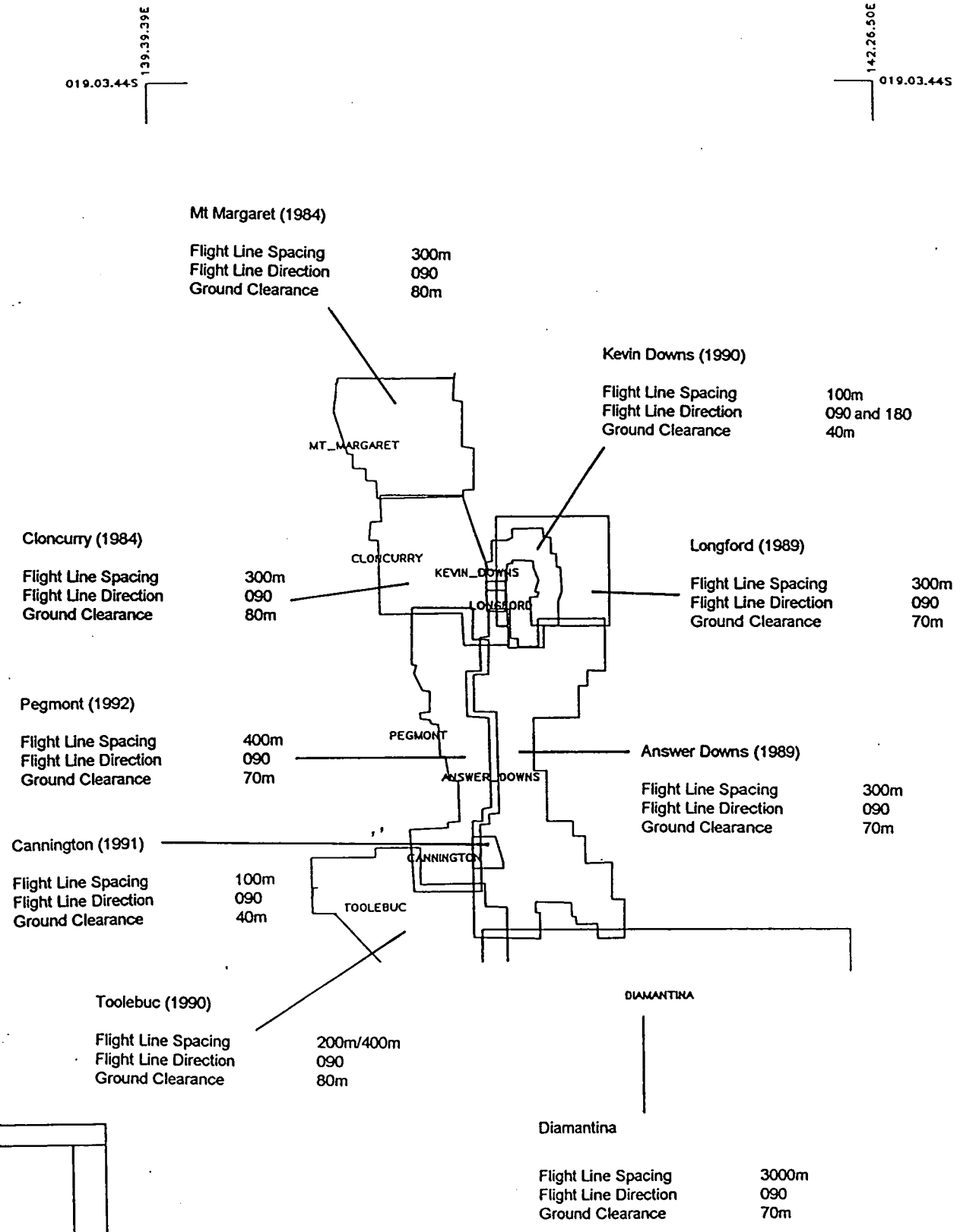

Figure 6.3 Regional aeromagnetic survey locations and specifications, Soldiers Cap Group, Eastern Succession, Australia.

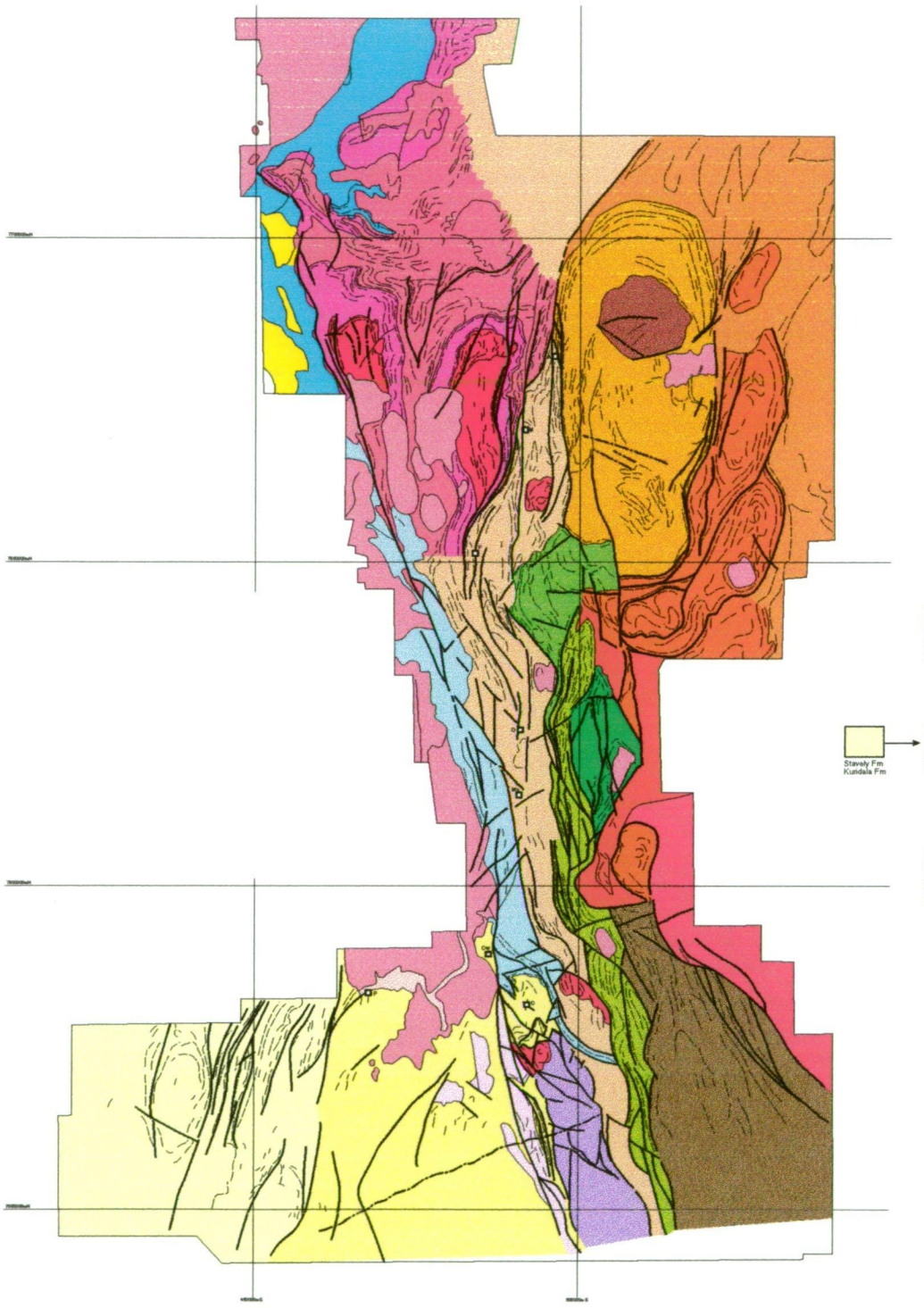

B H P MINERALS

Soldiers Gap Group

Eastern Succession, Mt Isa Block, Australia

AEROMAGNETIC INTERPRETATION

0 10 20km

Interpretation by T.Karr

Figure 6.4

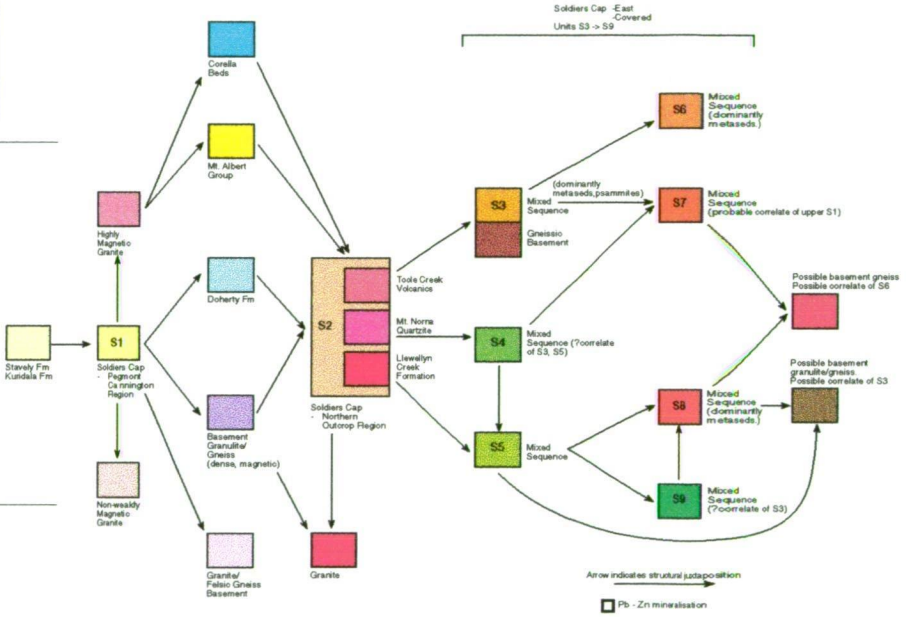

Figure 6.5 Regional Aeromagnetic Interpretation
Draped on Vertical Derivative
Soldiers cap Group, Eastern Succession.

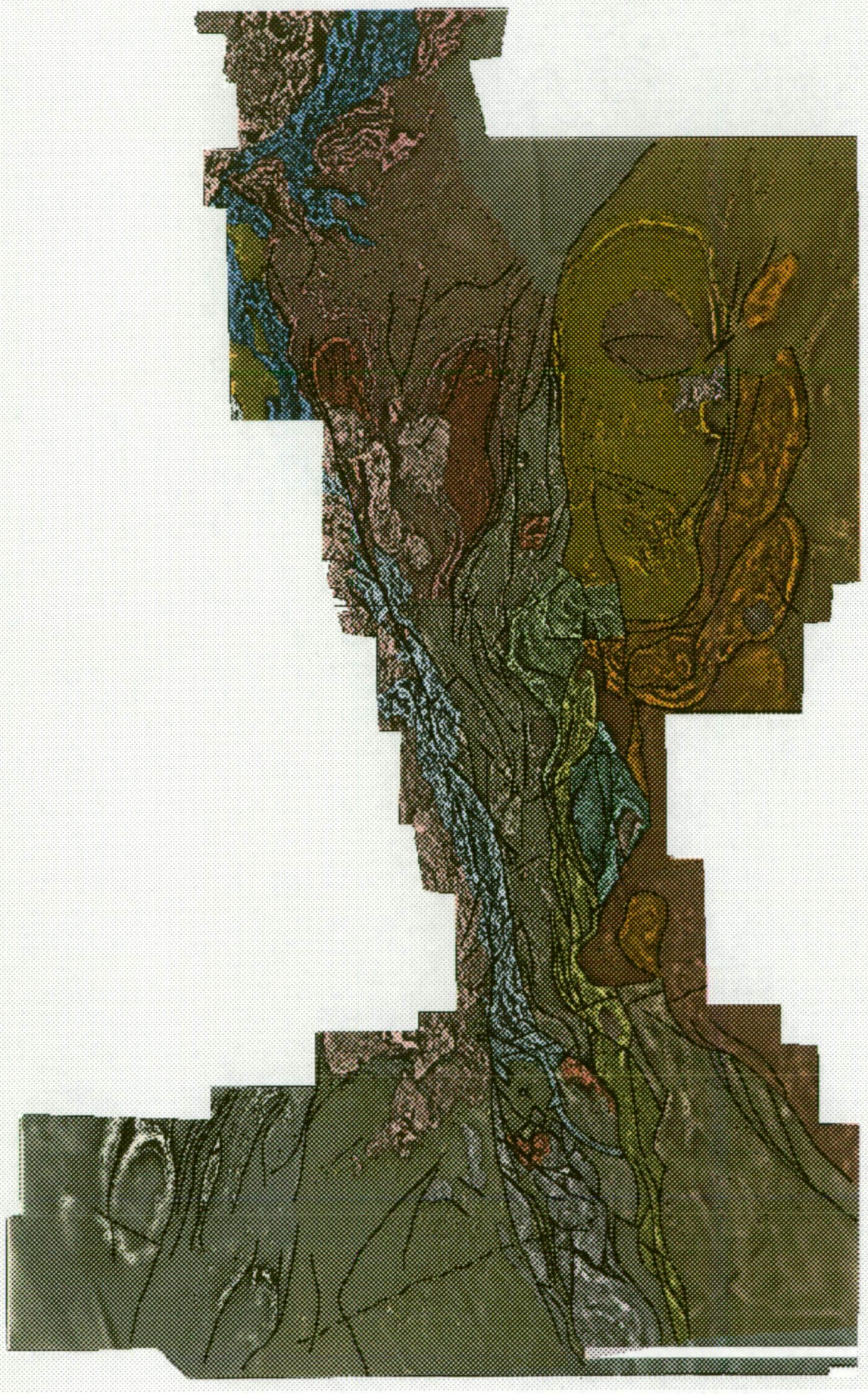

The Mt Stavely and Kuridala Formations have not been separately mapped in the magnetic interpretation as they appear to have very similar magnetic characteristics. The Osborne (Trough Tank) Au-Cu deposit appears to occur in exactly the same sequence as the Starra Au-Cu deposits , although the former is mapped as occurring in the Kuridala Formation and the latter in the Mt Stavely Formation (Figure 5.3). The Kuridala-Mt Stavely Formations are characterised by strongly magnetic (up to 1200 nT) linear BIF units. The distinct style of dome and basin folding results in the magnetic units defining elongate ellipsoids and extensive linear magnetic features, in stark contrast with the adjoining Soldiers Cap Group.

Further north the western boundary of the Soldiers Cap Group is in contact with the Doherty Metasomatic Zone. This zone of intense Na metasomatism is strongly and irregularly magnetic , with alteration resulting in plagioclase-actinolite-diopside-quartz-scapolite-magnetite assemblages. Further north again, in the type area of the Soldiers Cap Group, the western boundary of the Solders cap Group adjoins the Corella Formation, also strongly and irregularly magnetic. It has a magnetic signature which is very similar to the Doherty Formation.

East of outcrop the Soldiers Cap Group can be seen to extend a considerable distance under cover. A number of individual formations can be identified on the basis of unique magnetic character. None of these sequences outcrops. Many show very different magnetic character to any of the outcropping sequences, and so are likely to be new formations. Many boundaries between magnetic packages are structural and so a magnetic lithostratigraphy is difficult to develop. Magnetic units tend to be BIF, quartz magnetite rocks, amphibolite and magnetite in metasedimentary rocks. Magnetic contact aureoles around granites are also evident.

Regionally, BHT mineralisation is generally magnetically quite distinctive. BHT prospects and deposits are shown in Figures 6.4 and 6.5 (Plates 11 and 12). It is clear that the mineralisation is generally intimately associated with magnetite. The anomalous magnetic response in each case has a limited strike length, as opposed to laterally extensive, uniformly magnetic amphibolites and BIFs. However the mineralisation may be associated with less magnetic, linearly extensive marker horizons such as BIF.

Cannington and Pegmont, the most economically significant known occurrences, have aeromagnetic anomalies of the order of 450nT and 150 nT respectively. Altia (3500 nT), Maronan (2500 nT) and Fairmile (1000nT) are strongly magnetic while Dingo (50 nT), Marramungee (100nT) and Cowie (30 nT) have more subtle responses in the aeromagnetic data.

Cowie has a relatively weak response despite being intimately associated with BIF, showing that BIF and magnetite-related deposits need not have a strong aeromagnetic signature. The magnetic field falls off rapidly with distance, at a power of -3, particularly for thin or discontinuous units. Hence a two metre thick BIF may give a weak response in a regional aeromagnetic survey. Cannington's aeromagnetic anomaly increases in strength to 1100 nT in a low level detailed aeromagnetic survey (altitude decreasing from 70m to 40m), and increases to 2600 nT in ground magnetic data.

Certainly the most significant mineralisation is not associated with the strongest aeromagnetic anomalies. More important is the anomalous nature of the magnetic response within the immediate surroundings.

In summary, the Soldiers Cap Group is characterised by three main types of aeromagnetic signatures:

1. relatively non-magnetic host sequences with uncommon linear magnetic units of significant strikelength (Transitional and Upper Sequence);

2. relatively non-magnetic host sequences with uncommon linear magnetic units of short strikelength (Transitional and Upper Sequence);

3. "stripy" magnetic host sequences with abundant linear magnetic units of significant strikelength (? Lower Sequence).

Significant mineralisation within the Soldiers Cap Group is closely associated with magnetite. Magnetic signatures are of two types:

1. A strongly magnetic localised zone within a moderately magnetic linear unit of significant strike extent (e.g. Altia and Maronan);

2. Moderately magnetic short strike length anomalies within a relatively non-magnetic background (e.g. Cannington and Pegmont).

6.2 Aeromagnetic Interpretation of the Pegmont - Cannington Region

Regional aeromagnetic images covering the Pegmont-Cannington region are presented as Figures 6.6 and 6.7, and Plates 13 and 14. The images incorporate a number of separate surveys. Survey specifications are detailed in Table 6.1 while the survey locations are shown in Figure 6.3.

An interpretation of the aeromagnetic data is presented in Figure 6.8 and Plate 15. The interpretation is draped on the aeromagnetic data in Figure 6.9 and Plate 16.

Soldiers Cap Group

The formation within the Soldiers Cap Group which hosts the Pegmont and Cannington deposits (unit S1) has a uniformly flat, relatively non-magnetic signature. Within this relatively quiet background a number of weakly and moderately magnetic units occur.

Figure 6.6 Regional Aeromagnetic Data
Pegmont - Cannington Region, Australia.
Reduction To Pole

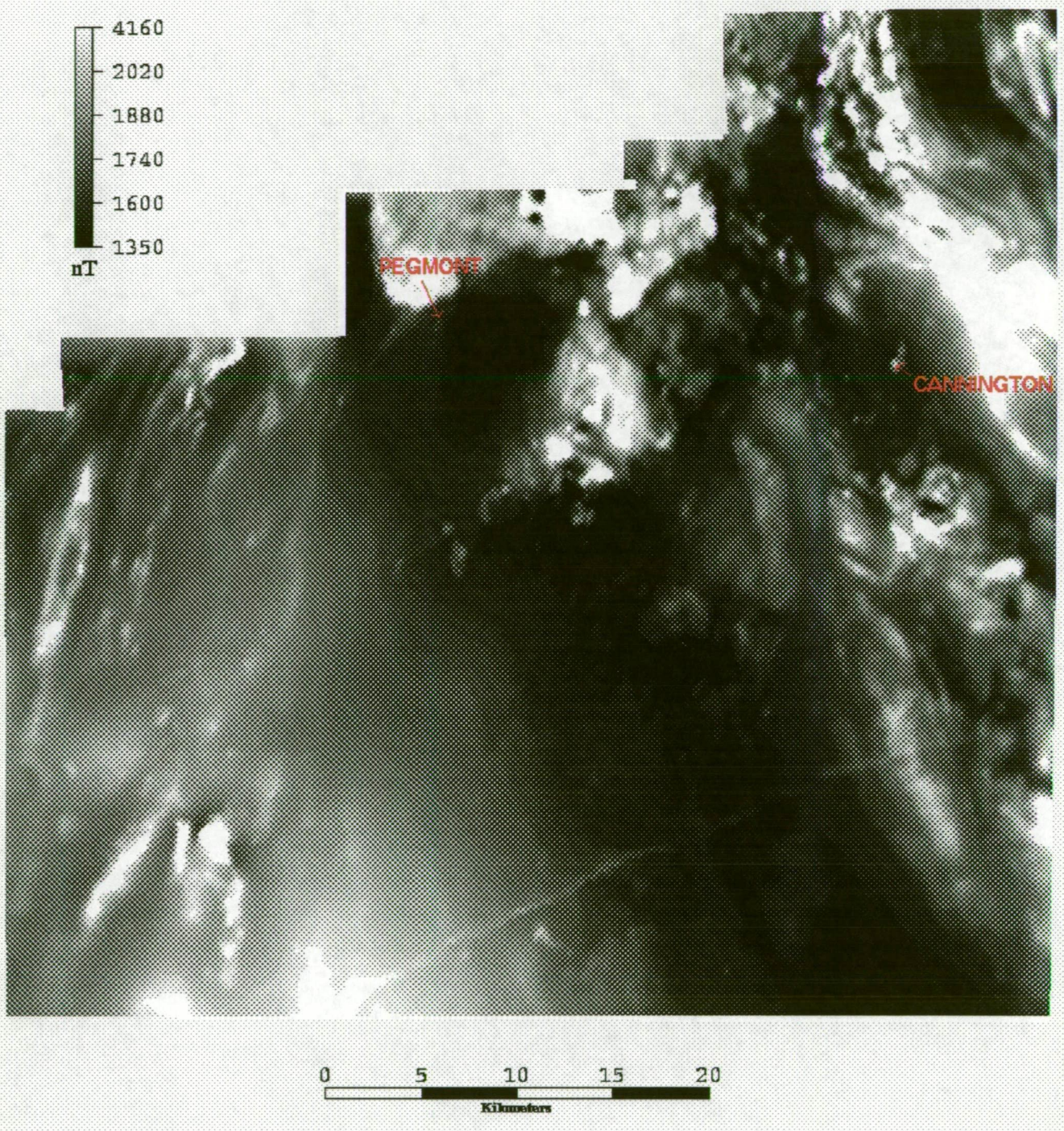

Figure 6.7 Regional Aeromagnetic Data
Pegmont-Cannington region, Australia.
Reduction To Pole - 1st Vertical Derivative

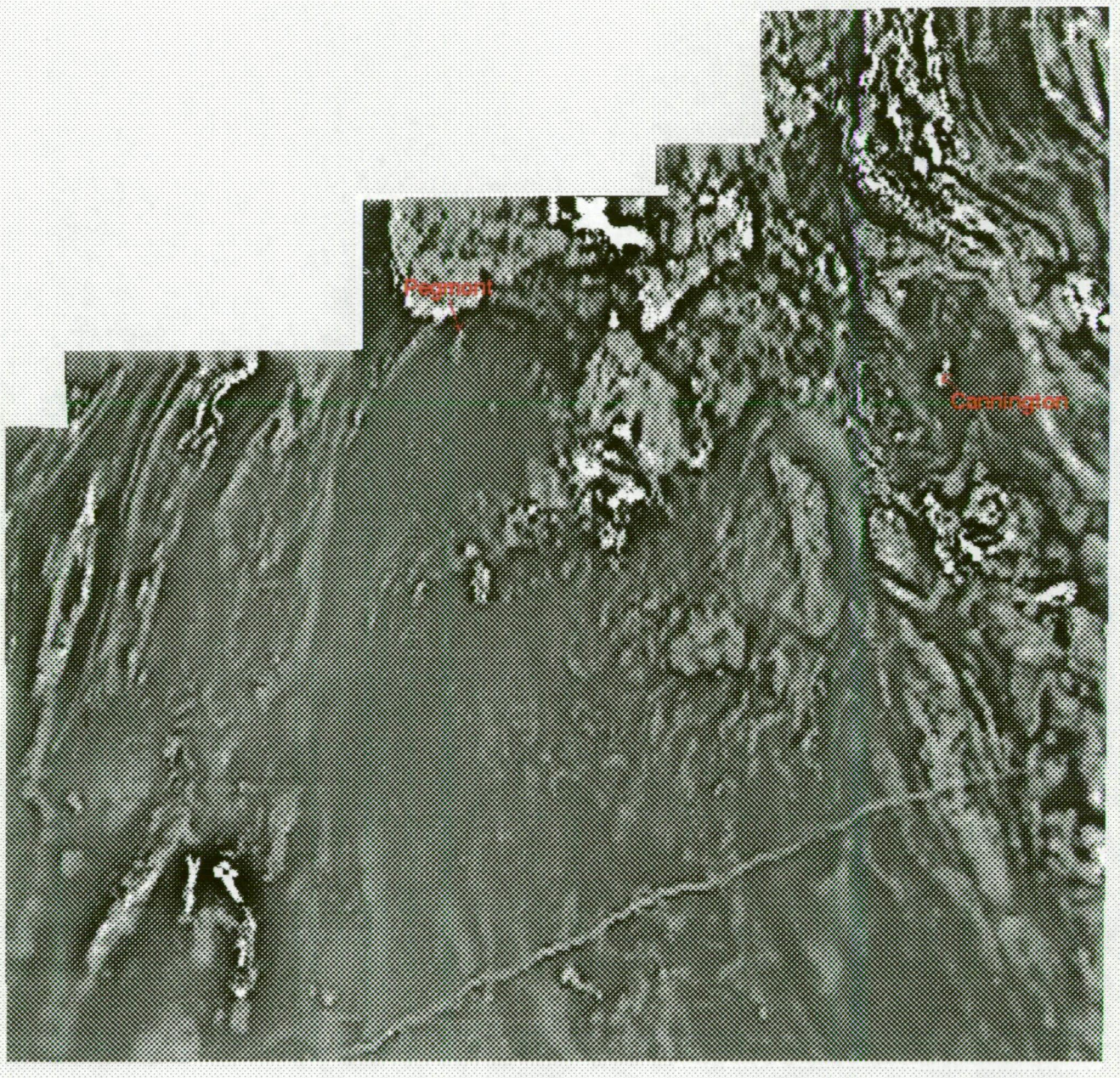

B H P MINERALS

Pegmont - Cannington Region
Eastern Succession, Mt Isa Block, Australia
AEROMAGNETIC INTERPRETATION

0 10km

Interpretation by T.Kerr

Figure 6.8

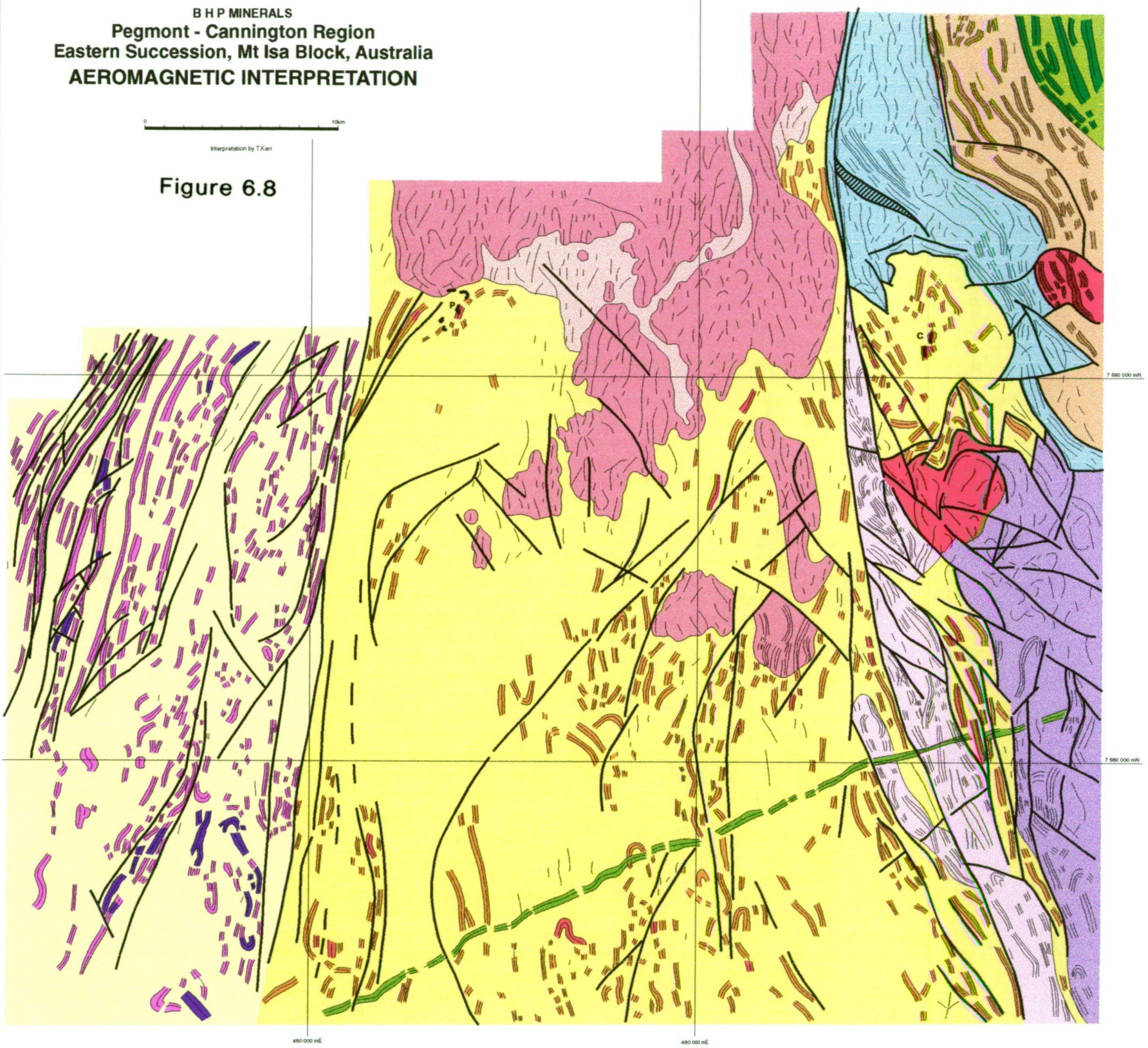

Dyke

Highly magnetic granite

Non - weakly magnetic granite

Doherty Fm

Mt. Stavely / Kuridala Fm
highly magnetic unit -iron formation
moderately magnetic unit -magnetite exhalites, BIF -amphibolites

Mafic granulite / gneiss basement

Soldiers Cap - Pegmont / Cannington Region - Unit S1
highly magnetic unit -magnetite - amphibolites -magnetite - exhalites, BIF
moderately to weakly magnetic -amphibolites -magnetite - exhalites, BIF

Felsic gneiss /granite basement

Soldiers Cap - Northern Outcropping Region - S2
magnetic unit -magnetite - exhalite, BIF -amphibolite -magnetite in shear zones

Magnetic granite

Shear zone

Soldiers Cap - Unit S5
magnetic unit -metasediments/metavolcanics

BHT mineralisation

Figure 6.9 Regional Aeromagnetic Interpretation (Colour) Draped On Vertical Derivative (Intensity) Pegmont-Cannington Region, Australia.

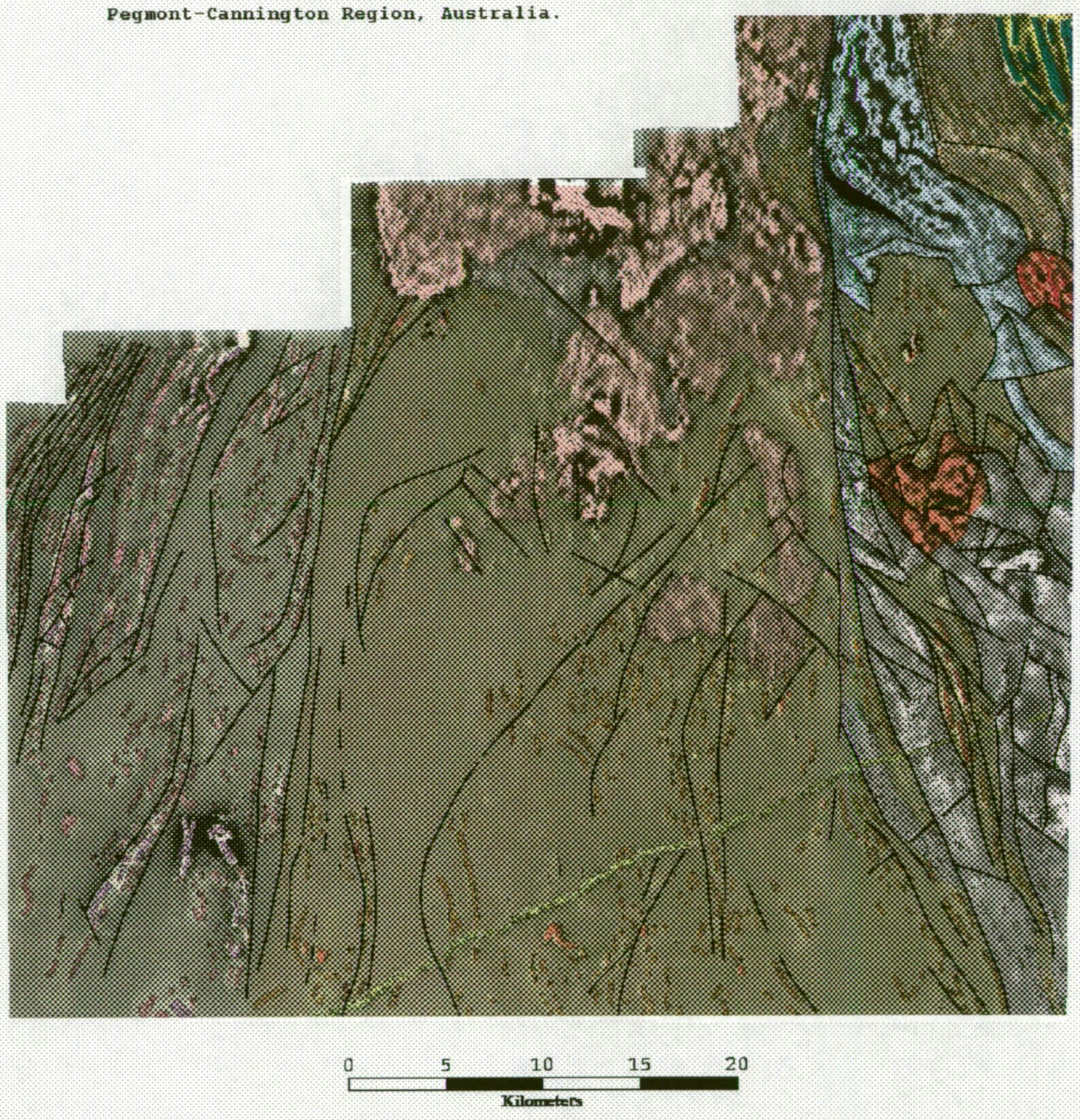

The weakly magnetic units have amplitudes of less than 50 nT, commonly of the order of 10 nT. The moderately magnetic units have amplitudes ranging from 90 to 450 nT, most commonly approximately 150 nT. The anomaly associated with the Cannington deposit is the strongest anomaly within this Soldiers Cap unit.

The magnetic units within this formation are relatively short in strike length, generally less than 2km. The magnetic units are commonly magnetite-bearing amphibolites, metasedimentary rocks and exhalites.

Further east, two stripy formations within the Soldiers Cap Group occur under cover. Unit S2 corresponds to the outcropping Soldiers Cap Group formation occurring further north. It is characterised by linear moderately magnetic units (30 to 150 nT) within a flat relatively non-magnetic background. These magnetic units are more frequent and laterally continuous than the magnetic units within Unit S1. Magnetic units within Unit S2 are likely to be magnetite-bearing metasediments, amphibolites, and exhalites such as BIF and magnetite in shear zones.

Unit S5 is similar in texture to Unit S2, but the linear magnetic units are considerably more magnetic (200 - 500 nT). Magnetic units are likely to be magnetic amphibolites and exhalites such as BIF.

Mt Stavely - Kuridala Formation

As mentioned in the previous section there is a notable change in magnetic character across the interpreted boundary between the Soldiers Cap Group and the Kuridala - Mt Stavely Formation. Once again linear magnetic units occur in a relatively non-magnetic background. However magnetic units within the Kuridala-Mt Stavely Formation are generally considerably more magnetic and have a larger strike length than magnetic units within Unit S1 of the Soldiers Cap Group. Magnetic units are also more common within the Kuridala-Mt Stavely Formations.

Magnetic units classed as strongly magnetic have amplitudes of the order of 400 - 2000 nT. BIF units are the source of these magnetic anomalies. Weak to moderately magnetic units have amplitudes of up to 200 nT. These units are likely to be thinner or less magnetic BIF, magnetic amphibolite or magnetite-bearing metasedimentary rocks.

Doherty Metasomatic Zone

The Doherty Metasomatic Zone is a strongly magnetic unit with some indication of poorly defined linear magnetic zones. The low zones between the linear magnetic bands may be due to magnetite destruction in shear zones, and hence the banding may not be stratigraphic. Amplitudes range from 300 to 1000 nT, commonly of the order of 500 nT.

Felsic Gneiss/Granite Basement

A number of sequences of felsic gneiss/granite basement have been interpreted. They are all characterised by an irregular, contorted, moderate to strongly magnetic signature, suggesting a gneissic rock fabric. A much greater percentage of these basement gneiss formations are magnetic compared to the younger, less deformed metasedimentary/metavolcanic rock sequences.

6.3 Detailed Aeromagnetic Interpretation of the Cannington Region

A detailed aeromagnetic survey was flown over the immediate surrounds of the Cannington deposit in 1991. This survey was flown at an altitude of 40m, with a 100m line spacing. Images of this survey are presented in Figures 6.10 and 6.11, and Plates 17 and 18. An interpretation of this survey is presented in Figure 6.12 and Plate 19. The interpretation is draped over the aeromagnetic data in Figure 6.13, Plate 20.

Within the Soldiers Cap Group, the formation surrounding the deposits, Unit S1, has been further subdivided using the detailed data set.

Unit 1 hosts the Cannington deposit. This unit is interpreted to be sediment dominated. Magnetic units within the relatively non-magnetic host have been subdivided into three types, based on amplitude. Very strongly magnetic units have amplitudes of 500 to 1200 nT and represent BIF and magnetite intimately associated with base metals. Strongly magnetic units have amplitudes of the order of 100 nT and may be magnetite-bearing exhalites or amphibolites. Moderately magnetic units have amplitudes of the order of tens of nanoteslas and are likely to be magnetite-bearing metasedimentary rocks, moderately magnetic amphibolites and thin or weakly magnetic exhalites.

Unit 2 has a slightly stronger magnetic background and magnetic units are more common. This unit is interpreted to be volcanic rock dominated. Strongly magnetic units (100 to 500 nT) are magnetic amphibolite. Moderately magnetic units (less than 100 nT) are interpreted to be probable magnetic amphibolite, or possibly magnetite exhalites.

South of Unit 2, two sequences have been mapped as probable moderate and strongly magnetic granites, or possible contact metamorphosed Soldiers Cap Group. The moderately magnetic sequence has amplitudes of the order of 300 nT while the strongly magnetic sequence has amplitudes of 500 to 800 nT.

West of Unit 2, weak to moderately magnetic (100 to 300 nT) basement felsic gneiss or granite has been interpreted.

It is clear that within the metasedimentary rock-dominated Soldiers Cap Group the Cannington deposit has by far the strongest magnetic anomaly. Note the increase in amplitude from 450 nT in the regional survey to 1200 nT in the detailed lower-altitude survey. Magnetic amphibolite is the most common source of moderate magnetic anomalies.

Figure 6.10 Detailed Aeromagnetic Data, Cannington, QLD, Australia
Reduction To Pole

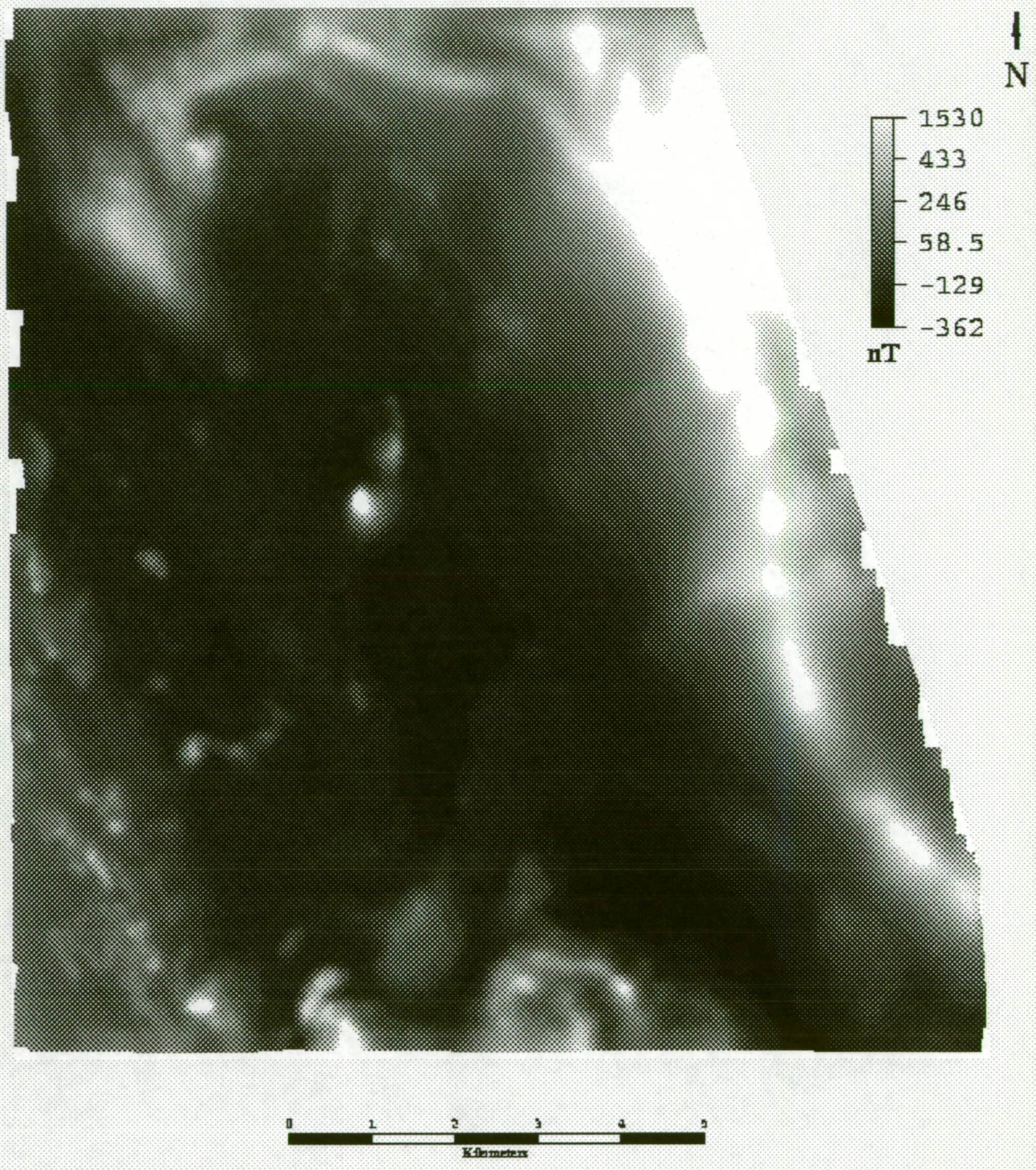

Figure 6.11 Detailed Aeromagnetic Data, Cannington, QLD, Australia
Reduction To Pole - 1st Vertical Derivative

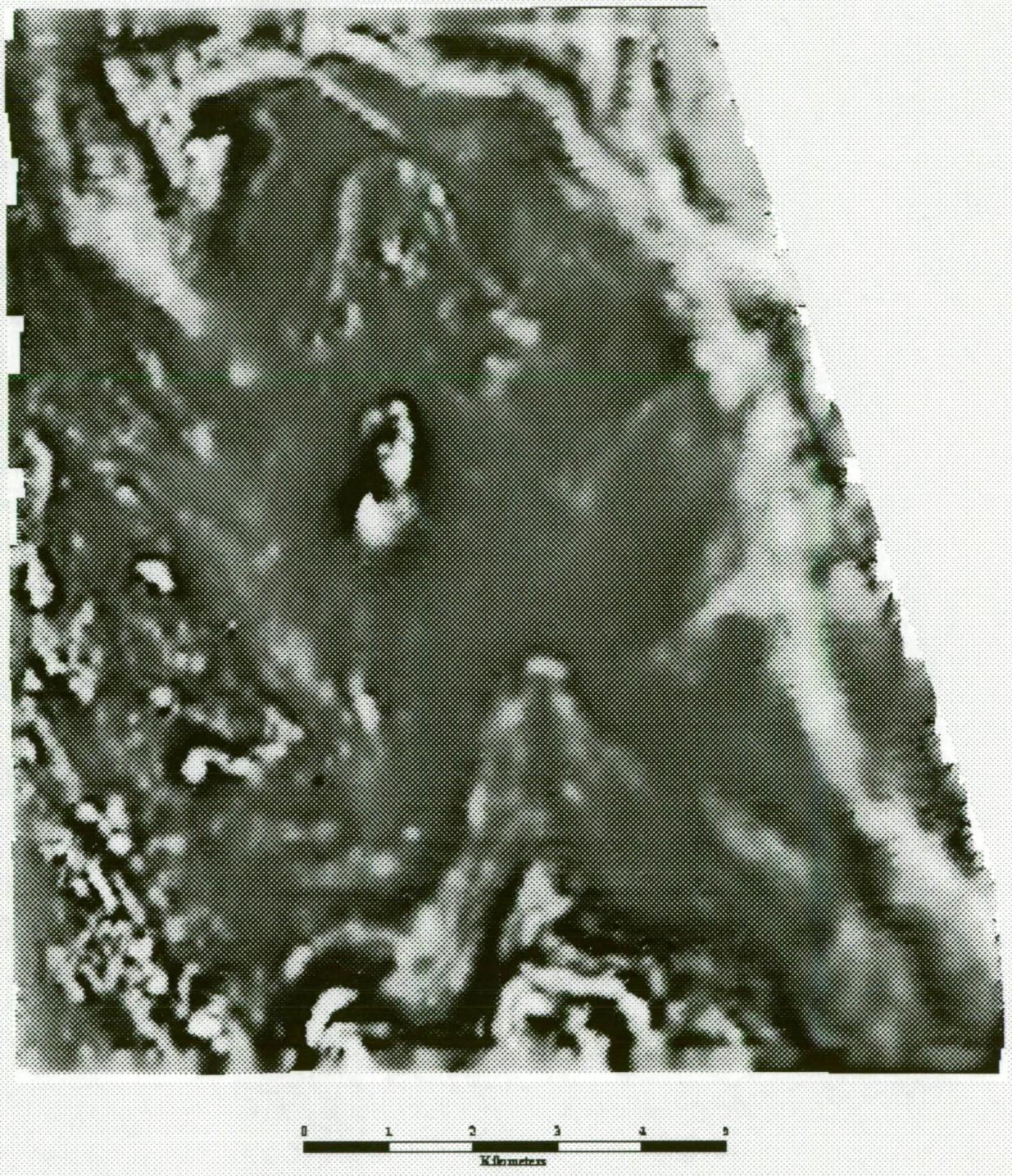

Figure 6.12

B H P MINERALS

Cannington, Qld, Australia

DETAILED AEROMAGNETIC SURVEY INTERPRETATION

0 2km

Interpretation by T.Kerr

Doherty Formation
Highly magnetic unit

Soldiers Gap Group - sediment dominated
Weak to non magnetic psammites, pelites, quartz-feldspar schists, gneisses, amphibolites with a low frequency of magnetic units
Very highly magnetic : BIF-mt-base metals
Highly magnetic : mt-exhalite-BM
Moderately magnetic : mt-exhalite / mt-amphibolite
Magnetite destruction alteration zone
Magnetite-amphibolite

Soldiers Gap Group - volcanic dominated
Weak to moderately magnetic with a high frequency of magnetic units
Highly magnetic : probable magnetite-amphibolite, possible magnetite-exhalite
Highly magnetic : magnetite-amphibolite
Moderatley magnetic : probable magnetite-amphibolite, possible magnetite-exhalite

?Soldiers Gap Group - volcanic dominated
Moderately magnetic : probable correlation of volcanic dominated Soldiers Gap(contact metamorphosed), possible magnetic granite
Moderately magnetic unit

Magnetic Granite
Highly magnetic : probable magnetic granite, possible contact metamorphosed Soldiers Gap
Highly magnetic unit

?Basement
Moderately magnetic : granite / felsic granite
Magnetic unit

Cannington Ag-Pb-Zn mineralisation

7 585 000 mN
7 580 000 mN
7 575 000 mN
490 000 mE
495 000 mE

Figure 6.13 Detailed Aeromagnetic Interpretation (Colour)
Draped On Vertical Derivative (Intensity)
Cannington, QLD, Australia.

6.4 Magnetic Characteristics of the Cannington Deposit

From the aeromagnetic data it is apparent that magnetite is intimately associated with the deposit. The distribution of magnetite within the deposit itself will now be considered.

A representative cross section through the deposit was shown in Figure 5.6. The ore zone is subdivided into five lodes and 10 mineralisation types which are summarised in Table 5.2.

Down hole susceptibility measurements for a selection of holes on section 4700N are presented in Appendix A. From these measurements it is clear that the Nithsdale, Colwell, Kheri and Burnham lodes are generally strongly magnetic. Susceptibilities up of more than 100 000 x 10^{-5} SI are common. The magnetite at Cannington is preferentially associated with the high grade footwall and hanging wall Pb lodes (Nithsdale and Burnham lodes) and with the low grade Zn lodes (Kheri and Colwell).

The high grade Zn lodes (Cuckadoo and Glenholme) have been severely overprinted by metasomatic alteration, resulting in silicification and magnetite destruction. Prior to this overprinting these lodes could have had similar compositions to the Kheri/Colwell lodes (Cuckadoo) and Nithsdale/Colwell lodes (Glenholme). Hence the magnetite could have originally been equally distributed between the Pb and Zn lodes.

A magnetic model of section 4700N was constructed by assigning susceptibilities to the individual units using the data presented in Appendix A. The model results are compared to a ground magnetic profile in Figure 6.14, while susceptibilities used in modelling are summarised in Table 6.1 . The amplitude of the model data is approximately **two orders of magnitude** greater than the ground magnetic anomaly. The peaks of the model and field profiles are also displaced. The model program is based on the 2D Talwani algorithm and assumes an infinite strikelength. It does not incorporate the effects of self demagnetisation or remanence. Clearly a more sophisticated modelling approach which incorporates remanence, self-demagnetisation and 3D effects is required.

6.5 Magnetic Characteristics of the Pegmont Deposit

From the aeromagnetic data it is clear that the Pegmont deposit shows an anomalous magnetic response, with mineralisation being intimately associated with magnetite.

A plan view of the geology of the Pegmont deposit is presented as Figure 5.8. Mineralogical variations across the mound or basin are summarised in Table 5.6 and Figure 5.10.

The thickest Pb-Zn mineralisation is intimately associated with magnetite. Intermediate Pb-Zn mineralisation is associated with pyrite-pyrrhotite, and pyrrhotite is associated with weak Cu-Zn mineralisation at the margins. There is no preferential association of magnetite with Pb or Zn within the high grade portion of the deposit.

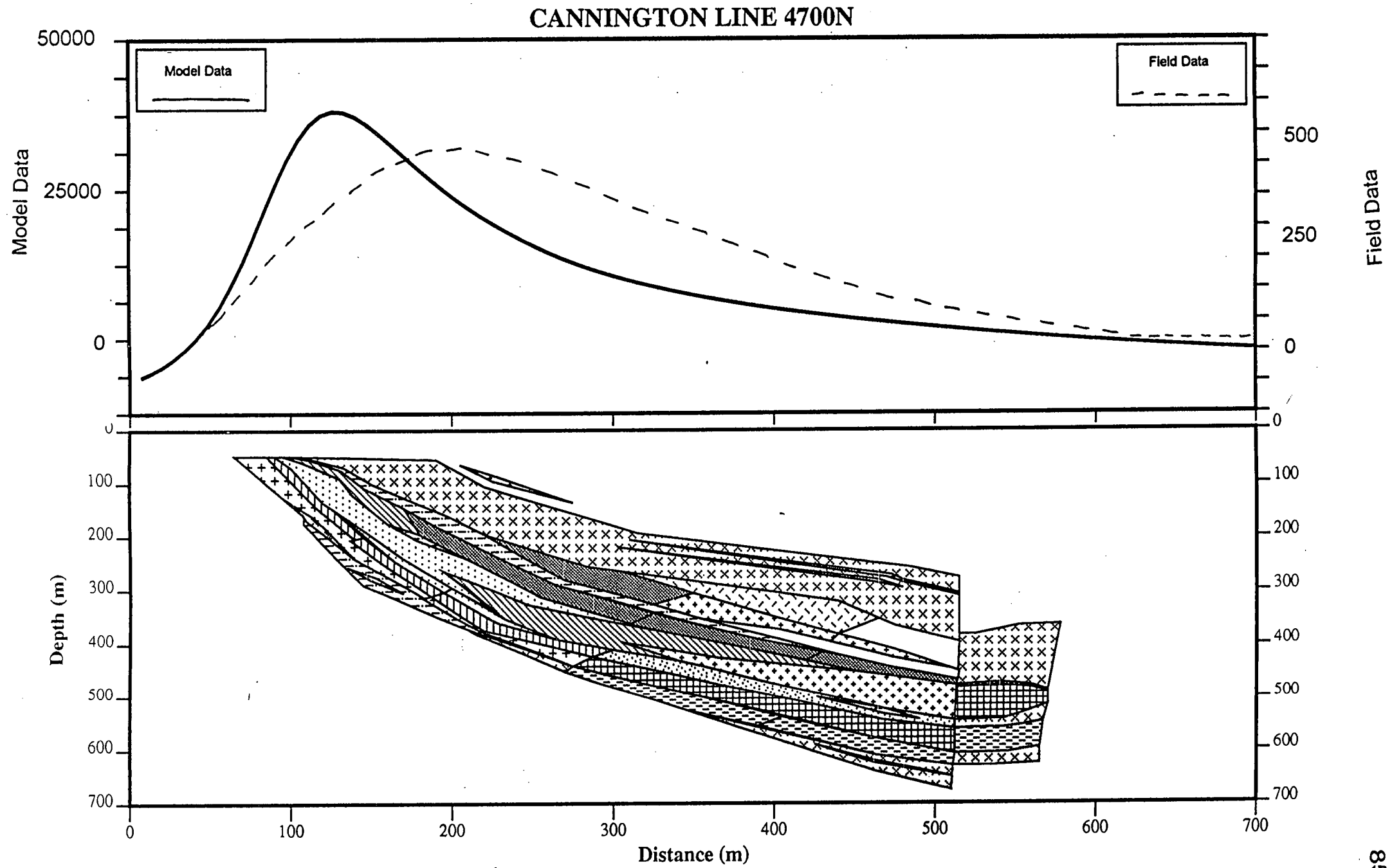

Figure 6.14 Ground magnetic profile and model, Cannington.

Ground magnetic data over the Pegmont deposit show a 450 nT anomaly over the mineralised outcrop. This compares to a 150 nT anomaly in the regional aeromagnetic survey. An important feature is the greater strike extent of the ground magnetic anomaly associated with the lode horizon, when compared to the aeromagnetic anomaly.

LITHOLOGY	SUSCEPTIBILITY (SI x 10^{-5})
Pegmatite	0
SHMU Halo	0
Amphibolite	0, 40 000 - 100 000
Broadlands BL1	0, 1000
Broadlands BL2/3	1000
Burnham BM2	40 000
Nithsdale	1000, 100 000
Warenda	1000, 10 000
Kheri (KH1)	20 000, 30 000, 100 000
Colwell (CW1)	30 000, 100 000
Colwell (CW2)	10 000
Glenholme	0, 10 000
Cuckadoo	0, 1000, 100 000
Silicified Quartzite	0

Table 6.1 Magnetic susceptibilities used in modelling of section 4700N, Cannington.

7. GEOLOGY AND MINERALISATION OF THE BERGSLAGEN DISTRICT, SWEDEN.

The Bergslagen District is significant because it hosts the second largest economic BHT deposit presently being mined. The district is also significant because it is one of the few BHT provinces which also hosts significant VHMS mineralisation.

7.1 Regional Geology

The Bergslagen District is located in south central Sweden (Figure 7.1). The Bergslagen Supracrustal Sequence (1.9 - 1.86 Ba) is comprised of felsic metavolcanic and metasedimentary rock sequences confined to a series of long narrow tectonically controlled grabens. These narrow grabens display a similar stratigraphic sequence despite being spatially separated. They are enclosed by extensive syn to post orogenic granitoid rocks. The supracrustal sequences were later deformed and metamorphosed to amphibolite facies during the Svecokarelian Orogeny (1.9 - 1.7 Ma). The basement to the Bergslagen Supracrustal Sequence is unknown, a common feature of BHT host provinces.

Stratigraphy

Three separate sequences are recognised within the Bergslagen Supracrustal Sequence:

Lower Sequence	- subaerial felsic ignimbrites and air-fall deposits
Transitional Sequence	- decrease in explosive volcanism and increase in volcaniclastic rocks and metasedimentary rocks of volcanic derivation (tuffites)
Upper Sequence	- metasedimentary rocks, including greywackes, shales and mass flow deposits

There is a lateral variation from west to east. Felsic volcanic rocks in the west form a pile more than 10km thick which thins to less than 900m in the east. As the proportion of felsic volcanic rocks decreases the metasedimentary component of the stratigraphy increases to the east. Nevertheless the same vertical zonation is observed, albeit with differing proportions (Baker and Hellingwerf, 1988).

There is also a vertical zonation from lower Na-rich units to upper K-rich units. This is interpreted to represent regional hydrothermal alteration (Walters, 1992), and has been described in other BHT provinces (e.g., Eastern Succession, Mt Isa Block).

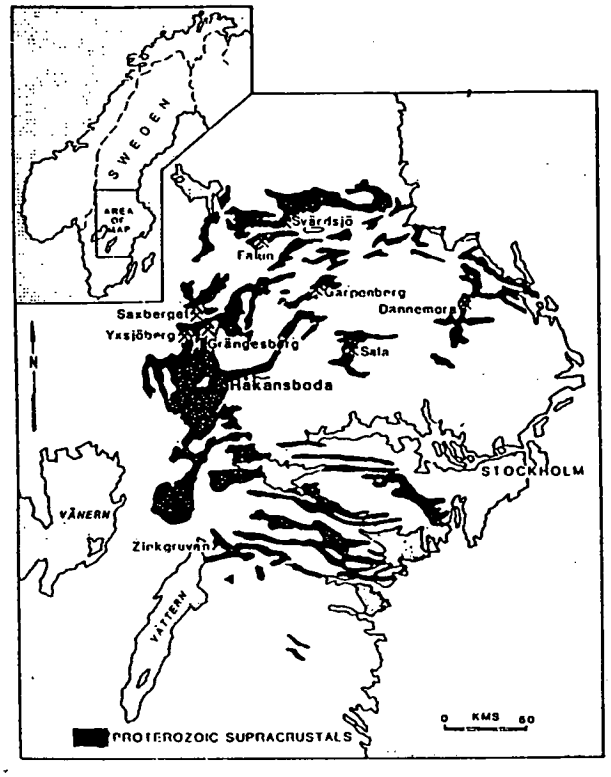

Figure 7.1 Location plan, Bergslagen District.
(Walters, 1992)

Structure

Deformation during the Svecokarelian orogeny (1.87 - 1.7 Ba) resulted in isoclinal folding of the supracrustal sequence sandwiched between the more competent early to syn-orogenic granitoids. Metamorphism reached upper amphibolite facies, with migmatization and partial melting of the biotite-rich rocks in the Upper (metasedimentary) Sequence. Later brittle fracturing is marked by north-north-east trending fault systems with block movements of hundreds of metres (Hedstrom *et al.*, 1989).

Mineralisation

The Bergslagen district is a very mineralised district, with three main classes of stratiform and stratabound Fe-Cu-Pb-Zn-W mineralisation recognised:

Iron/Manganese Ores	- Quartz-banded iron ore - Skarn iron ore - Apatite iron ore - Mn oxide-silicate ore
Base Metal Sulfide Ores	- Falun Type (VHMS) Cu-Zn-Pb sulfide ore - Zinkgruvan Type (BHT) Zn-Pb sulfide ore
Scheelite skarn ores	

These ore types are confined to the Lower and Transitional Sequences. The iron ores are by far the most common deposits mined historically. They generally contain high levels of base metals and are considered to have been formed by exhalative processes (Walters, 1992).

Fe-oxide rich iron ores are concentrated in the felsic volcanic dominated Lower Sequence and have much lower base metal and manganese contents than stratigraphically higher iron-rich exhalites. They have been directly compared to the quartz-magnetite horizons within the Thackaringa Group, Broken Hill, Australia (Walters 1992).

The Transitional Sequence, which is comprised of mixed tuffite-fine grained clastic-carbonate units, hosts a concentration of Mn-Fe-Ca-base metal rich exhalites. These exhalites show complex gradations from BIF to skarn-like Mn-Fe ores to dolomite, carbonate and base metal sulfide ore zones.

Stratabound base metal mineralisation is associated with numerous horizons of various exhalites and alterites within the Transitional Sequence. Many small tonnage deposits occur but the most significant are Falun (VHMS) and Zinkgruvan (BHT), which form two end members of a spectrum of base metal sulfide deposits.

Falun-style base metal deposits are the dominant style of base metal mineralisation within the Bergslagen District. The characteristic feature of this style of deposit is widespread Mg alteration/enrichment.

Mg alteration envelopes the sulfide ore lenses in the footwall of Falun style deposits. Mg alteration is generally evident in the form of phlogopite, with subordinate cordierite, staurolite, and anthophyllite. There is a gradation from unaltered host rocks toward increasing Mg- alteration toward the ore lenses. Mg enrichment is not confined to the footwall and may be present within the ore lenses and in laterally equivalent exhalites distal to the deposit. It may be evident as dolomite or cordierite-anthophyllite quartzites. Mg enrichment is not a feature of the BHT holotype. It represents a significant input of sea water in shallow, near surface convection cells characteristic of more volcanic rock-dominated sequences (Walters 1992).

The best examples of Falun type mineralisation are Falun (approx. 40 Mt grading 2-5% Zn, 2% Pb, 40 g/t Ag, 0.5% Cu, 0.3 g/t Au) and Garpenberg (total resource estimate unavailable but now being mined at a rate of 200,000 tonnes per year at a grade of 5% Zn, 4% Pb, 0.4% Cu, 130 g/t Ag, 0.9 g/t Au).

7.2 Garpenberg Ore Deposit - Falun Style VHMS Mineralisation

Garpenberg is much better documented than Falun (Vivallo, 1985). It is comprised of ore lenses which show a vertical zonation (Figure 7.2).

Stratigraphic Top
- Zn-Pb-Ag rich ores consisting of sphalerite, galena, chalcopyrite, pyrite and pyrrhotite (Strandgruvan and Zinkgruvan orebodies - not the Zinkgruvan BHT deposit)
- hosted by calc-silicate gneisses (tremolite-talc-chlorite skarns) and "quartz-gneisses/mica schists" (quartz-phlogopite-chlorite)
- Strandgruvan shows further zonation from chalcopyrite-galena-pyrrhotite at base to sphalerite-pyrite in hanging wall, very low magnetite content within ore body but very high magnetite content at the margins

Stratigraphic Centre
- Massive and disseminated Cu-Pb-Zn ore lenses comprised of pyrrhotite with subordinate chalcopyrite, sphalerite, galena and pyrite (Rodgruvan orebody) higher Ag and lower Au than footwall stockwork zone
- hosted by phlogopite, tremolite, talc, mica rich calc-silicate gneisses

Stratigraphic Base
- irregular footwall stockwork of Cu-Py-Po bearing qtz-fluorite veins (Stockenstrom and Printz ore bodies)
- hosted by quartz gneiss and mica schist

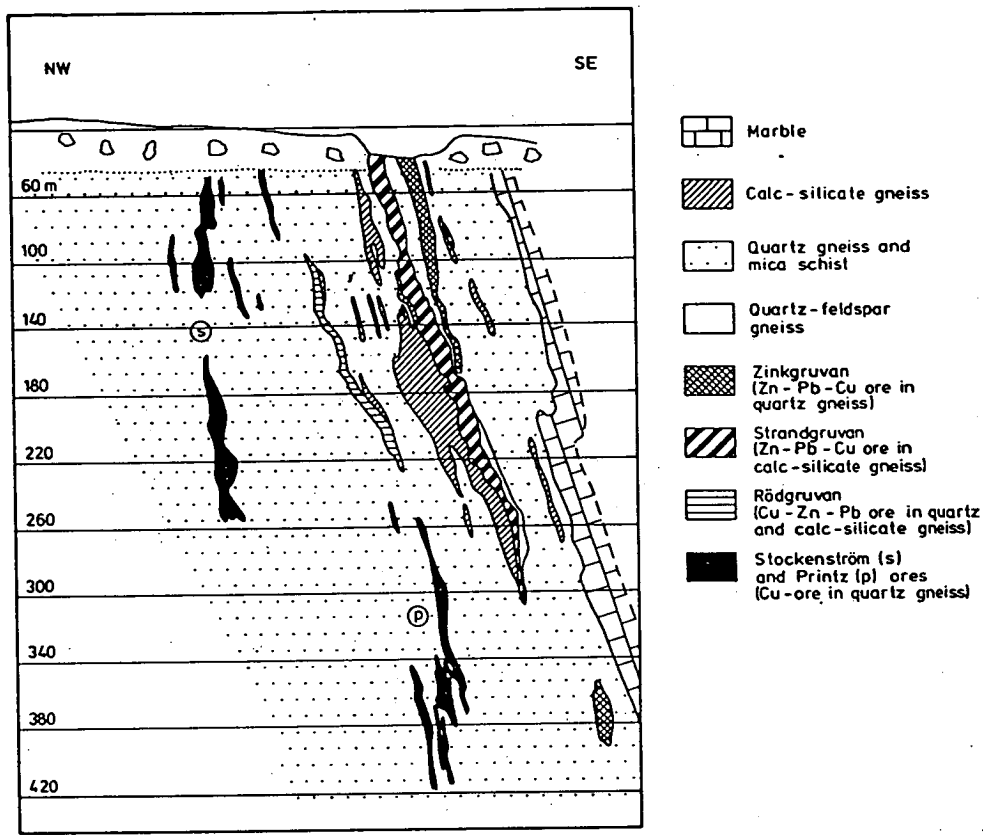

Figure 7.2 Cross section of the Garpenberg ore deposit. (Vivallo, 1985)

The ore lenses are enclosed in a distinctive zone of "quartz gneisses" and "mica schists" which are dominated by quartz-phlogopite with subordinate cordierite, staurolite, andalusite, anthophyllite and minor gahnite. There is a gradation from unaltered host rocks toward increasing Mg- alteration toward the ore lenses.

7.3 Zinkgruvan Ore Deposit - BHT Mineralisation

The Zinkgruvan deposit is the second largest economic BHT deposit currently being mined in the world. Historical production and present reserves total approximately 40 Mt (Hedstrom *et al.*, 1989). The deposit is currently exploited from two separate underground mines, Nygruvan and Knalla (Figure 7.3). Ore in the Knalla mine has an average grade of 6% Zn, 5.5% Pb, 100 g/t Ag while at Nygruvan the average grade is 10% Zn, 1% Pb, 45 g/t Ag.

The Zinkgruvan deposit is situated within an east-west striking syncline of early Proterozoic rocks of 1.9 - 1.88 Ba age. The Lower, Transitional and Upper Sequences are all present within near the mine (Figure 7.4).

The deposit is located within the metavolcano-metasedimentary Transitional Sequence, close to the contact with the overlying Upper metasedimentary rock sequence. It consists of tabular-shaped ore bodies within a 5 to 25m thick stratiform zone. The deposit has a strike length of approximately 5000m and extends down dip more than 1300m. A steeply dipping north-north-east trending fault (Figure 7.3) separates the deposit into the Knalla mine and the Nygruvan mine. The Zinkgruvan deposit is notably less folded and deformed than other BHT deposits.

The following description of the Zinkgruvan deposit is largely derived from Hedstrom *et al* (1989) and Walters (1992). Detailed cross sections and plan views of the geology in the vicinity of the Nygruvan and Knalla mines are presented in Figures 7.5 to 7.8. A detailed stratigraphic section is presented in Figure 7.9.

A schematic reconstruction of the Zinkgruvan ore deposit is presented in Figure 7.10 .

Footwall Sequence of the Zinkgruvan Deposit

North of the Zinkgruvan deposit pink quartz-microcline rock occurs over an area of 7km^2 in the stratigraphic footwall (Figures 7.3 and 7.4). The rock is comprised of pink fine grained massive qtz microcline rock with less than 5% biotite. The rock is interpreted to be a product of hydrothermal alteration. The intensity of the alteration increases toward the stockwork Cu mineralisation at Knalla mine. This association between BHT mineralisation and footwall potassic alteration has been noted elsewhere, e.g. Broken Hill, Australia (Walters, 1992).

The stratigraphic footwall sequence of the Nygruvan deposit varies from west to east. These variations are summarised in Figure 7.9. The main difference is that marbles and diopsidic calc-silicate rocks are more prevalent in the western footwall.

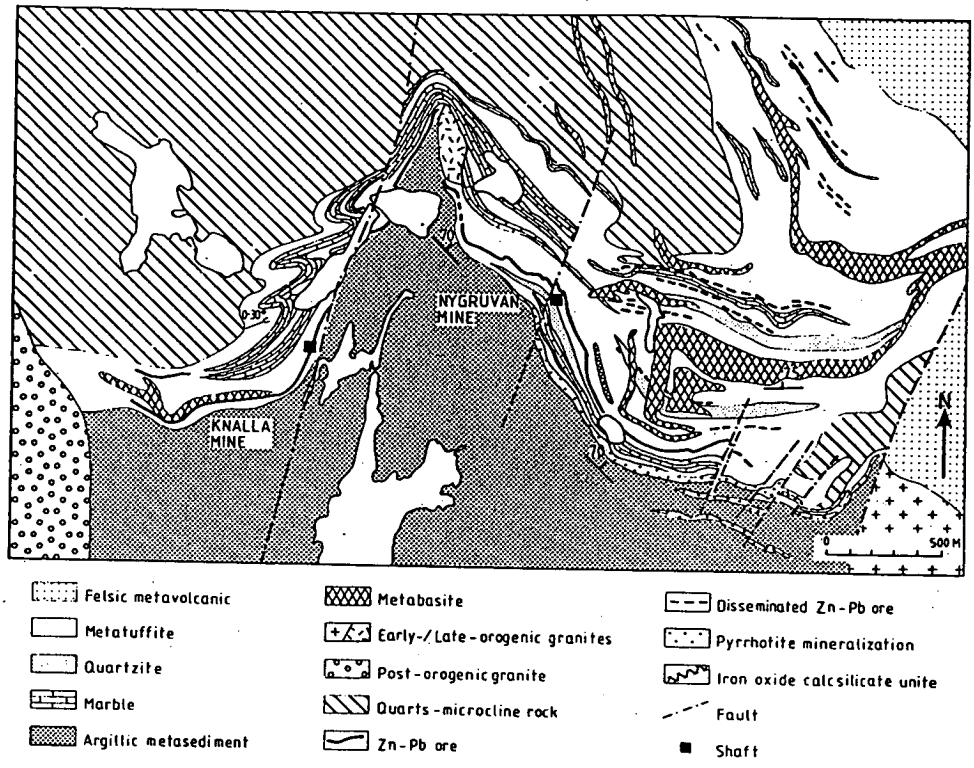

Figure 7.3 Geological map of the Zinkgruvan mine area. (Hedstrom, 1989)

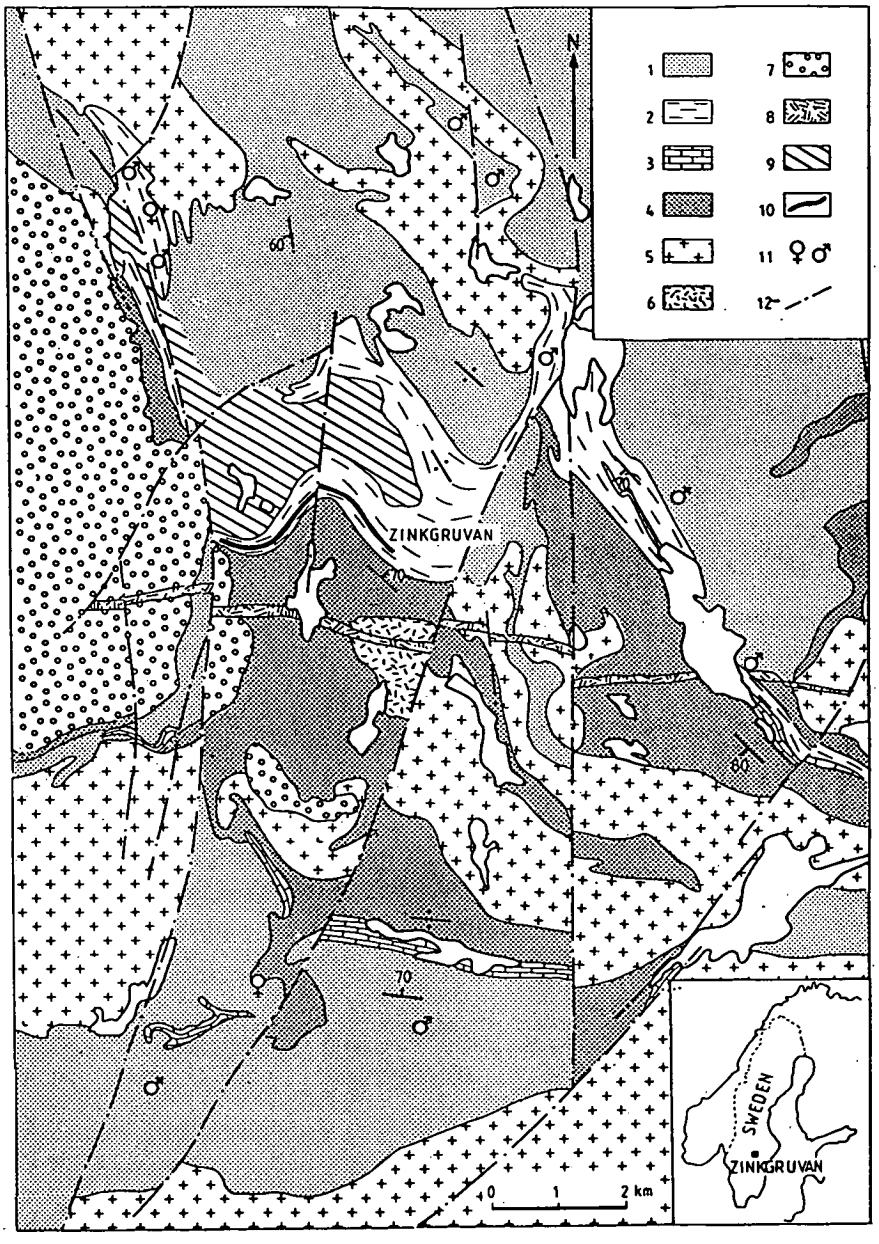

1 = felsic metavolcanic rock, 2 = metatuffite, 3 = marble, 4 = argillic metasediment, 5 = early orogenic granitoids, 6 = late orogenic granites and pegmatites, 7 = postorogenic granites, 8 = dolerite, 9 = quartz-microcline rock, 10 = Zinkgruvan ore deposit, 11 = sulfide iron oxide mineralization, 12 = fault.

Figure 7.4 Regional geological map, Zinkgruvan. (Hedstrom, 1989)

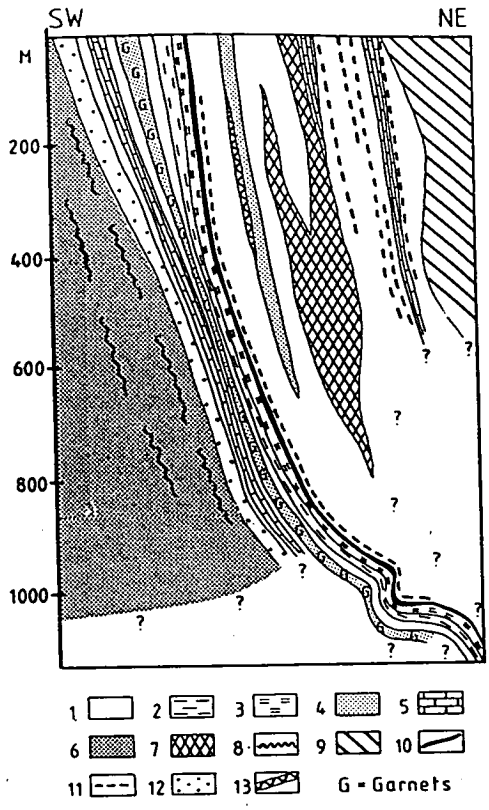

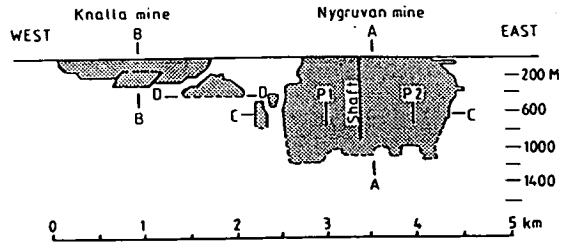

1 = metatuffite, 2 = metatuffite bedded, 3 = metatuffite calc-silicate bedded, 4 = quartzite, 5 = marble, 6 = argillic metasediment, 7 = metabasite, 8 = thin exhalite beds in the argillic metasediments, 9 = quartz-microcline rock, 10 = massive Zn-Pb ore, 11 = disseminated Zn-Pb ore, 12 = pyrrhotite mineralization, 13 = iron oxide calc-silicate unit.

Figure 7.5 Cross section through the Nygruvan Mine (section A-A) (Hedstrom, 1989)

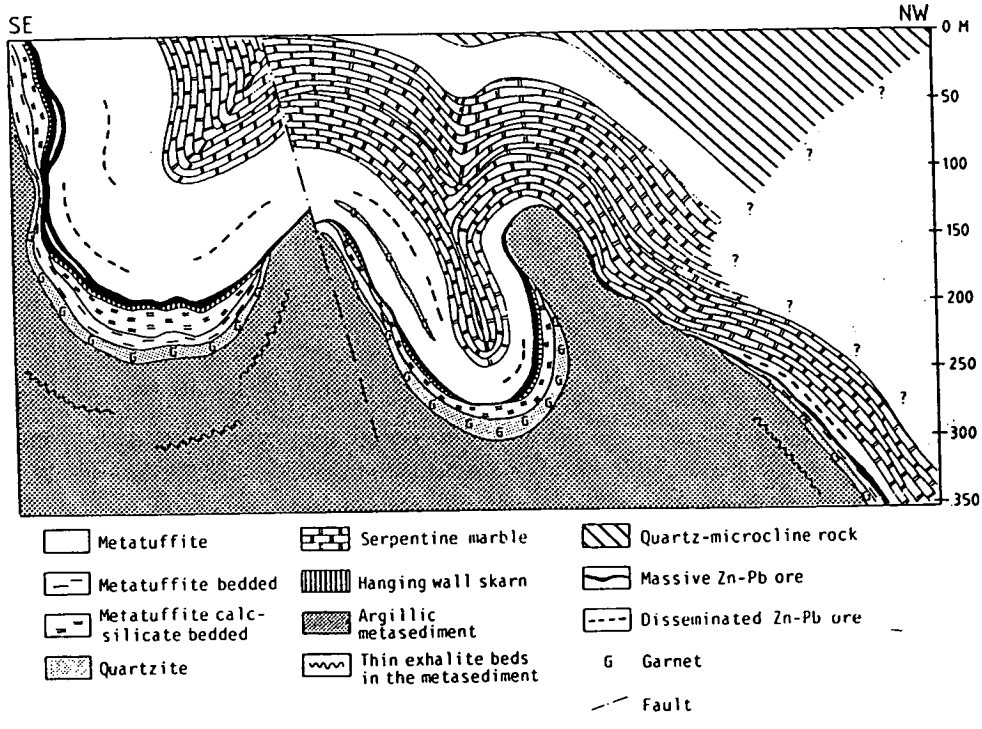

Figure 7.6 Cross section through the Knalla Mine (section B-B) (Hedstrom, 1989)

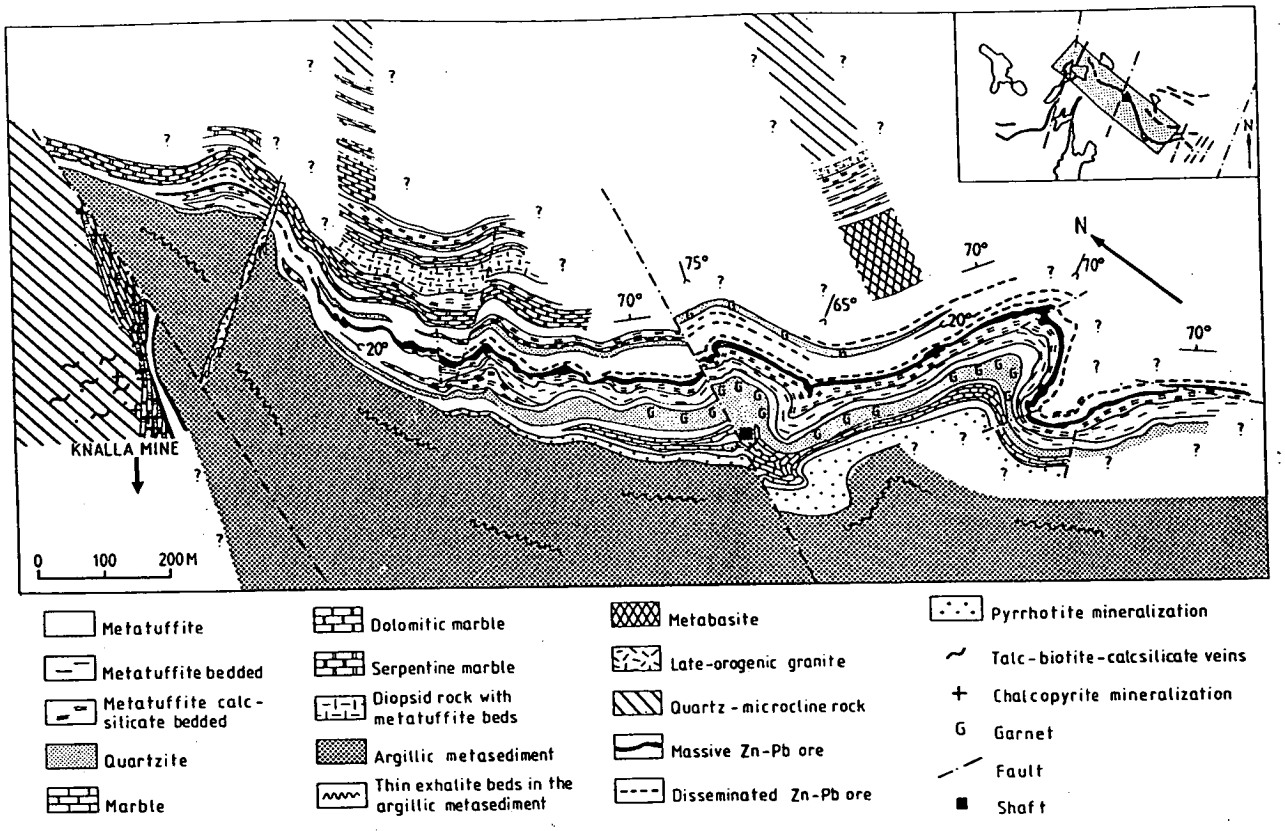

Figure 7.7 Geology plan of level 650, Nygruvan Mine. (Hedstrom, 1989)

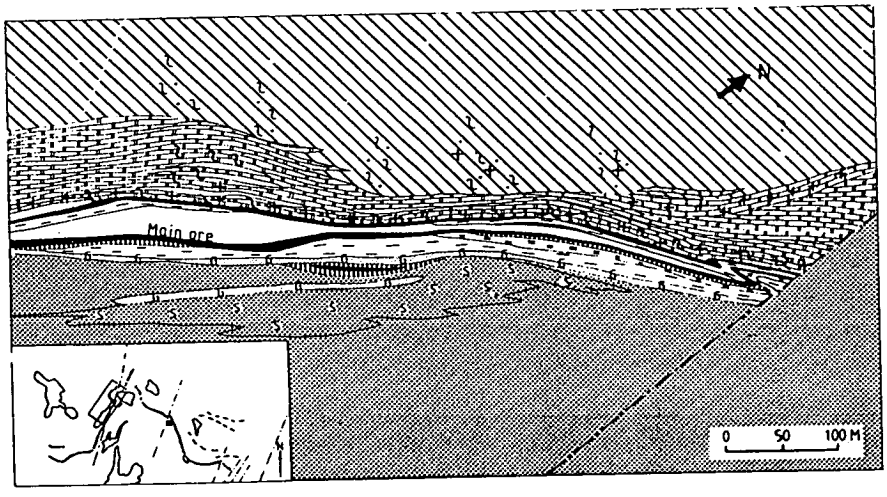

Figure 7.8 Geology plan of level 350, Knalla Mine. (Hedstrom, 1989)

A - west of the shaft fault

B - east of the shaft fault

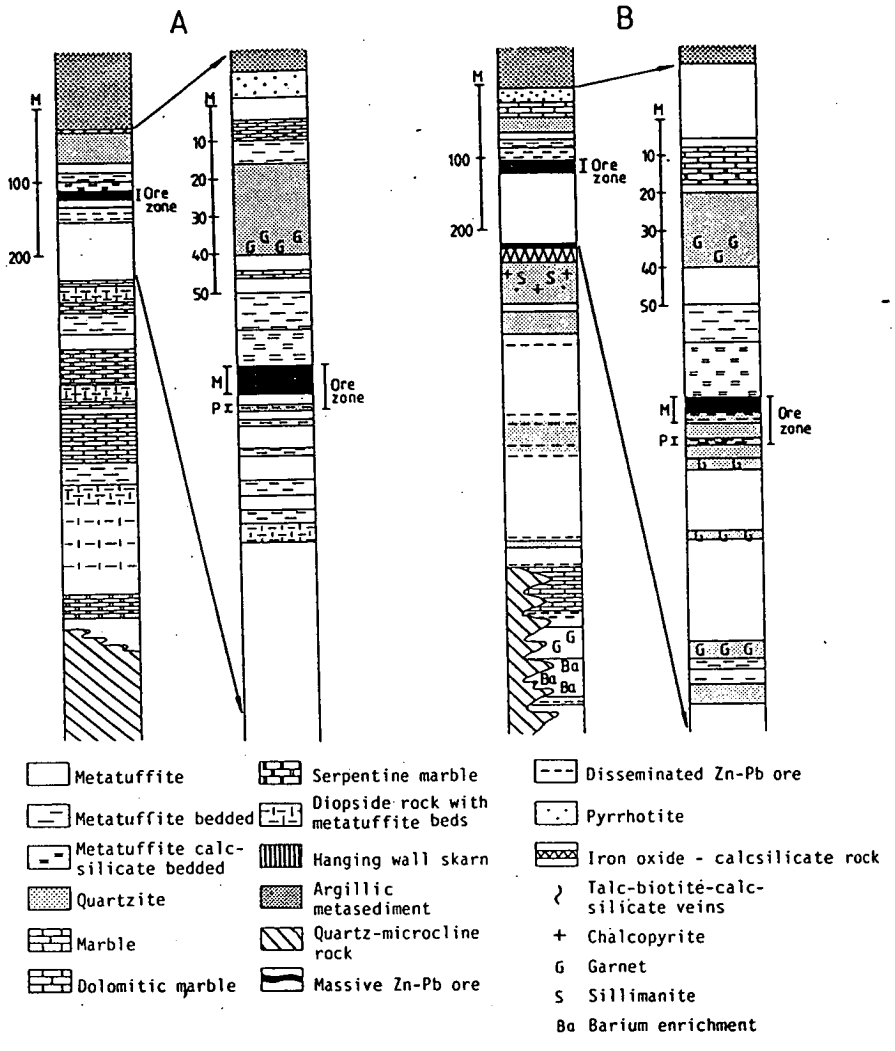

M - Main ore bed

P - Parallel ore bed

Figure 7.9 Stratigraphic section, Nygruvan Mine (Hedstrom, 1989)

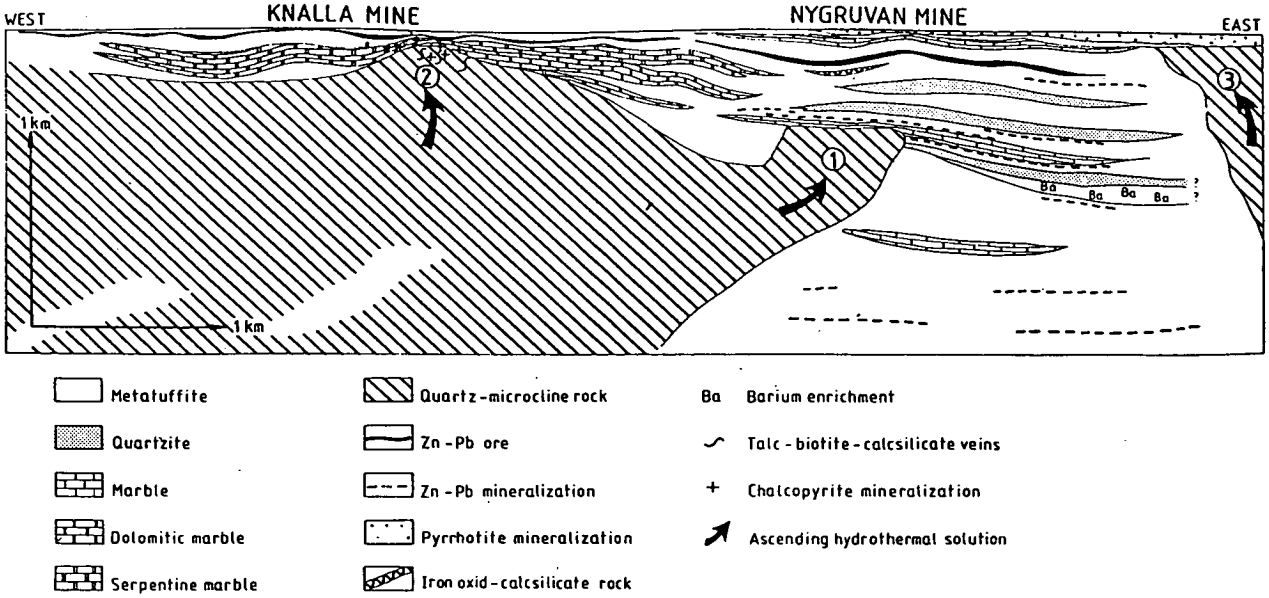

Figure 7.10 Schematic reconstruction of the Zinkgruvan deposit. (Hedstrom, 1989)

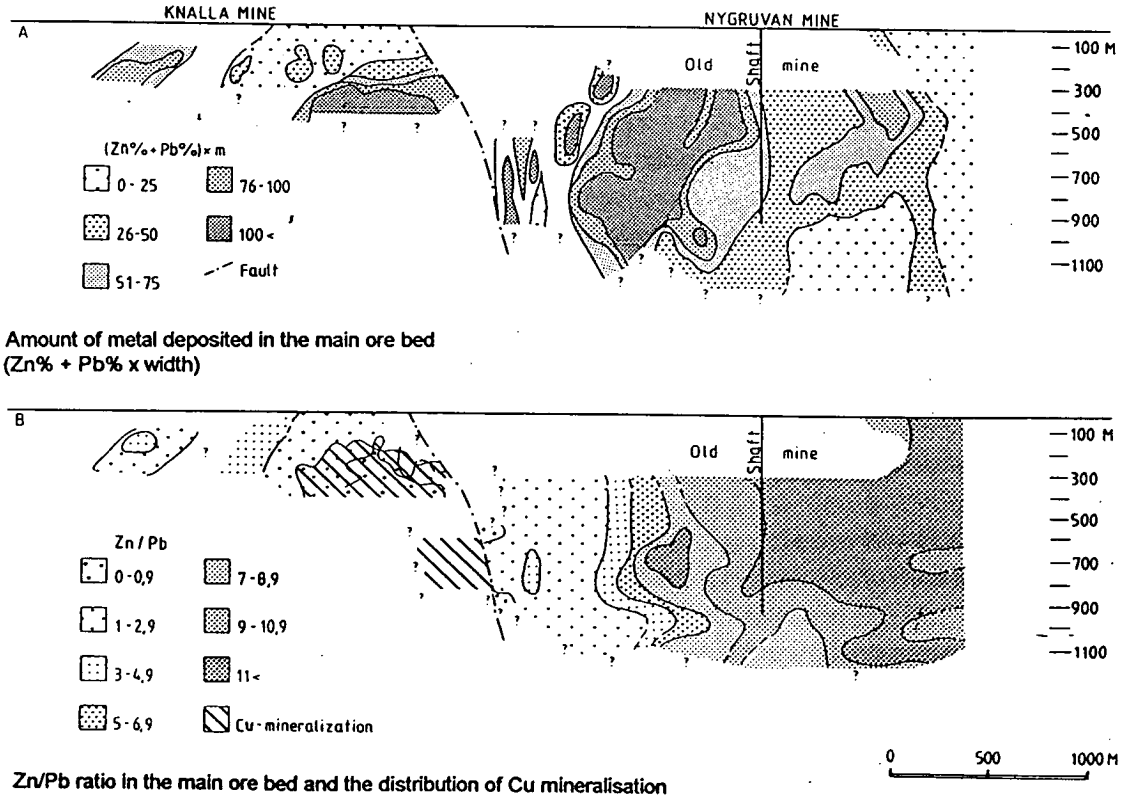

A. Amount of metal deposited in the main ore bed (Zn% + Pb% x width)

B. Zn/Pb ratio in the main ore bed and the distribution of Cu mineralisation

Figure 7.11 Metal zonation within the Zinkgruvan ore deposit. (Hedstrom, 1989)

In the western footwall of the Nygruvan mine serpentine marble (Figure 7.9) contains magnetite and serpentine as pseudomorphs after olivine.

In the central footwall of the Nygruvan mine there is a 10 to 30m thick manganese rich iron oxide-calc-silicate unit which occurs 50 to 100m stratigraphically below the ore zone. The unit has a limited lateral extent of 200 to 500m. Within the calc-silicate rock massive beds of Mn-rich magnetite occur, commonly with disseminated pyrrhotite and sphalerite. At the stratigraphic top of the unit the Mn-rich calc-silicate rock ends with a magnetite rich ore bed which is directly overlain by a 1 to 2m thick massive sphalerite ore bed with less than 0.05% Pb. This is the only occurrence of iron oxide-base metal mineralisation at Zinkgruvan.

In the eastern footwall of the Nygruvan mine, numerous weak stratiform base metal occurrences occur stratigraphically below the main deposit. 700m below the ore zone, a 30 to 40m thick bed of gneissic quartzitic metatuffite contains 0.5 to 4 wt% barite (Figure 7.9) as well as disseminated pyrrhotite and pyrite. Further up stratigraphy (600m below the deposit) marbles (Figure 7.9) are overlain and underlain by quartzitic metatuffite beds with stratified disseminated galena and sphalerite. Another 100 to 200m further up stratigraphy (400 - 500m below the ore zone) well bedded quartzitic units (Figure 7.9) 0.5 to 2m thick contain disseminated galena and sphalerite (0.5 - 5% Zn, 0.1 - 0.5% Pb). These beds alternate with barren massive metatuffite units of similar thickness.

The stratigraphic footwall of the Knalla mine is largely comprised of serpentine marble.

Hanging Wall Sequence

At the contact between the Transitional Sequence and the metasedimentary Upper Sequence in the eastern part of the Nygruvan mine there are numerous stratiform beds of disseminated pyrrhotite with elevated Zn (up to 0.5%), Pb, Cu and SiO_2 contents. These beds are confined within a 5 to 50m interval which increases in thickness to the east before being terminated by a fault (Fig. 7.7). It wedges out toward the west and has not been recognised at Knalla mine. Higher in the sequence 10cm to 50cm thick beds of quartz-garnet-biotite rock with minor pyrrhotite and calc-silicate minerals occur rarely.

Ore Zones

The ore zone consists of two lenses, the Main and Parallel ore lenses. The Parallel ore lens is absent in the Knalla mine.

The ore is dominantly comprised of sphalerite and galena, with minor but common chalcopyrite (less than 2% Cu) present as inclusions within sphalerite. Pyrrhotite and arsenopyrite are also present. The ore is hosted by quartzitic metatuffite with minor garnet, diopside, tremolite, calcite and lesser vesuvianite and clinozoisite. The laminations of the ore are defined by differing amounts of these minerals.

Nygruvan Mine

The Nygruvan mine is divided into eastern and western zones by the shaft fault (Figure 7.3). The thickness of the ore zone increases to the east from a few metres to 20-25m.

The Parallel ore zone is best developed in the east. Its thickness varies from 0.5 - 4m. It consists of quartzitic metatuffite with 1-10cm layers defined by varying amounts of sphalerite and galena. There is a systematic increase in Zn and Pb grade toward the stratigraphic hanging wall. Gangue minerals include quartz, sericite-feldspar, garnet, tremolite, biotite, calcite and vesuvianite.

The Main and Parallel ore zones are separated by a gneissic metatuffite 3-8m thick which becomes more quartzitic and garnetiferous toward the Main ore zone.

In the eastern part of the Nygruvan mine, the Main ore zone has an upper and lower lens separated by a calc-silicate and carbonate bedded quartzitic metatuffite with less than 6% combined Pb and Zn. The lower lens is comprised of garnet bearing quartzitic metatuffite with up to three layers of disseminated sphalerite and galena, each approximately 1m thick with grades of up to 15% Zn and 3% Pb. The lenses are compositionally laminated.

The lower unit of the main ore lens is missing from the western part of the Nygruvan mine. Instead a 1m thick quartzitic metatuffite bed with sphalerite-galena mineralisation occurs.

The upper unit of the Main ore lens is a 1.5 to 8m thick massive Zn-Pb sulfide unit overlain by a 0.5-1.5m thick hanging wall skarn. The massive Zn-Pb sulfide ore has grades of up to 45% Zn and 10% Pb. The upper unit and the hanging wall skarn can be traced along the entire Nygruvan mine (more than 1800m).

The hanging wall skarn defines the top of the ore zone. It is a calc-silicate bed with abundant disseminated pyrrhotite throughout. Sphalerite and galena content is low, but increases stratigraphically downward toward the Main lens.

Knalla Mine

The parallel ore bed is less obvious and the ore body is comprised only of the Main ore lens, underlain by stockwork Cu mineralisation in the eastern part of the Knalla mine. Also, stratigraphically below the main lens a 2-4m thick unit, containing 0.5-1m thick beds of sphalerite-galena bearing metatuffite, occurs locally.

The Main ore lens is generally 3m wide and is composed of two to four layers of massive sphalerite-galena ore with intercalated metatuffite. Galena is more abundant than sphalerite in the lower layers. The hanging wall skarn varies in width from 0-2.5m and contains a calcite layer with 2-5% Pb.

Stockwork Cu mineralisation occurs in the eastern part of the Knalla mine where the ore zone is in contact with serpentinite marbles and close to the pink quartz microcline

rock. The stockwork mineralisation consists of sulfide-bearing silicate veins and disseminated and veined chalcopyrite and pyrrhotite. The stockwork is hosted by the upper part of the serpentinite marbles. Locally below the Zn-Pb ore lenses sphalerite veins occur.

Metal Zonation at Zinkgruvan

The Zinkgruvan deposit has a distinct lateral metal zonation. The Zn/Pb ratio increases away from the Cu stockwork mineralisation, with decreasing metal content (Figure 7.11). No similar vertical zonation is evident but both the main and parallel ore beds show a systematic increase in grade toward their hanging wall.

8. MAGNETIC CHARACTERISTICS OF STRATIGRAPHY AND BHT MINERALISATION OF THE BERGSLAGEN DISTRICT, SWEDEN.

8.1 Regional Aeromagnetic Characteristics

Aeromagnetic data over the Bergslagen District were obtained from the Swedish Geological Survey. Data were acquired at a line spacing of 200m and a survey altitude of 30 to 40m and was provided as a 200m x 200m grid.

Images of the aeromagnetic data are presented as Figures 8.1 and 8.2, Plates 21 and 22. An interpretation of the aeromagnetic data is presented in Figure 8.3 and Plate 23. The interpretation is draped over the aeromagnetic data in Figure 8.4, Plate 24.

The interpretation was carried out at a scale of 1: 50 000, with reference to 1:50 000 scale geological maps from the Swedish Geological Survey (Wikstrom, 1989a,b).

The most striking feature of the Bergslagen region is the percentage of stratigraphy comprised of granitoids. These syn- to post-orogenic granitoids dominate the aeromagnetic image. This results in a magnetic character more commonly associated with Archaean granite greenstone sequences, where narrow greenstone belts with narrow linear magnetic anomalies are interspersed between extensive granitoid batholiths with a characteristic fractured magnetic texture. Greenstone belts make up a small percentage of the outcrop geology, which is dominated by the granite batholiths.

In the Bergslagen District the majority of very strongly magnetic units with significant strike extent occur within the volcanic Lower Sequence. These units are closely associated with iron ore deposits. The Transitional Sequence contains moderate to strongly magnetic units but these are of much shorter strike length and considerably less common. The metasedimentary Upper Sequence contains even fewer magnetic units and these probably occur within undifferentiated Transitional Sequence, or are actually situated within the underlying volcanic sequence.

Lower Sequence

The Lower Sequence consists of subaerial felsic ignimbrites and air fall deposits. It has been subdivided on the basis of magnetic character into a variably magnetic, stripy sequence and a less extensive, relatively non-magnetic sequence.

The variably magnetic sequence has a background magnetic intensity of the order of 500 nT. Within this irregularly magnetic sequence a number of moderate to strongly magnetic linear units of significant strike length occur. Magnetic intensity varies from 300 nT to 7000 nT, commonly 500 to 1000 nT. Very strongly magnetic units are intimately associated with iron oxide deposits, while less magnetic units are associated with amphibolites and magnetite exhalites. The Lower Sequence is easily mapped using the aeromagnetic data.

Figure 8.1 Regional Aeromagnetic Data, Bergslagen, Sweden.
Reduction To Pole

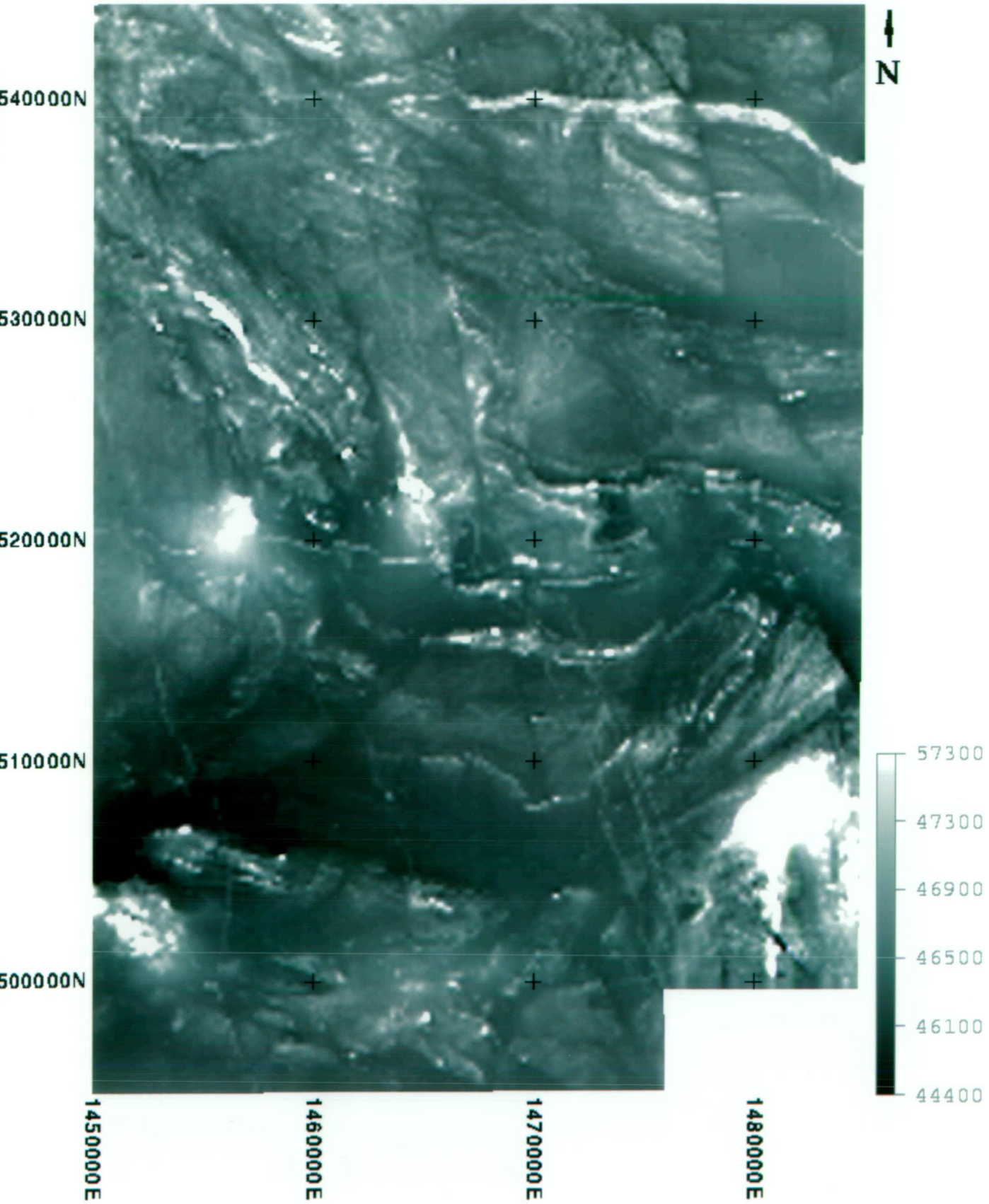

Figure 8.2 Regional Aeromagnetic Data, Bergslagen, Sweden.
Reduction To Pole – 1st Vertical Derivative

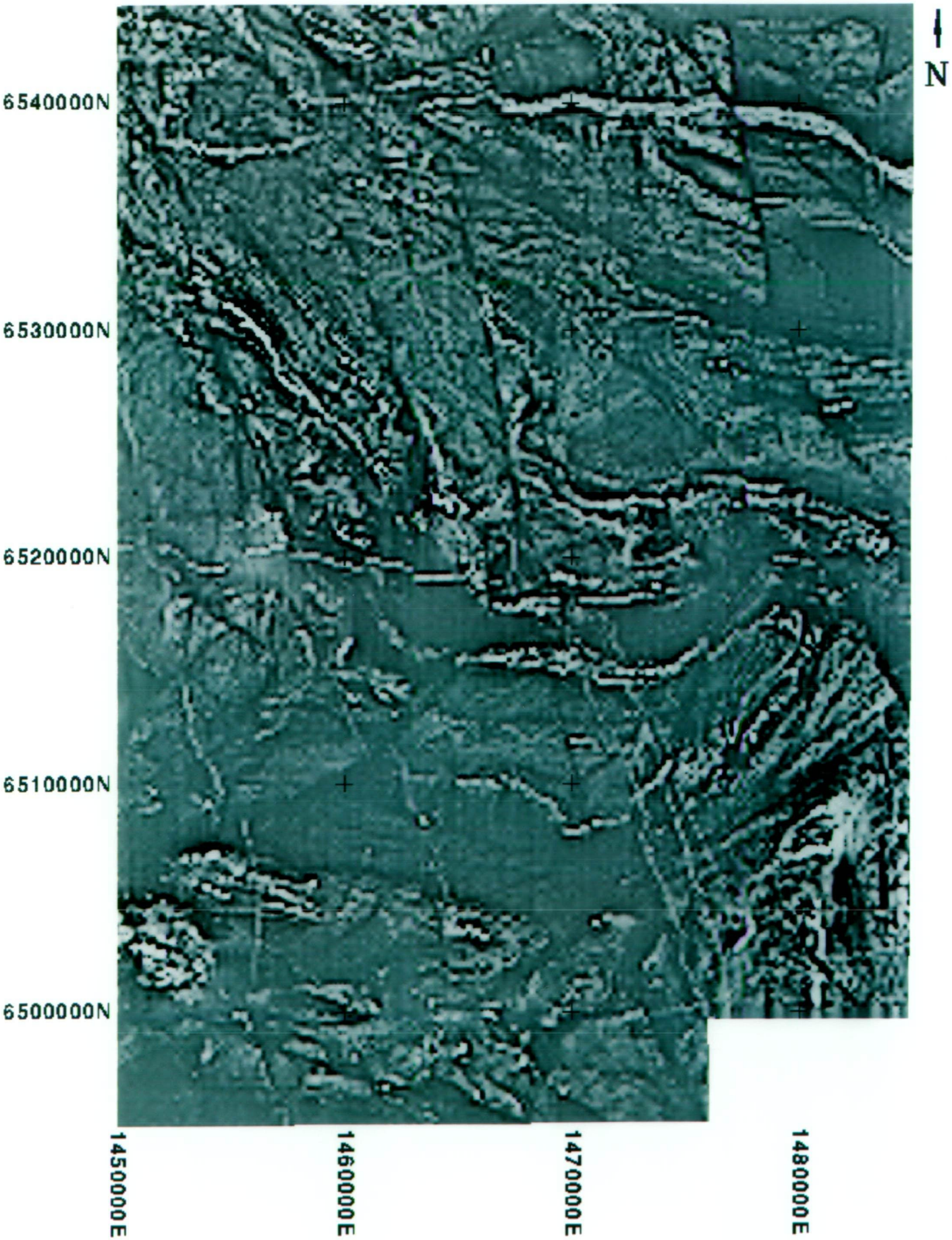

Figure 8.3

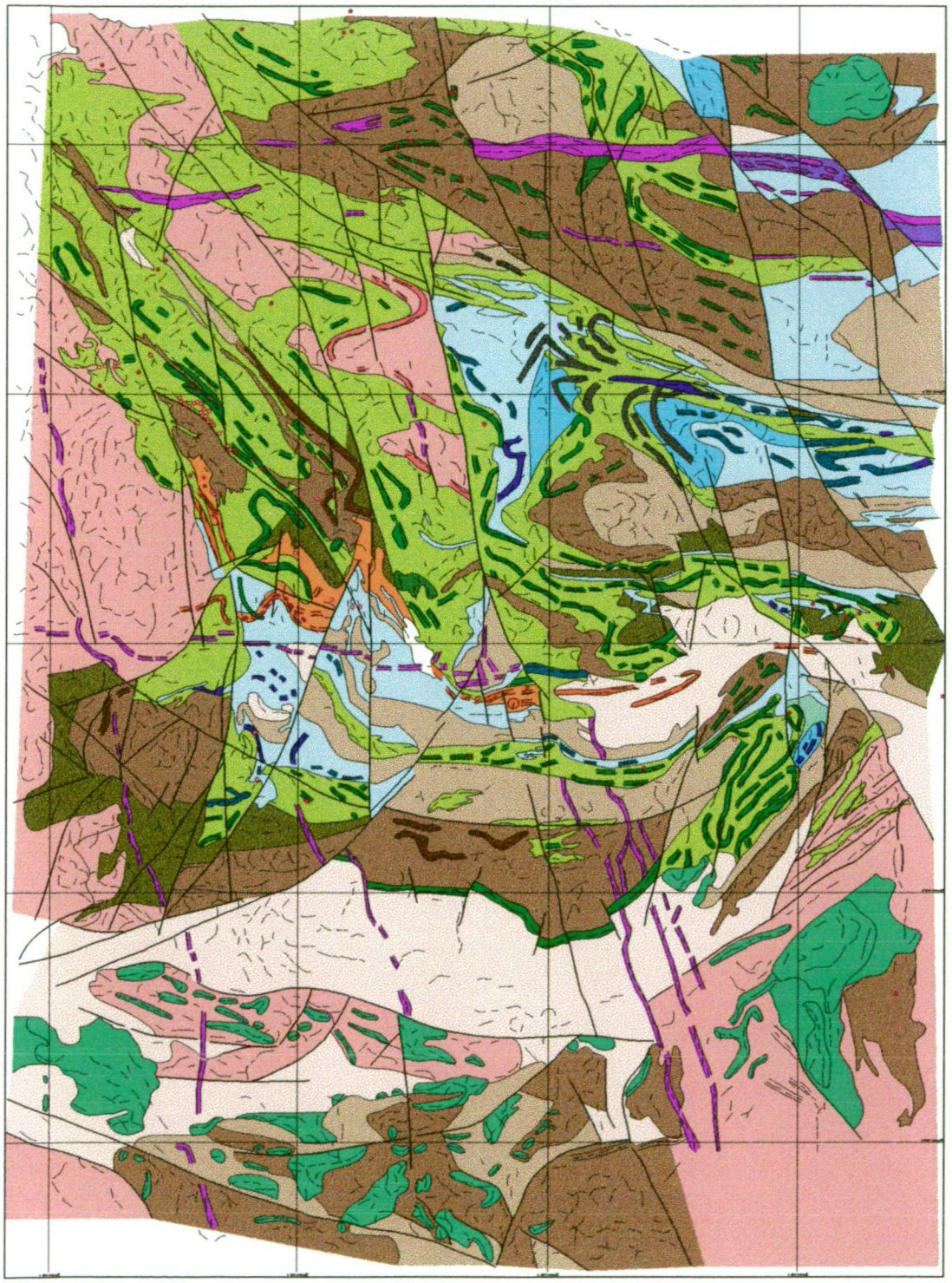

ZINKGRUVAN, SWEDEN
AEROMAGNETIC INTERPRETATION

0 5km

Interpretation by T.Kerr

EARLY OROGENIC GRANITES
- Flat uniform relatively non magnetic
- Magnetic unit intercalated, (possible mafic intrusive)
- Variably moderately magnetic (in part due to mafic intrusives?)
- Magnetic unit intercalated, (possible mafic intrusive)
- Magnetic unit

YOUNGER GRANITES
- Flat uniform relatively non magnetic
- Variably moderately magnetic (in part due to mafic intrusives)
- Magnetic unit

SEDIMENTS
- Variably moderately magnetic (thin cover over volcanics?)
- Flat uniform relatively non magnetic
- Magnetic unit - (within meta sediments, possible mafic intrusive-mafic volcanic unit)
- Discordant magnetic unit - underlying volcanic or mafic intrusives
- Highly magnetic unit (?calc silicate)

VOLCANICS
- Flat uniform relatively non magnetic
- Magnetic unit -Iron formation, magnetic volcanics, mafic intrusives
- Variably magnetic "stripy"
- Magnetic unit -Iron formation, magnetic volcanics, mafic intrusives
- Discordant magnetic unit, magnetic volcanics or mafic intrusives

MAFIC INTRUSIVES
- Magnetic
- Relatively non magnetic

DIORITE DYKES
- Magnetic
- Less magnetic

MIXED
- Flat uniform relatively non magnetic
- Magnetic unit (in places trangressive, possibly not well mapped or intrusive)

- Zinkgruvan Deposit
- Oxide deposit
- Sulfide deposit

Figure 8.4 Regional Aeromagnetic Interpretation (Colour)
Draped On Vertical Derivative (Intensity)
Bergslagen, Sweden.

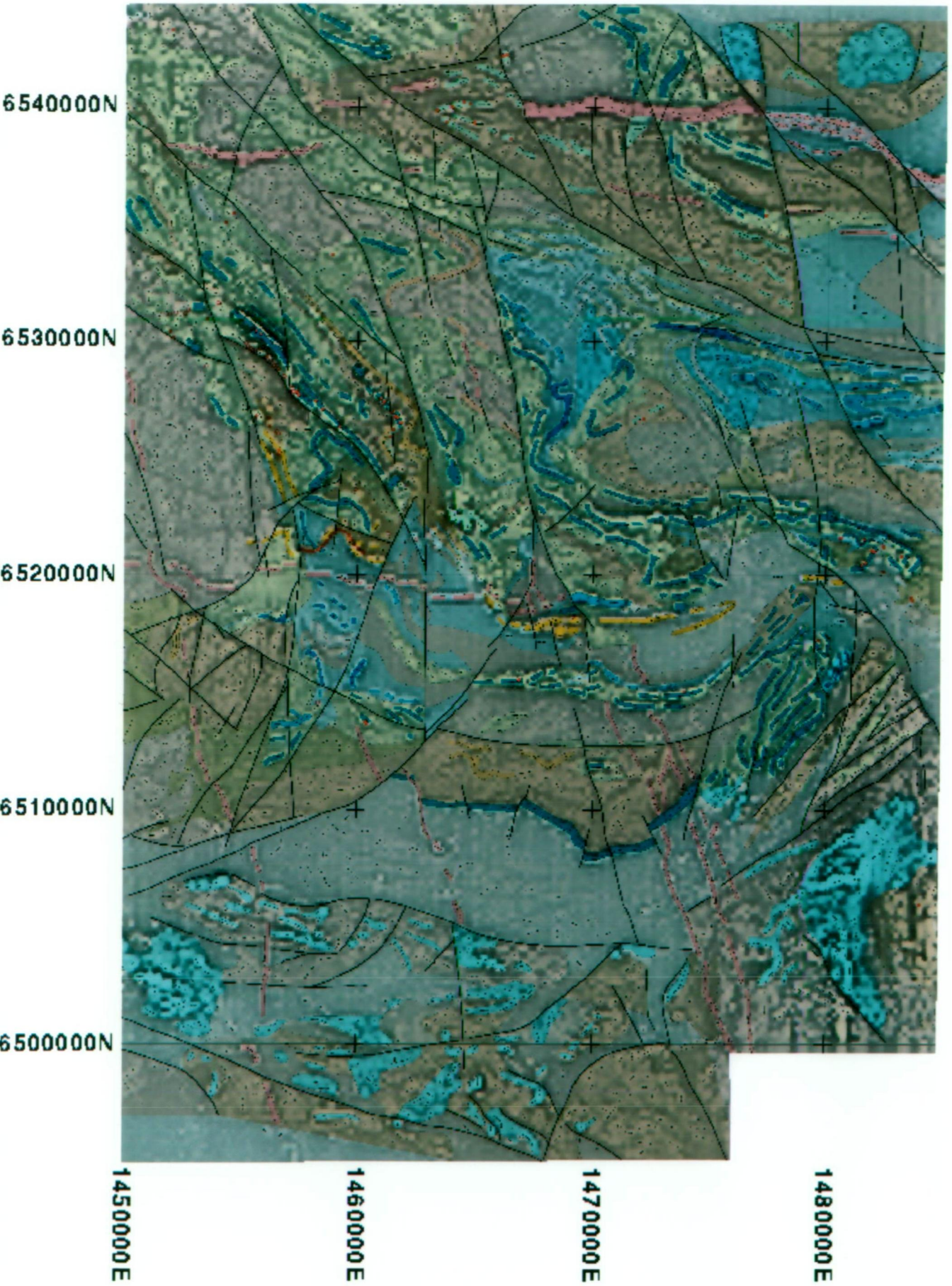

Transitional Sequence

The Transitional Sequence has only been mapped as a separate sequence near the Zinkgruvan deposit. Elsewhere it has not been subdivided from the volcanic and sedimentary rock dominated sequences in the published geology maps. In these areas it is assumed that the Transitional Sequence occurs near the boundary of the volcanic and sedimentary rock dominated sequences.

The Transitional Sequence is characterised by linear magnetic units within a relatively non-magnetic background. Compared to many of the other BHT provinces the Transitional Sequence is relatively narrow in outcrop and is considerably less extensive. Calc-silicate rocks and magnetite exhalites are a feature of the Transitional Sequence and form prominent magnetic horizons.

Upper Sequence

The Upper Sequence is comprised of greywackes, shales and mass flow deposits. It is relatively non-magnetic but contains linear magnetic units. In some areas it appears to display a weak irregularly magnetic character. In these areas the metasedimentary sequence is interpreted to be thin and relatively flat lying. The magnetic character is probably derived from the underlying metavolcanic sequence.

Many discordant magnetic units have been identified which cross-cut the boundary of the metasedimentary and metavolcanic sequences. These discordant magnetic units may be situated within the volcanic sequence, and appear to cross cut boundaries where the overlying sedimentary sequence is flat lying and thin and behaves transparently. Alternatively, the geological mapping within these areas may require revision.

Within the sedimentary sequence magnetic units which occur near the contact within the volcanic sequence may actually represent calc-silicates and magnetite exhalites of the Transitional Sequence, which has not been differentiated in the published mapping. Some of these units reach amplitudes of 2000 nT.

Intrusions

The early orogenic granites have been subdivided into relatively non-magnetic and weak to moderately magnetic (approximately 300 nT) classes. Within the weak to moderately magnetic granitoids linear magnetic units have been identified. These units have been interpreted to be previously unmapped magnetic units of the volcanic Lower Sequence. Some of these units attain amplitudes of more than 1000 nT and are associated with iron ore deposits.

The younger post orogenic granitoid rocks are subdivided into a relatively non-magnetic class and a weak to moderately magnetic class. The relatively non-magnetic class is associated with a deep magnetic low zone normally associated with very thick sedimentary sequences. The weak to moderately magnetic sequence has a background amplitude of 200 to 300 nT.

The granitoid rocks are intruded by moderate to strongly magnetic mafic intrusions which attain amplitudes up to 4500 nT.

The stratigraphy is also intruded by dolerite dykes. An east-west striking dolerite suite in the northern part of the image has magnetic responses in the range of 1000 to 1500 nT. North-north-west striking dolerite dykes have much lower amplitudes ranging from 100 to 300 nT.

Mineralisation

Mineralisation within the Lower Sequence is dominated by iron oxide deposits, generally intimately associated with strongly magnetic stratigraphy. Sulfide ore deposits occur within the Lower and Transitional Sequences, where they are closely associated, but not necessarily coincident, with more moderately magnetic units (less than 1000 nT).

8.2 Magnetic Characteristics of the Zinkgruvan Deposit

The Zinkgruvan deposit is not described in the literature as containing any magnetic minerals. However magnetite and pyrrhotite are described in the footwall and hanging wall respectively (see Section 7.3).

In the aeromagnetic image the Zinkgruvan deposit itself is not magnetic, but it is closely associated with a prominent magnetic horizon within the regional image. This magnetic horizon has a similar strike length to the Zinkgruvan deposit.

Most of the magnetic horizon occurs in the hanging wall of the Nygruvan mine. This magnetic signature is interpreted to correspond to stratiform beds rich in pyrrhotite (Figure 7.7). Magnetic susceptibility measurements on hand specimens of this pyrrhotitic unit have confirmed that the pyrrhotite is of the magnetic monoclinic variety.

Magnetic units within the footwall of the Zinkgruvan deposit are interpreted to correspond to magnetite in calc-silicate rocks and serpentine marbles (Figures 7.3 and 7.9).

Although these magnetic units occur in the footwall and hanging wall, rather than within the ore deposit itself, the limited strike length and very regionally anomalous character of the associated magnetic anomaly suggests that they are related to the ore forming process.

9. GEOLOGY AND MINERALISATION OF THE AGGENYS - GAMSBERG DISTRICT, BUSHMANLAND, SOUTH AFRICA.

9.1 Regional Geology

The Aggenys-Gamsberg deposits occur within the Bushmanland Sub-Province of the Namaqualand Metamorphic Complex. The only deposit to be developed to date is the Broken Hill deposit at Aggenys. This deposit is comprised of 85 Mt grading 3.57% Pb, 1.77% Zn, 0.34% Cu, 48 g/t Ag and 48.9% magnetite. The South African deposits, while large in tonnage, are considerably lower in grade than deposits from the other BHT provinces. However they represent a significant sub-type of BHT mineralisation directly associated with magnetite .

Stratigraphy

The stratigraphy of the Bushmanland region is difficult to interpret due to limited outcrop, complex deformation and granulite-amphibolite facies metamorphism. The stratigraphy is summarised below (after Joubert, 1986; Rozendaal, 1986; Ryan *et al.*, 1986) :

Lower Sequence

- quartzofeldspathic sequence
- **Lower Grey Augen Gneiss** (microperthite augen in quartz-plagioclase-microcline-biotite groundmass) overlain by **Pink Gneiss/Haramoep Gneiss** (quartz- microcline-plagioclase granite gneiss with thin lenses of amphibolite, quartzite and schist units interpreted to be metamorphosed felsic pyroclastic rocks)

Transitional Sequence

- metasedimentary/?metavolcanic sequence
- **Aluminous Schist/Namies Schist** (quartz-muscovite-K feldspar-biotite-sillimanite metasedimentary rocks with widespread metaexhalites)
- **White Quartzite Formation/Pella Quartzite** (glassy, recrystallized quartz with minor muscovite, sillimanite, biotite and magnetite, with thin interbands of sillimanite schist, metaconglomerate, quartzite and magnetite-quartzite)
- **Aggenys/Gams Ore Formations** - complex chemical metasedimentary rocks interbedded with sillimanite-rich schists, calc-silicates and quartzites.

Upper Sequence

- **Amphibolite and Leucocratic Grey Gneiss Formation/Nousees Mafic Gneiss** (metaconglomerates interbedded with a highly variable succession of leucocratic (quartz-feldspar-muscovite) and mafic (biotite-amphibole-magnetite) gneisses and amphibolites.

Structure and Metamorphism

The earliest phase of deformation is evident as tight intrafolial folds within gneissic layering. This phase is significant within the Broken Hill (South Africa) mine.

The main phase of deformation, the Namaqua event, is associated with the highest prograde metamorphic event. The Namaqua event resulted in large and small scale recumbent folds. Large scale thrusting toward the south is described by Joubert (1986), although evidence is not well documented. This event resulted in large scale tectonic duplication of stratigraphy and the recrystallization and remobilisation of the Aggenys-Gamsberg mineral deposits into hinge zones.

The third phase of deformation consists of open folds associated with dextral movement along north-west trending shear zones. *En echelon* folds were developed by this dextral strike slip regime, evident (from west to east) as the Aggenys, Gamsberg, Namies and Samoep synforms. An alternative view is that the F3 *en echelon* synforms are apparent and actually result from the interference of an F3 synform with F2 en echelon synforms (Joubert, 1986). The open synforms are separated by narrow antiforms with strong shearing in the hinge zones. They are separated from one another by east-north-east trending cusp-like steep zones or shears (Joubert, 1986). A three dimensional picture of the resulting structure of the Aggenys Gamsberg mineral deposits is presented in Figure 9.1.

The fourth phase of deformation is evident as shear zones and fractures in a north-north-west orientation, commonly marked by quartz veins and pegmatites. Large monoclinal folds are associated. This phase of deformation is thought to be associated with the final phase of uplift of the Bushmanland sequence.

The main phase of metamorphism was associated with the Namaqua event and reached amphibolite-granulite facies. Retrogressive metamorphism has resulted in alteration of garnets to chlorite, sillimanite to sericite and plagioclase to sericite and epidote.

The sequence and timing of metamorphic and structural events is summarised in Table 9.1.

Mineralisation

The Aggenys and Gamsberg deposits occur toward the top of the Transitional Sequence, in the Aggenys and Gams Ore Formations. Distally the ore horizon is evident as a distinctive quartzite-aluminous schist couplet which hosts base metal and barite occurrences, iron formations and blue quartzites (Walters 1992).

There is an apparent regional metal zonation between the Aggenys-Gamsberg deposits with decreasing copper and increasing zinc from west to east (Ryan et. al., 1986).

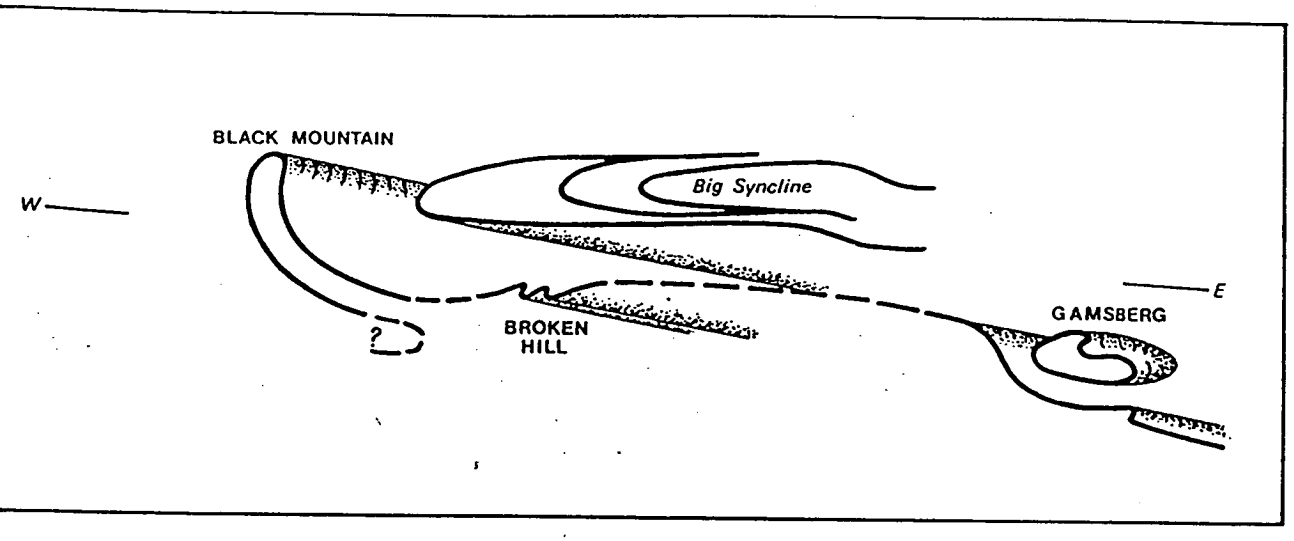

Figure 9.1 Structure of the Aggenys-Gamsberg deposits, based on the distribution of quartzite.
(Joubert, 1986)

1 000 Ma	Open folding	Emplacement of pegmatites Emplacement of noritoid bodies
1 070 ± 20 Ma	Steep structure formation	Emplacement of Rietberg Granite
1 166 ± 26 Ma	E–W open folding	Emplacement of Concordia Granite
1 213 ± 22 Ma	Recumbent folding and regional metamorphism	
1 850 Ma		Emplacement of Vioolsdrif Granite and perhaps Modderfontein Granite

Table 9.1 Sequence and timing of structural events in Namaqualand and Bushmanland.
(Joubert, 1986)

9.2 Broken Hill Ore Deposit, Aggenys.

The Broken Hill ore deposit (Figure 9.2) is the only deposit of the Aggenys-Gamsberg group to be mined to date. It is comprised of 85 Mt grading 4.57% Pb, 1.77% Zn, 0.34% Cu, 48 g/t Ag and 48.9% magnetite. The surface geology of the deposit is shown in Figure 9.3. The deposit outcrops as a 600m long east-west striking magnetite rich gossan. The limits of the ore body have not been completely defined but it has a down-plunge extent of at least 1200m.

The deposit consists of two ore bodies, the Upper and the Lower, which are partly separated by an unmineralised sillimanite-quartz schist. The stratigraphy is described in Table 9.2. The sequence has been recumbently folded and then refolded, resulting in the lower formations occurring in both the hanging wall and footwall (Figure 9.4).

Of particular note is the spatial relationship between the massive sulfide ore, magnetite quartzite and magnetite amphibolite. The magnetite quartzite directly overlies the sulfide ore and is in turn overlain by magnetite amphibolite. The magnetite quartzite is comprised of thin alternating bands of magnetite and quartz, with magnetite content ranging from 40 to 60%. Other minerals include garnet (up to 15%), and minor biotite. Galena, sphalerite and chalcopyrite occur throughout.

The magnetite amphibolite consists of thin alternating bands rich in quartz, spessartine garnet, magnetite, orthopyroxene, grunerite, cummingtonite and fayalite, with a slightly higher base metal content than the magnetite quartzite.

The bulk of the mineralisation in the Upper ore body is hosted by well banded pyrrhotite and pyrite rock (unit 3.9, Table 9.2). The combined pyrrhotite content ranges from 15 to 50%.

The irregular nature of the footwall garnet quartzite has lead Walters (1992) to speculate that it may be a footwall alteration zone.

The mineralogy of the Broken Hill deposit is summarised in Figure 9.5 and Table 9.3. Ryan *et al.* (1986) propose that the oxide , sulfide and silicate facies are all well defined at Broken Hill, with relative positions indicated in Figure 9.4. He proposes that these are facies changes representing changes from deep water conditions in the centre of the basin to shallow water conditions at the margins.

9.3 Black Mountain Ore Deposit, Aggenys.

The Black Mountain ore deposit (Fig. 9.2) is comprised of 81.6 Mt grading 0.75% Cu, 2.67% Pb, 0.59% Zn and 30 g/t Ag. The surface geology is presented in Figure 9.6. The deposit is open at depth.

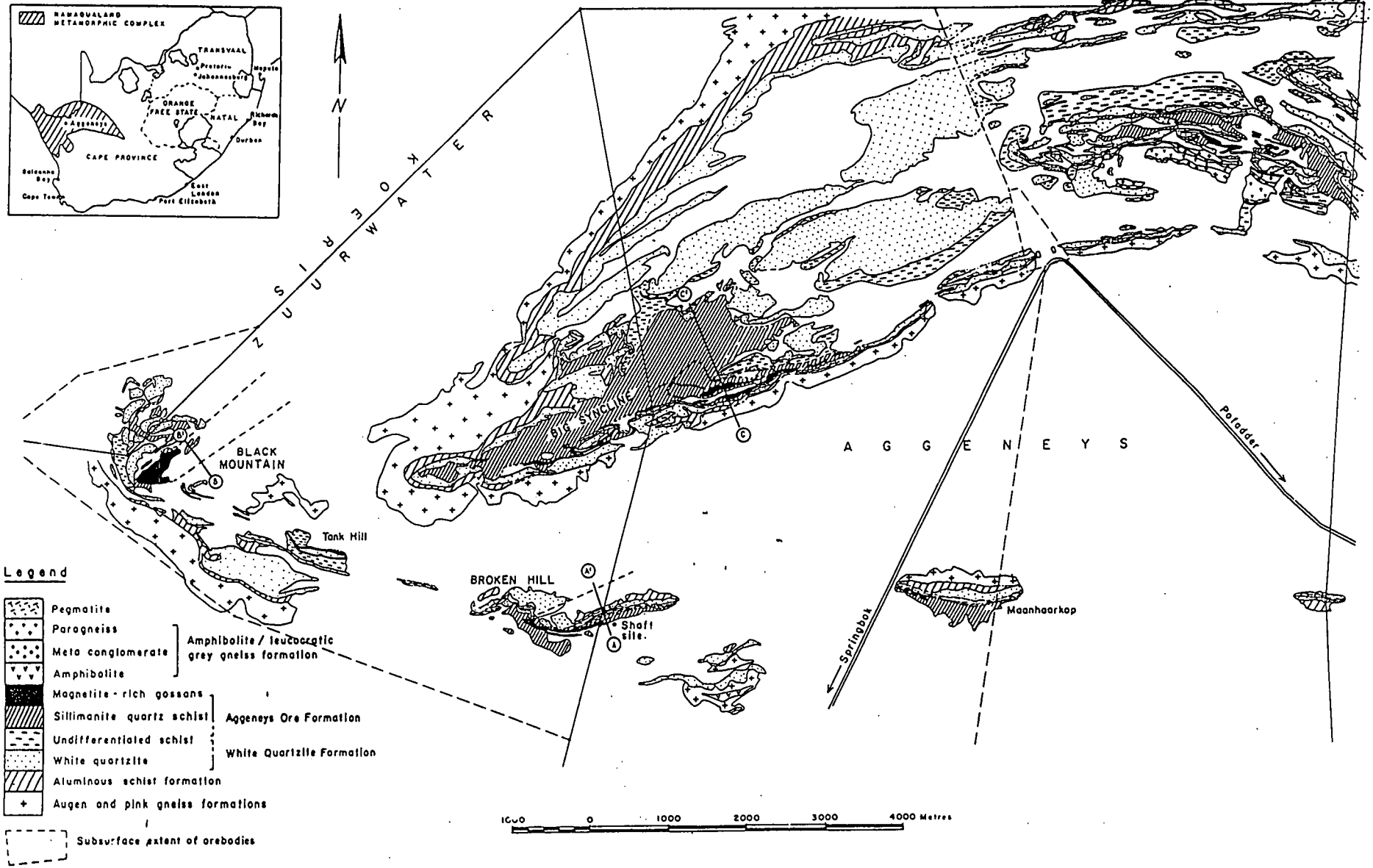

Figure 9.2 Geological plan of the Aggenys district.
(Ryan,et al, 1986)

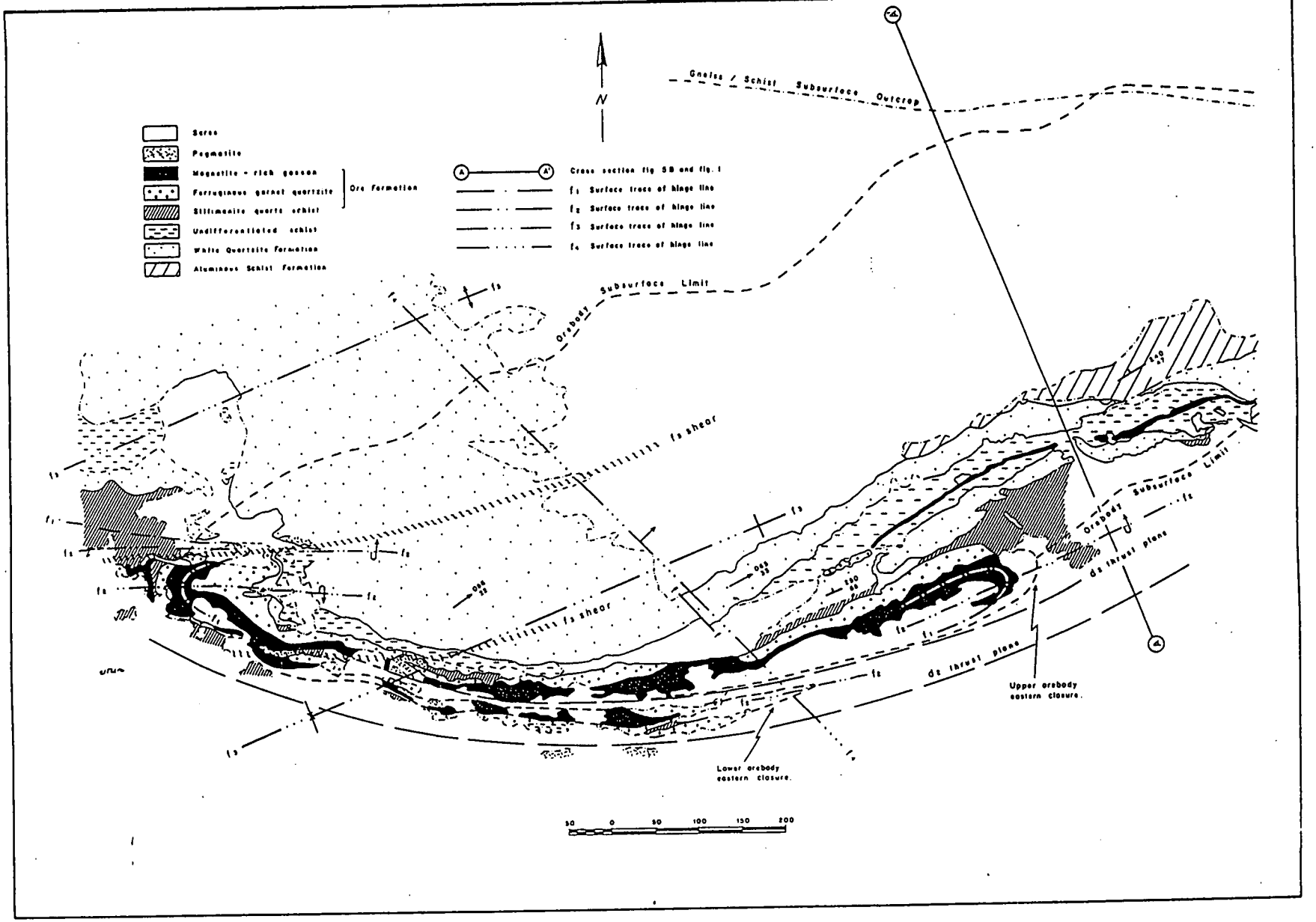

Figure 9.3 Geological plan of the Broken Hill (SA) deposit.
(Ryan,et al, 1986)

		THICKNESS		
1.	PINK GNEISS FORMATION			
2.	ALUMINOUS SCHIST FORMATION			
3.	WHITE QUARTZITE FORMATION			
4.1	Sillimanite–quartz schist	(5–15m)	Lower Ore Body	AGGENEYS ORE FORMATION
4.2	Ferruginous garnet quartzite	(5–25m)		
4.3	Magnetite quartzite	(5–10m)		
4.4	Magnetite amphibolite	(10–30m)		
4.5	Magnetite quartzite	(3– 5m)		
4.6	Baritic massive sulphide	(2– 5m)		
4.7	Massive sulphide	(2– 5m)		
4.8	Sulphide quartzite	(1– 5m)		
4.9	Banded massive sulphide	(5–15m)		
4.10	Magnetite quartzite	(2– 7m)		
4.11	Magnetite amphibolite	(5–20m)		
4.12	Magnetite quartzite	(1– 5m)		
4.13	Ferruginous garnet quartzite	(1– 2m)		
5.1	Sillimanite–quartz schist	(0–10m)	Upper Ore Body	
5.2	Ferruginous garnet quartzite	(2–10m)		
5.3	Magnetite amphibolite	(5–10m)		
5.4	Massive sulphide	(2– 5m)		
5.5	Magnetite amphibolite	(5–10m)		
5.6	Ferruginous garnet quartzite	(1– 2m)		
6.0	Pyritic graphitic biotite schist	(5–20m)	Spring Schist Succ.?	
7.0	Pyritic sillimanite–quartz–biotite schist	(>100m)		

Table 9.2 Stratigraphy of the Broken Hill (SA) deposit. (Ryan et al, 1986)

Facies	Rock Types	Minerals	Mineralization
Silicate	Magnetite Amphibolite	Quartz Magnetite Grunerite Cummingtonite Spessartine garnet Fayalite	Moderate mineralization with galena > sphalerite > chalcopyrite
Oxide	Magnetite Quartzite	Magnetite, Quartz, Garnet, Biotite	Moderate mineralization with galena > sphalerite > chalcopyrite
	Ferruginous Garnet Quartzite	Quartz, Magnetite, Garnet, Biotite	Very weak mineralization with sphalerite > chalcopyrite > galena
Sulphide	Massive Sulphide	Pyrrhotite, Pyrite, Quartz	High grade mineralization with galena > sphalerite > chalcopyrite
	Sulphide Quartzite	Quartz, Pyrrhotite, Pyrite	Moderate to high grade mineralization with galena >sphalerite > chalcopyrite

Table 9.3 Rock types, gangue and ore mineralogy at Broken Hill, SA. (Ryan et al, 1986)

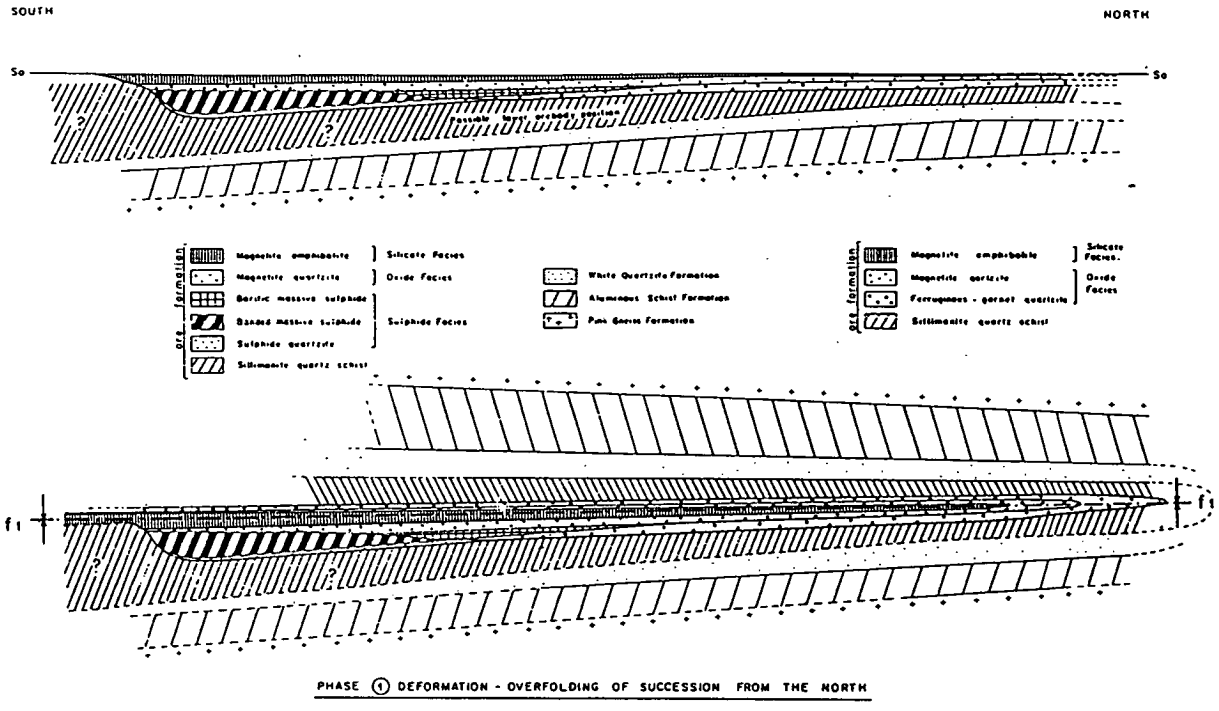

PHASE ① DEFORMATION - OVERFOLDING OF SUCCESSION FROM THE NORTH

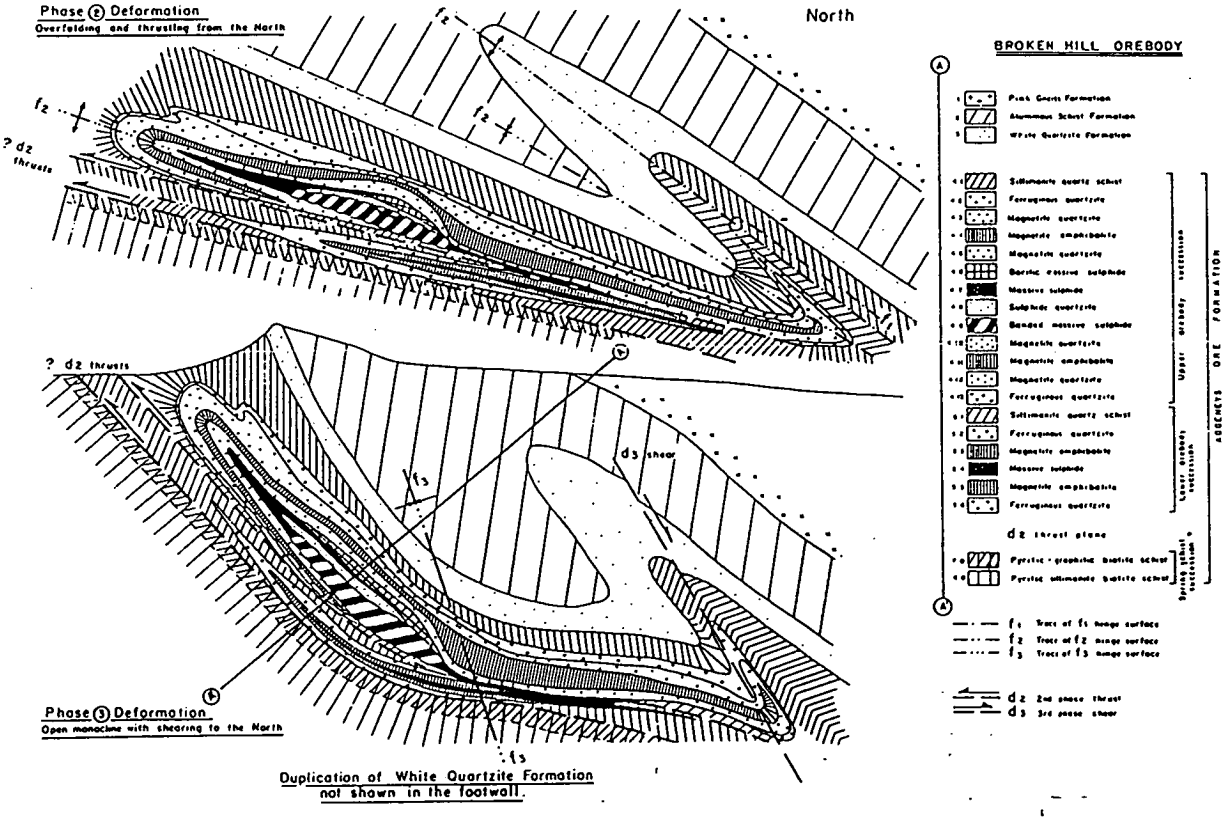

Figure 9.4 Deposition and folding of the Broken Hill (SA) deposit. (Ryan,et al, 1986)

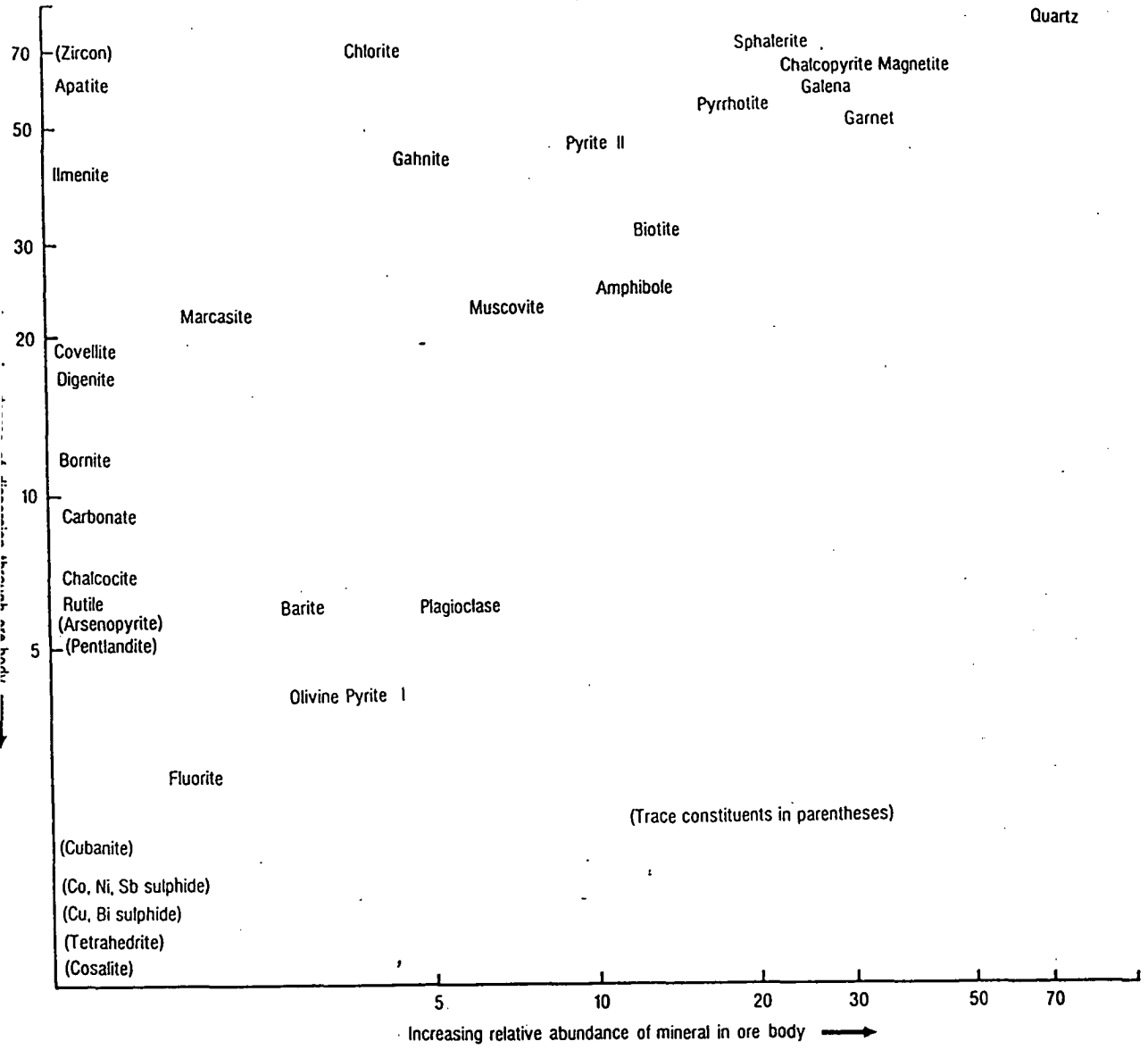

Figure 9.5 Mineralogy of the Broken Hill (SA) deposit. (Ryan,et al, 1986)

The stratigraphy of the deposit is summarised in Table 9.4. It is hosted in a recumbent fold and hence the stratigraphy in the upper limb is overturned (Figure 9.7). The deposit consists of two ore bodies, the Upper (economic) ore body and the Lower ore body. The stratigraphy is possibly overturned so the Upper ore body could be the stratigraphically lower lower of the two. It is hosted by magnetite quartzite and magnetite amphibolite which grades laterally and vertically into magnetite-barite rock (Ryan *et al.*, 1986).

The mixed zone forms the stratigraphic footwall to the Upper ore body. There is a progression from banded schist to garnet quartz schist and then to garnet quartzite toward the ore body. There is an increase in the K-feldspar, sillimanite and muscovite content of the schists toward the ore. The garnet quartzite thickens markedly in the vicinity of the ore, with no sympathetic thickening of the overlying magnetite quartzite. This footwall zone of K-feldspar, sillimanite and muscovite grading into garnet quartzite may be a footwall alteration zone (Walters, 1992).

The garnet quartzite consists of approximately 80% quartz with subordinate almandine garnet and biotite and accessory cordierite and sillimanite. Sulfide content increases toward the hinge zone. Pyrite is dominant, with subordinate chalcopyrite. Minor sphalerite, galena and pyrrhotite occur near the contact with the overlying magnetite quartzite.

The magnetite quartzite is dominantly comprised of quartz and magnetite with accessory almandine-spessartine garnet, biotite, chlorite and rare apatite. The dominant sulfide is pyrite, followed by pyrrhotite. Galena is the dominant base metal sulfide, followed by chalcopyrite, with accessory sphalerite.

The magnetite amphibolite is dominantly comprised of magnetite and grunerite, with lesser pyroxmangite, quartz, hedenbergite, spessartine garnet, fayalite and apatite. The dominant sulfide is pyrrhotite, followed by pyrite. Galena and sphalerite are the dominant base metal sulfides, with accessory chalcopyrite and minor arsenopyrite.

The magnetite-barite rock consists of 25 to 70% barite with up to 10% magnetite. Quartz is also a major constituent. Accessory minerals include orange garnet and mica.

The Upper ore body displays a vertical stratigraphic metal zoning, from chalcopyrite in the garnet quartzite to galena-chalcopyrite in the magnetite quartzite and galena-sphalerite in the magnetite amphibolite. This is accompanied by an upward increase in the pyrrhotite/pyrite ratio.

The stratigraphic position of the Lower ore body is problematical. It may be a separate unit stratigraphically above or below the Upper ore body or it may be the stratigraphic equivalent of the Upper ore body. If it is a stratigraphic equivalent then it is inferred by Ryan *et al.* (1986) to have formed in a separate sub-basin, as there is no continuity of sulfide between the two ore zones.

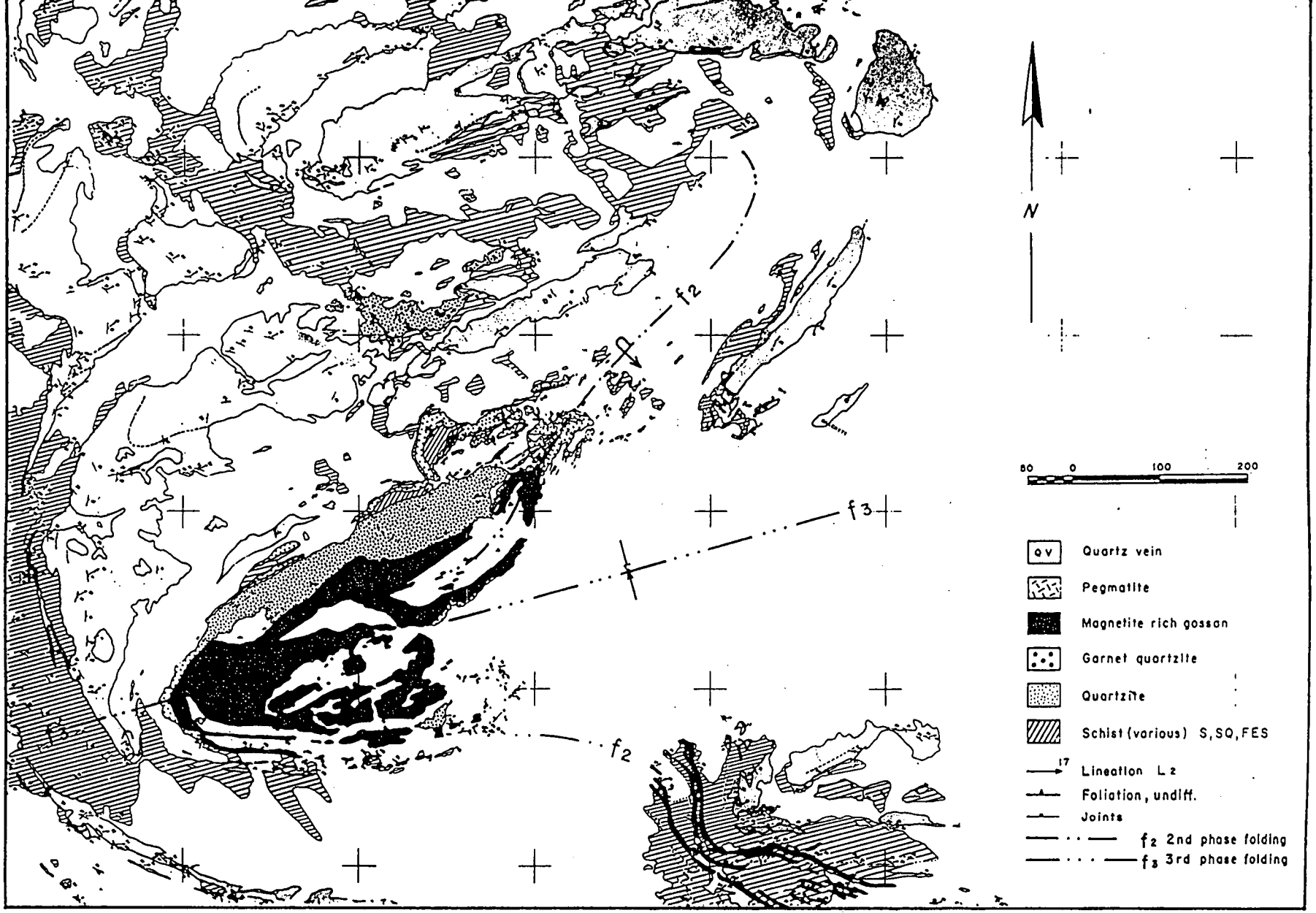

Figure 9.6 Geological plan of the Black Mountain deposit.
(Ryan,et al, 1986)

Stratigraphic Unit			Thickness (m)
7.	Lower ore body	AGGENEYS ORE FORMATION	(5–25)
6.	Baritic quartz schist		(10–25)
5.	Magnetite–barite rock		(0–45)
4.	Magnetite amphibolite		(0–20)
3.	Magnetite quartzite		
2.	Mixed zone consisting of gradations between garnet quartzite and various quartz schists	Economic ore body	(30–65)
1.	Banded quartz schist		(10–25)
	WHITE QUARTZITE FORMATION		
	ALUMINOUS SCHIST FORMATION		
	PINK GNEISS FORMATION		

Table 9.4 Stratigraphy of the Black Mountain deposit. (Ryan et al, 1986)

Stratigraphic Unit		Thickness (m)	
6. —	Spring Schist and Quartzite Member	5–300	AGGENEYS ORE FORMATION
5. —	Calc-silicate Member	0–50	
4.	Nodular Schist Member	0–10	
3. —	Pyribolite Member	0–20	
2. —	Magnetite Quartzite Member	0–60	
1. —	Fly Scist Member	0–200	
	WHITE QUARTZITE FORMATION		

Table 9.5 Stratigraphy of the Big Syncline deposit. (Ryan et al, 1986)

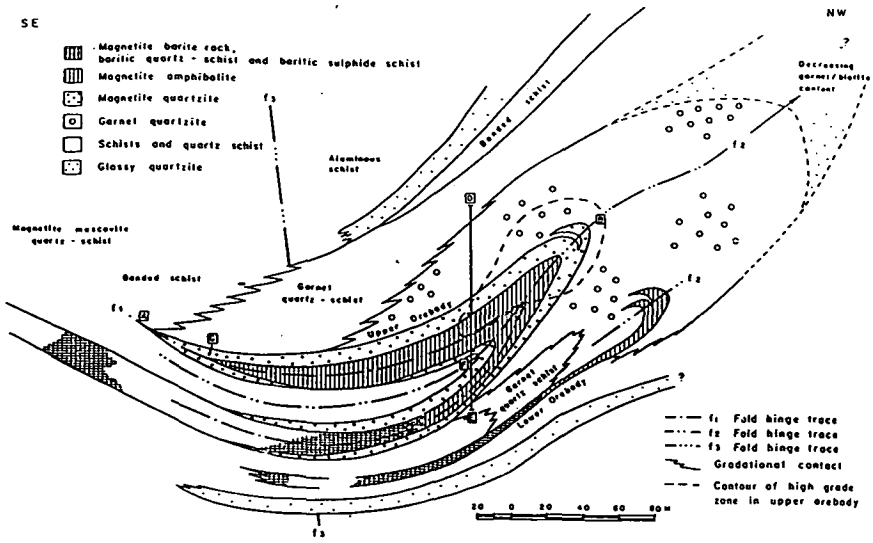

A. Generalised cross section of the Black Mountain ore body showing fold phases 1 to 3

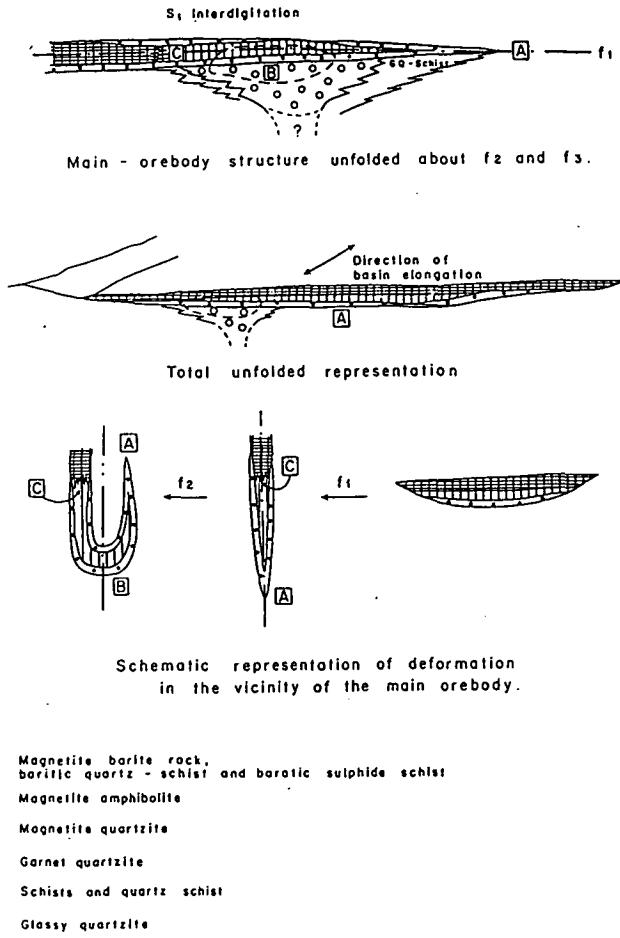

B. Schematic diagram illustrating the sequential unfolding of the Black Mountain upper ore body.

Figure 9.7 Folding of the Black Mountain deposit. (Ryan,et al, 1986)

The lower ore body is comprised of garnet quartzite, magnetite amphibolite and sulfide schist. The magnetite amphibolite differs from that associated with the Upper ore body in that grunerite is dominant over spessartine, and magnetite content is markedly lower. Ore mineralogy is different with sphalerite and galena dominating, whereas galena dominates in the Upper ore body. Down dip the magnetite amphibolite grades into baritic sulfidic schist, which commonly grades to massive sulfide with dominant pyrite and subordinate galena and sphalerite. Gahnite is a common gangue mineral, together with quartz, white mica and hematite.

9.4 Big Syncline Ore Deposit, Aggenys.

The Big Syncline deposit (Fig. 9.2) consists of 101 Mt grading 0.09% Cu, 1.01% Pb, 2.45% Zn and 12.9 g/t Ag. The deposit is hosted by the Spring Schist and Quartzite Member. The stratigraphy is summarised in Table 9.5 and a cross section is presented as Figure 9.8.

Of particular interest is the fact that the magnetite rich units in the southern portion of the deposit do not occur in the northern part of the deposit. It is inferred by Ryan *et al.* (1986) that this may reflect a facies change from shallow water oxide facies (Magnetite Quartzite member) to deeper basin sulfide facies (Spring Schist and Quartzite member).

The Magnetite Quartzite Member consists of interbanded quartz rich and magnetite rich layers which locally grade to garnet quartzite, at the expense of magnetite. Disseminated pyrite and chalcopyrite occur throughout.

The Pyribolite (pyroxene-amphibole) Member occurs as sporadic boudins of baritic pyribole with magnetite or pyrrhotite bearing rock in the extreme southern part of the Aggenys Ore Formation. Coarse clusters and disseminations of sphalerite and galena (almost economic) occur with pyrite, pyrrhotite, marcasite and chalcopyrite.

The Calc-silicate Member is comprised of layers dominated by spessartine garnet and epidote minerals and a layer dominated by andradite garnet and wollastonite in a calcite matrix. This Member contains sphalerite, galena, chalcopyrite, pyrite and pyrrhotite.

The Spring Schist hosts the stratiform Big Syncline deposit. Sphalerite, galena, coarse grained pyrite, pyrrhotite and marcasite are hosted by a coarse grained schistose silicate assemblage consisting of quartz, muscovite, K-feldspar, biotite, sillimanite and garnet.

The Spring Quartzite is comprised of altered calcic plagioclase, muscovite, biotite and skeletal garnet, with low concentrations of pyrite, pyrrhotite, sphalerite and galena.

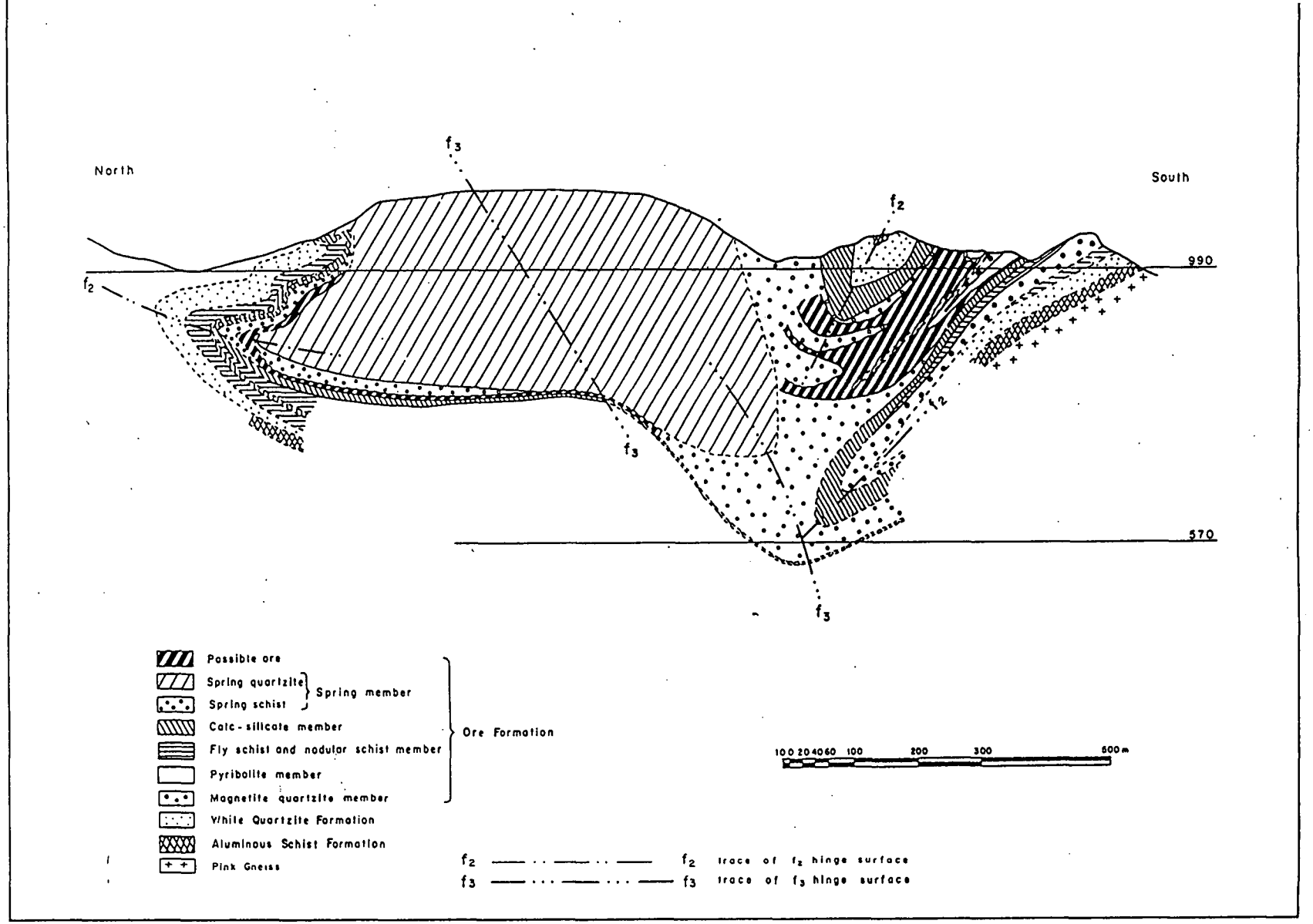

Figure 9.8 Generalised cross section of the Big Syncline deposit. (Ryan,et al, 1986)

9.5 Gamsberg Ore Deposit, Gamsberg.

The Gamsberg Ore Deposit contains 150 Mt grading 7.1% Zn and 0.5% Pb. A plan of the geology of the deposit is presented in Figure 9.9 and the stratigraphy is summarised in Table 9.6. Cross sections are presented in Figures 9.10 and 9.11.

The deposit is hosted by the Gams Ore Formation which is characterised by diverse magnetite-carbonate-garnet rich assemblages (Rozendaal, 1986; Walters, 1992). The Gams Ore Formation is subdivided into the A, B and C Members. The A Member has a maximum width of 10m and is not economically mineralised. The B Member hosts the mineralisation. Its width varies from 0 to 50m, averaging 25m. Sulfide minerals, in decreasing order of abundance, are pyrite, pyrrhotite, sphalerite and galena. Small amounts of chalcopyrite, alabandite, magnetite, ilmenite and graphite are present. Laterally the B Member grades into barren sillimanite quartzite. Vertically the B Member grades up into the C Member. The silicate mineralogy does not change much from B to C but magnetite and hematite occur instead of sulfides in the C Member. The thickness of the C member varies from 0 to 9m.

Detailed mineral assemblages for the members of the Gams Ore Formation are summarised in Table 9.7. Within the A Member, garnet shows a vertical zonation from almandine to spessartine toward the ore. Magnetite is the major opaque mineral in unit A2, but disseminated pyrite and pyrrhotite dominate in A3 and A4. Carbonate is mainly manganoan calcite.

Within the B Member sphalerite is the dominant ore mineral, increasing toward the top of the member. Chalcopyrite has a sympathetic distribution to sphalerite. Pyrite is dominant in unit B1, instead of silicate gangue. Pyrrhotite is dominant in unit B2 and is dominantly associated with sphalerite. Magnetite is absent in the lower part of the mineralised zone, but forms a minor constituent of the upper zinc-rich portion where it occurs as grains embedded in massive sphalerite. Graphite is dominantly found in the quartz-muscovite-sillimanite schist at the base of the B Member. It occurs as flakes aligned parallel to foliation or interlayered with slightly elongated pyrite and sphalerite grains.

The C Member is marked by a change from base metal sulfides to iron silicates and oxides. Composition of the silicates is similar to the B Member except for the occurrence of pyroxenoid. C Member displays considerable lateral and vertical variation. Pyroxenoid-amphibole-garnet-clinopyroxene rocks of unit C1 occur directly over mineralised B Member, but grade laterally to banded magnetite hematite quartzite $\pm$ interbedded barite, magnetite-garnet-sillimanite-quartz rock or garnet rich quartzite. Barite occurs within C Member as massive recrystallised layers and banded hematite rich units which increase in thickness from south to east as B Member thins.

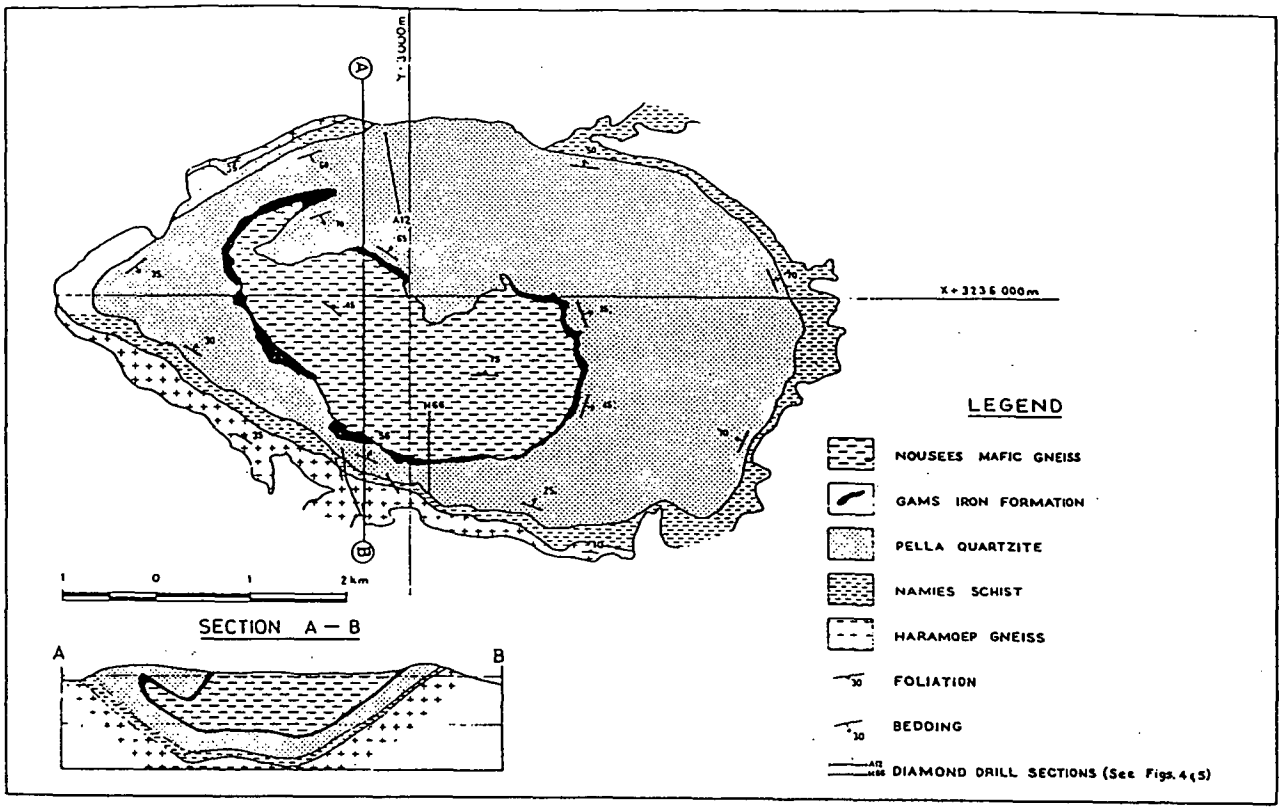

Figure 9.9 Geological map of the Gamsberg deposit. (Rozendaal, 1986)

Aggeneys–Pofadder Area (Joubert, 1974)		Gamsberg (Rozendaal, 1977)	
	Formation	Formation	Lithology
Bushmanland Group	Nousees Mafic Gneiss	Nousees Mafic Gneiss	Amphibolite, quartz–feldspar–amphibole gneiss/fels, pyroxene–plagioclase—quartz (± amphibole) fels. Quartz–muscovite schist, interbedded quartzite bands and conglomerate lenses, feldspathic schist ± biotite.
		(Unconformity)	
	Pella Quartzite	Gams Iron Formation (Gams Formation)	C Member: Garnet–pyroxenoid rhythmite, pyroxenoid–amphibole–garnet–clinopyroxene rock, quartz–garnet–amphibole–magnetite rock and magnetite–hematite quartzite with interbedded barite. B Member: Mineralized quartz–sericite–sillimanite schist, mineralized quartz–grunerite–garnet rock. A Member: Quartz–garnet–feldspar–clinopyroxene rock, carbonate–quartz–garnet–clinopyroxene marble, garnet–pyroxene–amphibole rock.
		Pella Quartzite	Dark recrystallized quartzite, with conglomerate and quartz–biotite–muscovite–sillimanite schist bands. Quartz–biotite–muscovite–sillimanite schist, quartz–muscovite schist, interbedded quartzite bands. Massive recrystallized milky quartzite.
	Namies Schist	Namies Schist	Quartz–biotite–muscovite–sillimanite schist, interbedded quartzite bands and lenticular massive sillimanite bodies.
	Haramoep Gneiss	Haramoep Gneiss	Pink granite–gneiss

Table 9.6 Stratigraphy of the Gamsberg deposit. (Rozendaal, 1986)

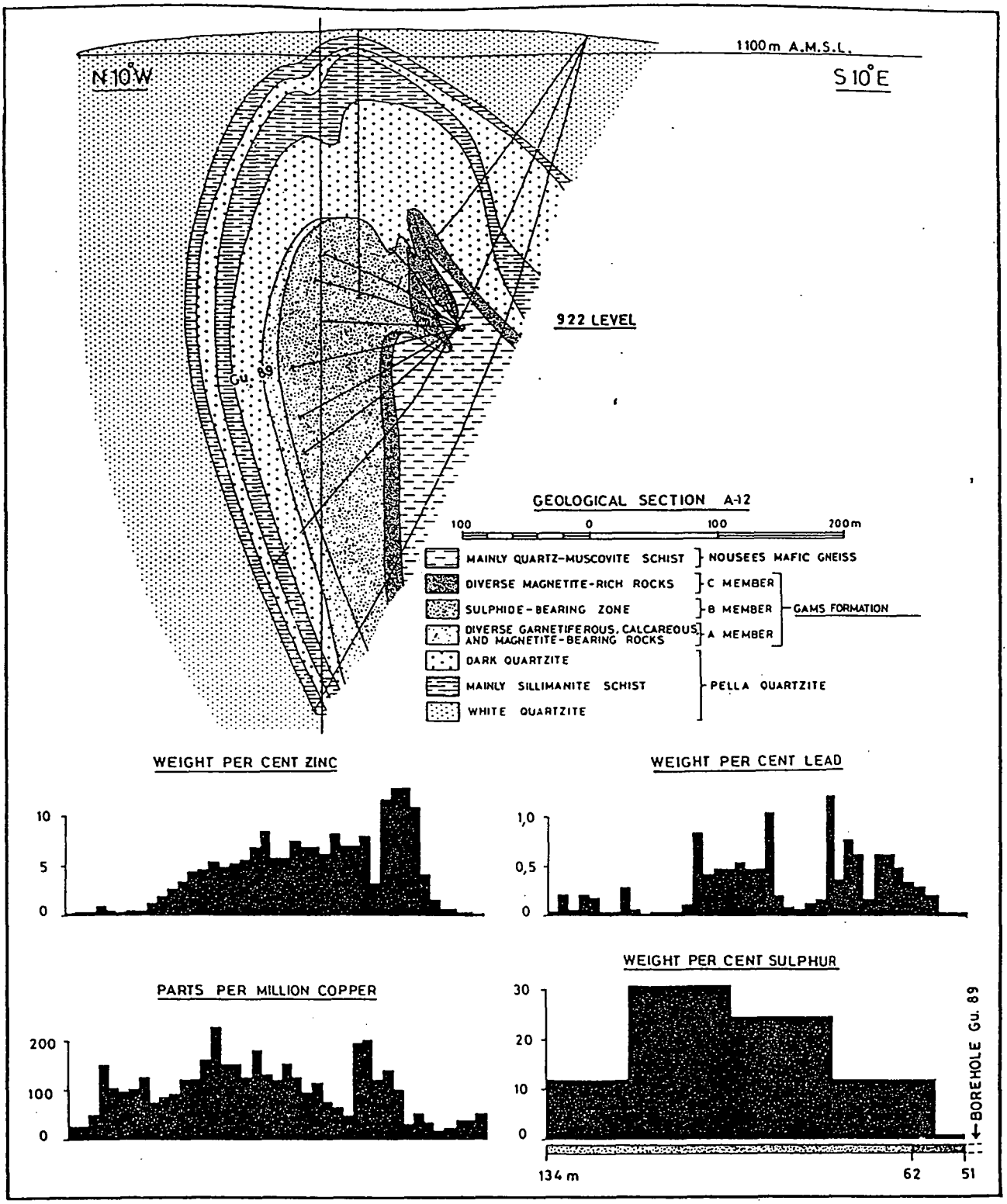

Figure 9.10 Cross section of the Gamsberg deposit (northern part). (Rozendaal, 1986)

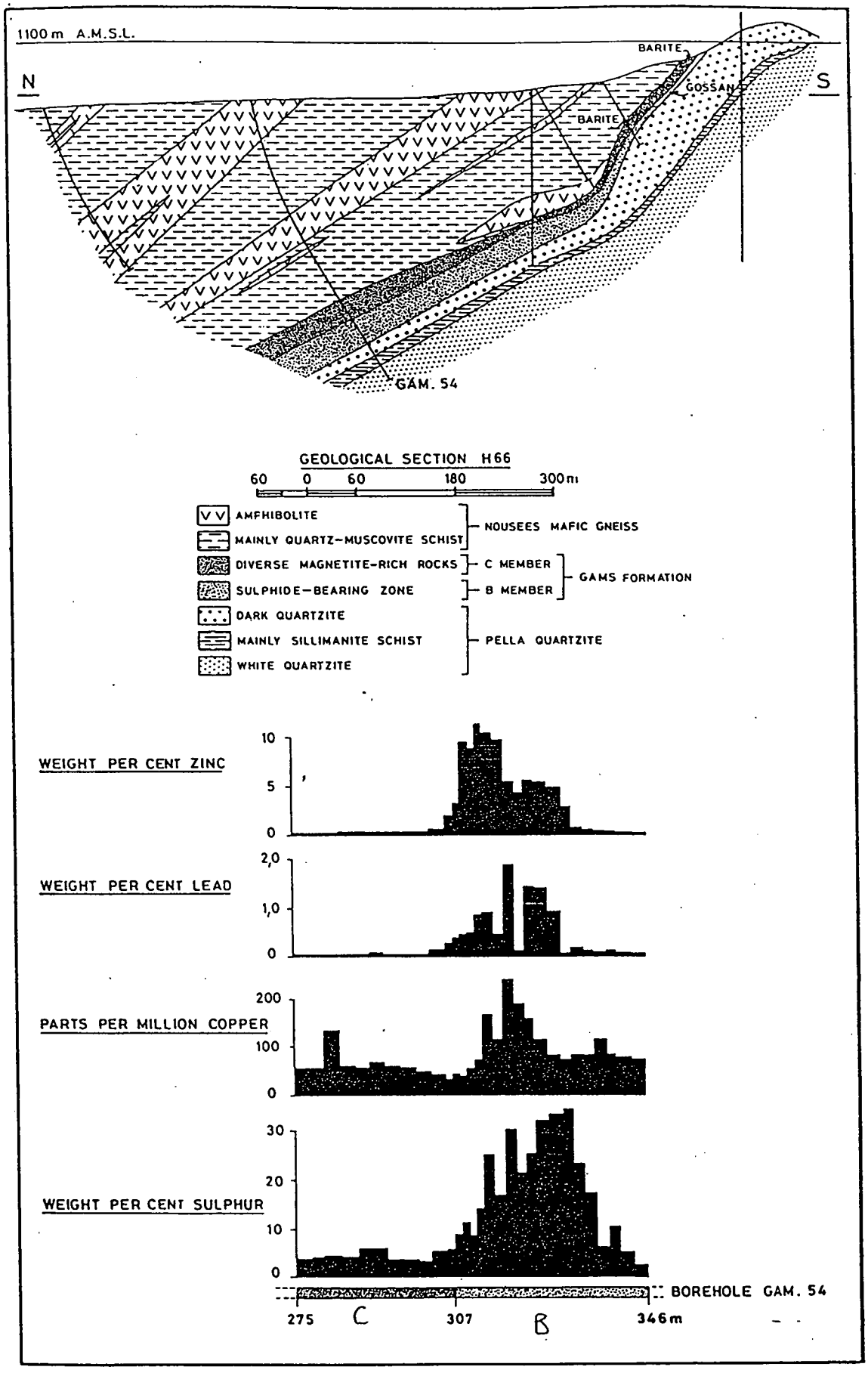

Figure 9.11 Cross section of the Gamsberg deposit (southern part). (Rozendaal, 1986)

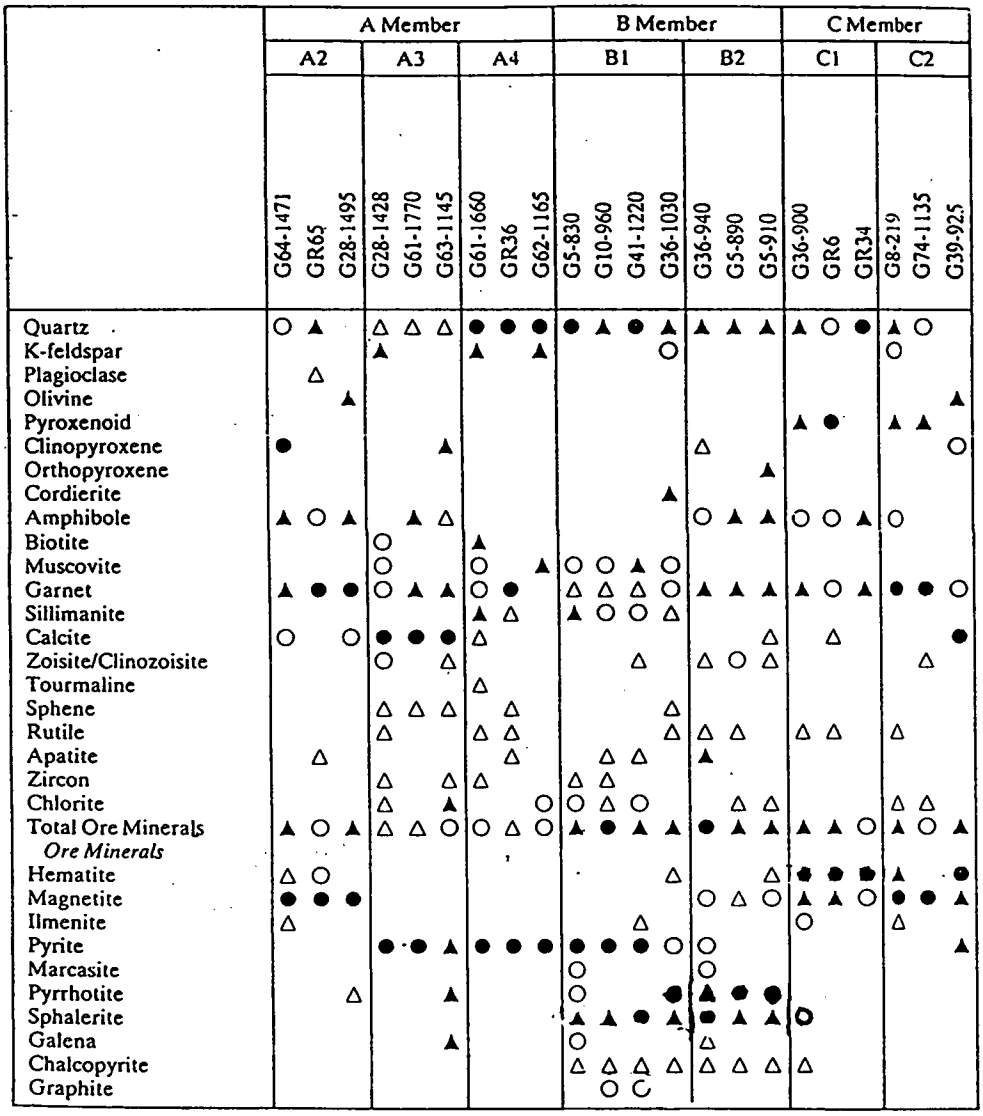

● Major constituents >40 %
▲ Subordinate constituents 10–40 %
○ Minor constituents 1–10 %
△ Accessory constituents <1 %

Table 9.7 Mineralogy of the Gamsberg deposit. (Rozendaal, 1986)

10. MAGNETIC CHARACTERISTICS OF STRATIGRAPHY AND MINERALISATION OF THE AGGENYS-GAMSBERG DISTRICT, SOUTH AFRICA

10.1 Regional Aeromagnetic Characteristics

Aeromagnetic data over the Aggenys-Gamsberg district were acquired at a line spacing of 1000m and a survey altitude of 100m and gridded using a 200m x 200m mesh size.

Interpretation of this data set was difficult due to the coarse flight line spacing, as well as limited outcrop and inconsistent stratigraphic terminology in published maps and papers.

Images of the aeromagnetic data are presented as Figures 10.1 and 10.2, Plates 25 and 26. An interpretation of the aeromagnetic data is presented in Figure 10.3 and Plate 27. The interpretation is draped over the aeromagnetic data in Figure 10.4, Plate 28.

The interpretation was conducted at a scale of 1: 100 000, with reference to the 1:100 000 scale Stratigraphic Map of Central Bushmanland (Colliston *et al*, 1986).

The regional aeromagnetic characteristics of this province differ significantly from the other BHT provinces. The magnetic image is dominated by magnetic units which in plan view appear sinusoidal and swirling , reflecting the structural style of the province. The most strongly magnetic units occur within the Transitional Sequence, rather than the Lower and Basement Sequences, and are intimately associated with the ore deposits.

Stratigraphy

The Basement and Lower Sequences within the Aggenys Gamsberg district are comprised of undifferentiated granites and quartzofeldspathic gneisses interpreted to be felsic pyroclastic rocks. These sequences have not been differentiated in the aeromagnetic interpretation. They have a relatively, uniform, weak to moderately magnetic character. Magnetic units within this sequence have amplitudes up to 300 nT. They may be amphibolites, calc-silicates or magnetite in metasedimentary rocks within the Lower Sequence. Alternately they may be weak to moderately magnetic undifferentiated units of the Transitional Sequence.

The Transitional and Upper Sequences generally have a weak to moderately magnetic background response, similar to the Lower and Basement Sequences. They have not been differentiated in the magnetic interpretation. However there are limited regions in which the Transitional Sequence has a relatively higher background magnetic response. Within the Transitional Sequence numerous moderate to strongly magnetic units occur. The strongly magnetic units are magnetite exhalites (iron formations), calc-silicates and amphibolites. Weaker magnetic units are probably magnetic amphibolites and magnetite in metasedimentary rocks.

Figure 10.1 Regional Aeromagnetic Data, Aggenys–Gamsberg, South Africa.
Reduction To Pole

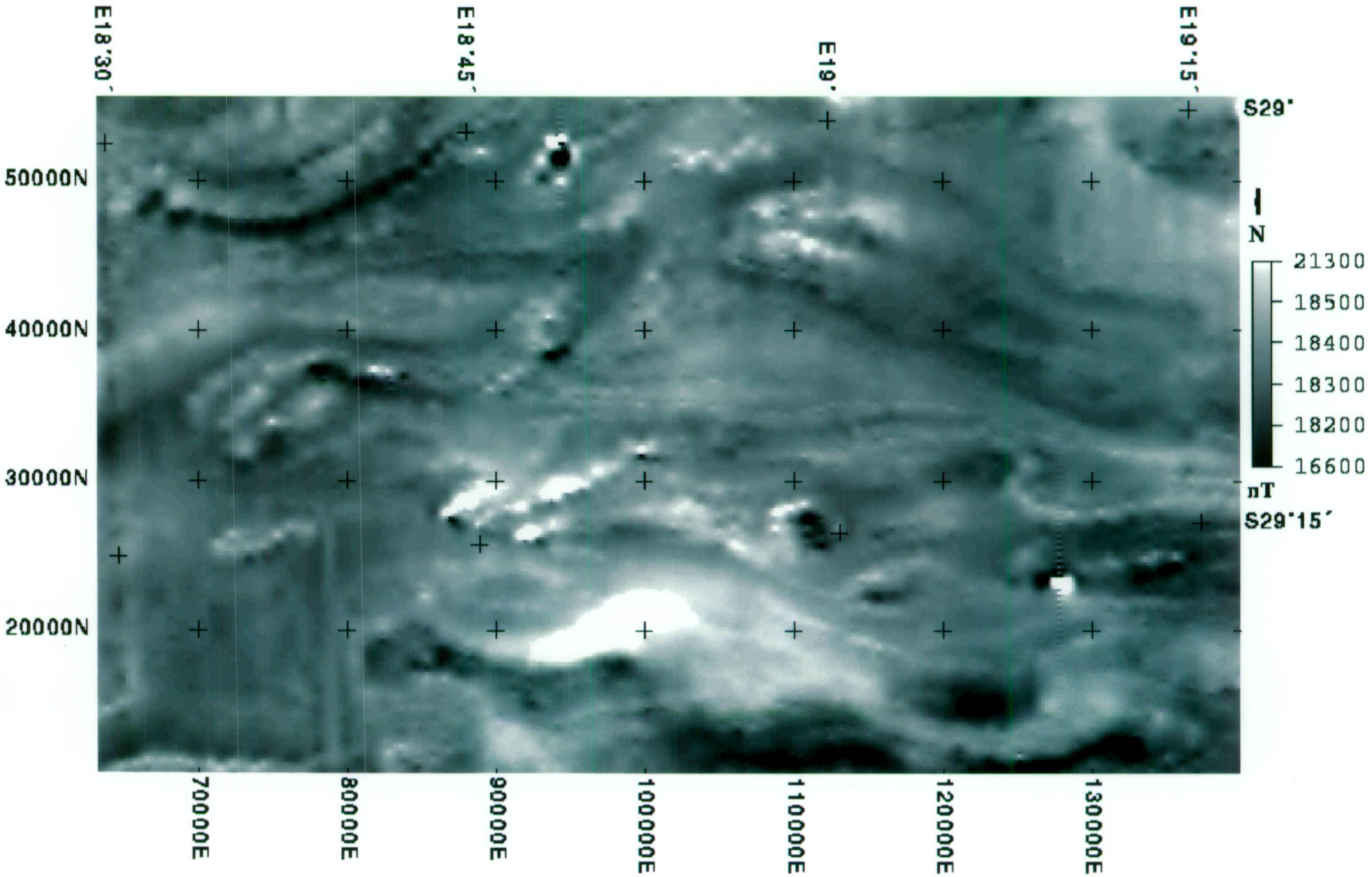

Figure 10.2 Regional Aeromagnetic Data, Aggenys–Gamsberg, South Africa.
Reduction To Pole – 1st Vertical Derivative

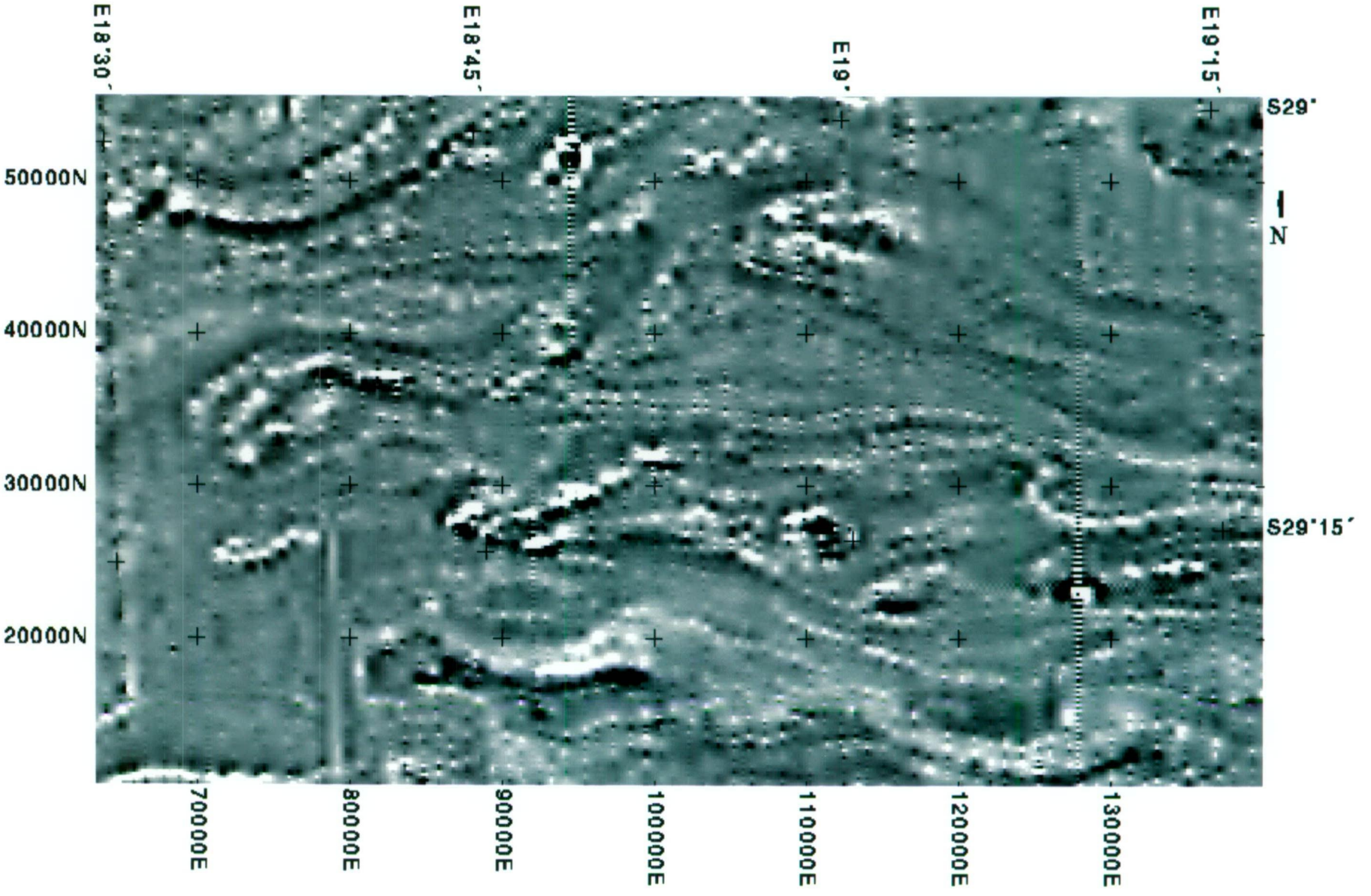

Figure 10.3

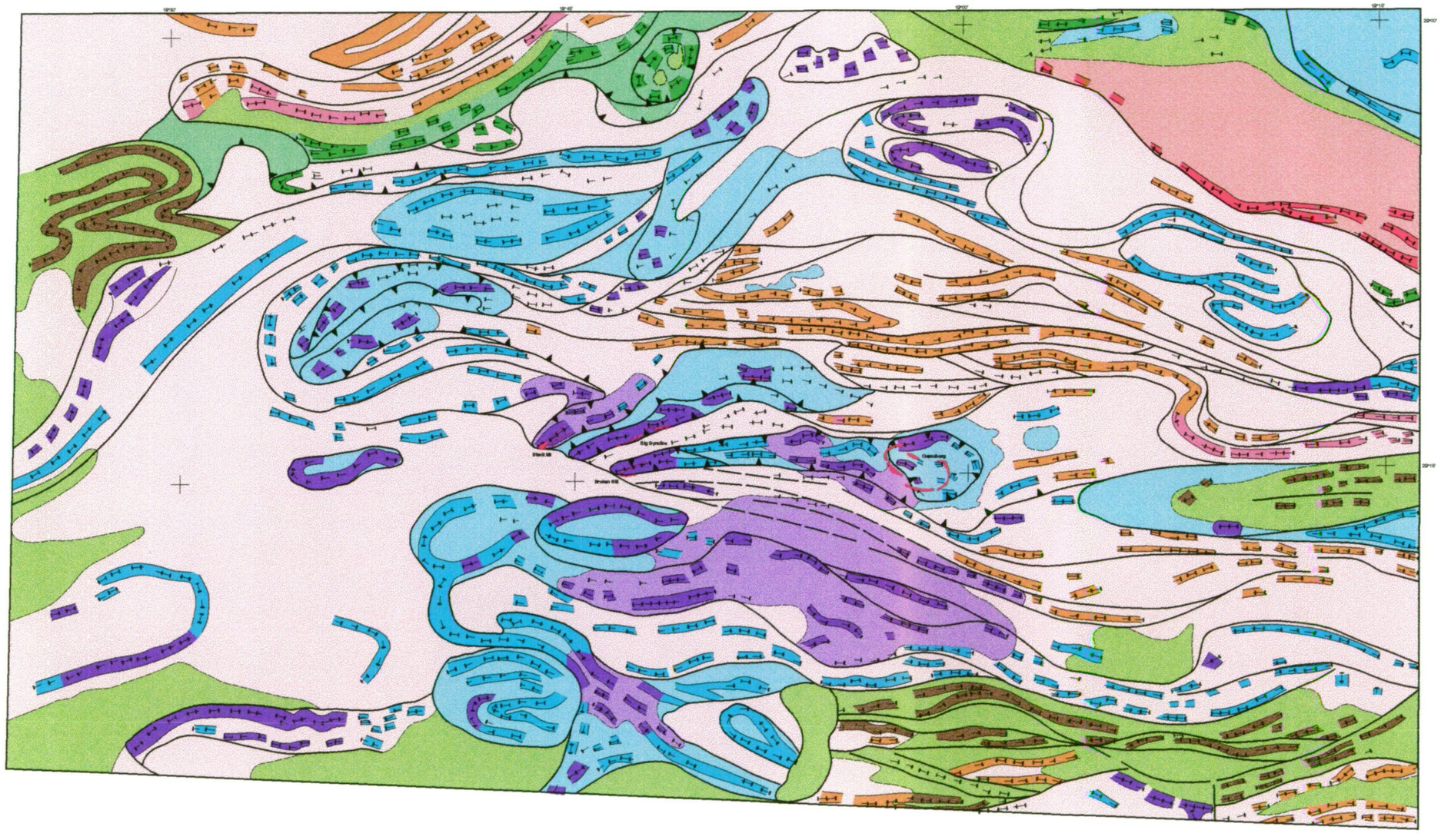

B H P MINERALS

Aggenys - Gamsberg District, Namaqualand, South Africa

AEROMAGNETIC INTERPRETATION

0 10km

Interpretation by T.Kerr

Surface projection of deposit

Outcropping magnetite gossan

INTRUSIVE

Pella Granite

- magnetic unit (probable intercalated calc silicates)

STRATIGRAPHY

Unknown Sequence : weakly to ? negatively magnetised

Possible correlative of Haib Subgroup or unassigned meta quartzites and schists outcropping in core of Namiesberg

- magnetic unit (iron formation / calc silicate / amphibolite / ultramafic)

Middle Sequence

Aggenys Subgroup (includes minor occurences of Upper and Lower Sequences)

Regionally weak to moderately magnetic

Highly magnetic

- Moderately magnetic units
- Highly magnetic units

] Iron formation / calc silicates / amphibolite of the Namies / Aluminous Schist, Pella / White Quartzite and Aggenys / Gams Iron Formation

"Basement" and "Lower Sequence"

Undifferentiated quartzofeldspathic gneisses and granites : regionally weak to moderately magnetic (includes the "Lower Sequence" haramoep Gneiss and Pink and augen Gneiss, may also include unrecognised non magnetic middle sequence)

- Magnetic unit
- Highly magnetic unit

] Iron formation / amphibolite / calc silicates

Haib Subgroup: may be weakly to ? negatively magnetised

- Layered matic and felsic gneiss
- Magnetic unit (probable calc silicates / amphibolites / ultramafic)

Figure 10.4 Regional Aeromagnetic Interpretation (Colour)
Draped On Vertical Derivative (Intensity)
Aggenys–Gamsberg District, South Africa

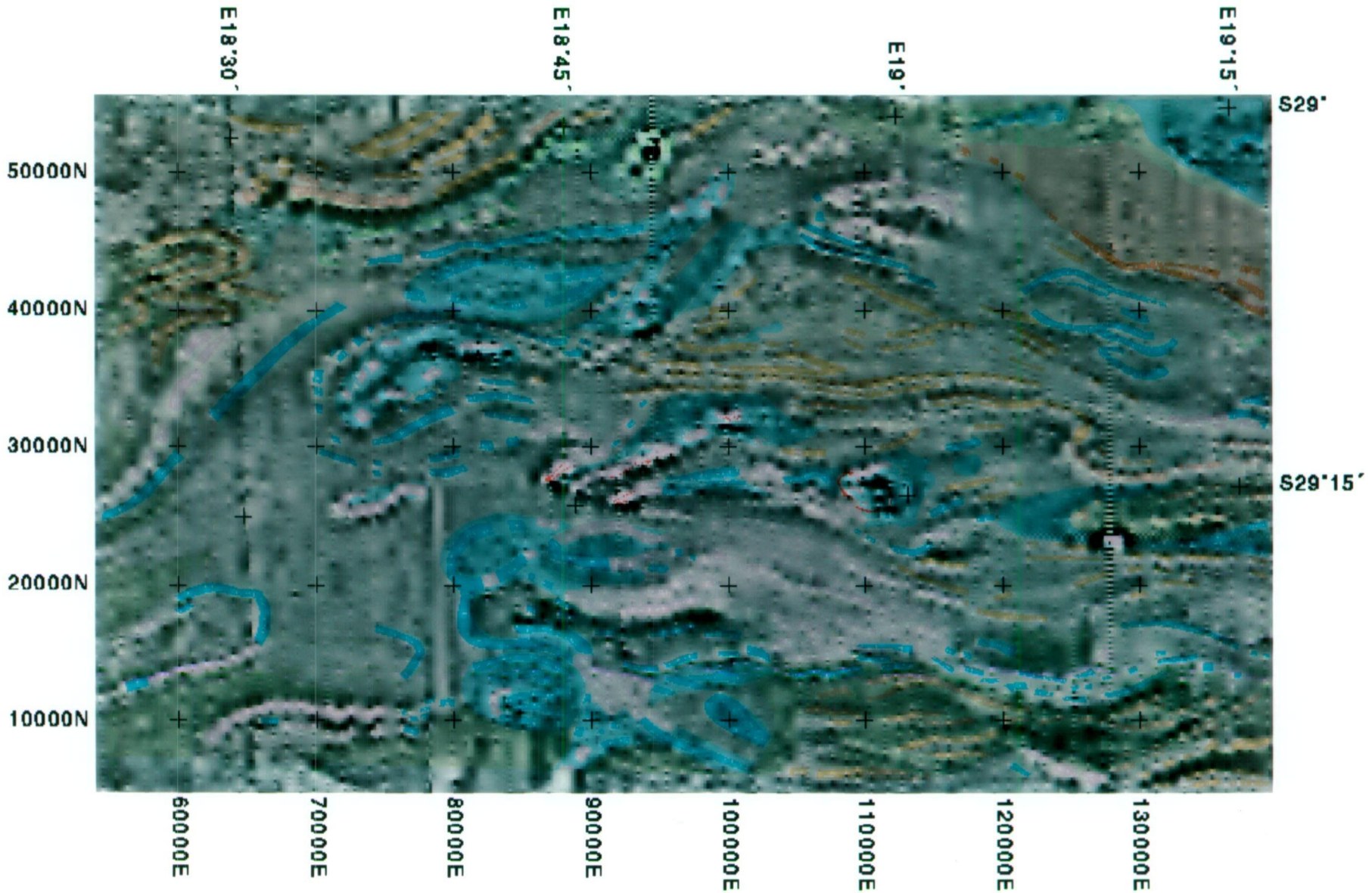

The Upper Sequence is mapped as conglomerate, amphibolite, magnetite bearing gneisses and quartz-muscovite-feldspar gneisses. The sequence has a very limited extent in outcrop. The Upper Sequence appears to be relatively non-magnetic in the regional aeromagnetic data, despite the description of amphibolites and magnetite bearing mafic gneisses. Hence it was not able to be differentiated from the background response of the Transitional Sequence.

An unidentified sequence was mapped within the aeromagnetic data. This sequence has a relatively low background magnetic response compared to the sequences described above. It may correspond to unassigned meta-quartzites and schists outcropping in the core of Namiesberg or it may be a correlative of the Haib Subgroup.

The Haib subgroup is interpreted by some authors (e.g., Walters, 1992). to grade into metasedimentary rocks of the Bushmanland region. It is characterised by a lower, rarely negative, magnetic background response compared to the BHT host stratigraphy. This sequence consists of layered mafic and felsic gneisses. Magnetic units within this sequence attain amplitudes of 350 nT.

Mineralisation

The strongest magnetic anomalies in the entire regional survey correspond to the Aggenys group of deposits. The Broken Hill (South Africa) and Black Mountain deposits have aeromagnetic anomalies with amplitudes of approximately 1000 nT. Big Syncline has an aeromagnetic anomaly of approximately 600 nT. The Gamsberg deposit is closely associated with a magnetic anomaly of 400 nT.

I was unable to obtain an accurate position for the Gamsberg deposit. Based on available information it appears to be displaced to the west of the magnetic unit, but this may be a positioning problem rather than a true displacement.

Elsewhere in the region it is rare for magnetic units to have amplitudes greater than 300 nT.

10.2 Magnetic Characteristics of the Aggenys and Gamsberg Deposits

From the regional aeromagnetic data it is clear that each of the deposits is intimately associated with a strongly anomalous magnetic response of similar strike length to the deposit itself, at a scale of 1:100 000. The following discussion considers the spatial relationship between magnetic units and ore lenses on a deposit scale. The geology of the each of the deposits was described in detail in Section 9.

The Broken Hill (South Africa) deposit contains 48% magnetite and hence would be expected to have a strong magnetic anomaly. Ore lenses contain base metals hosted by banded pyrite and pyrrhotite rock, with pyrrhotite content ranging from 15 to 50%. Immediately overlying the ore lenses (less than 5m above the massive sulfide) are units of magnetite quartzite and magnetite amphibolite with up to 60% magnetite.

The Black Mountain deposit differs from the Broken Hill (SA) deposit in that economic ore lenses contain magnetite as gangue. Magnetite is present in magnetite quartzite, magnetite amphibolite and magnetite barite rock.

The stratigraphically lower part of the Upper Ore Body is hosted by garnet quartzite and quartz schists. Pyrite is the dominant sulfide within the garnet quartzite and schist, with subordinate chalcopyrite. Magnetite quartzite overlies the garnet quartzite and quartz schists. Pyrite is the dominant sulfide with subordinate pyrrhotite. Economic mineralisation is dominantly galena, followed by chalcopyrite and accessory sphalerite. Magnetite amphibolite occurs stratigraphically above the magnetite quartzite. Pyrrhotite is the dominant iron sulfide, with galena and sphalerite both abundant. The overlying magnetite barite rock contains up to 10% magnetite.

The Lower Ore Body is a thin magnetite rich sulfide ore body comprised of garnet quartzite, magnetite amphibolite and sulfidic schist. It contains less magnetite and galena than the Upper Ore body.

The Big Syncline ore deposit is hosted by the Spring Schist and Quartzite member. The deposit consists of sphalerite and galena in association with coarse grained pyrite, pyrrhotite and marcasite. Highly magnetic units occur in the footwall less than 60m below the deposit and include magnetite quartzite and magnetite pyribole.

The Gamsberg deposit is hosted by the Gams Formation, an iron formation stratigraphically equivalent to the Aggenys ore formation. The Gams Formation contains three members, the A, B and C Members. The B Member (50m thick) is economically mineralised, containing pyrite, pyrrhotite, marcasite and sphalerite in order of decreasing abundance. Within the B Member magnetite (< 10%) is a minor constituent of the upper zinc rich portion. The base of the A Member (less than 10m below the economic mineralisation) contains more than 40 % magnetite. The C Member contains zones of more than 40% magnetite and hematite and directly overlies the economic mineralisation.

As previously mentioned I had some problems obtaining an accurate position for the Gamsberg deposit. Available information indicated the position shown in Figure 10.3 and Plate 27 but it is likely that the ore deposit is actually situated further east, corresponding the 450 nT aeromagnetic anomaly. No other comparable magnetic units (e.g. more than 40% magnetite) are described near the deposit (Table 9.7).

Distal extensions of the Aggenys and Gamsberg deposits are represented by banded calc-silicate horizons contain sub-economic mineralisation.

11. DISCUSSION AND SYNTHESIS OF MAGNETIC CHARACTERISTICS OF BHT DEPOSITS AND HOST PROVINCES

11.1 Discussion of Regional Aeromagnetic Characteristics

Figure 11.1 shows an aeromagnetic image of the regional aeromagnetic data for each of the four provinces. At first glance it is clear that the Australian provinces show some similarity. The Bergslagen and Aggenys-Gamsberg provinces have very different aeromagnetic characteristics, although magnetic characteristics of individual stratigraphic sequences share many similarities with their Australian equivalents. Many of the differences in the aeromagnetic images are related to structural style and magnetic characteristics of basement stratigraphy, rather than magnetic properties of BHT host stratigraphy.

The Lower Sequence of the Broken Hill Block and the Bergslagen Province have very similar magnetic properties. In both provinces the Lower Sequence is volcanic rock dominated and is characterised by a variably magnetic background containing strongly magnetic linear anomalies related to magnetite rich units .

The Lower Sequence of the Soldiers Cap Group is likely to occur east of the outcropping areas. Sequences of stripy magnetic packages interpreted to be metavolcanic rocks probably correspond to the Lower Sequence. If so, then the magnetic characteristics of the Lower Sequence within this province are consistent with the Broken Hill and Bergslagen provinces.

The Lower Sequence within the Aggenys-Gamsberg district appears to have a very different aeromagnetic signature from the other provinces. It is interpreted to be dominantly comprised of metamorphosed felsic pyroclastics. It has a relatively flat, uniform, weak to moderately magnetic background response, very similar to the metasedimentary rock-dominated sequence. Weak to moderately magnetic linear units within the Lower Sequence include amphibolites, calc-silicates and magnetite in metasedimentary rocks. Strongly magnetic units are absent.

The Transitional Sequence of the Broken Hill Block and the Soldiers Cap Group have very similar background magnetic responses. Both are extensive and have a very low, relatively non-magnetic response. Within this low background response moderate to strongly magnetic units correspond to magnetic exhalites and amphibolites. However in the Broken Hill Block and northern Soldiers Cap Group the magnetic units have significant strike extent. In contrast, the southern Soldiers Cap Group sequence, which hosts the Pegmont and Cannington deposits, has relatively few magnetic units and they are characterised by much shorter strike lengths.

The Transitional Sequence of the Bergslagen province has not been differentiated over much of the region in the published mapping. Where it has been differentiated it has a similar magnetic character to the Transitional Sequences of the Broken Hill Group and Soldiers Cap Group, but it is considerably less extensive. Moderate to strongly magnetic units within the low background response correspond to magnetic calc-silicate exhalites and magnetic amphibolite.

Figure 11.1 Comparison of Regional Aeromagnetic Characteristics.

a) Broken Hill, Australia

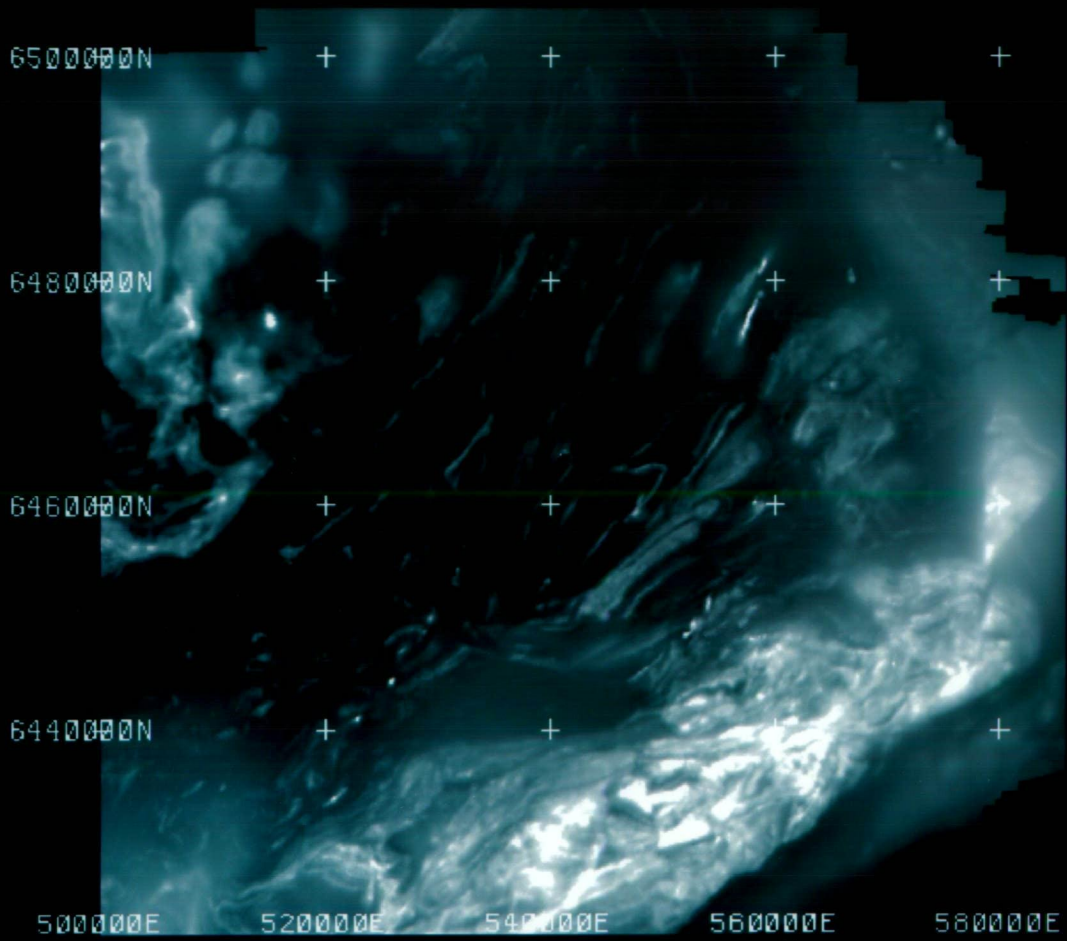

b) Eastern Succession, Australia

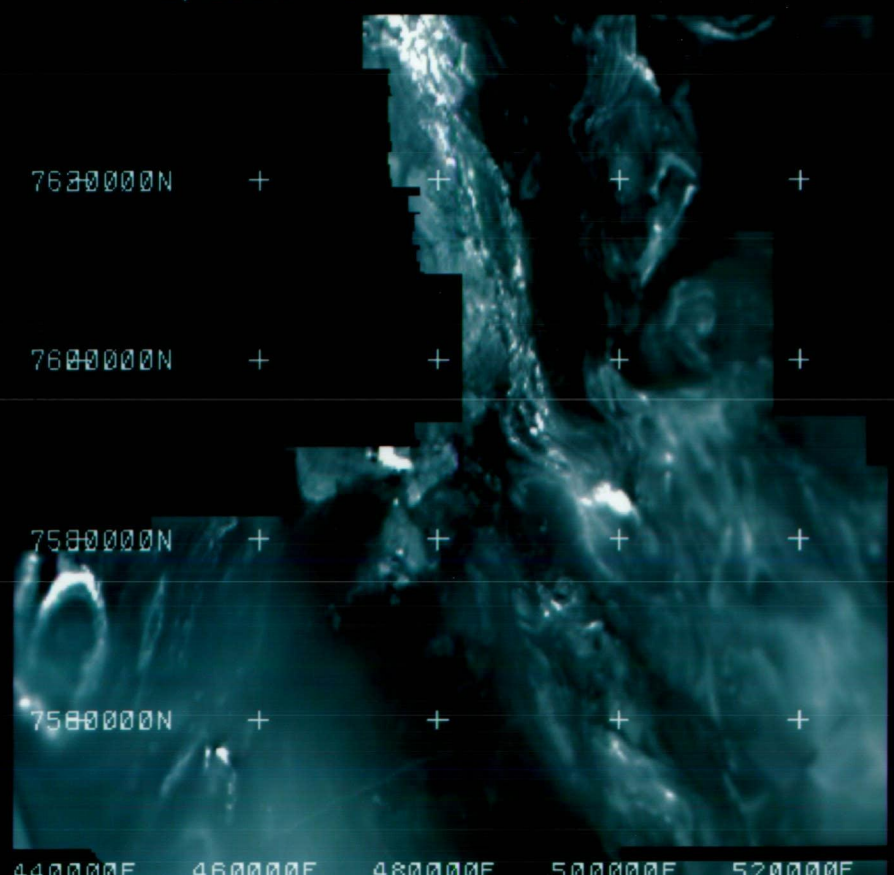

Figure 11.1 Comparision of Regional Aeromagnetic Characteristics.

c) Bergslagen, Sweden

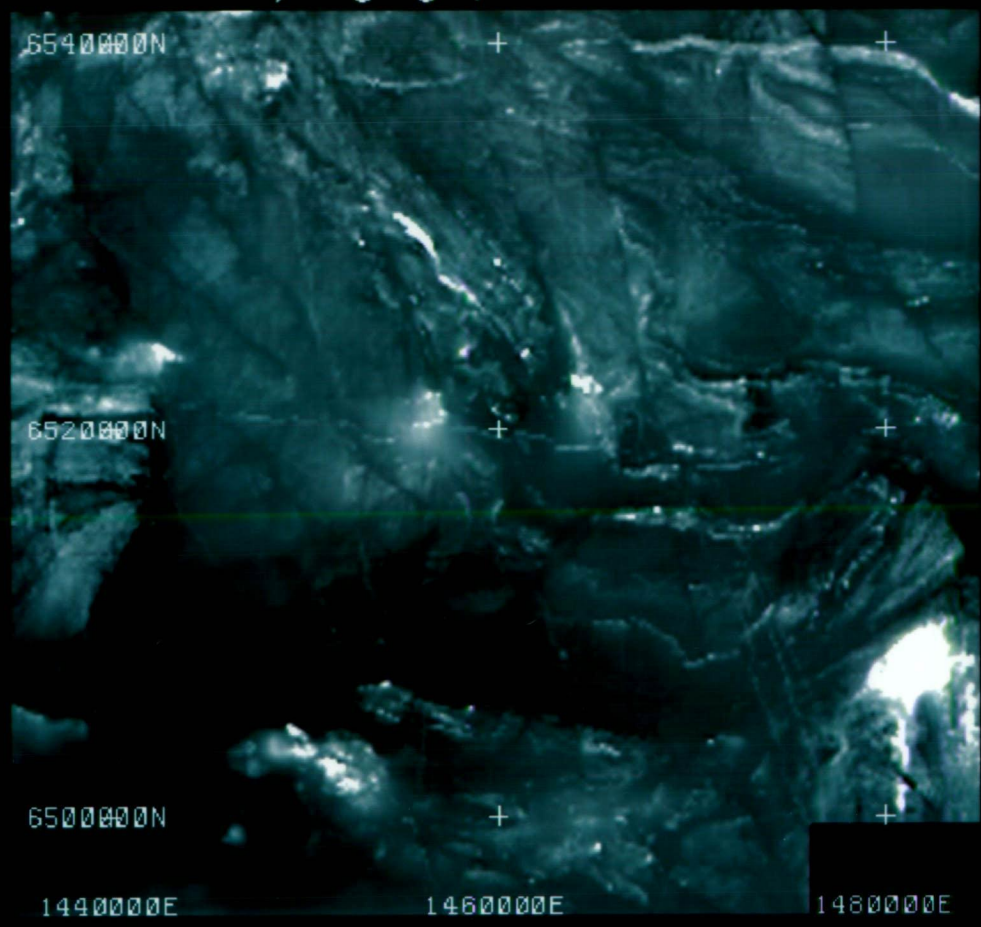

d) Aggenys–Garnsberg, South Africa

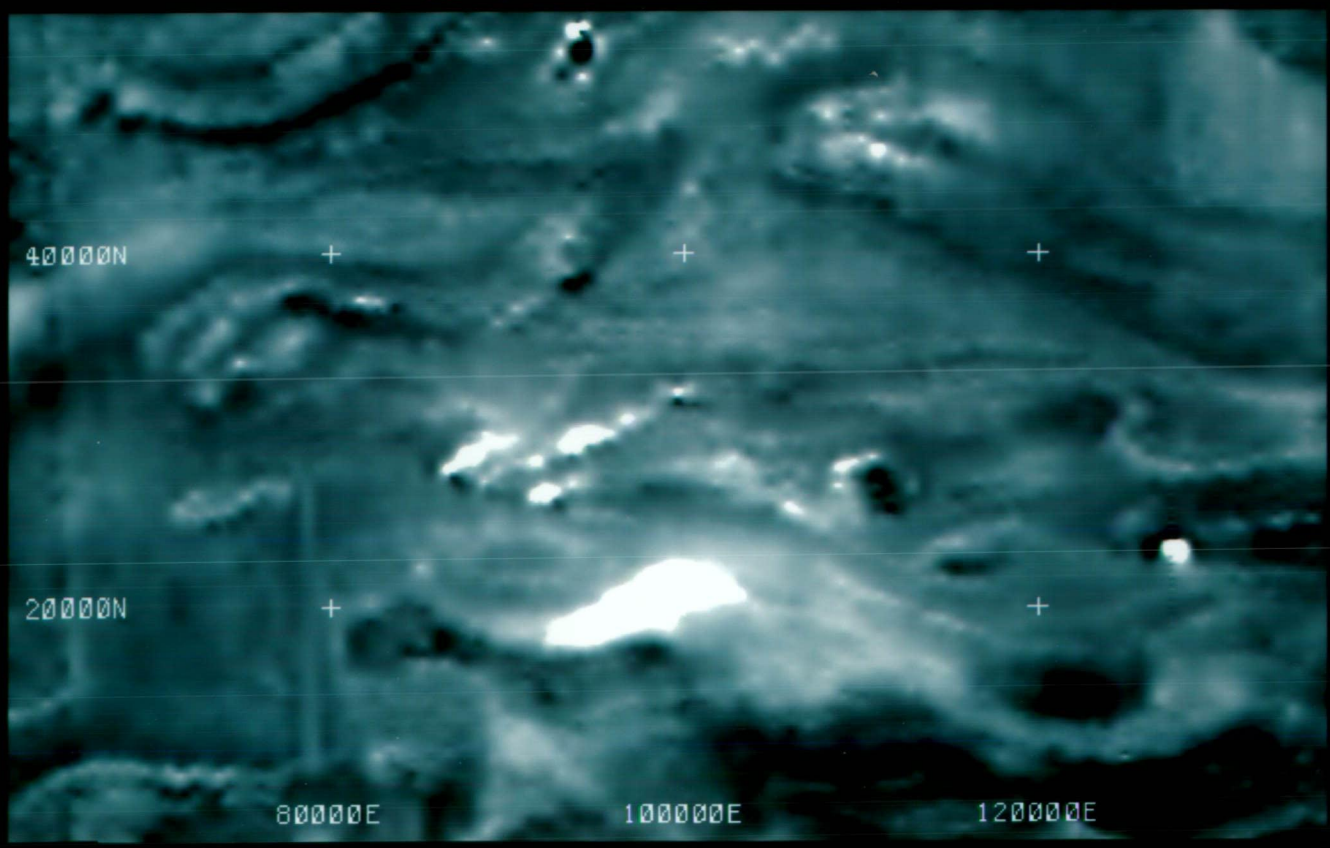

The Transitional Sequence of the Aggenys-Gamsberg district has a weak to moderately magnetic background response similar to the Lower and Basement Sequences. However there are limited regions in which the Transitional Sequence has a relatively higher background magnetic response. Within this background response the Transitional Sequence contains extensive linear, moderately to strongly magnetic units corresponding to iron formations and other magnetite-bearing exhalites.

The Upper Sequence of the Broken Hill Block largely consists of relatively non-magnetic metasedimentary rocks. The notable exception is one strongly magnetic unit at the base of the sequence which reflects magnetite within a metasedimentary unit. This magnetite may be related to waning hydrothermal activity from the main vent which sourced the Broken Hill deposit. Rare, weak to moderately magnetic units correspond to calc-silicates.

The Upper Sequence of the Soldiers Cap Group corresponds in the type area to the Toole Creek Volcanics, a sequence of interbedded shales, quartzites and calc-silicates with extensive mafic igneous rocks which may be sills. The sequence is similar to the Upper Sequence of the Broken Hill Group in that it marks a change to finer grained sedimentation. These finer grained sedimentary rocks have a relatively non-magnetic response. However the extensive mafic igneous rocks have an influence on the magnetic signature resulting in narrow weakly magnetic linear units where the stratigraphy is steeply dipping, and more extensive weak, very irregular magnetic zones where the stratigraphy is flat lying. The Upper Sequence does not contain any strongly magnetic units.

Further south the Upper Sequence may correspond to relatively non-magnetic stratigraphy within areas mapped as the Glen Idol Schist/New Hope Arkose, interpreted to be thick bedded quartzofeldspathic psammites with minor psammopelites and psammites.

The Upper Sequence of the Bergslagen district consists of greywackes, shales and mass flow deposits, similar to the Upper Sequence of the Broken Hill Block. The Bergslagen Upper Sequence is relatively non-magnetic. However much of it displays a weak irregularly magnetic character. In these areas the metasedimentary sequence is interpreted to be thin and relatively flat lying. The magnetic character is probably derived from the underlying volcanic sequence.

Within the metasedimentary sequence linear magnetic units may be units of the undifferentiated Transitional Sequence, mafic intrusions or magnetic units within underlying metavolcanic rocks.

The Upper Sequence of the Aggenys-Gamsberg District has a very limited areal extent in published mapping. It has a similar, if not slightly lower, background response to the Lower and Transitional Sequences. Despite the description of magnetite-bearing schists and amphibolite within the metasedimentary rocks the sequence as mapped does not contain magnetic units, although this may be a reflection of the limited outcrop and poor stratigraphic understanding.
Hence it is clear that the Broken Hill, Bergslagen and Soldiers Cap regions have BHT stratigraphic sequences with similar magnetic properties. Despite this, the Bergslagen

district looks quite different in the aeromagnetic data. This is due to the extent and magnetic character of the granitoids compared to the BHT stratigraphy and the relatively undeformed nature of the sequence. The granitoids comprise more than 50 % of the outcrop. The distinctive, fractured pattern of the younger granites dominates the image. The very low, uniform areas in the image look very similar to the Transitional Sequences of the Broken Hill and Soldiers Cap Groups, but correspond to the older granites in the published mapping.

The Transitional and Upper Sequences are very spatially limited in the Bergslagen district compared to the Broken Hill and Soldiers cap provinces. This reflects the development of the Bergslagen sequences in a series of narrow grabens. The Upper Sequence of the Bergslagen district often appears weakly and irregularly magnetic due to the magnetic characteristics of the underlying metavolcanic rocks. The metasedimentary rock sequence in these zones is thin and relatively flat-lying and behaves transparently. The Broken Hill and Soldiers Cap Upper Sequences would also appear transparent if they were flat-lying, thin and underlain by a magnetic sequence.

The aeromagnetic character of the Aggenys-Gamsberg district differs significantly from the other three provinces studied. The structural style within the Aggensys-Gamsberg district is an important factor. The area is characterised by recumbent folding and nappe tectonics, with many limbs still relatively flat lying, and this gives rise to the wavy, swirling nature of the aeromagnetic image. The Broken Hill and Soldiers Cap regions are also thought to have undergone similar deformation, but this has been overprinted by numerous deformations resulting in stratigraphy that is generally isoclinally folded and steeply dipping.

The other major difference between the Aggenys-Gamsberg district and the other provinces is the magnetic character of the Lower Sequence. The Lower Sequence appears to have a very uniform flat signature compared to Lower Sequences of the other provinces. This may be apparent only, due to the coarse flight line spacing. A more irregular texture may become apparent with a more detailed line spacing. Alternately the uniform flat signature may be a true reflection of the magnetic character of this sequence. The Lower Sequence is also notably devoid of linear magnetic units. The Lower Sequences of the other provinces are host to the strongest magnetic units of the BHT host stratigraphy, commonly with amplitudes of thousands of nanoteslas.

There are significant problems with the lack of outcrop and conflicting stratigraphic interpretation in the Aggenys - Gamsberg district, and this, combined with the coarse nature of the aeromagnetic data, should be borne in mind when extrapolating these observations to other regions.

11.2 Discussion of Deposit Scale Magnetic Characteristics

The Broken Hill (Australia) ore deposit is notable for its lack of a magnetic response. No magnetite has been described within the deposit itself and pyrrhotite enveloping one of the lodes is non-magnetic.

It appears, however, that there is a regional increase in iron content of the lode horizon toward the deposit. Further, it appears that there is a gradual increase in magnetite within the lode horizon toward the deposit, before an abrupt disappearance of magnetite within the ore zone itself (see Section 4.2).

In the stratigraphic hanging wall a magnetite rich unit at the base of the Upper Sequence may be related to exhalation from the main vent. In the footwall a sequence containing magnetite and BIF may represent an earlier exhalation event. This footwall magnetic unit displays **a notable decrease in magnetic intensity directly below the deposit**, suggesting possible footwall alteration resulting in magnetite destruction, or a primary annular distribution of magnetite around the vent.

The Zinkgruvan deposit shows many similarities in magnetic character to the Broken Hill (Australia) deposit. There is no magnetite within the ore zone itself. However Zinkgruvan differs in that it has magnetic units of limited strike length in the hanging wall and footwall of the deposit which are much more closely associated with the ore zone. In the hanging wall a stratabound pyrrhotitic unit is magnetic. This pyrrhotite is interpreted in the literature to be related to the mineralising event (Hedstrom *et al.*, 1989). In the footwall serpentinite marble and a magnetite rich calc-silicate unit occur. The magnetite rich calc-silicate unit is interpreted to be related to the mineralising process.

The magnetic characteristics of deposits of the Aggenys - Gamsberg district and the Soldiers Cap Group contrast markedly with the Broken Hill (Australia) and Zinkgruvan deposits.

The Broken Hill (South Africa) deposit contains 48% magnetite but much of this is situated in the hanging wall, in magnetite quartzite and magnetite amphibolite. The magnetite quartzite is in direct contact with the sulfide ore and contains up to 60% magnetite. Magnetite has not been described within the sulfide ore.

The Black Mountain deposit differs from the Broken Hill (SA) deposit in that economic ore lenses contain magnetite as gangue. Magnetite is present in magnetite quartzite, magnetite amphibolite and magnetite barite rock, and preferentially associated with galena rich ore, although it also occurs in galena-sphalerite ore.

Big Syncline shares some similarities with Broken Hill (Australia) and Zinkgruvan in that there is no magnetite in the ore. Sphalerite and galena occur with pyrrhotite, but it is not known if the pyrrhotite is the magnetic variety. Strongly magnetic units occur in the footwall less than 60m below the deposit and include magnetite quartzite and magnetite pyribole (pyroxene-amphibole rock). For the purpose of regional aeromagnetic interpretation the deposit is intimately associated with a strong magnetic anomaly.

The Gamsberg deposit contains pyrrhotite and magnetite in association with sphalerite-rich ore. Strongly magnetite rich units (more than 40% magnetite) also occur immediately above and below the ore.

Within the Soldiers Cap Group the Pegmont and Cannington deposits are also intimately associated with magnetite. At Cannington magnetite is preferentially associated with the high grade Pb lodes and with the low grade Zn lodes. The high grade Zn lodes have been severely overprinted by metasomatic alteration. Prior to this overprinting these lodes may have had similar magnetite compositions to the high grade Pb lodes. Hence it is possible that magnetite may have originally been equally distributed between Pb and Zn lodes.

At Pegmont the thickest Pb-Zn mineralisation is intimately associated with magnetite. There is no preferential association of magnetite with Pb or Zn within the high grade portion of the deposit.

11.3 Synthesis

The BHT stratigraphy in each of the provinces shares many similarities in magnetic properties. However the interpreter must consider the influence of variations in spatial extent, structural style, basement magnetic character and Lower Sequence magnetic character when assessing an aeromagnetic image for BHT prospectivity.

It appears that we have two classes of BHT deposits: those that are intimately associated with magnetic minerals, and those that are not. The Broken Hill (SA) deposit may provide an intermediate example where magnetite is not present in the ore but immediately overlies it. However the Broken Hill (SA) ore itself may still be magnetic if the pyrrhotite is of the magnetic variety.

BHT deposits which are not intimately associated with magnetite or magnetic pyrrhotite may still display an anomalous magnetic signature when the lateral variations along strike and characteristics of the immediate hanging wall and footwall are considered, even if the ore itself is not magnetic.

When considering implications for exploration it is important to consider whether a spectrum of BHT deposits could occur between the magnetite-rich and magnetite-poor end members. Could a BHT deposit exist which contains a low to moderate magnetic mineral content and is weakly magnetic, rather than strongly magnetic or non-magnetic? Metamorphic processes will be a siginifcant factor, but could these variations occur as a primary feature of the mineralising process? Could the deposits from the four provinces be sourced from a fluid with similar composition, with differing magnetic characteristics related to variation in conditions at the point of exhalation?

The following chapter describes thermodynamic modelling of an exhalation event, undertaken to address these questions.

12. THERMODYNAMIC MODELLING OF A BHT MINERALISING EVENT

Thermodynamic modelling of a BHT fluid was undertaken to study whether a common BHT fluid could be used to model the existing deposits. The proposition to be tested was that differences in mineralogy, particularly magnetite distribution, may be explained purely by differing pre-metamorphic mineral assemblages resulting from variations in the environment at the point of exhalation. The question of whether magnetite associated with the deposits could be primary rather than metamorphic was also of interest.

12.1 Construction of a BHT fluid

The first stage in the process was the construction of a model BHT fluid. This a difficult task as there are no primary fluid inclusion data available. Broken Hill type deposits are commonly strongly metamorphosed with later metasomatic overprinting.

Temperature, salinity, oxygen fugacity, sulfur molality and pH.

Fluid parameters to be determined in the first stage included temperature, salinity, oxygen fugacity, sulfur fugacity and pH.

The temperature of the model BHT fluid was inferred by considering the mineralogy of the deposits. The temperature of a BHT fluid is likely to be slightly lower than that of VHMS deposits, based on lower copper and magnesium content and a more distal relationship with magmatic activity. Temperatures of 250 C and 300 C were selected for the purpose of the trials.

Estimation of salinity required two parameters: the NaCl equivalent total weight percent and the ratio of NaCl : KCl : $CaCl_2$. Two salinity ratios were used.

The first ratio (DC) chosen was 8.16 : 1 : 1. This ratio was obtained from Cooke (1993) and is based on data from a number of modern geothermal systems.

The second ratio (SS) was obtained from data on the Salton Sea geothermal system (Barnes, 1979; Mc Kibben and Elders, 1985; McKibben *et al.* 1988). It was considered that the Salton Sea geothermal system is the closest modern analogue to a likely BHT fluid in terms of the tectonic setting and stratigraphy. Examples of published Salton Sea brine compositions are presented in Tables 12.1 to 12.4. The Salton Sea ratio used was 5.03 : 1.31 : 3.04. The Salton Sea fluids contain considerably more $CaCl_2$ than the ratio used by Cooke (1993).

Trials were conducted for fluids with salinities of 10, 15 and 25 wt% equivalent NaCl. The 25 wt% salinity may seem high, but was obtained from salinity estimates of the Salton Sea brines presented in Tables 12.1 to 12.4.

Constituent	Shallow (well B-1R)	Deep (well S2-14)
Na	15,000	52,700
Ca	2,500	26,500
K	2,500	16,500
Fe	86	1,550
Mn	60	1,390
Zn	11	506
SiO_2	255	>475
Sr	112	405
NH_4	103	336
B	92	253
Ba	45	194
Li	55	190
Pb	3	95
Mg	54	36
Cu	nd	6
Cd	nd	2
As	nd	5
Cl	31,000	154,000
Br	24	99
SO_4	53	110
H_2S	nd	7
CO_2	10,100	1,660
Total dissolved solids	62,100	257,000
Flow zone depth	950 m	1,870 m
Flow zone temperature	240°C	305°C

Data from Williams and McKibben (1988) and Williams (unpub.); concentrations in ppm; concentrations of Ba and SO_4 may be too high due to contamination by drilling fluids; analyses have been corrected for steam loss during flashing to yield true downhole concentrations; nd = no data

Table 12.1 Chemical compositions of Salton Sea Brines. (McKibben and Elders, 1985)

	IID 1	IID 1	IID 2	State of California 1	Woolsey 1	Magmamax 1
	Skinner et al. (1967)[1]	White (1968)[1]	Helgeson (1968)[1]	Helgeson (1968)[1]	Palmer (1975) (maximum ppm values from Magma Power Co.)[2]	Palmer (1975)[2]
Zn	790	540	500	500	—	—
Pb	84	102	80	80	—	—
Cu	8	8	3	2	—	—
Ag	0.8	1.4	2	<1	—	—
Fe	2,090	2,290	2,000	1,200	244	93
Mn	1,560	1,400	1,370	950	488	200
Na	50,400	50,400	53,000	47,800	49,729	52,500
Ca	28,000	28,000	27,800	21,200	12,658	25,000
K	17,500	17,500	16,500	14,000	6,510	5,000
Li	215	215	210	180	90	—
Cl	155,000	155,000	155,000	127,000	83,183	—
SO_4	5	5.4	30 (total S)	—	—	—
Sulfide S	16	16		30	—	—
Silica	400	400	400	—	181	500
pH	5.2	5.2	4.64	—	6.25	6.65
TDS	258,360	~250,000	258,769	219,500	151,237	>100,000
S.G.	—	—	—	—	1.106	1.022
BHT	316°C	340°C	332°C	305°C	238°C	265°C

	Magmamax 1	Woolsey 1	Sportsman 1	Sinclair 4
	Needham et al. (1980) (Average of Jan. 1977 tests)	Needham et al. (1980) (Average chemical analyses Feb. 1977)	Palmer (1975)[2]	Palmer (1975)[2]
Zn	290[3]	—	—	600
Pb	44	—	—	60
Cu	0.5	—	—	3
Ag	0.8	—	—	1
Fe	280	235	4,200	1,300
Mn	635	—	—	1,700
Na	38,300	40,000	70,000	78,000
Ca	21,100	16,700	34,470	37,735
K	10,400	9,100	24,000	20,690
Li	150 to 200[3]	140	150	400
Cl	128,700	99,000	201,757	210,700
SO_4	—	—	34	75
Sulfide S	—	—	—	—
Silica	239[3]	—	5	625
pH	5.5	5.44	4.82 to 6.10	5.0
TDS	>200,000	>150,000	334,987	387,500
S.G.	—	—	1.207	—
BHT	—	200°C	310°C	260°C

All compositions are given in ppm unless otherwise noted; not all analyzed constituents are listed

[1] Known to be corrected for steam loss

[2] Not known if corrected for steam loss

[3] Concentrations from samplings in 1976

TDS = total dissolved solids in ppm by wt; S.G. = specific gravity at 20° to 25°C; BHT = bottom hole temperature; — = not reported

Table 12.2 Analyses of typical shallow, low salinity and deep, hypersaline brines from the eastern Salton Sea geothermal field. (McKibben et al, 1988)

Location	Complex-Forming			Species (molalities)		Metals (ppm)				
	ΣCl	ΣSO_4	$-\Sigma S^{2-}$	ΣNH_3	ΣCO_3	Zn	Pb	Cu	pH at T°C	
Ore Deposits[a]										
Creede, Colo.[b]	0.9-1.9	0.02-0.3	$10^{-3.8}$-$10^{-3.7}$	—	—	$10^{-2.8}$	$10^{-3.3}$ (Fe: 1)	$10^{-2.8}$	5.4	250
Darwin, Cal.[c]	>4.3	~0.01	—	—	0.15 ± 0.06	<7700	—	740	4.8-6.7	350
Yatani, Japan[d]	0.1-0.2	10^{-6}-10^{-10}	$\sim 10^{-2}$	—	—	—	—	—	~6	250
Providencia, Mex.[e]	0.03->4.3	<0.7	—	—	—	220-890	—	<70-530	—	300
Echo Bay, N.W.T.[f]	~7	10^{-2}-10^{-3}	—	—	1 to 0.1		(Ag: 0.1-1.)		4.2 ± .5	200
Kuroko Deposits, Japan[g]	0.4-1.5	—	$<10^{-1.7}$	—	—	—	—	—	5.5 ± .5	250
Pasto Bueno, Peru[h]	0.4 to 3.5								—	175-290
Tribag, Ontario[i]	—	$<H_2S$	10^{-2}-10^{-3}	—	—				—	—
Messina, S. Africa[i]	—								—	—
S. W. Wisconsin, U.S.[j]	4.2->5.1	—	$>10^{-3}$	—	0.03-0.9	8700	~500	400	6.0 ± .3	150
Eureka, Col.[k]	0.1-0.6	$10^{-2.2}$	$10^{-1.4}$	—	0.01-0.2	>1-<1000	>1-<1000	(Au 10^{-2}-10^{-3})	4.3-5.9	300
Geothermal Fluids										
El Tatio, Chile[m]	0.2	—	$10^{-3.7}$	$10^{-3.9}$	$10^{-1.1}$	—	—	—	—	263
									7	25
Imperial Valley[n]										
Salton Sea, Cal.	2.4	$<10^{-4.0}$	$10^{-3.7}$	$10^{-1.5}$	$10^{-3.0}$	380	70	3	—	240
									6.1	25
Cerro Prieto, Mex.	0.3	$10^{-3.8}$	—	—	$10^{-3.0}$	—	—	—	—	100
									7.9	25
Cheleken, U.S.S.R.[o]	3.1	$10^{-2.8}$	$10^{-4.0}$	—	$10^{-2.4}$	0.19	3.6	0.9	5.5	54
	2.9	$10^{-2.5}$	—	—	$10^{-3.4}$	2.3-4.7	3.6	0.8	5.4	80
Central Miss. U.S.A.[p]	5.9	—	—	$10^{-2.1}$		124	6.8			158
Eastern Kansas, U.S.A.[q]	6.0	$10^{-1.9}$	$10^{-2.9}$	$10^{-3.0}$	$10^{-2.4}$	.06	1.7	.14	7.03	~20
	4.0	$10^{-2.9}$	$10^{-2.2}$	$10^{-3.4}$	$10^{-2.2}$	.13	1.1	<.1	6.88	~20

[a] Where sufficient data are available, the concentrations of the ore-depositing stage were selected.
[b] A vein deposit of Ag-Pb-Zn-Cu-Au in volcanics (Barton et al., 1977).
[c] A contact metasomatic Pb-Zn-Ag deposit in skarn (Rye et al., 1974).
[d] Pb-Zn and Au-Ag veins in volcanics (Hattori, 1975).
[e] Pb-Zn pipes in carbonates (Rye and Haffty, 1969).
[f] Vein deposit of U-Ni-Ag-Cu (Robinson and Ohmoto, 1973).
[g] Urabe (1974).
[h] Vein deposit of W-Cu-Zn-Pb (Landis and Rye, 1974; Norman, et al., 1976).
[i] Cu breccia pipe deposit (Norman, et al., 1976).
[j] Mississippi-Valley type Zn-Pb deposits (McLimans, 1977).
[k] Au-Ag-Pb-Zn-Cu-Cd veins in volcanics in stage 4 mineralization (Casadevall and Ohmoto, 1977).
[l] These are selected for their relatively high concentrations of metals and/or sulfide. Other examples are given by White in the first edition and in Chapters 13 and 15 of this edition.
[m] Cusicanqui et al. (1976).
[n] Wells sampled are Magmamax No. 1 near the Salton Sea and No. M-5 at Cerro Prieto (Phillips et al., 1977; Rimstidt and Barnes, 1977; and unpublished data).
[o] Analyses are of fluids from an upper, H_2S-rich aquifer and a lower, metal-rich aquifer. Metallic sulfides precipitate where they mix, either in surface tanks or by natural subsurface circulation. A general range of metal contents is 0.2-5.4 ppm Zn and 2-77 ppm Pb (Lebedov, 1967, 1972).
[p] Norphlet brine of the Pelahatchie oil Field (Carpenter et al., 1974).
[q] The upper analyses are for oil field brine from the Arbuckle Formation and the lower from the Viola Formation (McClure, 1973).

Table 12.3 Chemical compositions of hydrothermal solutions. (Barnes, 1979)

	Modern solutions			Ancient solutions		
Element	1	2	3	4	5	6
Cl	155,000	157,000	158,200	87,000	46,500	295,000
Na	50,400	76,140	59,500	40,400	19,700	152,000
Ca	28,000	19,708	36,400	8,600	7,500	4,400
K	17,500	409	538	3,500	3,700	67,000
Sr	400	636	1,110	—	—	—
Ba	235	—[a]	61	—	—	—
Li	215	7.9	—	—	—	—
Rb	135	1.0	—	—	—	—
Cs	14	0	—	—	—	—
Mg	54	3,080	1,730	5,600	570	—
B	390	—	—	<100	185	—
Br	120	526.5	870	—	—	—
I	18	31.7	—	—	—	—
F	15	—	—	—	—	—
NH_4	409	—	39	—	—	—
HCO_3^-	>150	31.9	—	—	—	—
H_2S	16[b]	0	—	—	—	—
SO_4^{2-}	5	309	310	1,200	1,600	11,000
Fe	2,290	14.0	298	—	—	8,000
Mn	1,400	46.5	—	450	690	—
Zn	540	3.0	300	10,900	1,330	—
Pb	102	9.2	80	—	—	—
Cu	8	1.4	—	9,100	140	—

[a] Not determined.
[b] Sulfide present; all S reported as H_2S.

Concentrations in ppm. 1 = Salton Sea geothermal brine (Muffler and White, 1969); 2 = Cheleken geothermal brine (Lebedev and Nikitina, 1968); 3 = oil field brine, Gaddis Farms D-1 well, Lower Rodessa reservoir, central Mississippi, 11,000 ft (Carpenter et al., 1974); 4 = fluid inclusion in fluorite, Cave-in-Rock District, Ill. (Roedder et al., 1963); 5 = fluid inclusion in sphalerite, OH vein, Creede Colo., recalculated by Skinner and Barton (1973); 6 = fluid inclusions, core zone at Bingham Canyon (Roedder, 1971).

Table 12.4 Compositions of modern and ancient hydrothermal solutions. (Barnes, 1979)

Predominance area diagrams were calculated for carbon species (Figure 12.1), kaolinite-muscovite-K feldspar (Figure 12.2) and iron species (Figure 12.3) in order to select oxygen fugacity, sulfur molality and pH.

VHMS systems typically contain sulfur molalities of the order of 0.001. BHT systems are inferred to be relatively sulfur poor as base metals remain in sufficient quantities to precipitate as oxides and other non-sulfide species after all sulfur is consumed. Reducing the sulfur molality by an order of magnitude from the typical VHMS molality resulted in an incursion of hematite into the pyrite field (Figure 12.3 (d)). Molality was increased from 0.0001 to 0.00025 resulting in the disappearance of this incursion. This value of 0.00025 molal was then adopted as the sulfur molality for the model BHT fluid.

Oxygen fugacity was determined using the predominance diagrams for carbon and iron species. Oxygen fugacity was chosen to produce a slightly reduced fluid. The fluid was positioned in the upper part of the magnetite field to avoid dropping into the pyrite field too quickly with decreasing temperature, and to avoid the graphite field.

A pH of one unit acid was selected, placing the fluid in the just into the calcite stability field. This pH plots in the muscovite predominance field for most of the fluids, with the 25 wt% salinity fluid just entering the K feldspar stability field.

The resulting suite of fluids generated for trial are summarised in Table 12.5.

Fluid Code	Salinity Ratio	Salinity (wt%) (NaCl, KCl, $CaCl_2$)	wt% NaCl equiv.	Temperature °C	log fO_2	S (molal)	pH
DC10_1	DC	8.16, 1, 1	10	250	-36.5	0.00025	4.58
DC15_1	DC	12.24, 1.5, 1.5	15	250	-36.5	0.00025	4.58
DC10_2	DC	8.16, 1, 1	10	300	-33.0	0.00025	4.65
DC15_2	DC	12.24, 1.5, 1.5	15	300	-33.0	0.00025	4.65
SS10_1	SS	5.03, 1.31, 3.04	10	250	-33.0	0.00025	4.58
SS15_1	SS	7.54, 1.96, 4.56	15	250	-36.5	0.00025	4.58
SST_1	SS	12.8, 3.34, 7.76	25	250	-36.5	0.00025	4.58
SS10_2	SS	5.03, 1.31, 3.04	10	300	-36.5	0.00025	4.65
SS15_2	SS	7.54, 1.96, 4.56	15	300	-33.0	0.00025	4.65
SST_2	SS	12.8, 3.34, 7.76	25	300	-33.0	0.00025	4.65

Table 12.5 Summary of Suite of Theoretical BHT Fluids Generated For Thermodynamic Modelling

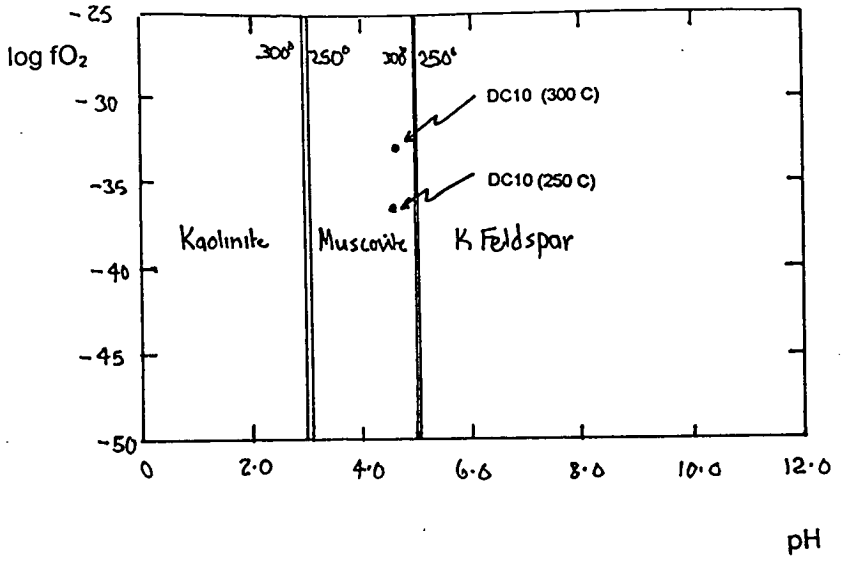

A. Salinity ratio DC, 10 wt. % eq. NaCl

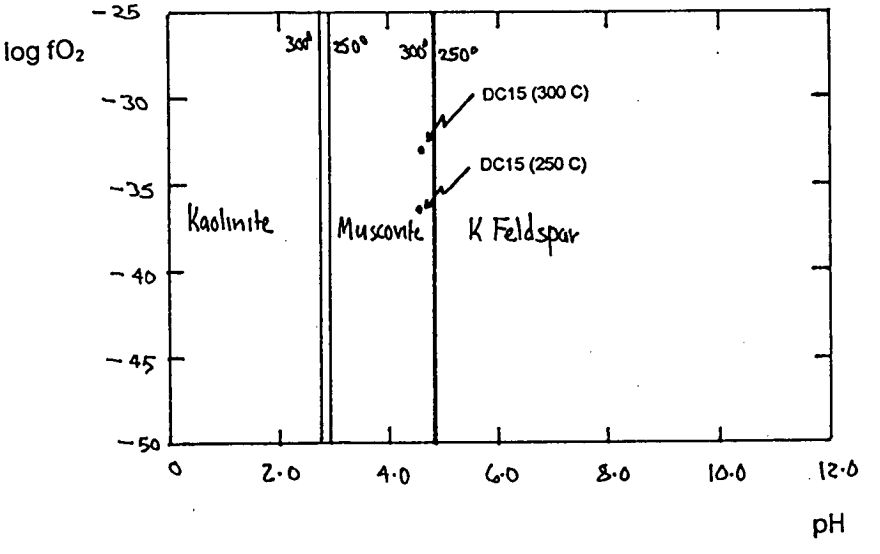

B. Salinity ratio DC, 15 wt. % eq. NaCl

Figure 12.1 Predominance area diagram, showing stability fields for kaolinite, muscovite and k-feldspar.

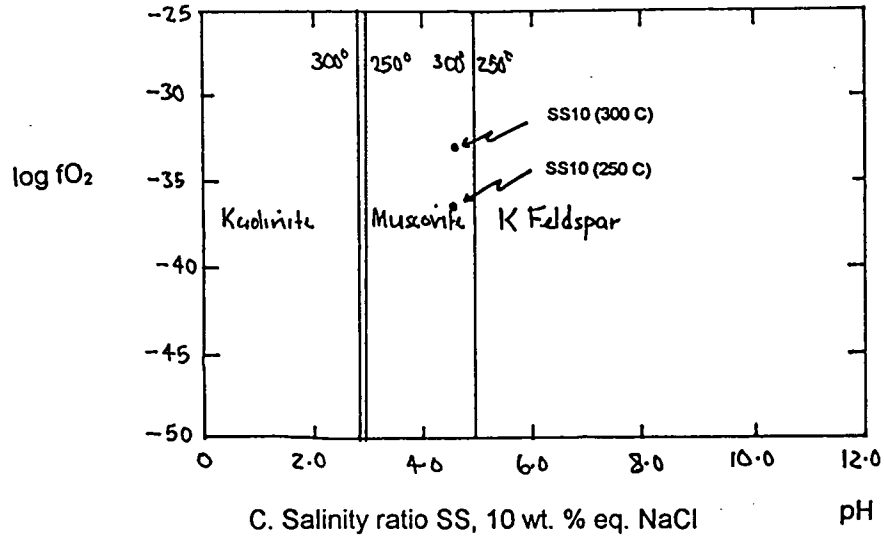

C. Salinity ratio SS, 10 wt. % eq. NaCl

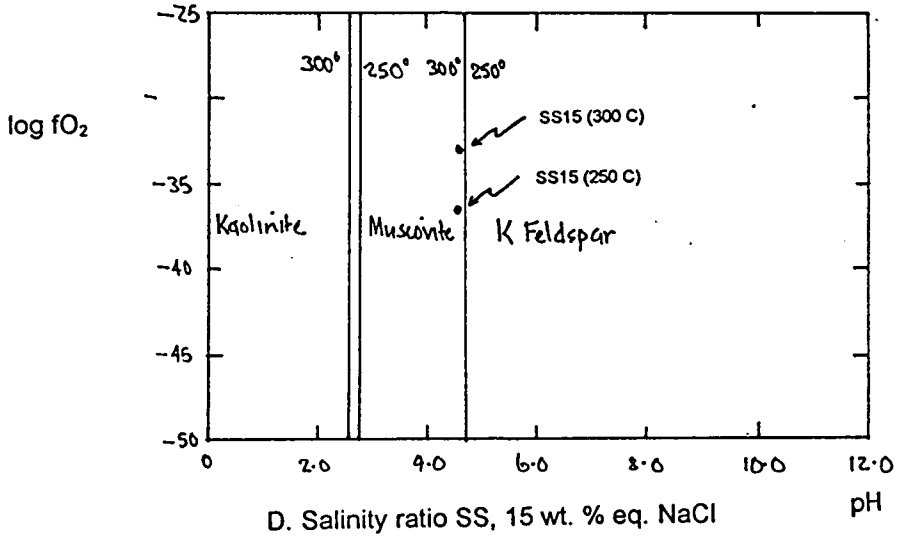

D. Salinity ratio SS, 15 wt. % eq. NaCl

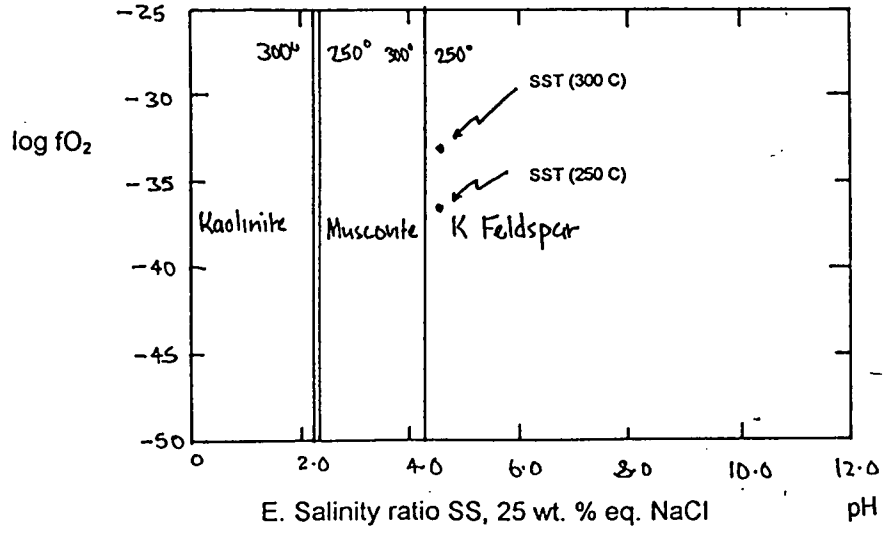

E. Salinity ratio SS, 25 wt. % eq. NaCl

Figure 12.1 Predominance area diagram, showing stability fields for kaolinite, muscovite and k-feldspar.

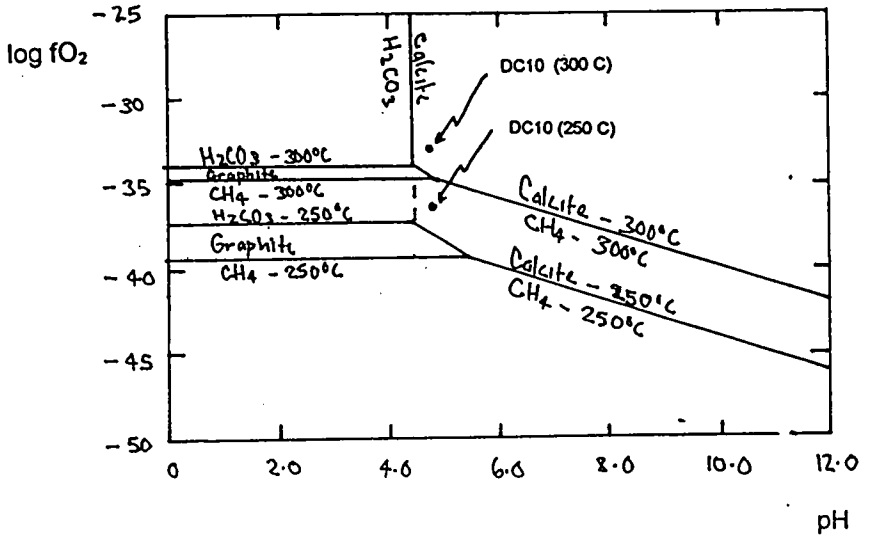

A. Salinity ratio DC, 10 wt. % eq. NaCl

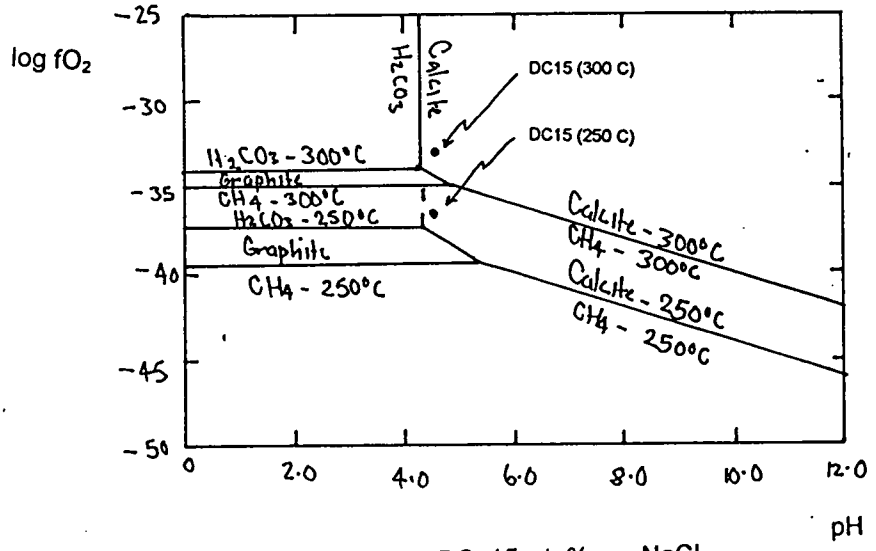

B. Salinity ratio DC, 15 wt. % eq. NaCl

Figure 12.2 Predominance area diagram, showing stability fields for calcite, graphite, methane and carbon species.

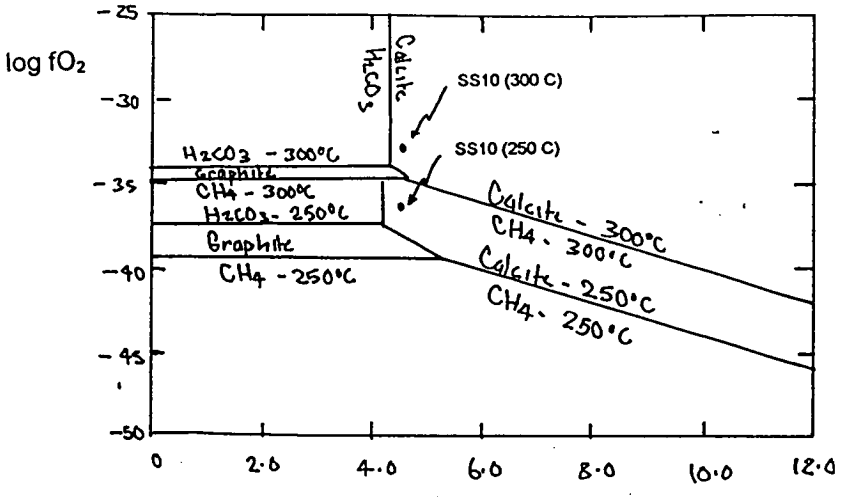

C. Salinity ratio SS, 10 wt. % eq. NaCl

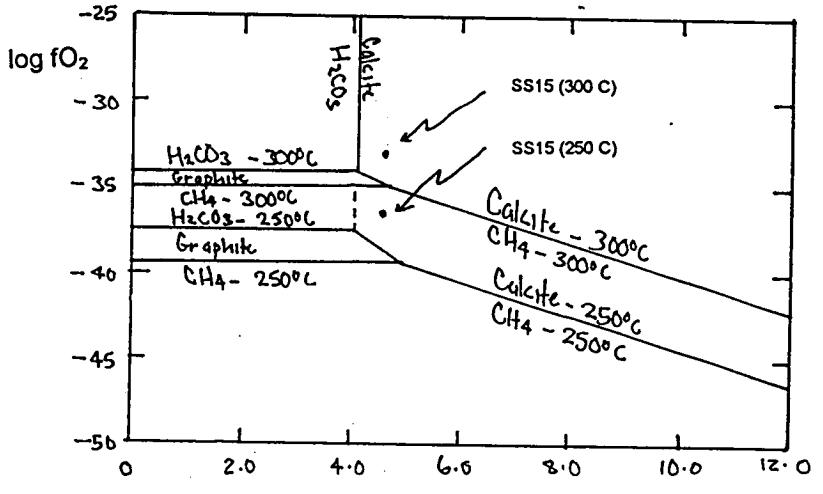

D. Salinity ratio SS, 15 wt. % eq. NaCl

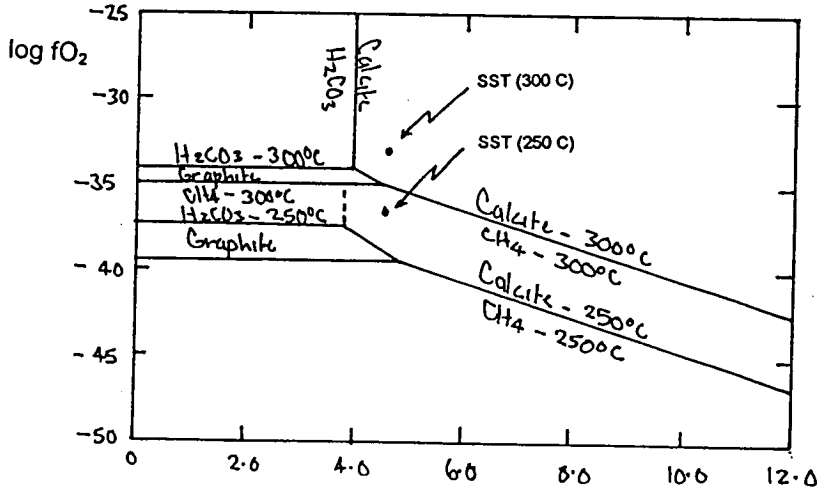

E. Salinity ratio SS, 25 wt. % eq. NaCl.

Figure 12.2 Predominance area diagram, showing stability fields for calcite, graphite, methane and carbon species.

A. **Temperature = 300°C; a(ΣS) = 0.0015**

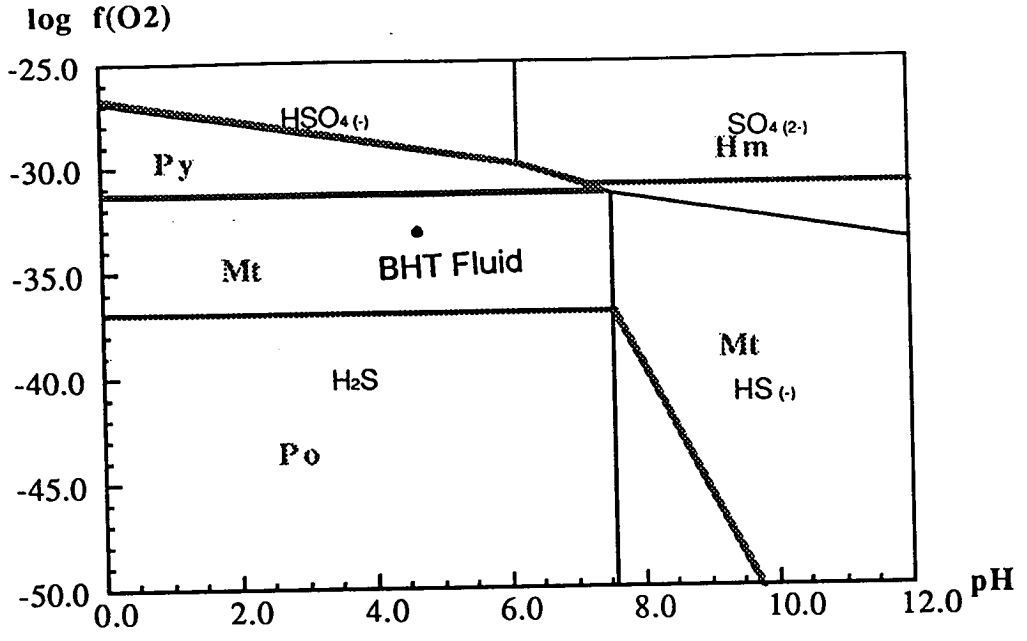

B. **Temperature = 300°C; a(ΣS) = 0.0010**

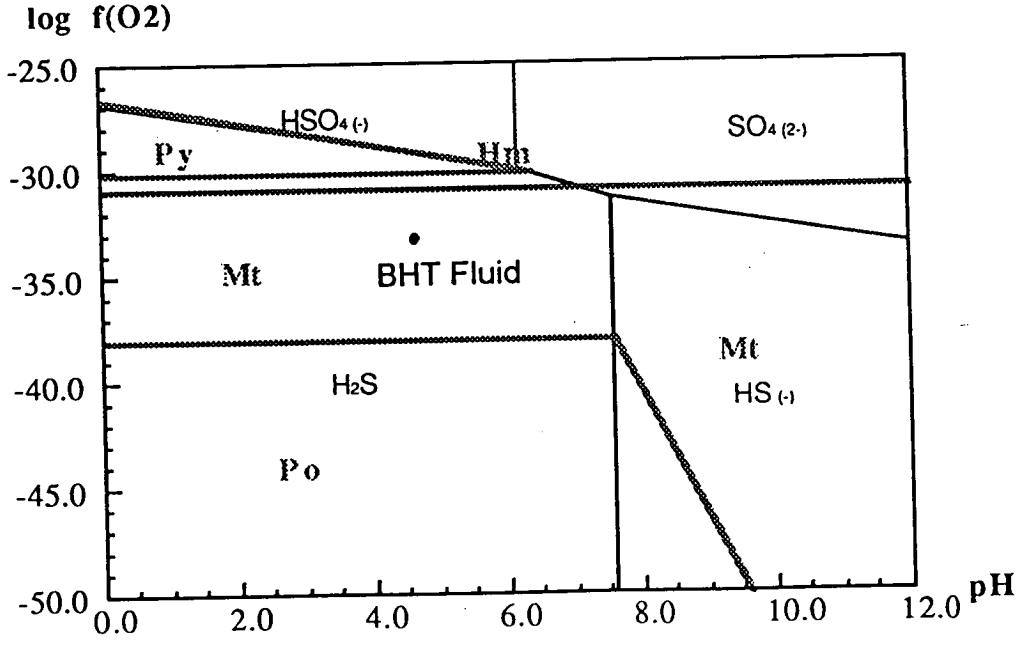

Figure 12.3 Stability fields of Fe-oxides and sulfides at 300°C as a function of oxygen fugacity and pH .

C. Temperature = 300°C; a(ΣS) = 0.0001

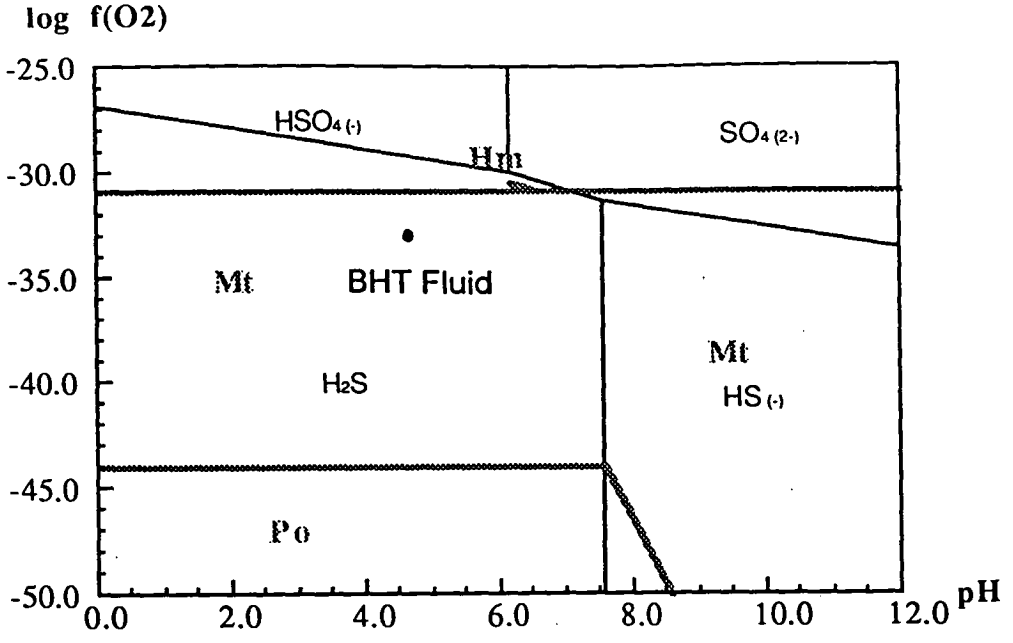

D. Temperature = 300°C; a(ΣS) = 0.00025

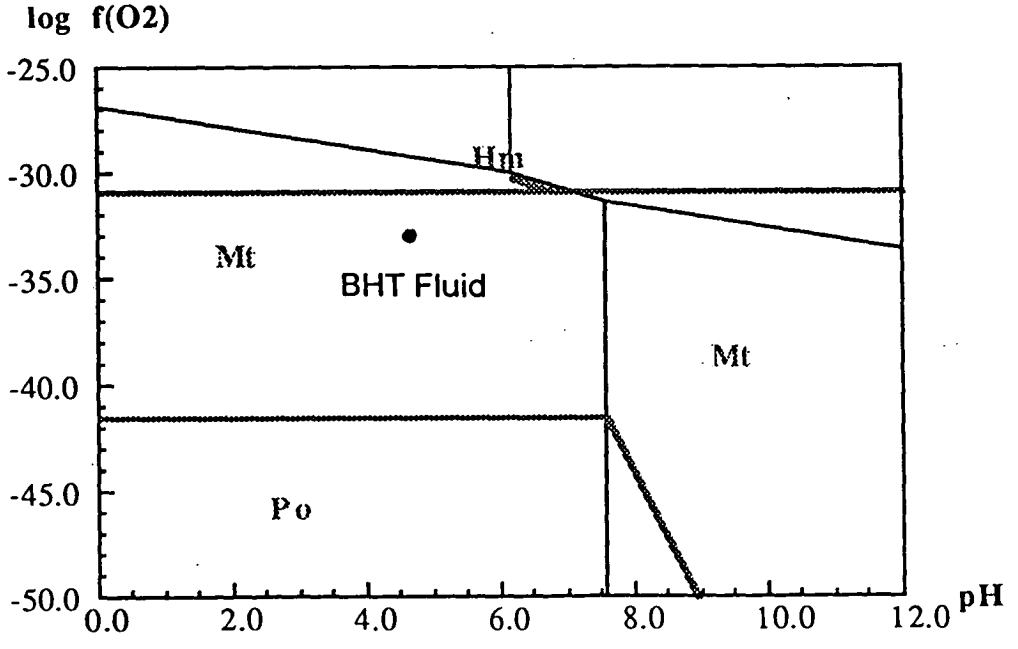

Figure 12.3 Stability fields of Fe-oxides and sulfides at 300°C as a function of oxygen fugacity and pH .

A. **Temperature = 250°C; a(ΣS) = 0.0015**

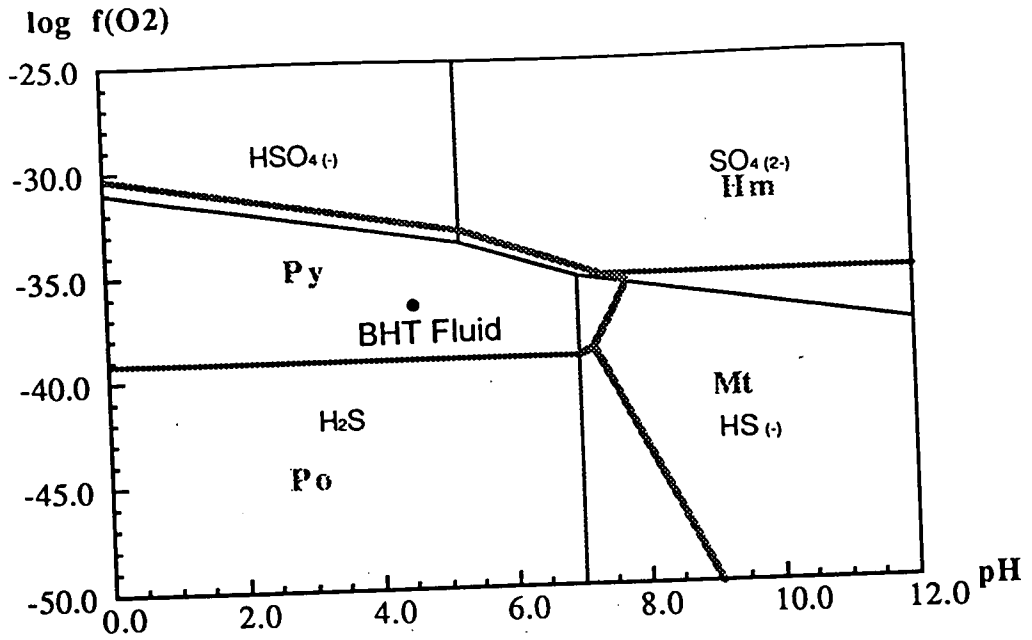

B. **Temperature = 250°C; a(ΣS) = 0.0010**

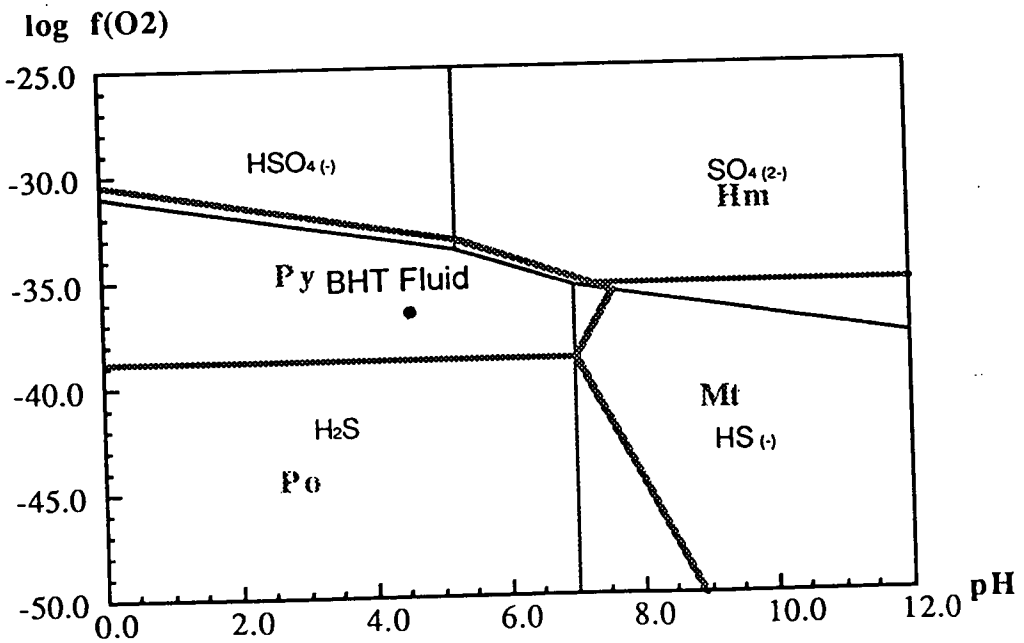

Figure 12.4 Stability fields of Fe-oxides and sulfides at 250°C as a function of oxygen fugacity and pH .

C. **Temperature = 250°C; a(ΣS) = 0.0001**

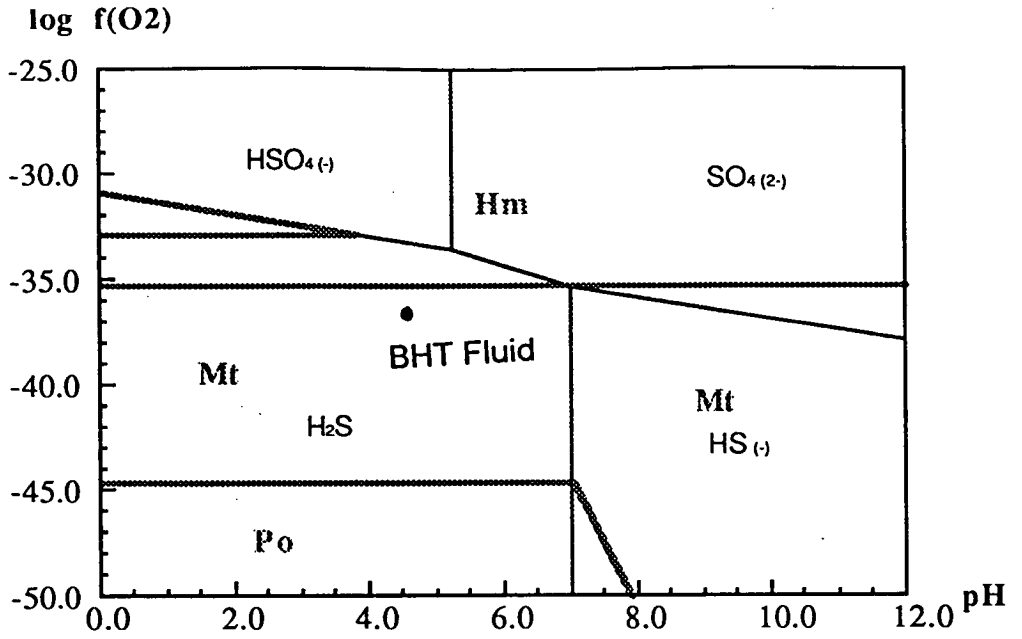

D. **Temperature = 250°C; a(ΣS) = 0.00025**

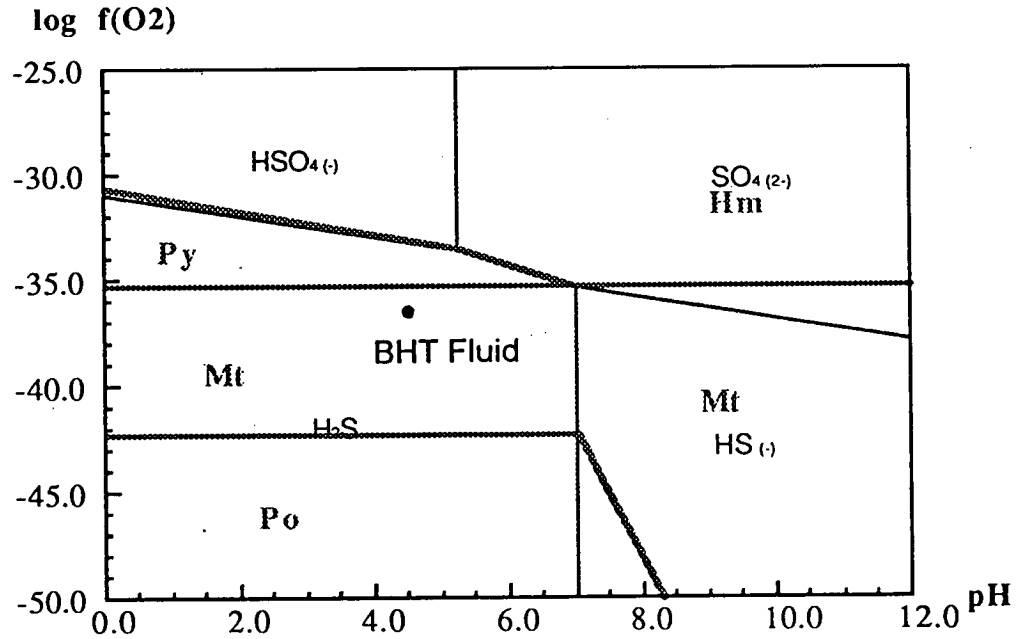

Figure 12.4 Stability fields of Fe-oxides and sulfides at 250°C as a function of oxygen fugacity and pH .

Component Elements and Concentrations

The next stage involved the determination of component elements and their concentrations. It was desirable to limit the suite of elements as far as possible to optimise the computer simulation. The following elements were chosen for inclusion in the fluid, after studying the mineralogy of Broken Hill Type deposits:

H, O, Cl, S, Si, Al, Ca, Mg, Fe, K, Na, Mn, Zn, Cu, Pb, Ag, Au, Ba, F, P

The fluid was created using the program SOLVEQ (Spycher and Reed, 1990b). This program allows the user to specify temperature, salinity, pH, oxygen fugacity, sulfur molality and CO_2 molality. Additional chemical components were then added one by one to the brine. Mineral equilibrium was forced, after each addition, within SOLVEQ. Occasionally a component was too soluble (Mn, Ba), causing the program to crash. That component was then limited to a value obtained from the composition of Salton Sea brines.

The resulting fluids were saturated with respect to SiO_2, Al^{3+}, Ca^{2+}, Mg^{2+}, Fe^{2+}, Zn^{2+}, Cu^{2+}, Pb^{2+}, Ag^{+}, $AuCl_2^{-}$, Ba^{2+}, F^{-} and HPO_4^{2-}.

Compositions of the fluids, in terms of molality and parts per million (ppm), are presented in Appendix B.

An interesting feature observed was the change in saturation concentrations of component species after each addition of a new species in SOLVEQ. The most significant change involved aluminium and fluorine. The concentration of Al^{3+} dissolved in the fluid increased by two orders of magnitude after the addition of F^{-}.

Another important feature to note is the amount of metal that these fluids are capable of transporting. Concentrations of base and precious metals are presented for each of the fluids in Table 12.6. The Salton Sea brine concentrations are included for comparison.

The ore forming window is generally thought to be 1 to 10 ppm for base metals and 0.3 to 1 ppm for gold (Cooke, pers. com., 1993). While Au lies below the ore forming window (as expected for a BHT deposit) it is clear that the concentrations of base metals in the fluids listed in Table 12.6 above far exceed the range of the ore forming window.

The upper limit of the ore forming window has been positioned because of concerns that a fluid which can carry more than 10 ppm may run into a source rock problem. The fluid may then be critically undersaturated, requiring a very efficient deposition mechanism (Cooke, pers.com., 1994).

Fluid Code	Temp (°C)	Salinity (wt% eq. NaCl)	Zn^{2+} (ppm)	Pb^{2+} (ppm)	Cu^{2+} (ppm)	Ag^{+} (ppm)	$AuCl_2^-$ (ppb)
DC10_1	250	10	148	74.5	0.199	6.49	.32
DC15_1	250	15	372	189	0.420	14.7	.27
DC10_2	300	10	3380	2290	21.8	53.6	.026
DC15_2	300	15	8180	5670	37.7	172.3	.035
SS10_1	250	10	108	52.6	.194	4.63	.23
SS15_1	250	15	342	173	.388	13.8	.28
SST_1	250	25	1590	788	1.09	102	.33
SS10_2	300	10	3250	2190	21.1	53.5	.027
SS15_2	300	15	9260	6410	41.4	254	.041
SST_2	300	25	24950	17250	122	3460	.058
Salton Sea	305	25 (approx.)	506	95	6	N/A	N/A

Table 12.6 Base and Precious Metal Compositions of Trial Fluids.

12.2 Computer Simulations of Cooling, Boiling and Mixing with Oxidised and Reduced Seawater

Once the fluid composition was balanced using SOLVEQ, the program CHILLER was used to model mineral precipitation due to cooling, boiling and fluid mixing during exhalation.

Cooling simulations involved cooling the BHT fluid from its initial temperature (250°C or 300°C) down to 20°C in 5 °C steps. Boiling simulations involved allowing the fluid to boil as the temperature was reduced by 5°C steps from the initial temperature (250°C or 300°C) to 100°C.

Fluid mixing simulations involved adding small amounts of oxidised or reduced seawater to the BHT fluid. The compositions of the oxidised and reduced sea water are listed in Table 12.7. These compositions were obtained by Cooke (1993) from Drever (1994 - oxidised sea water) and Huston (pers.com. 1993 - reduced seawater, largely Black Sea data).

Results of boiling, cooling, and oxidised and reduced seawater mixing for the 10 variations of a BHT fluid listed in Table 12.1 are summarised in the spreadsheets and graphs in Appendices C and D respectively.

Results - Cooling

Results of the cooling simulation are presented in Appendices C and D. The results for fluid SS15 at 250°C and 300°C were reasonably typical and are presented in Figures

	Oxidised seawater	Anoxic seawater
pH	8.02	7.50
log $f_{(O_2)}$	-2.71	-76.40
H^+	0.001	0.101
H_2O	1 kg	1 kg
Cl^-	15205.8	21306.1
SO_4^{-2}	2726.2	80.8
HCO_3^-	142.8	27.9
HS^-	-	9.7
$SiO_{2\ (aq)}$	0.503	-
Al^{+3}	0.0009	-
Ca^{+2}	120.9	411.1
Mg^{+2}	11.9	1286.7
Fe^{+2}	4.22 E-08	4.23 E-11
K^+	401.1	379.1
Na^+	10821.9	10741.6
Mn^{+2}	0.0002	0.269
Zn^{+2}	0.002	0.000006
Cu^+	0.0005	0.003
Pb^{+2}	0.00003	5.63 E-14
Ag^+	0.00004	-
$AuCl_2^-$	0.000005	-
Ba^{+2}	0.002	1.50 E-07
$O_{2\ (aq)}$ *	0.101	-

Modern-day oxidised and anoxic seawater compositions used in the mixing simulations (note the difference in oxygen fugacities for the two waters). All concentrations expressed as ppm, with the exception of H_2O (kg). The composition of oxidised seawater is taken from Drever (1984). Note that the seawater analysis as originally published is supersaturated with respect to muscovite, hematite, calcite and dolomite at 5°C. Consequently, the concentrations of K^+, Fe^{+2}, Ca^{+2} and Mg^{+2} have been reduced to 90% of saturation levels. Anoxic seawater composition compiled by D. Huston (pers. commun., 1993), mostly from data on the Black Sea.

Table 12.7 Compostions of oxidised and reduced seawater. (Cooke, 1993)

12.5 and 12.6. The precipitation sequence for the entire suite of fluids is summarised in Table 12.8 .

Cooling was not generally an effective mechanism for precipitating iron oxides, particularly at low temperature and low salinity. Nor was it effective in precipitating sphalerite. At higher salinities and temperatures only gold, silver, bornite and acanthite were precipitated.

Results - Boiling

A complete set of results is presented in Appendices C and D. Results from fluid SS15 are presented in Figures 12.7 and 12.8. Results for the entire suite of fluids are summarised in Table 12.9 .

Boiling was very effective in producing primary magnetite, together with chamosite and hematite. The only base metal to be precipitated was copper, in the form of bornite and chalcocite, and this was a rare occurrence. Fluorite and quartz were precipitated proximally, with muscovite being precipitated in the intermediate region.

Results - Oxidised Fluid Mixing

A complete set of results is presented in Appendices C and D. Results from fluid SS15 are presented in Figures 12.9 and 12.10 to provide a representative example. Results for the entire suite of fluids are summarised in Table 12.10.

Mixing with oxidised sea water was effective in precipitating chamosite, hematite and pyrite, but not magnetite. Once again Cu was the major base metal precipitated, in the form of chalcocite. Galena was precipitated only by lower salinity, 300°C fluids. Barite precipitated proximally, anhydrite precipitated in the intermediate zone and kaolinite and gibbsite precipitated distally. Muscovite precipitated distally for the 250°C SS fluids, and both proximally and distally for the higher temperature fluids.

The SST fluids showed similar behaviour to the lower salinity fluids. The most notable exceptions were the precipitation of magnetite and fluorite for SST at 250°C, and the disappearance of clinochlor from the precipitation sequence.

Results - Reduced Fluid Mixing

A complete set of results is presented in Appendices C and D. Results from fluid SS15 are presented in Figures 12.11 and 12.12. Results for the entire suite of fluids are summarised in Table 12.11.

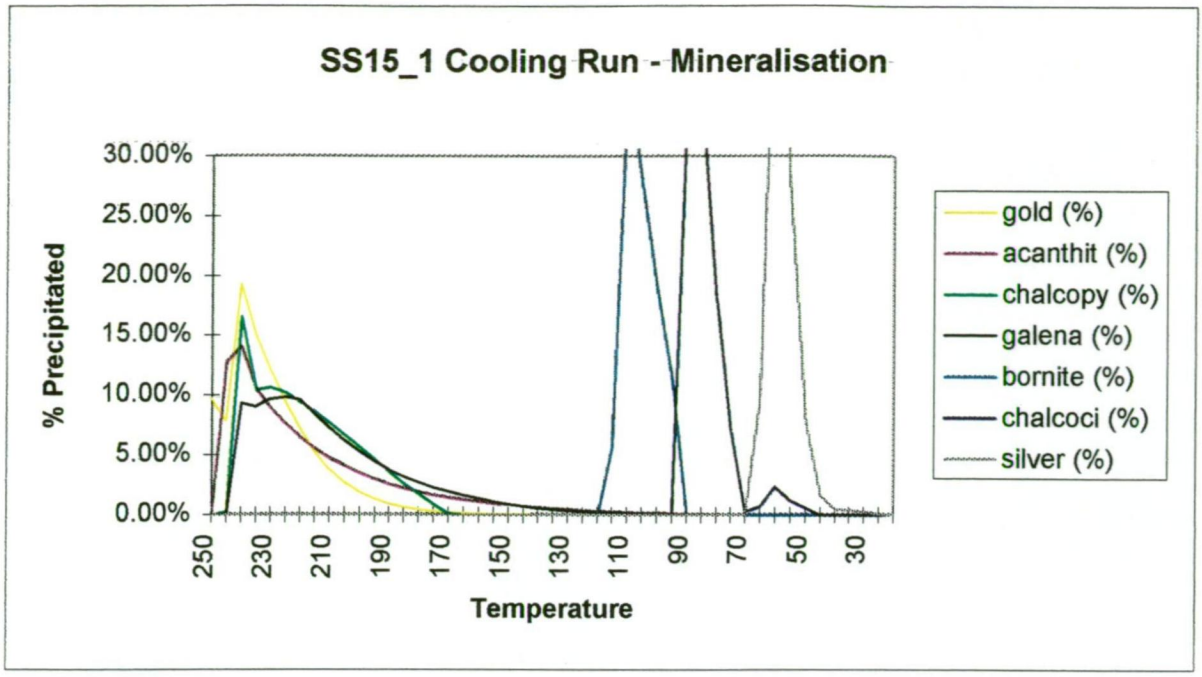

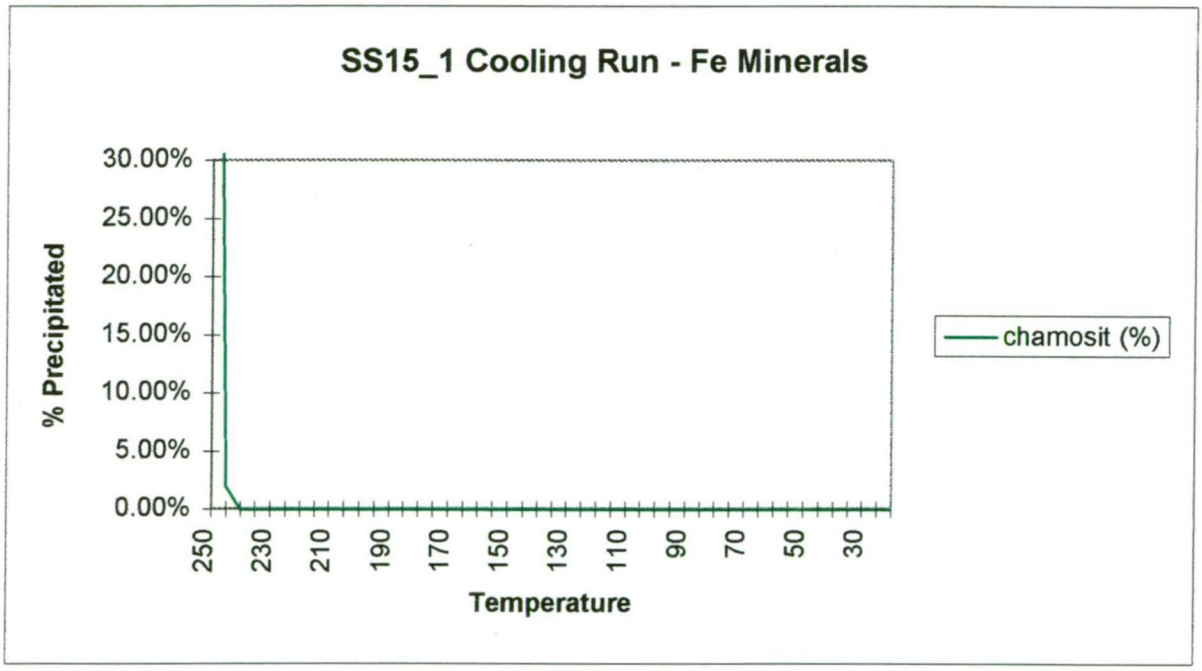

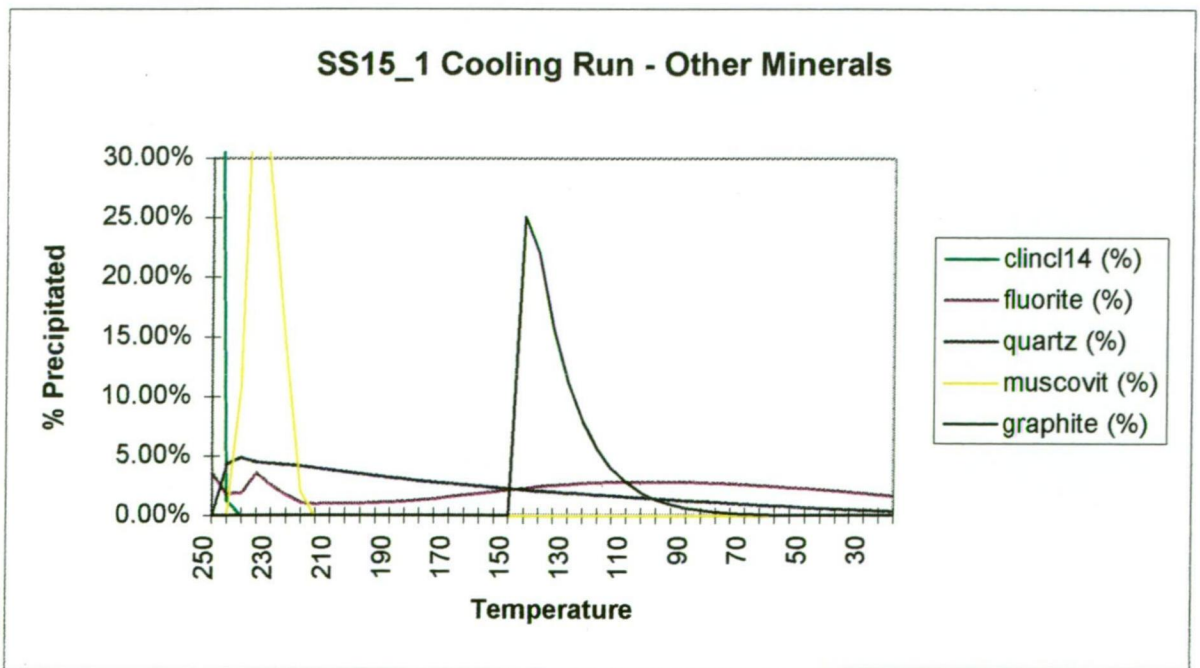

Figure 12.5 Mineral precipitation from Fluid SS15 during cooling from 250°C to 20°C in steps of 5°C

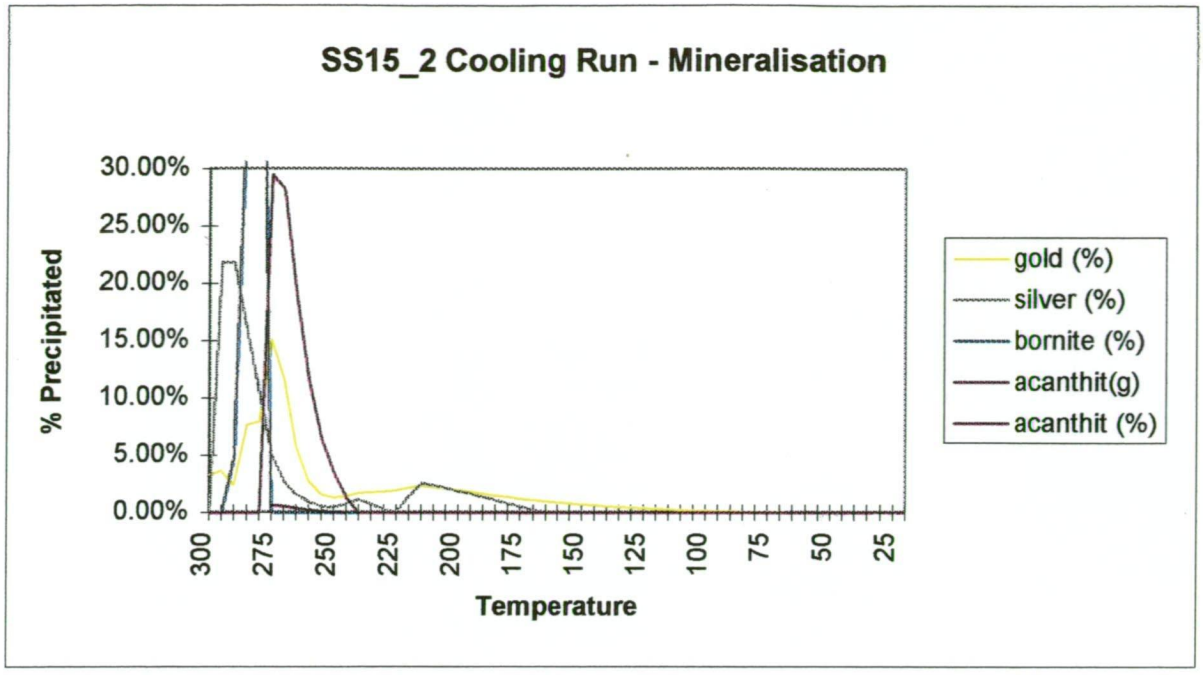

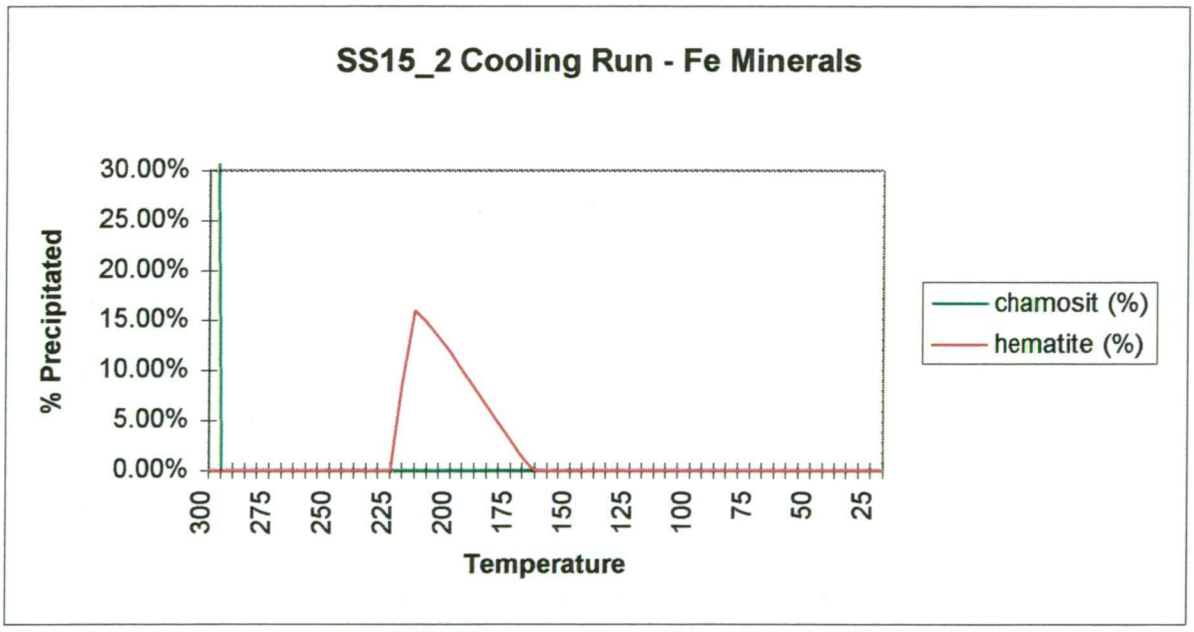

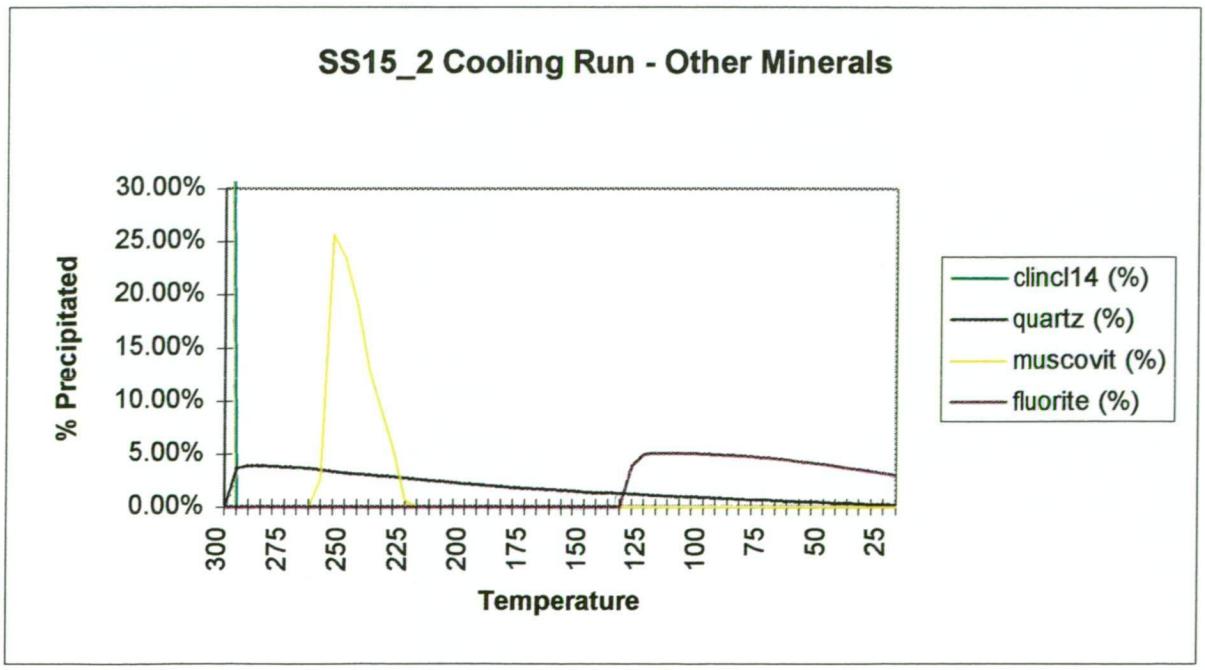

Figure 12.6 Mineral precipitation from Fluid SS15 during cooling from 300°C to 20°C in steps of 5°C

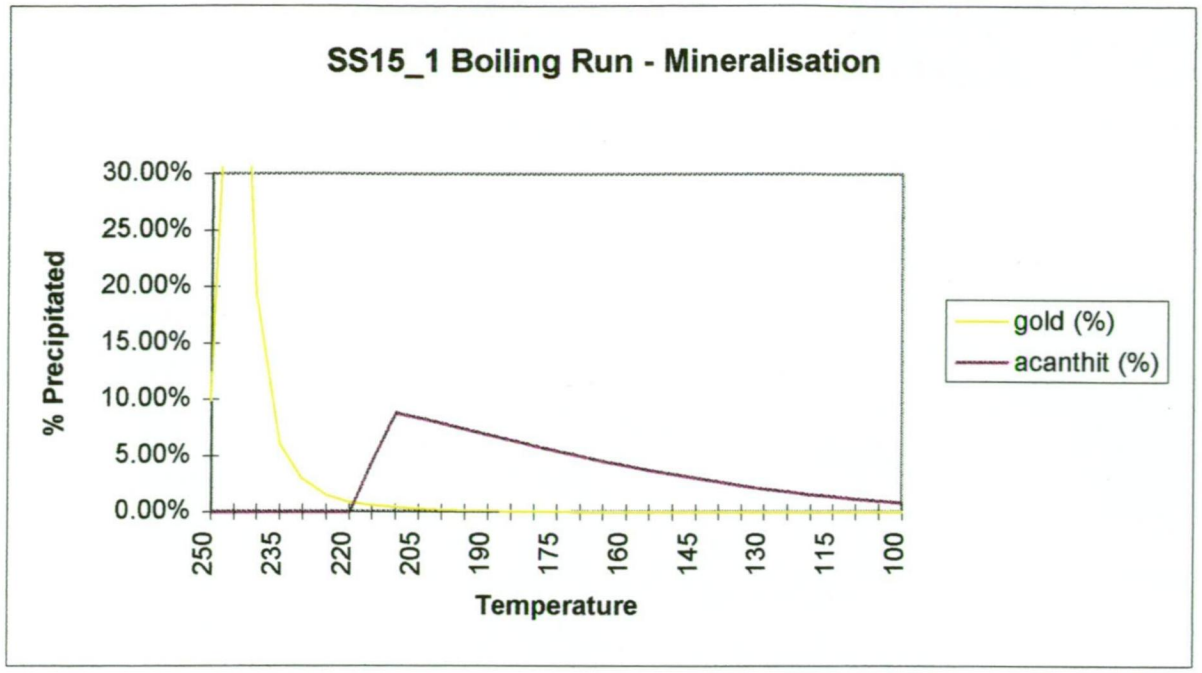

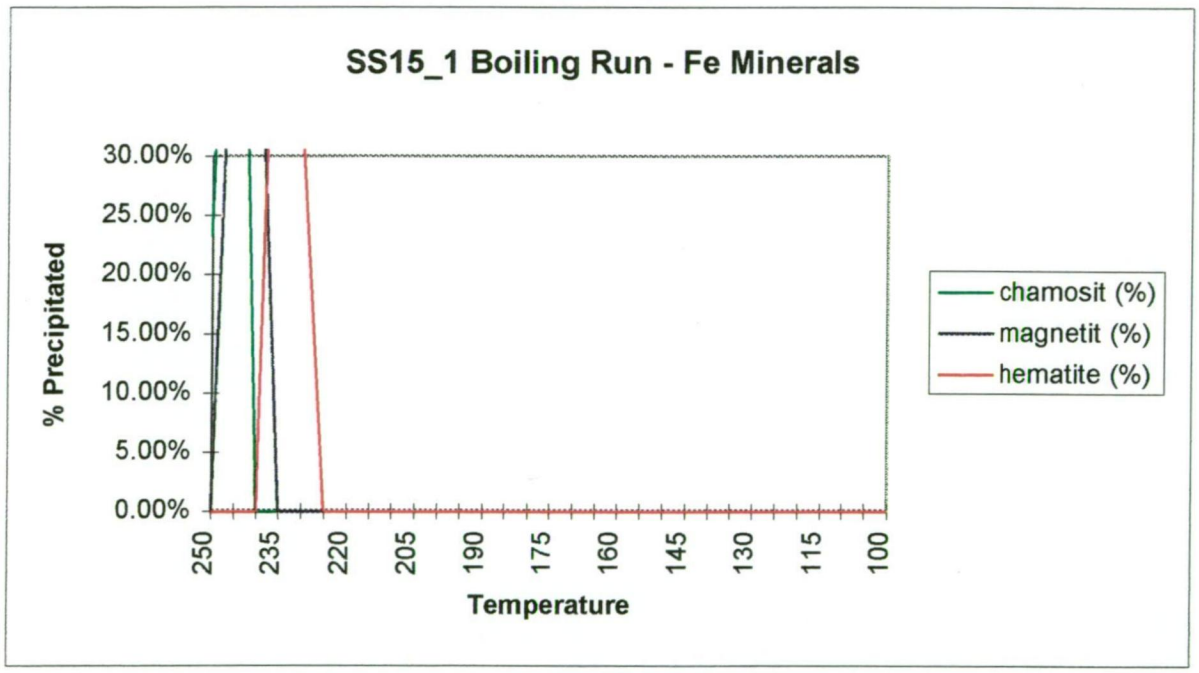

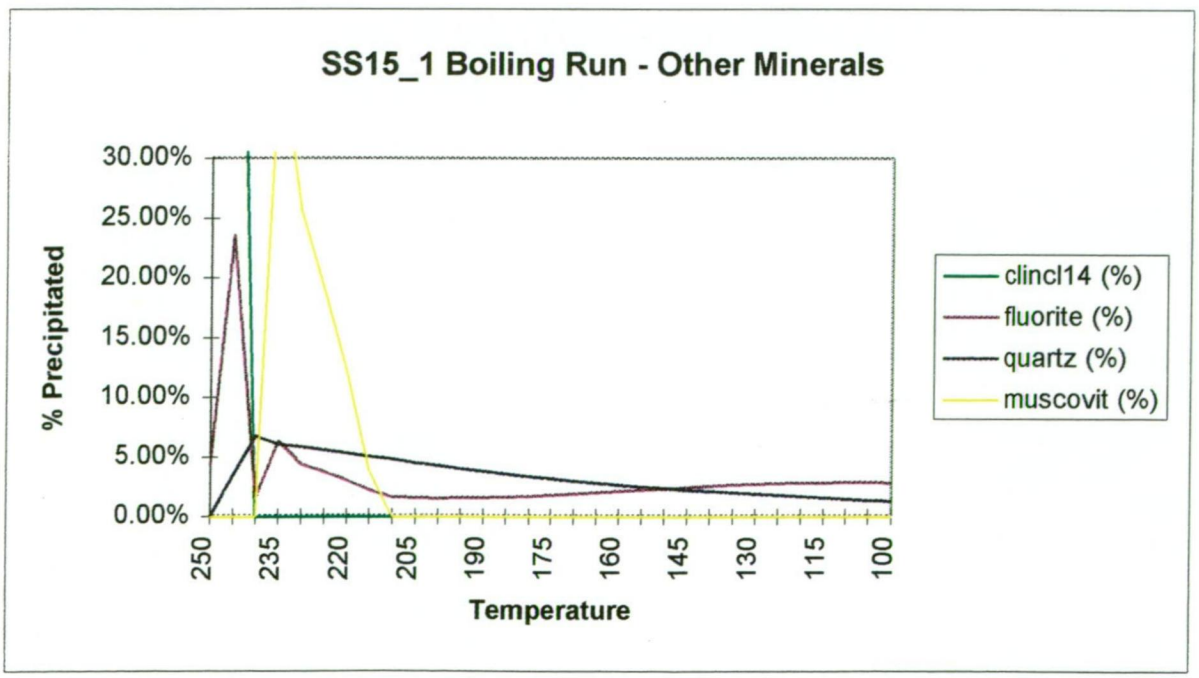

Figure 12.7 Mineral precipitation from Fluid SS15 during boiling from 250°C to 100°C in steps of 5°C

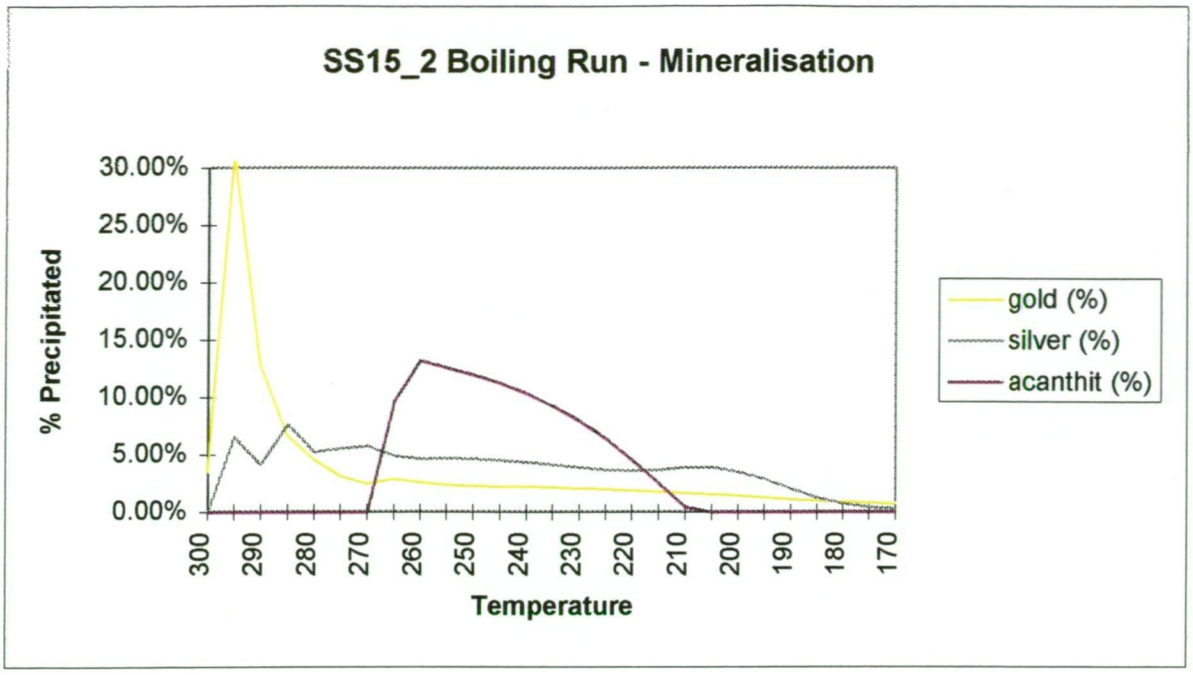

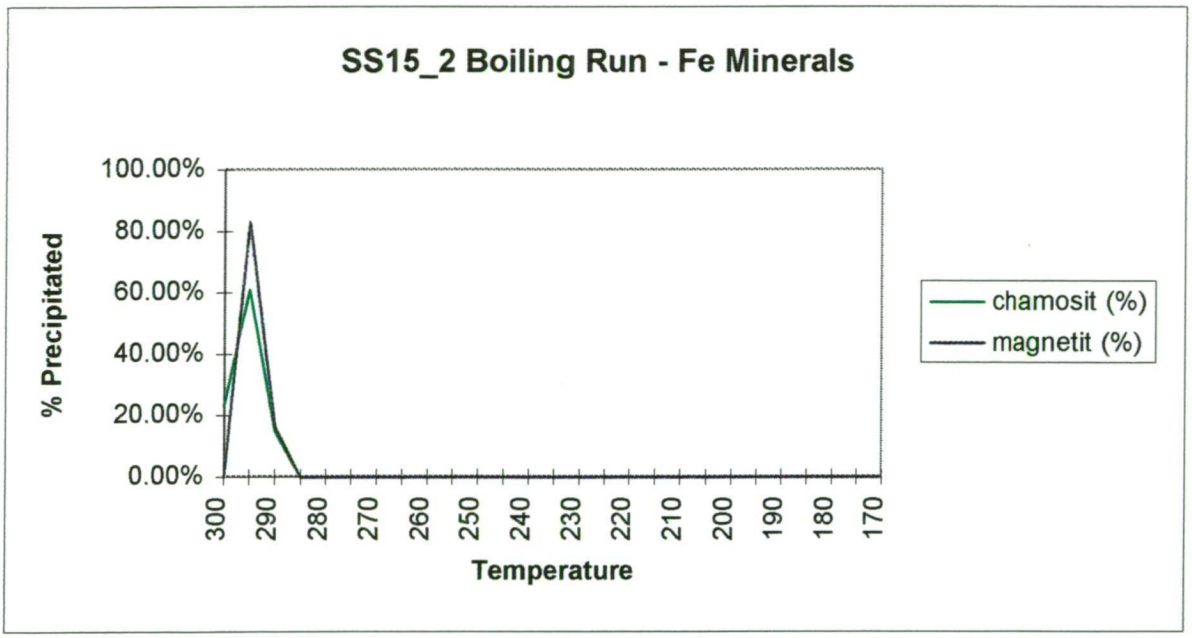

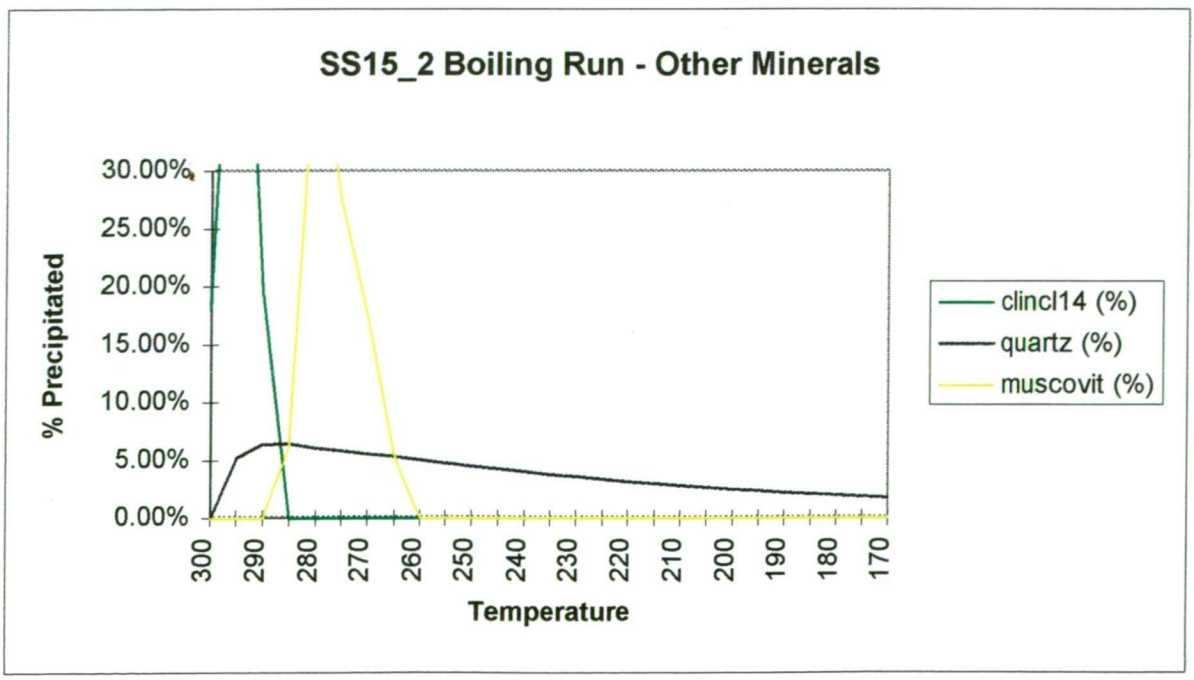

Figure 12.8 Mineral precipitation from Fluid SS15 during boiling from 300°C to 100°C in steps of 5°C

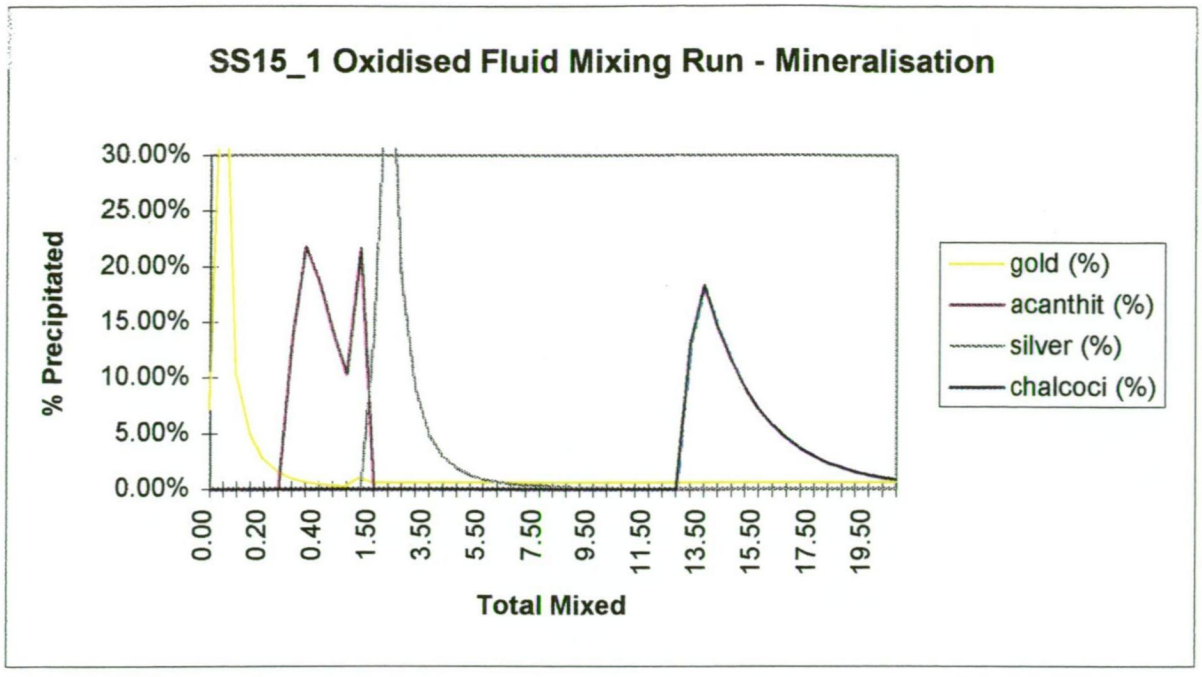

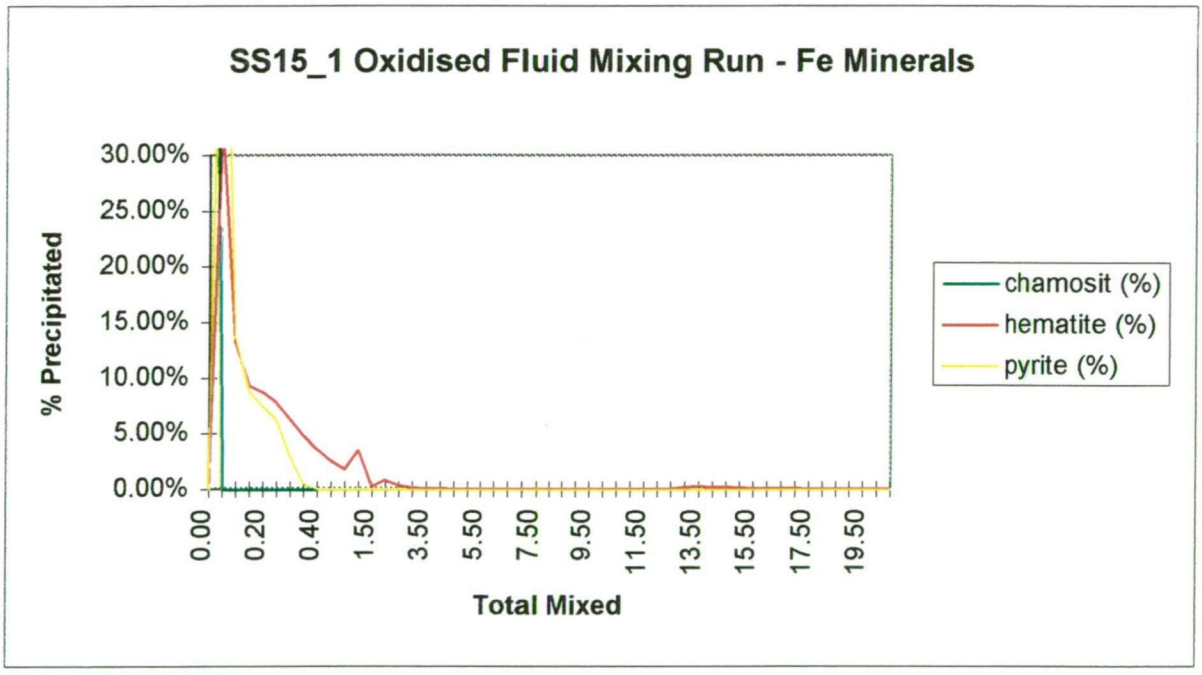

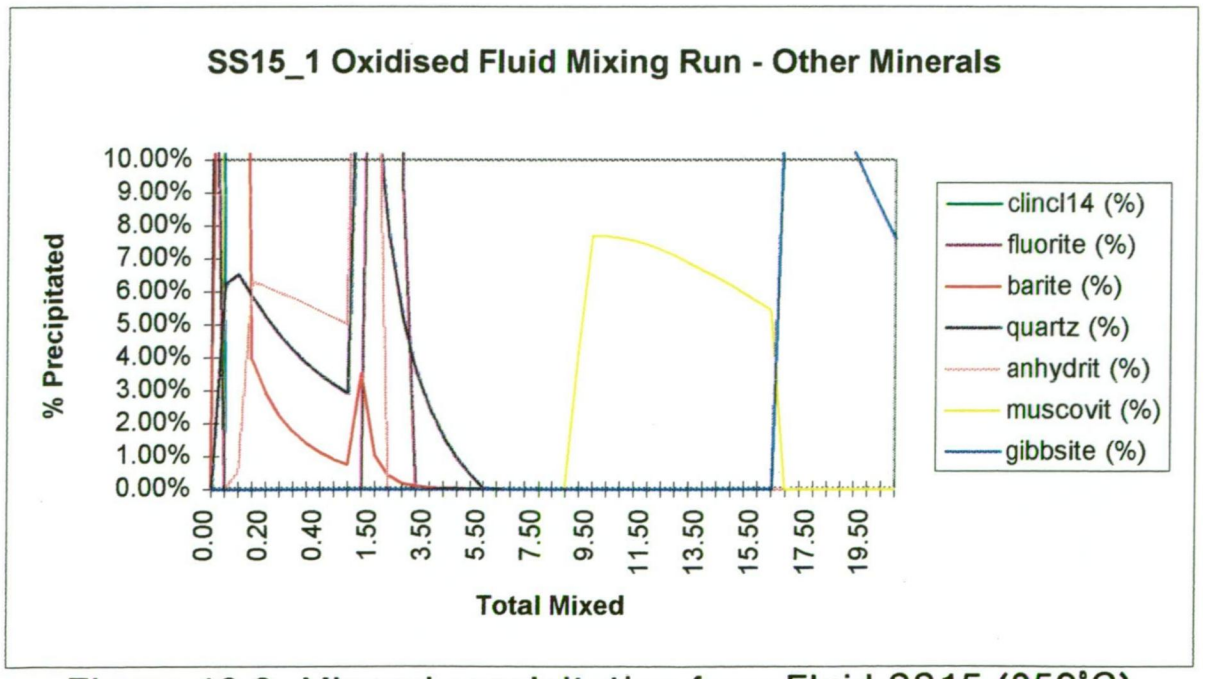

Figure 12.9 Mineral precipitation from Fluid SS15 (250°C) during oxidised fluid mixing

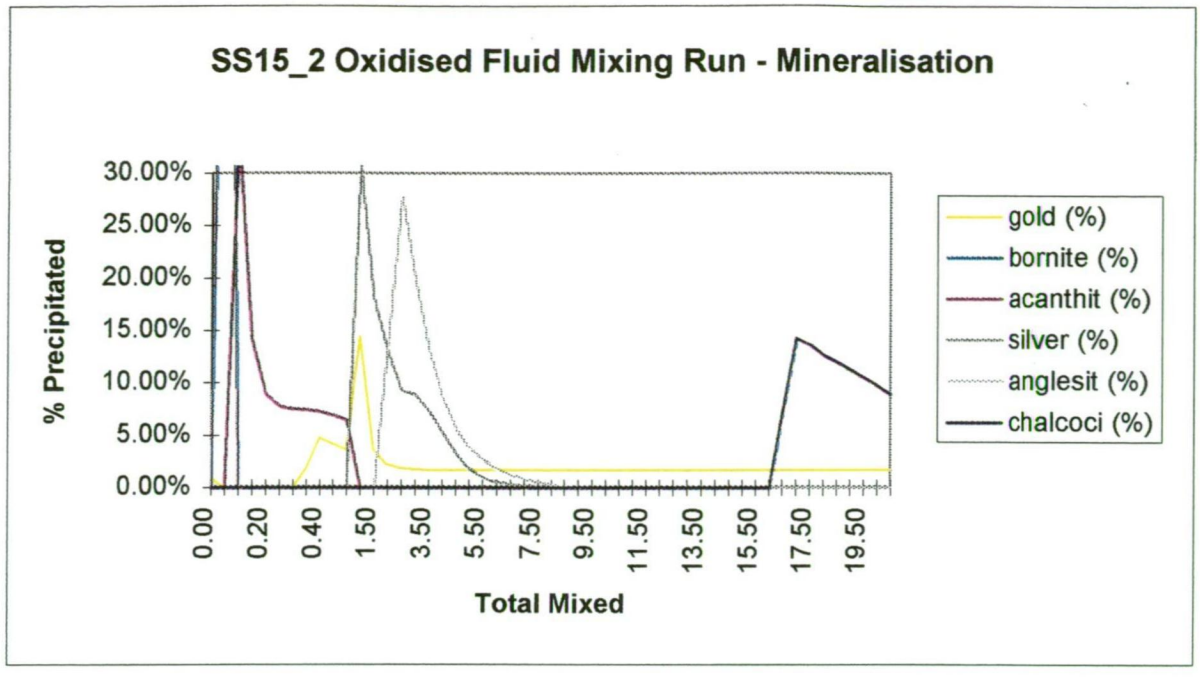

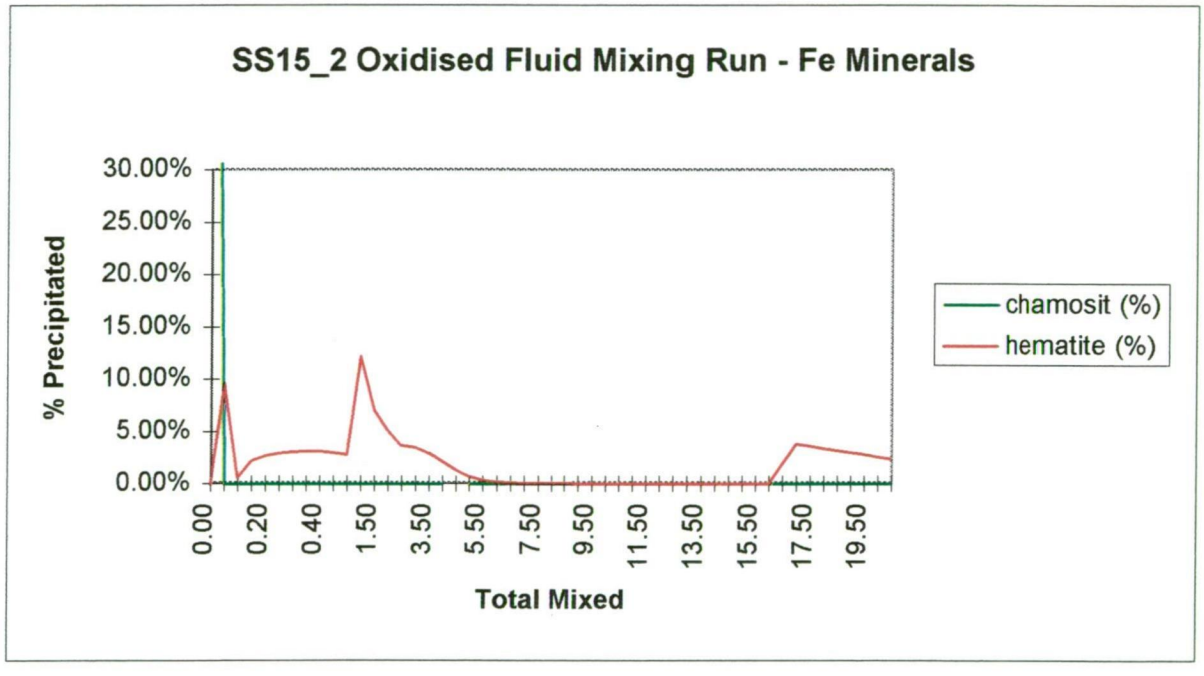

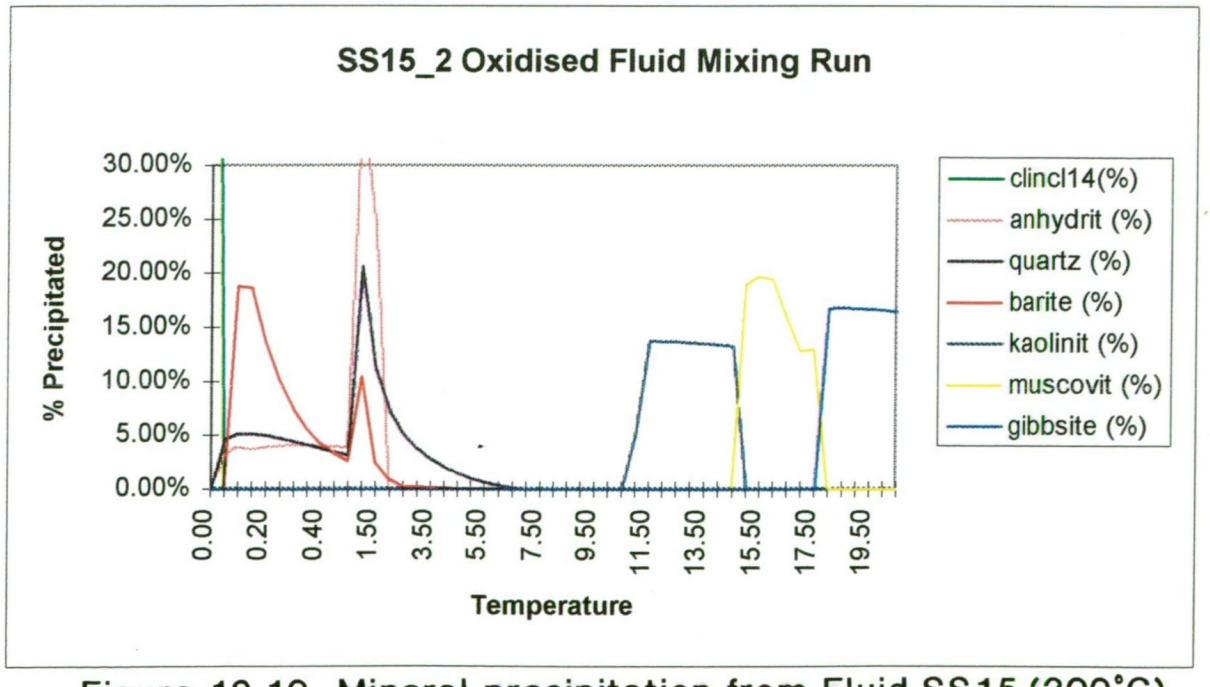

Figure 12.10 Mineral precipitation from Fluid SS15 (300°C) during oxidised fluid mixing

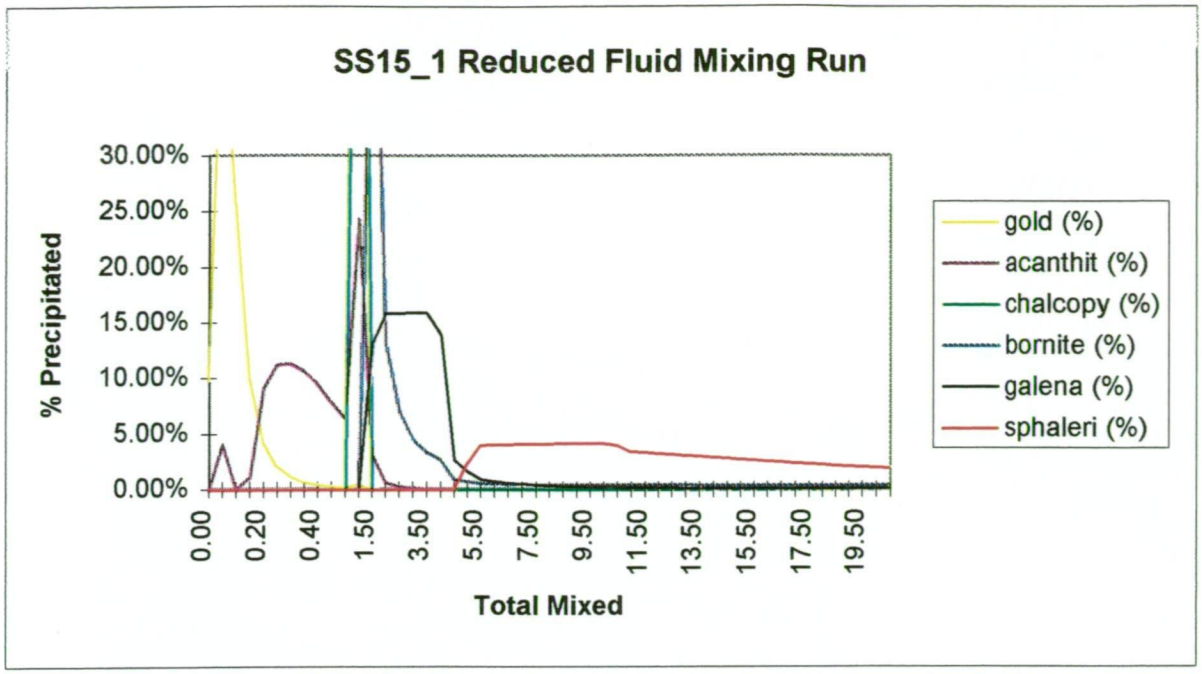

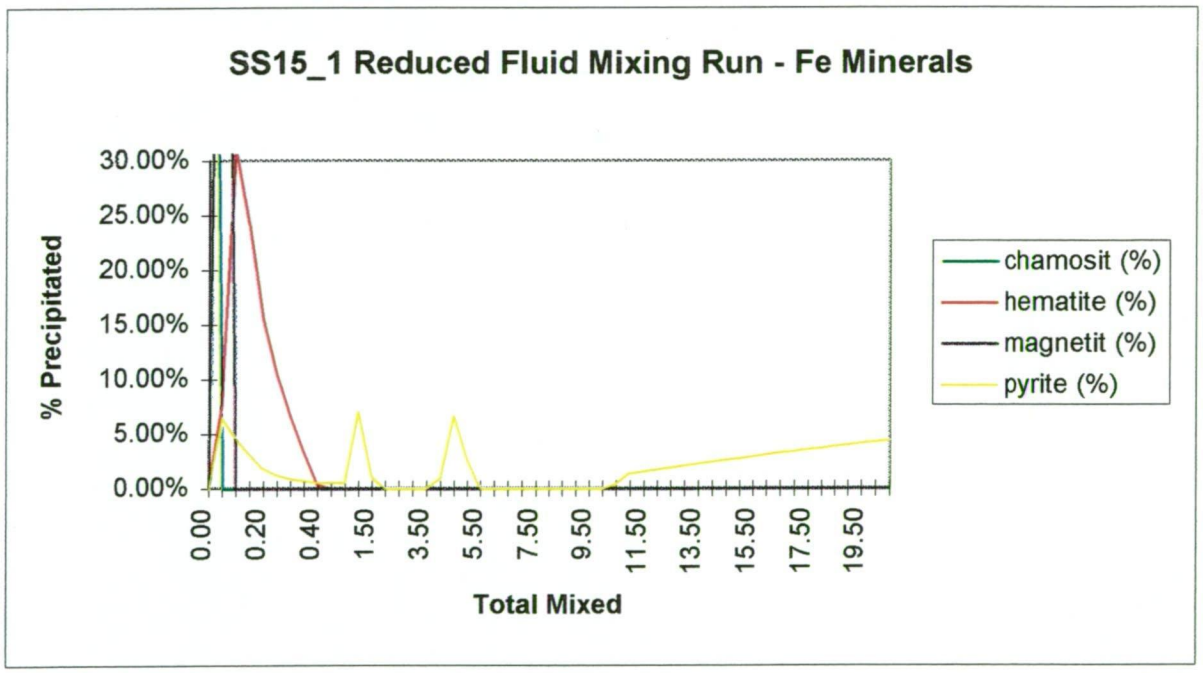

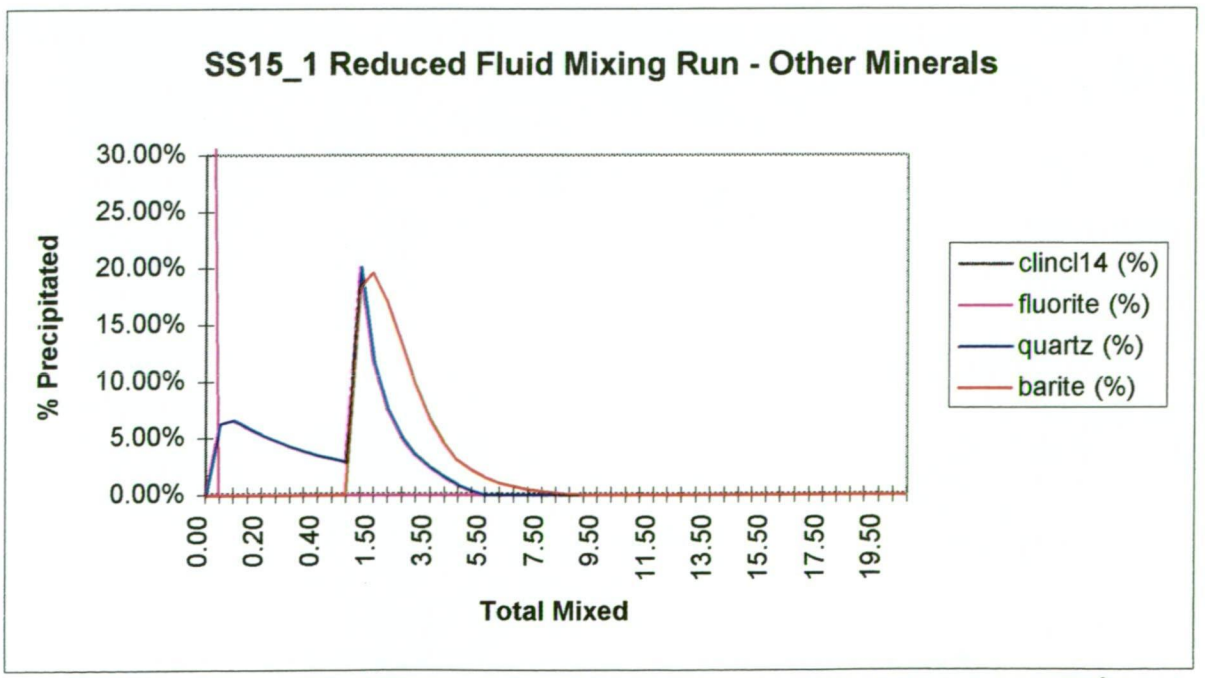

Figure 12.11 Mineral precipitation from Fluid SS15 (250°C) during reduced fluid mixing

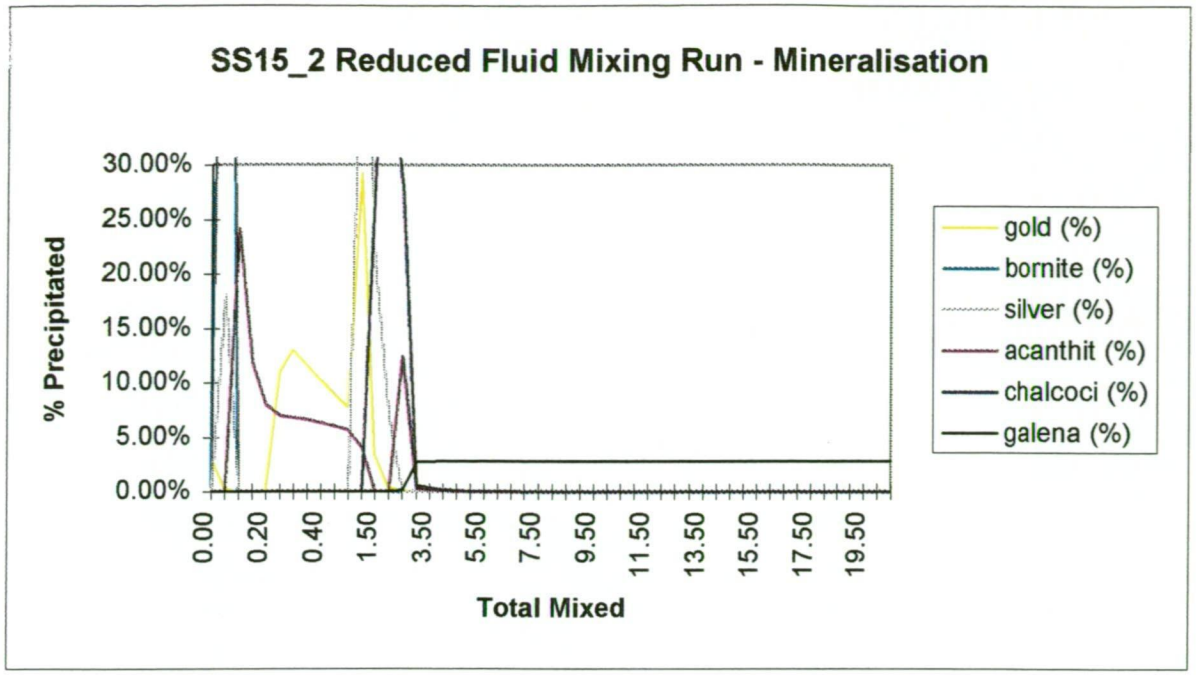

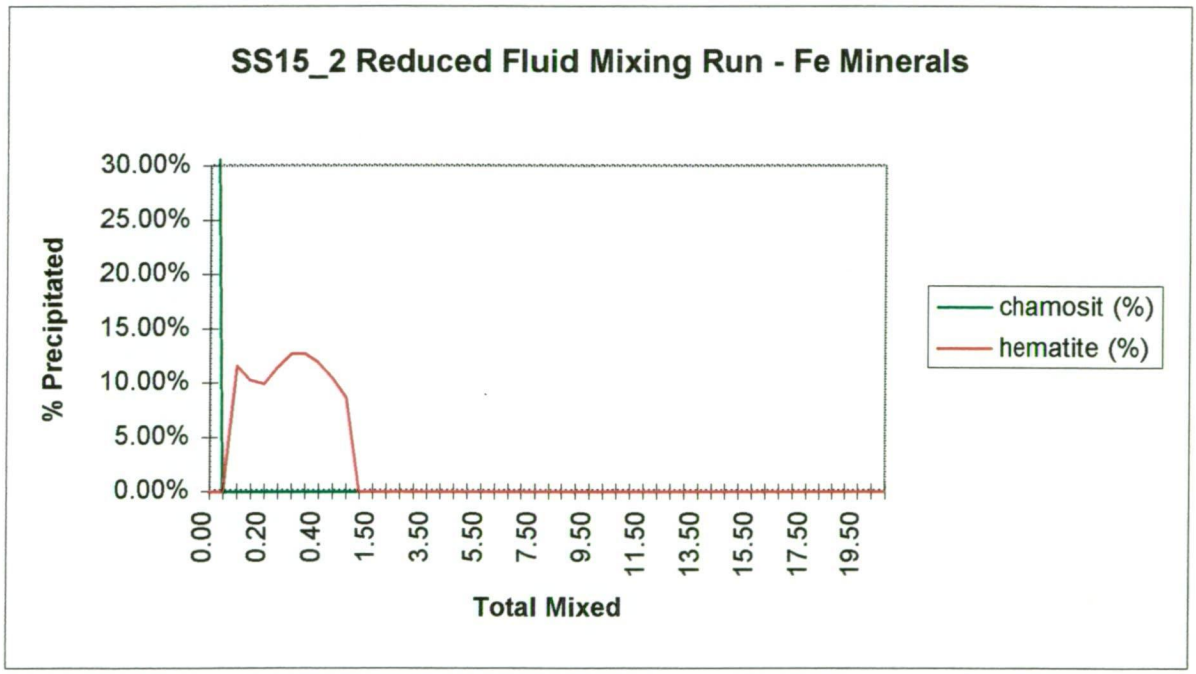

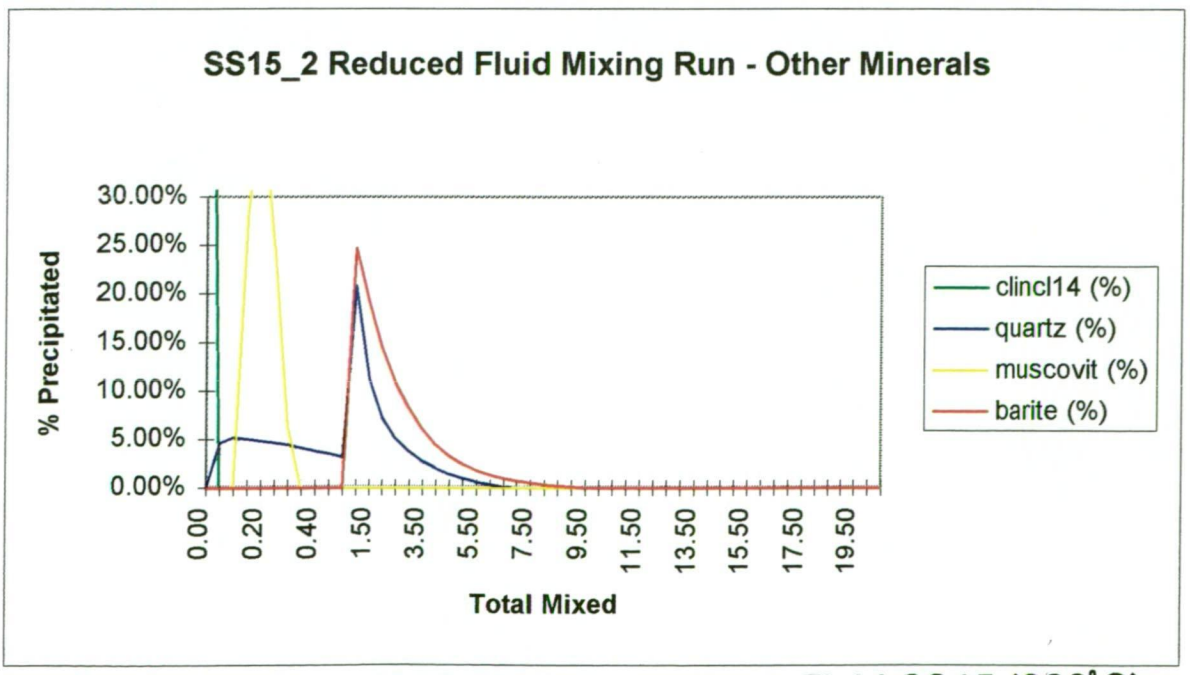

Figure 12.12 Mineral precipitation from Fluid SS15 (300°C) during reduced fluid mixing

Cooling Precipitation Sequence for DC10, DC15, SS10, SS15 at 250°C

	Proximal	Intermediate	Distal
Mineralisation	**gold, acanthite, chalcopyrite, galena**	**galena (sphalerite - SS10 only)**	**bornite, chalcocite, silver**
Fe Minerals	**chamosite**	**(pyrite - 10 wt% NaCl equiv. only)**	
Other Minerals	**clinclor14, quartz, fluorite, muscovite**	**graphite**	**fluorite**

Cooling Precipitation Sequence for DC10, DC15, SS10, SS15 at 300°C

	Proximal	Intermediate	Distal
Mineralisation	**gold, silver, bornite, acanthite, (galena - 10 wt % NaCl equiv. only)**		
Fe Minerals	**chamosite**	**hematite**	
Other Minerals	**clinclor14, quartz, muscovite**	**graphite**	**fluorite**

Cooling Precipitation Sequence for SST at 250°C

	Proximal	Intermediate	Distal
Mineralisation	**gold, acanthite, silver**		
Fe Minerals	**magnetite**	**hematite (siderite)**	
Other Minerals	**fluorite, muscovite, quartz**		**fluorite**

Cooling Precipitation Sequence for SST at 300°C

	Proximal	Intermediate	Distal
Mineralisation	**gold, silver, acanthite**	**silver**	**gold**
Fe Minerals		**hematite**	
Other Minerals	**quartz**		**fluorite**

Table 12.8 Summary of Cooling Precipitation Sequences

Boiling Precipitation Sequence for DC10, DC15, SS10, SS15 at 250°C

	Proximal	Intermediate	Distal
Mineralisation	**gold**	**acanthite**	**chalcocite (SS10 only)**
Fe Minerals	**chamosite, magnetite, hematite**		
Other Minerals	**clinclor14, fluorite, quartz**	**muscovite**	**fluorite**

Boiling Precipitation Sequence for DC10, DC15, SS10, SS15 at 300°C

	Proximal	Intermediate	Distal
Mineralisation	**gold, bornite (SS10 only)**	**silver, acanthite (higher salinity only)**	**chalcocite (lower salinity only)**
Fe Minerals	**chamosite, magnetite (SS fluids only)**		
Other Minerals	**clinclor14, quartz,**	**muscovite**	**fluorite (SS10 only)**

Boiling Precipitation Sequence for SST at 250°C

	Proximal	Intermediate	Distal
Mineralisation	**gold**	**acanthite, silver**	**chalcocite**
Fe Minerals	**magnetite**		
Other Minerals	**fluorite, muscovite, quartz**		**fluorite**

Boiling Precipitation Sequence for SST at 300°C

	Proximal	Intermediate	Distal
Mineralisation	**gold, silver**	**acanthite**	**silver**
Fe Minerals	**magnetite**		
Other Minerals	**quartz, apatite-fluorite, muscovite**		

Table 12.9 Summary of Boiling Precipitation Sequences

Oxidised Fluid Mixing Precipitation Sequence for DC10, DC15, SS10, SS15 at 250°C

	Proximal	Intermediate	Distal
Mineralisation	**gold**	**acanthite, silver**	**chalcocite (higher salinity only)**
Fe Minerals	**(chamosite), hematite, pyrite**		
Other Minerals	**clinclor14, barite, quartz**	**fluorite, quartz (anhydrite and barite - SS only)**	**kaolinite, gibbsite, (muscovite - SS only)**

Oxidised Fluid Mixing Precipitation Sequence for DC10, DC15, SS10, SS15 at 300°C

	Proximal	Intermediate	Distal
Mineralisation	**gold, bornite, acanthite (galena - lower salinity only)**	**silver, anglesite (chalcocite - lower salinity only)**	**chalcocite (higher salinity only)**
Fe Minerals	**chamosite, hematite**	**hematite**	**hematite (high salinity only)**
Other Minerals	**clinclor14, barite, (muscovite - exception SS15)**	**quartz, anhydrite, barite**	**muscovite, kaolinite, gibbsite**

Oxidised Fluid Mixing Precipitation Sequence for SST at 250°C

	Proximal	Intermediate	Distal
Mineralisation	**gold**	**acanthite, silver**	**galena**
Fe Minerals	**(magnetite), hematite, pyrite**	**hematite**	**hematite**
Other Minerals	**fluorite, muscovite, barite, quartz**	**fluorite, quartz, anhydrite, barite**	**muscovite, gibbsite**

Oxidised Fluid Mixing Precipitation Sequence for SST at 300°C

	Proximal	Intermediate	Distal
Mineralisation	**gold, acanthite**	**gold, anglesite**	**gold, anglesite, silver**
Fe Minerals	**hematite**		**hematite**
Other Minerals	**quartz, anhydrite, barite**		

Table 12.10 Summary of Oxidised Fluid Mixing Precipitation Sequence

Reduced Fluid Mixing Precipitation Sequence for DC10, DC15, SS10, SS15 at 250°C

	Proximal	Intermediate	Distal
Mineralisation	**gold, acanthite**	**galena, chalcopyrite, bornite**	**sphalerite, chalcocite**
Fe Minerals	**(chamosite, magnetite) hematite,**	**pyrite**	**pyrite**
Other Minerals	**clinclor14, quartz**	**fluorite, quartz, barite**	

Reduced Fluid Mixing Precipitation Sequence for DC10, DC15, SS10, SS15 at 300°C

	Proximal	Intermediate	Distal
Mineralisation	**gold, bornite, silver, acanthite, minor galena**	**gold, silver, acanthite, chalcocite**	**galena**
Fe Minerals	**chamosite**	**hematite**	
Other Minerals	**clinclor14, muscovite, quartz**	**quartz, barite**	

Reduced Fluid Mixing Precipitation Sequence for SST at 250°C

	Proximal	Intermediate	Distal
Mineralisation	**gold, acanthite**	**acanthite, bornite, chalcocite, galena**	**galena, sphalerite**
Fe Minerals	**(magnetite), hematite, pyrite**	**pyrite**	
Other Minerals	**fluorite, muscovite, quartz**	**quartz, barite**	

Reduced Fluid Mixing Precipitation Sequence for SST at 300°C

	Proximal	Intermediate	Distal
Mineralisation	**gold, acanthite, silver**	**gold, silver**	**chalcocite, acanthite**
Fe Minerals	**hematite**		**hematite**
Other Minerals	**quartz**	**quartz, barite**	

Table 12.11 Summary of Reduced Fluid Mixing Precipitation Sequence

Mixing with a reduced sea water was the most effective way of precipitating base metals, particularly sphalerite. Sphalerite was , however, only precipitated by the 250°C fluids. Note that galena precipitated more proximally than sphalerite in all cases.

Mixing with a reduced sea water was also effective in precipitating iron oxides, with magnetite precipitated by the 250°C fluids and hematite precipitated by the 300° C fluids. Pyrite was by far the most dominant species however and was precipitated by all fluids except SST at 300°C. Chamosite was precipitated proximally by all fluids except SST.

Fluorite was only precipitated by the lower temperature fluids.

12.3 Comparison of Precipitation Mechanisms

The most efficient mechanisms for precipitation of each mineral are summarised in Table 12.12 below.

Mineral	Mechanism
magnetite	boiling (reduced fluid mixing of 250°C fluids)
hematite	oxidation (reduced fluid mixing)
chamosite	boiling
pyrite	reduced fluid mixing
gold	all similar
silver	cooling - 300°C fluids
acanthite	reduced fluid mixing
anglesite	oxidized fluid mixing - 300°Cfluids
chalcopyrite	cooling - 250°C fluids
chalcocite	oxidized fluid mixing - 250°C fluids cooling - 300°C fluids
galena	reduced fluid mixing - cooling
sphalerite	reduced fluid mixing - 250°C fluids
fluorite	cooling
muscovite	cooling
kaolinite	oxidized fluid mixing
gibbsite	oxidized fluid mixing
graphite	cooling

Table 12.12 Summary of most effective precipitation mechanism for various minerals.

Fe Minerals

Boiling precipitated magnetite very efficiently. Hematite was also precipitated by the 250°C fluids. Chamosite was precipitated by all except the SST fluids.

Cooling precipitated predominantly chamosite. Magnetite and hematite were only precipitated by the higher salinity, higher temperature fluids. Pyrite was precipitated by the low temperature 10 wt% eq. salinity fluids only.

Mixing with oxidised sea water precipitated hematite, pyrite and chamosite from the 250°C series and hematite and chamosite from the 300°C temperature series. Magnetite was precipitated by only one of the ten trial fluids as a result of mixing with oxidised sea water.

Mixing with reduced sea water resulted in the precipitation of pyrite, hematite, magnetite and pyrite from the 250°C fluids. The 300°C fluids precipitated hematite and chamosite only.

Mineralisation

Cooling precipitated gold, silver, acanthite, bornite, and lead bearing minerals. Boiling precipitated only gold, silver and copper. Mixing with oxidised sea water precipitated a similar suite to cooling. Mixing with reduced seawater was the only process to precipitate zinc mineralisation, in addition to gold, silver, copper and lead.

The failure of any other mechanism to precipitate sphalerite warrants further consideration. The fluids used in the trial were saturated with respect to base metals and carried far higher concentrations than the upper limit of the normal ore forming window. This, coupled with the fact that the fluid was designed to be relatively sulfur poor, may have resulted in available sulfur being consumed in precipitating silver, copper and lead sulfides. Sphalerite may have been precipitated when the fluid mixed with reduced sea water because of extra sulfur provided by the mixing fluid.

It is likely that sphalerite would be precipitated by additional mechanisms if base metals were undersaturated within the fluid.

Other Minerals

Clinochlore was precipitated by all trials by the 10 and 15 wt% eq. fluids, but was at no stage precipitated by the SST fluids.

Quartz was precipitated proximally in almost all trials, and continued to precipitate at a decreasing level more distally. The notable exception occurred when mixing the 300°C fluids with oxidised seawater, where quartz was precipitated in the intermediate, rather than proximal zone.

Anhydrite, kaolinite and gibbsite were produced by oxidised fluid mixing only.

Barite was precipitated by mixing with both oxidised and reduced fluids. However, barite tended to precipitate proximally during oxidised fluid mixing, whereas it precipitated in the intermediate to distal zone during reduced fluid mixing.

Muscovite was precipitated proximally during cooling. Boiling favoured precipitation in the more intermediate zone for lower salinities. Muscovite was precipitated proximally by boiling the SST fluids. Mixing with oxidised sea water resulted in precipitation of muscovite distally for the 250°C fluids and both proximally and distally for the 300°C fluids (except SST). Mixing with reduced seawater resulted in proximal precipitation of muscovite for 300°C 10 and 15 wt% eq. fluids and the 250°C SST fluid.

Fluorite was precipitated both proximally and distally during cooling of 250°C fluids and distally for the 300°C fluids. Boiling showed similar results, except for the 300°C SST fluid which precipitated fluorite proximally. Oxidised fluid mixing resulted in precipitation of fluorite in the intermediate zone by 10 and 15 wt% eq. 250°C fluids, and the proximal and intermediate zones for SST 250°C fluids. 300°C fluids did not precipitate fluorite at all when mixed with oxidised seawater. Reduced seawater mixing showed similar results to oxidised sea water mixing except the 250°C SST fluid precipitated fluorite in the proximal zone only.

Graphite was only precipitated by cooling of the 10 and 15 wt% eq. fluids.

Fluor-apatite was precipitated by boiling of the SST 300°C fluid only.

12.4 Comparison of Modelling Results To Mineral Assemblages of BHT Deposits

To compare the mineral assemblages of BHT deposits with those generating by modelling, it is necessary to consider the likely pre-metamorphic mineral assemblages of the BHT deposits. Table 12.13 shows common prograde metamorphic reactions common in iron rich units. This table will be referred to frequently in the following discussion.

Mineralogical zonation at Broken Hill, South Africa, is summarised in Table 12.14 Trace chalcocite, fluorite and muscovite are described in the literature, but their position relative to mineralisation is not known (Ryan *et al.*, 1986, Walters, 1992).

Comparison of this zonation to that obtained in the modelling trials suggests that the proximal assemblage is best represented by the process of reduced fluid mixing with a 250°C model BHT fluid. This is implied by the proximal occurrence of pyrite, pyrrhotite. The minor amount of magnetite precipitated proximally in the modelling results may have been converted to pyrite and pyrrhotite during metamorphism (Table 12.13).

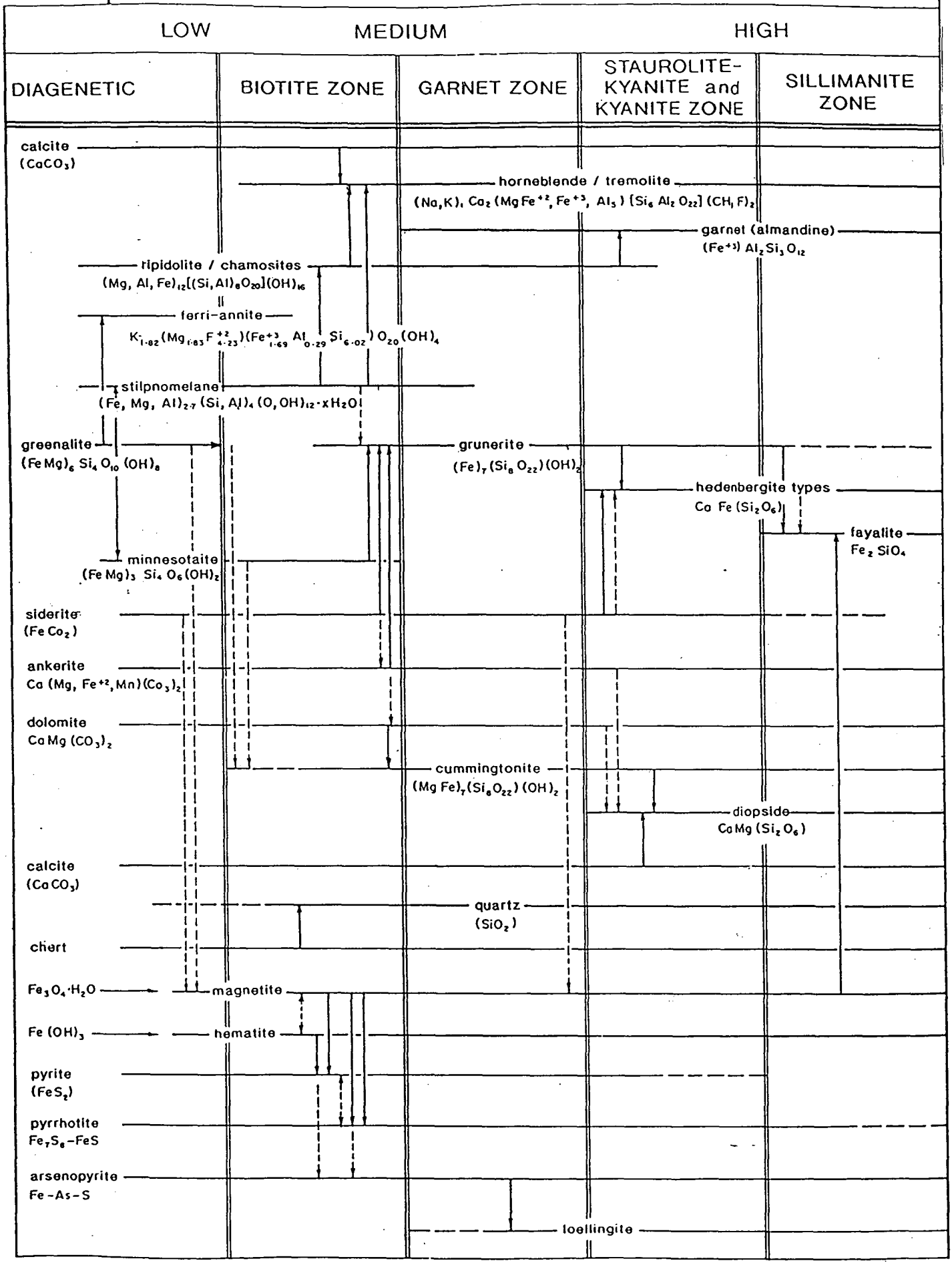

Table 12.13 Common prograde metamorphic reaction pathways in iron formations.
(Sheppard, 1993)

	Mineralisation	Fe Minerals	Other Minerals
Proximal	galena, sphalerite, silver	pyrrhotite, pyrite	quartz
	galena, sphalerite, silver	pyrrhotite, pyrite	barite
	galena, sphalerite, chalcopyrite	magnetite	quartz, garnet, biotite
	sphalerite, galena, chalcopyrite	magnetite, orthopyroxene, grunerite, fayalite, cummingtonite	quartz, spessartine garnet
Distal	trace base metals	magnetite, (? hematite)	quartz, barite, aluminous schist

Table 12.14 Mineralogical Zonation at Broken Hill, South Africa.

Distal mineral assemblages are best modelled by oxidised fluid mixing with higher salinity BHT fluids. The absence of pyrite, and the presence of magnetite, barite and aluminous schist is interpreted to best correspond to a modelled pre-metamorphic assemblage of hematite, quartz, barite, kaolinite and gibbsite.

The precursors to amphibole and pyroxene minerals are not well represented in the modelling results. These minerals are commonly derived from decarbonation reactions between calcite, siderite, ferroan dolomite, calcite and quartz. Carbonates were only produced when fluid SST was cooled from 250°C, and then only as siderite. This was despite the fact that the model fluid contained 1 wt% CO_2.

The Pb and Zn zonation at Broken Hill (South Africa) agrees well with the modelling results, with galena being proximal relative to sphalerite. Distal chalcopyrite mineralisation may be the metamorphic equivalent of distal chalcocite in the modelling results.

The other deposits of the Aggenys-Gamsberg district show similar zonations, on varying scales. However, Big Syncline and Gamsberg have the opposite Pb/Zn zonation, with sphalerite occurring proximally rather than galena. It should be noted that both Big Syncline and Gamsberg are zinc rich and Pb poor relative to the other

deposits of the province. Differences in the primary Zn/Pb ratio of the fluid may have a significant impact on the base metal zonation.

Metal zonation at Pegmont is summarised in Table 12.15 below:

Central	Intermediate	Edge
High grade mineralization; galena > sphalerite	Lower grade mineralization; sphalerite > galena	Insignificant mineralization; sphalerite ≈ chalcopyrite
Magnetite	Magnetite pyrite pyrrhotite	Pyrrhotite (>> pyrite)
Quartz absent	Some quartz	Abundant quartz
Garnet present, but subordinate	Garnet present, becoming more abundant	Abundant garnet dominates
Abundant fayalite	Minor fayalite sometimes present	Fayalite absent
Green hornblende, clinopyroxene and grunerite weakly developed	Green hornblende and pyroxene dominant; hornblende > pyroxene	Traces of green hornblende sometimes persist
Constant apatite	Constant apatite	Constant apatite
Minor biotite	Minor biotite	Abundant biotite

Table 12.15 Mineralogical Zonation Across the Pegmont Basin
(Stanton and Vaughan, 1979)

Pegmont mineral zonation features proximal magnetite, fayalite and galena, intermediate magnetite, pyrite, pyrrhotite, amphibole and pyroxene and distal pyrrhotite, pyrite, quartz and garnet. The mineral assemblage is best represented by a combination of boiling and mixing of 250°C fluids with reduced seawater.

Mineral zonation at Cannington is summarised in Table 12.16. The base metal zonation at Cannington is not well simulated by the modelling. The Fe mineral and fluorite distributions compare most favourably with boiling and oxidised fluid mixing results. The distal concentration of garnet is not well modelled. Chamosite, the interpreted precursor (Stanton, 1976) to metamorphic garnet, is generally precipitated proximally in the model results. Similarly to Broken Hill (SA), the amphibole-pyroxene distribution at Cannington is again not well modelled .

	Mineralisation	Fe Minerals	Other Minerals
Proximal	sphalerite, galena, silver	magnetite, hedenbergite, pyrrhotite, (fayalite) (hornblende) (pyrite)	fluorite, (quartz)
	galena, sphalerite, (chalcopyrite, freibergite)	magnetite, hedenbergite, pyroxmangite, (fayalite) (hornblende)	fluorite (talc) (chlorite)
	galena, (sphalerite)	magnetite, orthopyroxene, grunerite, fayalite, cummingtonite	garnet, quartz (talc) (chlorite) (fluorite)
Distal	trace base metals	magnetite, (? hematite)	

Table 12.16 Mineralogical Zonation at Cannington

Mineral zonation at Broken Hill (Australia) is summarised in Table 12.17. The Fe mineral content of the BHT deposit is best modelled by cooling, which primarily precipitates chamosite. Very distal assemblages are best reflected by oxidised fluid mixing. The manganese, carbonate and amphibole mineralogy is once again not well modelled. Nor is the base metal distribution.

Mineral zonation at Zinkgruvan is summarised in Table 12.18. Zinkgruvan is best modelled by proximal reduced fluid mixing and possible distal oxidised fluid mixing (magnetite-calc-silicate rocks). The base metal zonation agrees with modelling, with proximal galena and distal sphalerite. Precursors of the dominant calc-silicate lithologies were not well modelled.

	Mineralisation	Fe Minerals	Other Minerals
Proximal	sphalerite, (galena)	pyrrhotite, Mn-hedenbergite ? garnet	quartz, garnet biotite, rhodonite
	galena, sphalerite, (chalcopyrite)	Mn hedenbergite,	quartz, calcite, rhodonite, fluorite
	gahnite (trace Pb, Zn, Cu)	Pyrrhotite (magnetite, hematite), ?garnet	quartz, garnet
Distal	trace base metals	BIF (magnetite, hematite, amphiboles)	

Table 12.17 Mineral Zonation at Broken Hill, Australia

	Mineralisation	Fe Minerals	Other Minerals
Proximal	Cu	pyrrhotite,	quartz
	galena, sphalerite, (chalcopyrite)	pyrrhotite, biotite, ?garnet,	quartz, calcite, diopside, tremolite, garnet, sericitic feldspar,
	sphalerite	Pyrrhotite ?chlorite ? amphibole ? garnet	diopside, chlorite, amphibole, quartz, garnet
Distal	trace base metals	magnetite	calc-silicates

12.18 Mineral Zonation at Zinkgruvan, Bergslagen, Sweden

12.5 Summary

Thermodynamic modelling was successful in demonstrating that mineral assemblages precipitated by a fluid of constant composition are strongly influenced by the environment of precipitation. The relative significance of cooling, boiling, mixing with reduced sea water and mixing with oxidised sea water is very important in controlling the partitioning of Fe into oxide, silicate, sulfide or carbonates.

Modelling indicated that BHT deposits with significant pyrite and pyrrhotite in association with magnetite are best modelled by proximal reduced sea water mixing, with distal oxidised sea water mixing. BHT deposits with proximal magnetite and minimal Fe sulfide may be modelled by boiling and oxidised sea water mixing.

The Broken Hill deposit, which is characterised by a deficiency in both iron oxides and sulfides, was best modelled by cooling and very distal oxidised fluid mixing. This may reflect a mineralising event in which the mineralising fluid completely dominated the host environment and very little fluid mixing occurred. It is interesting to note that the Broken Hill deposit is by far the largest BHT deposit.

Proximal base and precious metal assemblages were dominated by gold, silver and copper. Galena was precipitated in the proximal to intermediate zone. Sphalerite was only precipitated by reduced fluid mixing, and only distally. The dominance of the ore mineralogy of the proximal zone by precious metals and copper does not compare well with the ore mineralogy of the deposits. This is probably due to the exceptionally high dissolved metals in the saturated fluids used in the trials. Sulfur was probably consumed by precipitation of silver and lead sulfides, forcing zinc to stay in solution. More realistic model results would probably be obtained by using undersaturated metal concentrations.

Thermodynamic modelling was not successful in commonly precipitating carbonate minerals, despite containing 1 wt. % CO_2. As a result metamorphic amphibole, pyroxene and calc-silicate assemblages were not well modelled.

12.6 Future Work

An important factor to model is the role of undersaturation.

Attempts to model an undersaturated 300°C SS15 fluid by reducing Au and Ag content by three orders of magnitude and base metals by 75% have precipitated proximal fluoro-apatite, clinochlore, chamosite, dolomite, magnetite, sphalerite, talc and minnesotaite during cooling and boiling from 300°C to 295°C and 260°C respectively. This compares to a saturated mineral assemblage of chlinoclore, chamosite and gold.

The undersaturated assemblage is greatly different. It contains carbonate minerals and minnesotaite which would form amphiboles and pyroxenes on metamorphism. It contains proximal magnetite and sphalerite which have not been previously precipitated

by cooling. It does not contain proximal galena, so the zonation of the two minerals has been reversed.

Unfortunately from this point on the computer modelling becomes unstable and crashes, despite repeated attempts with minor adjustments. This is currently being addressed.

Modelling of the actual Salton sea concentrations listed in Table 12.1 (Well S2-14) is another important trial to be completed, as this is our closest modern analogue. Unfortunately to date modelling has not been successful due to software instability problems similar to those described above. This is also currently being addressed.

13. SYNTHESIS

13.1 Magnetic Characteristics of BHT Host Provinces

It has long been recognised that host provinces of BHT deposits possess common geological characteristics, enabling the development of a regional geological model for BHT ore deposits. This study has shown that these common geological characteristics are reflected in common magnetic characteristics of host provinces of BHT deposits.

The quartzofeldspathic/acid-volcanic dominant Lower Sequences are generally characterised by a moderate, variably magnetic, background response. Within this moderately magnetic background, strongly magnetic units with significant strike extent may occur. These magnetic units commonly include magnetic amphibolites and quartz-iron-oxide related mineralisation. A clear exception to this pattern appears to be the Lower Sequence of the Aggenys Gamsberg district, which is relatively non-magnetic and contains few moderate to strongly magnetic units.

The metavolcanic/metasedimentary Transitional Sequence is generally characterised by a relatively non-magnetic background response within which linear, moderate to strongly magnetic units may occur. These magnetic units may include magnetic amphibolites or exhalites.

0The metasediment-dominated Upper Sequence is also relatively non-magnetic with even fewer intercalated magnetic units. These magnetic units may be metasedimentary rocks, calc-silicates or mafic intrusions containing magnetite.

Despite the similar physical properties, within the four provinces, of the Lower, Transitional and Upper Sequences, there are striking differences in the aeromagnetic images, particularly when comparing the Australian provinces to the Aggenys-Gamsberg and Bergslagen districts. These differences are largely a function of differing basement stratigraphy, differences in the extent of the BHT stratigraphy and differing structural styles.

13.2 Deposit Scale Characteristics - Implications for Exploration

BHT deposits may be grouped into two classes: those that are intimately associated with magnetic minerals, and those which are not.

Deposits which are intimately associated with magnetic minerals are commonly associated with magnetic anomalies which are amongst the strongest within the Transitional Sequence. These magnetic anomalies generally have a strike length of the order of the strike length of the deposit. In aeromagnetic data they may range from 400 nT to more than 1000 nT. The amplitude of the magnetic response increases markedly in ground magnetic data as the distance between sensor and source is reduced.

Deposits which do not contain magnetic minerals within the ore itself may be associated with a locally anomalous signature when the strike extensions and hanging and footwall sequences are considered. In the footwall and hanging wall magnetic minerals may occur which are related to the mineralising event. Magnetite destruction may be evident in the footwall. Alternately the non-magnetic ore may show a lateral gradation into distal magnetic minerals.
The most economically significant deposit, Broken Hill (Australia), deposit is of this type.

It is clear that BHT deposits display a range of magnetic characteristics. Thermodynamic modelling was conducted in order to explore the range of possible magnetic signatures. Controls on mineral assemblages may include the relative significance of boiling (related to water depth and temperature), cooling and fluid mixing to mineral precipitation. Other significant factors include the rate of fluid expulsion, which would influence the degree of fluid mixing, and the degree of undersaturation of the fluid .

The thermodynamic modelling discussed in Section 12 studied the roles in mineral precipitation and zonation of cooling, boiling, mixing with oxidised sea water and mixing with reduced seawater. This modelling showed that a single fluid could produce a variety of mineral assemblages and zonations. Magnetite and hematite could be precipitated in a proximal, intermediate and/or distal position depending on the precipitation mechanism. Cooling failed to precipitate iron oxides for most trials.

Comparison with mineral assemblages of deposits showed that precipitation may have involved more than one mechanism. The dominant mechanism may have varied from proximal to distal positions, and from one deposit to another.

Some deposits rich in proximal magnetite could be modelled by a combination of boiling and mixing with an oxidised fluid, suggesting a shallow oxidised basin.

Other deposits with proximal iron sulfides and intermediate to distal iron oxides were best modelled by proximal mixing with a reduced fluid and distal mixing with an oxidised fluid. This could represent a progression from the more reduced deep water basin centre to the shallower more oxidised basin margins.

The Broken Hill (Australia) deposit, by far the the most economically significant, may be modelled by assuming cooling was the predominant proximal and intermediate precipitation mechanism for iron minerals. This would result in proximal precipitation of the iron silicate precursor to garnet and virtually no precipitation of iron sulfides or oxides. This could occur if the rate of fluid expulsion was very rapid such that there was a swamping of the seafloor environment resulting in limited fluid mixing. Expulsion into very deep water would prevent boiling. On the margins of the pond of ore fluid limited sea water mixing could occur, resulting in abrupt iron oxide deposition on the edge of the proximal to intermediate iron oxide free zone. Iron oxide precipitation would then taper off distally as fluid mixing continued and the amount of available iron decreased with distance from the vent. Magnetic units above and below the ore position possibly reflect minor exhalation from the main vent before and after the main mineralising event.

14. CONCLUSIONS

Host provinces to BHT deposits share common magnetic characteristics which reflect common geological characteristics. However significant differences in the aeromagnetic character occur and are related to differences in volume of BHT host stratigraphy, basement stratigraphy and structural style of the host province. The interpreter must carefully consider these aspects when assessing the BHT prospectivity of a province based on aeromagnetic data.

BHT deposits may be classified on the presence or absence of magnetic minerals within the ore. Deposits which contain magnetic minerals within the ore are commonly associated with magnetic anomalies which are amongst the strongest within the metasedimentary/metavolcanic Transitional Sequence. Deposits of the Aggenys-Gamsberg and Eastern Succession regions are of this type. Deposits which do not contain magnetic minerals within the ore itself may be associated with a locally anomalous signature when the strike extensions and hanging and footwall sequences are considered. The most economically signifcant deposit, Broken Hill (Australia), is of this type.

Thermodynamic modelling showed that a single fluid can give rise to a spectrum of iron oxide distribution, including total absence, depending on whether the dominant precipitation mechanism was boiling, cooling, mixing with oxidised sea water or mixing with reduced sea water. The interpreter must carefully consider the range of likely environments of deposition consistent with the known geology and define a suite of potential aeromagnetic signatures.

REFERENCES

BAKER, J.H. and HELLINGWERF, R.M., (Editors), 1988, Special Issue on the Berglagen Province (Editors): Geol. Mijnbouw, 67: 117-458.

BARNES, H.L., 1979, Geochemistry of Hydrothermal Ore Deposits; 2nd Edition: Publ. by John Wiley & Sons Inc., USA.

BARNES, R.G., 1980, Types of Mineralisation in the Broken Hill Block and their Relationship to Stratigraphy: New South Wales Geolog. Survey - Records 20 Part 1, pp 33-70.

BARNES, R.G., 1983, Mineralisation of the Broken Hill Block: Broken Hill Conference, AUSIMM, pp 71-80.

BARNES, R.G., 1986, A Summary Record of Mineral Deposits in the Broken Hill Blocl Excluding the South Eastern Portion: New South Wales Geological Survey - Records Volume 22, Part 2, pp 163-367.

BARNES, R.G., 1988, Metallogenic Studies of the Broken Hill and Euriowie Blocks, New South Wales: New South Wales Geol. Survey Bulletin 32.

BARRETT, T.J. and ANDERSON, G.M., 1982, The Solubility of Sphalerite and Galena in Nacl Brines: Econ. Geol. Vol. 77, pp 1923-1933.

BARRETT, T.J. and ANDERSON, G.M., 1988, The Solubility of Sphalerite and Galena in 1-5 m Nacl Solutions to 300 Deg C: Geochemica et Cosmochimica Acta, Vol. 52, pp 813-820.

BEARDSMORE, T.J., NEWBERRY, S.P. and LAING, W.P., 1988, The Maronan Supergroup: an Inferred Early Volcano-Sedimentary Rift Sequence in the Mount Isa Inlier, and its Implications for Ensialic Rifting in the Middle Proterozoic of Northwest Queensland: Precambrian Res., 40-41: 487-508.

BEESON, R., 1990, Broken Hill-Type Lead Zinc Deposits - An Overview of their Occurrence and Geological Setting: Trans. Instn. Min. Metal., Sept-Dec 1990, pp B163-B175 .

BHP EXPLORATION, 1990, Broken Hill Field Visit 1990: Unpublished BHP Company Report.

BLAKE, D.H., 1987, Geology of the Mount Isa Inliers and Environs, Queensland and Northern Territory: BMR Bulletin 225.

BLAKE, D.H., JAQUES, A.L. and DONCHAK, P.J.T, 1983, 1:100,000 Geological Map and Commentary, Selwyn Region, Qld: Publ. by Australian Government Publishing Service, Canberra.

BLAKE, D.H., *et al.*, 1983, 1:250,000 Geology of the Duchess-Urandangi Region: Publ. by Bureau of Mineral Resources, Geology and Geophysics, Department of National Development and Energy.

BLAKE, D.H. and STEWART, A.J., 1992, Stratigraphic and Tectonic Framework, Mount Isa Inlier, in Stewart, A.J. and Blake, D.H. (Eds): Detailed Studies of the Mount Isa Inlier, BMR Bulletin 243.

BRADLEY, G.M., 1984, Mount Gipps 1:25,000 Geology Sheet, 7234-III-S, New South Wales Geological Survey, Sydney.

BROWN, R.E., WILLIS, I.L., STROUD, W.J. and STEVENS, B.P.J, The Relationship between Mapped Rock Units and the Stratigraphic Subdivision in Key Areas of the Broken Hill Block: Broken Hill Conference, 1983, AUSIMM, pp 51-70.

BROWN, R.E., 1984, Pinnacles 1:25,000 Geological Sheet, 7133-I-N, New South Wales Geological Survey, Sydney.

BROWN, R.E., 1984, Broken Hill 1:25,000 Geology Sheet, 7134-UU-S, New South Wales Geological Survey, Sydney.

BUNTING, W.F. and WALTERS, S.J., 1984, Eyre Peninsular: Regional Evaluation of the Hutchison Group for Broken Hill Style Base Metal Mineralisation Potential: Unpublished BHP Company Report CR 4480.

CAMPBELL, G. and MASON, R., 1979, The Application of Airborne and Ground Techniques to the Search for Magnetite Quartzite Associated Base Metal Deposits in Southern Africa: Geoph. and Geochem. in search for Metall. Ores, Geol. Surv. Canada, Econ. Geol. Rpt 31, pp 757-777.

CARVALHO, I.G., 1982, Geology of the Pb-Zn District of Boquira; Bahia State, Brazil: Quinto Congreso Latinoamericano de Geologia, Vol. II.

CARVALHO, I.G., 1988, Host Rock Geochemistry and its Contribution to the Genetic Interpretation of the Boquira Pb-Zn Deposits, Bahia State, Brazil: Annals of VII Latino-Amer. Geol. Conf., 1988, Congresso Latino-Americano de Geologia, Vol. 7.

COLLISTON, W.P. (Editor), PRAEKELT, H.E., STRYDOM, D and PRETORIUS, J.J., 1986, Stratigraphic Map of Central Bushmanland: Publ. by University of Orange Free State, Bloemfontein.

COOK, D.R., 1993, Transport and Deposition of Base Metals from High Temperature (250°C) Sedimentary Brines. AMIRA/ARC Project P 384, Report No. 4, pp 111-129.

COOK, D.R., HUSTON, D.L., LARGE, R.R. and GAMMONS, C.H., 1993, Hydrothermal Geochemistry: In CODES Masters of Economic Geology Course Work Manual 12, 2nd Edition, pp 1-35.

DARDENNE, M.A., 1988, Geologia do Chumbo E Zinco: Principais Depositos Minerais Do Brasil - Volume III.

DREVER, J.I., 1984, The Geochemistry of Natural Waters. Prentice Hall, N.J.

DONCHAK, P.J.T., BLAKE, D.H., NOON, T.A. and JAQUES, A.L., 1983, 1:100,000 Geological Map and Commentary, Kuridala Region, Queensland: Publ. by Australian Government Publishing Service, Canberra.

EDWARDS, A. and WINDRIM, D.P., 1986, A Preliminary Report on Overseas Visit to USA and Brazil by AC Edwards and DP Windrim: Unpublished BHP Company Memo CM 2210.

ESPOURTEILLE, F. and FLEISCHER, R., 1986, Mina De Chumbo De Boquira, Bahia: Principais Depositos Minerais Do Brasil Vol. 3.

FREITCH, R., 1982, A Model for the Formation of the Iron, Manganese and Sulphide Ores of Central Sweden: Geol. RDSCH. Vol. 71 pp 206-212.

FROESE, E., 1981, Applications of Thermodynamics in the Study of Mineral Deposits: Geol. Surv. of Canada, Paper 80-28.

FRONDEL, C. and BAUM, J.L., 1974, Structure and Mineralogy of the Franklin Zinc-Iron-Manganese Deposit, New Jersey: Econ. Geol. Vol. 69 No. 2, pp 157-180.

FROST, B.R., 1979, Metamorphism of Iron Formation: Paragenesis in the System Fe-Si-C-O-H: Econ. Geol. Vol. 74 pp 775-785.

GRANT, F.S., 1984, Aeromagnetics, Geology and Ore Environments, I, Magnetite in Igneous, Sedimentary and Metamorphic Rocks: An Overview: Geoexploration, Vol. 23 pp 303-333.

GRANT, F.S., 1984, Aeromagnetics, Geology and Ore Environments, II. Magnetite and Ore Environments: Geoexploration, Vol. 23 pp 335-362.

HAGGERTY, S.E., 1979, Aeromagnetic Mineralogy of Igneous Rocks: Canadian Journal of Earth Science Vol. 16, pp 1281-1293.

HAYDON, R.C. and McCONACHY, G.W., 1987, The Stratigraphic Setting of Pb-Zn-Ag Mineralisation at Broken Hill: Econ. Geol. Vol. 82 pp 826-856.

HEDSTROM, P., SIMEONOV, A. and MALMSTROM, L., 1989, The Zinkgruvan Ore Deposit, South Central Sweden: A Proterozoic, Proximal Zn-Pb-Ag Deposit in Distal Volcanic Facies: Econ. Geol. Vol. 84 pp 1235-1261.

HEMLEY, J.J., CYGAN, G.L., FEIN, J.B., ROBINSON, G.R. and D'ANGELO, W.M., 1992, Hydrothermal Ore Forming Processes in Light of Studies in Rock-Buffered Systems: I. Iron-Copper-Zinc-Lead Solubility Relations: Econ. Geol. Vol. 87 pp 1-22.

HEMLEY, J.J. and HUNT, J.P., 1992, Hydrothermal Ore Forming Processes in Light of Studies in Rock-Buffered Systems: II. Some General Geologic Applications: Econ. Geol. Vol. 87 pp 23-43.

HIGGINS, M.L., BERG, R.C. and HELLSTEN, K.J., Menninnie Dam Lead-Zinc-Silver Prospect, Eyre Peninsular, in HUGHES, F.E. (Editor), 1990, Geology of Mineral Deposits of Aust. and PNG, Monograph 14, AUSIMM, pp 1055-1058.

HILL, E.J., LOOSVELD, R.J.H. and PAGE, R.W., 1992, Structure and Geochronology of the Tommy Creek Block, Mount Isa Inlier, in Stewart, A.J. and Blake, D.H. (Eds): Detailed Studies of the Mount Isa Inlier, BMR Bulletin 243, pp 349-361.

HOLMES, R. and TOOMS, J.S., 1973, Dispersion from a Submarine Exhalative Ore Body: in JONES, M.J. (Editor), 1973, Geochem. Exploration, Inst. Min. Metal. London .

HUTCHISON, R.W., 1982, Syndepositional Hydrothermal Processes and Precambrian Sulphide Deposits, in HUTCHISON, R.W. *et al.* (Editors), 1982, Precambrian Sulphide Deposits, Geol. Assoc. of Canada, Special Paper 25.

ISLES, D.J., 1983, A Regional Geophysical Study of the Broken Hill Block, N.S.W. Australia: PhD Thesis, University of Adelaide.

JAMES, H.L., 1954, Sedimentary Facies of Iron Formation: Econ. Geol. Vol. 49 No. 3, pp 235-281.

JOUBERT, P., 1986, The Namaqualand Metamorphis Complex - a Summary, in ANHAEUSSER, C.R. and MASKE, S (Eds), Mineral Deposits of Southern Africa, Geol. Soc, South Africa, pp 1395-1420.

KLAU, W. and LARGE, D.E., 1980, Submarine Exhalative Cu-Pb-Zn Deposits - A Discussion of their Classification and Metallogenesis: Geologisches Jahrbuch D40, pp 13-58.

KLEIN, C., 1983, Diagenesis and Metamorphism of Precambrian Iron Formations in Iron Formations: Facts and Problems (Eds Trendall, A.F. and Morris, R.C.), Developments in Precambrian Geology 6, pp 417-470.

KOARK, H., KRESTEN, P., LAUFELD, S. and SANDWALL, J., 1986, Geology of the Falun Mine, Geological Survey of Sweden.

LAING, W.P., 1980, Stratigraphic Interpretation of the Broken Hill Mines Area: New South Wales Geolog. Survey - Records 20 Part 1, pp 71-85.

LAING, W.P., 1993, Structural/Metasomatic Controls on Ore Deposits in the East Mount Isa Block: the Key to Tonnes and Grade, in Symposium on Recent Advances in the Mount Isa Block: AIG Bull., 13:17-24.

LAING, W.P., MARJORIBANKS, R.W. and RUTLAND, R.W.R., 1978, Structure of the Broken Hill Mine Area and its Significance for the Genesis of the Orebodies: Econ. Geol., 73: pp 1112-1136.

LARGE, D.E., 1980, Geological parameters associated with Sediment Hosted, Submarine Exhalative Pb-Zn Deposits: An Empirical Model for Mineral Exploration: Geologisches Jahrbuch D40 pp 59-129.

LOCSEI, J., 1977, Pegmont: A Stratiform Lead-Zinc Deposit in the Precambrian of Northwest Queensland: Proc. Aust. Inst. Min. Metall. Vol. 262, pp 25-28.

LOTTERMOSER, B.G., 1989, Rare Earth Element Study of Exhalites within the Willyama Supergroup, Broken Hill Block Australia: Mineralium Deposita, Vol. 24, pp 92-99.

LOTTERMOSER, B.G, 1991, Trace Element Composition of Exhalites associated with the Broken Hill Sulfide Deposit, Australia: Econ. Geol. Vol. 86, pp 870-877.

MACKENZIE, D.H. and DAVIES, R.H., 1990, Broken Hill Lead-Silver-Zinc Deposit at ZC Mines: in HUGHES, F.E. (Editor), 1990, Geology of Mineral Deposits of Aust. and PNG, Monograph 14, AUSIMM, pp 1079-1084.

MARJORIBANKS, R.W., RUTLAND, R.W.R., GLEN, R.A. and LAING, W.P., 1980, The Structure and Tectonic Evaluation of the Broken Hill Region, Australia: Precambrian Res. Vol 13, pp 209-240.

MCINTYRE, J.I., 1979, Aeromagnetics - An Effective Geological Mapping Aid for the Willyama Complex? Bull. Aust. Soc. Explor. Geophys. V10 No. 1, pp 42-53.

MCINTYRE, J.I., 1980, Geological Significance of Magnetic Patterns Related to Magnetite in Sediments and Metasediments - a Review: Bull. Aust. Soc. Explor. Geophys. V11 No. 1/2.

MCINTYRE, J.I. and WYATT, B.W., 1978, Contributions to the Regional Geology of the Broken Hill Area from Geophysical Data: BMR Journal of Geol. and Geophys, Vol. 3, pp 265-280.

McKIBBEN, M.A. and ELDERS, W.A., 1985, Fe-Zn-Cu-Pb Mineralisation in the Salton Sea Geothermal System, Imperial Valley, California: Econ. Geol. Vol. 80 pp 539-559.

McKIBBEN, M.A., ANDES, J.P. JNR and WILLIAMS, A.E., 1988, Active One Formation at a Brine Interface in Metamorphosed Deltaic Lacustrine Sediments: The Salton Sea Geothermal System, California: Econ. Geol. Vol. 83 pp 511-523.

MEL'NIK, Y.P., 1982, Precambrian Banded Iron Formations - Physiochemical Conditions of Formation: Developments in Precambrian Geology 5, Publ. by Elsevier, Amsterdam.

OPPY, I., 1992, Magnetic Susceptibility Readings at Pasminco Southern Operations: Unpublished Poster Presentation, Australian Geological Conference, 1992.

PALACHE, C., 1935, The Minerals of Franklin and Sterling Hill, Sussex County, New Jersey: USGS Professional Paper 180.

PARR, J., 1994, The Geology and Stratigraphic Setting of the Pinnacles Pb-Zn-Ag Deposit, Western NSW, Australia: Econ. Geol. Vol. 89, pp 778-790.

PETERSEN, U., 1965, Application of Saturation (Solubility) Diagrams to Problems in Ore Deposits: Econ. Geol. Vol. 60, pp 853-893.

PLIMER, I.R., 1984, The Role of Fluorine in Submarine Exhalative Systems with Special Reference to Broken Hill Australia: Mineralium Deposita, Vol. 19, pp 19-25.

PLIMER, I.R., 1985, Broken Hill Pb-Zn-Ag Deposit - A Product of Mantle Metasomatism: Mineralium Deposita, 20: 147-153.

PLIMER, I.R., 1986, Sediment-Hosted Exhalative Pb-Zn Deposits - Products of Contrasting Ensialic Rifting: Trans. Geol. Soc. South Africa, Vol. 89, pp 57-73.

PLIMER, I.R., 1988, Broken Hill, Australia and Bergslagen, Sweden - Why God and Mammon Bless the Antipodes! Geol. Mijnbowuw, 67: 265-278.

RICHARDS, S.M., 1966, The Banded Iron Formations at Broken Hill, Australia and their Relationship to the Lead Zinc Ore Bodies, Parts 1 and 2: Econ. Geol. Vol. 61, pp 72-96, 257-274.

ROCHE, M.T., 1994, The Cannington Silver Lead Zinc Deposit - at Feasibility: Darwin Conference, AUSIMM, pp 193-197.

ROZENDAAL, A., 1986, The Gamsberg Zinc Deposit, Namaqualand District, in ANHAEUSSER, C.R. and MASKE, S. (Editors), 1986, Mineral Deposits of Southern Africa, Geol. Soc. of Sth. Afr. Johann., pp 1477 - 1488.

RUBURN, B.J., WILSON, I.H., GRIMES, K.G. and HILL, R.M., 1988, 1:100,000 Geological Map and Commentary, Cloncurry, Queensland: Publ. by Australian Government Publishing Service, Canberra.

RUMBLE, D. (Editor), 1976, Oxide Minerals: Mineralogical Society of America Short Course Notes, Vol 3.

RUSSELL, M.J., SOLOMON, M. and WALSHE, J.L., 1981, The Genesis of Sediment Hosted, Exhalative Zinc-Lead Deposits: Mineralium Deposita, Vol. 16, pp 113-127.

RYAN, P.J., *et at*, 1986, The Aggenys Base Metal Sulphide Deposits, Namaqualand District, in ANHAEUSSER, C.R. and MASKE, S. (Editors), 1986, Mineral Deposits of Southern Africa, Geol. Soc. of Sth. Afr. Johann., pp 1447-1473 .

RYBURN, R.J., WILSON, I.H., GRIMES, K.G. and HILL, R.M., 1988, Cloncurry Qld, 1:100,000 Map Commentary, BMR, Australia.

SEGNIT, E.R., 1961, Petrology of the Zinc Lode, New Broken Hill Consolidated Ltd, Broken Hill, NSW: Proceedings of AUSIMM, NO. 199, pp 87-111.

SHEPPARD, M.J., 1993, Aspects Critical to the Development of Large Iron Formation Hosted Gold Deposits: Unpublished BHP Company Report CR 7712.

SHEPPY, N.R., 1975, Interim Assessment Report, pegmont Lead-Zinc Deposit, Northwest Queensland: Unpublished BHP Company Report EX 774.

SKRZECZYNSKI, R.H., 1993, From Concept to Cannington: A Decade of Exploration in the Eastern Succession, in Symposium on Recent Advances in the Mount Isa Block: AIG Bull., 13: 35-38.

SOLOMON, M. and WALSHE, J.L., 1979, The Formation of Massive Sulphide Deposits on the Sea Floor: Econ. Geol., Vol. 74, pp 797-813.

SPYCHER, N.F. and REED, M.H., 1990a, Users Guide for CHILLER: A Program for Computing Water-rock Reactions, Boiling, Mixing and Other Reaction Processes in Aqueous-Mineral-Gas Systems: University of Oregon (Unpublished).

SPYCHER, N.F. and REED, M.H., 1990b, Users Guide for SOLVEQ: A Computer Program for Computing Aqueous-Mineral-Gas Equilibria: University of Oregon (Unpublished).

SQUILLER, S.F. and SCLAR, C.B., 1980, Genesis of the Sterling Hill Deposit, Sussex County, New Jersey: Proceedings, 5th Symposium of Int. Assoc. of Geologists for Ore Deposits (IAGOD) Vol. 1, pp 759-766.

STANTON, R.L., 1983, Stratiform Ores and metamorphic processes: Some Thoughts Arising from Broken Hill: Proc. Broken Hill Conference, Aust. Inst. Min. Metall., pp 11-28.

STANTON, R.L., 1972, A Preliminary Account of Chemical Relationships between Sulfide Lode and "Banded Iron Formation" at Broken Hill, New South Wales: Econ. Geol., Vol. 67, pp 1128-1145.

STANTON, R.L., 1976, Petrochemical Studies of the Ore Environment at Broken Hill, New South Wales: 1 - Constitution of "Banded Iron Formation": Inst. of Mining and Metallurgy, Transactions, Section B, Vol. 85, pp 33-46.

STANTON, R.L., 1976, Petrochemical Studies of the Ore Environment at Broken Hill, New South Wales: 2 - Regional Metamorphism of BIFS and their Associates: Inst. of Mining and Metallurgy, Transactions, Section B, Vol. 85, pp 118-131.

STANTON, R.L., 1976, Petrochemical Studies of the Ore Environment at Broken Hill, New South Wales: 3 - BIFS and Sulfide Ore Bodies - Constitutional and Genetic Ties: Inst. of Mining and Metallurgy, Transactions, Section B, Vol. 85, pp 132-141.

STANTON, R.L., 1976, Petrochemical Studies of the Ore Environment at Broken Hill, New South Wales: 4 - Environmental Synthesis: Inst. of Mining and Metallurgy, Transactions, Section B, Vol. 85, pp 221-233.

STANTON, R.L. and VAUGHAN, J.P., 1978, Pegmont Petrochemical Research: Unpublished BHP Company Memo CM 126.

STANTON, R.L. and VAUGHAN, J.P., 1979, Facies of Ore Formation, A Preliminary Account of the Pegmont Deposit as an Example of Potential Relationships Between Small "Iron Formations" and Stratiform Sulfide Ores: AUSIMM Proceedings, No. 270, pp 25-38.

STEVENS, B.P.J., 1989, Geology of the Broken Hill Ore Body and Enclosing Rocks: Unpublished.

STEVENS, B.P.J., WILLIS, I.L., BROWN, R.E. and STROUD, W.J., 1983, The Early Proterozoic Willyama Supergroup: Definitions of Stratigraphic Units from the Broken Hill Block, New South Wales: New South Wales Geolog. Survey - Records 21 Part 2, pp 407-442.

STEVENS, B.P.J., BARNES, R.G. and FORBES, G.G., 1990, Willyama Block - Regional Geology and Minor Mineralisation: in HUGHES, F.E. (Editor), 1990, Geology of Mineral Deposits of Aust. and PNG, Monograph 14, AUSIMM.

STEVENS, B.P.J., BARNES, R.G., BROWN, R.E., STROUD, W.J. and WILLIS, I.L., 1988, The Willyama Supergroup in the Broken Hill and Eriowie Blocks, New South Wales: Precambrian Res., 40-41: 297-327.

STEWART, I.C. and BOYD, D.M., 1983, Enhancement of Aeromagnetic Trends from Broken Hill using the Second Derivative: Bull. Aust. Soc. Explor. Geophys (1983), pp 11-21.

SVERJENSKY, D.A., 1984, The Distribution of Divalent Trace Elements between Sulfides, Oxides, Silicates and Hydrothermal Solutions: Thermodynamic Basis: Geochemica Et Cosmochimica Acta, Vol. 49, pp 853-864.

TUCKER, D.H., 1983, The Characteristics and Interpretation of Regional Magnetic and Gravity Fields in the Broken hill District: Broken Hill Conference, 1983, AUSIMM, pp 81-114.

VAN DER HEYDEN, A. and EDGECOMBE, D.R., 1990, Silver-Lead-Zinc Deposit at South Mine, Broken Hill: in HUGHES, F.E. (Editor), 1990, Geology of Mineral Deposits of Aust. and PNG, Monograph 14, AUSIMM, pp 1073-1078.

VIVALLO, W., 1985, The Geology and Genesis of the Proterozoic Massive Sulfide Deposit at Garpenberg, Central Sweden: Econ. Geol. Vol. 80, pp 17-32.

WALTERS, S.G., 1984, A Review and Classification of Broken Hill Type Mineralisation - A Conceptual Model for Exploration: Unpublished BHP Company Report CR 4213.

WALTERS, S.G., 1992, Broken Hill Type Pb-Zn-Ag Deposits, Geological Characteristics and Exploration Models. Master of Economic Geology Course Work Manuals, CODES, University of Tasmania, pp 1.1-1.56.

WALTERS, S.G., 1994, Geology and Lode Characterisation, Cannington Southern Zone: Unpublished BHP Company Report CR 7997.

WHITING, T.H., 1991, Soldiers Cap Aeromagnetic Interpretation - Version 2: Unpublished Company Memo CM 4996.

WIKSTROM, A., 1989, 1:50,000 Geology Map SGU Ser. Af nr 165, Berggrundskarten, 9 F Finspang SV: Publ. by SGU, Uppsula, Sweden.

WIKSTROM, A., 1989, 1:50,000 Geology Map SGU Ser. Af nr 164, Berggrundskarten, 9 F Finspang NV: Publ. by SGU, Uppsula, Sweden.

WILLIAMS, P.J. and BLAKE, K.L., 1994, Alteration in the Cloncurry District. EGRU Contribution 49, James Cook University, Townsville, Australia.

WILLIS, I.L., 1989, Broken Hill Stratigraphic Map, NSW Geological Survey, Sydney.

WILLIS, I.L., BROWN, R.E., STROUD, W.J. and STEVENS, B.P.J., 1983, The Early Proterozoic Willyama Supergroup: Stratigraphic Subdivision and Interpretation of High to Low-grade Metamorphic Rocks in the Broken Hill Block, New South Wales: Geol. Soc. Australia Journal, 30: 195-224.

WILSON, I.H., GRIMES, K.G. and DERRICK, G.M. (Editors), 1983, 1:250,000 Geological Map, Cloncurry: Publ. by Department of Mines, Qld.

WINDRIM, D.P., 1984, Lower Proterozoic Stratiform Base Metal Mineralisation in the Berglagen District, South Central Sweden: Report on a Visit in September-October 1984: Unpublished BHP Company Report CR 4514.

WITHERLEY, K.E., 1984, Notes on Black Mountain Geophysics, Republic of South Africa: Internal BHP Company Memo (Unpublished).

WRIGHT, J.V., HAYDON, R.C. and McCONACHY, G.W., 1987, Sedimentary Model for the Giant Broken Hill Pb-Zn Deposit, Australia, in Geology, Vol 15, pp 598-602.

APPENDIX A

Susceptibility measurements on selected drill core,
section 4700N, Cannington.

CAD 07 - Magnetic Susceptibility

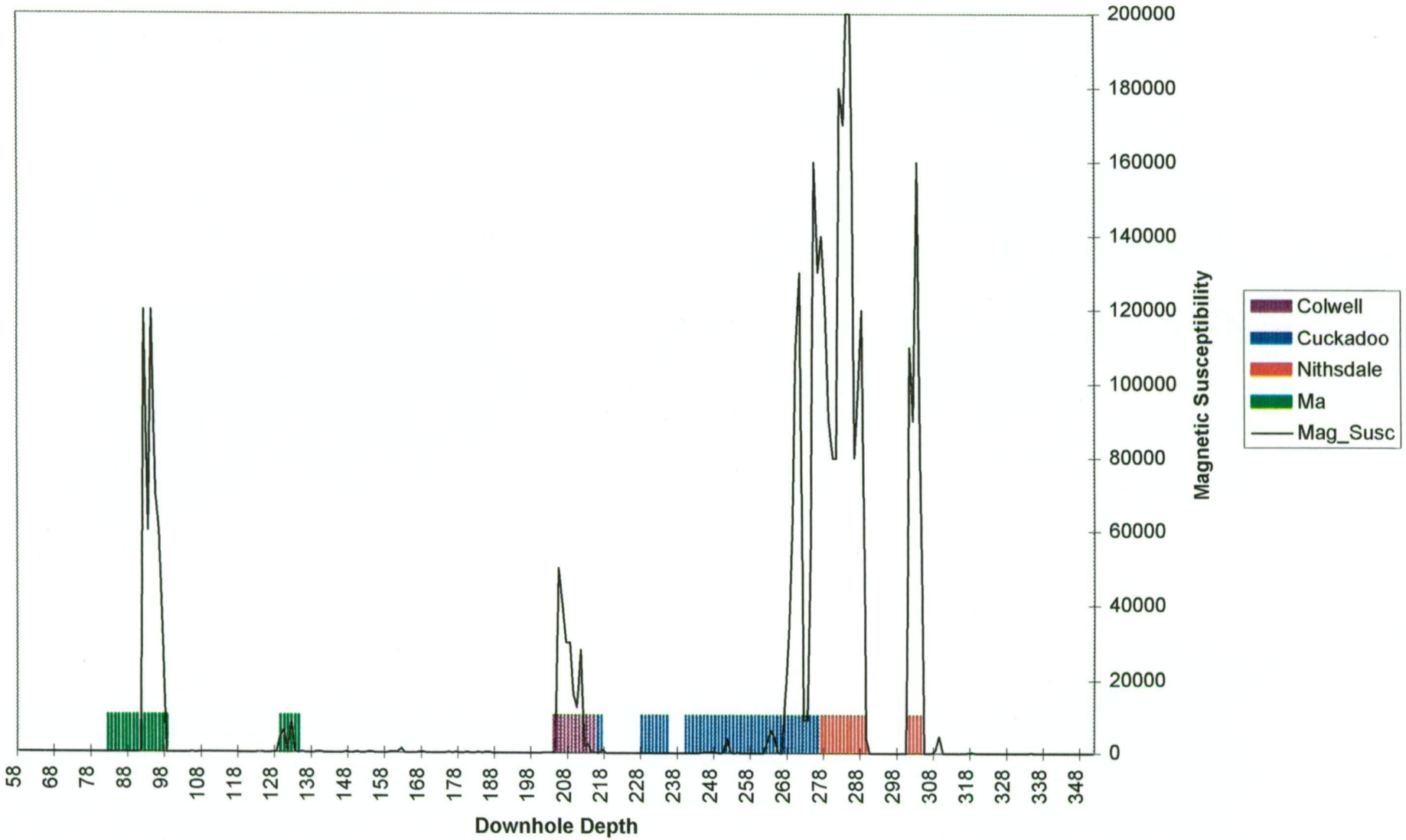

CAD 07 - Magnetic Susceptibility

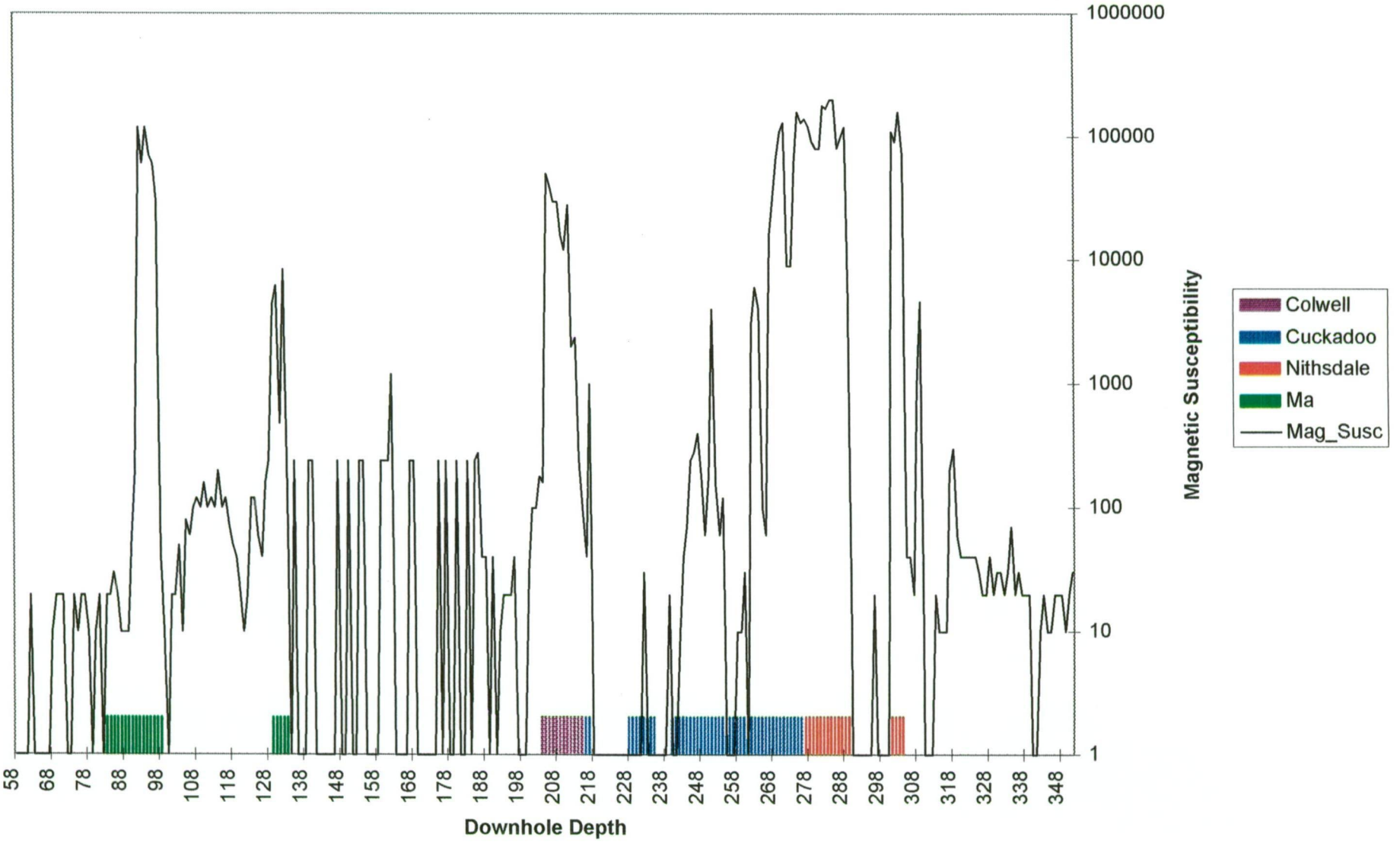

CAD 15 - Magnetic Susceptibility

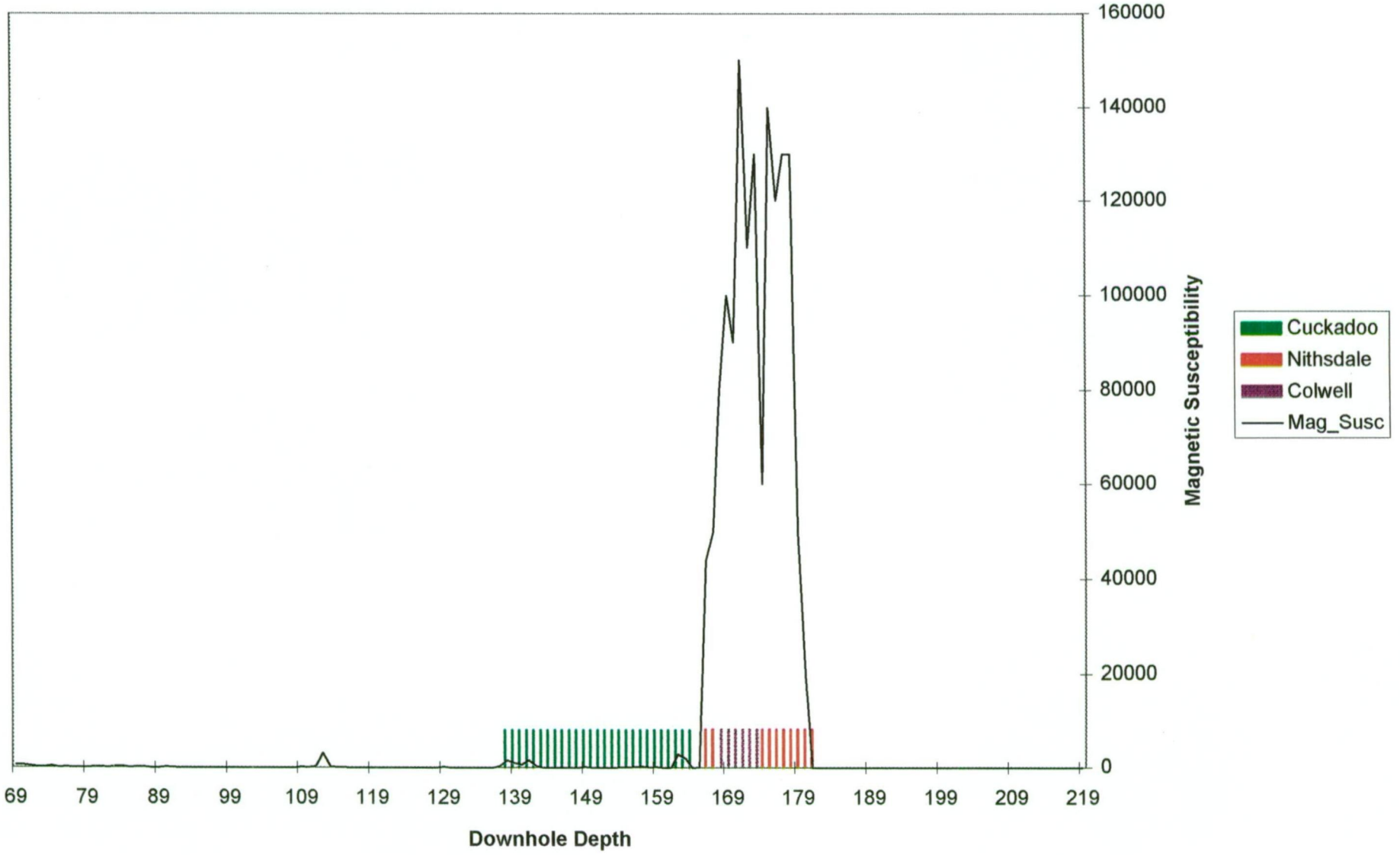

CAD 15 - Magnetic Susceptibility

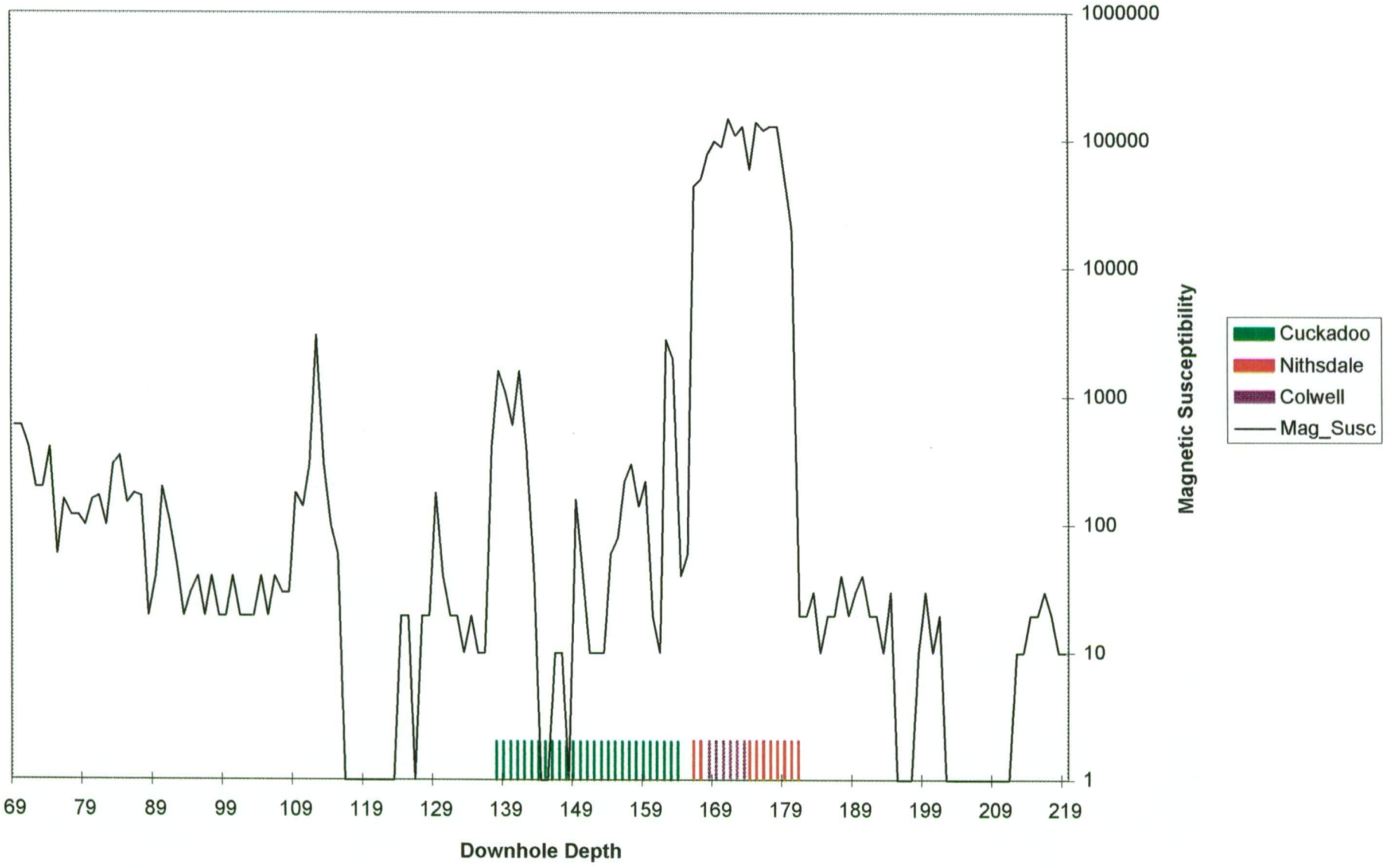

CAD 24 - Magnetic Susceptibility

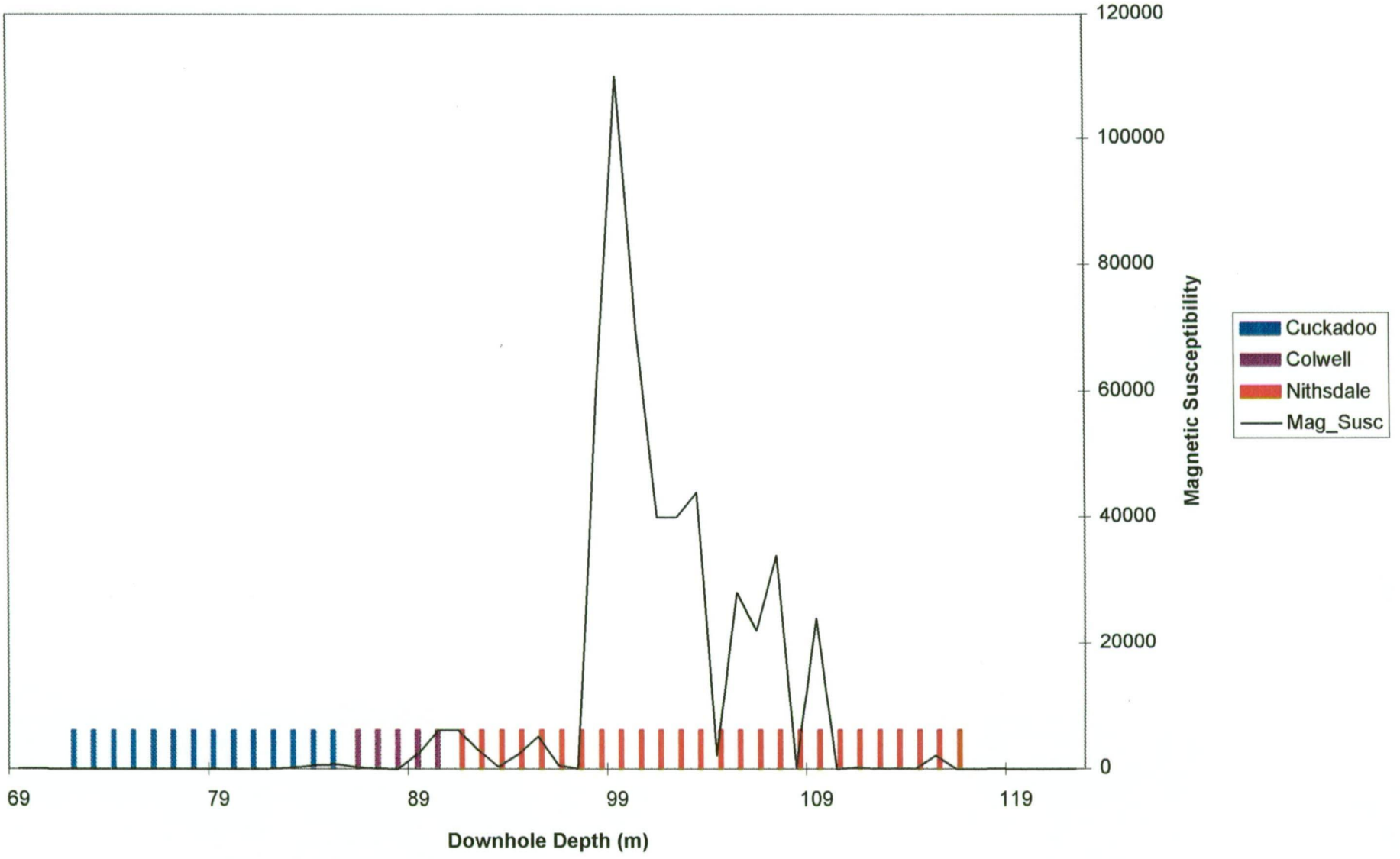

CAD 24 - Magnetic Susceptibility

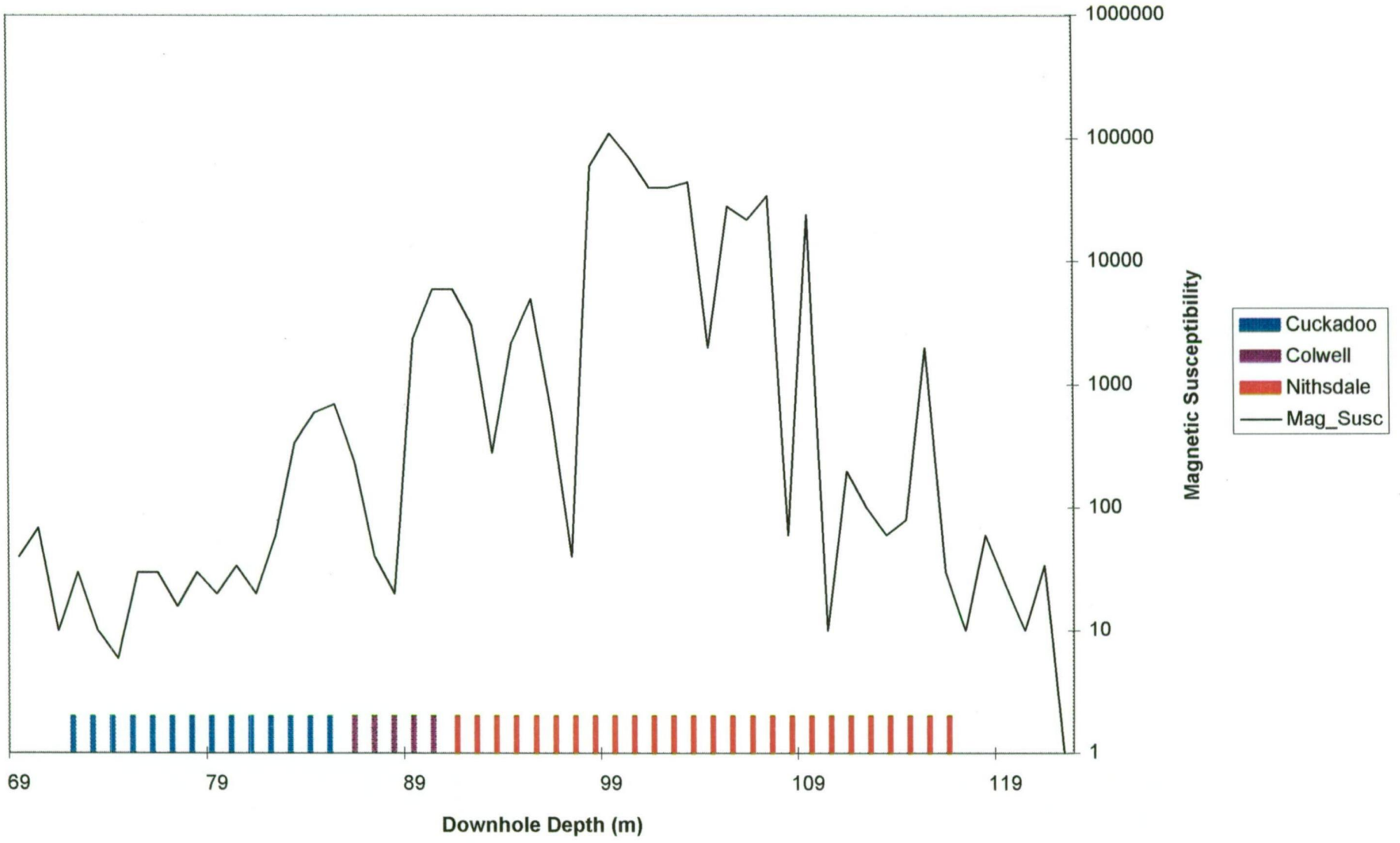

CAD 28 - Magnetic Susceptibility

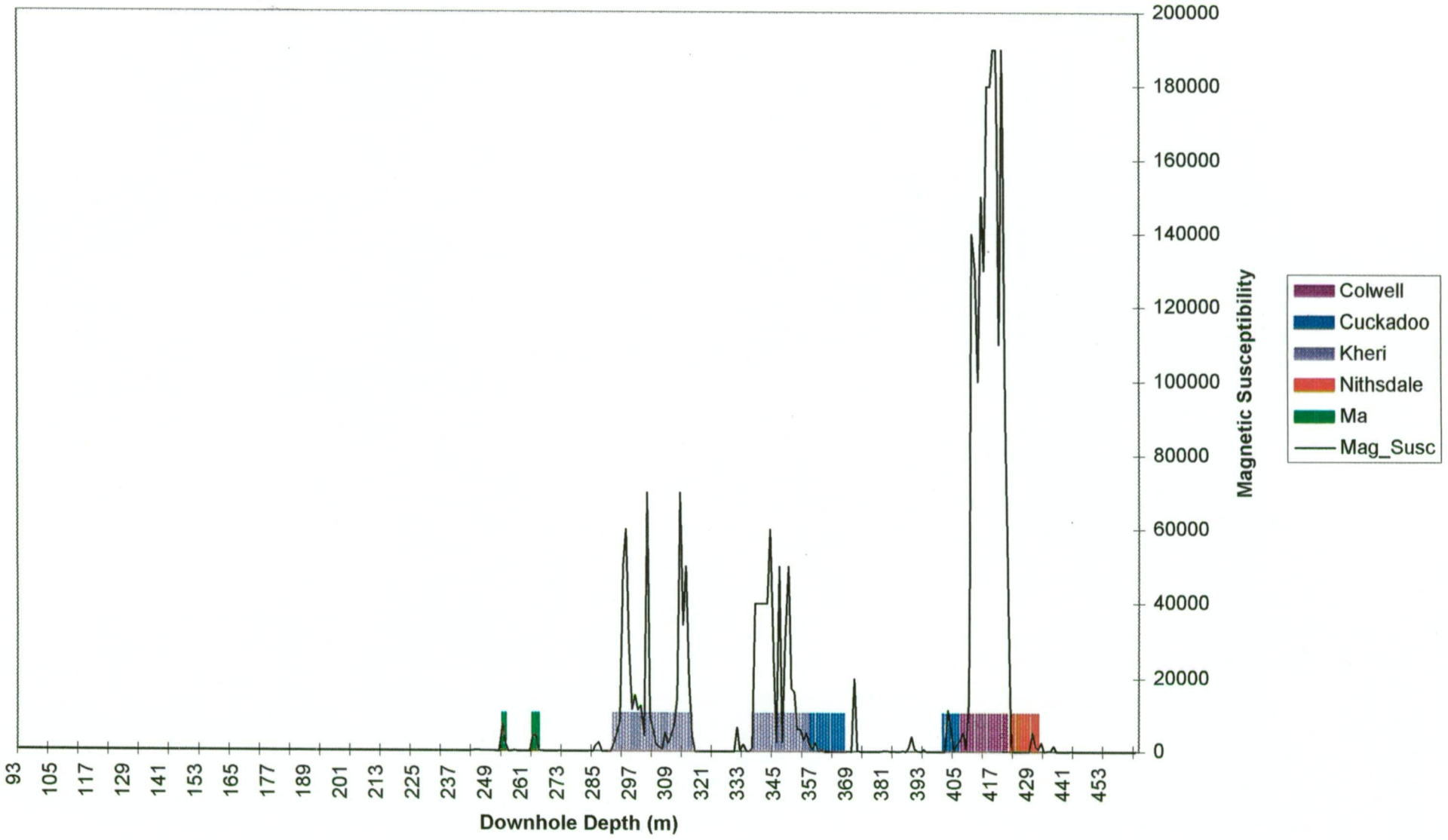

CAD 28 - Magnetic Susceptibility

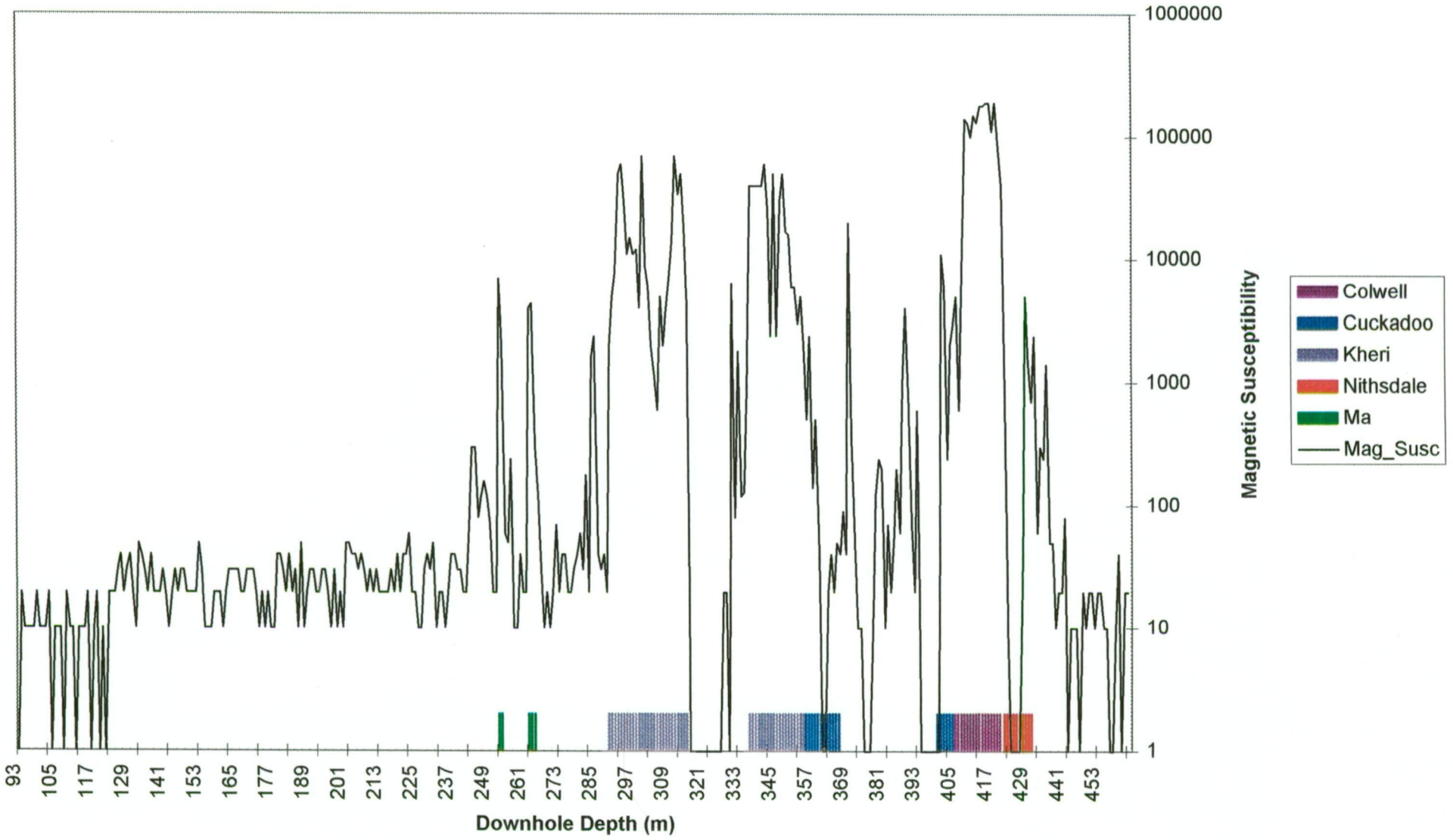

CAD 51 - Magnetic Susceptibility

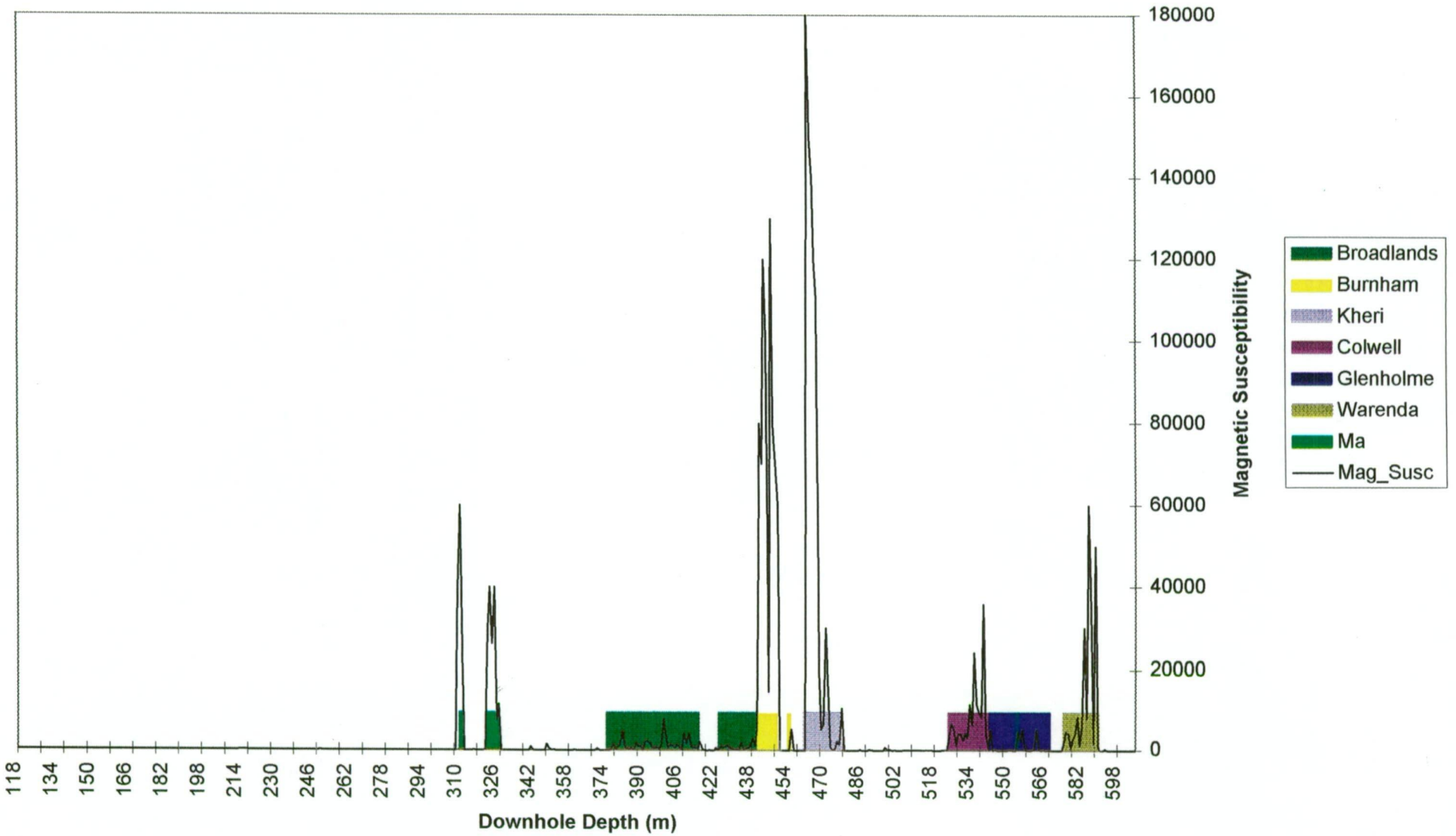

CAD 51 - Magnetic Susceptibility

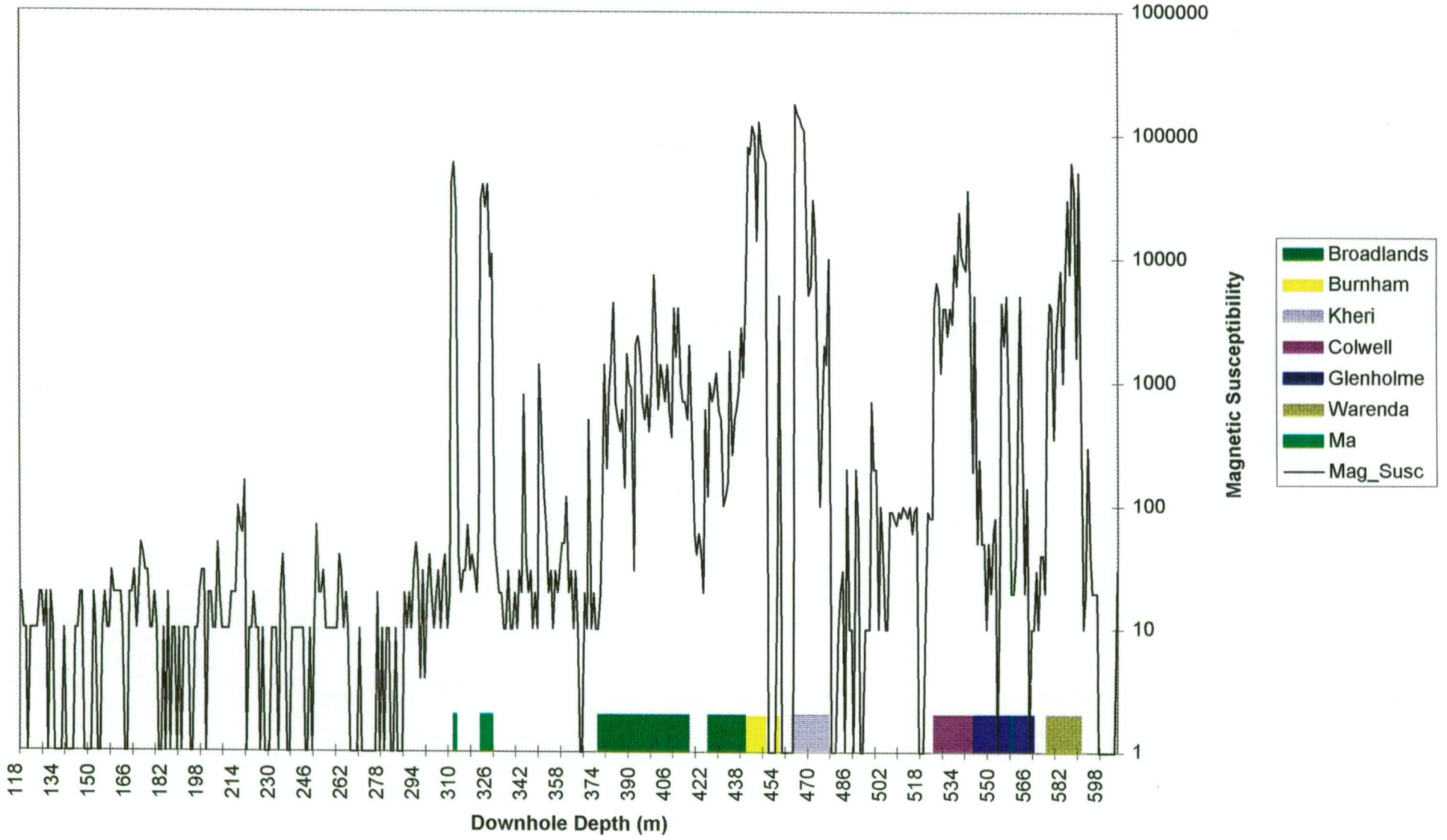

CAD 63 - Magnetic Susceptibility

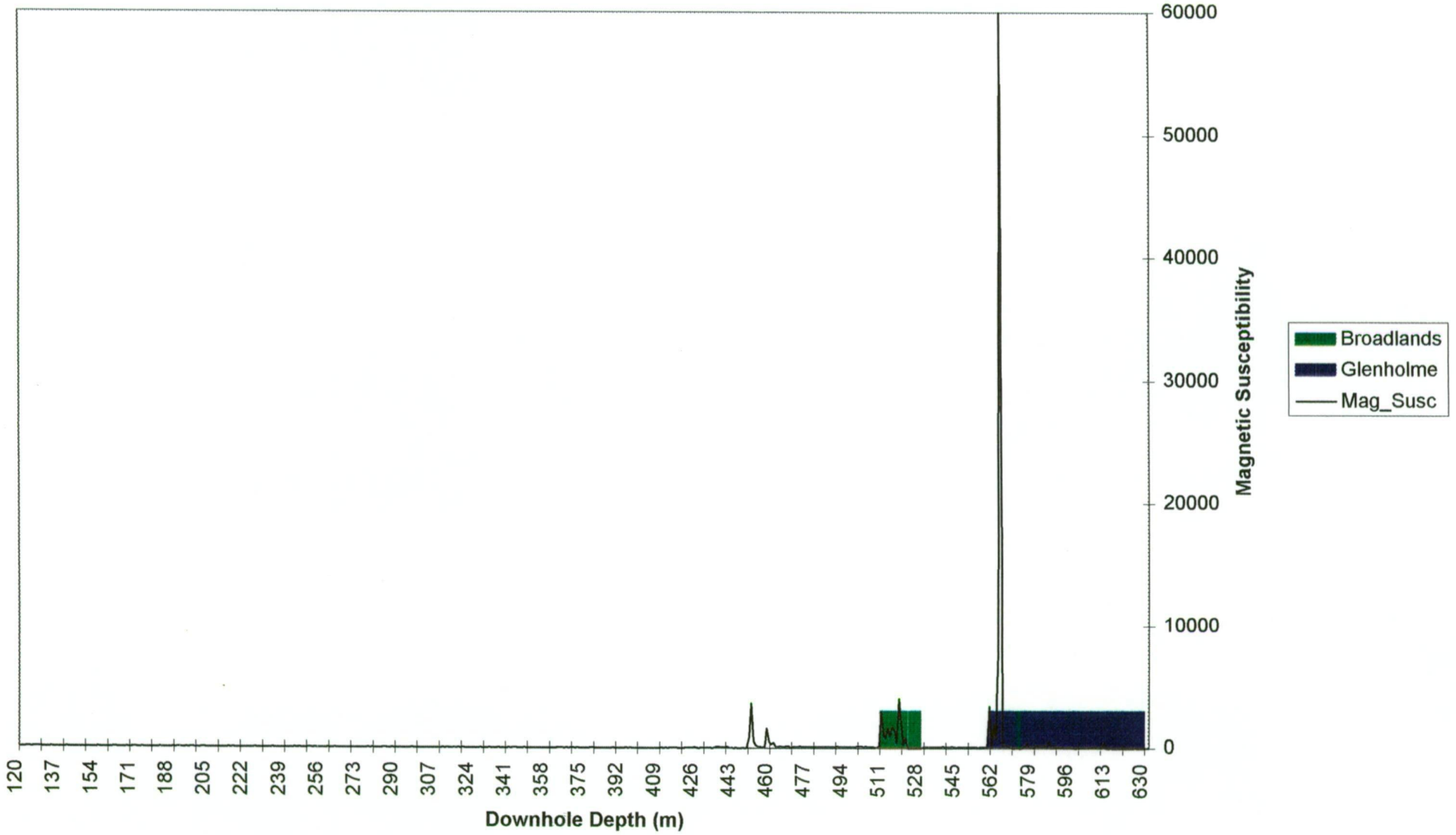

CAD 63 - Magnetic Susceptibility

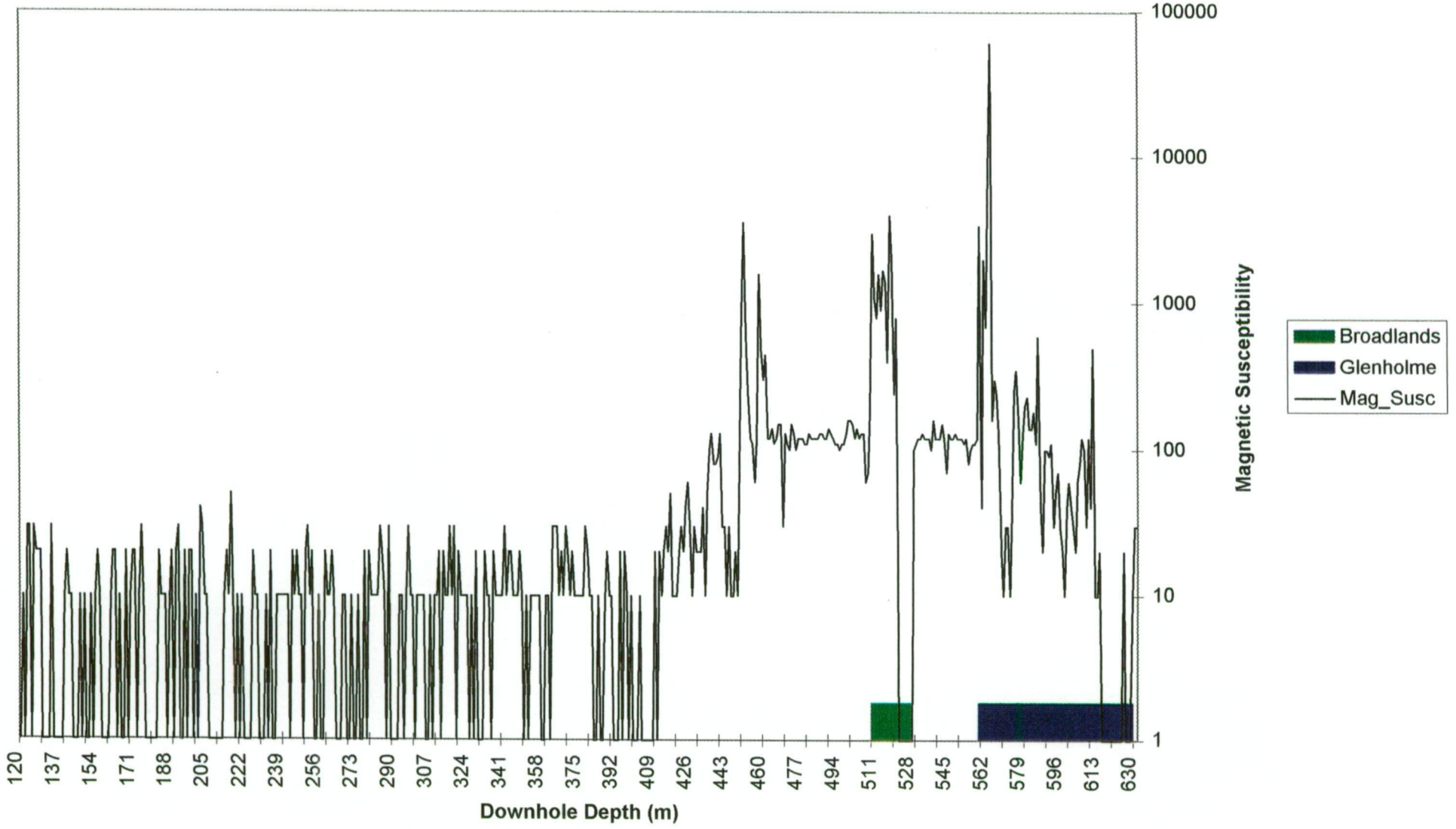

CAD 74 - Magnetic Susceptibility

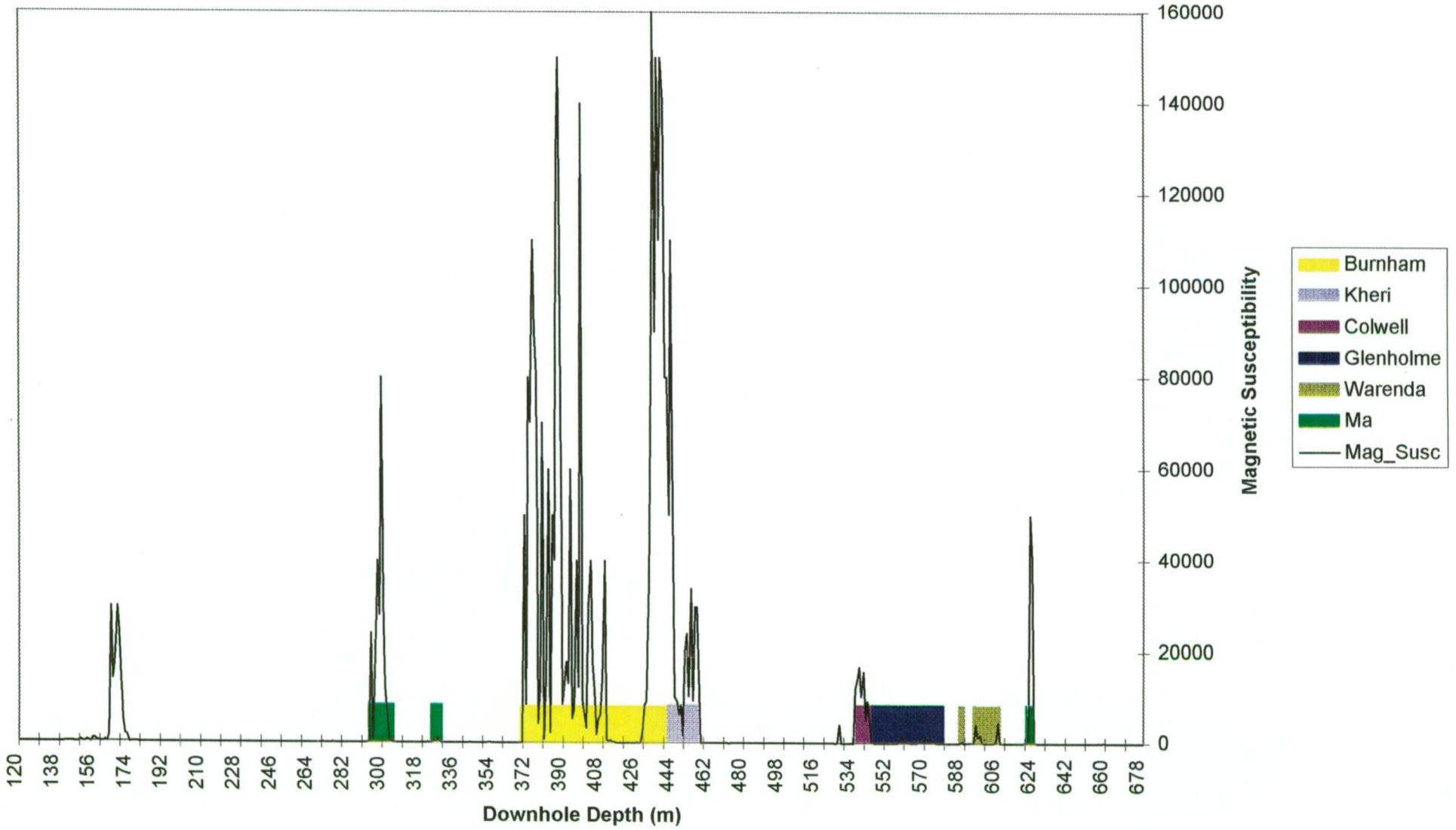

CAD 74 - Magnetic Susceptibility

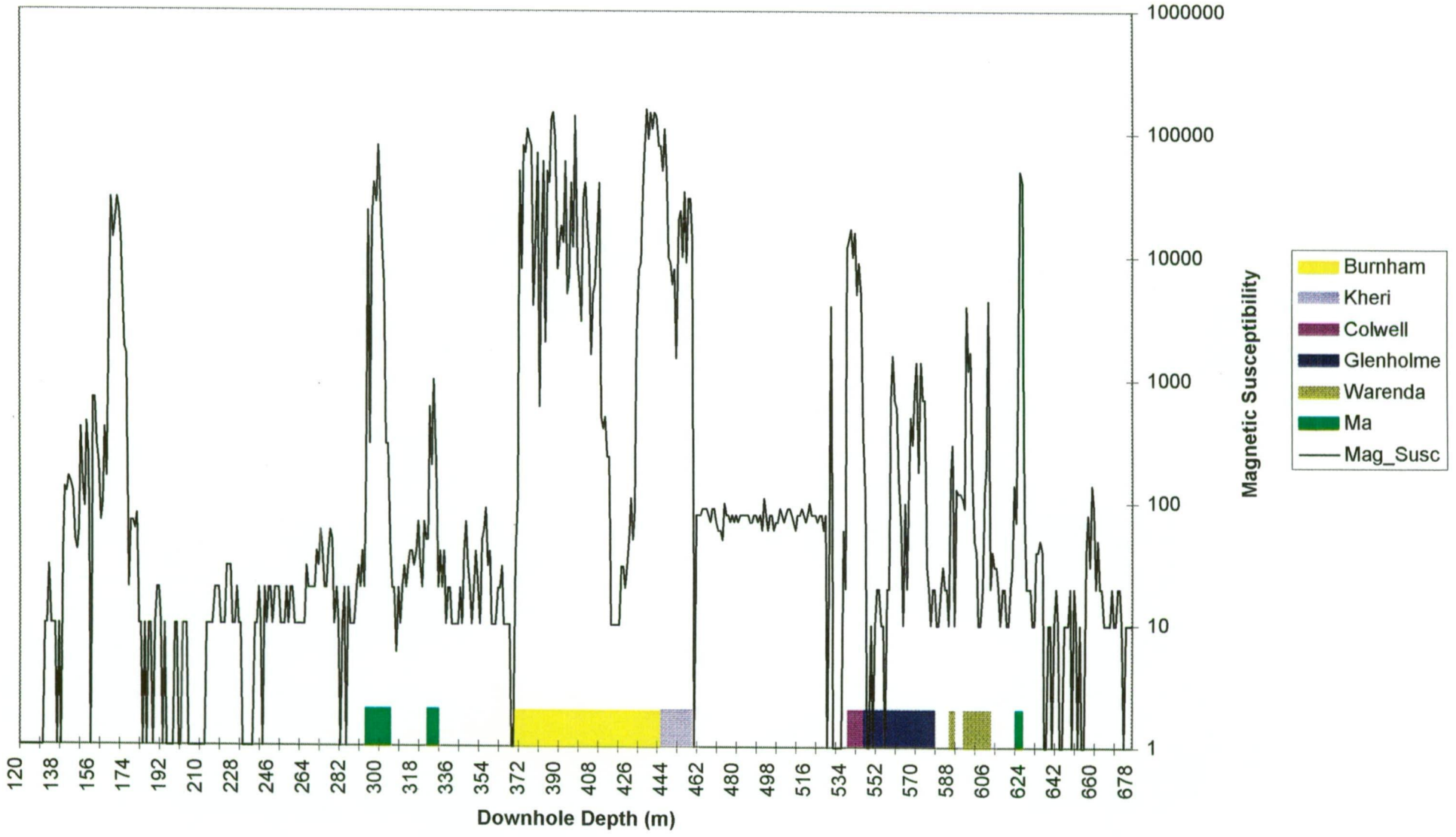

APPENDIX B

Compositions of model BHT fluids.

Chemical composition of Fluid DC10_1

Species	Molality	Total Moles		Concentration (ppm)
H+	.7444E-04	.2557E+00	CM	.227736E+03
H2O	.1000E+01	.5551E+02		.883572E+06
Cl-	.1182E+01	.1926E+01		.603326E+05
SO4--	.1490E-08	-.1450E-04		-.123072E+01
HCO3-	.5630E-03	.2558E+00		.137910E+05
HS-	.3265E-05	.2528E-03		.738721E+01
SiO2(aq)	.6185E-02	.6187E-02	EQ	.328445E+03
Al+++	.3105E-11	.5665E-02	EQ	.135043E+03
Ca++	.2128E-01	.1014E+00		.359095E+04
Mg++	.9070E-02	.1520E-01	EQ	.326475E+03
Fe++	.4962E-03	.2341E-01	EQ	.115534E+04
K+	.1178E+00	.1510E+00		.521698E+04
Na+	.9602E+00	.1432E+01	AD	.290928E+05
Mn++	.7229E-03	.2888E-01		.140189E+04
Zn++	.1825E-06	.2565E-02	EQ	.148167E+03
Cu+	.1063E-09	.3551E-05	EQ	.199339E+00
Pb++	.1484E-06	.4071E-03	EQ	.745345E+02
Ag+	.1532E-08	.6810E-04	EQ	.649113E+01
AuCl2-	.5877E-11	.1348E-08	EQ	.319118E-03
Ba++	.7783E-03	.1910E-02		.231779E+03
F-	.3119E-03	.2150E-01	EQ	.360986E+03
HPO4--	.5724E-11	.1523E-08	EQ	.129196E-03

Chemical composition of Fluid DC10_2

Species	Molality	Total Moles		Concentration (ppm)
H+	.8020E-04	.2268E+00	CM	.204150E+03
H2O	.1000E+01	.5551E+02		.892892E+06
Cl-	.8174E+00	.1711E+01		.541630E+05
SO4--	.2172E-10	-.1050E-03		-.900615E+01
HCO3-	.1602E-03	.2272E+00		.123783E+05
HS-	.7968E-06	.2246E-03		.663239E+01
SiO2(aq)	.9731E-02	.9733E-02	EQ	.522162E+03
Al+++	.8300E-12	.1308E-02	EQ	.315018E+02
Ca++	.2495E-01	.9007E-01		.322335E+04
Mg++	.2761E-02	.5908E-02	EQ	.128249E+03
Fe++	.1620E-03	.8921E-02	EQ	.444832E+03
K+	.9639E-01	.1341E+00		.468196E+04
Na+	.7108E+00	.1172E+01	AD	.240560E+05
Mn++	.2620E-03	.2548E-01		.124989E+04
Zn++	.9712E-06	.5786E-01	EQ	.337713E+04
Cu+	.1669E-07	.3848E-03	EQ	.218328E+02
Pb++	.1797E-05	.1237E-01	EQ	.228900E+04
Ag+	.1302E-07	.5564E-03	EQ	.535866E+02
AuCl2-	.4330E-10	.1087E-09	EQ	.260104E-04
Ba++	.4429E-03	.1747E-02		.214235E+03
F-	.1361E-04	.4200E-02		.712454E+02
HPO4--	.8479E-12	.5337E-09	EQ	.457333E-04

Chemical composition of Fluid DC15_1

Species	Molality	Total Moles		Concentration (ppm)
H+	.8203E-04	.2271E+00	CM	.195893E+03
H2O	.1000E+01	.5551E+02		.855920E+06
Cl-	.1426E+01	.2567E+01		.778956E+05
SO4--	.2064E-08	-.1300E-04		-.106888E+01
HCO3-	.5611E-03	.2272E+00		.118657E+05
HS-	.3095E-05	.2119E-03		.599826E+01
SiO2(aq)	.6185E-02	.6187E-02	EQ	.318167E+03
Al+++	.7657E-11	.5485E-02	EQ	.126662E+03
Ca++	.3401E-01	.1351E+00		.463465E+04
Mg++	.1575E-01	.2345E-01	EQ	.487933E+03
Fe++	.8134E-03	.6195E-01	EQ	.296147E+04
K+	.1492E+00	.1966E+00		.657986E+04
Na+	.1208E+01	.1864E+01	AD	.366851E+05
Mn++	.8535E-03	.2548E-01		.119814E+04
Zn++	.3224E-06	.6660E-02	EQ	.372656E+03
Cu+	.1298E-09	.7720E-05	EQ	.419856E+00
Pb++	.2471E-06	.1070E-02	EQ	.189816E+03
Ag+	.1652E-08	.1595E-03	EQ	.147292E+02
AuCl2-	.8290E-11	.1182E-08	EQ	.270945E-03
Ba++	.8161E-03	.1747E-02		.205364E+03
F-	.3350E-03	.2108E-01	EQ	.342836E+03
HPO4--	.8140E-11	.1503E-08	EQ	.123473E-03

Chemical composition of fluid DC15_2

Species	Molality	Total Moles		Concentration (ppm)
H+	.1027E-03	.2267E+00	CM	.194369E+03
H2O	.1000E+01	.5551E+02		.850507E+06
Cl-	.1026E+01	.2567E+01		.774030E+05
SO4--	.6132E-10	-.1025E-03		-.837438E+01
HCO3-	.2204E-03	.2272E+00		.117907E+05
HS-	.1040E-05	.2119E-03		.596033E+01
SiO2(aq)	.9731E-02	.9733E-02	EQ	.497387E+03
Al+++	.7270E-11	.1295E-02	EQ	.297277E+02
Ca++	.6633E-01	.1351E+00		.460534E+04
Mg++	.9834E-02	.1386E-01	EQ	.286526E+03
Fe++	.5275E-03	.2593E-01	EQ	.123160E+04
K+	.1441E+00	.1966E+00		.653825E+04
Na+	.1021E+01	.1606E+01	AD	.313981E+05
Mn++	.6784E-03	.2548E-01		.119056E+04
Zn++	.2797E-05	.1471E+00	EQ	.817581E+04
Cu+	.1825E-07	.6976E-03	EQ	.376970E+02
Pb++	.4406E-05	.3219E-01	EQ	.567179E+04
Ag+	.1497E-07	.1878E-02	EQ	.172289E+03
AuCl2-	.5763E-10	.1530E-09	EQ	.348504E-04
Ba++	.7412E-03	.1747E-02		.204065E+03
F-	.1814E-04	.4200E-02		.678635E+02
HPO4--	.2521E-11	.6957E-09	EQ	.567908E-04

Chemical composition of Fluid SS10_1

Species	Molality	Total Moles		Concentration (ppm)
H+	.7136E-04	.2267E+00	CM	.204658E+03
H2O	.1000E+01	.5551E+02		.895777E+06
Cl-	.1038E+01	.1715E+01		.544651E+05
SO4--	.1105E-08	-.1350E-04		-.116168E+01
HCO3-	.4751E-03	.2272E+00		.124183E+05
HS-	.2752E-05	.2254E-03		.667752E+01
SiO2(aq)	.6185E-02	.6187E-02	EQ	.332981E+03
Al+++	.1978E-11	.7037E-03	EQ	.170078E+02
Ca++	.5606E-01	.2740E+00		.983738E+04
Mg++	.7531E-02	.1302E-01	EQ	.283506E+03
Fe++	.4053E-03	.1325E-01	EQ	.662910E+03
K+	.1395E+00	.1755E+00		.614720E+04
Na+	.6072E+00	.8819E+00	AD	.181619E+05
Mn++	.5958E-03	.2548E-01		.125393E+04
Zn++	.1742E-06	.1838E-02	EQ	.107625E+03
Cu+	.1409E-09	.3409E-05	EQ	.194022E+00
Pb++	.1452E-06	.2832E-03	EQ	.525582E+02
Ag+	.1623E-08	.4788E-04	EQ	.462680E+01
AuCl2-	.4631E-11	.9782E-09	EQ	.234734E-03
Ba++	.6965E-03	.1747E-02		.214927E+03
F-	.1686E-03	.3070E-02	EQ	.522479E+02
HPO4--	.8665E-12	.2668E-09	EQ	.229355E-04

Chemical composition of Fluid SS10_2

Species	Molality	Total Moles		Concentration (ppm)
H+	.8149E-04	.2265E+00	CM	.203902E+03
H2O	.1000E+01	.5551E+02		.893149E+06
Cl-	.8095E+00	.1715E+01		.543053E+05
SO4--	.2365E-10	-.1050E-03		-.900874E+01
HCO3-	.1634E-03	.2272E+00		.123818E+05
HS-	.8224E-06	.2254E-03		.665793E+01
SiO2(aq)	.9731E-02	.9733E-02	EQ	.522313E+03
Al+++	.8889E-12	.1205E-02	EQ	.290482E+02
Ca++	.8153E-01	.2740E+00		.980851E+04
Mg++	.3116E-02	.6335E-02	EQ	.137567E+03
Fe++	.1759E-03	.8802E-02	EQ	.439046E+03
K+	.1272E+00	.1755E+00		.612916E+04
Na+	.4742E+00	.7718E+00	AD	.158479E+05
Mn++	.2877E-03	.2548E-01		.125025E+04
Zn++	.1033E-05	.5566E-01	EQ	.324991E+04
Cu+	.1661E-07	.3723E-03	EQ	.211307E+02
Pb++	.1889E-05	.1185E-01	EQ	.219355E+04
Ag+	.1313E-07	.5554E-03	EQ	.535085E+02
AuCl2-	.4196E-10	.1109E-09	EQ	.265320E-04
Ba++	.4690E-03	.1747E-02		.214296E+03
F-	.1390E-04	.3900E-02		.661755E+02
HPO4--	.1427E-12	.8470E-10	EQ	.726050E-05

Chemical composition of Fluid SS15_1

Species	Molality	Total Moles		Concentration (ppm)
H+	.8211E-04	.2264E+00	CM	.195512E+03
H2O	.1000E+01	.5551E+02		.856579E+06
Cl-	.1390E+01	.2572E+01		.781074E+05
SO4--	.2111E-08	-.1300E-04		-.106970E+01
HCO3-	.5613E-03	.2272E+00		.118749E+05
HS-	.3125E-05	.2130E-03		.603405E+01
SiO2(aq)	.6185E-02	.6187E-02	EQ	.318411E+03
Al+++	.7226E-11	.6829E-03	EQ	.157823E+02
Ca++	.1074E+00	.4109E+00		.141069E+05
Mg++	.1674E-01	.2454E-01	EQ	.511111E+03
Fe++	.8297E-03	.5733E-01	EQ	.274229E+04
K+	.2009E+00	.2633E+00		.881898E+04
Na+	.8208E+00	.1256E+01	AD	.247410E+05
Mn++	.8911E-03	.2548E-01		.119906E+04
Zn++	.3245E-06	.6099E-02	EQ	.341520E+03
Cu+	.1264E-09	.7137E-05	EQ	.388455E+00
Pb++	.2480E-06	.9775E-03	EQ	.173490E+03
Ag+	.1639E-08	.1494E-03	EQ	.138021E+02
AuCl2-	.7887E-11	.1207E-08	EQ	.276951E-03
Ba++	.8339E-03	.1747E-02		.205522E+03
F-	.1901E-03	.3056E-02	EQ	.497364E+02
HPO4--	.1508E-11	.2739E-09	EQ	.225187E-04

Chemical composition of Fluid SS15_2

Species	Molality	Total Moles		Concentration (ppm)
H+	.1138E-03	.2264E+00	CM	.193957E+03
H2O	.1000E+01	.5551E+02		.849936E+06
Cl-	.1044E+01	.2572E+01		.775017E+05
SO4--	.1036E-09	-.1025E-03		-.836875E+01
HCO3-	.2521E-03	.2272E+00		.117828E+05
HS-	.1227E-05	.2130E-03		.598725E+01
SiO2(aq)	.9731E-02	.9733E-02	EQ	.497060E+03
Al+++	.1808E-10	.1281E-02	EQ	.293848E+02
Ca++	.2537E+00	.4109E+00		.139975E+05
Mg++	.1734E-01	.2147E-01	EQ	.443574E+03
Fe++	.8820E-03	.3291E-01	EQ	.156189E+04
K+	.1973E+00	.2633E+00		.875058E+04
Na+	.6046E+00	.9152E+00	AD	.178838E+05
Mn++	.1118E-02	.2548E-01		.118976E+04
Zn++	.4217E-05	.1666E+00	EQ	.925857E+04
Cu+	.1787E-07	.7673E-03	EQ	.414376E+02
Pb++	.6175E-05	.3639E-01	EQ	.640842E+04
Ag+	.1558E-07	.2774E-02	EQ	.254318E+03
AuCl2-	.5584E-10	.1806E-09	EQ	.411261E-04
Ba++	.9225E-03	.1747E-02		.203928E+03
F-	.2086E-04	.4200E-02		.678179E+02
HPO4--	.8971E-12	.1695E-09	EQ	.138253E-04

Chemical composition of Fluid SST_1

Species	Molality	Total Moles		Concentration (ppm)
H+	.1120E-03	.2263E+00	CM	.178415E+03
H2O	.1000E+01	.5551E+02		.782016E+06
Cl-	.1647E+01	.4372E+01		.121213E+06
SO4--	.8874E-08	-.1200E-04		-.901463E+00
HCO3-	.7049E-03	.2272E+00		.108412E+05
HS-	.3605E-05	.1873E-03		.484412E+01
SiO2(aq)	.6185E-02	.6187E-02	EQ	.290691E+03
Al+++	.1957E-09	.1048E-02	EQ	.221145E+02
Ca++	.4110E+00	.6986E+00		.218964E+05
Mg++	.2648E-02	.2900E-02		.551360E+02
Fe++	.4637E-02	.3743E+00	EQ	.163473E+05
K+	.3337E+00	.4475E+00		.136839E+05
Na+	.1067E+01	.1648E+01	AD	.296267E+05
Mn++	.3614E-02	.2548E-01		.109468E+04
Zn++	.1539E-05	.3103E-01	EQ	.158639E+04
Cu+	.1024E-09	.2208E-04	EQ	.109696E+01
Pb++	.9600E-06	.4865E-02	EQ	.788337E+03
Ag+	.1595E-08	.1214E-02	EQ	.102446E+03
AuCl2-	.1067E-10	.1569E-08	EQ	.328742E-03
Ba++	.1313E-02	.1711E-02		.183765E+03
F-	.2612E-03	.4583E-02	EQ	.680882E+02
HPO4--	.7728E-11	.3701E-09	EQ	.277764E-04

Chemical composition of Fluid SST_2

Species	Molality	Total Moles		Concentration (ppm)
H+	.2183E-03	.2269E+00	CM	.175092E+03
H2O	.1000E+01	.5551E+02		.765736E+06
Cl-	.1032E+01	.4372E+01		.118690E+06
SO4--	.1709E-08	-.9300E-04		-.684090E+01
HCO3-	.4257E-03	.2272E+00		.106155E+05
HS-	.1974E-05	.1873E-03		.474328E+01
SiO2(aq)	.9731E-02	.9734E-02	EQ	.447841E+03
Al+++	.1023E-07	.6005E-03	EQ	.124060E+02
Ca++	.6831E+00	.6986E+00		.214406E+05
Mg++	.2879E-02	.2900E-02		.539882E+02
Fe++	.2346E-01	.1429E+00	EQ	.611008E+04
K+	.3750E+00	.4475E+00		.133990E+05
Na+	.7359E+00	.9232E+00	AD	.162525E+05
Mn++	.1442E-01	.2548E-01		.107190E+04
Zn++	.9025E-04	.4984E+00	EQ	.249470E+05
Cu+	.2184E-07	.2525E-02	EQ	.122859E+03
Pb++	.8460E-04	.1087E+00	EQ	.172498E+05
Ag+	.1984E-07	.4194E-01	EQ	.346450E+04
AuCl2-	.3961E-10	.2817E-09	EQ	.577787E-04
Ba++	.1651E-02	.1747E-02		.183726E+03
F-	.3178E-04	.2000E-02		.290950E+02
HPO4--	.3608E-09	.6377E-08	EQ	.468687E-03

APPENDIX C

Tables of results of thermodynamic modelling of BHT fluids

DC10, DC15, SS10, SS15, SST at 250°C and 300°C

T (C)	pH	log f(O2)	clincl14(%)	chamosit (%)	fluorite (%)	gold (%)	acanthit (%)	chalcopy (%)	quartz (%)	galena (%)	muscovit (%)	pyrite (%)	graphite (%)	bornite (%)	chalcoci (%)
250	4.53	-36.5	100%	100%	100%	10.77%									
245	4.49	-36.95			0%	0.95%	10.40%	0.99%	4.43%						
240	4.45	-37.41			0%	13.63%	14.23%	26.37%	4.93%	13.59%	2.38%				
235	4.39	-37.9			0%	15.93%	9.64%	8.33%	4.40%	2.69%	45.93%	13.29%			
230	4.34	-38.4			0%	14.27%	8.33%	7.15%	4.32%	1.28%	30.96%	17.15%			
225	4.3	-38.89			0%	11.52%	7.36%	7.44%	4.23%	2.07%	16.91%	16.83%			
220	4.26	-39.39			0%	8.96%	6.51%	7.61%	4.15%	3.37%	3.83%	14.94%			
215	4.22	-39.9			0%	6.63%	5.70%	7.24%	4.01%	3.47%		12.89%			
210	4.18	-40.41			0%	4.82%	4.99%	6.73%	3.85%	3.47%		10.58%			
205	4.14	-40.92			0%	3.45%	4.39%	6.26%	3.68%	4.11%		7.84%			
200	4.1	-41.44			0%	2.46%	3.87%	5.84%	3.51%	5.28%		4.81%			
195	4.06	-41.96			0%	1.75%	3.41%	5.47%	3.38%	6.91%		1.67%			
190	4.02	-42.5			0%	1.28%	2.99%	4.56%	3.21%	7.48%					
185	3.98	-43.04			0%	0.97%	2.58%	3.18%	3.07%	6.69%					
180	3.95	-43.6			0%	0.73%	2.23%	1.96%	2.93%	5.94%					
175	3.91	-44.17			0%	0.54%	1.93%	0.88%	2.82%	5.28%					
170	3.87	-44.75			0%	0.40%	1.67%		2.70%	4.66%					
165	3.84	-45.35			0%	0.29%	1.43%		2.59%	4.06%					
160	3.8	-45.96			0%	0.21%	1.24%		2.48%	3.51%					
155	3.77	-46.53			0%	0.14%	1.07%		2.38%	3.02%			20.96%		
150	3.73	-47.1			0%	0.09%	0.92%		2.28%	2.57%			22.61%		
145	3.7	-47.68			0%	0.07%	0.79%		2.18%	2.17%			16.32%		
140	3.67	-48.28			0%	0.05%	0.68%		2.09%	1.82%			11.71%		
135	3.63	-48.89			0%	0.03%	0.58%		2.00%	1.51%			8.37%		
130	3.6	-49.52			0%	0.02%	0.49%		1.91%	1.24%			5.96%		
125	3.57	-50.17			0%	0.01%	0.42%		1.83%	1.02%			4.22%		
120	3.54	-50.84			0%	0.01%	0.36%		1.75%	0.82%			2.98%		
115	3.51	-51.52			0%	0.01%	0.30%		1.67%	0.59%			2.11%	10.55%	
110	3.48	-52.22			0%	0.00%	0.26%		1.59%	0.39%			1.48%	20.34%	
105	3.46	-52.95			0%	0.00%	0.22%		1.51%	0.30%			1.03%	17.85%	
100	3.43	-53.69			0%	0.00%	0.18%		1.43%	0.22%			0.72%	15.62%	
95	3.4	-54.46			0%	0.00%	0.15%		1.35%	0.16%			0.50%	13.65%	
90	3.38	-55.25			0%	0.00%	0.13%		1.27%	0.11%			0.34%	11.80%	
85	3.36	-56.07			0%	0.00%	0.11%		1.19%	0.07%			0.23%	10.20%	
80	3.34	-56.91			0%	0.00%	0.09%		1.12%	0.06%			0.15%		19.40%
75	3.32	-57.77			0%	0.00%	0.07%		1.04%	0.03%			0.10%		18.90%
70	3.3	-58.66			0%	0.00%	0.06%		0.96%	0.02%			0.07%		15.52%
65	3.28	-59.58			0%	0.00%	0.05%		0.89%	0.01%			0.05%		12.72%
60	3.27	-60.52			0%	0.00%	0.04%		0.81%	0.00%			0.03%		10.38%
55	3.25	-61.49			0%	0.00%	0.03%		0.74%				0.02%		8.12%
50	3.24	-62.5			0%	0.00%	0.02%		0.67%				0.01%		6.01%
45	3.23	-63.53			0%	0.00%	0.02%		0.60%				0.01%		4.19%
40	3.22	-64.6			0%	0.00%	0.01%		0.53%				0.01%		2.70%
35	3.21	-65.69			0%	0.00%	0.01%		0.47%				0.00%		1.48%
30	3.21	-66.83			0%	0.00%	0.01%		0.42%				0.00%		0.57%
25	3.2	-67.99			0%	0.00%	0.01%		0.36%				0.00%		
20	3.2	-69.2			0%	0.00%	0.00%		0.31%				0.00%		
Total (m)			6.82E-06	7.46E-06	4.01E-03	1.35E-09	3.40E-05	2.21E-06	6.02E-03	9.50E-05	5.88E-03	5.20E-05	5.57E-05	1.52E-07	2.17E-07
Total (g)			3.79E-03	5.32E-03	5.32E-03	2.66E-07	8.43E-03	4.06E-04	3.61E-01	2.27E-02	1.48E-05	6.24E-03	6.68E-04	7.62E-06	3.46E-05

T (C)	P (bars)	pH	log f(O2)	clincl14 (%)	chamosit (%	fluorite (%	gold (%)	magnetit (%)	quartz (%	hematite (%)	muscovit (%)	acanthit (%
250	77.59	4.53	-36.5	32.57%	24.90%	0.18%	10.85%					
245	46.6	4.5	-36.17	67.43%	75.10%	8.04%	48.20%	100.00%	3.75%			
240	37.61	4.45	-36.27			4.86%	22.59%		6.19%	87.19%	29.03%	
235	32.65	4.39	-36.43			4.32%	8.44%		5.94%	12.81%	26.77%	
230	29	4.34	-36.69			3.87%	3.95%		5.76%		18.76%	
225	25.98	4.29	-37.01			3.56%	2.15%		5.51%		12.53%	
220	23.37	4.25	-37.37			3.36%	1.26%		5.29%		8.01%	
215	21.05	4.21	-37.77			3.22%	0.79%		5.04%		4.27%	
210	18.95	4.17	-38.2			3.09%	0.52%		4.82%		0.62%	2.30%
205	17.05	4.14	-38.65			2.95%	0.37%		4.54%			10.01%
200	15.32	4.1	-39.12			2.91%	0.26%		4.29%			9.42%
195	13.74	4.06	-39.61			2.88%	0.18%		4.04%			8.76%
190	12.29	4.02	-40.12			2.86%	0.13%		3.82%			8.10%
185	10.98	3.98	-40.65			2.85%	0.09%		3.60%			7.42%
180	9.77	3.94	-41.19			2.84%	0.06%		3.38%			6.77%
175	8.67	3.9	-41.75			2.85%	0.05%		3.19%			6.15%
170	7.68	3.86	-42.34			2.87%	0.03%		3.01%			5.56%
165	6.77	3.82	-42.93			2.88%	0.02%		2.84%			5.00%
160	5.95	3.78	-43.55			2.91%	0.02%		2.68%			4.49%
155	5.22	3.74	-44.19			2.93%	0.01%		2.53%			4.02%
150	4.55	3.7	-44.84			2.95%	0.01%		2.39%			3.57%
145	3.96	3.66	-45.52			2.98%	0.01%		2.26%			3.16%
140	3.42	3.63	-46.21			3.01%	0.00%		2.13%			2.79%
135	2.95	3.59	-46.92			3.03%	0.00%		2.01%			2.44%
130	2.53	3.55	-47.66			3.05%	0.00%		1.89%			2.13%
125	2.16	3.51	-48.41			3.07%	0.00%		1.78%			1.86%
120	1.84	3.47	-49.19			3.10%	0.00%		1.67%			1.61%
115	1.55	3.43	-49.99			3.12%	0.00%		1.57%			1.38%
110	1.3	3.39	-50.81			3.14%	0.00%		1.47%			1.19%
105	1.09	3.36	-51.66			3.16%	0.00%		1.37%			1.01%
100	0.9	3.32	-52.53			3.17%	0.00%		1.28%			0.86%
Total (m)				**2.21E-05**	**3.02E-05**	**2.82E-03**	**1.35E-09**	**1.15E-05**	**5.32E-03**	**2.25E-05**	**3.67E-05**	**3.27E-05**
Total (g)				**1.18E-02**	**2.16E-02**	**2.20E-01**	**2.66E-07**	**2.65E-03**	**3.20E-01**	**3.59E-03**	**1.46E-02**	**8.11E-03**

T (°C)	pH	TotMix	log f(O2)	clincl14 (%)	hamosit (%	fluorite (%)	gold (%)	barite (%)	hematite (%)	pyrite (%)	quartz (%)	acanthit (%)	silver (%)	kaolinit (%)	gibbsite (%)
250.00	4.53		-36.50	100.00%	100.00%	0.23%	8.15%								
239.90	4.18	0.05	-34.35				47.18%	52.79%	30.39%	52.46%	6.45%				
230.60	4.06	0.10	-34.74				9.77%	33.22%	15.39%	13.36%	6.66%				
221.90	3.97	0.15	-35.24				4.63%	7.42%	15.42%	11.36%	5.96%				
213.80	3.90	0.20	-35.80				2.46%	2.37%	13.48%	9.22%	5.33%				
206.40	3.85	0.25	-36.38				1.43%	1.13%	10.90%	7.19%	4.77%				
199.40	3.81	0.30	-36.97				0.90%	0.66%	7.92%	5.18%	4.28%				
192.90	3.80	0.35	-37.56			3.82%	0.59%	0.43%	3.34%	1.23%	3.86%	36.32%			
186.80	3.79	0.40	-38.10			6.24%	0.47%	0.31%	0.54%		3.50%	26.82%			
181.10	3.79	0.45	-38.61			5.98%	0.32%	0.23%			3.19%	14.49%			
175.80	3.78	0.50	-39.08			5.51%	0.20%	0.17%			2.92%	9.26%			
136.20	3.79	1.00	-42.87			38.58%	0.83%	0.72%			20.09%	13.11%			
111.80	3.86	1.50	-43.39			20.78%	0.60%	0.23%	0.02%		11.57%				
95.35	3.97	2.00	-45.13			11.27%	0.60%	0.12%	0.03%		7.53%				
83.49	4.08	2.50	-46.67			5.55%	0.59%	0.07%	0.21%		5.11%		11.91%		
74.66	4.18	3.00	-47.96			2.04%	0.59%	0.04%	0.56%		3.51%		34.94%		
67.90	4.28	3.50	-49.06				0.59%	0.03%	0.32%		2.38%		19.23%		
62.65	4.36	4.00	-49.98				0.59%	0.02%	0.20%		1.55%		10.99%		
58.62	4.44	4.50	-50.75				0.59%	0.01%	0.13%		0.91%		6.67%		
55.26	4.50	5.00	-51.41				0.59%	0.01%	0.09%		0.41%		4.28%		
52.66	4.56	5.50	-51.97				0.59%	0.01%	0.07%		0.01%		2.88%		
50.59	4.61	6.00	-52.45				0.59%	0.00%	0.06%				2.02%		
48.96	4.66	6.50	-52.86				0.59%	0.00%	0.05%				1.47%		
47.67	4.71	7.00	-53.21				0.59%	0.00%	0.05%				1.10%		
46.66	4.75	7.50	-53.52				0.59%		0.04%				0.84%		
45.88	4.79	8.00	-53.79				0.59%		0.04%				0.65%		
45.29	4.82	8.50	-54.03				0.59%		0.04%				0.52%		
44.85	4.85	9.00	-54.24				0.59%		0.04%				0.42%		
44.55	4.88	9.50	-54.42				0.59%		0.03%				0.34%		
44.35	4.91	10.00	-54.56				0.59%		0.03%				0.24%	10.42%	
44.24	4.93	10.50	-54.67				0.59%		0.03%				0.19%	15.08%	
44.20	4.95	11.00	-54.78				0.59%		0.03%				0.17%	15.08%	
44.23	4.97	11.50	-54.87				0.59%		0.03%				0.15%	15.03%	
44.30	4.99	12.00	-54.95				0.59%		0.03%				0.13%	14.94%	
44.42	5.01	12.50	-55.02				0.59%		0.03%				0.12%	14.81%	
44.58	5.03	13.00	-55.09				0.59%		0.03%				0.10%	14.65%	
44.76	5.04	13.50	-55.14				0.59%		0.03%				0.08%		5.37%
44.97	5.06	14.00	-55.17				0.59%		0.03%				0.07%		6.54%
45.20	5.07	14.50	-55.21				0.59%		0.03%				0.06%		6.60%
45.45	5.08	15.00	-55.24				0.59%		0.03%				0.05%		6.66%
45.71	5.10	15.50	-55.26				0.59%		0.03%				0.05%		6.71%
45.98	5.11	16.00	-55.28				0.59%		0.03%				0.05%		6.75%
46.26	5.12	16.50	-55.30				0.59%		0.03%				0.04%		6.78%
46.55	5.13	17.00	-55.32				0.59%		0.03%				0.04%		6.80%
46.84	5.14	17.50	-55.34				0.59%		0.03%				0.04%		6.82%
47.14	5.15	18.00	-55.35				0.59%		0.03%				0.04%		6.84%
47.44	5.16	18.50	-55.37				0.59%		0.03%				0.03%		6.84%
47.74	5.17	19.00	-55.38				0.59%		0.03%				0.03%		6.84%
48.04	5.18	19.50	-55.39				0.59%		0.03%				0.03%		6.83%
48.34	5.19	20.00	-55.40				0.59%		0.03%				0.03%		6.82%
48.64	5.20	20.50	-55.41				0.59%		0.03%				0.03%		6.80%
otal (m)				6.82E-06	7.46E-06	1.96E-03	1.78E-09	1.91E-03	1.13E-03	2.92E-04	4.46E-03	1.67E-05	3.45E-05	2.00E-04	1.58E-03
Total (g)				3.79E-03	5.32E-03	1.53E-01	3.51E-07	4.46E-01	1.81E-01	3.51E-02	2.68E-01	4.14E-03	3.72E-03	5.15E-02	1.23E-01

T (°C)	P (bars)	pH	TotMix	log f(O2)	clincl14 (%	hamosit (%	luorite (%	gold (%)	hematite (%	magnetit (%	pyrite (%)	quartz (%)	acanthit (%	barite (%)	halcopy (%	bornite (%)	galena (%	phaleri (%	chalcocl (%)
250.00	250.00	4.53		-36.50	100.00%	100.00%	0.27%	10.75%			3.35%	6.53%							
239.90	250.00	4.42	0.05	-36.29			6.67%	47.43%	4.92%	100.00%	2.04%	6.74%							
230.50	250.00	4.28	0.10	-36.48			1.67%	22.85%	29.67%		1.53%	6.03%							
221.80	250.00	4.16	0.15	-36.75			0.32%	9.68%	27.97%		1.05%	5.39%	8.00%						
213.80	250.00	4.06	0.20	-37.14			0.88%	4.27%	20.55%		0.71%	4.82%	11.94%						
206.30	250.00	4.00	0.25	-37.62			2.18%	2.09%	12.24%		0.47%	4.32%	12.81%						
199.30	250.00	3.96	0.30	-38.13			3.58%	1.12%	4.65%		0.33%	3.89%	11.99%						
192.80	250.00	3.93	0.35	-38.67			4.35%	0.63%			0.32%	3.53%	10.14%						
186.70	250.00	3.91	0.40	-39.21			4.04%	0.37%			0.31%	3.21%	8.63%	1.27%					
181.00	250.00	3.88	0.45	-39.78			3.80%	0.22%			0.31%	2.94%	7.03%	1.94%					
175.60	250.00	3.86	0.50	-40.34			3.63%	0.15%			3.24%	20.19%	24.77%	19.10%	100.00%				
136.10	250.00	3.72	1.00	-45.02			29.12%	0.39%			1.81%	11.57%	3.41%	18.49%		54.85%	17.06%		
111.70	250.00	3.66	1.50	-48.42			17.58%	0.05%			0.16%	7.49%	0.78%	16.74%		16.13%	36.12%		
95.21	250.00	3.64	2.00	-50.96			10.14%	0.01%			1.79%	5.05%	0.26%	13.13%		6.24%	17.68%		
83.36	250.00	3.65	2.50	-52.93			6.57%	0.00%			2.50%	3.43%	0.11%	9.53%		3.11%	9.61%		
74.54	250.00	3.67	3.00	-54.49			3.70%	0.00%			2.84%	2.29%	0.05%	6.52%		1.90%	5.72%		
67.79	250.00	3.70	3.50	-55.73			1.50%	0.00%			3.02%	1.46%	0.03%	4.37%		1.36%	3.65%		
62.55	250.00	3.74	4.00	-56.73				0.00%			3.13%	0.81%	0.02%	2.93%		1.08%	2.44%		
58.43	250.00	3.78	4.50	-57.54				0.00%			3.19%	0.31%	0.01%	2.00%		0.93%	1.71%		
55.17	250.00	3.81	5.00	-58.20				0.00%			2.99%		0.01%	1.38%		0.83%	1.22%	0.71%	
52.58	250.00	3.85	5.50	-58.73				0.00%			1.25%		0.00%	1.00%		0.76%	0.74%	5.77%	
50.53	250.00	3.87	6.00	-59.16				0.00%			1.37%		0.00%	0.68%		0.73%	0.59%	5.44%	
48.90	250.00	3.89	6.50	-59.51				0.00%			1.48%		0.00%	0.45%		0.70%	0.47%	5.19%	
47.61	250.00	3.92	7.00	-59.78				0.00%			1.56%		0.00%	0.28%			0.38%	4.97%	11.62%
46.61	250.00	3.94	7.50	-60.00				0.00%			1.63%		0.00%	0.15%			0.32%	4.79%	11.45%
45.83	250.00	3.96	8.00	-60.18				0.00%			1.69%		0.00%	0.04%			0.27%	4.62%	11.28%
45.25	250.00	3.98	8.50	-60.31							1.76%		0.00%				0.23%	4.45%	11.14%
44.81	250.00	4.00	9.00	-60.42							1.81%		0.00%				0.19%	4.29%	11.04%
44.51	250.00	4.02	9.50	-60.49							1.87%		0.00%				0.17%	4.13%	10.96%
44.31	250.00	4.04	10.00	-60.55							1.93%		0.00%				0.15%	3.98%	10.89%
44.21	250.00	4.06	10.50	-60.58							1.99%		0.00%				0.13%	3.82%	10.84%
44.17	250.00	4.07	11.00	-60.60							2.04%		0.00%				0.12%	3.67%	10.79%
44.20	250.00	4.09	11.50	-60.60							2.10%		0.00%			0.64%	0.10%	3.51%	
44.28	250.00	4.11	12.00	-60.60							2.15%					0.64%	0.09%	3.36%	
44.40	250.00	4.13	12.50	-60.58							2.20%					0.64%	0.09%	3.22%	
44.56	250.00	4.14	13.00	-60.56							2.25%					0.64%	0.08%	3.08%	
44.75	250.00	4.16	13.50	-60.53							2.30%					0.63%	0.07%	2.94%	
44.96	250.00	4.17	14.00	-60.50							2.35%					0.63%	0.07%	2.81%	
45.19	250.00	4.19	14.50	-60.46							2.39%					0.63%	0.06%	2.68%	
45.44	250.00	4.20	15.00	-60.41							2.44%					0.63%	0.06%	2.56%	
45.70	250.00	4.22	15.50	-60.37							2.48%					0.63%	0.05%	2.44%	
45.97	250.00	4.23	16.00	-60.32							2.52%					0.63%	0.05%	2.33%	
46.25	250.00	4.25	16.50	-60.27							2.56%					0.63%	0.05%	2.23%	
46.54	250.00	4.26	17.00	-60.22							2.59%					0.63%	0.04%	2.12%	
46.83	250.00	4.27	17.50	-60.17							2.63%					0.63%	0.04%	2.03%	
47.13	250.00	4.29	18.00	-60.12							2.66%					0.63%	0.04%	1.94%	
47.43	250.00	4.30	18.50	-60.06							2.69%					0.63%	0.04%	1.85%	
47.73	250.00	4.31	19.00	-60.01							2.72%					0.63%	0.04%	1.77%	
48.03	250.00	4.32	19.50	-59.95							2.75%					0.63%	0.03%	1.69%	
48.33	250.00	4.34	20.00	-59.90							2.77%					0.63%	0.03%	1.62%	
48.63	250.00	4.35	20.50	-59.85															
Total (m)					**6.82E-06**	**7.46E-06**	**1.70E-03**	**1.35E-09**	**3.79E-04**	**1.52E-05**	**2.59E-03**	**4.42E-03**	**3.40E-05**	**1.70E-03**	**4.56E-07**	**7.67E-07**	**3.99E-04**	**1.60E-03**	**1.14E-07**
Total (g)					**3.79E-03**	**5.32E-03**	**1.33E-01**	**2.66E-07**	**6.05E-02**	**3.53E-03**	**3.11E-01**	**2.66E-01**	**8.44E-03**	**3.97E-01**	**8.38E-05**	**3.85E-04**	**9.53E-02**	**1.56E-01**	**1.81E-05**

)	pH	log f(O2)	clinch14 (%)	chamosit (%)	gold (%)	bornite (%)	galena (%)	silver (%)	quartz (%	muscovit (%	chalcoci (%	graphite (%	fluorite (%)
300	4.61	-33	58.43%	62.54%	0.03%								
295	4.58	-33.36	41.57%	37.46%	0.21%	36.96%	1.19%	0.21%	0.10%				
290	4.53	-33.73			0.52%	63.04%	10.00%	0.44%	0.19%	1.74%			
285	4.46	-34.1			0.71%		16.65%	0.61%	0.29%	2.43%	0.25%		
280	4.4	-34.48			0.89%		13.68%	0.76%	0.39%	3.11%	0.45%		
275	4.34	-34.86			1.06%		11.56%	0.90%	0.48%	3.79%	0.63%		
270	4.28	-35.26			1.21%		10.03%	1.03%	0.58%	4.44%	0.79%		
265	4.23	-35.65			1.35%		8.87%	1.15%	0.67%	5.05%	0.94%		
260	4.18	-36.06			1.47%		7.88%	1.26%	0.76%	5.62%	1.08%		
255	4.13	-36.47			1.57%		6.89%	1.35%	0.84%	6.12%	1.22%		
250	4.09	-36.89			1.65%		5.75%	1.44%	0.93%	6.53%	1.35%		
245	4.05	-37.32			1.72%		4.35%	1.52%	1.01%	6.83%	1.47%		
240	4.01	-37.75			1.78%		2.62%	1.60%	1.08%	7.01%	1.60%		
235	3.98	-38.19			1.82%		0.51%	1.66%	1.16%	7.06%	1.71%		
230	3.95	-38.64			1.86%			1.72%	1.23%	6.95%	1.80%		
225	3.92	-39.1			1.89%			1.77%	1.30%	6.68%	1.87%		
220	3.9	-39.57			1.91%			1.81%	1.37%	6.26%	1.93%		
215	3.88	-40.05			1.92%			1.85%	1.44%	5.69%	1.97%		
210	3.86	-40.53			1.94%			1.88%	1.50%	4.96%	2.01%		
205	3.84	-41.03			1.94%			1.91%	1.57%	4.09%	2.03%		
200	3.82	-41.54			1.95%			1.94%	1.62%	3.08%	2.05%		
195	3.81	-42.06			1.95%			1.96%	1.68%	1.92%	2.06%		
190	3.8	-42.59			1.96%			1.97%	1.74%	0.64%	2.07%		
185	3.78	-43.13			1.96%			1.99%	1.79%		2.07%		
180	3.76	-43.69			1.96%			2.00%	1.84%		2.08%		
175	3.74	-44.26			1.96%			2.00%	1.88%		2.08%		
170	3.71	-44.84			1.96%			2.01%	1.93%		2.08%		
165	3.69	-45.43			1.96%			2.02%	1.97%		2.08%		
160	3.67	-46.04			1.96%			2.02%	2.01%		2.08%		
155	3.65	-46.6			1.96%			2.03%	2.04%		2.08%	1.03%	
150	3.62	-47.17			1.96%			2.03%	2.08%		2.08%	1.87%	
145	3.6	-47.75			1.96%			2.03%	2.12%		2.08%	2.47%	
140	3.58	-48.35			1.96%			2.03%	2.15%		2.08%	2.90%	
135	3.56	-48.96			1.96%			2.04%	2.18%		2.08%	3.21%	
130	3.54	-49.59			1.96%			2.04%	2.21%		2.08%	3.42%	
125	3.52	-50.24			1.96%			2.04%	2.24%		2.08%	3.58%	
120	3.5	-50.9			1.96%			2.04%	2.27%		2.08%	3.68%	
115	3.48	-51.59			1.96%			2.04%	2.30%		2.08%	3.76%	
110	3.47	-52.29			1.96%			2.04%	2.32%		2.08%	3.81%	
105	3.45	-53.02			1.96%			2.04%	2.35%		2.08%	3.85%	
100	3.43	-53.77			1.96%			2.04%	2.37%		2.08%	3.87%	
95	3.41	-54.53			1.96%			2.05%	2.39%		2.08%	3.89%	
90	3.4	-55.32			1.96%			2.05%	2.41%		2.08%	3.90%	
85	3.38	-56.14			1.96%			2.05%	2.43%		2.08%	3.90%	0.27%
80	3.36	-56.98			1.96%			2.05%	2.45%		2.08%	3.91%	1.40%
75	3.34	-57.84			1.96%			2.05%	2.47%		2.08%	3.91%	2.52%
70	3.32	-58.73			1.96%			2.05%	2.48%		2.08%	3.91%	3.63%
65	3.31	-59.65			1.96%			2.05%	2.49%		2.08%	3.91%	4.72%
60	3.29	-60.59			1.96%			2.05%	2.51%		2.08%	3.91%	5.79%
55	3.28	-61.57			1.96%			2.05%	2.52%		2.08%	3.91%	6.83%
50	3.27	-62.57			1.96%			2.05%	2.53%		2.08%	3.91%	7.86%
45	3.25	-63.6			1.96%			2.05%	2.54%		2.08%	3.91%	8.85%
40	3.25	-64.67			1.96%			2.05%	2.55%		2.08%	3.91%	9.82%
35	3.24	-65.77			1.96%			2.05%	2.56%		2.08%	3.91%	10.76%
30	3.23	-66.9			1.96%			2.05%	2.56%		2.08%	3.91%	11.66%
25	3.23	-68.07			1.96%			2.05%	2.57%		2.08%	3.91%	12.53%
20	3.23	-69.27			1.96%			2.05%	2.57%		2.08%	3.91%	13.36%
m)			6.39E-06	6.15E-06	5.54E-09	5.11E-06	1.09E-04	2.72E-02	3.75E-01	4.01E-04	5.75E-03	1.81E-03	3.37E-03
g)			3.55E-03	4.39E-03	1.09E-06	2.55E-03	2.62E-02	2.93E+00	2.25E+01	1.60E-01	9.15E-01	2.18E-02	2.63E-01

T (°C)	P (bars)	pH	log f(O2)	clincl14 (%)	chamosit (%)	gold (%)	quartz (%)	muscovit (%)	chalcoci (%)	silver (%)
300	116.26	4.61	-32.99	20.58%	25.22%	1.51%				
295	89.51	4.63	-32.87	56.88%	56.07%	17.34%	4.98%			
290	77.8	4.62	-32.83	22.23%	18.47%	11.03%	5.83%			
285	70.03	4.61	-32.93	0.32%	0.24%	10.61%	5.71%	17.80%		
280	63.83	4.58	-33.12			8.76%	5.44%	21.18%	0.87%	
275	58.49	4.53	-33.37			7.28%	5.22%	16.92%	1.79%	1.06%
270	53.71	4.48	-33.64			5.53%	4.99%	12.72%	0.84%	3.58%
265	49.37	4.43	-33.94			4.87%	4.75%	10.52%	1.05%	4.22%
260	45.37	4.37	-34.26			4.37%	4.52%	8.45%	1.45%	4.72%
255	41.68	4.32	-34.59			3.95%	4.29%	6.35%	1.95%	5.12%
250	38.26	4.27	-34.95			3.58%	4.07%	4.17%	2.51%	5.41%
245	35.08	4.22	-35.31			3.22%	3.86%	1.89%	3.11%	5.60%
240	32.12	4.17	-35.69			2.87%	3.66%		3.65%	5.67%
235	29.36	4.13	-36.08			2.49%	3.45%		3.92%	5.49%
230	26.81	4.08	-36.49			2.16%	3.25%		4.18%	5.29%
225	24.42	4.04	-36.91			1.85%	3.06%		4.42%	5.06%
220	22.22	3.99	-37.34			1.58%	2.89%		4.63%	4.82%
215	20.17	3.95	-37.79			1.33%	2.72%		4.81%	4.56%
210	18.26	3.91	-38.24			1.12%	2.56%		4.95%	4.30%
205	16.5	3.87	-38.72			0.93%	2.41%		5.04%	4.03%
200	14.88	3.83	-39.2			0.76%	2.27%		5.09%	3.76%
195	13.38	3.79	-39.7			0.63%	2.14%		5.08%	3.50%
190	12	3.76	-40.22			0.51%	2.02%		5.01%	3.24%
185	10.73	3.72	-40.75			0.41%	1.90%		4.89%	2.98%
180	9.57	3.69	-41.29			0.33%	1.79%		4.71%	2.73%
175	8.51	3.65	-41.86			0.26%	1.69%		4.47%	2.49%
170	7.54	3.62	-42.44			0.20%	1.60%		4.16%	2.26%
165	6.66	3.59	-43.03			0.16%	1.51%		3.80%	2.03%
160	5.86	3.56	-43.65			0.12%	1.42%		3.39%	1.82%
155	5.13	3.53	-44.28			0.09%	1.34%		2.95%	1.61%
150	4.48	3.51	-44.93			0.07%	1.27%		2.48%	1.42%
145	3.9	3.48	-45.61			0.05%	1.19%		2.02%	1.24%
140	3.37	3.45	-46.3			0.04%	1.13%		1.59%	1.08%
135	2.91	3.43	-47.01			0.03%	1.06%		1.20%	0.93%
Total (m)				**1.83E-05**	**1.53E-05**	**1.09E-10**	**8.54E-03**	**2.96E-05**	**1.16E-04**	**5.32E-04**
Total (g)				**1.01E-02**	**1.09E-02**	**2.14E-08**	**5.13E-01**	**1.18E-02**	**1.85E-02**	**5.73E-02**

T (°C)	pH	TotMix	log f(O2)	clinci14(%)	chamosit (%)	gold (%)	barite (%)	bornite (%)	hematite (%)	quartz (%)	anhydrit (%)	galena (%)	acanthit (%)	muscovit (%)	chalcoci (%)	silver (%)	anglesit (%)	kaolinit (%)	gibbsite (%)
300	4.61		-33	100.00%	100.00%	0.30%													
288.9	4.35	0.05	-30.42				55.81%	74.71%	22.68%	4.80%									
278.5	4.31	0.10	-30.91				27.67%	16.36%	3.67%	5.40%	5.27%	100.00%							
268.6	4.27	0.15	-31.5				4.25%	1.50%	0.60%	4.84%	13.27%		19.70%	29.07%					
259.4	4.21	0.20	-32.06				2.91%		3.78%	4.80%	12.50%		15.06%	21.84%					
250.7	4.15	0.25	-32.62				2.05%		5.99%	4.64%	11.58%		11.88%	14.83%					
242.5	4.09	0.30	-33.17			3.69%	1.48%		7.37%	4.41%	10.57%		10.63%	8.69%					
234.7	4.03	0.35	-33.71			4.77%	1.09%		8.03%	4.15%	9.54%		9.98%	3.74%					
227.4	3.98	0.40	-34.24			3.50%	0.83%	3.01%	8.23%	3.86%	8.50%		7.91%						
220.6	3.94	0.45	-34.76			2.64%	0.64%	4.42%	7.72%	3.53%	7.50%		6.25%						
214.1	3.91	0.50	-35.26			2.02%	0.50%		6.76%	3.22%	6.57%		5.09%		28.40%				
166	3.95	1.00	-39.25			6.80%	1.96%		17.97%	20.93%	14.70%		13.50%		71.60%				
136.1	4.01	1.50	-41.28			2.18%	0.36%		1.83%	11.25%						30.88%			
115.7	4.08	2.00	-42.86			1.99%	0.13%		1.30%	7.26%						21.71%	33.96%		
101	4.16	2.50	-44.27			1.96%	0.09%		0.93%	5.09%						15.25%	27.25%		
89.92	4.24	3.00	-45.48			1.95%	0.06%		0.60%	3.68%						9.65%	15.90%		
81.31	4.31	3.50	-46.52			1.95%	0.05%		0.39%	2.70%						6.07%	9.65%		
74.5	4.38	4.00	-47.41			1.95%	0.03%		0.27%	1.97%						3.96%	5.98%		
69.03	4.45	4.50	-48.17			1.95%	0.03%		0.19%	1.42%						2.70%	3.69%		
64.6	4.5	5.00	-48.83			1.95%	0.02%		0.15%	0.98%						1.92%	2.17%		
61	4.55	5.50	-49.39			1.95%	0.01%		0.12%	0.63%						1.41%	1.10%		
58.05	4.6	6.00	-49.88			1.95%	0.01%		0.10%	0.34%						1.06%	0.31%		
55.63	4.64	6.50	-50.31			1.95%	0.01%		0.08%	0.10%						0.83%			
53.65	4.68	7.00	-50.69			1.95%	0.01%		0.08%							0.68%			
52.02	4.72	7.50	-51.02			1.95%	0.00%		0.07%							0.56%			
50.7	4.76	8.00	-51.32			1.95%	0.00%		0.06%							0.47%			
49.63	4.79	8.50	-51.57			1.95%	0.00%		0.06%							0.37%		3.41%	
48.76	4.82	9.00	-51.79			1.95%			0.05%							0.30%		6.51%	
48.08	4.85	9.50	-51.99			1.95%			0.05%							0.26%		6.70%	
47.54	4.87	10.00	-52.16			1.95%			0.05%							0.22%		6.85%	
47.13	4.9	10.50	-52.32			1.95%			0.05%							0.20%		6.96%	
46.82	4.92	11.00	-52.46			1.95%			0.05%							0.17%		7.04%	
46.6	4.94	11.50	-52.59			1.95%			0.04%							0.15%		7.09%	
46.46	4.97	12.00	-52.71			1.95%			0.04%							0.14%		7.11%	
46.39	4.99	12.50	-52.82			1.95%			0.04%							0.12%		7.10%	
46.37	5.01	13.00	-52.91			1.95%			0.04%							0.11%		7.07%	
46.4	5.03	13.50	-53			1.95%			0.04%							0.10%		7.01%	
46.47	5.04	14.00	-53.08			1.95%			0.04%							0.09%		6.94%	
46.57	5.06	14.50	-53.16			1.95%			0.04%							0.08%		6.85%	
46.71	5.08	15.00	-53.23			1.95%			0.04%							0.07%		6.74%	
46.86	5.09	15.50	-53.29			1.95%			0.04%							0.07%		6.62%	
47.04	5.11	16.00	-53.35			1.95%			0.04%					21.83%		0.06%			
47.24	5.13	16.50	-53.4			1.95%			0.04%							0.05%			11.97%
47.45	5.14	17.00	-53.45			1.95%			0.04%							0.05%			12.59%
47.67	5.15	17.50	-53.5			1.95%			0.04%							0.04%			12.20%
47.9	5.17	18.00	-53.54			1.95%			0.04%							0.04%			11.78%
48.14	5.18	18.50	-53.58			1.95%			0.04%							0.04%			11.32%
48.39	5.19	19.00	-53.62			1.95%			0.04%							0.03%			10.82%
48.64	5.21	19.50	-53.66			1.95%			0.04%							0.03%			10.31%
48.9	5.22	20.00	-53.69			1.95%			0.04%							0.03%			9.77%
49.16	5.23	20.50	-53.73			1.95%			0.04%							0.03%			9.23%
Total (m)				3.74E-06	3.84E-06	5.40 E-10	1.74E-03	3.39E-05	9.09E-04	7.48E-03	8.20E-03	5.91E-05	2.25E-04	4.78E-05	1.99E-05	1.06E-04	8.31E-03	2.37E-04	3.28E-04
Total (g)				2.08E-03	2.74E-03	1.08E-07	4.07E-01	1.70E-02	1.45E-01	4.49E-01	1.12E+00	1.41E-02	5.57E-02	1.90E-02	3.17E-03	1.14E-02	2.52E+00	6.12E-02	2.55E-02

T (°C)	P (bars)	a(H+)	pH	TotMix	log f(O2)	clinc14 (%)	chamosit (%)	gold (%)	galena (%)	silver (%)	muscovit (%	quartz (%	bornite (%)	acanthit (%)	barite (%)	hematite (%)	chalcocl (%)
300	250	2.45E-05	4.61		-33	100.00%	100.00%	1.49%									
288.9	250	3.09E-05	4.51	0.05	-33.61			18.49%	1.09%	100.00%	3.86%	4.79%	17.05%				
278.4	250	3.84E-05	4.42	0.10	-33.51				0.89%		19.47%	5.06%	34.14%				
268.6	250	4.62E-05	4.34	0.15	-32.27						19.58%	5.05%	47.89%				
269.3	250	5.43E-05	4.27	0.20	-32.74						17.97%	4.90%	0.92%	12.98%			
260.6	250	6.22E-05	4.21	0.25	-33.26			6.37%			15.85%	4.64%		11.33%			
242.3	250	6.98E-05	4.16	0.30	-33.79			22.03%			13.04%	4.35%		9.45%	0.21%		
234.6	250	7.79E-05	4.11	0.35	-34.37			14.98%			8.06%	4.09%		8.56%	2.19%	13.98%	
227.3	250	8.70E-05	4.06	0.40	-34.93			9.75%			2.17%	3.86%		6.82%	2.03%	40.17%	3.33%
220.4	250	9.52E-05	4.02	0.45	-35.48			7.05%				3.57%		5.63%	2.04%	32.46%	4.53%
214	250	1.02E-04	3.99	0.50	-36			5.21%				3.25%		4.81%	2.09%	13.40%	4.64%
207.9	250	1.08E-04	3.97	0.55	-36.51			3.80%				2.97%		4.18%	2.12%		4.78%
168.8	250	1.56E-04	3.81	1.10	-41.59			10.21%	0.14%			20.92%		31.10%	21.35%		67.15%
129	250	1.83E-04	3.74	1.65	-45.14			0.53%	2.48%			11.04%		3.31%	18.14%		9.59%
109.1	250	1.95E-04	3.71	2.20	-47.84			0.06%	2.71%			7.02%		0.99%	14.52%		3.07%
94.95	250	1.97E-04	3.71	2.75	-49.95			0.01%	2.77%			4.81%		0.39%	10.77%		1.22%
84.36	250	1.94E-04	3.71	3.30	-51.64			0.00%	2.79%			3.39%		0.18%	7.57%		0.58%
76.23	250	1.89E-04	3.72	3.85	-53			0.00%	2.80%			2.40%		0.10%	5.23%		0.31%
69.87	250	1.82E-04	3.74	4.40	-54.12			0.00%	2.81%			1.67%		0.06%	3.63%		0.19%
64.81	250	1.75E-04	3.76	4.95	-55.04			0.00%	2.81%			1.12%		0.04%	2.55%		0.12%
60.77	250	1.68E-04	3.78	5.50	-55.79			0.00%	2.81%			0.69%		0.02%	1.81%		0.08%
57.5	250	1.61E-04	3.79	6.05	-56.42			0.00%	2.81%			0.35%		0.02%	1.29%		0.06%
54.87	250	1.54E-04	3.81	6.60	-56.93			0.00%	2.81%			0.06%		0.01%	0.92%		0.05%
52.74	250	1.48E-04	3.83	7.15	-57.36			0.00%	2.81%					0.01%	0.65%		0.04%
51.01	250	1.42E-04	3.85	7.70	-57.71			0.00%	2.81%					0.01%	0.44%		0.03%
49.63	250	1.37E-04	3.86	8.25	-57.99			0.00%	2.81%					0.00%	0.27%		0.02%
48.62	250	1.32E-04	3.88	8.80	-58.22			0.00%	2.81%					0.00%	0.14%		0.02%
47.64	250	1.28E-04	3.89	9.35	-58.41			0.00%	2.81%					0.00%	0.04%		0.02%
46.95	250	1.23E-04	3.91	9.90	-58.56			0.00%	2.81%					0.00%			0.02%
46.42	250	1.20E-04	3.92	10.45	-58.67			0.00%	2.81%					0.00%			0.01%
46.02	250	1.16E-04	3.94	11.00	-58.76			0.00%	2.81%					0.00%			0.01%
45.74	250	1.13E-04	3.95	11.55	-58.83			0.00%	2.81%					0.00%			0.01%
45.55	250	1.09E-04	3.96	12.10	-58.88			0.00%	2.81%					0.00%			0.01%
45.44	250	1.06E-04	3.97	12.65	-58.91			0.00%	2.81%					0.00%			0.01%
45.39	250	1.04E-04	3.98	13.20	-58.93			0.00%	2.81%								0.01%
45.4	250	1.01E-04	4	13.75	-58.93				2.81%								0.01%
45.46	250	9.87E-05	4.01	14.30	-58.93				2.81%								0.01%
45.66	250	9.64E-05	4.02	14.85	-58.92				2.81%								0.01%
45.7	250	9.42E-05	4.03	15.40	-58.9				2.81%								0.01%
45.86	250	9.22E-05	4.04	15.95	-58.87				2.81%								0.01%
46.04	250	9.02E-05	4.04	16.50	-58.85				2.81%								0.01%
46.25	250	8.84E-05	4.05	17.05	-58.81				2.81%								0.01%
46.47	250	8.66E-05	4.06	17.60	-58.78				2.81%								0.01%
46.7	250	8.49E-05	4.07	18.15	-58.74				2.81%								0.01%
46.95	250	8.33E-05	4.08	18.70	-58.7				2.81%								0.01%
47.2	250	8.18E-05	4.09	19.25	-58.65				2.81%								0.01%
47.47	250	8.03E-05	4.1	19.80	-58.61				2.81%								0.01%
47.74	250	7.89E-05	4.1	20.35	-58.56				2.81%								0.01%
Total (m)						3.74E-06	3.84E-06	1.09E-10	5.93E-03	9.02E-05	5.38E-05	7.39E-03	2.49E-05	2.33E-04	1.53E-03	2.66E-05	1.30E-04
Total (g)						2.08E-03	2.74E-03	2.14E-08	1.42E+00	9.73E-03	2.14E-02	4.44E-01	1.28E-02	5.77E-02	3.68E-01	4.24E-03	3.07E-02

T (°C)	pH	log f(O2)	clincl14 (%)	chamosit (%)	gold (%)	fluorite (%	acanthit (%)	quartz (%)	chalcopy (%)	galena (%)	muscovit (%	graphite (%	bornite (%)	chalcoci (%)
250	4.53	-36.49	57.19%	46.77%	0.25%									
245	4.49	-36.95	42.81%	53.23%	0.41%	0.10%	0.28%	0.14%						
240	4.45	-37.41			0.73%	0.27%	0.64%	0.28%	0.93%	0.03%	7.34%			
235	4.39	-37.87			1.07%	0.40%	0.90%	0.42%	1.49%	0.19%	9.83%			
230	4.34	-38.34			1.36%	0.51%	1.13%	0.56%	2.07%	0.41%	11.44%			
225	4.29	-38.81			1.61%	0.61%	1.32%	0.69%	2.62%	0.65%	12.27%			
220	4.25	-39.3			1.81%	0.70%	1.49%	0.82%	3.13%	0.91%	12.40%			
215	4.21	-39.79			1.96%	0.78%	1.63%	0.95%	3.57%	1.16%	11.91%			
210	4.17	-40.28			2.08%	0.86%	1.75%	1.07%	3.95%	1.41%	10.87%			
205	4.14	-40.79			2.17%	0.93%	1.86%	1.19%	4.26%	1.63%	9.34%			
200	4.12	-41.31			2.23%	1.00%	1.95%	1.31%	4.50%	1.83%	7.36%			
195	4.09	-41.83			2.27%	1.06%	2.02%	1.43%	4.68%	2.00%	4.99%			
190	4.07	-42.37			2.30%	1.12%	2.09%	1.54%	4.79%	2.14%	2.25%			
185	4.05	-42.91			2.32%	1.18%	2.15%	1.65%	4.87%	2.24%				
180	4.01	-43.47			2.33%	1.26%	2.20%	1.74%	5.00%	2.29%				
175	3.98	-44.04			2.33%	1.34%	2.24%	1.83%	5.08%	2.34%				
170	3.94	-44.63			2.34%	1.42%	2.28%	1.91%	5.12%	2.38%				
165	3.91	-45.22			2.34%	1.50%	2.31%	1.99%	5.12%	2.41%				
160	3.87	-45.84			2.34%	1.59%	2.34%	2.07%	5.08%	2.44%				
155	3.84	-46.46			2.35%	1.68%	2.37%	2.14%	5.01%	2.46%				
150	3.8	-47.1			2.35%	1.76%	2.39%	2.22%	4.89%	2.49%				
145	3.77	-47.69			2.35%	1.85%	2.41%	2.28%	4.87%	2.50%		1.12%		
140	3.74	-48.29			2.35%	1.94%	2.42%	2.35%	4.85%	2.52%		2.08%		
135	3.71	-48.9			2.35%	2.04%	2.44%	2.41%	4.79%	2.53%		2.76%		
130	3.68	-49.53			2.35%	2.13%	2.45%	2.47%	4.72%	2.54%		3.25%		
125	3.65	-50.18			2.35%	2.23%	2.46%	2.53%	4.62%	2.55%		3.59%		
120	3.62	-50.84			2.35%	2.32%	2.47%	2.58%		2.67%		3.70%	8.76%	
115	3.59	-51.53			2.35%	2.42%	2.47%	2.64%		2.66%		3.88%	9.53%	
110	3.56	-52.23			2.35%	2.52%	2.48%	2.69%		2.66%		4.00%	10.21%	
105	3.53	-52.96			2.35%	2.62%	2.49%	2.73%		2.66%		4.08%	10.81%	
100	3.51	-53.7			2.35%	2.72%	2.49%	2.78%		2.65%		4.14%	11.34%	
95	3.48	-54.47			2.35%	2.82%	2.49%	2.82%		2.65%		4.18%	11.79%	
90	3.46	-55.26			2.35%	2.92%	2.50%	2.86%		2.64%		4.21%	12.19%	
85	3.44	-56.07			2.35%	3.02%	2.50%	2.90%		2.64%		4.23%	12.54%	
80	3.42	-56.91			2.35%	3.12%	2.50%	2.93%		2.64%		4.24%	12.83%	
75	3.4	-57.77			2.35%	3.22%	2.50%	2.96%		2.68%		4.20%		7.75%
70	3.38	-58.66			2.35%	3.32%	2.51%	2.99%		2.68%		4.20%		7.93%
65	3.36	-59.58			2.35%	3.43%	2.51%	3.02%		2.68%		4.21%		8.08%
60	3.35	-60.52			2.35%	3.53%	2.51%	3.05%		2.68%		4.21%		8.20%
55	3.33	-61.49			2.35%	3.63%	2.51%	3.07%		2.67%		4.21%		8.30%
50	3.32	-62.5			2.35%	3.73%	2.51%	3.09%		2.67%		4.21%		8.39%
45	3.31	-63.53			2.35%	3.83%	2.51%	3.11%		2.67%		4.21%		8.45%
40	3.3	-64.6			2.35%	3.93%	2.51%	3.13%		2.67%		4.21%		8.51%
35	3.3	-65.69			2.35%	4.03%	2.51%	3.14%		2.67%		4.21%		8.55%
30	3.29	-66.82			2.35%	4.12%	2.51%	3.15%		2.67%		4.21%		8.59%
25	3.29	-67.99			2.35%	4.22%	2.51%	3.17%		2.67%		4.21%		8.62%
20	3.28	-69.19			2.35%	4.31%	2.51%	3.18%		2.67%		4.21%		8.64%
Total (m)			9.70E-06	1.18E-05	5.03E-08	9.25E-02	3.17E-03	1.92E-01	9.20E-05	4.32E-03	2.72E-04	6.17E-04	1.02E-05	4.34E-05
Total (g)			5.39E-03	8.45E-03	9.91E-06	7.22E+00	7.87E-01	1.16E+01	1.69E-02	1.03E+00	1.09E-01	7.41E-03	5.12E-03	6.91E-03

T (°C)	P (bars)	pH	log f(O2)	clincl14 (%)	chamosit (%)	gold (%)	fluorite (%)	magnetit (%)	quartz (%	hematite (%)	muscovit (%)	acanthit (%)
250	75.99	4.53	-36.49	27.81%	20.98%	10.75%						
245	44.34	4.5	-36.21	72.19%	79.02%	53.69%	8.02%	100.00%	4.03%			
240	36.04	4.45	-36.26			19.91%	5.17%		6.13%	86.45%	31.56%	
235	31.42	4.39	-36.43			7.16%	4.47%		5.94%	13.55%	25.48%	
230	27.97	4.33	-36.68			3.30%	4.04%		5.74%		18.04%	
225	25.1	4.29	-37			1.78%	3.74%		5.51%		12.26%	
220	22.59	4.24	-37.37			1.06%	3.54%		5.26%		7.95%	
215	20.36	4.2	-37.77			0.68%	3.39%		5.02%		4.34%	
210	18.34	4.16	-38.2			0.47%	3.21%		4.81%		0.37%	1.99%
205	16.5	4.12	-38.65			0.35%	2.98%		4.53%			8.98%
200	14.82	4.08	-39.12			0.24%	2.93%		4.27%			8.57%
195	13.29	4.04	-39.61			0.17%	2.88%		4.02%			8.09%
190	11.89	4	-40.12			0.12%	2.84%		3.79%			7.58%
185	10.61	3.96	-40.64			0.08%	2.81%		3.57%			7.06%
180	9.44	3.92	-41.19			0.06%	2.80%		3.37%			6.55%
175	8.38	3.88	-41.75			0.05%	2.79%		3.18%			6.05%
170	7.41	3.84	-42.33			0.03%	2.79%		3.00%			5.57%
165	6.54	3.8	-42.93			0.03%	2.80%		2.83%			5.11%
160	5.74	3.75	-43.55			0.02%	2.82%		2.67%			4.68%
155	5.03	3.71	-44.19			0.01%	2.84%		2.53%			4.26%
150	4.39	3.67	-44.84			0.01%	2.87%		2.38%			3.87%
145	3.81	3.63	-45.52			0.01%	2.90%		2.25%			3.50%
140	3.3	3.59	-46.21			0.01%	2.93%		2.12%			3.15%
135	2.84	3.55	-46.92			0.00%	2.96%		2.00%			2.81%
130	2.43	3.51	-47.66			0.00%	2.99%		1.89%			2.50%
125	2.08	3.47	-48.41			0.00%	3.02%		1.77%			2.21%
120	1.76	3.43	-49.19			0.00%	3.05%		1.67%			1.94%
115	1.49	3.39	-49.99			0.00%	3.07%		1.57%			1.70%
110	1.25	3.36	-50.82			0.00%	3.09%		1.47%			1.47%
105	1.04	3.32	-51.66			0.00%	3.11%		1.37%			1.27%
100	0.87	3.28	-52.53			0.00%	3.13%		1.28%			1.09%
Total (m)				**2.02E-05**	**2.68E-05**	**1.18E-09**	**2.85E-03**	**2.15E-05**	**5.33E-03**	**1.88E-05**	**3.73E-05**	**7.58E-05**
Total (g)				**1.12E-02**	**1.91E-02**	**2.33E-07**	**2.23E-01**	**4.98E-03**	**3.20E-01**	**3.00E-03**	**1.49E-02**	**1.88E-02**

T (°C)	pH	TotMix	log f(O2)	clinci14 (%)	chamosit (%)	gold (%)	barite (%)	hematite (%)	pyrite (%)	quartz (%)	acanthit (%)	fluorite (%)	silver (%)	kaolinit (%)	muscovit (%)	gibbsite (%)	chalcoci (%
260	4.53		-36.49	100.00%	100.00%	7.82%											
240	4.16	0.05	-34.26			42.11%	46.54%	26.53%	47.44%	6.52%							
230.8	4.04	0.10	-34.7			10.61%	33.20%	12.56%	12.88%	6.54%							
222.2	3.93	0.15	-35.2			5.13%	9.73%	12.88%	11.54%	5.87%							
214.2	3.85	0.20	-35.75			2.79%	3.60%	12.00%	10.02%	5.26%							
206.8	3.78	0.25	-36.31			1.69%	1.79%	10.52%	8.45%	4.72%							
199.9	3.73	0.30	-36.88			1.12%	1.07%	8.59%	6.76%	4.24%	0.18%						
193.4	3.7	0.35	-37.44			0.78%	0.71%	6.16%	2.08%	3.83%	34.37%						
187.4	3.68	0.40	-38			0.57%	0.50%	4.06%	0.82%	3.47%	29.89%						
181.7	3.67	0.45	-38.53			0.43%	0.38%	1.91%		3.17%	21.02%	1.85%					
176.4	3.66	0.50	-39			0.32%	0.29%	0.35%		2.90%	7.68%	5.02%					
137	3.66	1.00	-42.73			1.16%	1.25%			20.05%	6.86%	40.67%					
112.6	3.72	1.50	-43.86			0.68%	0.41%	0.02%		11.61%		24.94%					
96.02	3.84	2.00	-45.73			0.66%	0.20%	0.02%		7.59%		14.69%					
84.11	3.96	2.50	-47.37			0.65%	0.11%	1.26%		5.18%		7.78%	47.45%				
76.22	4.08	3.00	-48.85			0.65%	0.07%	0.70%		3.57%		3.84%	26.04%				
68.41	4.2	3.50	-50.12			0.65%	0.05%	0.34%		2.44%		1.21%	12.19%				
63.11	4.3	4.00	-51.18			0.65%	0.03%	0.18%		1.60%			5.86%				
58.94	4.39	4.50	-52.07			0.65%	0.02%	0.10%		0.95%			3.05%				
55.63	4.46	5.00	-52.81			0.65%	0.02%	0.07%		0.45%			1.73%				
53	4.53	5.50	-53.44			0.65%	0.01%	0.05%		0.04%			1.05%				
50.91	4.59	6.00	-53.97			0.65%	0.01%	0.04%					0.68%				
49.24	4.64	6.50	-54.42			0.65%	0.00%	0.03%					0.46%				
47.92	4.69	7.00	-54.82			0.65%	0.00%	0.03%					0.33%				
46.89	4.73	7.50	-55.16			0.65%	0.00%	0.03%					0.24%				
46.09	4.77	8.00	-55.45			0.65%		0.03%					0.18%				
45.48	4.81	8.50	-55.71			0.65%		0.03%					0.14%				
45.03	4.85	9.00	-55.94			0.65%		0.03%					0.11%				
44.7	4.88	9.50	-56.14			0.65%		0.02%					0.08%	5.66%			
44.49	4.9	10.00	-56.28			0.65%		0.02%					0.06%	23.65%			
44.37	4.93	10.50	-56.41			0.65%		0.02%					0.05%	23.66%			
44.32	4.95	11.00	-56.53			0.65%		0.02%					0.04%	23.59%			
44.34	4.97	11.50	-56.63			0.65%		0.02%					0.04%	23.44%			
44.41	4.99	12.00	-56.72			0.65%		0.02%					0.03%		33.17%		
44.62	5.01	12.50	-56.8			0.65%		0.02%					0.03%		33.61%		
44.67	5.03	13.00	-56.87			0.65%		0.02%					0.02%		33.22%		
44.85	5.04	13.50	-56.93			0.65%		0.02%					0.02%			5.80%	
45.06	5.06	14.00	-56.97			0.65%		0.02%					0.02%			6.57%	
45.27	5.07	14.50	-57.01			0.65%		0.16%					0.01%			6.60%	13.96%
45.52	5.09	15.00	-57.05			0.65%		0.17%					0.01%			6.64%	16.01%
45.77	5.1	15.50	-57.08			0.65%		0.15%					0.01%			6.69%	13.32%
46.04	5.11	16.00	-57.11			0.65%		0.13%					0.01%			6.73%	11.09%
46.32	5.13	16.50	-57.14			0.65%		0.11%					0.01%			6.76%	9.24%
46.6	5.14	17.00	-57.16			0.65%		0.10%					0.01%			6.78%	7.72%
46.89	5.15	17.50	-57.18			0.65%		0.08%					0.01%			6.79%	6.46%
47.18	5.16	18.00	-57.2			0.65%		0.07%					0.01%			6.80%	5.42%
47.48	5.17	18.50	-57.22			0.65%		0.07%					0.01%			6.80%	4.56%
47.77	5.18	19.00	-57.24			0.65%		0.06%					0.01%			6.79%	3.85%
48.07	5.19	19.50	-57.25			0.65%		0.05%					0.01%			6.78%	3.26%
48.37	5.2	20.00	-57.27			0.65%		0.05%					0.01%			6.75%	2.76%
48.67	5.21	20.50	-57.28			0.65%		0.04%					0.01%			6.72%	2.35%
Total (m)				5.55E-06	5.54E-06	1.61E-09	1.74E-03	1.45E-03	2.96E-04	4.45E-03	4.17E-05	2.06E-03	7.61E-05	1.34E-04	6.33E-05	1.62E-03	3.45E-06
Total (g)				3.08E-03	3.96E-03	3.18E-07	4.07E-01	2.32E-01	3.65E-02	2.68E-01	1.03E-02	1.61E-01	8.21E-03	3.47E-02	2.52E-02	1.26E-01	6.49E-04

T (°C)	pH	TotMix	log f(O2)	clinci14 (%)	chamosit (%)	gold (%)	acanthit (%)	fluorite (%)	hematite (%)	magnetit (%)	pyrite (%)	quartz (%	barite (%)	chalcopy (%)	bornite (%)	galena (%)	chalcoci (%)	sphaleri (%)
260	4.53		-36.49	100.00%	100.00%	10.68%												
240	4.41	0.05	-36.28			41.69%	3.77%	7.18%	8.06%	100.00%	6.49%	6.60%						
230.7	4.27	0.10	-36.52			25.97%	5.28%	2.46%	22.48%		4.37%	6.63%						
222.1	4.14	0.15	-36.81			10.98%	4.97%	0.43%	22.06%		3.41%	5.94%						
214.1	4.03	0.20	-37.19			4.86%	7.21%		18.66%		2.55%	5.32%						
206.7	3.95	0.25	-37.65			2.36%	8.91%	0.27%	14.21%		1.88%	4.77%						
199.8	3.9	0.30	-38.13			1.27%	9.42%	1.25%	9.43%		1.36%	4.28%						
193.3	3.86	0.35	-38.64			0.74%	9.23%	2.39%	4.72%		0.95%	3.86%						
187.2	3.83	0.40	-39.15			0.46%	8.59%	3.56%	0.37%		0.61%	3.50%						
181.6	3.81	0.45	-39.66			0.29%	7.32%	3.43%			0.59%	3.19%						
176.3	3.79	0.50	-40.17			0.19%	6.11%	3.28%			0.61%	2.92%						
136.8	3.65	1.00	-44.74			0.46%	24.32%	29.40%			7.05%	20.15%	15.40%	100.00%				
112.4	3.61	1.50	-48.13			0.04%	3.60%	21.07%			7.64%	11.62%	19.37%		66.24%			
96.88	3.58	2.00	-50.59			0.01%	0.68%	12.06%				7.55%	17.91%		14.41%	14.48%		
83.98	3.58	2.50	-52.5			0.00%	0.27%	7.39%				5.12%	14.34%		6.99%	14.51%		
76.1	3.59	3.00	-54.02			0.00%	0.13%	4.10%				3.50%	10.54%			14.53%	37.83%	
68.3	3.61	3.50	-55.26			0.00%	0.07%	1.73%				2.35%	7.30%			14.53%	26.20%	
63.01	3.63	4.00	-56.29			0.00%	0.05%					1.50%	4.95%			14.53%	18.29%	
58.85	3.65	4.50	-57.2				0.04%					0.86%	3.37%		1.90%	14.53%		
55.55	3.68	5.00	-57.92				0.02%				4.82%	0.35%	2.24%		1.14%	5.69%		
52.93	3.72	5.50	-58.46				0.01%				7.01%		1.53%		0.60%	1.69%		
50.84	3.76	6.00	-58.91				0.00%				7.24%		1.07%		0.53%	1.26%		
49.18	3.78	6.50	-59.26			0.00%	0.00%				2.34%		0.79%		0.46%	0.75%		2.81%
47.87	3.8	7.00	-59.54			0.00%	0.00%						0.55%		0.41%	0.45%		4.17%
46.84	3.82	7.50	-59.76			0.00%	0.00%						0.35%		0.40%	0.37%		4.20%
46.04	3.83	8.00	-59.93			0.00%	0.00%						0.20%		0.39%	0.31%		4.21%
45.44	3.85	8.50	-60.07			0.00%	0.00%						0.08%			0.26%	3.07%	4.23%
44.99	3.86	9.00	-60.17				0.00%									0.22%	3.01%	4.24%
44.67	3.88	9.50	-60.25				0.00%									0.19%	2.95%	4.25%
44.46	3.89	10.00	-60.3				0.00%									0.17%	2.91%	4.25%
44.34	3.91	10.50	-60.33				0.00%									0.15%	2.88%	4.26%
44.3	3.92	11.00	-60.35				0.00%									0.14%	2.85%	4.26%
44.31	3.93	11.50	-60.36				0.00%								0.35%	0.12%		4.27%
44.38	3.94	12.00	-60.35				0.00%				0.51%				0.35%	0.11%		4.00%
44.5	3.96	12.50	-60.33								1.10%				0.35%	0.09%		3.68%
44.65	3.97	13.00	-60.31								1.27%				0.35%	0.08%		3.59%
44.83	3.98	13.50	-60.28								1.43%				0.35%	0.08%		3.50%
45.03	4	14.00	-60.25								1.60%				0.34%	0.07%		3.41%
45.26	4.01	14.50	-60.21								1.77%				0.34%	0.07%		3.33%
45.5	4.02	15.00	-60.16								1.93%				0.34%	0.06%		3.24%
45.76	4.03	15.50	-60.12								2.09%				0.34%	0.06%		3.15%
46.03	4.05	16.00	-60.07								2.25%				0.34%	0.06%		3.06%
46.3	4.06	16.50	-60.02								2.41%				0.34%	0.06%		2.98%
46.59	4.07	17.00	-59.97								2.57%				0.34%	0.05%		2.89%
46.88	4.08	17.50	-59.92								2.72%				0.34%	0.05%		2.81%
47.17	4.1	18.00	-59.86								2.88%				0.34%	0.05%		2.73%
47.47	4.11	18.50	-59.81								3.03%				0.34%	0.05%		2.65%
47.77	4.12	19.00	-59.76								3.17%				0.34%	0.05%		2.57%
48.07	4.13	19.50	-59.7								3.31%				0.34%	0.05%		2.49%
48.37	4.14	20.00	-59.65								3.45%				0.34%	0.04%		2.42%
48.67	4.16	20.50	-59.59								3.59%				0.34%	0.04%		2.34%
Total (m)				5.55E-06	5.54E-06	1.18E-09	7.97E-05	1.73E-03	5.26E-04	1.30E-05	1.09E-03	4.41E-03	1.53E-03	7.39E-07	1.41E-06	1.04E-03	4.37E-07	3.62E-03
Total (g)				3.08E-03	3.95E-03	2.33E-07	1.98E-02	1.35E-01	8.40E-02	3.01E-03	1.31E-01	2.65E-01	3.57E-01	1.36E-04	7.07E-04	2.49E-01	6.95E-05	3.43E-01

T (°C)	pH	log f(O2)	clincl14 (%	chamosit (%)	gold (%)	silver (%)	quartz (%)	bornite (%)	chalcoci (%	acanthit (%)	muscovit (%)	fluorite (%)
300	4.61	-32.99	100.00%	100.00%	2.16%							
295	4.54	-33.33			2.38%	14.35%	3.62%					
290	4.45	-33.65			3.54%	17.33%	3.89%	20.07%				
285	4.37	-33.96			7.08%	14.99%	3.88%	79.93%				
280	4.29	-34.27			8.25%	13.01%	3.84%		14.03%			
275	4.21	-34.57			9.95%	11.11%	3.79%		20.72%			
270	4.15	-34.85			8.67%	9.37%	3.72%		21.62%			
265	4.09	-35.08			7.47%	7.21%	3.63%		22.76%			
260	4.04	-35.27			6.71%	4.75%	3.53%		20.86%	3.08%		
255	4	-35.47			9.38%	2.45%	3.43%			31.08%		
250	3.96	-35.64			6.07%	1.53%	3.31%			23.78%	2.41%	
245	3.93	-35.8			3.84%	0.90%	3.15%			16.37%	36.09%	
240	3.9	-35.93			2.61%	0.55%	3.04%			11.03%	30.83%	
235	3.87	-36.06			1.94%	0.34%	2.94%			7.06%	21.56%	
230	3.85	-36.19			1.61%	0.23%	2.84%			4.31%	9.11%	
225	3.83	-36.32			1.45%	0.24%	2.73%			2.40%		
220	3.81	-36.47			1.38%	0.40%	2.62%			0.89%		
215	3.79	-36.64			1.36%	0.62%	2.51%					
210	3.77	-36.81			1.28%	0.41%	2.40%					
205	3.74	-36.99			1.19%	0.15%	2.30%					
200	3.72	-37.18			1.13%	0.04%	2.20%					
195	3.7	-37.38			1.07%	0.01%	2.10%					
190	3.68	-37.6			1.01%	0.00%	2.01%					
185	3.66	-37.83			0.94%	0.00%	1.93%					
180	3.64	-38.07			0.87%	0.00%	1.84%					
175	3.62	-38.32			0.80%	0.00%	1.77%					
170	3.6	-38.59			0.73%	0.00%	1.69%					
165	3.58	-38.86			0.67%	0.00%	1.62%					
160	3.56	-39.15			0.60%	0.00%	1.55%					
155	3.54	-39.44			0.54%	0.00%	1.49%					
150	3.52	-39.75			0.49%	0.00%	1.42%					
145	3.5	-40.07			0.43%	0.00%	1.37%					
140	3.48	-40.41			0.38%	0.00%	1.31%					
135	3.46	-40.75			0.34%	0.00%	1.25%					
130	3.44	-41.12			0.29%	0.00%	1.20%					
125	3.42	-41.49			0.25%	0.00%	1.15%					
120	3.4	-41.88			0.22%	0.00%	1.09%					
115	3.38	-42.29			0.18%	0.00%	1.04%					
110	3.36	-42.71			0.16%	0.00%	0.99%					
105	3.35	-43.15			0.13%	0.00%	0.94%					
100	3.33	-43.61			0.11%	0.00%	0.89%					
95	3.31	-44.08			0.09%	0.00%	0.84%					
90	3.29	-44.6			0.07%	0.00%	0.79%					3.67%
85	3.27	-45.14			0.05%	0.00%	0.75%					7.91%
80	3.25	-45.71			0.04%	0.00%	0.70%					7.83%
75	3.22	-46.3			0.03%	0.00%	0.65%					7.73%
70	3.21	-46.9			0.02%	0.00%	0.60%					7.60%
65	3.19	-47.54			0.02%	0.00%	0.55%					7.46%
60	3.17	-48.19			0.01%	0.00%	0.51%					7.29%
55	3.15	-48.88			0.01%	0.00%	0.46%					7.10%
50	3.14	-49.59			0.01%	0.00%	0.42%					6.90%
45	3.12	-50.33			0.00%	0.00%	0.38%					6.69%
40	3.11	-51.1			0.00%	0.00%	0.33%					6.46%
35	3.1	-51.91			0.00%	0.00%	0.30%					6.22%
30	3.09	-52.75			0.00%	0.00%	0.26%					5.97%
25	3.08	-53.64			0.00%	0.00%	0.23%					5.71%
20	3.08	-54.56			0.00%	0.00%	0.19%					5.45%
Total (m)			4.13E-06	3.80E-06	5.30E-11	8.36E-04	9.61E-03	1.52E-06	4.91E-05	5.24E-05	4.67E-06	5.28E-04
Total (g)			2.30E-03	2.70E-03	3.01E-08	9.02E-02	5.78E-01	7.64E-04	7.82E-03	1.30E-02	1.86E-03	4.12E-02

T (°C)	P (bars)	pH	log f(O2)	clincl14 (%)	chamosit (%)	gold (%)	quartz (%	silver (%)	muscovit (%)	acanthit (%
300	121.91	4.61	-32.99	16.19%	21.95%	2.21%				
295	88.34	4.64	-32.87	56.36%	56.86%	24.20%	4.81%			
290	75.87	4.63	-32.81	19.83%	15.91%	12.16%	5.92%			
285	68.03	4.61	-32.9	7.63%	5.28%	8.97%	5.92%	1.43%		
280	61.89	4.56	-33.06			5.88%	5.60%	2.93%	33.55%	
275	56.63	4.5	-33.27			4.51%	5.38%	3.70%	24.86%	
270	51.95	4.44	-33.51			3.75%	5.14%	4.43%	18.05%	
265	47.7	4.38	-33.78			3.33%	4.90%	5.05%	12.58%	
260	43.8	4.32	-34.06			3.08%	4.66%	5.56%	7.75%	
255	40.2	4.26	-34.34			2.92%	4.43%	5.95%	3.20%	
250	36.87	4.2	-34.65			2.94%	4.20%	5.50%		4.37%
245	33.77	4.13	-34.98			2.90%	3.96%	4.65%		10.13%
240	30.9	4.08	-35.31			2.65%	3.74%	4.70%		9.94%
235	28.22	4.02	-35.65			2.44%	3.52%	4.68%		9.68%
230	25.74	3.96	-36			2.24%	3.32%	4.62%		9.34%
225	23.43	3.91	-36.34			2.05%	3.13%	4.50%		8.92%
220	21.3	3.86	-36.69			1.86%	2.95%	4.33%		8.41%
215	19.31	3.81	-37.04			1.68%	2.77%	4.12%		7.82%
210	17.48	3.77	-37.39			1.50%	2.61%	3.87%		7.14%
205	15.78	3.73	-37.74			1.33%	2.46%	3.59%		6.38%
200	14.21	3.69	-38.09			1.17%	2.32%	3.30%		5.55%
195	12.77	3.65	-38.44			1.03%	2.18%	3.02%		4.63%
190	11.44	3.61	-38.79			0.90%	2.06%	2.79%		3.64%
185	10.22	3.58	-39.14			0.79%	1.94%	2.65%		2.55%
180	9.1	3.55	-39.5			0.69%	1.83%	2.67%		1.37%
175	8.08	3.51	-39.87			0.61%	1.73%	2.85%		0.14%
170	7.15	3.48	-40.25			0.53%	1.63%	2.74%		
165	6.31	3.45	-40.63			0.46%	1.54%	2.37%		
160	5.55	3.42	-41.01			0.39%	1.45%	1.79%		
155	4.86	3.4	-41.37			0.33%	1.37%	1.15%		
150	4.23	3.37	-41.73			0.28%	1.29%	0.66%		
145	3.68	3.35	-42.1			0.24%	1.22%	0.38%		
Total (m)				**2.57E-05**	**1.74E-05**	**1.51E-10**	**8.37E-03**	**9.09E-04**	**1.40E-05**	**9.75E-05**
Total (%)				**1.43E-02**	**1.24E-02**	**2.98E-08**	**5.03E-01**	**9.81E-02**	**5.57E-03**	**2.42E-02**

T (°C)	pH	TotMix	log f(O2)	clincl14 (%)	chamosit (%)	gold (%)	barite (%)	bornite (%)	hematite (%)	quartz (%	acanthit (%)	anhydrit (%	muscovit (%	silver (%)	anglesit (%)	kaolinit (%)	chalcoci (%)	gibbsite (%)
300	4.61		-32.99	100.00%	100.00%	0.50%												
289.1	4.32	0.05	-30.34				27.17%	96.50%	7.99%	3.28%								
278.8	4.28	0.10	-30.82				21.08%	3.50%	1.27%	3.73%	11.09%	1.97%						
269.2	4.21	0.15	-31.3				4.06%		1.09%	3.62%	8.23%	7.67%	10.99%					
260	4.14	0.20	-31.77				2.90%		1.90%	3.41%	4.52%	7.24%	19.85%					
251.4	4.06	0.25	-32.25				2.10%		2.65%	3.32%	3.85%	6.69%	11.02%					
243.3	3.98	0.30	-32.73				1.54%		3.19%	3.19%	3.91%	6.07%	2.70%					
235.6	3.91	0.35	-33.2			1.38%	1.15%		3.49%	2.97%	4.02%	5.40%						
228.4	3.84	0.40	-33.67			4.01%	0.88%		3.62%	2.73%	4.07%	4.71%						
221.6	3.79	0.45	-34.13			3.49%	0.68%		3.62%	2.50%	4.01%	4.04%						
215.2	3.74	0.50	-34.58			3.03%	0.53%		3.47%	2.29%	3.82%	3.41%						
209.7	3.71	0.55	-34.99			14.40%	35.32%		28.18%	30.03%	52.48%	50.52%						
164.1	3.65	1.05	-38.56			10.85%	1.78%		9.06%	13.99%		2.30%		43.70%				
135.3	3.67	1.55	-40.33			2.37%	0.32%		3.28%	7.74%				15.72%	9.11%			
115.5	3.71	2.05	-41.77			1.82%	0.08%		2.02%	5.08%				9.67%	31.82%			
101.1	3.79	2.55	-43.18			1.69%	0.09%		2.20%	3.59%				10.50%	20.98%			
90.19	3.89	3.05	-44.56			1.64%	0.08%		1.74%	2.62%				8.29%	13.46%			
81.67	4	3.55	-45.88			1.62%	0.06%		1.11%	1.93%				5.29%	8.63%			
74.91	4.1	4.05	-47.08			1.61%	0.04%		0.62%	1.42%				2.92%	5.62%			
69.47	4.2	4.55	-48.12			1.61%	0.03%		0.33%	1.03%				1.53%	3.74%			
65.06	4.29	5.05	-49.01			1.61%	0.02%		0.18%	0.72%				0.83%	2.52%			
61.45	4.36	5.55	-49.77			1.61%	0.02%		0.11%	0.47%				0.48%	1.70%			
58.48	4.43	6.05	-50.42			1.61%	0.01%		0.07%	0.26%				0.29%	1.13%			
56.06	4.48	6.55	-50.97			1.61%	0.01%		0.05%	0.09%				0.19%	0.72%			
54.05	4.54	7.05	-51.45			1.61%	0.01%		0.04%					0.13%	0.41%			
52.41	4.58	7.55	-51.86			1.61%	0.01%		0.03%					0.09%	0.17%			
51.07	4.63	8.05	-52.22			1.61%	0.00%		0.03%					0.07%				
49.97	4.67	8.55	-52.54			1.61%	0.00%		0.02%					0.05%				
49.09	4.7	9.05	-52.82			1.61%	0.00%		0.02%					0.04%				
48.38	4.73	9.55	-53.06			1.61%	0.00%		0.02%					0.03%		3.21%		
47.83	4.76	10.05	-53.26			1.61%			0.02%					0.02%		8.02%		
47.4	4.79	10.55	-53.45			1.61%			0.02%					0.02%		8.10%		
47.08	4.82	11.05	-53.61			1.61%			0.01%					0.02%		8.15%		
46.84	4.84	11.55	-53.76			1.61%			0.01%					0.01%		8.18%		
46.69	4.87	12.05	-53.9			1.61%			0.01%					0.01%		8.20%		
46.61	4.89	12.55	-54.02			1.61%			0.01%					0.01%		8.19%		
46.57	4.91	13.05	-54.14			1.61%			0.01%					0.01%		8.16%		
46.59	4.93	13.55	-54.24			1.61%			0.01%					0.01%		8.12%		
46.66	4.95	14.05	-54.34			1.61%			0.01%					0.01%		8.05%		
46.76	4.97	14.55	-54.42			1.61%			0.01%					0.01%		7.97%		
46.87	4.99	15.05	-54.51			1.61%			0.01%					0.01%		7.88%		
47.02	5.01	15.55	-54.58			1.61%			0.01%					0.01%		7.77%		
47.19	5.02	16.05	-54.65			1.61%			0.01%				27.12%	0.00%				
47.37	5.04	16.55	-54.72			1.61%			0.01%				28.32%	0.00%				
47.58	5.05	17.05	-54.75			1.61%			1.99%					0.00%			10.77%	15.07%
47.79	5.06	17.55	-54.75			1.61%			3.08%					0.00%			16.73%	14.46%
48.02	5.07	18.05	-54.75			1.61%			2.96%					0.00%			16.08%	14.39%
48.26	5.08	18.55	-54.76			1.61%			2.83%					0.00%			15.35%	14.27%
48.5	5.09	19.05	-54.77			1.61%			2.68%					0.00%			14.56%	14.13%
48.75	5.1	19.55	-54.77			1.61%			2.53%					0.00%			13.71%	13.95%
49	5.12	20.05	-54.78			1.61%			2.36%					0.00%			12.81%	13.73%
Total (m)				4.13E-05	3.80E-06	6.63E-10	2.68E-03	3.36E-05	2.86E-03	1.04E-02	6.65E-04	1.34E-02	4.02E-05	1.19E-03	2.69E-02	2.16E-04	1.13E-04	2.39E-04
Total (g)				2.30E-03	2.71E-03	1.29E-07	6.26E-01	1.69E-02	4.66E-01	6.27E-01	1.62E-01	1.83E+00	1.60E-02	1.28E-01	8.16E+00	5.66E-02	2.09E-02	1.86E-02

T (°C)	pH	TotMix	log f(O2)	clincl14 (%	chamosit (%	gold (%)	bornite (%)	galena (%)	silver (%)	quartz (%	acanthit (%	muscovit (%	hematite (%)	barite (%)	chalcocl (%)
300	4.61		-32.99	100.00%	100.00%	2.16%									
289	4.47	0.05	-33.37			1.37%	35.81%	0.44%	22.15%	4.66%					
278.8	4.38	0.10	-31.85				64.19%			5.00%	2.59%	20.53%			
269.1	4.3	0.15	-32.07							4.93%	12.34%	26.99%			
259.9	4.23	0.20	-32.47			0.88%				4.75%	7.48%	28.59%			
251.3	4.16	0.25	-32.93			17.45%				4.64%	6.41%	16.99%	11.17%		
243.2	4.08	0.30	-33.41			13.16%				4.45%	6.29%	6.90%	17.42%		
236.5	4.01	0.35	-33.9			11.02%				4.20%	6.24%		19.87%		
228.3	3.94	0.40	-34.38			9.37%				3.86%	6.04%		19.22%		
221.5	3.89	0.45	-34.85			8.03%				3.53%	5.79%		17.55%		
215.1	3.84	0.50	-35.32			6.92%				3.23%	5.47%		14.77%	0.21%	
167.2	3.59	1.00	-39.71			26.52%			52.73%	21.06%	20.41%			23.28%	
137.2	3.5	1.50	-43.1			2.66%			25.13%	11.35%				18.66%	43.21%
116.8	3.5	2.00	-45.9			0.38%				7.34%	13.10%			14.45%	37.03%
102	3.5	2.50	-48.74			0.07%		1.36%		5.14%	7.09%			11.50%	17.84%
90.83	3.52	3.00	-50.45			0.01%		2.67%		3.73%	0.30%			8.71%	0.74%
82.16	3.53	3.50	-51.85			0.00%		2.70%		2.73%	0.16%			6.41%	0.40%
75.27	3.55	4.00	-53.01			0.00%		2.71%		1.99%	0.09%			4.67%	0.23%
69.74	3.57	4.50	-53.98			0.00%		2.72%		1.42%	0.06%			3.41%	0.15%
65.25	3.59	5.00	-54.79			0.00%		2.72%		0.98%	0.04%			2.50%	0.10%
61.59	3.61	5.50	-55.47			0.00%		2.73%		0.62%	0.03%			1.85%	0.07%
58.59	3.63	6.00	-56.04			0.00%		2.73%		0.32%	0.02%			1.37%	0.05%
56.12	3.65	6.50	-56.51			0.00%		2.73%		0.07%	0.01%			1.01%	0.04%
54.1	3.67	7.00	-56.9			0.00%		2.73%			0.01%			0.74%	0.03%
52.43	3.69	7.50	-57.23			0.00%		2.73%			0.01%			0.53%	0.02%
51.08	3.71	8.00	-57.5			0.00%		2.73%			0.01%			0.36%	0.02%
49.97	3.72	8.50	-57.73			0.00%		2.73%			0.00%			0.22%	0.01%
49.08	3.74	9.00	-57.91			0.00%		2.73%			0.00%			0.11%	0.01%
48.36	3.76	9.50	-58.06			0.00%		2.73%			0.00%			0.02%	0.01%
47.8	3.77	10.00	-58.18			0.00%		2.73%			0.00%				0.01%
47.37	3.79	10.50	-58.27			0.00%		2.73%			0.00%				0.01%
47.04	3.8	11.00	-58.34			0.00%		2.73%			0.00%				0.01%
46.81	3.81	11.50	-58.39			0.00%		2.73%			0.00%				0.00%
46.66	3.83	12.00	-58.43			0.00%		2.73%							0.00%
46.56	3.84	12.50	-58.45			0.00%		2.73%							0.00%
46.53	3.85	13.00	-58.46			0.00%		2.73%							0.00%
46.56	3.86	13.50	-58.46			0.00%		2.73%							0.00%
46.61	3.87	14.00	-58.45					2.73%							0.00%
46.7	3.88	14.50	-58.44					2.73%							0.00%
46.82	3.89	15.00	-58.42					2.73%							0.00%
46.97	3.91	15.50	-58.39					2.73%							0.00%
47.14	3.92	16.00	-58.36					2.73%							0.00%
47.33	3.92	16.50	-58.33					2.73%							0.00%
47.53	3.93	17.00	-58.29					2.73%							
47.75	3.94	17.50	-58.25					2.73%							
47.98	3.95	18.00	-58.21					2.73%							
48.21	3.96	18.50	-58.16					2.73%							
48.46	3.97	19.00	-58.12					2.73%							
48.71	3.98	19.50	-58.07					2.73%							
48.96	3.99	20.00	-58.03					2.73%							
49.22	3.99	20.50	-57.98					2.73%							
Total (m)				4.13E-06	3.80E-06	1.53E-10	3.09E-06	6.55E-03	1.10E-03	7.39E-03	3.90E-04	3.50E-05	1.61E-04	1.51E-03	2.71E-04
Total (g)				2.30E-03	2.71E-03	3.01E-08	1.55E-02	1.33E+00	1.18E-01	4.44E-01	9.67E-02	1.40E-02	2.67E-02	3.53E-01	4.31E-02

T (C)	P (bars)	pH	log f(O2)	clincl14 (%)	chamosit (%	fluorite (%)	gold (%)	acanthit (%)	chalcopy (%)	quartz (%	galena (%)	muscovit (%	sphaleri (%)	pyrite (%)	graphite (%)	bornite (%	chalcoci (%)
250	250	4.53	-36.5	98.45%	97.63%	1.04%	10.22%										
245	250	4.5	-36.95	1.55%	2.37%	1.67%	0.26%	11.27%	6.33%	4.63%							
240	250	4.46	-37.41			0.98%	15.47%	13.71%	20.05%	4.90%	10.91%						
235	250	4.41	-37.87			2.95%	12.30%	10.66%	14.75%	4.51%	8.45%	54.74%					
230	250	4.36	-38.34			2.11%	10.99%	9.25%	13.44%	4.40%	8.48%	34.63%	12.79%				
225	250	4.32	-38.81			1.16%	10.51%	7.79%	10.44%	4.30%	6.86%	10.62%	87.21%				
220	250	4.28	-39.31			0.89%	9.50%	6.67%	7.84%	4.16%	6.09%			18.91%			
215	250	4.24	-39.82			0.96%	8.12%	5.51%	4.94%	3.99%	3.52%			28.97%			
210	250	4.2	-40.33			1.01%	5.95%	4.80%	4.47%	3.82%	3.51%			23.25%			
205	250	4.16	-40.85			1.06%	4.32%	4.22%	4.08%	3.65%	3.82%			16.58%			
200	250	4.13	-41.37			1.13%	3.12%	3.72%	3.76%	3.49%	4.37%			9.58%			
195	250	4.09	-41.89			1.21%	2.27%	3.27%	3.49%	3.34%	5.04%			2.72%			
190	250	4.05	-42.43			1.32%	1.72%	2.84%	2.80%	3.20%	5.06%						
185	250	4.02	-42.98			1.45%	1.34%	2.43%	1.92%	3.06%	4.60%						
180	250	3.98	-43.53			1.59%	1.04%	2.08%	1.17%	2.93%	4.16%						
175	250	3.95	-44.11			1.74%	0.79%	1.78%	0.53%	2.80%	3.75%						
170	250	3.91	-44.69			1.88%	0.60%	1.53%		2.68%	3.35%						
165	250	3.88	-45.28			2.03%	0.44%	1.30%		2.57%	2.96%						
160	250	3.84	-45.9			2.16%	0.32%	1.11%		2.46%	2.60%						
155	250	3.81	-46.52			2.28%	0.23%	0.95%		2.36%	2.26%						
150	250	3.78	-47.16			2.39%	0.16%	0.81%		2.26%	1.94%						
145	250	3.75	-47.75			2.50%	0.10%	0.69%		2.17%	1.65%				26.48%		
140	250	3.72	-48.35			2.59%	0.07%	0.58%		2.08%	1.39%				21.45%		
135	250	3.69	-48.96			2.66%	0.05%	0.49%		1.99%	1.16%				15.35%		
130	250	3.66	-49.59			2.73%	0.03%	0.42%		1.90%	0.96%				10.93%		
125	250	3.64	-50.24			2.79%	0.02%	0.35%		1.82%	0.78%				7.76%		
120	250	3.61	-50.9			2.83%	0.01%	0.30%		1.74%	0.62%				5.48%	3.98%	
115	250	3.58	-51.59			2.86%	0.01%	0.25%		1.66%	0.44%				3.87%	21.81%	
110	250	3.56	-52.29			2.89%	0.01%	0.21%		1.58%	0.34%				2.71%	19.14%	
105	250	3.54	-53.02			2.90%	0.00%	0.18%		1.50%	0.26%				1.89%	16.75%	
100	250	3.52	-53.76			2.90%	0.00%	0.15%		1.42%	0.20%				1.31%	14.61%	
95	250	3.49	-54.53			2.89%	0.00%	0.12%		1.34%	0.14%				0.90%	12.70%	
90	250	3.48	-55.32			2.87%	0.00%	0.10%		1.26%	0.10%				0.62%	11.00%	
85	250	3.46	-56.14			2.83%	0.00%	0.09%		1.18%	0.08%				0.42%		17.01%
80	250	3.44	-56.97			2.79%	0.00%	0.07%		1.11%	0.05%				0.28%		17.19%
75	250	3.42	-57.84			2.75%	0.00%	0.06%		1.03%	0.04%				0.19%		14.13%
70	250	3.41	-58.73			2.69%	0.00%	0.05%		0.95%	0.02%				0.13%		11.59%
65	250	3.4	-59.64			2.63%	0.00%	0.04%		0.88%	0.02%				0.08%		9.48%
60	250	3.39	-60.59			2.56%	0.00%	0.03%		0.81%	0.01%				0.06%		7.73%
55	250	3.38	-61.56			2.48%	0.00%	0.03%		0.73%	0.01%				0.04%		6.29%
50	250	3.37	-62.57			2.40%	0.00%	0.02%		0.66%	0.00%				0.02%		5.10%
45	250	3.36	-63.6			2.31%	0.00%	0.02%		0.60%	0.00%				0.02%		4.13%
40	250	3.35	-64.66			2.22%	0.00%	0.01%		0.53%					0.01%		3.08%
35	250	3.35	-65.76			2.13%	0.00%	0.01%		0.47%					0.01%		2.10%
30	250	3.35	-66.89			2.03%	0.00%	0.01%		0.41%					0.00%		1.30%
25	250	3.35	-68.06			1.93%	0.00%	0.01%		0.36%					0.00%		0.67%
20	250	3.35	-69.26			1.83%	0.00%	0.00%		0.31%					0.00%		0.22%
Total (m)				4.60E-06	4.85E-06	7.52E-04	9.78E-10	2.39E-05	2.53E-06	6.05E-03	1.39E-04	7.49E-06	5.96E-06	1.85E-05	3.69E-05	9.75E-08	1.66E-07
Total (g)				2.56E-03	3.46E-03	5.87E-02	1.93E-07	5.93E-03	4.64E-04	3.64E-01	3.33E-02	2.98E-03	6.81E-04	2.22E-03	4.43E-04	4.89E-05	2.64E-05

T (C)	P (bars)	pH	log f(O2)	clincl14(%)	chamosit (%)	fluorite (%	gold (%)	magnetit (%)	quartz (%	hematite (%	muscovit (%	acanthit (%	chalcoci (%
250	71.83	4.53	-36.49	24.71%	18.57%	1.28%	10.29%						
245	45.12	4.51	-36.27	75.29%	81.43%	20.79%	49.90%	46.98%	4.16%				
240	37.07	4.47	-36.44			1.58%	21.99%	53.02%	6.71%				
235	32.41	4.42	-36.61			6.30%	7.93%		5.99%	100.00%	37.94%		
230	28.89	4.37	-36.86			4.83%	3.84%		5.75%		27.35%		
225	25.95	4.33	-37.18			3.62%	2.13%		5.51%		17.41%		
220	23.38	4.29	-37.55			2.97%	1.27%		5.25%		11.06%		
215	21.08	4.25	-37.95			2.52%	0.81%		4.99%		5.92%	1.98%	
210	19	4.22	-38.37			1.99%	0.56%		4.76%		0.32%	10.25%	
205	17.11	4.18	-38.82			1.93%	0.38%		4.48%			9.68%	
200	15.38	4.15	-39.3			1.92%	0.26%		4.22%			8.98%	
195	13.8	4.11	-39.79			1.94%	0.18%		3.98%			8.26%	
190	12.35	4.08	-40.3			1.98%	0.13%		3.75%			7.55%	
185	11.03	4.04	-40.83			2.04%	0.09%		3.53%			6.86%	
180	9.83	4.01	-41.38			2.11%	0.07%		3.33%			6.20%	
175	8.73	3.97	-41.94			2.19%	0.05%		3.14%			5.58%	
170	7.73	3.94	-42.53			2.27%	0.03%		2.97%			4.99%	
165	6.82	3.9	-43.13			2.35%	0.02%		2.80%			4.45%	
160	6	3.87	-43.74			2.43%	0.02%		2.64%			3.94%	
155	5.25	3.83	-44.38			2.51%	0.01%		2.50%			3.48%	
150	4.59	3.8	-45.04			2.58%	0.01%		2.36%			3.05%	
145	3.99	3.76	-45.71			2.65%	0.01%		2.22%			2.67%	
140	3.45	3.73	-46.41			2.70%	0.00%		2.10%			2.32%	
135	2.98	3.69	-47.12			2.75%	0.00%		1.98%			2.00%	
130	2.55	3.66	-47.85			2.79%	0.00%		1.86%			1.72%	
125	2.18	3.63	-48.61			2.82%	0.00%		1.75%			1.48%	
120	1.85	3.6	-49.39			2.84%	0.00%		1.65%			1.26%	
115	1.56	3.57	-50.19			2.85%	0.00%		1.55%			1.06%	
110	1.32	3.53	-51.01			2.85%	0.00%		1.45%			0.89%	11.53%
105	1.1	3.5	-51.86			2.83%	0.00%		1.35%			0.75%	48.22%
100	0.91	3.47	-52.73			2.82%	0.00%		1.26%			0.62%	40.25%
Total (m)				**1.86E-05**	**2.59E-05**	**6.51E-04**	**9.78E-10**	**5.72E-05**	**5.39E-03**	**4.15E-06**	**1.91E-05**	**2.33E-05**	**6.18E-07**
Total (g)				**1.04E-02**	**1.85E-02**	**5.08E-02**	**1.93E-07**	**1.32E-02**	**3.24E-01**	**6.62E-04**	**7.62E-03**	**5.78E-03**	**9.83E-05**

T (°C)	P (bars)	pH	Tot Mix	log f(O2)	clincl14 (%)	chamosit (%)	fluorite (%)	gold (%)	barite (%)	hematite (%	pyrite (%)	quartz (%	anhydrit (%)	acanthit (%)	silver (%)	kaolinit (%	muscovit (%)	gibbsite (%)
250	250	4.53		-36.5	100.00%	100.00%	5.85%	7.09%										
239.9	250	4.19	0.06	-34.33				37.35%	59.17%	42.42%	61.78%	6.78%						
230.6	250	4.07	0.10	-34.77				12.07%	27.19%	17.90%	14.81%	6.65%	1.63%					
221.8	250	4	0.15	-35.41				5.75%	2.62%	10.95%	8.58%	5.95%	6.42%					
213.8	250	3.95	0.20	-36.05				3.08%	1.95%	9.47%	6.69%	5.32%	6.31%					
206.3	250	3.92	0.26	-36.68				1.74%	1.48%	7.47%	5.01%	4.76%	6.18%					
199.3	250	3.9	0.30	-37.3				1.05%	1.15%	5.04%	2.13%	4.27%	6.06%	21.93%				
192.8	250	3.89	0.35	-37.9				0.67%	0.91%	2.92%	0.88%	3.85%	5.92%	21.70%				
186.7	250	3.9	0.40	-38.5				0.45%	0.74%	1.12%	0.12%	3.49%	5.76%	17.28%				
181	250	3.92	0.45	-39.06				0.36%	0.60%	0.08%		3.18%	5.56%	11.35%				
176.7	250	3.93	0.50	-39.59				0.25%	0.50%			2.91%	5.33%	8.10%				
136.1	250	4.04	1.00	-43.64			41.41%	1.02%	2.36%			20.03%	38.97%	19.64%				
111.7	250	4.14	1.50	-44.81			45.24%	0.75%	0.72%	0.01%		11.53%	11.86%					
96.23	250	4.23	2.00	-46.42			7.50%	0.75%	0.27%	0.05%		7.49%						
83.38	250	4.32	2.50	-47.72				0.75%	0.13%	0.05%		5.08%						
74.56	250	4.4	3.00	-48.8				0.75%	0.07%	0.13%		3.49%			13.20%			
67.8	250	4.47	3.50	-49.71				0.75%	0.05%	0.17%		2.36%			20.92%			
62.66	250	4.54	4.00	-50.48				0.75%	0.03%	0.13%		1.53%			14.56%			
58.44	250	4.6	4.50	-51.13				0.75%	0.02%	0.11%		0.90%			10.49%			
55.18	250	4.65	5.00	-51.69				0.75%	0.01%	0.10%		0.40%			7.78%			
52.69	250	4.7	5.50	-52.17				0.75%	0.01%	0.09%		0.00%			5.91%			
50.63	250	4.75	6.00	-52.58				0.75%	0.01%	0.08%					4.58%			
48.9	250	4.79	6.50	-52.93				0.75%	0.00%	0.07%					3.62%			
47.62	250	4.83	7.00	-53.24				0.75%	0.00%	0.07%					2.90%			
46.61	250	4.86	7.50	-53.51				0.75%	0.00%	0.07%					2.36%			
45.84	250	4.9	8.00	-53.73				0.75%		0.06%					1.81%	39.38%		
45.26	250	4.92	8.50	-53.92				0.75%		0.06%					1.46%	60.62%		
44.82	250	4.95	9.00	-54.09				0.75%		0.06%					1.23%		8.32%	
44.51	250	4.98	9.50	-54.23				0.75%		0.06%					1.06%		8.39%	
44.32	250	5	10.00	-54.36				0.75%		0.06%					0.92%		8.37%	
44.21	250	5.02	10.50	-54.48				0.75%		0.06%					0.81%		8.30%	
44.18	250	5.04	11.00	-54.58				0.75%		0.06%					0.71%		8.20%	
44.2	250	5.07	11.50	-54.67				0.75%		0.06%					0.63%		8.06%	
44.28	250	5.08	12.00	-54.75				0.75%		0.06%					0.56%		7.89%	
44.4	250	5.1	12.50	-54.82				0.75%		0.06%					0.50%		7.69%	
44.56	250	5.12	13.00	-54.89				0.75%		0.06%					0.45%		7.47%	
44.75	250	5.14	13.50	-54.95				0.75%		0.06%					0.41%		7.23%	
44.96	250	5.15	14.00	-55				0.75%		0.06%					0.37%		6.97%	
45.19	250	5.17	14.50	-55.05				0.75%		0.06%					0.34%		6.70%	
45.44	250	5.19	15.00	-55.1				0.75%		0.06%					0.31%		6.42%	
45.7	250	5.2	15.50	-55.14				0.75%		0.06%					0.28%			12.74%
45.97	250	5.22	16.00	-55.18				0.75%		0.06%					0.25%			12.26%
46.25	250	5.23	16.50	-55.22				0.75%		0.06%					0.23%			11.45%
46.54	250	5.24	17.00	-55.25				0.75%		0.06%					0.22%			10.62%
46.83	250	5.26	17.50	-55.28				0.75%		0.06%					0.20%			9.80%
47.13	250	5.27	18.00	-55.31				0.75%		0.06%					0.19%			9.00%
47.43	250	5.28	18.50	-55.34				0.75%		0.06%					0.17%			8.23%
47.73	250	5.29	19.00	-55.37				0.75%		0.06%					0.16%			7.48%
48.03	250	5.3	19.50	-55.4				0.75%		0.06%					0.15%			6.78%
48.33	250	5.32	20.00	-55.42				0.75%		0.06%					0.14%			6.12%
48.63	250	5.33	20.50	-55.45				0.75%		0.06%					0.13%			5.51%
Total (m)					4.53E-06	4.74E-06	1.33E-04	1.41E-09	1.74E-03	5.94E-04	2.00E-04	4.48E-03	1.77E-02	2.06E-05	6.46E-06	2.22E-05	1.12E-04	2.07E-04
Total (g)					2.52E-03	3.38E-03	1.04E-02	2.78E-07	4.07E-01	9.49E-02	2.39E-02	2.69E-01	2.41E+00	5.11E-03	6.97E-04	5.74E-03	4.46E-02	1.61E-02

T (°C)	P (bars)	pH	Tot Mix	log f(O2)	clincl14 (%)	chamosit (%)	fluorite (%)	gold (%)	acanthit (%)	hematite (%)	magnetit (%)	pyrite (%)	quartz (%	barite (%)	chalcopy (%)	galena (%)	bornite (%)	sphaleri (%
260	250	4.53		-36.5	100.00%	100.00%	100.00%	0.21%										
239.8	250	4.43	0.05	-36.29				0.87%	0.07%	1.05%	100.00%	0.13%	0.23%					
230.6	250	4.27	0.10	-36.31				1.53%		7.98%		0.24%	0.43%					
221.8	250	4.14	0.15	-36.5				1.79%		11.20%		0.30%	0.61%					
213.7	250	4.07	0.20	-36.97				1.90%	0.20%	12.76%		0.34%	0.77%					
206.2	250	4.02	0.25	-37.51				1.96%	0.55%	13.42%		0.37%	0.92%					
199.2	250	4	0.30	-38.08				1.99%	0.88%	13.39%		0.38%	1.05%					
192.7	250	3.99	0.35	-38.67				2.01%	1.19%	12.63%		0.40%	1.16%	0.02%				
186.6	250	4	0.40	-39.3				2.02%	1.46%	11.17%		0.41%	1.27%	0.10%				
180.9	250	4.02	0.45	-39.9				2.03%	1.66%	9.31%		0.41%	1.37%	0.17%				
175.6	250	4.04	0.50	-40.49				2.03%	1.82%	7.10%		0.42%	1.46%	0.25%				
136	250	4.01	1.00	-45.22				2.04%	2.24%			0.45%	2.06%	0.86%	100.00%	0.75%		
111.6	250	3.94	1.50	-48.61				2.04%	2.29%			0.51%	2.41%	1.36%		1.72%	1.97%	
95.11	250	3.92	2.00	-51.16				2.04%	2.30%			0.62%	2.63%	1.76%		2.12%	2.16%	
83.28	250	3.91	2.50	-53.11				2.04%	2.30%			0.59%	2.79%	2.08%		2.28%	2.24%	0.45%
74.46	250	3.91	3.00	-54.65				2.04%	2.30%			0.58%	2.89%	2.30%		2.37%	2.28%	0.83%
67.72	250	3.92	3.50	-55.88				2.04%	2.31%			0.62%	2.96%	2.44%		2.44%	2.31%	1.13%
62.48	250	3.94	4.00	-56.88				2.04%	2.31%			0.68%	3.00%	2.53%		2.48%	2.34%	1.35%
58.37	250	3.97	4.50	-57.69				2.04%	2.31%			0.77%	3.02%	2.60%		2.51%	2.36%	1.54%
55.12	250	3.99	5.00	-58.34				2.04%	2.31%			0.86%	3.03%	2.64%		2.53%	2.38%	1.70%
52.54	250	4.02	5.50	-58.88				2.04%	2.31%			0.97%	3.03%	2.67%		2.55%	2.40%	1.84%
50.48	250	4.05	6.00	-59.31				2.04%	2.31%			1.08%	3.02%	2.69%		2.56%	2.42%	1.97%
48.86	250	4.07	6.50	-59.66				2.04%	2.31%			1.19%	3.00%	2.70%		2.57%	2.43%	2.08%
47.58	250	4.1	7.00	-59.94				2.04%	2.31%			1.31%	2.97%	2.71%		2.58%	2.45%	2.19%
46.58	250	4.12	7.50	-60.16				2.04%	2.31%			1.43%	2.93%	2.72%		2.58%	2.47%	2.29%
45.8	250	4.14	8.00	-60.34				2.04%	2.31%			1.55%	2.89%	2.72%		2.59%	2.48%	2.39%
45.22	250	4.16	8.50	-60.48				2.04%	2.31%			1.68%	2.84%	2.72%		2.59%	2.50%	2.48%
44.79	250	4.18	9.00	-60.58				2.04%	2.31%			1.81%	2.79%	2.71%		2.60%	2.52%	2.56%
44.49	250	4.2	9.50	-60.66				2.04%	2.31%			1.94%	2.74%	2.71%		2.60%	2.53%	2.65%
44.29	250	4.22	10.00	-60.71				2.04%	2.31%			2.07%	2.68%	2.70%		2.60%	2.55%	2.72%
44.19	250	4.24	10.50	-60.75				2.04%	2.31%			2.20%	2.61%	2.69%		2.61%	2.56%	2.80%
44.16	250	4.26	11.00	-60.77				2.04%	2.31%			2.33%	2.54%	2.69%		2.61%	2.58%	2.87%
44.19	250	4.28	11.50	-60.77				2.04%	2.31%			2.47%	2.47%	2.68%		2.61%	2.60%	2.94%
44.27	250	4.29	12.00	-60.77				2.04%	2.31%			2.61%	2.40%	2.67%		2.61%	2.61%	3.00%
44.39	250	4.31	12.50	-60.75				2.04%	2.31%			2.74%	2.32%	2.65%		2.61%	2.63%	3.06%
44.56	250	4.33	13.00	-60.73				2.04%	2.31%			2.88%	2.24%	2.64%		2.61%	2.65%	3.12%
44.74	250	4.34	13.50	-60.7				2.04%	2.31%			3.03%	2.16%	2.63%		2.62%	2.66%	3.17%
44.95	250	4.35	14.00	-60.67				2.04%	2.31%			3.17%	2.08%	2.62%		2.62%	2.68%	3.22%
45.18	250	4.37	14.50	-60.63				2.04%	2.31%			3.31%	1.99%	2.60%		2.62%	2.69%	3.27%
45.43	250	4.38	15.00	-60.58				2.04%	2.31%			3.45%	1.90%	2.59%		2.62%	2.71%	3.32%
45.69	250	4.4	15.50	-60.54				2.04%	2.31%			3.60%	1.81%	2.57%		2.62%	2.73%	3.37%
45.96	250	4.41	16.00	-60.49				2.04%	2.31%			3.74%	1.71%	2.56%		2.62%	2.74%	3.41%
46.26	250	4.42	16.50	-60.44				2.04%	2.31%			3.89%	1.62%	2.54%		2.62%	2.76%	3.45%
46.53	250	4.43	17.00	-60.39				2.04%	2.31%			4.04%	1.52%	2.53%		2.62%	2.77%	3.49%
46.83	250	4.45	17.50	-60.34				2.04%	2.31%			4.19%	1.42%	2.51%		2.62%	2.79%	3.52%
47.12	250	4.46	18.00	-60.28				2.04%	2.31%			4.34%	1.31%	2.49%		2.62%	2.80%	3.56%
47.42	250	4.47	18.50	-60.23				2.04%	2.31%			4.48%	1.21%	2.47%		2.62%	2.82%	3.59%
47.72	250	4.48	19.00	-60.18				2.04%	2.31%			4.63%	1.10%	2.46%		2.62%	2.84%	3.62%
48.03	250	4.49	19.50	-60.12				2.04%	2.31%			4.79%	1.00%	2.44%		2.62%	2.85%	3.66%
48.33	250	4.5	20.00	-60.07				2.04%	2.31%			4.94%	0.89%	2.42%		2.62%	2.87%	3.68%
48.63	250	4.51	20.50	-60.01				2.04%	2.31%			5.09%	0.77%	2.40%		2.63%	2.88%	3.71%
Total (m)					4.53E-06	4.74E-06	7.78E-06	4.79E-08	1.04E-03	1.98E-03	3.29E-06	6.31E-02	1.47E-01	6.71E-02	2.36E-06	1.06E-02	3.04E-06	3.79E-02
Total (g)					2.62E-03	3.38E-03	6.08E-04	9.44E-06	2.67E-01	3.16E-01	7.62E-03	6.37E+00	8.86E+00	1.22E+01	4.32E-04	2.66E+00	1.63E-02	3.69E+00

C)	pH	log f(O2)	clincl14 (%)	chamosit (%)	gold (%)	bornite (%	galena (%)	silver (%)	quartz (%	muscovit (%	chalcoci (%	graphite (%	fluorite (%
300	4.61	-33	56.28%	59.84%	0.04%								
295	4.58	-33.36	43.72%	40.16%	0.26%	37.53%	1.51%	0.24%	0.10%				
290	4.53	-33.72			0.62%	62.47%	6.91%	0.51%	0.19%	1.27%			
285	4.47	-34.09			0.85%		11.06%	0.70%	0.29%	1.89%	0.24%		
280	4.41	-34.46			1.05%		10.59%	0.87%	0.39%	2.52%	0.44%		
275	4.36	-34.85			1.21%		10.16%	1.02%	0.48%	3.15%	0.62%		
270	4.31	-35.24			1.35%		9.73%	1.15%	0.57%	3.76%	0.78%		
265	4.26	-35.64			1.47%		9.25%	1.26%	0.66%	4.34%	0.93%		
260	4.21	-36.04			1.57%		8.66%	1.36%	0.75%	4.89%	1.07%		
255	4.17	-36.45			1.65%		7.94%	1.45%	0.84%	5.38%	1.20%		
250	4.13	-36.87			1.71%		7.08%	1.53%	0.92%	5.80%	1.32%		
245	4.09	-37.3			1.76%		6.05%	1.60%	1.00%	6.14%	1.45%		
240	4.06	-37.73			1.80%		4.88%	1.66%	1.08%	6.39%	1.56%		
235	4.03	-38.18			1.83%		3.55%	1.71%	1.15%	6.53%	1.68%		
230	4	-38.63			1.86%		2.10%	1.76%	1.23%	6.56%	1.79%		
225	3.97	-39.09			1.88%		0.54%	1.80%	1.30%	6.47%	1.90%		
220	3.95	-39.56			1.89%			1.83%	1.37%	6.25%	1.96%		
215	3.92	-40.04			1.90%			1.86%	1.43%	5.91%	2.00%		
210	3.9	-40.53			1.91%			1.88%	1.50%	5.46%	2.02%		
205	3.89	-41.03			1.92%			1.91%	1.56%	4.90%	2.04%		
200	3.87	-41.54			1.92%			1.92%	1.62%	4.22%	2.06%		
195	3.85	-42.06			1.92%			1.94%	1.68%	3.44%	2.07%		
190	3.84	-42.59			1.93%			1.95%	1.73%	2.57%	2.07%		
185	3.83	-43.13			1.93%			1.96%	1.78%	1.60%	2.08%		
180	3.82	-43.69			1.93%			1.97%	1.84%	0.55%	2.08%		
175	3.8	-44.26			1.93%			1.98%	1.88%		2.08%		
170	3.78	-44.84			1.93%			1.98%	1.93%		2.08%		
165	3.76	-45.43			1.93%			1.99%	1.97%		2.08%		
160	3.73	-46.04			1.93%			1.99%	2.01%		2.08%		
155	3.71	-46.6			1.93%			2.00%	2.05%		2.08%	1.01%	
150	3.69	-47.17			1.93%			2.00%	2.08%		2.08%	1.85%	
145	3.66	-47.75			1.93%			2.00%	2.12%		2.08%	2.46%	
140	3.64	-48.35			1.93%			2.00%	2.15%		2.08%	2.89%	
135	3.62	-48.96			1.93%			2.00%	2.19%		2.08%	3.20%	
130	3.6	-49.59			1.93%			2.00%	2.22%		2.08%	3.42%	0.13%
125	3.57	-50.24			1.93%			2.01%	2.25%		2.08%	3.57%	0.52%
120	3.55	-50.91			1.93%			2.01%	2.27%		2.08%	3.68%	0.91%
115	3.52	-51.59			1.93%			2.01%	2.30%		2.08%	3.76%	1.31%
110	3.5	-52.29			1.93%			2.01%	2.33%		2.08%	3.81%	1.71%
105	3.48	-53.02			1.93%			2.01%	2.35%		2.08%	3.85%	2.11%
100	3.46	-53.77			1.93%			2.01%	2.37%		2.08%	3.87%	2.50%
95	3.44	-54.53			1.93%			2.01%	2.39%		2.08%	3.89%	2.90%
90	3.42	-55.32			1.93%			2.01%	2.41%		2.08%	3.90%	3.30%
85	3.4	-56.14			1.93%			2.01%	2.43%		2.08%	3.91%	3.69%
80	3.38	-56.98			1.93%			2.01%	2.45%		2.08%	3.91%	4.08%
75	3.36	-57.84			1.93%			2.01%	2.47%		2.08%	3.92%	4.46%
70	3.35	-58.73			1.93%			2.01%	2.48%		2.08%	3.92%	4.84%
65	3.34	-59.65			1.93%			2.01%	2.50%		2.08%	3.92%	5.22%
60	3.32	-60.59			1.93%			2.01%	2.51%		2.08%	3.92%	5.58%
55	3.31	-61.56			1.93%			2.01%	2.52%		2.08%	3.92%	5.94%
50	3.3	-62.57			1.93%			2.01%	2.53%		2.08%	3.92%	6.29%
45	3.29	-63.6			1.93%			2.01%	2.54%		2.08%	3.92%	6.63%
40	3.29	-64.67			1.93%			2.01%	2.55%		2.08%	3.92%	6.96%
35	3.28	-65.76			1.93%			2.01%	2.56%		2.08%	3.92%	7.28%
30	3.28	-66.9			1.93%			2.01%	2.57%		2.08%	3.92%	7.59%
25	3.28	-68.06			1.93%			2.01%	2.57%		2.08%	3.92%	7.88%
20	3.28	-69.27			1.93%			2.01%	2.58%		2.08%	3.92%	8.16%
al (m)			5.87E-06	5.28E-06	5.74E-09	4.96E-06	2.44E-04	2.76E-02	3.74E-01	5.74E-04	5.78E-03	1.82E-02	7.09E-03
al (g)			3.26E-03	3.77E-03	1.13E-06	2.49E-03	6.86E-02	2.98E+00	2.25E+01	2.29E-01	9.20E-01	2.18E-02	5.54E-01

T (°C)	P (bars)	pH	log f(O2)	clincl14 (%)	chamosit (%	gold (%)	magnetit (%)	quartz (%)	bornite (%)	silver (%)	chalcoci (%	muscovit (%)	fluorite (%
300	116.67	4.61	-32.99	13.49%	16.96%	1.89%							
295	89.57	4.64	-32.9	54.03%	55.36%	19.98%	68.62%	4.86%					
290	77.81	4.63	-32.87	20.45%	17.96%	12.59%	31.38%	5.79%					
285	70.03	4.62	-32.97	12.02%	9.71%	10.67%		5.74%	100.00%	1.23%			
280	63.83	4.58	-33.14			8.50%		5.49%		3.89%	2.98%	20.69%	
275	58.48	4.53	-33.37			6.43%		5.23%		3.70%	1.85%	20.27%	
270	53.7	4.48	-33.64			5.30%		4.99%		4.13%	1.53%	16.67%	
265	49.35	4.43	-33.94			4.58%		4.75%		4.51%	1.59%	13.75%	
260	45.36	4.38	-34.25			4.07%		4.52%		4.83%	1.87%	11.09%	
255	41.67	4.32	-34.59			3.66%		4.29%		5.08%	2.29%	8.48%	
250	38.24	4.27	-34.95			3.29%		4.07%		5.25%	2.78%	5.81%	
245	35.06	4.22	-35.31			2.95%		3.86%		5.36%	3.31%	3.05%	
240	32.1	4.18	-35.69			2.63%		3.67%		5.39%	3.85%	0.20%	
235	29.35	4.13	-36.09			2.28%		3.46%		5.18%	4.08%		
230	26.79	4.09	-36.5			1.96%		3.26%		4.94%	4.29%		
225	24.41	4.04	-36.92			1.68%		3.07%		4.69%	4.47%		
220	22.2	4	-37.36			1.42%		2.89%		4.43%	4.63%		
215	20.15	3.96	-37.81			1.19%		2.72%		4.16%	4.75%		
210	18.25	3.92	-38.27			0.99%		2.56%		3.89%	4.84%		
205	16.49	3.88	-38.75			0.82%		2.41%		3.62%	4.88%		
200	14.87	3.84	-39.24			0.67%		2.27%		3.35%	4.89%		
195	13.37	3.81	-39.74			0.55%		2.14%		3.09%	4.84%		
190	11.99	3.77	-40.26			0.44%		2.02%		2.84%	4.75%		
185	10.72	3.74	-40.8			0.35%		1.90%		2.59%	4.60%		
180	9.56	3.7	-41.35			0.28%		1.80%		2.35%	4.40%		
175	8.5	3.67	-41.92			0.21%		1.69%		2.02%	3.91%		3.48%
170	7.53	3.63	-42.51			0.16%		1.60%		1.65%	3.27%		10.25%
165	6.65	3.59	-43.12			0.13%		1.51%		1.50%	3.05%		10.79%
160	5.85	3.55	-43.74			0.10%		1.42%		1.36%	2.80%		11.34%
155	5.13	3.51	-44.38			0.08%		1.34%		1.23%	2.52%		11.88%
150	4.48	3.47	-45.04			0.06%		1.27%		1.10%	2.21%		12.39%
145	3.89	3.43	-45.72			0.04%		1.20%		0.99%	1.90%		12.87%
140	3.37	3.39	-46.41			0.03%		1.13%		0.88%	1.58%		13.31%
135	2.9	3.36	-47.13			0.02%		1.06%		0.77%	1.28%		13.70%
Total (m)				**2.47E-05**	**1.88E-05**	**1.11E-10**	**2.22E-05**	**8.53E-03**	**4.31E-07**	**5.31E-04**	**1.15E-04**	**2.37E-05**	**1.97E-04**
Total (g)				**1.37E-02**	**1.34E-02**	**2.18E-08**	**5.14E-03**	**5.12E-01**	**2.16E-04**	**5.73E-02**	**1.82E-02**	**9.45E-03**	**1.54E-02**

T (°C)	pH	TotMix	log f(O2)	clincl14 (%	chamosit (%)	gold (%)	anhydrit (%)	barite (%)	bornite (%)	hematite (%)	quartz (%	galena (%)	muscovit (%)	acanthit (%)	chalcocl (%)	silver (%)	anglesit (%)	kaolinit (%)	gibbsite (%)
300	4.61		-33	100.00%	100.00%	0.38%													
288.9	4.35	0.05	-30.53				1.91%	29.82%	91.46%	31.01%	4.81%								
278.6	4.32	0.10	-31.14				3.63%	19.03%	8.54%		5.32%	100.00%	0.97%						
268.7	4.27	0.15	-31.71				3.93%	12.76%		0.09%	4.80%		12.45%	26.03%					
259.6	4.21	0.20	-32.26				4.06%	8.83%		4.13%	4.79%		8.88%	16.61%					
250.8	4.14	0.25	-32.8			2.20%	4.11%	6.27%		6.12%	4.63%		6.11%	12.66%					
242.6	4.08	0.30	-33.34			5.24%	4.12%	4.56%		7.22%	4.40%		3.61%	10.93%					
234.9	4.02	0.35	-33.86			3.64%	4.09%	3.39%		7.66%	4.14%		1.57%	9.96%					
227.6	3.97	0.40	-34.38			2.75%	4.05%	2.58%		7.56%	3.85%		0.08%	9.11%					
220.8	3.93	0.45	-34.89			2.14%	4.00%	2.00%		6.86%	3.53%			7.97%					
214.3	3.9	0.50	-35.39			1.68%	3.94%	1.57%		5.91%	3.22%			6.74%					
166.3	3.95	1.00	-39.4			6.04%	34.81%	6.33%		14.53%	20.94%				100.00%	45.04%			
136.3	4.04	1.50	-41.65			2.15%	21.40%	1.60%		3.77%	11.27%					28.51%			
116.9	4.12	2.00	-43.31			1.97%	5.97%	0.62%		1.29%	7.28%					9.51%			
101.2	4.19	2.50	-44.65			1.95%		0.24%		0.66%	5.10%					4.69%	22.99%		
90.08	4.27	3.00	-45.81			1.94%		0.12%		0.47%	3.70%					3.27%	31.29%		
81.46	4.34	3.50	-46.8			1.94%		0.08%		0.32%	2.71%					2.13%	18.57%		
74.63	4.4	4.00	-47.65			1.94%		0.06%		0.23%	1.98%					1.46%	11.39%		
69.16	4.46	4.50	-48.39			1.94%		0.04%		0.18%	1.43%					1.04%	7.11%		
64.71	4.51	5.00	-49.02			1.94%		0.03%		0.14%	0.99%					0.77%	4.40%		
61.1	4.56	5.50	-49.56			1.94%		0.02%		0.12%	0.64%					0.58%	2.58%		
58.14	4.61	6.00	-50.04			1.94%		0.02%		0.10%	0.35%					0.45%	1.30%		
56.71	4.65	6.50	-50.45			1.94%		0.01%		0.09%	0.11%					0.36%	0.35%		
53.72	4.69	7.00	-50.81			1.94%		0.01%		0.08%						0.30%			
52.09	4.73	7.50	-51.13			1.94%		0.01%		0.08%						0.25%			
50.76	4.76	8.00	-51.42			1.94%		0.00%		0.07%						0.21%			
49.68	4.79	8.50	-51.66			1.94%		0.00%		0.07%						0.17%		6.11%	
48.81	4.82	9.00	-51.87			1.94%		0.00%		0.06%						0.14%		9.69%	
48.12	4.85	9.50	-52.06			1.94%				0.06%						0.13%		10.02%	
47.58	4.87	10.00	-52.23			1.94%				0.06%						0.11%		10.27%	
47.16	4.9	10.50	-52.39			1.94%				0.06%						0.10%		10.47%	
46.86	4.92	11.00	-52.53			1.94%				0.06%						0.09%		10.61%	
46.64	4.94	11.50	-52.65			1.94%				0.05%						0.08%		10.69%	
46.49	4.96	12.00	-52.77			1.94%				0.05%						0.07%		10.73%	
46.42	4.98	12.50	-52.87			1.94%				0.05%						0.06%		10.73%	
46.4	5	13.00	-52.97			1.94%				0.05%						0.06%		10.68%	
46.43	5.02	13.50	-53.05			1.94%				0.05%			9.19%			0.05%			
46.49	5.04	14.00	-53.13			1.94%				0.05%			9.48%			0.04%			
46.59	5.06	14.50	-53.2			1.94%				0.05%			9.36%			0.04%			
46.73	5.07	15.00	-53.27			1.94%				0.05%			9.22%			0.04%			
46.88	5.09	15.50	-53.33			1.94%				0.05%			9.05%			0.03%			
47.06	5.11	16.00	-53.39			1.94%				0.05%			8.86%			0.03%			
47.26	5.12	16.50	-53.44			1.94%				0.05%			8.64%			0.03%			
47.46	5.14	17.00	-53.49			1.94%				0.05%			2.53%			0.03%			9.24%
47.68	5.15	17.50	-53.54			1.94%				0.05%						0.02%			14.83%
47.91	5.16	18.00	-53.58			1.94%				0.05%						0.02%			14.27%
48.16	5.18	18.50	-53.62			1.94%				0.05%						0.02%			13.66%
48.4	5.19	19.00	-53.66			1.94%				0.05%						0.02%			13.02%
48.65	5.2	19.50	-53.7			1.94%				0.05%						0.02%			12.35%
48.91	5.22	20.00	-53.74			1.94%				0.05%						0.02%			11.66%
49.17	5.23	20.50	-53.77			1.94%				0.05%						0.02%			10.97%
Total (m)				3.30E-06	3.16E-06	5.42E-10	2.92E-02	1.74E-03	2.88E-05	7.42E-04	7.47E-03	7.30E-05	1.14E-04	1.80E-04	1.84E-05	1.94E-04	7.13E-03	1.48E-04	2.50E-04
Total (g)				1.84E-03	2.25E-03	1.07E-07	3.97E+00	4.07E-01	1.44E-02	1.18E-01	4.49E-01	1.76E-02	4.55E-02	4.47E-02	2.93E-03	2.10E-02	2.16E+00	3.82E-02	1.95E-02

T (°C)	pH	TotMix	log f(O2)	clincl14 (%)	chamosit (%	gold (%)	bornite (%)	galena (	silver (%)	muscovit (%)	quartz (%	hematite (%	acanthit (%	barite (%)	chalcocl (%)
300	4.61		-33	100.00%	100.00%	1.86%									
288.9	4.52	0.05	-33.58			25.89%	15.36%	1.22%	100.00%	7.00%	4.74%				
278.6	4.44	0.10	-33.14				38.43%	0.81%		23.17%	4.96%				
268.7	4.34	0.15	-32.28				39.98%			17.27%	5.09%	24.71%			
259.4	4.27	0.20	-32.73				0.63%			18.18%	4.88%	8.20%	14.14%		
250.7	4.2	0.25	-33.26			4.93%				14.37%	4.67%	12.42%	12.32%		
242.5	4.14	0.30	-33.8			18.05%	2.15%			9.69%	4.42%	17.05%	10.12%		
234.8	4.08	0.35	-34.37			13.67%	3.45%			6.41%	4.13%	14.10%	8.39%	1.66%	
227.5	4.04	0.40	-34.93			9.75%				3.12%	3.84%	12.20%	6.85%	2.09%	4.54%
220.6	4	0.45	-35.47			7.00%				0.80%	3.55%	8.74%	5.70%	2.11%	5.38%
214.2	3.98	0.50	-36			5.12%					3.26%	2.59%	4.84%	2.16%	5.38%
166.1	3.82	1.00	-40.78			12.84%		0.13%			21.16%		31.16%	20.03%	64.90%
136.1	3.75	1.50	-44.24			0.78%		2.15%			11.34%		4.10%	17.21%	11.89%
116.8	3.71	2.00	-46.91			0.10%		2.40%			7.31%		1.27%	14.30%	4.04%
101	3.7	2.50	-49.02			0.02%		2.47%			5.10%		0.50%	11.19%	1.64%
89.98	3.71	3.00	-50.74			0.01%		2.50%			3.68%		0.24%	8.30%	0.78%
81.36	3.71	3.50	-52.14			0.00%		2.51%			2.68%		0.13%	5.98%	0.42%
74.56	3.73	4.00	-53.3			0.00%		2.52%			1.95%		0.07%	4.29%	0.25%
69.08	3.74	4.50	-54.27			0.00%		2.52%			1.38%		0.05%	3.09%	0.16%
64.65	3.76	5.00	-55.08			0.00%		2.52%			0.94%		0.03%	2.25%	0.11%
61.04	3.78	5.50	-55.75			0.00%		2.52%			0.58%		0.02%	1.65%	0.08%
58.08	3.79	6.00	-56.32			0.00%		2.52%			0.29%		0.02%	1.21%	0.06%
55.66	3.81	6.50	-56.79			0.00%		2.52%			0.05%		0.01%	0.88%	0.05%
53.68	3.83	7.00	-57.18			0.00%		2.52%					0.01%	0.64%	0.04%
52.05	3.84	7.50	-57.51			0.00%		2.52%					0.01%	0.45%	0.03%
50.73	3.86	8.00	-57.78			0.00%		2.52%					0.00%	0.29%	0.02%
49.65	3.87	8.50	-58			0.00%		2.52%					0.00%	0.17%	0.02%
48.79	3.89	9.00	-58.18			0.00%		2.52%					0.00%	0.07%	0.02%
48.1	3.9	9.50	-58.33			0.00%		2.52%					0.00%		0.02%
47.66	3.91	10.00	-58.45			0.00%		2.52%					0.00%		0.01%
47.14	3.93	10.50	-58.54			0.00%		2.52%					0.00%		0.01%
46.83	3.94	11.00	-58.61			0.00%		2.52%					0.00%		0.01%
46.62	3.95	11.50	-58.66			0.00%		2.52%					0.00%		0.01%
46.48	3.96	12.00	-58.7			0.00%		2.52%					0.00%		0.01%
46.4	3.97	12.50	-58.72			0.00%		2.52%							0.01%
46.38	3.98	13.00	-58.73			0.00%		2.52%							0.01%
46.41	3.99	13.50	-58.74					2.52%							0.01%
46.48	4	14.00	-58.73					2.52%							0.01%
46.68	4.01	14.50	-58.72					2.52%							0.01%
46.72	4.02	15.00	-58.7					2.52%							0.01%
46.87	4.03	15.50	-58.68					2.52%							0.01%
47.05	4.04	16.00	-58.65					2.52%							0.01%
47.24	4.05	16.50	-58.62					2.52%							0.01%
47.46	4.05	17.00	-58.58					2.52%							0.01%
47.67	4.06	17.50	-58.55					2.52%							0.01%
47.91	4.07	18.00	-58.51					2.52%							0.01%
48.15	4.08	18.50	-58.47					2.52%							0.01%
48.39	4.09	19.00	-58.43					2.52%							0.01%
48.65	4.09	19.50	-58.38					2.52%							0.01%
48.9	4.1	20.00	-58.34					2.52%							0.01%
49.16	4.11	20.50	-58.3					2.52%							0.01%
Total (m)				3.30E-06	3.16E-06	1.11E-10	2.68E-05	6.00E-03	1.16E-04	5.33E-05	7.37E-03	8.59E-05	2.20E-04	1.53E-03	1.19E-04
Total (g)				1.84E-03	2.25E-03	2.18E-08	1.35E-02	1.44E+00	1.25E-02	2.12E-02	4.43E-01	1.37E-02	6.44E-02	3.66E-01	1.90E-02

T (C)	pH	log f(O2)	clincl14 (%)	chamosit (%)	fluorite (%)	gold (%)	acanthit (%)	chalcopy (%)	quartz (%	galena (%)	muscovit (%	graphite (%)	bornite (%)	chalcoci (%)	silver (%)
250	4.53	-36.49	98.70%	98.00%	3.67%	9.75%									
245	4.5	-36.95	1.30%	2.00%	1.82%	7.91%	12.82%	0.26%	4.36%						
240	4.46	-37.41			1.88%	19.37%	14.12%	16.66%	4.86%	9.34%	11.05%				
235	4.4	-37.87			3.60%	15.16%	10.59%	10.43%	4.48%	9.01%	44.60%				
230	4.35	-38.34			2.56%	12.21%	9.01%	10.65%	4.39%	9.66%	28.07%				
225	4.31	-38.81			1.74%	9.61%	7.67%	10.25%	4.28%	9.82%	14.11%				
220	4.27	-39.3			1.10%	7.39%	6.54%	9.42%	4.17%	9.57%	2.17%				
215	4.23	-39.79			1.00%	5.39%	5.57%	8.61%	4.01%	8.41%					
210	4.19	-40.28			1.01%	3.87%	4.75%	7.69%	3.83%	7.19%					
205	4.16	-40.79			1.03%	2.76%	4.07%	6.68%	3.67%	6.13%					
200	4.12	-41.31			1.05%	1.96%	3.49%	5.64%	3.51%	5.20%					
195	4.08	-41.83			1.09%	1.39%	3.01%	4.61%	3.36%	4.40%					
190	4.05	-42.37			1.15%	0.98%	2.60%	3.61%	3.21%	3.72%					
185	4.02	-42.91			1.22%	0.69%	2.25%	2.66%	3.07%	3.15%					
180	3.98	-43.47			1.32%	0.49%	1.95%	1.77%	2.94%	2.67%					
175	3.95	-44.04			1.43%	0.34%	1.69%	0.93%	2.82%	2.28%					
170	3.92	-44.63			1.57%	0.24%	1.47%	0.12%	2.70%	1.94%					
165	3.88	-45.22			1.71%	0.16%	1.28%		2.58%	1.62%					
160	3.85	-45.84			1.87%	0.11%	1.11%		2.48%	1.33%					
155	3.82	-46.46			2.02%	0.08%	0.97%		2.37%	1.09%					
150	3.79	-47.1			2.16%	0.05%	0.84%		2.27%	0.88%					
145	3.76	-47.69			2.30%	0.03%	0.72%		2.18%	0.71%		25.12%			
140	3.73	-48.29			2.42%	0.02%	0.62%		2.09%	0.56%		22.00%			
135	3.7	-48.9			2.53%	0.01%	0.54%		2.00%	0.44%		15.71%			
130	3.68	-49.53			2.62%	0.01%	0.46%		1.91%	0.34%		11.17%			
125	3.65	-50.18			2.70%	0.01%	0.40%		1.83%	0.25%		7.91%			
120	3.62	-50.84			2.75%	0.00%	0.34%		1.75%	0.19%		5.57%			
115	3.6	-51.53			2.79%	0.00%	0.29%		1.66%	0.11%		3.92%	5.75%		
110	3.57	-52.23			2.82%	0.00%	0.21%		1.58%			2.77%	37.09%		
105	3.55	-52.96			2.84%	0.00%	0.17%		1.50%			1.92%	27.36%		
100	3.53	-53.7			2.84%	0.00%	0.14%		1.43%			1.32%	18.65%		
95	3.5	-54.47			2.83%	0.00%	0.12%		1.35%			0.91%	11.15%		
90	3.48	-55.26			2.80%	0.00%	0.08%		1.27%			0.61%		35.54%	
85	3.46	-56.07			2.76%	0.00%	0.04%		1.19%			0.41%		34.30%	
80	3.45	-56.91			2.72%	0.00%	0.03%		1.11%			0.28%		17.96%	
75	3.43	-57.77			2.66%	0.00%	0.02%		1.04%			0.19%		7.12%	
70	3.41	-58.66			2.59%	0.00%	0.02%		0.96%			0.12%		0.26%	
65	3.4	-59.58			2.52%	0.00%	0.01%		0.88%			0.07%		0.68%	10.01%
60	3.39	-60.42			2.44%	0.00%			0.81%					2.37%	53.36%
55	3.38	-61.2			2.35%	0.00%			0.74%					1.19%	26.20%
50	3.37	-61.94			2.26%	0.00%			0.67%					0.59%	7.66%
45	3.36	-62.69			2.17%	0.00%	0.00%		0.60%						1.58%
40	3.35	-63.46			2.07%	0.00%	0.00%		0.53%						0.43%
35	3.34	-64.27			1.97%	0.00%	0.00%		0.47%						0.40%
30	3.34	-65.12			1.86%	0.00%			0.41%						0.25%
25	3.34	-66.01			1.76%	0.00%			0.36%						0.08%
20	3.33	-66.95			1.65%	0.00%			0.31%						0.02%
Total (m)			7.92E-06	7.36E-06	7.97E-04	1.21E-09	7.42E-05	4.44E-06	6.02E-03	1.16E-04	1.14E-05	2.71E-05	1.19E-07	1.24E-07	1.84E-07
Total (g)			4.40E-03	4.40E-03	6.22E-02	2.38E-07	1.84E-02	8.16E-04	3.62E-01	2.78E-02	4.55E-03	3.25E-04	6.98E-05	1.97E-05	1.99E-05

T (°C)	P (bars)	pH	log f(O2)	clincl14 (%)	chamosit (%)	fluorite (%)	gold (%)	magnetit (%)	quartz (%	hematite (%	muscovit (	acanthit (%)
250	76.1	4.53	-36.49	30.76%	23.25%	4.40%	9.83%					
245	44.32	4.51	-36.38	69.24%	76.75%	23.64%	57.42%	54.20%	3.44%			
240	36.02	4.47	-36.55			1.56%	19.08%	45.80%	6.76%			
235	31.4	4.42	-36.71			6.36%	6.20%		6.04%	67.11%	39.32%	
230	27.95	4.37	-36.98			4.37%	2.95%		5.83%	32.89%	25.50%	
225	25.08	4.33	-37.3			3.73%	1.57%		5.54%		19.05%	
220	22.57	4.28	-37.66			3.05%	0.94%		5.28%		12.20%	
215	20.34	4.25	-38.06			2.19%	0.63%		5.05%		3.93%	4.51%
210	18.32	4.21	-38.49			1.61%	0.44%		4.79%			8.80%
205	16.48	4.17	-38.94			1.55%	0.29%		4.51%			8.36%
200	14.8	4.13	-39.41			1.53%	0.19%		4.25%			7.89%
195	13.27	4.09	-39.91			1.54%	0.13%		4.00%			7.39%
190	11.87	4.05	-40.42			1.57%	0.09%		3.77%			6.88%
185	10.6	4.01	-40.95			1.63%	0.07%		3.56%			6.38%
180	9.43	3.97	-41.5			1.70%	0.05%		3.35%			5.89%
175	8.37	3.93	-42.06			1.79%	0.04%		3.16%			5.42%
170	7.4	3.9	-42.64			1.89%	0.03%		2.99%			4.97%
165	6.53	3.86	-43.25			2.00%	0.02%		2.82%			4.54%
160	5.74	3.82	-43.86			2.11%	0.01%		2.66%			4.12%
155	5.02	3.78	-44.5			2.23%	0.01%		2.51%			3.73%
150	4.38	3.75	-45.16			2.34%	0.01%		2.37%			3.36%
145	3.8	3.71	-45.83			2.44%	0.01%		2.24%			3.01%
140	3.29	3.67	-46.53			2.54%	0.00%		2.11%			2.67%
135	2.83	3.64	-47.24			2.63%	0.00%		1.99%			2.36%
130	2.43	3.6	-47.97			2.70%	0.00%		1.88%			2.07%
125	2.07	3.57	-48.73			2.76%	0.00%		1.77%			1.81%
120	1.76	3.54	-49.51			2.80%	0.00%		1.66%			1.56%
115	1.48	3.5	-50.31			2.83%	0.00%		1.56%			1.34%
110	1.25	3.47	-51.13			2.85%	0.00%		1.46%			1.15%
105	1.04	3.44	-51.98			2.85%	0.00%		1.36%			0.97%
100	0.86	3.41	-52.85			2.84%	0.00%		1.27%			0.82%
Total (m)				2.58E-05	3.14E-05	6.81E-04	1.21E-09	7.41E-05	5.36E-03	6.65E-06	1.82E-05	7.21E-05
Total (g)				1.43E-02	2.24E-02	5.32E-02	2.38E-07	1.71E-02	3.22E-01	1.06E-03	7.24E-03	1.79E-02

T (°C)	pH	TotMix	log f(O2)	clinci14 (%)	chamosit (%)	fluorite (%)	gold (%)	barite (%)	hematite (%)	pyrite (%)	quartz (%	anhydrit (%	acanthit (%	silver (%)	muscovit (%	chalcoci (%)	gibbsite (%)
260	4.53		-36.49	100.00%	100.00%	19.29%	7.18%										
240	4.15	0.05	-34.24				44.06%	47.23%	33.23%	59.90%	6.22%						
230.8	4.02	0.10	-34.69				10.28%	31.95%	13.23%	13.63%	6.53%	0.55%					
222.3	3.93	0.15	-35.31				5.08%	3.99%	9.32%	8.90%	5.86%	6.33%					
214.3	3.85	0.20	-35.91				2.75%	2.98%	8.75%	7.57%	5.25%	6.18%					
206.9	3.79	0.25	-36.5				1.62%	2.28%	7.84%	6.36%	4.71%	6.00%					
200	3.74	0.30	-37.08				1.03%	1.78%	6.42%	3.05%	4.24%	5.82%	13.35%				
193.6	3.71	0.35	-37.65				0.70%	1.41%	4.92%	0.57%	3.83%	5.63%	21.82%				
187.6	3.7	0.40	-38.21				0.50%	1.13%	3.62%	0.02%	3.48%	5.44%	18.68%				
181.9	3.69	0.45	-38.75				0.37%	0.92%	2.62%		3.17%	5.23%	14.10%				
176.6	3.69	0.50	-39.27				0.28%	0.76%	1.83%		2.91%	5.03%	10.32%				
137.2	3.82	1.00	-43.15				1.07%	3.54%	3.59%		20.11%	38.12%	21.73%				
112.8	3.96	1.50	-45.67			35.54%	0.66%	1.07%	0.28%		11.67%	15.67%		14.22%			
96.23	4.08	2.00	-47.55			36.10%	0.64%	0.44%	0.84%		7.64%			43.63%			
84.3	4.18	2.50	-49.07			9.07%	0.64%	0.20%	0.38%		5.22%			18.51%			
75.39	4.28	3.00	-50.32				0.64%	0.11%	0.20%		3.60%			8.95%			
68.67	4.36	3.50	-51.34				0.64%	0.07%	0.12%		2.46%			4.84%			
63.26	4.44	4.00	-52.2				0.64%	0.05%	0.09%		1.62%			2.87%			
59.07	4.5	4.50	-52.93				0.64%	0.03%	0.07%		0.97%			1.83%			
55.75	4.56	5.00	-53.55				0.64%	0.02%	0.06%		0.46%			1.22%			
53.11	4.62	5.50	-54.07				0.64%	0.02%	0.05%		0.05%			0.86%			
51	4.67	6.00	-54.53				0.64%	0.01%	0.05%					0.62%			
49.33	4.71	6.50	-54.92				0.64%	0.01%	0.04%					0.46%			
48	4.76	7.00	-55.26				0.64%	0.00%	0.04%					0.35%			
46.96	4.8	7.50	-55.56				0.64%	0.00%	0.04%					0.28%			
46.15	4.83	8.00	-55.82				0.64%	0.00%	0.04%					0.22%			
45.54	4.86	8.50	-56.05				0.64%		0.04%					0.18%			
45.08	4.89	9.00	-56.24				0.64%		0.04%					0.13%	4.20%		
44.76	4.92	9.50	-56.4				0.64%		0.04%					0.11%	7.71%		
44.53	4.95	10.00	-56.55				0.64%		0.04%					0.09%	7.70%		
44.41	4.97	10.50	-56.68				0.64%		0.04%					0.08%	7.65%		
44.36	4.99	11.00	-56.79				0.64%		0.04%					0.07%	7.56%		
44.37	5.02	11.50	-56.9				0.64%		0.04%					0.06%	7.44%		
44.44	5.04	12.00	-56.99				0.64%		0.03%					0.05%	7.30%		
44.56	5.06	12.50	-57.08				0.64%		0.03%					0.04%	7.12%		
44.69	5.08	13.00	-57.15				0.64%		0.23%					0.04%	6.89%	13.10%	
44.87	5.09	13.50	-57.22				0.64%		0.30%					0.03%	6.66%	18.35%	
45.07	5.11	14.00	-57.29				0.64%		0.25%					0.03%	6.44%	14.54%	
45.29	5.13	14.50	-57.35				0.64%		0.20%					0.03%	6.21%	11.51%	
45.53	5.14	15.00	-57.4				0.64%		0.17%					0.02%	5.96%	9.13%	
45.79	5.16	15.50	-57.45				0.64%		0.14%					0.02%	5.71%	7.25%	
46.06	5.17	16.00	-57.5				0.64%		0.12%					0.02%	5.44%	5.77%	
46.33	5.19	16.50	-57.55				0.64%		0.10%					0.02%		4.59%	13.60%
46.61	5.2	17.00	-57.59				0.64%		0.09%					0.02%		3.65%	14.23%
46.9	5.22	17.50	-57.63				0.64%		0.08%					0.02%		2.95%	13.20%
47.19	5.23	18.00	-57.66				0.64%		0.07%					0.01%		2.39%	12.19%
47.49	5.24	18.50	-57.7				0.64%		0.06%					0.01%		1.94%	11.19%
47.79	5.26	19.00	-57.73				0.64%		0.06%					0.01%		1.58%	10.23%
48.08	5.27	19.50	-57.76				0.64%		0.05%					0.01%		1.30%	9.31%
48.38	5.28	20.00	-57.79				0.64%		0.05%					0.01%		1.07%	8.44%
48.68	5.29	20.50	-57.82				0.64%		0.05%					0.01%		0.88%	7.62%
Total (m)				7.81E-06	7.21E-06	1.52E-04	1.64E-09	1.74E-03	9.54E-04	2.19E-04	4.44E-03	1.68E-02	5.70E-05	3.53E-05	1.25E-04	3.51E-06	1.67E-04
Total (g)				4.34E-03	5.15E-03	1.19E-02	3.23E-07	4.07E-01	1.52E-01	2.63E-02	2.67E-01	2.29E+00	1.41E-02	3.81E-03	4.99E-02	5.68E-04	1.30E-02

T (°C)	pH	TotMix	log f(O2)	clincl14 (%)	chamosit (%	fluorite (	gold (%)	acanthit (%	hematite (%)	magnetit (%)	pyrite (%)	quartz (%	barite (%)	chalcopy (%	bornite (%)	galena (%)	sphaleri (%)
260	4.53		-36.49	100.00%	100.00%	100.00%	9.75%										
240	4.41	0.05	-36.27				44.42%	4.11%	7.90%	100.00%	6.61%	6.30%					
230.8	4.24	0.10	-36.35				25.86%		31.21%		4.70%	6.61%					
222.2	4.09	0.15	-36.55				10.15%	1.03%	24.27%		3.21%	5.93%					
214.3	3.99	0.20	-36.96				4.32%	9.11%	15.57%		1.88%	5.31%					
206.8	3.92	0.25	-37.45				2.16%	11.25%	10.51%		1.29%	4.76%					
199.9	3.87	0.30	-37.98				1.20%	11.29%	6.74%		0.96%	4.28%					
193.6	3.83	0.35	-38.51				0.72%	10.58%	3.40%		0.75%	3.87%					
187.4	3.81	0.40	-39.05				0.46%	9.51%	0.40%		0.59%	3.51%					
181.8	3.8	0.45	-39.58				0.29%	7.89%			0.59%	3.20%					
176.6	3.78	0.50	-40.1				0.19%	6.45%			0.62%	2.93%					
137	3.71	1.00	-44.74				0.45%	24.37%			7.11%	20.21%	18.30%	100.00%			
112.6	3.67	1.50	-48.13				0.03%	3.25%			1.17%	11.67%	19.66%		55.76%	13.10%	
96.11	3.66	2.00	-50.59				0.01%	0.61%				7.60%	17.16%		13.07%	15.81%	
84.19	3.66	2.50	-52.52				0.00%	0.25%				5.16%	13.58%		6.99%	15.83%	
75.3	3.68	3.00	-54.06				0.00%	0.12%				3.53%	9.91%		4.45%	15.84%	
68.48	3.69	3.50	-55.35				0.00%	0.07%				2.38%	6.87%		3.31%	15.84%	
63.17	3.72	4.00	-56.47					0.05%			0.96%	1.53%	4.66%		2.62%	13.95%	
59	3.76	4.50	-57.29					0.01%			6.70%	0.87%	3.07%		0.87%	2.62%	
55.68	3.78	5.00	-57.96				0.00%	0.01%			2.79%	0.36%	2.21%		0.67%	1.55%	2.34%
53.06	3.8	5.50	-58.49				0.00%	0.01%					1.59%		0.54%	0.85%	3.99%
50.96	3.82	6.00	-58.92				0.00%	0.00%					1.11%		0.50%	0.67%	4.04%
49.28	3.84	6.50	-59.27				0.00%	0.00%					0.77%		0.47%	0.54%	4.07%
47.96	3.86	7.00	-59.55				0.00%	0.00%					0.52%		0.44%	0.44%	4.10%
46.92	3.87	7.50	-59.78				0.00%	0.00%					0.33%		0.43%	0.36%	4.12%
46.12	3.89	8.00	-59.95				0.00%	0.00%					0.19%		0.42%	0.30%	4.14%
45.6	3.9	8.50	-60.09					0.00%					0.07%		0.41%	0.26%	4.15%
45.06	3.92	9.00	-60.2					0.00%							0.40%	0.22%	4.16%
44.73	3.93	9.50	-60.27					0.00%							0.40%	0.20%	4.16%
44.61	3.94	10.00	-60.33					0.00%							0.39%	0.17%	4.17%
44.39	3.96	10.50	-60.36					0.00%			0.38%				0.39%	0.15%	3.97%
44.34	3.97	11.00	-60.38					0.00%			1.41%				0.38%	0.12%	3.44%
44.36	3.99	11.50	-60.39					0.00%			1.58%				0.38%	0.11%	3.36%
44.42	4	12.00	-60.39					0.00%			1.76%				0.38%	0.10%	3.27%
44.53	4.01	12.50	-60.37								1.93%				0.38%	0.09%	3.18%
44.68	4.03	13.00	-60.35								2.11%				0.38%	0.08%	3.09%
44.86	4.04	13.50	-60.32								2.28%				0.38%	0.08%	3.00%
45.06	4.06	14.00	-60.29								2.45%				0.37%	0.07%	2.91%
45.28	4.07	14.50	-60.25								2.62%				0.37%	0.07%	2.82%
45.52	4.08	15.00	-60.21								2.78%				0.37%	0.06%	2.74%
45.78	4.1	15.50	-60.16								2.95%				0.37%	0.06%	2.65%
46.05	4.11	16.00	-60.11								3.11%				0.37%	0.06%	2.57%
46.32	4.12	16.50	-60.06								3.27%				0.37%	0.05%	2.48%
46.6	4.14	17.00	-60.01								3.42%				0.37%	0.05%	2.40%
46.89	4.15	17.50	-59.96								3.58%				0.37%	0.05%	2.32%
47.19	4.16	18.00	-59.91								3.72%				0.37%	0.05%	2.25%
47.48	4.17	18.50	-59.86								3.87%				0.37%	0.04%	2.17%
47.78	4.19	19.00	-59.8								4.01%				0.37%	0.04%	2.10%
48.08	4.2	19.50	-59.75								4.15%				0.37%	0.04%	2.02%
48.38	4.21	20.00	-59.69								4.28%				0.37%	0.04%	1.95%
48.68	4.22	20.50	-59.64								4.41%				0.37%	0.04%	1.89%
Total (m)				7.81E-06	7.21E-06	2.93E-06	1.21E-09	7.47E-05	3.63E-04	2.69E-05	1.08E-03	4.40E-03	1.63E-03	1.58E-06	1.30E-06	9.66E-04	3.69E-03
Total (g)				4.34E-03	6.16E-03	2.29E-03	2.38E-07	1.86E-05	5.66E-02	6.23E-03	1.30E-01	2.64E-01	3.67E-01	2.91E-04	6.52E-04	2.29E-01	3.50E-01

C)	pH	log f(O2)	clincl14 (%)	chamosit (%)	gold (%)	silver (%)	quartz (%)	bornite (%)	acanthit (%)	muscovit (%)	hematite (%)	fluorite (%)
300	4.61	-32.99	100.00%	100.00%	3.25%							
295	4.51	-33.28			3.70%	21.81%	3.65%					
290	4.41	-33.51			2.50%	21.80%	3.90%	4.82%				
285	4.32	-33.7			7.70%	15.92%	3.89%	38.37%				
280	4.24	-33.82			7.96%	10.44%	3.86%	56.81%				
275	4.18	-33.92			15.14%	5.05%	3.80%		29.57%			
270	4.13	-34			11.80%	2.77%	3.73%		28.32%			
265	4.09	-34.05			5.78%	1.60%	3.64%		19.09%			
260	4.06	-34.08			2.82%	0.91%	3.53%		11.70%	2.75%		
255	4.03	-34.13			1.61%	0.53%	3.32%		6.45%	25.83%		
250	4	-34.2			1.36%	0.46%	3.22%		3.54%	23.62%		
245	3.97	-34.28			1.47%	0.72%	3.13%		1.34%	19.17%		
240	3.94	-34.38			1.73%	1.14%	3.04%			13.07%		
235	3.91	-34.49			1.82%	0.75%	2.94%			9.26%		
230	3.89	-34.59			1.87%	0.25%	2.83%			5.67%		
225	3.87	-34.71			1.95%	0.07%	2.74%			0.64%		
220	3.83	-34.91			2.22%	1.39%	2.63%				8.73%	
215	3.79	-35.19			2.36%	2.54%	2.52%				16.12%	
210	3.74	-35.48			2.26%	2.35%	2.41%				14.91%	
205	3.7	-35.76			2.13%	2.12%	2.31%				13.50%	
200	3.66	-36.04			1.98%	1.87%	2.21%				11.93%	
195	3.63	-36.33			1.83%	1.61%	2.11%				10.22%	
190	3.6	-36.6			1.68%	1.33%	2.02%				8.44%	
185	3.57	-36.88			1.53%	1.04%	1.93%				6.64%	
180	3.54	-37.15			1.38%	0.76%	1.85%				4.86%	
175	3.52	-37.42			1.25%	0.49%	1.77%				3.14%	
170	3.5	-37.69			1.13%	0.24%	1.70%				1.51%	
165	3.48	-37.96			1.01%	0.00%	1.62%					
160	3.46	-38.25			0.91%	0.00%	1.56%					
155	3.44	-38.54			0.82%	0.00%	1.49%					
150	3.43	-38.84			0.73%	0.00%	1.43%					
145	3.41	-39.16			0.65%	0.00%	1.37%					
140	3.39	-39.49			0.58%	0.00%	1.31%					
135	3.37	-39.83			0.51%	0.00%	1.26%					
130	3.34	-40.22			0.44%	0.00%	1.20%					3.90%
125	3.32	-40.62			0.38%	0.00%	1.15%					5.00%
120	3.29	-41.04			0.33%	0.00%	1.10%					5.03%
115	3.27	-41.47			0.28%	0.00%	1.05%					5.05%
110	3.24	-41.91			0.23%	0.00%	1.00%					5.05%
105	3.22	-42.38			0.19%	0.00%	0.95%					5.03%
100	3.2	-42.85			0.16%	0.00%	0.90%					5.00%
95	3.18	-43.35			0.13%	0.00%	0.85%					4.96%
90	3.15	-43.86			0.10%	0.00%	0.80%					4.90%
85	3.13	-44.4			0.08%	0.00%	0.75%					4.83%
80	3.12	-44.95			0.06%	0.00%	0.70%					4.74%
75	3.1	-45.52			0.05%	0.00%	0.65%					4.64%
70	3.08	-46.12			0.04%	0.00%	0.60%					4.53%
65	3.06	-46.74			0.03%	0.00%	0.56%					4.42%
60	3.05	-47.39			0.02%	0.00%	0.51%					4.29%
55	3.03	-48.07			0.01%	0.00%	0.46%					4.15%
50	3.02	-48.77			0.01%	0.00%	0.42%					4.00%
45	3	-49.51			0.01%	0.00%	0.38%					3.84%
40	2.99	-50.28			0.00%	0.00%	0.34%					3.68%
35	2.98	-51.08			0.00%	0.00%	0.30%					3.51%
30	2.97	-51.93			0.00%	0.00%	0.26%					3.34%
25	2.96	-52.81			0.00%	0.00%	0.23%					3.15%
20	2.95	-53.74			0.00%	0.00%	0.19%					2.97%
(m)			4.08E-06	3.47E-06	1.81E-10	1.02E-03	9.58E-03	6.28E-06	8.16E-05	1.41E-05	7.98E-05	7.21E-04
(g)			2.27E-03	2.48E-03	3.56E-08	1.10E-01	5.76E-01	3.15E-03	2.02E-02	5.63E-03	1.27E-02	5.63E-02

°C)	P (bars)	pH	TotMix	log f(O2)	clincl14 (%)	chamosit (%)	gold (%)	silver (%)	magnetit (%)	quartz (%	muscovit (%)	acanthit (%)
300	126.1	4.61		-32.99	17.99%	23.31%	3.46%					
295	88.88	4.63		-32.86	62.67%	61.30%	31.25%	6.58%	83.26%	5.16%		
290	75.99	4.61		-32.76	19.33%	15.39%	12.81%	4.08%	16.74%	6.38%		
285	68.07	4.58		-32.76			6.67%	7.62%		6.43%	6.28%	
280	61.89	4.52		-32.88			4.61%	5.21%		6.04%	43.19%	
275	56.62	4.45		-33.05			3.21%	5.48%		5.80%	27.45%	
270	51.93	4.39		-33.25			2.54%	5.71%		5.54%	17.65%	
265	47.68	4.31		-33.48			2.89%	4.89%		5.29%	5.42%	9.61%
260	43.77	4.24		-33.74			2.67%	4.62%		5.03%		13.20%
255	40.17	4.18		-34			2.41%	4.64%		4.75%		12.59%
250	36.83	4.11		-34.27			2.32%	4.60%		4.49%		11.96%
245	33.74	4.05		-34.54			2.27%	4.49%		4.24%		11.22%
240	30.86	3.99		-34.81			2.23%	4.32%		4.00%		10.33%
235	28.19	3.94		-35.08			2.18%	4.10%		3.77%		9.25%
230	25.71	3.89		-35.35			2.10%	3.87%		3.55%		7.94%
225	23.4	3.85		-35.62			2.00%	3.67%		3.35%		6.38%
220	21.26	3.8		-35.9			1.90%	3.58%		3.15%		4.56%
215	19.28	3.76		-36.18			1.80%	3.65%		2.97%		2.53%
210	17.45	3.72		-36.47			1.70%	3.90%		2.79%		0.44%
205	15.75	3.68		-36.78			1.59%	3.86%		2.63%		
200	14.18	3.64		-37.09			1.45%	3.51%		2.48%		
195	12.74	3.6		-37.4			1.30%	2.89%		2.34%		
190	11.41	3.57		-37.69			1.15%	2.05%		2.20%		
185	10.2	3.55		-37.97			1.02%	1.25%		2.08%		
180	9.08	3.52		-38.24			0.91%	0.71%		1.96%		
175	8.06	3.5		-38.52			0.82%	0.42%		1.85%		
170	7.14	3.48		-38.8			0.74%	0.26%		1.74%		
tal (m)					2.29E-05	1.51E-05	1.72E-10	1.05E-03	3.13E-05	7.83E-03	8.47E-06	8.93E-05
tal (g)					1.28E-02	1.08E-02	3.39E-08	1.13E-01	7.25E-03	4.70E-01	3.37E-03	2.21E-02

T (°C)	pH	TotMix	log f(O2)	clincl14(%)	chamosit (%	gold (%)	anhydrit (%	bornite (%	hematite (%)	quartz (%	acanthit (%)	barite (%)	silver (%)	anglesit (%)	kaolinit (%)	muscovit (%	chalcoci (%)	gibbsite (%)
300	4.61		-32.99	100.00%	100.00%	0.96%												
289.1	4.29	0.05	-30.41				3.21%	100.00%	9.69%	4.50%								
278.9	4.21	0.10	-30.85				3.92%		0.60%	5.11%	33.70%	18.85%						
269.3	4.12	0.15	-31.29				3.77%		2.18%	5.15%	14.09%	18.69%						
260.2	4.03	0.20	-31.74				3.95%		2.69%	5.00%	8.92%	13.75%						
251.6	3.95	0.25	-32.2				4.06%		2.93%	4.74%	7.74%	10.12%						
243.6	3.87	0.30	-32.67				4.10%		3.08%	4.43%	7.49%	7.51%						
236.9	3.79	0.35	-33.14			1.87%	4.10%		3.14%	4.10%	7.42%	5.66%						
228.7	3.73	0.40	-33.6			4.78%	4.07%		3.12%	3.77%	7.27%	4.33%						
221.9	3.67	0.45	-34.05			4.23%	4.02%		3.01%	3.45%	6.95%	3.36%						
216.6	3.63	0.50	-34.49			3.70%	3.96%		2.79%	3.16%	6.43%	2.65%						
167.7	3.47	1.00	-37.48			14.48%	35.77%		12.26%	20.69%		10.50%	30.90%					
137.8	3.48	1.50	-39.27			3.77%	25.08%		7.11%	11.22%		2.55%	17.87%					
117.3	3.53	2.00	-40.75			2.29%			5.17%	7.29%		0.94%	12.98%	13.92%				
102.4	3.59	2.50	-42.04			1.90%			3.69%	5.13%		0.25%	9.26%	27.84%				
91.26	3.67	3.00	-43.26			1.79%			3.52%	3.74%		0.23%	8.84%	19.67%				
82.63	3.77	3.50	-44.47			1.75%			2.95%	2.76%		0.18%	7.38%	13.14%				
76.61	3.87	4.00	-45.67			1.73%			2.14%	2.03%		0.13%	5.35%	8.61%				
70.06	3.98	4.50	-46.84			1.72%			1.33%	1.48%		0.09%	3.31%	5.69%				
66.64	4.09	5.00	-47.91			1.72%			0.73%	1.04%		0.06%	1.80%	3.83%				
61.86	4.19	5.50	-48.85			1.72%			0.38%	0.68%		0.05%	0.94%	2.61%				
58.82	4.27	6.00	-49.66			1.72%			0.21%	0.39%		0.03%	0.50%	1.79%				
56.33	4.35	6.50	-50.34			1.72%			0.12%	0.14%		0.02%	0.28%	1.22%				
54.29	4.42	7.00	-50.93			1.72%			0.08%			0.02%	0.17%	0.81%				
52.61	4.47	7.50	-51.43			1.72%			0.06%			0.01%	0.11%	0.50%				
51.24	4.53	8.00	-51.87			1.72%			0.04%			0.01%	0.07%	0.27%				
50.12	4.57	8.50	-52.24			1.72%			0.03%			0.01%	0.05%	0.08%				
49.21	4.61	9.00	-52.57			1.72%			0.03%			0.00%	0.04%					
48.48	4.65	9.50	-52.86			1.72%			0.02%			0.00%	0.03%					
47.91	4.69	10.00	-53.11			1.72%			0.02%			0.00%	0.02%					
47.47	4.72	10.50	-53.35			1.72%			0.02%			0.00%	0.02%					
47.13	4.75	11.00	-53.54			1.72%			0.02%				0.01%		5.18%			
46.89	4.78	11.50	-53.71			1.72%			0.02%				0.01%		13.74%			
46.73	4.81	12.00	-53.86			1.72%			0.02%				0.01%		13.71%			
46.64	4.83	12.50	-54			1.72%			0.01%				0.01%		13.66%			
46.6	4.85	13.00	-54.13			1.72%			0.01%				0.01%		13.59%			
46.61	4.88	13.50	-54.25			1.72%			0.01%				0.01%		13.49%			
46.66	4.9	14.00	-54.35			1.72%			0.01%				0.00%		13.38%			
46.75	4.92	14.50	-54.45			1.72%			0.01%				0.00%		13.24%			
46.87	4.94	15.00	-54.54			1.72%			0.01%				0.00%			18.95%		
47.02	4.96	15.50	-54.63			1.72%			0.01%				0.00%			19.73%		
47.18	4.97	16.00	-54.7			1.72%			0.01%				0.00%			19.45%		
47.37	4.99	16.50	-54.75			1.72%			1.91%				0.00%			16.05%	7.15%	
47.57	5	17.00	-54.76			1.72%			3.80%				0.00%			12.84%	14.24%	
47.78	5.01	17.50	-54.77			1.72%			3.64%				0.00%			12.98%	13.66%	
48.01	5.02	18.00	-54.78			1.72%			3.37%				0.00%				12.66%	16.74%
48.24	5.03	18.50	-54.79			1.72%			3.20%				0.00%				11.99%	16.78%
48.48	5.04	19.00	-54.8			1.72%			3.00%				0.00%				11.26%	16.76%
48.73	5.05	19.50	-54.81			1.72%			2.80%				0.00%				10.49%	16.70%
48.98	5.06	20.00	-54.83			1.72%			2.59%				0.00%				9.69%	16.59%
49.24	5.08	20.50	-54.84			1.72%			2.37%				0.00%				8.87%	16.44%
Total (m)				4.08E-06	3.47E-06	6.12E-10	2.75E-02	3.64E-05	2.74E-03	7.64E-03	2.99E-04	1.74E-03	2.18E-03	3.07E-02	1.36E-04	6.24E-05	1.82E-04	2.11E-04
Total (g)				2.27E-03	2.48E-03	1.21E-07	3.75E+00	1.83E-02	4.37E-01	4.53E-01	7.41E-02	4.07E-01	2.35E-01	9.30E+00	3.51E-02	2.48E-02	2.89E-02	1.65E-02

T (°C)	pH	TotMix	log f(O2)	clinc14 (%)	chamosit (%	gold (%)	bornite (%)	silver (%)	quartz (%)	acanthit (%)	hematite (%)	muscovit (%)	barite (%)	chalcocl (%)	galena (%)
300	4.61		-32.99	100.00%	100.00%	3.25%									
289.1	4.44	0.05	-33.01			0.36%	100.00%	18.11%	4.58%						
278.9	4.31	0.10	-31.62						5.20%	24.24%	11.64%				
269.2	4.2	0.15	-31.88						5.07%	11.89%	10.32%	27.58%			
260.1	4.11	0.20	-32.27						4.84%	7.96%	9.92%	40.87%			
251.6	4.03	0.25	-32.72			11.03%			4.67%	7.01%	11.49%	25.07%			
243.4	3.95	0.30	-33.19			13.07%			4.45%	6.80%	12.71%	6.48%			
235.8	3.87	0.35	-33.66			11.71%			4.15%	6.61%	12.73%				
228.6	3.81	0.40	-34.13			10.34%			3.81%	6.36%	11.88%				
221.8	3.76	0.45	-34.6			9.03%			3.49%	6.04%	10.54%				
215.4	3.71	0.50	-35.06			7.79%			3.20%	5.66%	8.77%				
167.6	3.41	1.00	-39.44			29.36%		54.51%	20.90%	4.15%			24.79%		
137.6	3.34	1.50	-42.82			3.47%		20.51%	11.29%				19.17%	30.01%	
117.1	3.34	2.00	-45.53			0.48%		6.87%	7.31%				14.50%	40.11%	
102.3	3.36	2.50	-48.64			0.10%			5.13%	12.51%			10.91%	28.28%	0.14%
91.15	3.38	3.00	-50.35			0.01%			3.72%	0.31%			8.24%	0.62%	2.72%
82.44	3.4	3.50	-51.76			0.00%			2.73%	0.16%			6.09%	0.33%	2.75%
75.63	3.43	4.00	-52.93			0.00%			1.99%	0.10%			4.46%	0.20%	2.76%
69.98	3.45	4.50	-53.9			0.00%			1.43%	0.06%			3.28%	0.12%	2.77%
65.47	3.47	5.00	-54.71			0.00%			0.99%	0.04%			2.43%	0.08%	2.77%
61.79	3.5	5.50	-55.39			0.00%			0.63%	0.03%			1.81%	0.06%	2.77%
58.77	3.52	6.00	-55.97			0.00%			0.33%	0.02%			1.35%	0.04%	2.77%
56.29	3.54	6.50	-56.44			0.00%			0.08%	0.01%			1.00%	0.03%	2.78%
54.26	3.56	7.00	-56.84			0.00%				0.01%			0.73%	0.02%	2.78%
52.58	3.58	7.50	-57.17			0.00%				0.01%			0.52%	0.02%	2.78%
51.21	3.6	8.00	-57.45			0.00%				0.01%			0.36%	0.01%	2.78%
50.09	3.62	8.50	-57.67			0.00%				0.00%			0.22%	0.01%	2.78%
49.19	3.64	9.00	-57.86			0.00%				0.00%			0.11%	0.01%	2.78%
48.46	3.66	9.50	-58.01			0.00%				0.00%			0.02%	0.01%	2.78%
47.89	3.67	10.00	-58.13			0.00%				0.00%				0.01%	2.78%
47.46	3.69	10.50	-58.22			0.00%				0.00%				0.01%	2.78%
47.12	3.71	11.00	-58.29			0.00%				0.00%				0.00%	2.78%
46.88	3.72	11.50	-58.34			0.00%				0.00%				0.00%	2.78%
46.72	3.73	12.00	-58.38			0.00%								0.00%	2.78%
46.62	3.75	12.50	-58.4			0.00%								0.00%	2.78%
46.69	3.76	13.00	-58.42			0.00%								0.00%	2.78%
46.6	3.77	13.50	-58.42			0.00%								0.00%	2.78%
46.66	3.79	14.00	-58.41											0.00%	2.78%
46.74	3.8	14.50	-58.4											0.00%	2.78%
46.86	3.81	15.00	-58.38											0.00%	2.78%
47.01	3.82	15.50	-58.35											0.00%	2.78%
47.18	3.83	16.00	-58.32												2.78%
47.36	3.84	16.50	-58.29												2.78%
47.56	3.85	17.00	-58.25												2.78%
47.78	3.86	17.50	-58.21												2.78%
48	3.87	18.00	-58.17												2.78%
48.24	3.88	18.50	-58.13												2.78%
48.48	3.89	19.00	-58.08												2.78%
48.73	3.9	19.50	-58.04												2.78%
48.98	3.91	20.00	-57.99												2.78%
49.24	3.92	20.50	-57.94												2.78%
Total (m)				4.08E-06	3.47E-06	1.81E-10	1.91E-05	1.99E-03	7.45E-03	3.92E-04	3.16E-04	1.44E-05	1.51E-03	3.35E-04	5.46E-03
Total (g)				2.27E-03	2.48E-03	3.66E-08	9.60E-03	2.14E-01	4.47E-01	9.73E-02	5.04E-02	5.72E-03	3.62E-01	5.33E-02	1.31E+00

T (°C)	P (bars)	pH	log f(O2)	fluorite (%)	gold (%)	magnetit (%)	muscovit (%)	acanthit (%)	quartz (%	silver (%)	hematite (%)	siderite (%)
250	250	4.57	-36.51	2.53%	4.50%	100.00%	16.90%					
245	250	4.49	-36.96	7.21%	56.79%		25.84%	32.84%	4.36%			
240	250	4.41	-37.42	5.81%	24.61%		20.17%	25.20%	4.58%			
235	250	4.35	-37.88	5.10%	9.14%		17.73%	16.91%	4.43%			
230	250	4.29	-38.23	3.28%	2.80%		7.83%	9.50%	4.43%	15.71%		
225	250	4.23	-38.42	2.41%	1.01%		3.05%	5.91%	4.33%	18.10%		
220	250	4.19	-38.56	2.67%	0.48%		4.92%	4.12%	4.11%	6.74%		
215	250	4.14	-38.68	2.43%	0.20%		3.57%	2.52%	3.96%	2.35%		
210	250	4.1	-38.87	1.46%	0.09%			1.32%	3.85%	6.29%	10.11%	
205	250	4.05	-39.17	0.66%	0.05%			0.65%	3.69%	13.09%	23.84%	
200	250	3.99	-39.47	0.67%	0.04%			0.44%	3.53%	10.94%	20.02%	
195	250	3.95	-39.78	0.72%	0.03%			0.29%	3.38%	8.90%	16.29%	
190	250	3.91	-40.09	0.80%	0.03%			0.18%	3.23%	6.99%	12.70%	
185	250	3.87	-40.41	0.90%	0.02%			0.10%	3.09%	5.25%	9.28%	
180	250	3.83	-40.72	1.02%	0.02%			0.02%	2.96%	3.71%	6.03%	
175	250	3.8	-41.03	1.13%	0.02%				2.83%	1.43%	1.72%	21.38%
170	250	3.76	-41.36	1.08%	0.02%				2.71%	0.29%		59.75%
165	250	3.73	-41.68	1.30%	0.02%				2.60%	0.13%		18.87%
160	250	3.7	-42.02	1.45%	0.02%				2.49%	0.05%		
155	250	3.67	-42.37	1.53%	0.01%				2.38%	0.02%		
150	250	3.64	-42.73	1.62%	0.01%				2.29%	0.01%		
145	250	3.61	-43.1	1.72%	0.01%				2.19%	0.00%		
140	250	3.58	-43.48	1.83%	0.01%				2.10%	0.00%		
135	250	3.56	-43.88	1.93%	0.01%				2.01%	0.00%		
130	250	3.53	-44.28	2.04%	0.01%				1.92%	0.00%		
125	250	3.5	-44.7	2.14%	0.01%				1.84%	0.00%		
120	250	3.48	-45.13	2.23%	0.01%				1.75%	0.00%		
115	250	3.45	-45.57	2.30%	0.01%				1.67%	0.00%		
110	250	3.43	-46.03	2.37%	0.00%				1.59%	0.00%		
105	250	3.4	-46.5	2.42%	0.00%				1.51%	0.00%		
100	250	3.38	-46.99	2.45%	0.00%				1.43%	0.00%		
95	250	3.36	-47.49	2.47%	0.00%				1.35%	0.00%		
90	250	3.34	-48.01	2.47%	0.00%				1.28%	0.00%		
85	250	3.32	-48.56	2.46%	0.00%				1.20%	0.00%		
80	250	3.3	-49.12	2.43%	0.00%				1.12%	0.00%		
75	250	3.28	-49.71	2.39%	0.00%				1.04%	0.00%		
70	250	3.26	-50.33	2.33%	0.00%				0.96%	0.00%		
65	250	3.25	-50.97	2.26%	0.00%				0.89%	0.00%		
60	250	3.23	-51.64	2.19%	0.00%				0.81%	0.00%		
55	250	3.22	-52.35	2.10%	0.00%				0.74%	0.00%		
50	250	3.2	-53.08	2.00%	0.00%				0.67%	0.00%		
45	250	3.19	-53.86	1.90%	0.00%				0.60%	0.00%		
40	250	3.18	-54.67	1.79%	0.00%				0.54%	0.00%		
35	250	3.16	-55.53	1.67%	0.00%				0.47%	0.00%		
30	250	3.15	-56.43	1.56%	0.00%				0.42%	0.00%		
25	250	3.14	-57.38	1.44%	0.00%				0.36%	0.00%		
20	250	3.13	-58.38	1.32%	0.00%				0.31%	0.00%		
Total (m)				1.18E-03	1.57E-09	3.77E-06	3.70E-05	1.75E-04	5.99E-03	2.31E-04	6.16E-05	1.66E-05
Total (g)				9.20E-02	3.09E-07	8.73E-04	1.48E-02	4.33E-02	3.60E-01	2.50E-02	9.84E-03	1.93E-03

T (°C)	P (bars)	pH	log f(O2)	fluorite (%)	gold (%)	magnetit (%)	muscovit (%)	quartz (%	acanthit (%	silver (%)
250	85.61	4.57	-36.51	2.83%	4.76%	3.75%	6.28%			
245	42.1	4.51	-36.71	35.48%	74.78%	87.34%	63.24%	2.63%		
240	33.55	4.44	-36.75	10.13%	12.65%	8.91%	15.78%	5.96%		
235	29.08	4.38	-36.89	6.56%	3.72%		9.18%	6.01%		
230	25.81	4.32	-37.14	4.64%	1.61%		5.52%	5.86%	0.03%	
225	23.1	4.26	-37.46	1.78%	1.10%			5.83%	13.28%	
220	20.75	4.21	-37.82	1.51%	0.51%			5.49%	12.57%	
215	18.66	4.15	-38.22	1.36%	0.27%			5.17%	11.67%	
210	16.77	4.09	-38.65	1.29%	0.15%			4.87%	10.62%	
205	15.06	4.04	-39.1	1.27%	0.10%			4.58%	9.46%	
200	13.5	3.99	-39.57	1.27%	0.07%			4.32%	8.26%	
195	12.07	3.94	-39.99	0.77%	0.04%			4.07%	4.63%	8.30%
190	10.78	3.88	-40.4	0.71%	0.03%			3.83%	3.80%	9.44%
185	9.6	3.83	-40.83	0.77%	0.03%			3.61%	3.51%	8.93%
180	8.52	3.77	-41.26	0.84%	0.03%			3.41%	3.23%	8.40%
175	7.54	3.72	-41.71	0.94%	0.02%			3.22%	2.96%	7.88%
170	6.66	3.68	-42.16	1.04%	0.02%			3.03%	2.69%	7.34%
165	5.86	3.63	-42.63	1.16%	0.02%			2.86%	2.43%	6.81%
160	5.13	3.58	-43.1	1.29%	0.02%			2.70%	2.17%	6.26%
155	4.48	3.54	-43.57	1.43%	0.01%			2.55%	1.91%	5.69%
150	3.9	3.5	-44.05	1.57%	0.01%			2.41%	1.66%	5.11%
145	3.38	3.46	-44.52	1.71%	0.01%			2.27%	1.41%	4.51%
140	2.91	3.42	-45.01	1.84%	0.01%			2.15%	1.16%	3.92%
135	2.5	3.38	-45.49	1.97%	0.01%			2.02%	0.93%	3.34%
130	2.14	3.34	-45.98	2.08%	0.01%			1.91%	0.71%	2.83%
125	1.82	3.3	-46.47	2.17%	0.00%			1.79%	0.50%	2.41%
120	1.54	3.27	-46.97	2.24%	0.00%			1.69%	0.30%	2.15%
115	1.29	3.23	-47.48	2.29%	0.00%			1.58%	0.09%	2.12%
110	1.08	3.19	-48	2.32%	0.00%			1.48%		2.02%
105	0.9	3.16	-48.53	2.36%	0.00%			1.39%		1.55%
100	0.74	3.13	-49.08	2.39%	0.00%			1.29%		0.99%
Total (m)				1.09E-03	1.57E-09	1.13E-04	1.03E-04	5.27E-03	1.73E-04	3.34E-04
Total (g)				8.51E-02	3.09E-07	2.61E-02	4.09E-02	3.17E-01	4.29E-02	3.61E-02

T (°C)	pH	TotMix	log f(O2)	fluorite (%)	gold (%)	magnetit (%)	muscovit (%	barite (%)	hematite (%)	pyrite (%)	quartz (%	acanthit (%	anhydrit (%)	silver (%)	chalcocl (%)	galena (%)	gibbsite (%)
260	4.57		-36.51	11.75%	3.53%	100.00%	69.50%										
240.4	4.07	0.05	-34.07		56.93%			3.10%	6.68%	79.38%	6.36%						
231.5	3.91	0.10	-34.55		7.28%			45.26%	2.29%	16.89%	6.16%						
223.3	3.79	0.15	-35.1		3.50%			14.78%	1.83%	3.73%	5.57%	11.45%	6.21%				
216.5	3.68	0.20	-35.58		2.37%			6.83%	1.65%		5.03%	15.70%	8.46%				
208.3	3.59	0.25	-36.07		1.06%			5.26%	1.52%		4.54%	12.62%	8.05%				
201.6	3.53	0.30	-36.56		0.76%			4.10%	1.37%		4.10%	10.55%	7.64%				
195.3	3.48	0.35	-37.04		0.63%			3.23%	1.20%		3.72%	8.91%	7.21%				
189.4	3.44	0.40	-37.51		0.55%			2.57%	1.03%		3.39%	7.52%	6.77%				
183.9	3.42	0.45	-37.97		0.47%			2.07%	0.88%		3.10%	6.32%	6.31%				
178.7	3.4	0.50	-38.41		0.40%			1.68%	0.74%		2.85%	5.28%	5.85%				
139.6	3.4	1.00	-42.09		1.83%			7.31%	3.10%		19.97%	21.65%	35.62%				
116.2	3.47	1.50	-44.39		0.66%			2.01%	1.39%		11.81%		7.89%	29.17%			
98.48	3.54	2.00	-46.07		0.55%			0.79%	1.45%		7.85%			30.42%			
86.38	3.65	2.50	-47.65	33.18%	0.53%			0.39%	0.92%		5.44%			19.40%			
77.29	3.77	3.00	-49.21	31.90%	0.53%			0.22%	0.54%		3.82%			11.37%			
70.3	3.91	3.50	-50.72	17.26%	0.53%			0.13%	0.26%		2.65%			5.47%			
64.83	4.04	4.00	-52.06	5.91%	0.53%			0.09%	0.11%		1.78%			2.27%			
60.6	4.16	4.50	-53.19		0.53%			0.06%	0.05%		1.11%			0.94%			
57.06	4.25	5.00	-54.13		0.53%			0.04%	0.02%		0.58%			0.42%			
54.28	4.34	5.50	-54.9		0.53%			0.03%	0.01%		0.15%			0.21%			
52.07	4.41	6.00	-55.54		0.53%			0.02%	0.03%					0.12%	0.01%		
50.29	4.47	6.50	-56.06		0.53%			0.02%	0.23%					0.07%	0.07%		
48.88	4.52	7.00	-56.52		0.53%			0.01%	0.14%					0.04%	0.04%		
47.76	4.57	7.50	-56.91		0.53%			0.01%	0.09%					0.03%	0.02%		
46.88	4.62	8.00	-57.26		0.53%			0.00%	0.06%					0.02%	0.01%		
46.2	4.66	8.50	-57.56		0.53%			0.00%	0.04%					0.02%	0.01%		
45.68	4.69	9.00	-57.83		0.53%			0.00%	0.03%					0.01%	0.01%		
45.3	4.73	9.50	-58.06		0.53%				0.02%					0.01%	0.00%		
45.04	4.76	10.00	-58.27		0.53%				0.01%					0.01%	0.00%		
44.87	4.79	10.50	-58.41		0.53%				0.90%					0.00%	0.00%	1.23%	
44.78	4.8	11.00	-58.43		0.53%				2.89%					0.00%	0.00%	3.99%	
44.76	4.81	11.50	-58.44		0.53%				3.03%					0.00%	0.00%	4.20%	
44.79	4.82	12.00	-58.43		0.53%				3.16%					0.00%	0.00%	4.38%	
44.87	4.82	12.50	-58.42		0.53%				3.28%					0.00%	0.00%	4.53%	
44.99	4.83	13.00	-58.4		0.53%				3.38%					0.00%	0.00%	4.67%	
45.15	4.83	13.50	-58.37		0.53%				3.46%					0.00%	0.00%	4.79%	
45.33	4.84	14.00	-58.34		0.53%				3.54%					0.00%	0.00%	4.89%	
45.53	4.84	14.50	-58.3		0.53%				3.60%						0.00%	4.98%	
45.76	4.85	15.00	-58.26		0.53%				3.66%						0.00%	5.06%	
46	4.85	15.50	-58.21		0.53%				3.71%						0.00%	5.13%	
46.26	4.86	16.00	-58.16		0.53%				3.75%						0.00%	5.19%	
46.51	4.86	16.50	-58.12		0.53%				3.79%						0.00%	5.24%	
46.78	4.86	17.00	-58.06		0.53%				3.82%						0.00%	5.28%	
47.06	4.86	17.50	-58.01		0.53%		6.49%		3.82%						0.00%	5.29%	
47.34	4.87	18.00	-57.96		0.53%		24.01%		3.79%						0.00%	5.25%	
47.63	4.87	18.50	-57.91		0.53%				3.73%						0.00%	5.16%	18.43%
47.92	4.87	19.00	-57.85		0.53%				3.73%						0.00%	5.15%	20.77%
48.21	4.87	19.50	-57.8		0.53%				3.74%						0.00%	5.18%	20.52%
48.5	4.87	20.00	-57.74		0.53%				3.75%						0.00%	5.19%	20.26%
48.79	4.87	20.50	-57.69		0.53%				3.77%						0.00%	5.21%	20.01%
Total (m)				2.53E-04	2.00E-09	3.77E-06	9.01E-06	1.71E-03	7.26E-03	1.89E-04	4.40E-03	2.62E-04	1.24E-02	6.89E-04	1.09E-05	1.31E-03	8.31E-05
Total (g)				1.98E-02	3.94E-07	8.73E-04	3.69E-03	3.98E-01	1.16E+00	2.27E-02	2.64E-01	6.50E-02	1.69E+00	7.43E-02	1.73E-03	3.14E-01	6.48E-03

T (°C)	pH	TotMix	log f(O2)	fluorite (%)	gold (%)	magnetit (%	muscovit (%	acanthit (%)	hematite (%)	pyrite (%)	quartz (%)	barite (%)	bornite (%)	galena (%)	chalcoci (%	sphaleri (%)
260	4.57		-36.51	71.35%	4.50%	10.65%	100.00%									
240.4	4.34	0.05	-36.24	28.65%	65.10%	89.35%		23.01%	15.27%	1.51%	6.44%					
231.6	4.13	0.10	-36.22		17.73%			12.06%	24.87%	4.58%	6.24%					
223.2	3.96	0.15	-36.39		5.96%			9.29%	18.54%	1.62%	5.64%					
216.6	3.84	0.20	-36.76		2.67%			7.63%	13.01%		5.09%					
208.2	3.75	0.25	-37.2		1.28%			6.13%	9.84%		4.59%					
201.6	3.68	0.30	-37.67		0.72%			5.09%	7.39%		4.15%					
196.2	3.63	0.35	-38.15		0.48%			4.31%	5.28%		3.76%					
189.3	3.59	0.40	-38.63		0.35%			3.70%	3.44%		3.42%					
183.7	3.57	0.45	-39.11		0.27%			3.20%	1.85%		3.13%					
178.6	3.55	0.50	-39.58		0.21%			2.80%	0.51%		2.88%					
139.6	3.48	1.00	-44.06		0.65%			19.41%		10.60%	20.09%	0.04%				
116	3.48	1.50	-47.44		0.06%			2.52%		38.78%	11.82%	19.48%	52.88%			
98.36	3.51	2.00	-50.02		0.01%			0.56%		42.91%	7.82%	18.27%	37.76%			
86.26	3.52	2.50	-51.91		0.00%			0.12%			5.39%	16.23%	6.14%	3.27%		
77.19	3.53	3.00	-53.4		0.00%			0.06%			3.74%	12.78%	3.23%	3.28%		
70.21	3.56	3.50	-54.6		0.00%			0.03%			2.57%	9.54%		3.29%	20.99%	
64.74	3.58	4.00	-55.57		0.00%			0.02%			1.69%	6.91%		3.29%	13.22%	
60.42	3.6	4.50	-56.36		0.00%			0.01%			1.02%	4.95%		3.30%	8.83%	
56.98	3.62	5.00	-57		0.00%			0.01%			0.49%	3.55%		3.30%	6.28%	
54.22	3.65	5.50	-57.53		0.00%			0.01%			0.05%	2.56%		3.30%	4.71%	
52.01	3.67	6.00	-57.96		0.00%			0.00%				1.85%		3.30%	3.68%	
50.24	3.69	6.50	-58.31		0.00%			0.00%				1.34%		3.30%	2.99%	
48.83	3.71	7.00	-58.59		0.00%			0.00%				0.96%		3.30%	2.52%	
47.71	3.73	7.50	-58.82		0.00%			0.00%				0.67%		3.30%	2.17%	
46.84	3.75	8.00	-59		0.00%			0.00%				0.45%		3.30%	1.92%	
46.16	3.76	8.50	-59.15		0.00%			0.00%				0.27%		3.30%	1.74%	
45.65	3.78	9.00	-59.26		0.00%			0.00%				0.13%		3.30%	1.61%	
45.27	3.8	9.50	-59.35		0.00%			0.00%				0.02%		3.30%	1.51%	
45.01	3.81	10.00	-59.41		0.00%			0.00%						3.30%	1.43%	
44.84	3.83	10.50	-59.46		0.00%			0.00%						3.30%	1.38%	
44.76	3.84	11.00	-59.49		0.00%			0.00%						3.30%	1.35%	
44.74	3.85	11.50	-59.51		0.00%			0.00%						3.30%	1.33%	
44.77	3.87	12.00	-59.52		0.00%			0.00%						3.30%	1.32%	
44.86	3.88	12.50	-59.52					0.00%						3.30%	1.33%	
44.98	3.89	13.00	-59.51					0.00%						3.30%	1.34%	
45.13	3.9	13.50	-59.5					0.00%						3.30%	1.37%	
45.32	3.92	14.00	-59.49					0.00%						3.30%	1.41%	
45.52	3.93	14.50	-59.48					0.00%						3.30%	1.46%	
45.75	3.94	15.00	-59.47					0.00%						3.30%	1.53%	
45.99	3.95	15.50	-59.46					0.00%						3.30%	1.63%	
46.24	3.96	16.00	-59.45					0.00%						3.30%	1.75%	
46.5	3.97	16.50	-59.46					0.00%						3.30%	1.92%	
46.77	3.98	17.00	-59.49					0.00%						3.30%	2.18%	
47.05	3.99	17.50	-59.47					0.00%						1.07%	1.24%	10.11%
47.33	3.99	18.00	-59.41												0.65%	14.98%
47.62	4	18.50	-59.36												0.64%	14.98%
47.91	4.01	19.00	-59.3												0.64%	14.98%
48.2	4.02	19.50	-59.24												0.64%	14.98%
48.49	4.03	20.00	-59.18												0.63%	14.98%
48.78	4.03	20.50	-59.12												0.63%	14.98%
Total (m)				4.17E-05	1.57E-09	3.64E-05	6.26E-06	6.07E-04	5.97E-04	1.90E-04	4.36E-03	1.44E-03	3.93E-06	4.59E-03	1.61E-06	1.01E-03
Total (g)				3.26E-03	3.09E-07	8.19E-03	2.49E-03	1.60E-01	9.64E-02	2.28E-02	2.62E-01	3.36E-01	1.97E-03	1.10E+00	2.66E-04	9.86E-02

T (°C)	pH	log f(O2)	gold (%)	quartz (%	silver (%)	acanthit (%	hematite (%)	fluorite (%)
300	4.63	-32.98	5.07%	0.00%				
295	4.45	-33.17	13.05%	3.86%	19.16%			
290	4.31	-33.2		3.88%	14.18%			
285	4.21	-33.16	30.91%	3.86%	6.07%	44.17%		
280	4.13	-33	9.14%	3.83%	2.80%	32.90%		
275	4.08	-32.77		3.77%	1.36%	16.98%		
270	4.03	-32.55		3.70%	1.29%	5.94%		
265	3.99	-32.35		3.62%	2.12%			
260	3.95	-32.14		3.52%	0.65%			
255	3.92	-31.94		3.42%	0.08%			
250	3.87	-31.84		3.30%	1.09%		2.11%	
245	3.79	-31.91		3.19%	3.13%		6.17%	
240	3.71	-32.01		3.07%	3.28%		6.47%	
235	3.63	-32.13		2.96%	3.40%		6.71%	
230	3.56	-32.27		2.84%	3.48%		6.88%	
225	3.49	-32.44		2.72%	3.52%		6.95%	
220	3.42	-32.62		2.61%	3.50%		6.92%	
215	3.36	-32.82		2.50%	3.43%		6.79%	
210	3.31	-33.03		2.39%	3.32%		6.55%	
205	3.26	-33.26		2.29%	3.15%		6.23%	
200	3.21	-33.49		2.19%	2.95%		5.84%	
195	3.17	-33.73		2.10%	2.73%		5.39%	
190	3.13	-33.98		2.00%	2.48%		4.90%	
185	3.09	-34.24		1.92%	2.23%		4.40%	
180	3.06	-34.5		1.84%	1.97%		3.88%	
175	3.03	-34.76		1.76%	1.71%		3.37%	
170	3	-35.03		1.68%	1.46%		2.87%	
165	2.98	-35.31		1.61%	1.21%		2.38%	
160	2.95	-35.59		1.55%	0.97%		1.91%	
155	2.93	-35.87		1.48%	0.74%		1.46%	
150	2.91	-36.17		1.42%	0.52%		1.02%	
145	2.89	-36.46	4.35%	1.36%	0.31%		0.60%	
140	2.88	-36.77	5.26%	1.30%	0.10%		0.19%	
135	2.86	-37.09	4.78%	1.25%	0.01%			
130	2.84	-37.42	4.30%	1.19%	0.01%			
125	2.83	-37.77	3.82%	1.14%	0.01%			
120	2.81	-38.13	3.37%	1.09%	0.01%			
115	2.8	-38.52	2.93%	1.04%	0.01%			
110	2.78	-38.91	2.52%	0.99%	0.02%			
105	2.76	-39.33	2.15%	0.94%	0.02%			
100	2.75	-39.76	1.80%	0.89%	0.02%			
95	2.73	-40.22	1.49%	0.84%	0.03%			
90	2.72	-40.69	1.21%	0.79%	0.03%			
85	2.7	-41.19	0.97%	0.74%	0.04%			
80	2.69	-41.71	0.77%	0.69%	0.05%			
75	2.67	-42.26	0.59%	0.65%	0.06%			
70	2.65	-42.82	0.45%	0.60%	0.07%			
65	2.64	-43.43	0.33%	0.55%	0.08%			7.47%
60	2.62	-44.07	0.24%	0.51%	0.08%			13.39%
55	2.6	-44.74	0.17%	0.46%	0.10%			12.63%
50	2.58	-45.44	0.12%	0.42%	0.11%			11.86%
45	2.56	-46.16	0.08%	0.37%	0.12%			11.08%
40	2.54	-46.92	0.05%	0.33%	0.13%			10.30%
35	2.53	-47.72	0.03%	0.29%	0.14%			9.51%
30	2.51	-48.55	0.02%	0.26%	0.15%			8.73%
25	2.49	-49.42	0.01%	0.22%	0.16%			7.92%
20	2.48	-50.33	0.01%	0.19%	0.16%			7.10%
Total (m)			2.82E-10	9.65E-03	1.68E-03	8.71E-05	4.25E-04	2.52E-04
Total (g)			5.55E-08	5.80E-01	1.81E-01	2.26E-02	6.79E-02	1.97E-02

T (°C)	P (bars)	pH	log f(O2)	gold (%)	quartz (%	apat-flu (%	silver (%)	magnetit (%	muscovit (%)	acanthit (%)
300	139.87	4.63	-32.98	6.88%	0.00%					
295	84.95	4.6	-32.76	66.07%	7.18%	39.00%	13.67%	100.00%	39.08%	
290	71.1	4.57	-32.6	17.62%	7.66%	61.00%	3.92%		38.54%	
285	63.27	4.51	-32.61	6.75%	7.58%		4.68%		16.61%	
280	57.32	4.43	-32.7	2.34%	7.32%		5.90%		5.77%	
275	52.28	4.35	-32.82	0.32%	7.02%		6.79%			
270	47.83	4.26	-32.97	0.00%	6.67%		5.92%			21.15%
265	43.8	4.17	-33.13		6.33%		6.10%			24.90%
260	40.11	4.08	-33.29		5.99%		6.42%			22.87%
255	36.72	4	-33.43		5.67%		6.69%			18.47%
250	33.59	3.93	-33.56		5.36%		7.22%			11.14%
245	30.69	3.85	-33.7		5.06%		8.30%			1.47%
240	28.01	3.78	-33.85		4.77%		8.51%			
235	25.52	3.71	-33.97		4.50%		7.38%			
230	23.22	3.67	-34.04		4.24%		4.68%			
225	21.08	3.63	-34.07		4.00%		2.12%			
220	19.11	3.6	-34.1		3.76%		0.94%			
215	17.28	3.58	-34.13		3.55%		0.49%			
210	15.6	3.55	-34.19		3.34%		0.28%			
Total (m)				**2.08E-10**	**6.57E-03**	**3.20E-10**	**1.13E-03**	**4.29E-05**	**1.49E-05**	**5.62E-05**
Total (g)				**4.10E-08**	**3.94E-01**	**1.61E-07**	**1.22E-01**	**9.94E-03**	**5.93E-03**	**1.39E-02**

T (°C)	pH	TotMix	log f(O2)	gold (%)	quartz (%	acanthit (%)	hematite (%)	anhydrit (%	barite (%)	silver (%)	anglesit (%)
300	4.63		-32.98	2.00%	0.00%						
289.6	4.24	0.05	-30.33		4.57%	53.14%	1.88%				
279.8	4.08	0.10	-30.33		4.91%	26.68%	0.87%				
270.6	3.94	0.15	-30.52		5.00%	12.50%	1.06%	3.36%			
261.7	3.81	0.20	-30.85		4.90%	7.69%	0.79%	7.24%			
253.4	3.67	0.25	-31.06		4.70%		0.74%	5.11%	13.51%	0.79%	
245.5	3.53	0.30	-31.18		4.43%		0.95%	4.24%	14.30%	1.00%	
238.1	3.42	0.35	-31.38		4.13%		0.98%	3.89%	12.29%	1.03%	
231.1	3.32	0.40	-31.64		3.82%		0.99%	3.70%	10.16%	1.03%	
224.4	3.25	0.45	-31.93		3.53%		0.98%	3.57%	8.23%	1.02%	
218.2	3.18	0.50	-32.24		3.25%		0.95%	3.48%	6.60%	1.00%	
212.2	3.13	0.55	-32.54		2.99%		0.92%	3.40%	5.29%	0.97%	
206.6	3.09	0.60	-32.83		2.75%		0.88%	3.32%	4.27%	0.92%	
201.3	3.05	0.65	-33.11		2.54%		0.84%	3.26%	3.47%	0.88%	
196.2	3.02	0.70	-33.38		2.35%		0.79%	3.19%	2.84%	0.83%	
191.5	2.99	0.75	-33.63		2.17%		0.75%	3.13%	2.34%	0.78%	
186.9	2.97	0.80	-33.87		2.02%		0.70%	3.07%	1.95%	0.73%	
182.6	2.95	0.85	-34.09		1.88%		0.66%	3.02%	1.64%	0.69%	
178.4	2.94	0.90	-34.31		1.76%		0.62%	2.96%	1.39%	0.65%	
174.5	2.92	0.95	-34.51		1.65%		0.59%	2.90%	1.19%	0.61%	
170.8	2.91	1.00	-34.7		1.56%		0.55%	2.84%	1.03%	0.58%	
167.2	2.9	1.05	-34.89		1.47%		0.53%	2.78%	0.89%	0.55%	
163.7	2.89	1.10	-35.06		1.39%		0.50%	2.72%	0.78%	0.52%	
160.4	2.89	1.15	-35.23		1.32%		0.48%	2.65%	0.68%	0.50%	
157.3	2.88	1.20	-35.4	1.52%	1.25%		0.46%	2.59%	0.60%	0.48%	
154.2	2.88	1.25	-35.55	3.44%	1.20%		0.44%	2.52%	0.54%	0.46%	
151.3	2.87	1.30	-35.71	3.14%	1.14%		0.42%	2.45%	0.48%	0.44%	
148.5	2.87	1.35	-35.86	2.86%	1.09%		0.41%	2.37%	0.43%	0.43%	
145.8	2.86	1.40	-36	2.61%	1.05%		0.39%	2.30%	0.39%	0.41%	
143.2	2.86	1.45	-36.14	2.39%	1.01%		0.38%	2.23%	0.35%	0.40%	
140.7	2.86	1.50	-36.28	2.19%	0.97%		0.37%	2.15%	0.31%	0.39%	
138.3	2.86	1.55	-36.42	2.01%	0.93%		0.36%	2.07%	0.29%	0.37%	
136	2.86	1.60	-36.55	1.84%	0.90%		0.35%	1.99%	0.26%	0.36%	
133.7	2.85	1.65	-36.68	1.70%	0.87%		0.34%	1.92%	0.24%	0.35%	
131.5	2.85	1.70	-36.8	1.56%	0.84%		0.33%	1.84%	0.22%	0.35%	
129.4	2.85	1.75	-36.93	1.44%	0.81%		0.32%	1.76%	0.20%	0.34%	
127.4	2.85	1.80	-37.05	1.31%	0.78%		0.08%		0.01%	0.09%	1.51%
125.4	2.85	1.85	-37.17	1.22%	0.76%		0.07%			0.07%	1.59%
123.5	2.85	1.90	-37.29	1.13%	0.73%		0.08%		0.00%	0.08%	1.57%
121.6	2.85	1.95	-37.4	1.05%	0.71%		0.09%		0.00%	0.09%	1.55%
119.8	2.85	2.00	-37.51	0.98%	0.69%		0.10%		0.01%	0.10%	1.53%
118.1	2.85	2.05	-37.62	0.91%	0.66%		0.10%		0.01%	0.11%	1.52%
116.4	2.86	2.10	-37.73	0.85%	0.64%		0.11%		0.01%	0.12%	1.50%
114.7	2.86	2.15	-37.84	0.79%	0.62%		0.12%		0.01%	0.12%	1.48%
113.2	2.86	2.20	-37.94	0.74%	0.60%		0.12%		0.01%	0.13%	1.47%
111.6	2.86	2.25	-38.05	0.69%	0.58%		0.13%		0.02%	0.13%	1.46%
110.1	2.86	2.30	-38.15	0.65%	0.56%		0.13%		0.02%	0.14%	1.44%
108.7	2.86	2.35	-38.24	0.61%	0.54%		0.14%		0.02%	0.14%	1.43%
107.3	2.86	2.40	-38.34	0.58%	0.52%		0.14%		0.02%	0.15%	1.41%
105.9	2.87	2.45	-38.44	0.54%	0.51%		0.15%		0.02%	0.15%	1.40%
104.6	2.87	2.50	-38.53	0.51%	0.49%		0.15%		0.02%	0.16%	1.39%
103.3	2.87	2.55	-38.62	0.49%	0.47%		0.15%		0.02%	0.16%	1.37%
102	2.87	2.60	-38.71	0.46%	0.45%		0.16%		0.03%	0.16%	1.36%
100.8	2.87	2.65	-38.8	0.44%	0.43%		0.16%		0.03%	0.17%	1.35%
99.69	2.88	2.70	-38.88	0.41%	0.42%		0.16%		0.03%	0.17%	1.33%
98.55	2.88	2.75	-38.96	0.40%	0.40%		0.17%		0.03%	0.17%	1.32%
97.45	2.88	2.80	-39.05	0.38%	0.38%		0.17%		0.03%	0.18%	1.31%
96.38	2.88	2.85	-39.12	0.36%	0.37%		0.17%		0.03%	0.18%	1.30%
95.35	2.88	2.90	-39.2	0.34%	0.35%		0.17%		0.03%	0.18%	1.28%
94.35	2.89	2.95	-39.28	0.33%	0.33%		0.18%		0.03%	0.18%	1.27%
93.38	2.89	3.00	-39.35	0.32%	0.32%		0.18%		0.03%	0.19%	1.26%
92.44	2.89	3.05	-39.42	0.31%	0.30%		0.18%		0.03%	0.19%	1.24%
91.53	2.89	3.10	-39.49	0.29%	0.29%		0.18%		0.03%	0.19%	1.23%
90.65	2.9	3.15	-39.56	0.28%	0.27%		0.18%		0.03%	0.19%	1.22%
89.8	2.9	3.20	-39.63	0.27%	0.26%		0.19%		0.03%	0.20%	1.20%
88.98	2.9	3.25	-39.69	0.27%	0.24%		0.19%		0.03%	0.20%	1.19%
88.19	2.9	3.30	-39.76	0.26%	0.23%		0.19%		0.03%	0.20%	1.17%
87.42	2.91	3.35	-39.82	0.25%	0.21%		0.19%		0.03%	0.20%	1.16%
86.69	2.91	3.40	-39.88	0.24%	0.20%		0.20%		0.03%	0.21%	1.14%
85.97	2.91	3.45	-39.93	0.24%	0.18%		0.20%		0.03%	0.21%	1.13%
85.28	2.91	3.50	-39.99	0.23%	0.17%		0.20%		0.03%	0.21%	1.11%
84.62	2.92	3.55	-40.04	0.22%	0.16%		0.20%		0.03%	0.21%	1.10%
83.98	2.92	3.60	-40.1	0.22%	0.14%		0.20%		0.03%	0.21%	1.08%
83.36	2.92	3.65	-40.15	0.21%	0.13%		0.21%		0.03%	0.22%	1.07%
82.77	2.92	3.70	-40.2	0.21%	0.12%		0.21%		0.03%	0.22%	1.05%

82.2	2.92	3.75	-40.24	0.21%	0.10%		0.21%		0.03%	0.22%	1.04%
81.65	2.93	3.80	-40.29	0.20%	0.09%		0.21%		0.03%	0.22%	1.02%
81.12	2.93	3.85	-40.33	0.20%	0.08%		0.21%		0.03%	0.23%	1.00%
80.61	2.93	3.90	-40.38	0.20%	0.07%		0.22%		0.03%	0.23%	0.99%
80.12	2.93	3.95	-40.42	0.19%	0.05%		0.22%		0.03%	0.23%	0.97%
79.65	2.94	4.00	-40.46	0.19%	0.04%		0.22%		0.03%	0.23%	0.95%
79.2	2.94	4.05	-40.49	0.19%	0.03%		0.22%		0.03%	0.23%	0.94%
78.77	2.94	4.10	-40.53	0.18%	0.02%		0.22%		0.03%	0.24%	0.92%
78.35	2.94	4.15	-40.57	0.18%	0.01%		0.23%		0.03%	0.24%	0.90%
77.95	2.95	4.20	-40.6	0.18%			0.23%		0.03%	0.24%	0.88%
77.57	2.95	4.25	-40.63	0.18%			0.23%		0.03%	0.24%	0.87%
77.2	2.95	4.30	-40.66	0.18%			0.23%		0.03%	0.24%	0.85%
76.85	2.95	4.35	-40.69	0.17%			0.23%		0.03%	0.25%	0.83%
76.52	2.95	4.40	-40.72	0.17%			0.24%		0.03%	0.25%	0.81%
76.2	2.96	4.45	-40.75	0.17%			0.24%		0.03%	0.25%	0.80%
75.89	2.96	4.50	-40.78	0.17%			0.24%		0.03%	0.25%	0.78%
75.6	2.96	4.55	-40.8	0.17%			0.24%		0.03%	0.25%	0.76%
75.32	2.96	4.60	-40.83	0.17%			0.24%		0.03%	0.26%	0.74%
75.05	2.96	4.65	-40.85	0.17%			0.24%		0.03%	0.26%	0.73%
74.8	2.97	4.70	-40.87	0.17%			0.25%		0.03%	0.26%	0.71%
74.56	2.97	4.75	-40.89	0.16%			0.25%		0.02%	0.26%	0.69%
74.33	2.97	4.80	-40.91	0.16%			0.25%		0.02%	0.26%	0.67%
74.11	2.97	4.85	-40.93	0.16%			0.25%		0.02%	0.26%	0.66%
73.9	2.97	4.90	-40.95	0.16%			0.25%		0.02%	0.27%	0.64%
73.7	2.98	4.95	-40.96	0.16%			0.25%		0.02%	0.27%	0.62%
73.52	2.98	5.00	-40.98	0.16%			0.26%		0.02%	0.27%	0.61%
73.52	2.98	5.00	-40.98	0.16%			0.26%		0.02%	0.27%	0.61%
69.08	3	5.50	-41.39	1.72%	0.07%		1.97%		0.26%	2.08%	6.11%
65.38	3.02	6.00	-41.75	1.64%	0.95%		2.00%		0.21%	2.11%	4.70%
62.28	3.05	6.50	-42.05	1.58%	0.63%		2.02%		0.16%	2.14%	3.54%
59.69	3.07	7.00	-42.32	1.55%	0.35%		2.03%		0.12%	2.15%	2.67%
57.52	3.09	7.50	-42.54	1.53%	0.12%		2.04%		0.09%	2.16%	2.02%
55.7	3.1	8.00	-42.74	1.51%			2.05%		0.07%	2.17%	1.55%
54.17	3.12	8.50	-42.9	1.50%			2.06%		0.05%	2.17%	1.20%
52.9	3.14	9.00	-43.04	1.50%			2.07%		0.04%	2.18%	0.95%
51.85	3.15	9.50	-43.16	1.49%			2.08%		0.03%	2.19%	0.75%
50.98	3.17	10.00	-43.27	1.49%			2.09%		0.02%	2.19%	0.60%
50.27	3.18	10.50	-43.35	1.48%			2.09%		0.02%	2.20%	0.49%
49.69	3.19	11.00	-43.42	1.48%			2.10%		0.01%	2.20%	0.40%
49.23	3.2	11.50	-43.48	1.48%			2.10%		0.01%	2.20%	0.33%
48.87	3.22	12.00	-43.53	1.48%			2.10%		0.01%	2.20%	0.27%
48.6	3.23	12.50	-43.58	1.48%			2.11%		0.01%	2.20%	0.22%
48.4	3.24	13.00	-43.61	1.48%			2.11%		0.00%	2.20%	0.18%
48.26	3.25	13.50	-43.64	1.48%			2.11%		0.00%	2.20%	0.14%
48.18	3.26	14.00	-43.66	1.48%			2.10%		0.00%	2.20%	0.12%
48.15	3.27	14.50	-43.68	1.48%			2.10%			2.19%	0.09%
48.16	3.28	15.00	-43.69	1.48%			2.10%			2.19%	0.07%
48.2	3.29	15.50	-43.7	1.48%			2.09%			2.18%	0.05%
48.28	3.3	16.00	-43.71	1.48%			2.09%			2.18%	0.04%
48.38	3.3	16.50	-43.72	1.48%			2.08%			2.17%	0.02%
48.51	3.31	17.00	-43.72	1.48%			2.07%			2.16%	0.01%
48.65	3.32	17.50	-43.73	1.48%			2.07%			2.15%	0.00%
48.81	3.33	18.00	-43.73	1.48%			2.06%			2.14%	
48.99	3.34	18.50	-43.73	1.47%			2.05%			2.13%	
49.18	3.35	19.00	-43.73	1.47%			2.04%			2.12%	
49.38	3.36	19.50	-43.73	1.47%			2.03%			2.11%	
49.58	3.36	20.00	-43.73	1.47%			2.02%			2.10%	
49.8	3.37	20.50	-43.73	1.47%			2.00%			2.09%	
Total (m)				7.14E-10	7.19E-03	3.21E-04	1.16E-02	3.06E-02	1.74E-03	2.22E-02	1.01E-01
Total (g)				1.41E-07	4.32E-01	7.94E-02	1.86E+00	4.16E+00	4.06E-01	2.40E+00	3.06E+01

T (°C)	pH	TotMix	log f(O2)	gold (%)	quartz (%	acanthit (%)	silver (%)	hematite (%)	barite (%)	chalcoci (%)
300	4.63		-32.98	5.07%	0.00%					
289.5	4.37	**0.05**	-32.42	43.36%	4.45%	56.34%	0.81%			
279.7	4.22	**0.10**	-31.35		4.78%	33.39%		4.99%		
270.4	4.04	**0.15**	-31.27		4.86%		0.50%	2.96%		
261.6	3.86	**0.20**	-31.14		4.77%		0.53%	6.70%		
253.3	3.7	**0.25**	-31.15		4.56%		0.55%	7.96%		
245.4	3.56	**0.30**	-31.27		4.30%		0.57%	8.62%		
238	3.45	**0.35**	-31.47		4.00%		0.57%	8.82%		
230.9	3.35	**0.40**	-31.73		3.70%		0.57%	8.64%		
224.3	3.28	**0.45**	-32.02		3.41%		0.55%	8.19%		
218	3.21	**0.50**	-32.32		3.14%		0.53%	7.57%		
170.7	2.94	**1.00**	-34.82		20.82%		4.06%	35.55%	12.83%	
140.7	2.88	**1.50**	-36.51		11.44%		2.92%		24.54%	
120.1	2.84	**2.00**	-37.92	25.78%	7.48%		2.93%		18.04%	
105.1	2.82	**2.50**	-39.13	12.88%	5.31%		2.93%		12.95%	
93.7	2.8	**3.00**	-40.18	5.92%	3.90%		2.93%		9.09%	
84.79	2.79	**3.50**	-41.09	2.93%	2.90%		2.93%		6.35%	
77.69	2.79	**4.00**	-41.9	1.55%	2.15%		2.93%		4.49%	
71.96	2.78	**4.50**	-42.61	0.87%	1.57%		2.93%		3.22%	
67.29	2.78	**5.00**	-43.23	0.51%	1.11%		2.93%		2.35%	
63.45	2.77	**5.50**	-43.79	0.32%	0.74%		2.93%		1.74%	
60.29	2.77	**6.00**	-44.28	0.21%	0.43%		2.93%		1.30%	
57.68	2.77	**6.50**	-44.73	0.14%	0.17%		2.93%		0.97%	
55.52	2.77	**7.00**	-45.12	0.10%			2.93%		0.72%	
53.74	2.77	**7.50**	-45.48	0.07%			2.92%		0.53%	
52.27	2.77	**8.00**	-45.8	0.05%			2.92%		0.38%	
51.06	2.77	**8.50**	-46.1	0.04%			2.92%		0.26%	
50.08	2.77	**9.00**	-46.38	0.03%			2.92%		0.16%	
49.28	2.77	**9.50**	-46.64	0.02%			2.92%		0.07%	
48.64	2.77	**10.00**	-46.88	0.02%			2.92%		0.00%	
48.14	2.77	**10.50**	-47.12	0.02%			2.92%			
47.75	2.77	**11.00**	-47.35	0.01%			2.92%			
47.46	2.77	**11.50**	-47.59	0.01%			2.92%			
47.25	2.77	**12.00**	-47.83	0.01%			2.92%			
47.12	2.77	**12.50**	-48.08	0.01%			2.92%			
47.04	2.78	**13.00**	-48.34	0.01%			2.92%			
47.02	2.78	**13.50**	-48.64	0.01%			2.92%			
47.04	2.78	**14.00**	-48.97	0.01%			2.92%			
47.11	2.78	**14.50**	-49.37	0.01%			2.92%			
47.2	2.78	**15.00**	-49.87	0.01%			2.92%			
47.32	2.78	**15.50**	-50.54	0.01%			2.92%			
47.47	2.78	**16.00**	-51.65	0.01%			2.92%			
47.63	2.78	**16.50**	-55.16	0.01%			2.88%			0.16%
47.82	2.79	**17.00**	-55.19	0.00%			0.02%			12.71%
48.01	2.81	**17.50**	-55.22	0.00%			0.02%			12.71%
48.22	2.82	**18.00**	-55.27	0.00%			0.02%			12.70%
48.44	2.83	**18.50**	-55.32	0.00%			0.02%			12.69%
48.67	2.84	**19.00**	-55.4	0.00%			0.03%			12.68%
48.91	2.85	**19.50**	-55.51	0.00%			0.03%			12.66%
49.15	2.86	**20.00**	-55.71	0.00%			0.04%			12.61%
49.39	2.87	**20.50**	-56.1	0.00%		10.28%				11.08%
Total (m)				**2.82E-10**	**7.42E-03**	**1.97E-04**	**4.15E-02**	**6.62E-04**	**1.54E-03**	**1.18E-03**
Total (g)				**5.55E-08**	**4.46E-01**	**4.88E-02**	**4.47E+00**	**1.06E-01**	**3.59E-01**	**1.89E-01**

APPENDIX D

Graphs of results of thermodynamic modelling of BHT fluids

DC10, DC15, SS10, SS15, SST at 250°C and 300°C

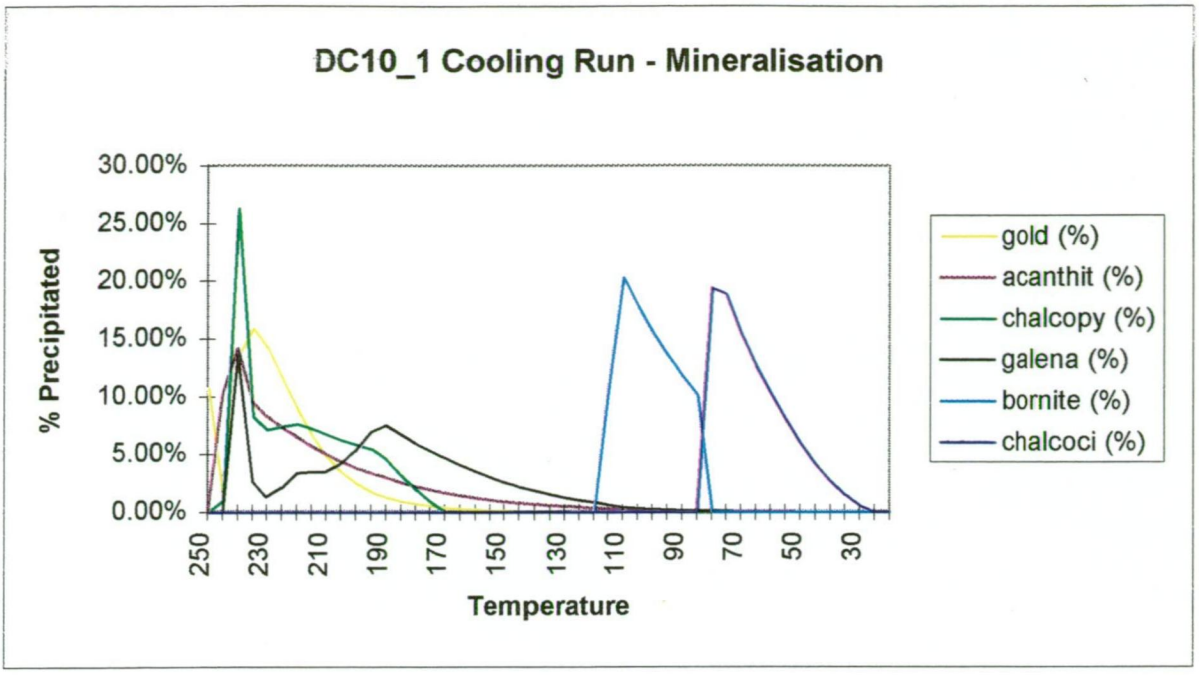
DC10_1 Cooling Run - Mineralisation
% Precipitated
30.00%
25.00%
20.00%
15.00%
10.00%
5.00%
0.00%
250
230
210
190
170
150
130
110
90
70
50
30
Temperature
gold (%)
acanthit (%)
chalcopy (%)
galena (%)
bornite (%)
chalcoci (%)

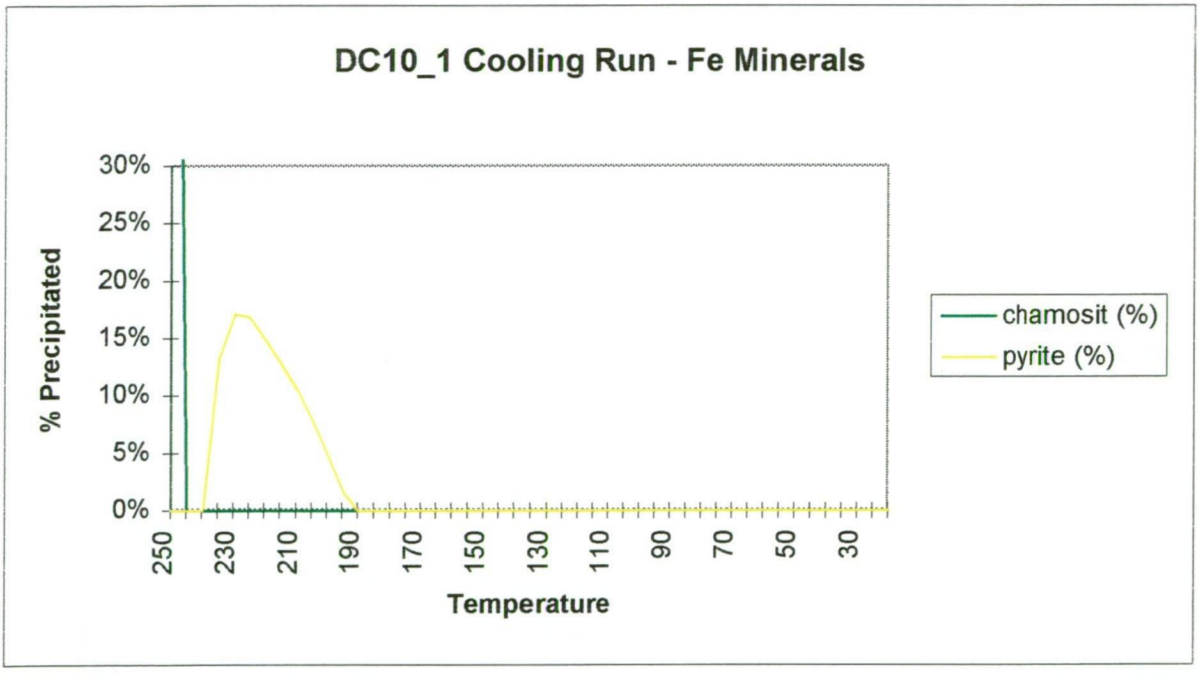
DC10_1 Cooling Run - Fe Minerals
% Precipitated
30%
25%
20%
15%
10%
5%
0%
250
230
210
190
170
150
130
110
90
70
50
30
Temperature
chamosit (%)
pyrite (%)

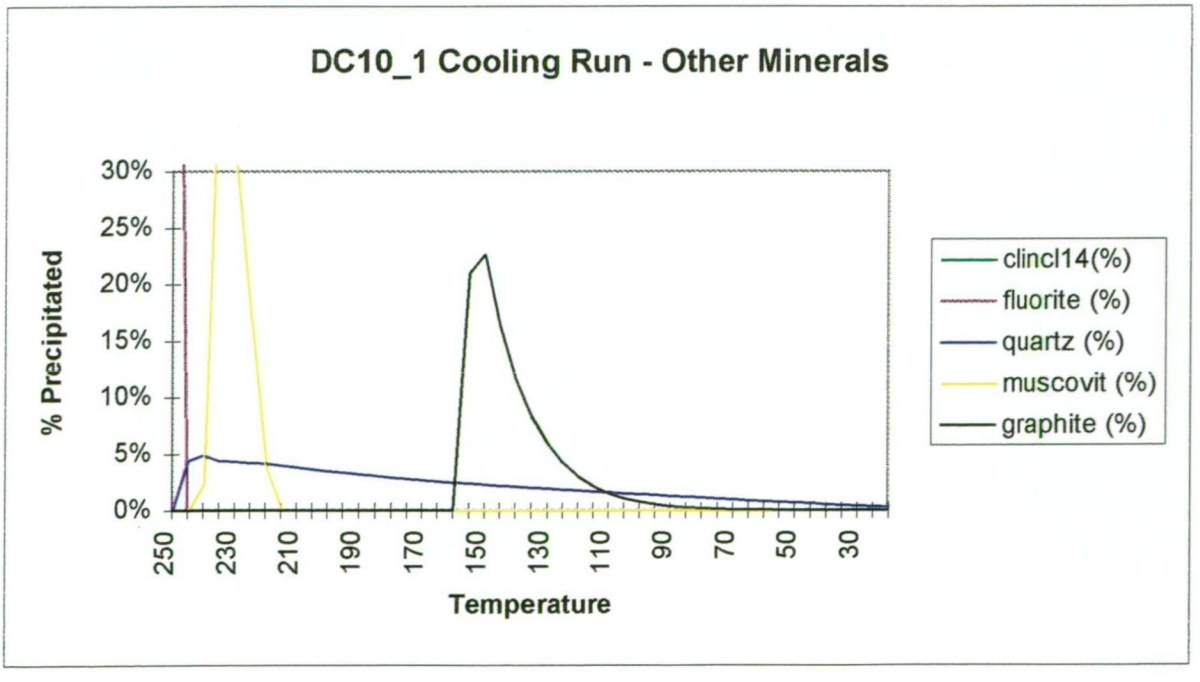
DC10_1 Cooling Run - Other Minerals
% Precipitated
30%
25%
20%
15%
10%
5%
0%
250
230
210
190
170
150
130
110
90
70
50
30
Temperature
clincl14(%)
fluorite (%)
quartz (%)
muscovit (%)
graphite (%)

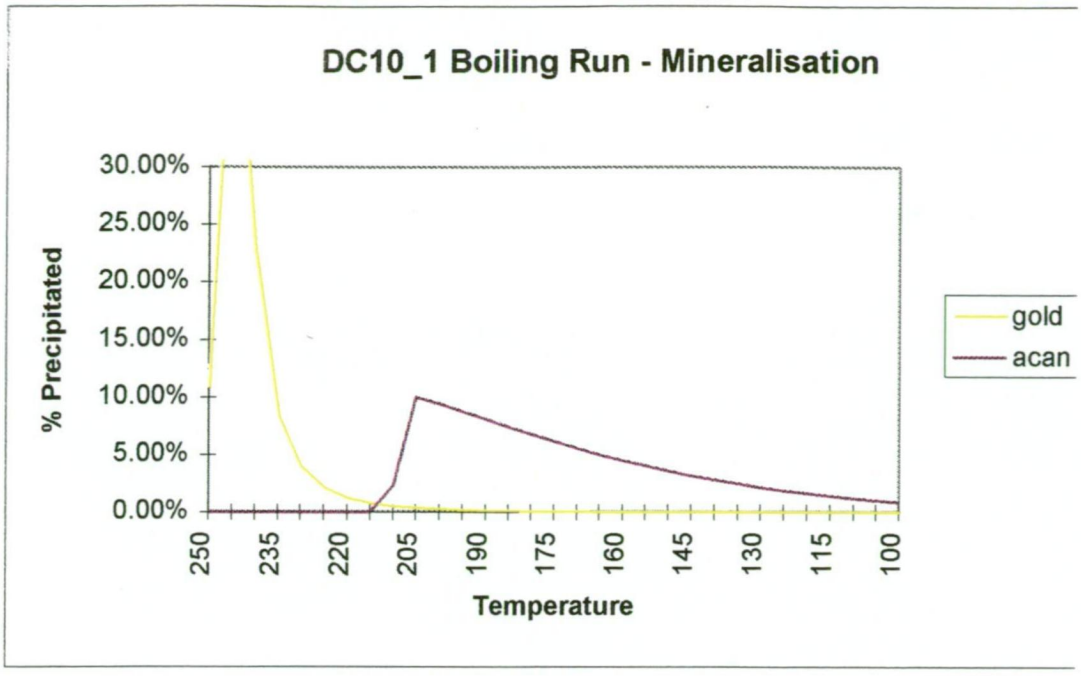
DC10_1 Boiling Run - Mineralisation
% Precipitated
30.00%
25.00%
20.00%
15.00%
10.00%
5.00%
0.00%
250
235
220
205
190
175
160
145
130
115
100
Temperature
gold
acan

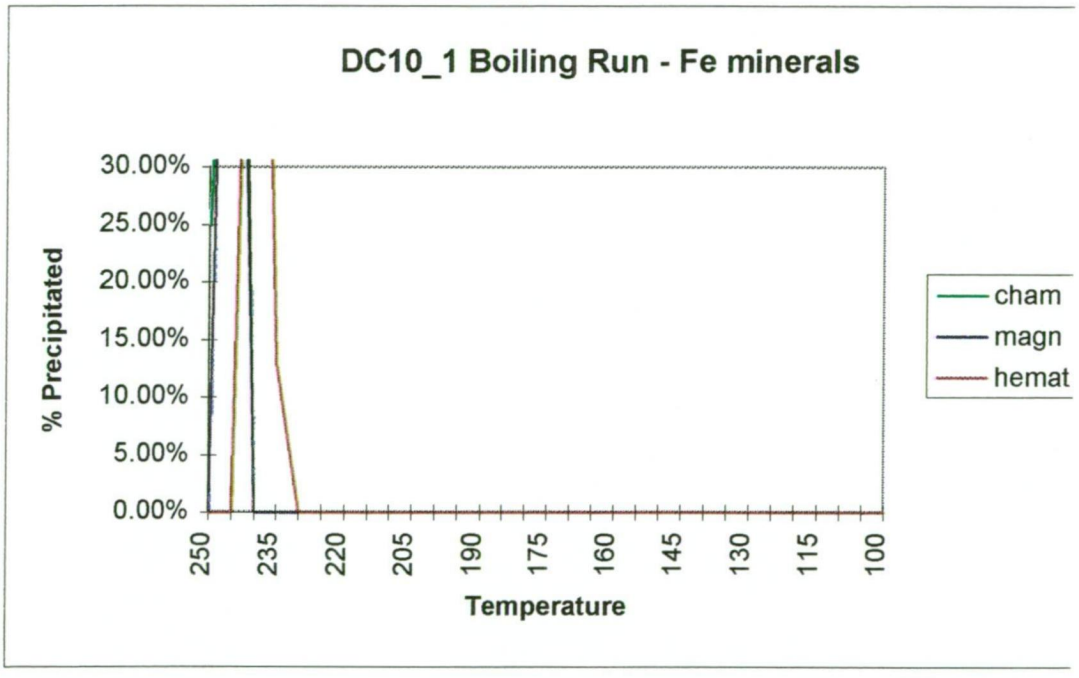
DC10_1 Boiling Run - Fe minerals
% Precipitated
30.00%
25.00%
20.00%
15.00%
10.00%
5.00%
0.00%
250
235
220
205
190
175
160
145
130
115
100
Temperature
cham
magn
hemat

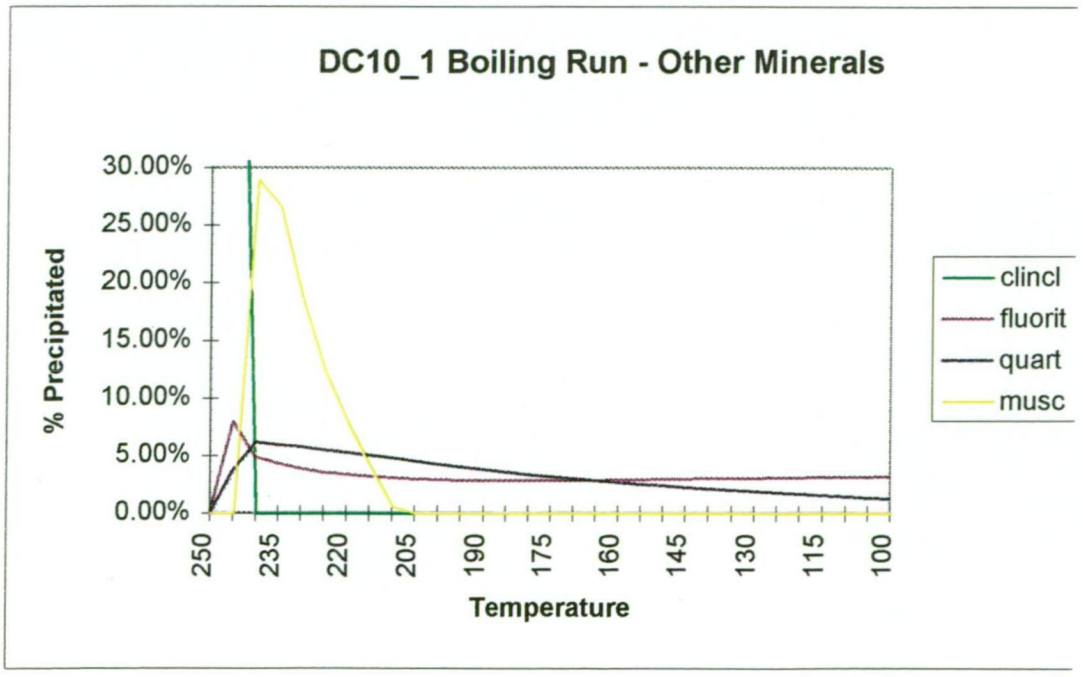
DC10_1 Boiling Run - Other Minerals
% Precipitated
30.00%
25.00%
20.00%
15.00%
10.00%
5.00%
0.00%
250
235
220
205
190
175
160
145
130
115
100
Temperature
clincl
fluorit
quart
musc

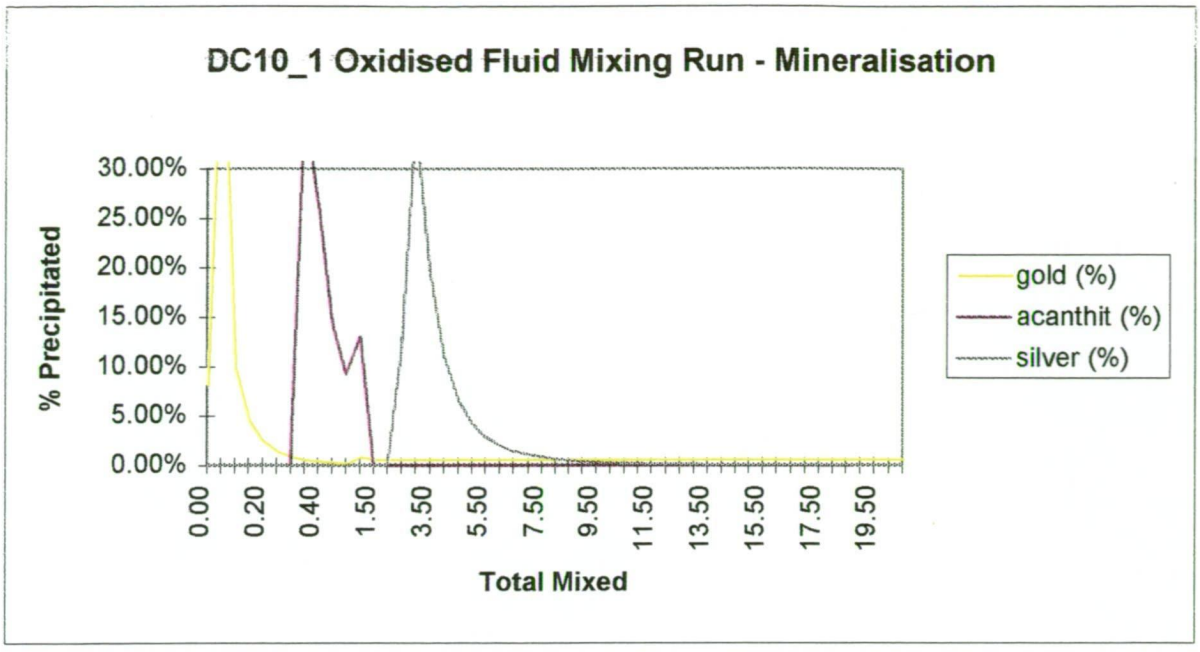
DC10_1 Oxidised Fluid Mixing Run - Mineralisation
% Precipitated
30.00%
25.00%
20.00%
15.00%
10.00%
5.00%
0.00%
0.00
0.20
0.40
1.50
3.50
5.50
7.50
9.50
11.50
13.50
15.50
17.50
19.50
Total Mixed
gold (%)
acanthit (%)
silver (%)

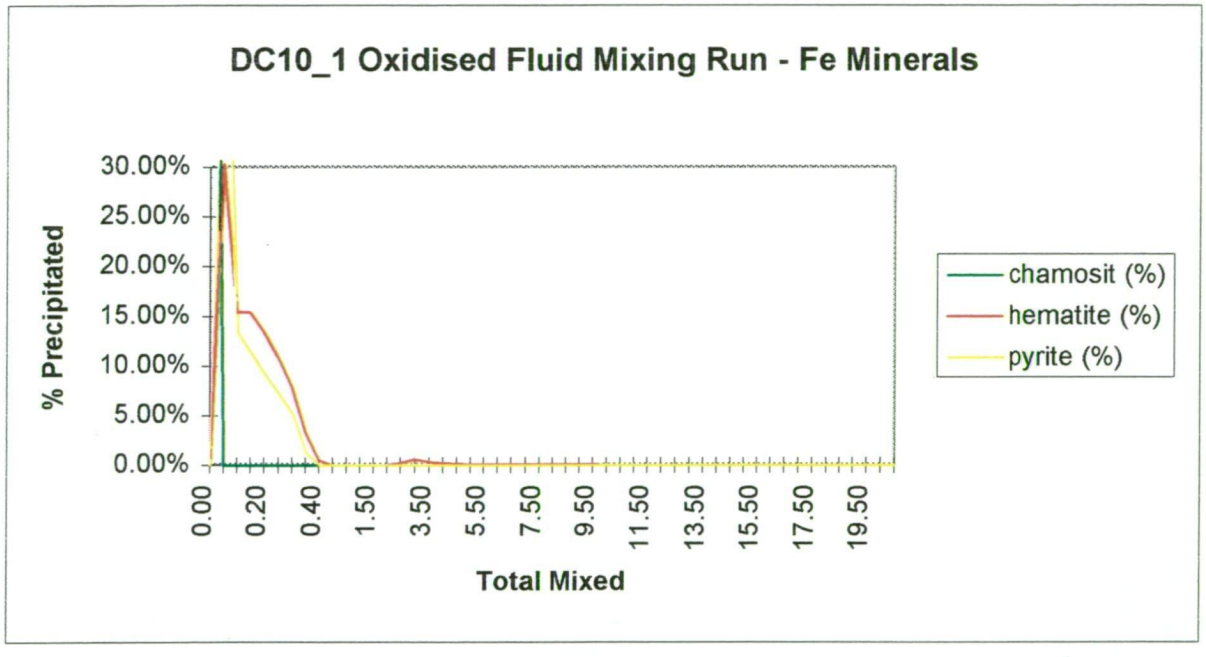
DC10_1 Oxidised Fluid Mixing Run - Fe Minerals
% Precipitated
30.00%
25.00%
20.00%
15.00%
10.00%
5.00%
0.00%
0.00
0.20
0.40
1.50
3.50
5.50
7.50
9.50
11.50
13.50
15.50
17.50
19.50
Total Mixed
chamosit (%)
hematite (%)
pyrite (%)

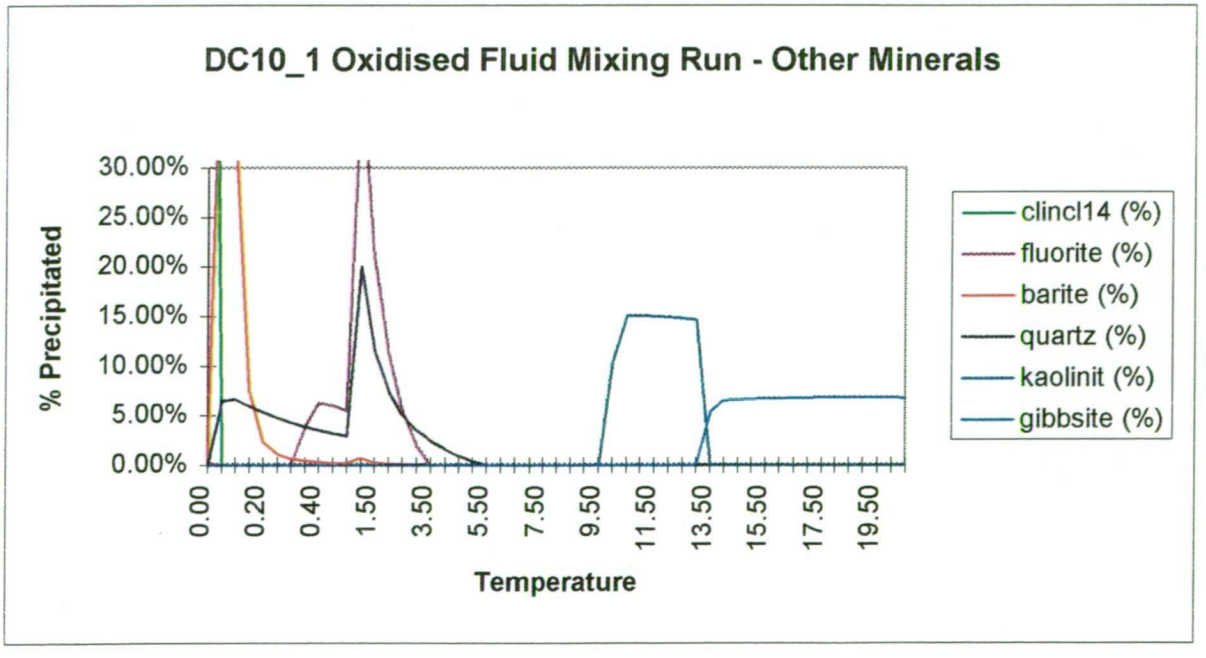
DC10_1 Oxidised Fluid Mixing Run - Other Minerals
% Precipitated
30.00%
25.00%
20.00%
15.00%
10.00%
5.00%
0.00%
0.00
0.20
0.40
1.50
3.50
5.50
7.50
9.50
11.50
13.50
15.50
17.50
19.50
Temperature
clincl14 (%)
fluorite (%)
barite (%)
quartz (%)
kaolinit (%)
gibbsite (%)

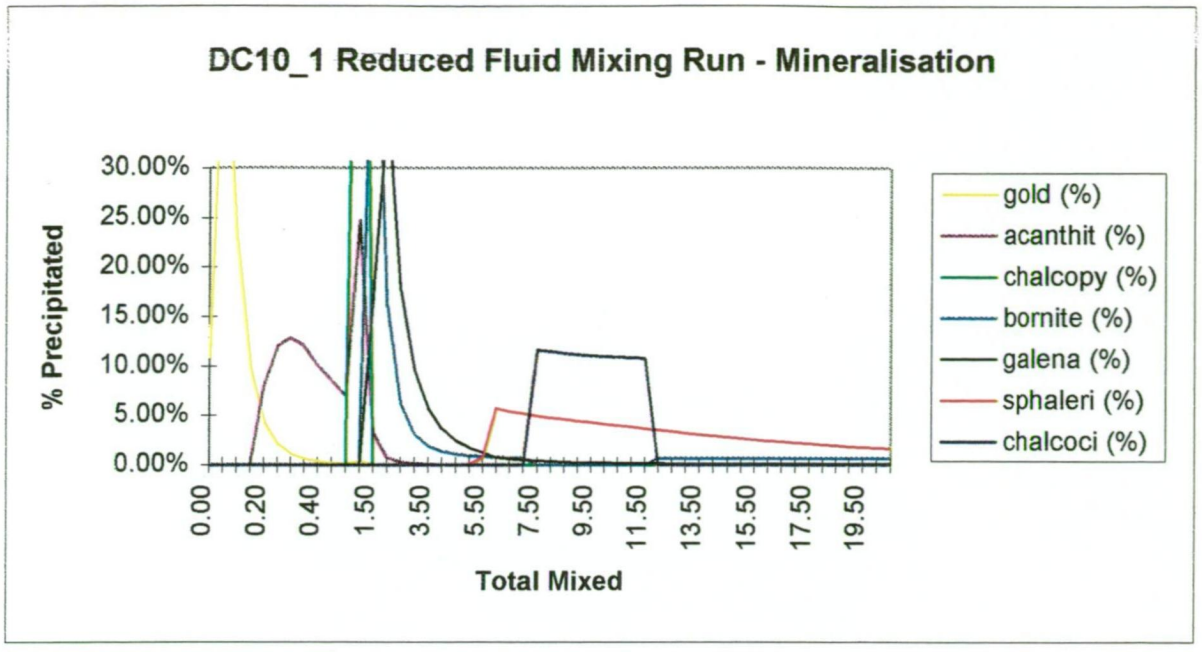
DC10_1 Reduced Fluid Mixing Run - Mineralisation
% Precipitated
30.00%
25.00%
20.00%
15.00%
10.00%
5.00%
0.00%
0.00
0.20
0.40
1.50
3.50
5.50
7.50
9.50
11.50
13.50
15.50
17.50
19.50
Total Mixed
gold (%)
acanthit (%)
chalcopy (%)
bornite (%)
galena (%)
sphaleri (%)
chalcoci (%)

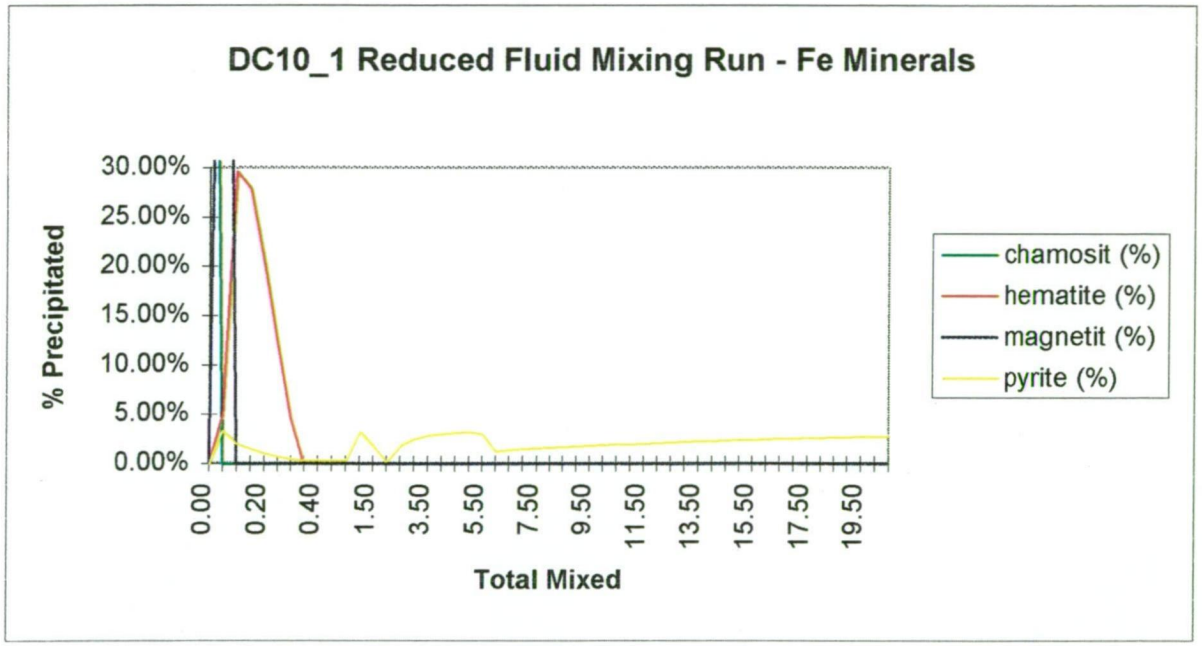
DC10_1 Reduced Fluid Mixing Run - Fe Minerals
% Precipitated
30.00%
25.00%
20.00%
15.00%
10.00%
5.00%
0.00%
0.00
0.20
0.40
1.50
3.50
5.50
7.50
9.50
11.50
13.50
15.50
17.50
19.50
Total Mixed
chamosit (%)
hematite (%)
magnetit (%)
pyrite (%)

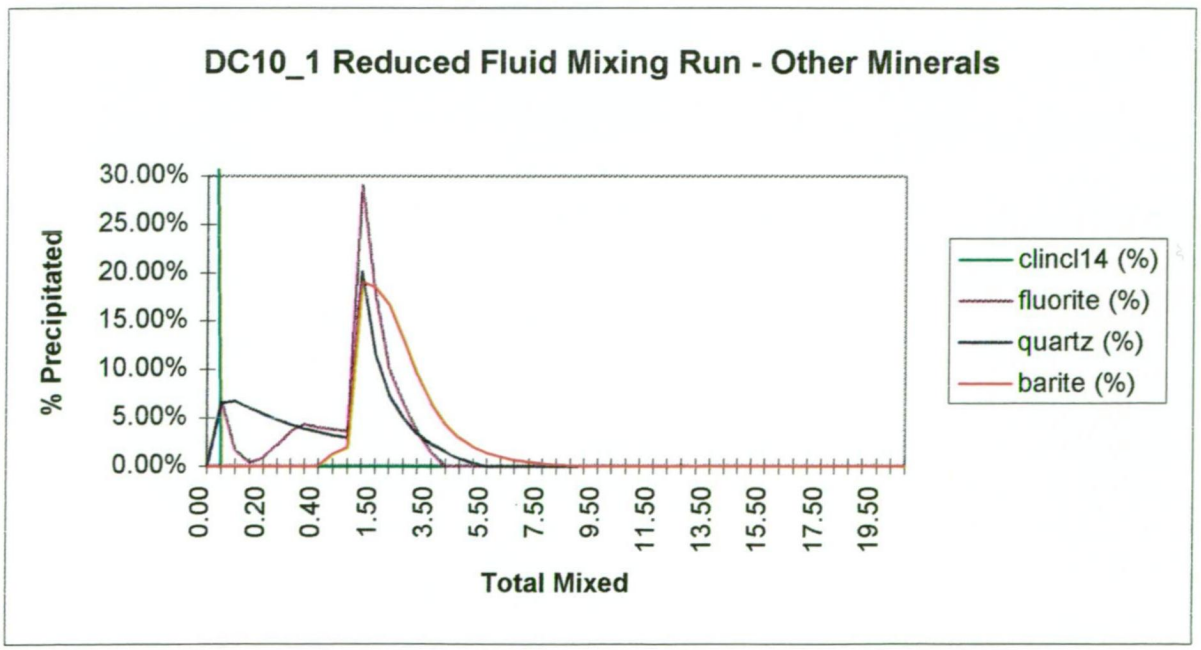
DC10_1 Reduced Fluid Mixing Run - Other Minerals
% Precipitated
30.00%
25.00%
20.00%
15.00%
10.00%
5.00%
0.00%
0.00
0.20
0.40
1.50
3.50
5.50
7.50
9.50
11.50
13.50
15.50
17.50
19.50
Total Mixed
clincl14 (%)
fluorite (%)
quartz (%)
barite (%)

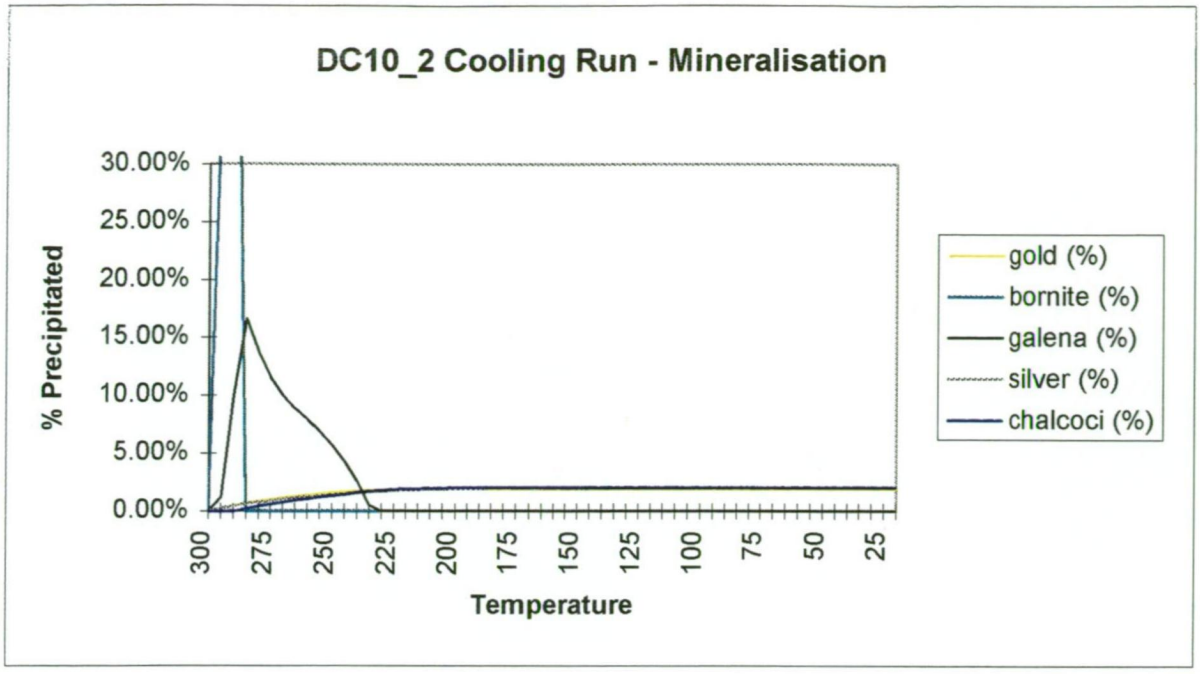
DC10_2 Cooling Run - Mineralisation
% Precipitated
30.00%
25.00%
20.00%
15.00%
10.00%
5.00%
0.00%
300
275
250
225
200
175
150
125
100
75
50
25
Temperature
gold (%)
bornite (%)
galena (%)
silver (%)
chalcoci (%)

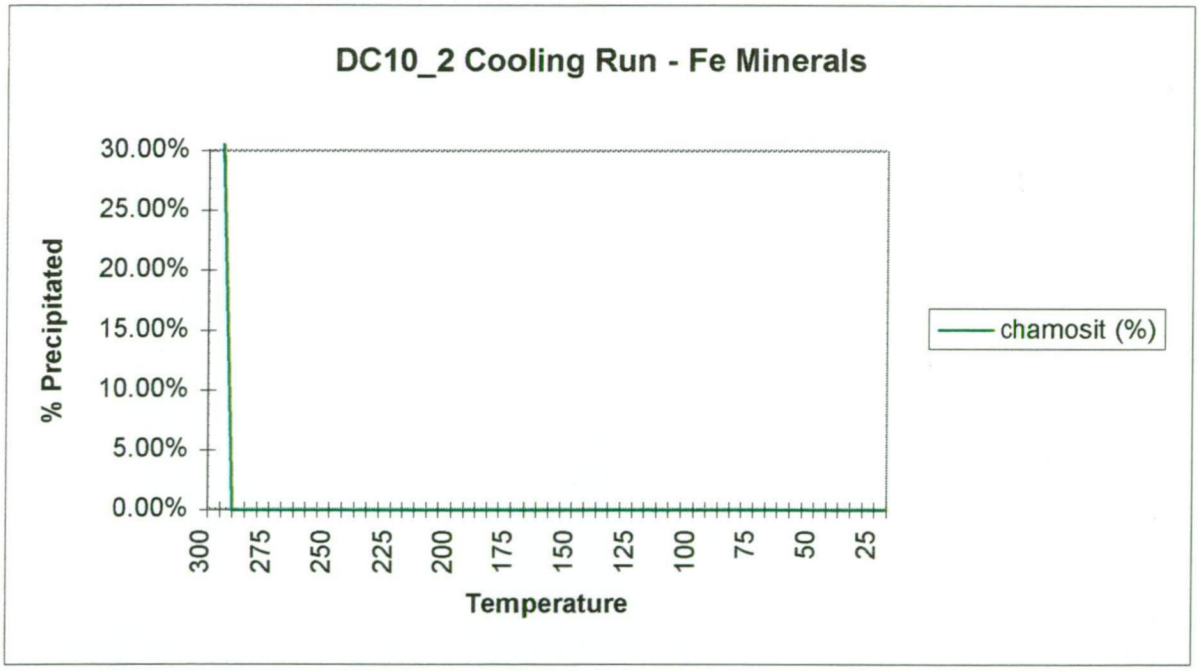
DC10_2 Cooling Run - Fe Minerals
% Precipitated
30.00%
25.00%
20.00%
15.00%
10.00%
5.00%
0.00%
300
275
250
225
200
175
150
125
100
75
50
25
Temperature
chamosit (%)

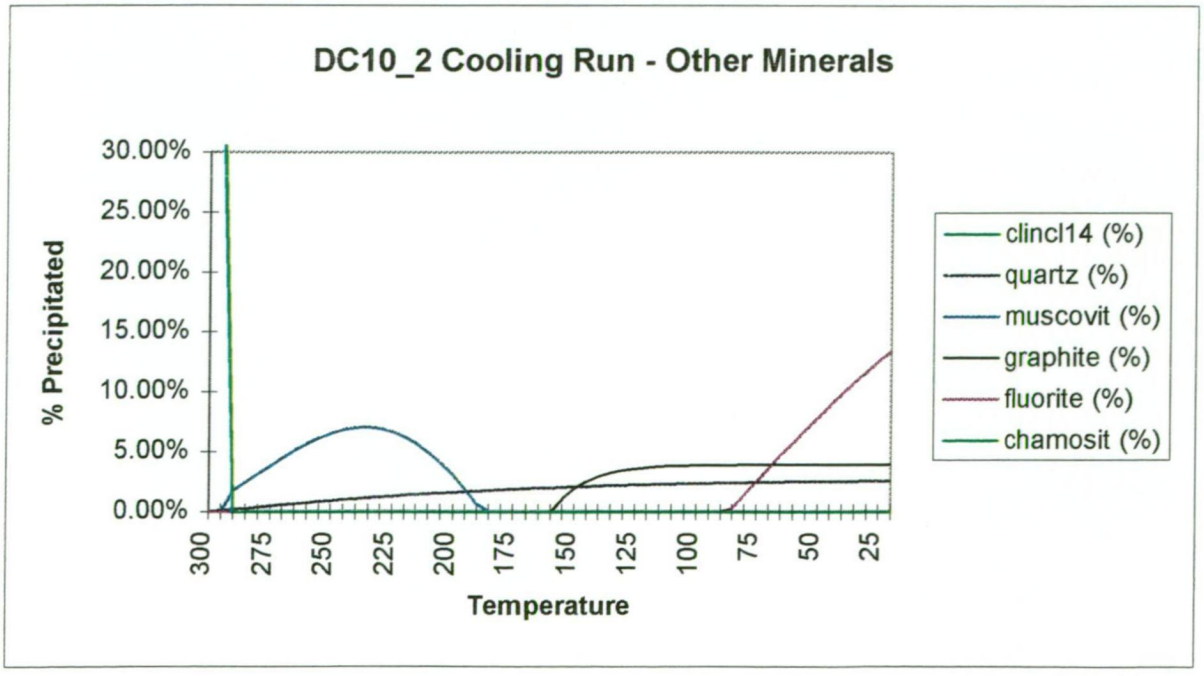
DC10_2 Cooling Run - Other Minerals
% Precipitated
30.00%
25.00%
20.00%
15.00%
10.00%
5.00%
0.00%
300
275
250
225
200
175
150
125
100
75
50
25
Temperature
clincl14 (%)
quartz (%)
muscovit (%)
graphite (%)
fluorite (%)
chamosit (%)

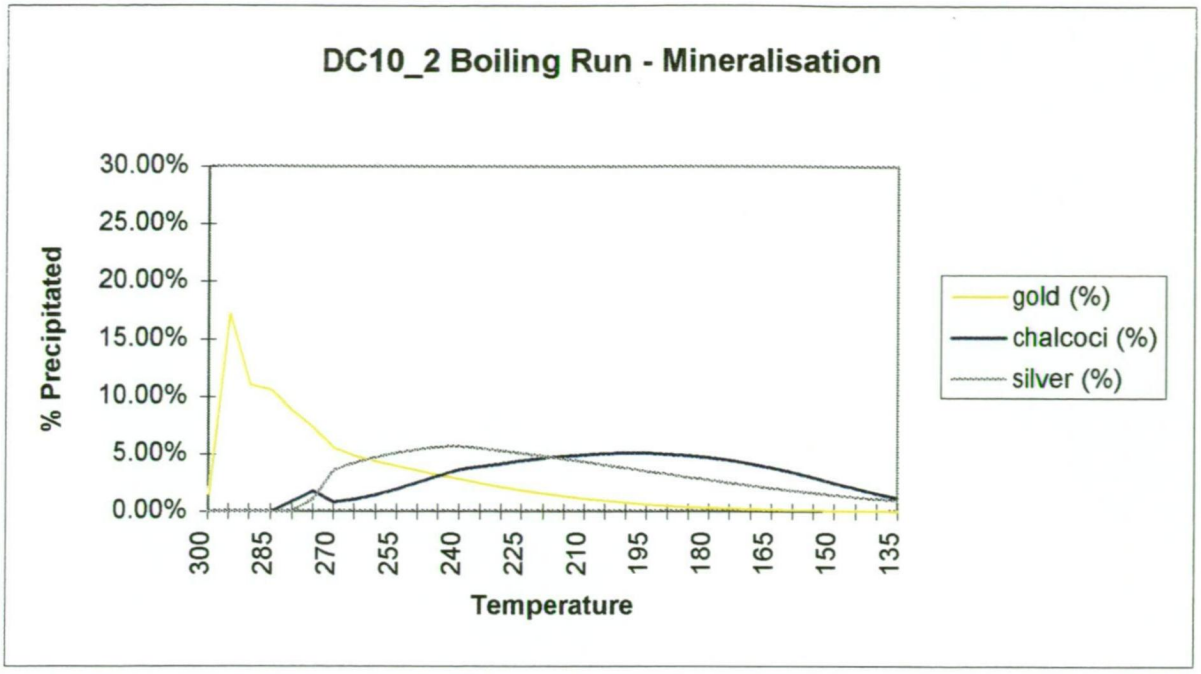
DC10_2 Boiling Run - Mineralisation
% Precipitated
30.00%
25.00%
20.00%
15.00%
10.00%
5.00%
0.00%
300
285
270
255
240
225
210
195
180
165
150
135
Temperature
gold (%)
chalcoci (%)
silver (%)

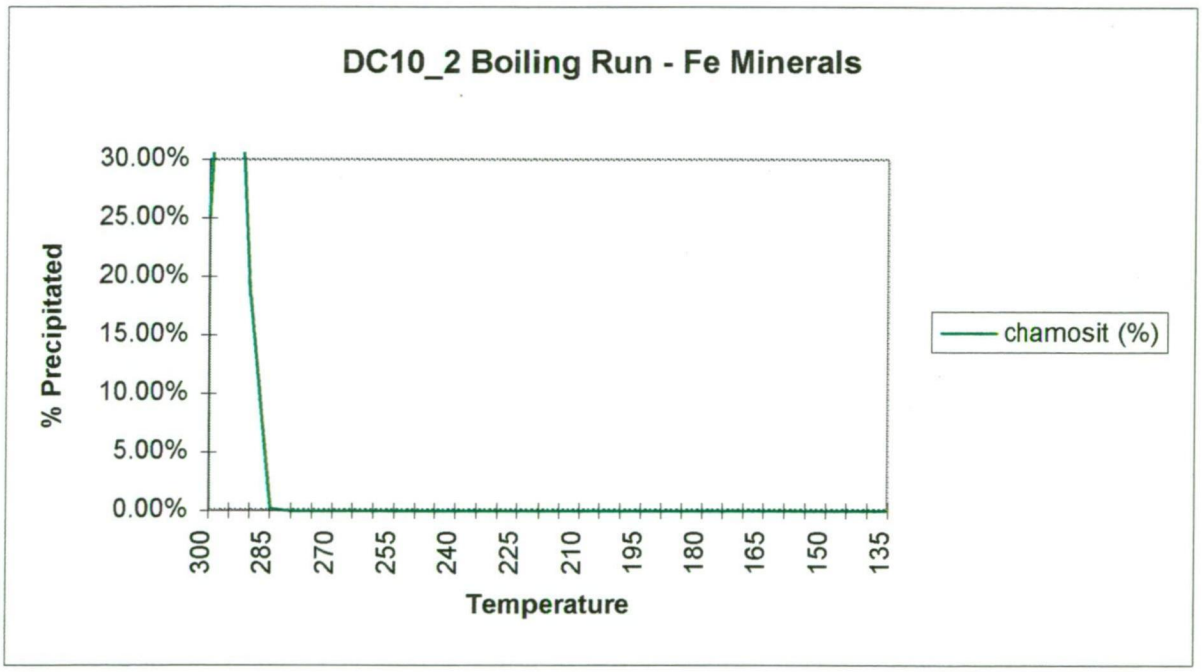
DC10_2 Boiling Run - Fe Minerals
% Precipitated
30.00%
25.00%
20.00%
15.00%
10.00%
5.00%
0.00%
300
285
270
255
240
225
210
195
180
165
150
135
Temperature
chamosit (%)

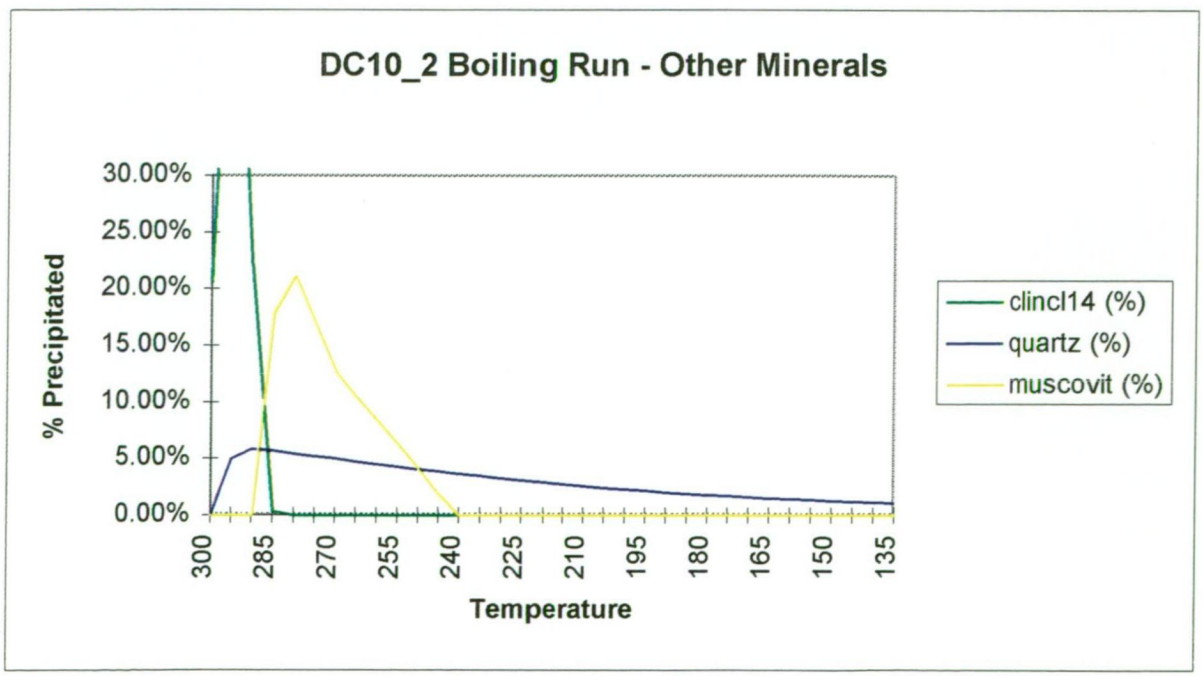
DC10_2 Boiling Run - Other Minerals
% Precipitated
30.00%
25.00%
20.00%
15.00%
10.00%
5.00%
0.00%
300
285
270
255
240
225
210
195
180
165
150
135
Temperature
clincl14 (%)
quartz (%)
muscovit (%)

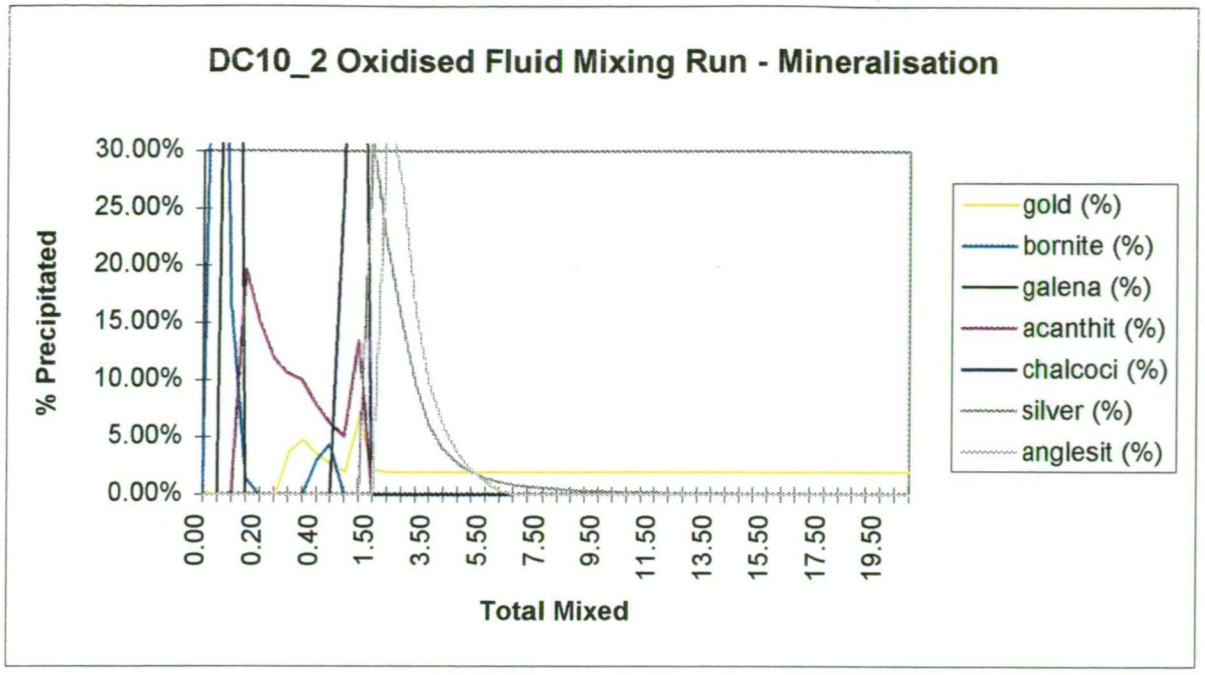
DC10_2 Oxidised Fluid Mixing Run - Mineralisation
% Precipitated
30.00%
25.00%
20.00%
15.00%
10.00%
5.00%
0.00%
0.00
0.20
0.40
1.50
3.50
5.50
7.50
9.50
11.50
13.50
15.50
17.50
19.50
Total Mixed
gold (%)
bornite (%)
galena (%)
acanthit (%)
chalcoci (%)
silver (%)
anglesit (%)

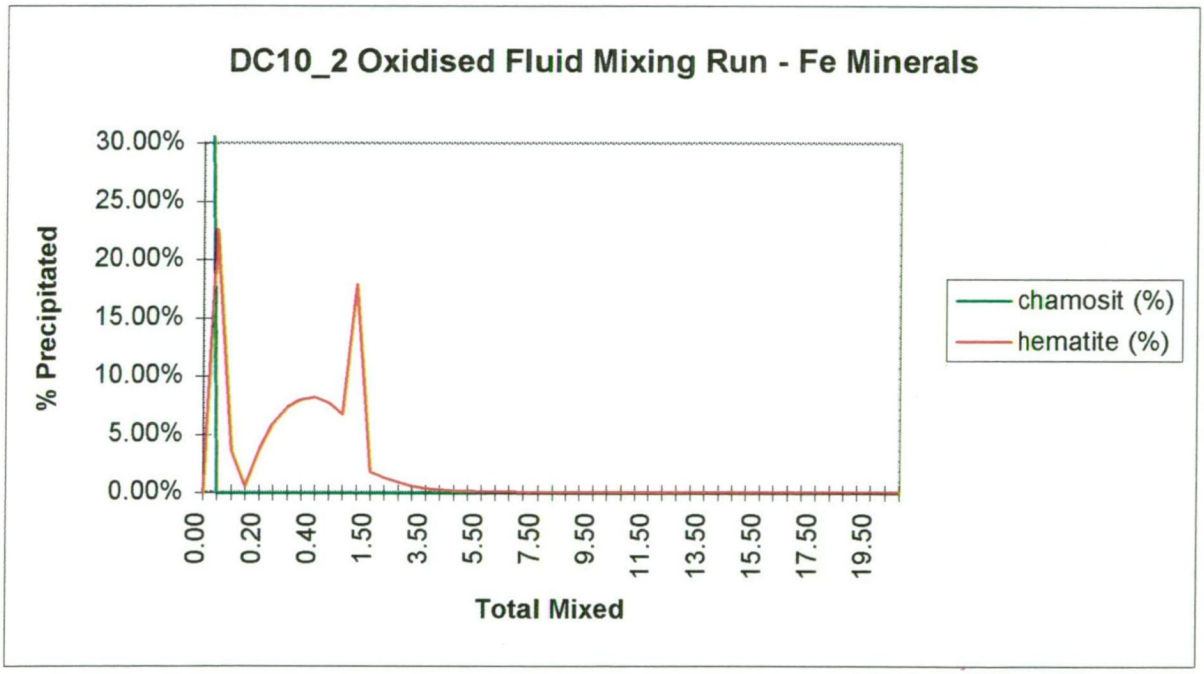
DC10_2 Oxidised Fluid Mixing Run - Fe Minerals
% Precipitated
30.00%
25.00%
20.00%
15.00%
10.00%
5.00%
0.00%
0.00
0.20
0.40
1.50
3.50
5.50
7.50
9.50
11.50
13.50
15.50
17.50
19.50
Total Mixed
chamosit (%)
hematite (%)

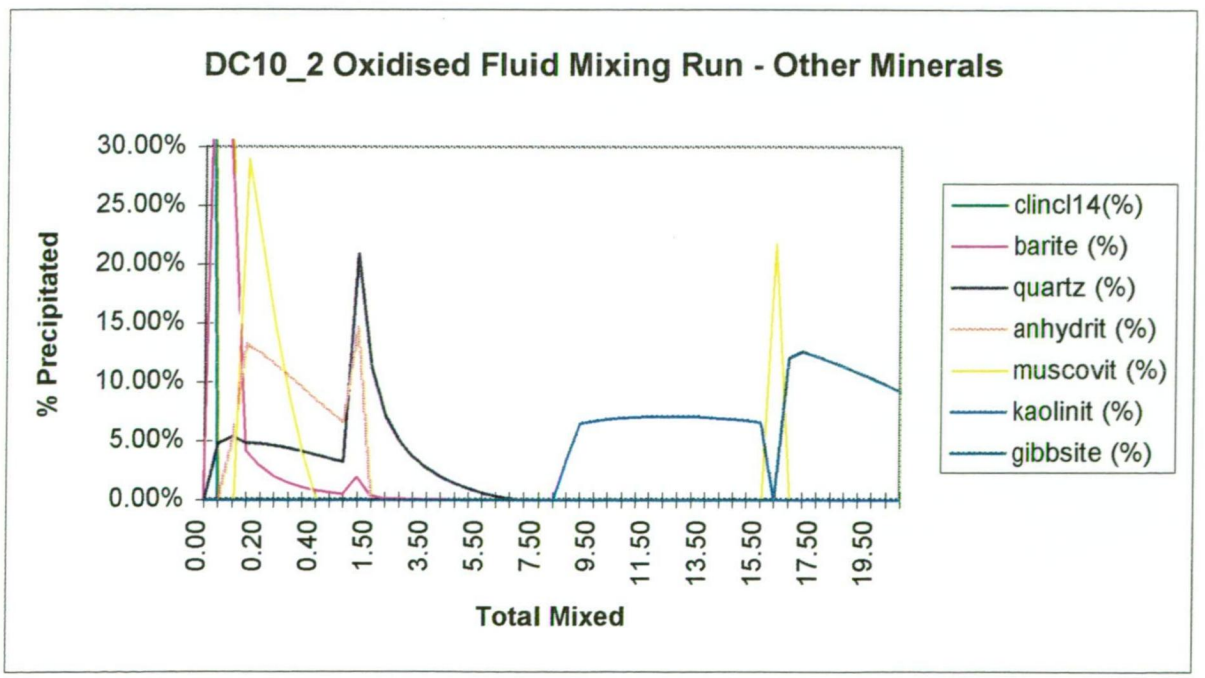
DC10_2 Oxidised Fluid Mixing Run - Other Minerals
% Precipitated
30.00%
25.00%
20.00%
15.00%
10.00%
5.00%
0.00%
0.00
0.20
0.40
1.50
3.50
5.50
7.50
9.50
11.50
13.50
15.50
17.50
19.50
Total Mixed
clincl14(%)
barite (%)
quartz (%)
anhydrit (%)
muscovit (%)
kaolinit (%)
gibbsite (%)

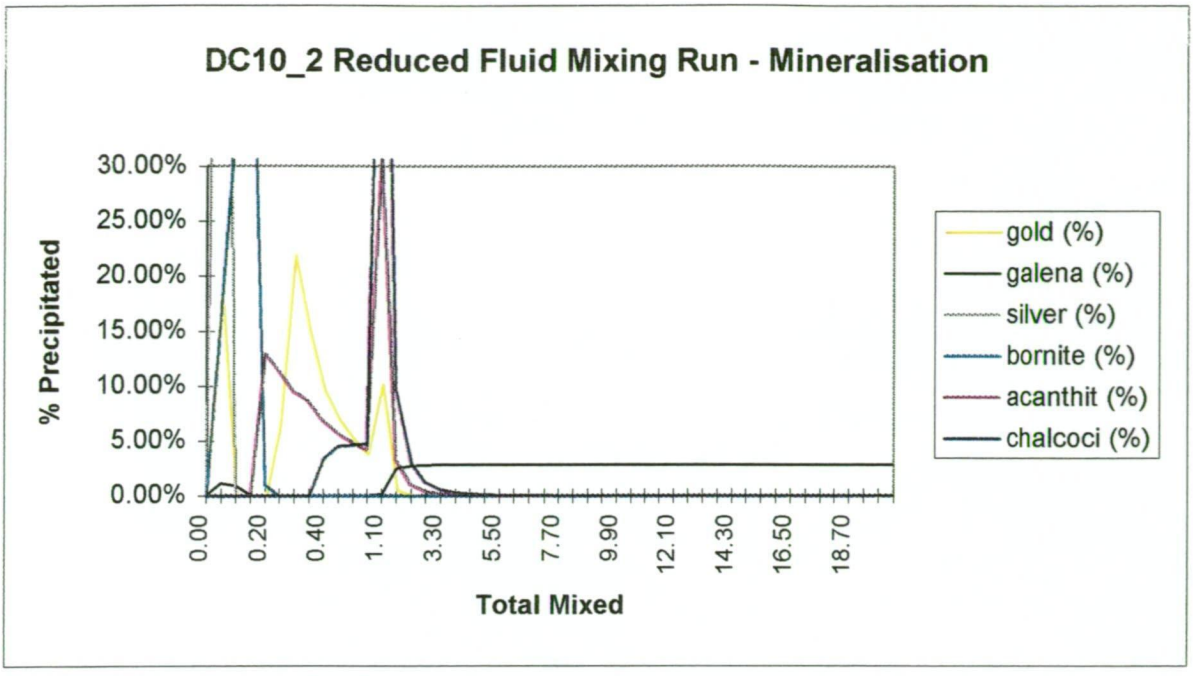
DC10_2 Reduced Fluid Mixing Run - Mineralisation
% Precipitated
30.00%
25.00%
20.00%
15.00%
10.00%
5.00%
0.00%
0.00
0.20
0.40
1.10
3.30
5.50
7.70
9.90
12.10
14.30
16.50
18.70
Total Mixed
gold (%)
galena (%)
silver (%)
bornite (%)
acanthit (%)
chalcoci (%)

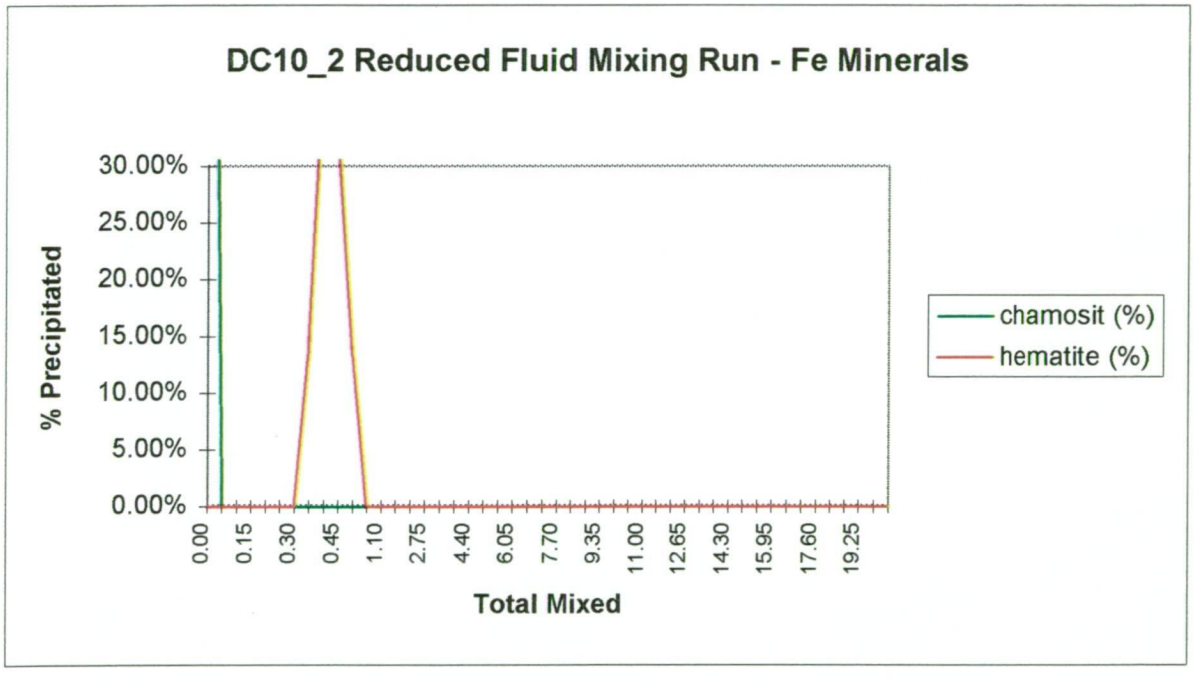
DC10_2 Reduced Fluid Mixing Run - Fe Minerals
% Precipitated
30.00%
25.00%
20.00%
15.00%
10.00%
5.00%
0.00%
0.00
0.15
0.30
0.45
1.10
2.75
4.40
6.05
7.70
9.35
11.00
12.65
14.30
15.95
17.60
19.25
Total Mixed
chamosit (%)
hematite (%)

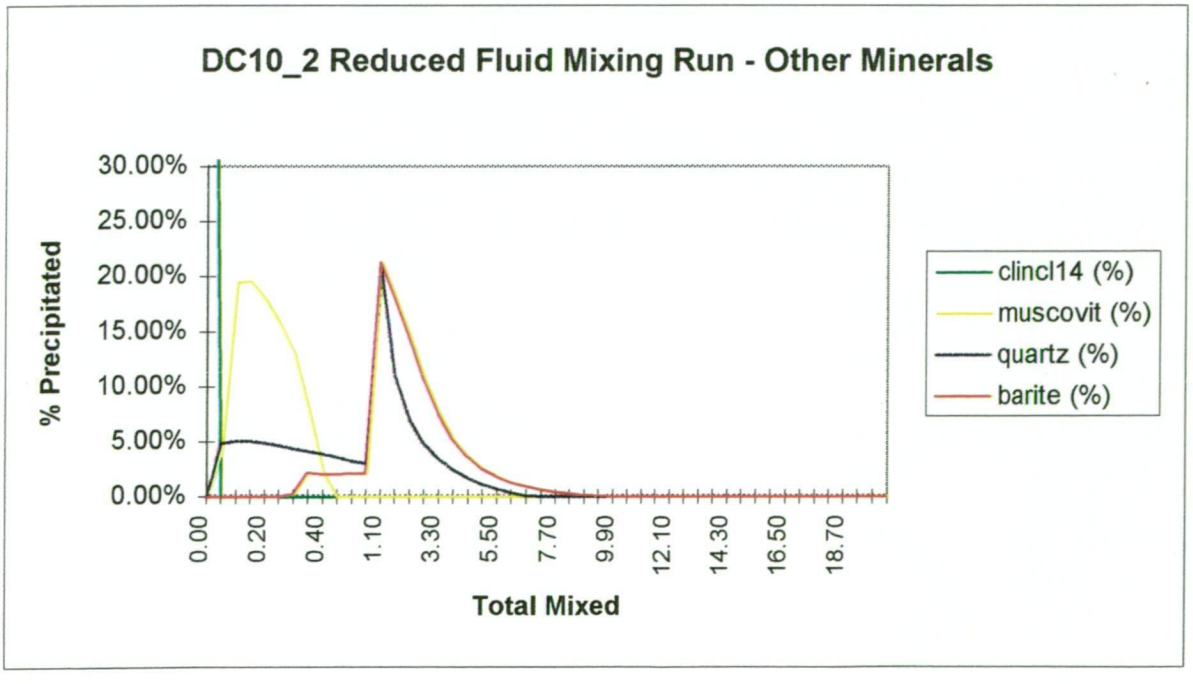
DC10_2 Reduced Fluid Mixing Run - Other Minerals
% Precipitated
30.00%
25.00%
20.00%
15.00%
10.00%
5.00%
0.00%
0.00
0.20
0.40
1.10
3.30
5.50
7.70
9.90
12.10
14.30
16.50
18.70
Total Mixed
clincl14 (%)
muscovit (%)
quartz (%)
barite (%)

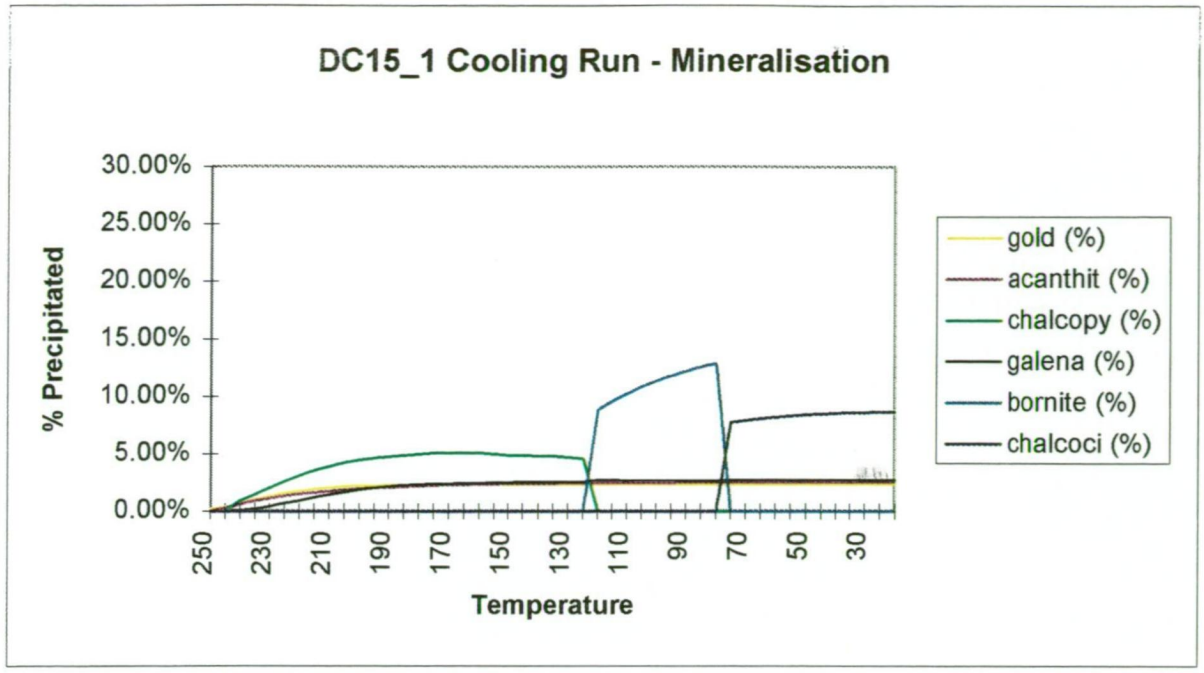
DC15_1 Cooling Run - Mineralisation
% Precipitated
30.00%
25.00%
20.00%
15.00%
10.00%
5.00%
0.00%
250
230
210
190
170
150
130
110
90
70
50
30
Temperature
gold (%)
acanthit (%)
chalcopy (%)
galena (%)
bornite (%)
chalcoci (%)

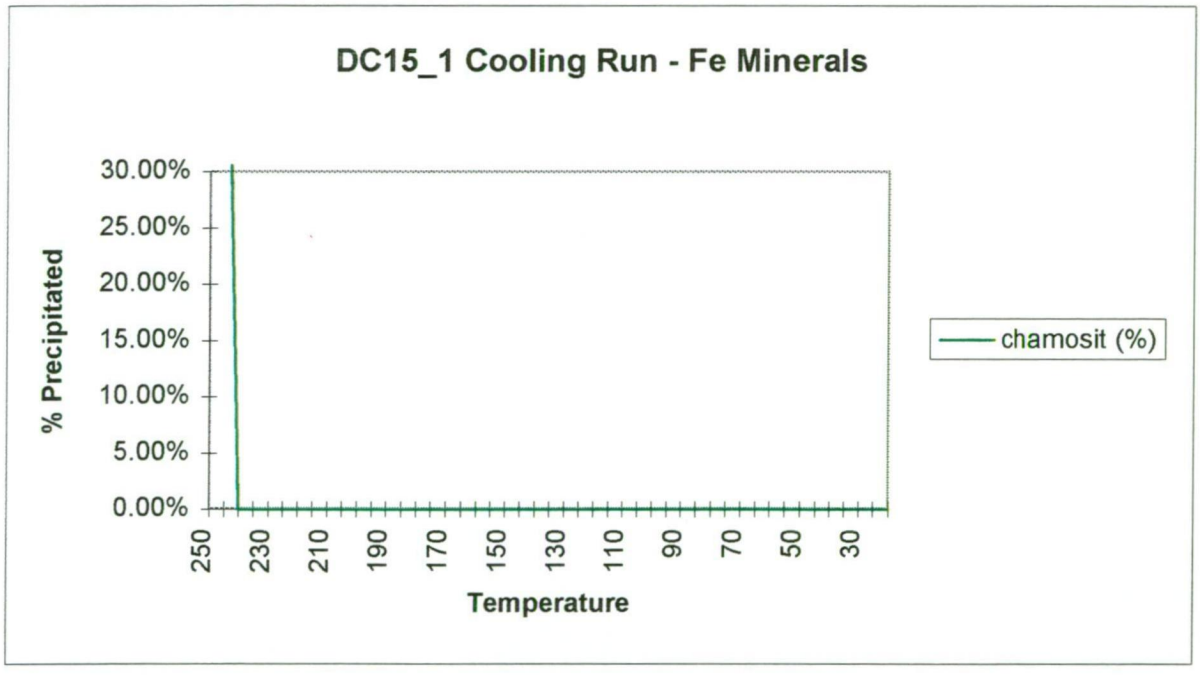
DC15_1 Cooling Run - Fe Minerals
% Precipitated
30.00%
25.00%
20.00%
15.00%
10.00%
5.00%
0.00%
250
230
210
190
170
150
130
110
90
70
50
30
Temperature
chamosit (%)

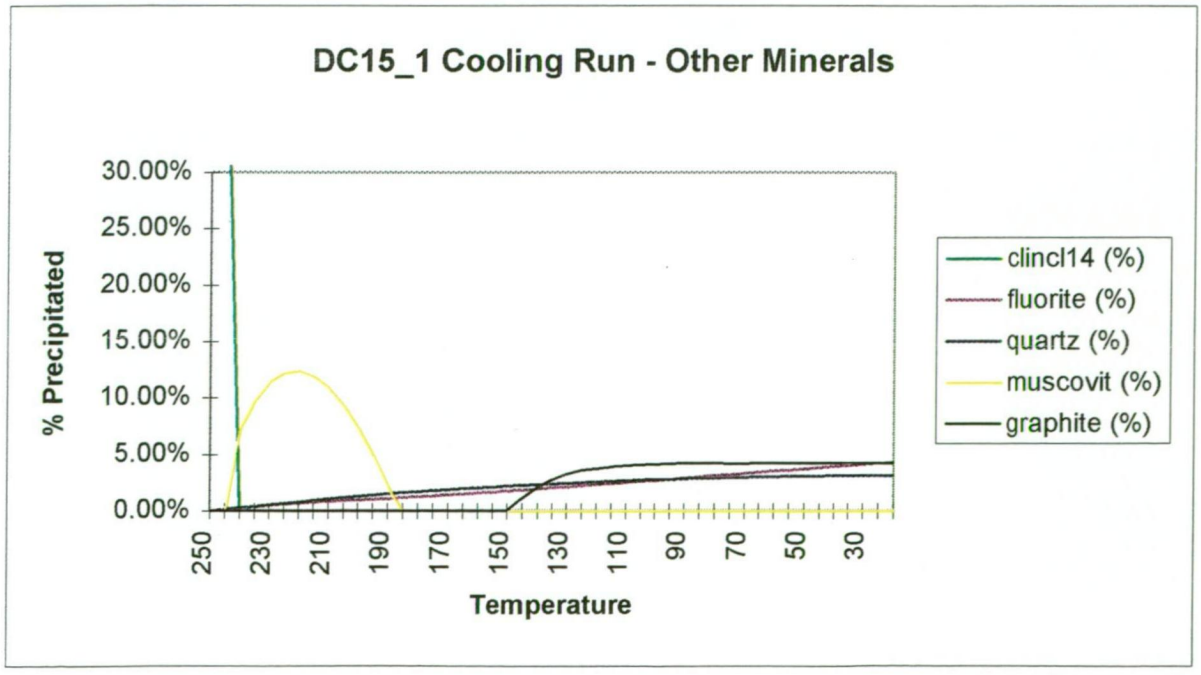
DC15_1 Cooling Run - Other Minerals
% Precipitated
30.00%
25.00%
20.00%
15.00%
10.00%
5.00%
0.00%
250
230
210
190
170
150
130
110
90
70
50
30
Temperature
clincl14 (%)
fluorite (%)
quartz (%)
muscovit (%)
graphite (%)

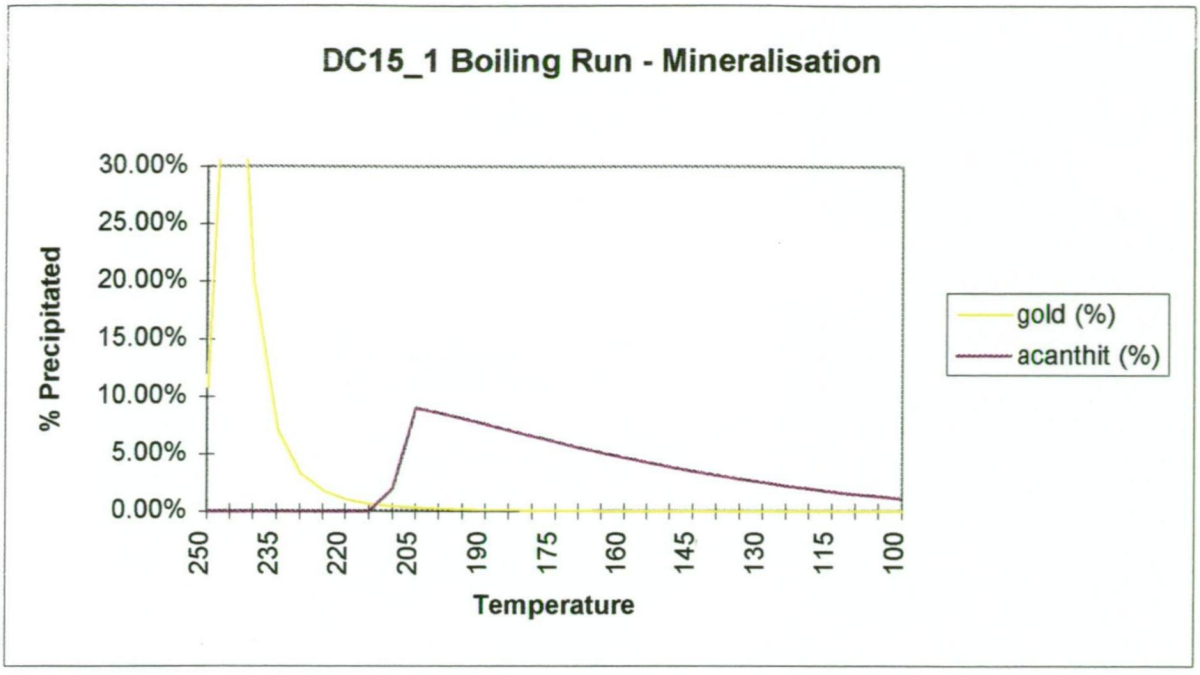
DC15_1 Boiling Run - Mineralisation
% Precipitated
30.00%
25.00%
20.00%
15.00%
10.00%
5.00%
0.00%
250
235
220
205
190
175
160
145
130
115
100
Temperature
gold (%)
acanthit (%)

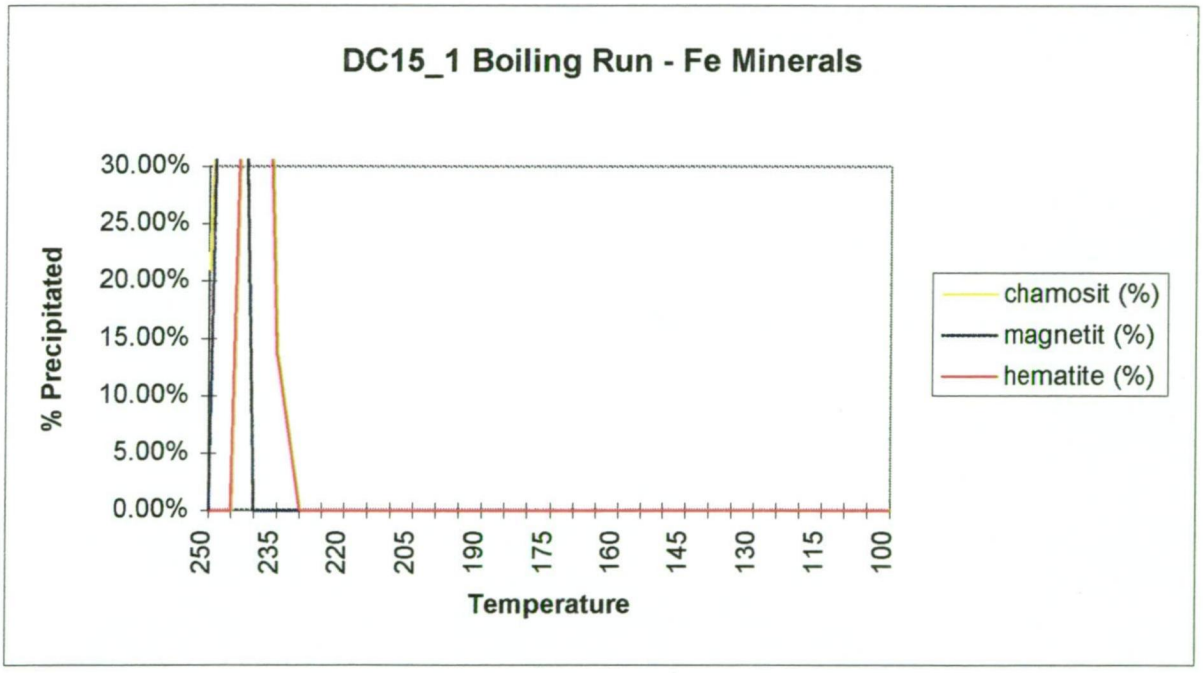
DC15_1 Boiling Run - Fe Minerals
% Precipitated
30.00%
25.00%
20.00%
15.00%
10.00%
5.00%
0.00%
250
235
220
205
190
175
160
145
130
115
100
Temperature
chamosit (%)
magnetit (%)
hematite (%)

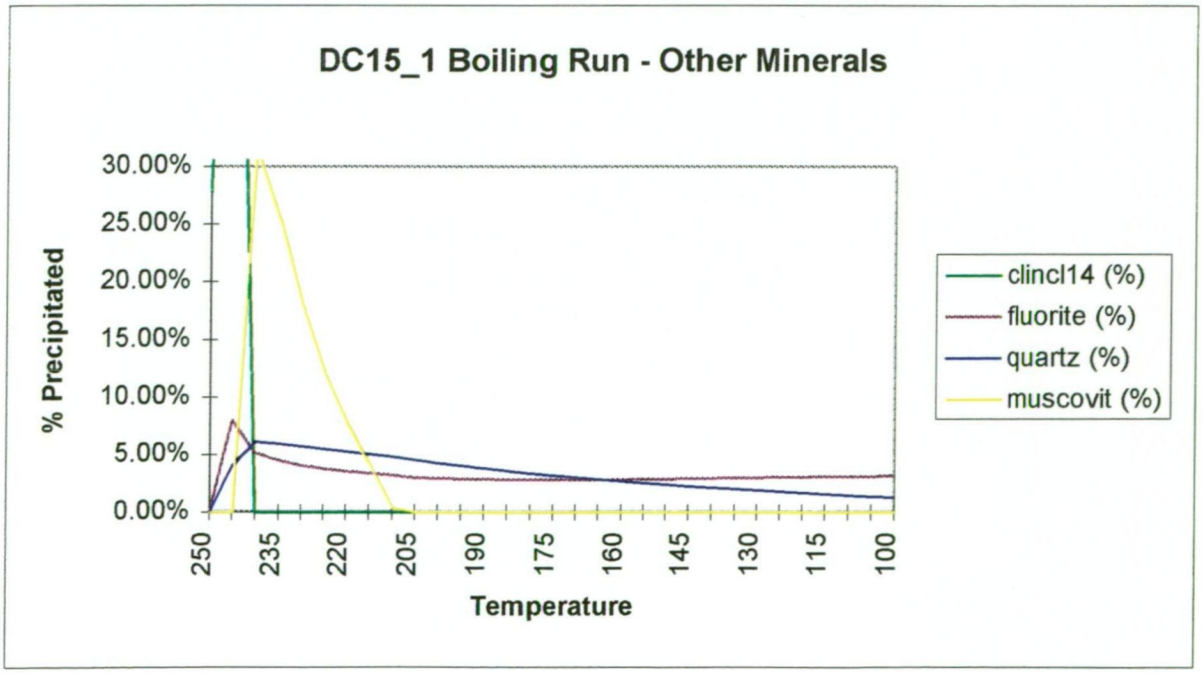
DC15_1 Boiling Run - Other Minerals
% Precipitated
30.00%
25.00%
20.00%
15.00%
10.00%
5.00%
0.00%
250
235
220
205
190
175
160
145
130
115
100
Temperature
clincl14 (%)
fluorite (%)
quartz (%)
muscovit (%)

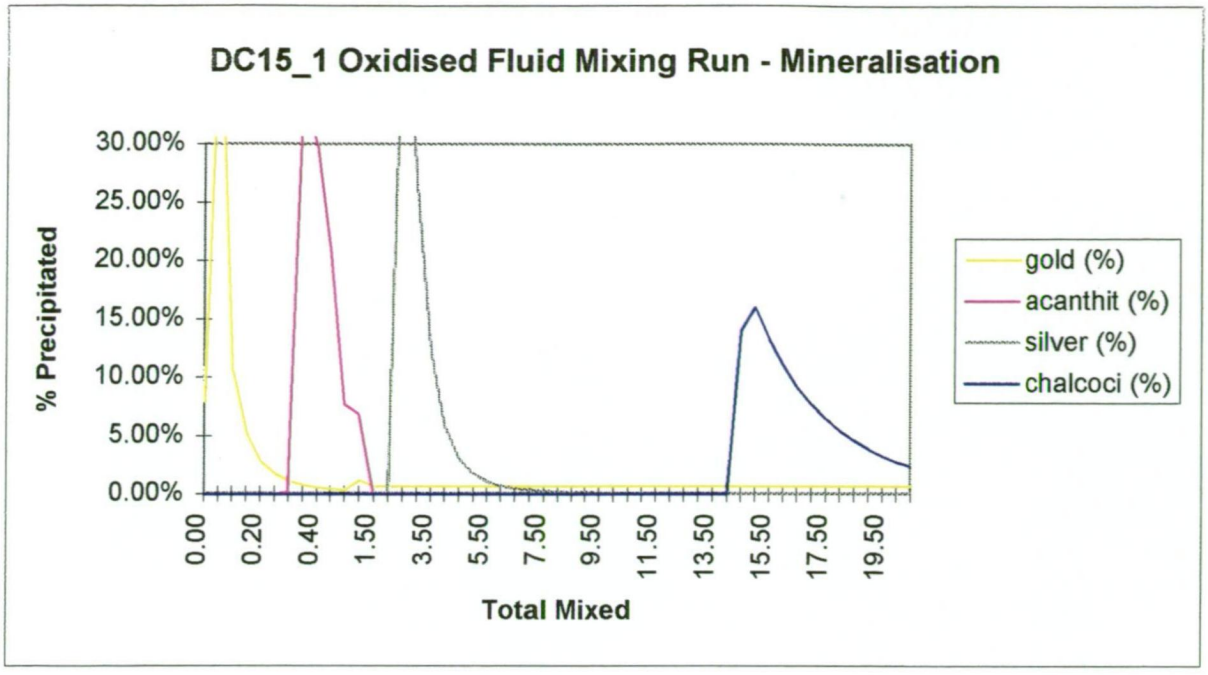
DC15_1 Oxidised Fluid Mixing Run - Mineralisation
% Precipitated
30.00%
25.00%
20.00%
15.00%
10.00%
5.00%
0.00%
0.00
0.20
0.40
1.50
3.50
5.50
7.50
9.50
11.50
13.50
15.50
17.50
19.50
Total Mixed
gold (%)
acanthit (%)
silver (%)
chalcoci (%)

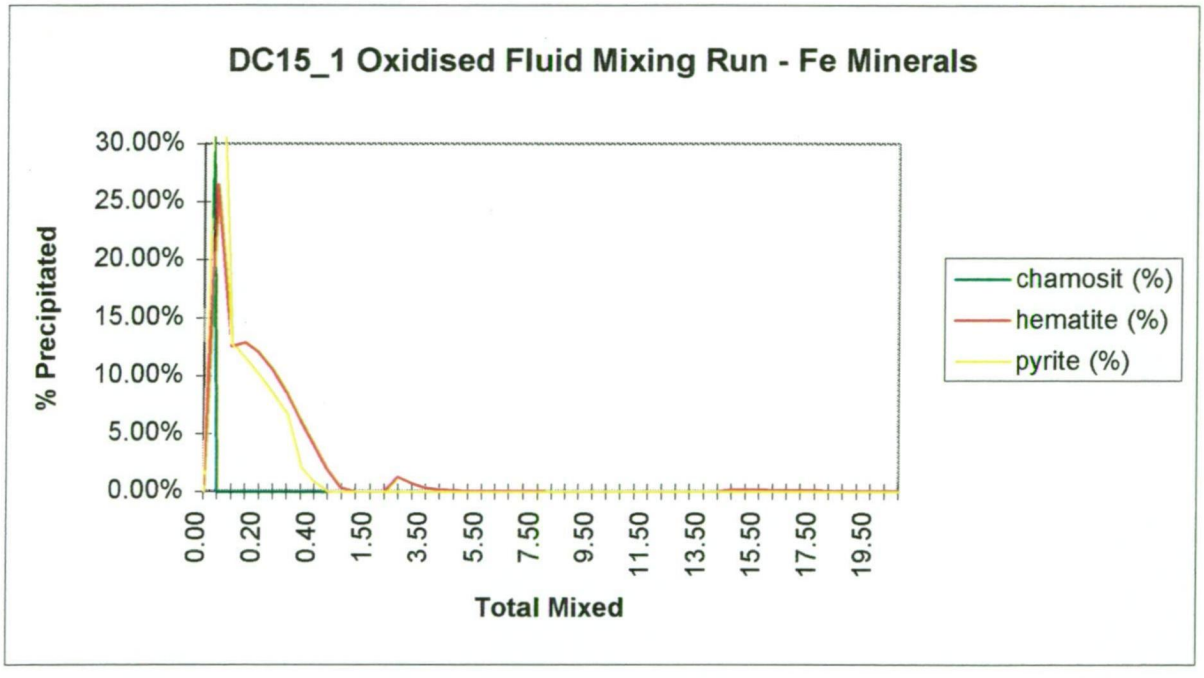
DC15_1 Oxidised Fluid Mixing Run - Fe Minerals
% Precipitated
30.00%
25.00%
20.00%
15.00%
10.00%
5.00%
0.00%
0.00
0.20
0.40
1.50
3.50
5.50
7.50
9.50
11.50
13.50
15.50
17.50
19.50
Total Mixed
chamosit (%)
hematite (%)
pyrite (%)

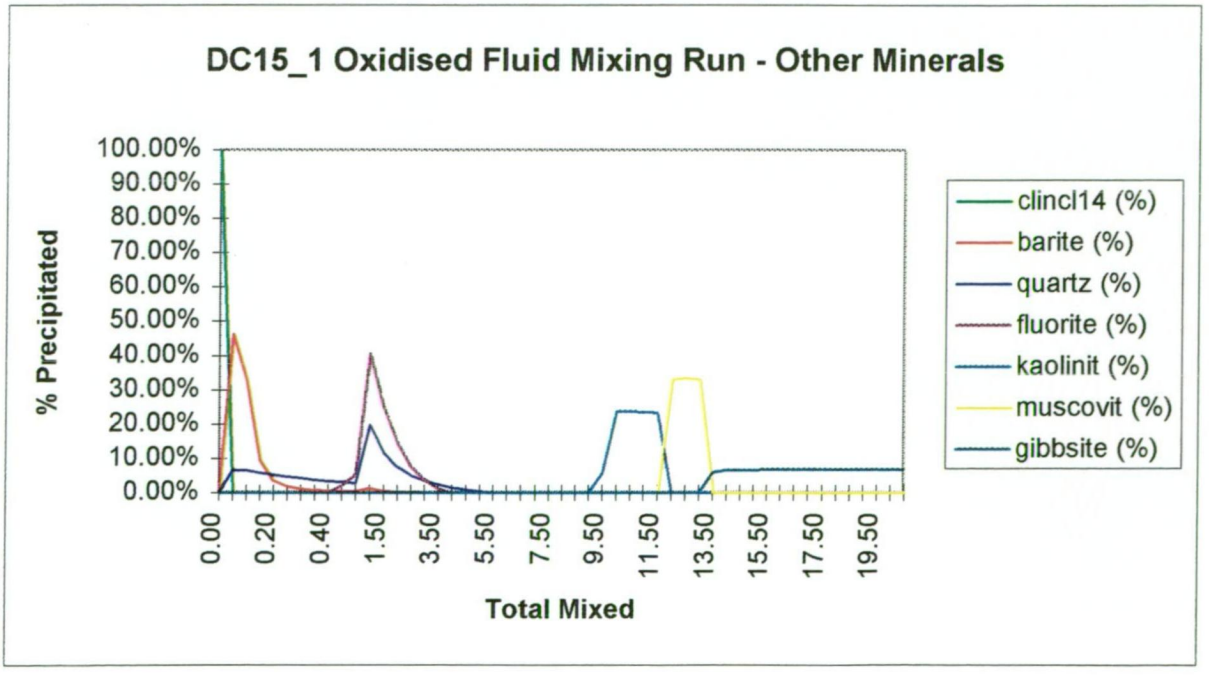
DC15_1 Oxidised Fluid Mixing Run - Other Minerals
% Precipitated
100.00%
90.00%
80.00%
70.00%
60.00%
50.00%
40.00%
30.00%
20.00%
10.00%
0.00%
0.00
0.20
0.40
1.50
3.50
5.50
7.50
9.50
11.50
13.50
15.50
17.50
19.50
Total Mixed
clincl14 (%)
barite (%)
quartz (%)
fluorite (%)
kaolinit (%)
muscovit (%)
gibbsite (%)

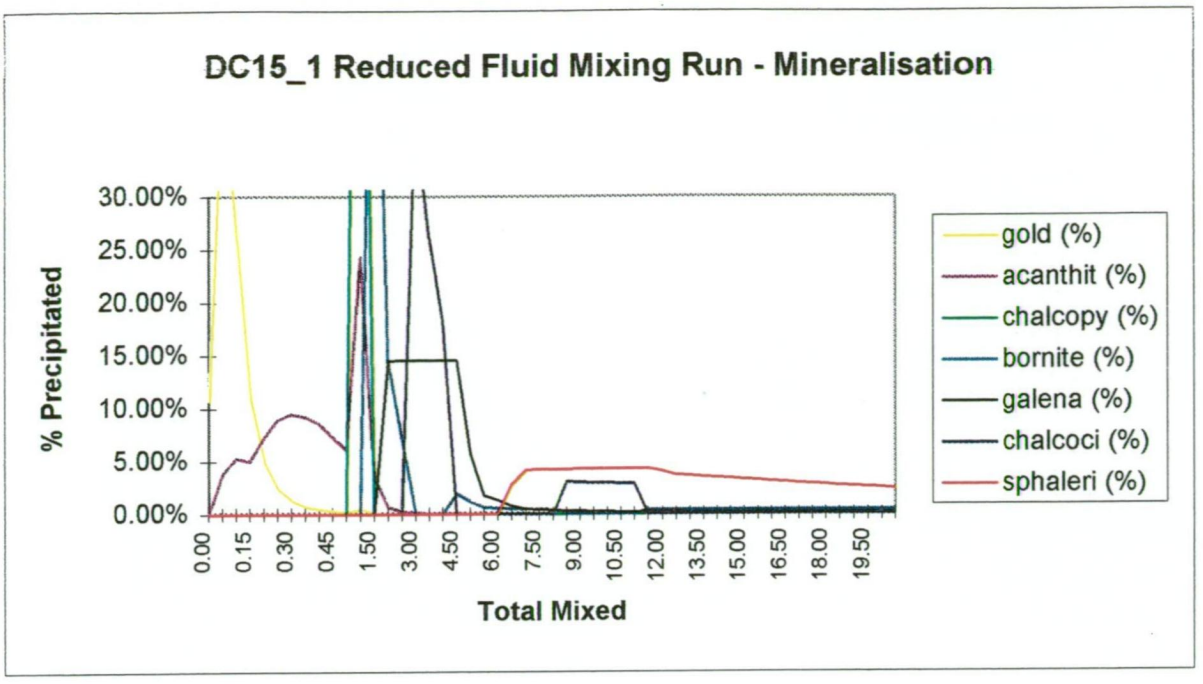
DC15_1 Reduced Fluid Mixing Run - Mineralisation
% Precipitated
30.00%
25.00%
20.00%
15.00%
10.00%
5.00%
0.00%
0.00 0.15 0.30 0.45 1.50 3.00 4.50 6.00 7.50 9.00 10.50 12.00 13.50 15.00 16.50 18.00 19.50
Total Mixed
gold (%)
acanthit (%)
chalcopy (%)
bornite (%)
galena (%)
chalcoci (%)
sphaleri (%)

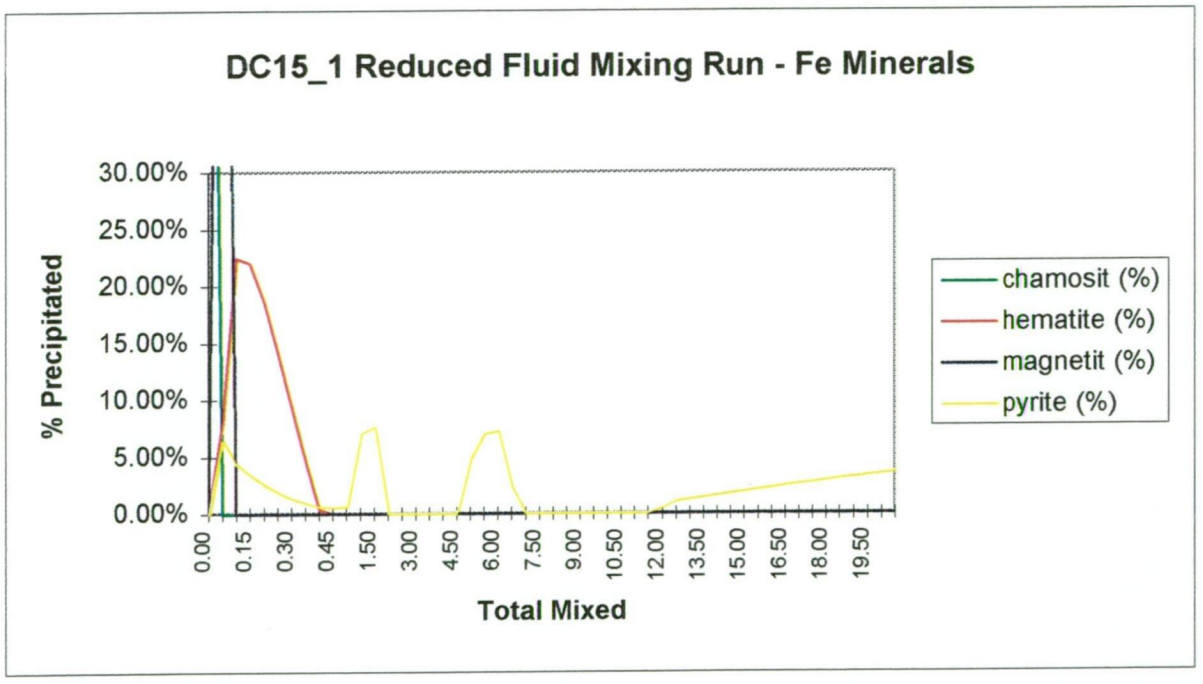
DC15_1 Reduced Fluid Mixing Run - Fe Minerals
% Precipitated
30.00%
25.00%
20.00%
15.00%
10.00%
5.00%
0.00%
0.00 0.15 0.30 0.45 1.50 3.00 4.50 6.00 7.50 9.00 10.50 12.00 13.50 15.00 16.50 18.00 19.50
Total Mixed
chamosit (%)
hematite (%)
magnetit (%)
pyrite (%)

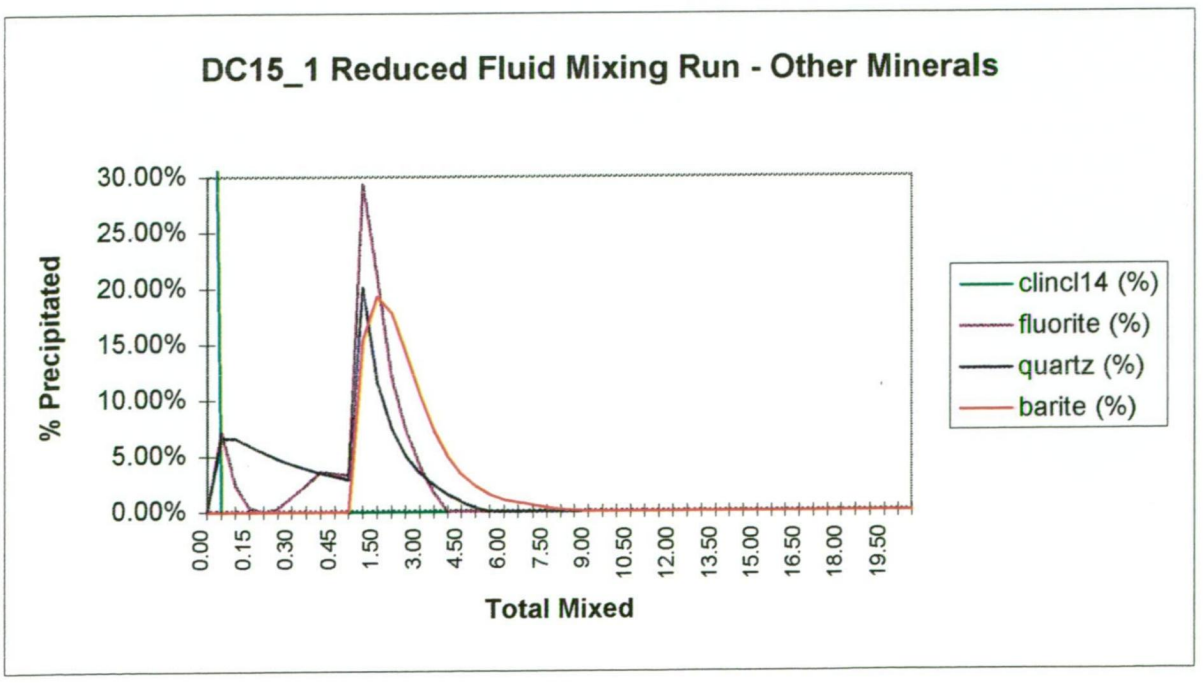
DC15_1 Reduced Fluid Mixing Run - Other Minerals
% Precipitated
30.00%
25.00%
20.00%
15.00%
10.00%
5.00%
0.00%
0.00 0.15 0.30 0.45 1.50 3.00 4.50 6.00 7.50 9.00 10.50 12.00 13.50 15.00 16.50 18.00 19.50
Total Mixed
clincl14 (%)
fluorite (%)
quartz (%)
barite (%)

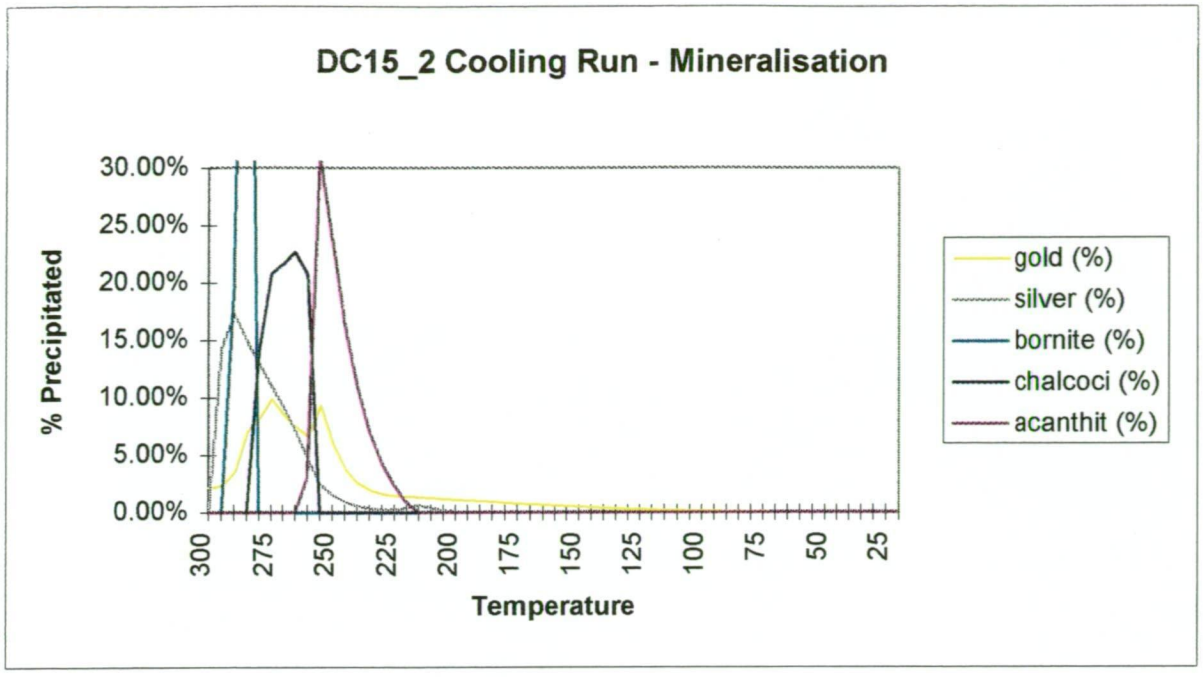
DC15_2 Cooling Run - Mineralisation
% Precipitated
30.00%
25.00%
20.00%
15.00%
10.00%
5.00%
0.00%
300
275
250
225
200
175
150
125
100
75
50
25
Temperature
gold (%)
silver (%)
bornite (%)
chalcoci (%)
acanthit (%)

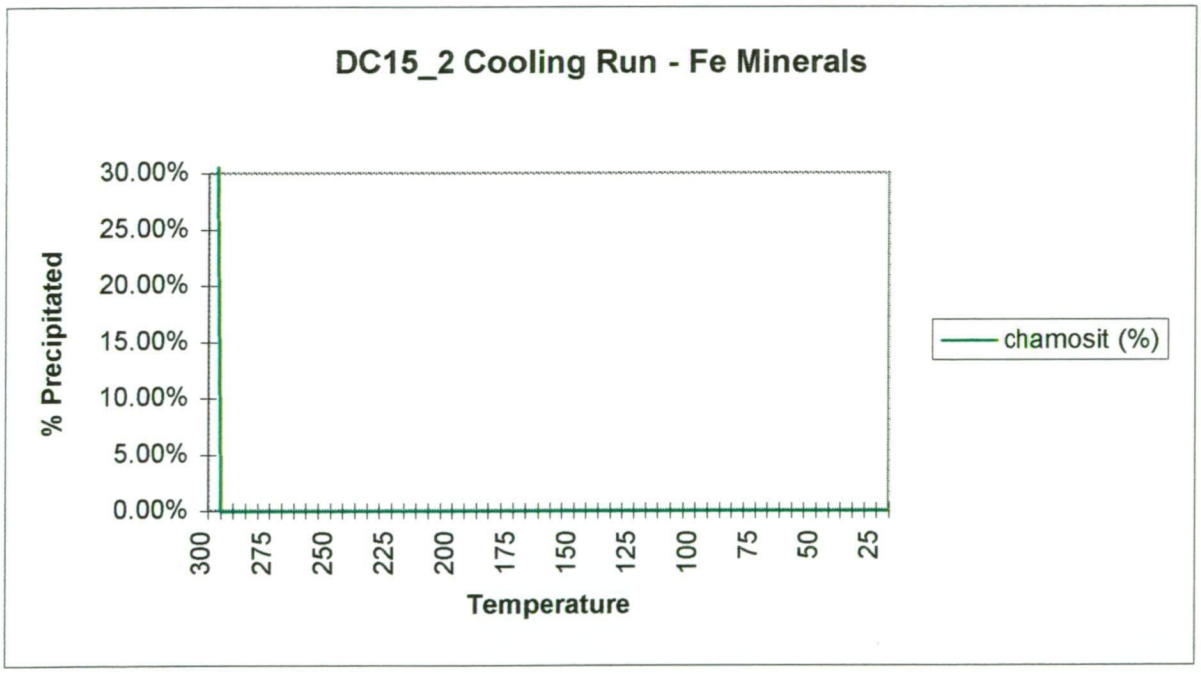
DC15_2 Cooling Run - Fe Minerals
% Precipitated
30.00%
25.00%
20.00%
15.00%
10.00%
5.00%
0.00%
300
275
250
225
200
175
150
125
100
75
50
25
Temperature
chamosit (%)

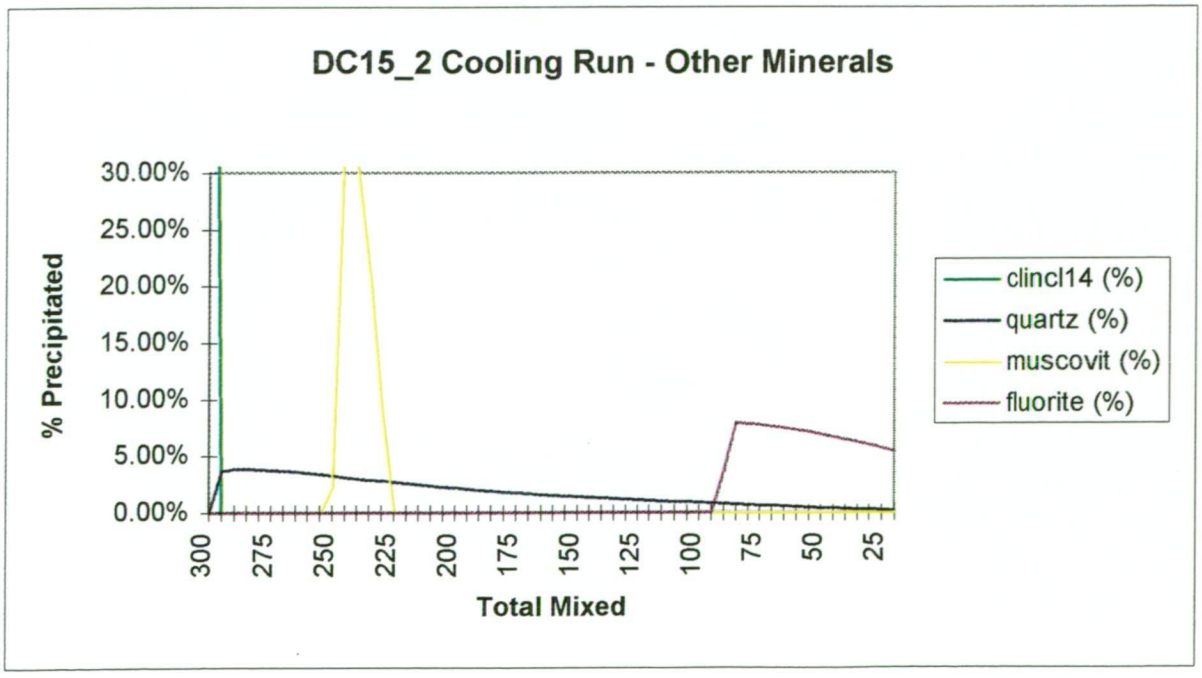
DC15_2 Cooling Run - Other Minerals
% Precipitated
30.00%
25.00%
20.00%
15.00%
10.00%
5.00%
0.00%
300
275
250
225
200
175
150
125
100
75
50
25
Total Mixed
clincl14 (%)
quartz (%)
muscovit (%)
fluorite (%)

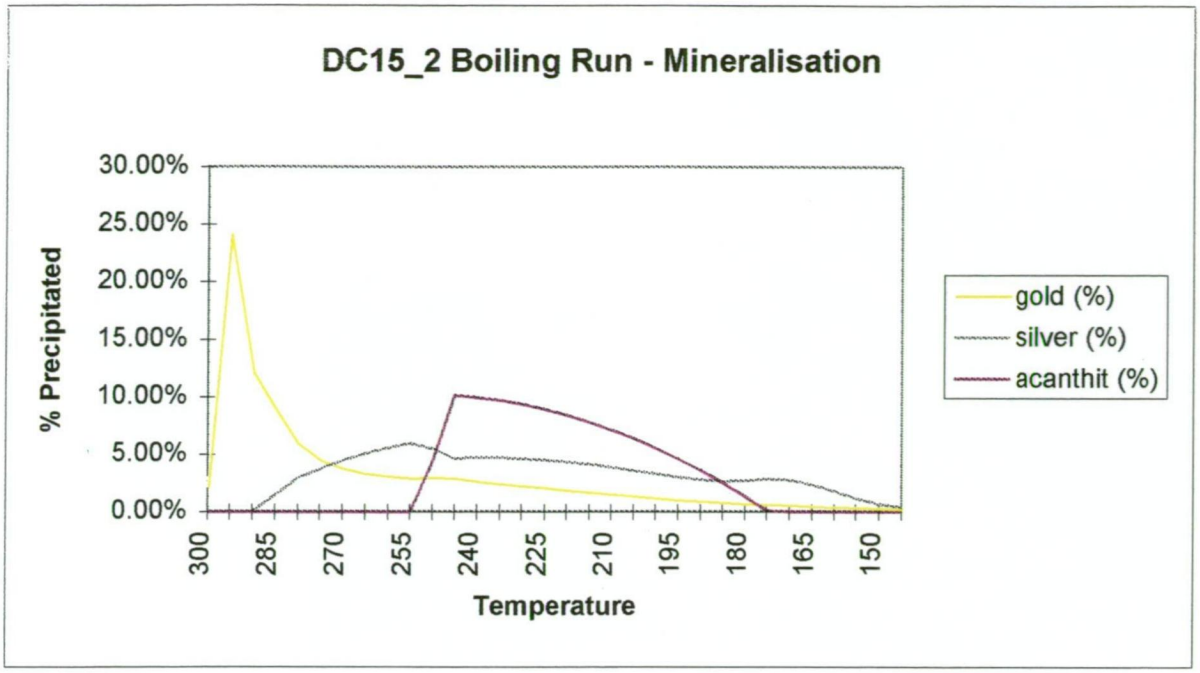
DC15_2 Boiling Run - Mineralisation
% Precipitated
30.00%
25.00%
20.00%
15.00%
10.00%
5.00%
0.00%
300
285
270
255
240
225
210
195
180
165
150
Temperature
gold (%)
silver (%)
acanthit (%)

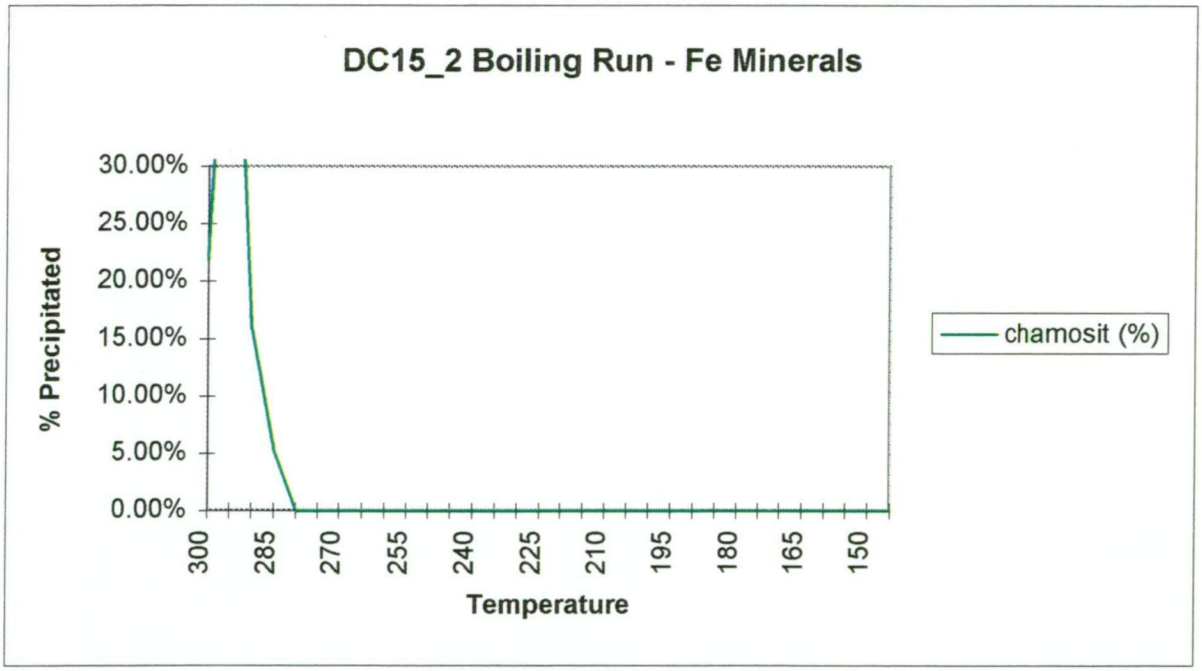
DC15_2 Boiling Run - Fe Minerals
% Precipitated
30.00%
25.00%
20.00%
15.00%
10.00%
5.00%
0.00%
300
285
270
255
240
225
210
195
180
165
150
Temperature
chamosit (%)

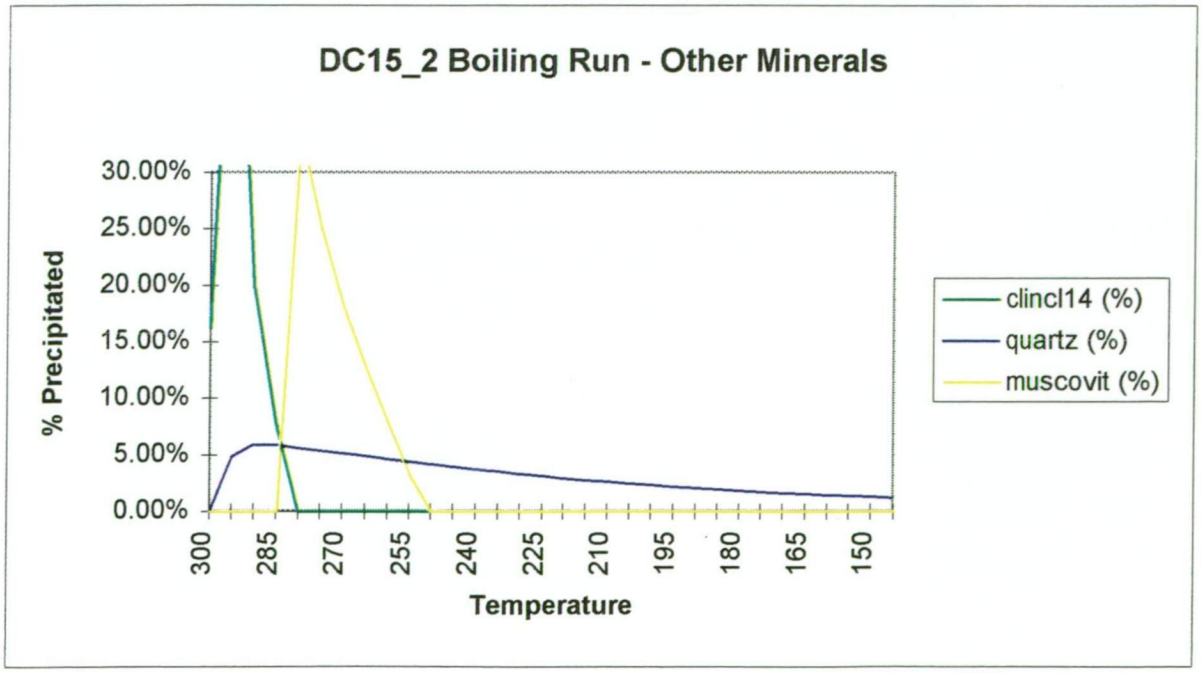
DC15_2 Boiling Run - Other Minerals
% Precipitated
30.00%
25.00%
20.00%
15.00%
10.00%
5.00%
0.00%
300
285
270
255
240
225
210
195
180
165
150
Temperature
clincl14 (%)
quartz (%)
muscovit (%)

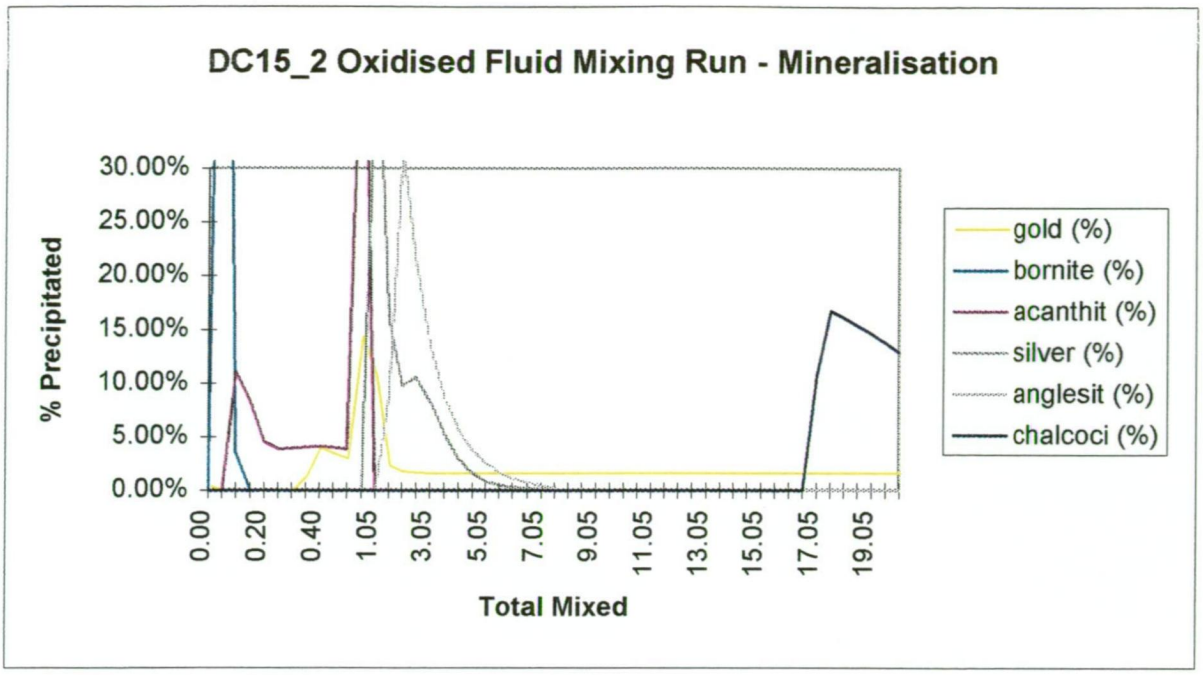
DC15_2 Oxidised Fluid Mixing Run - Mineralisation
% Precipitated
30.00%
25.00%
20.00%
15.00%
10.00%
5.00%
0.00%
0.00
0.20
0.40
1.05
3.05
5.05
7.05
9.05
11.05
13.05
15.05
17.05
19.05
Total Mixed
gold (%)
bornite (%)
acanthit (%)
silver (%)
anglesit (%)
chalcoci (%)

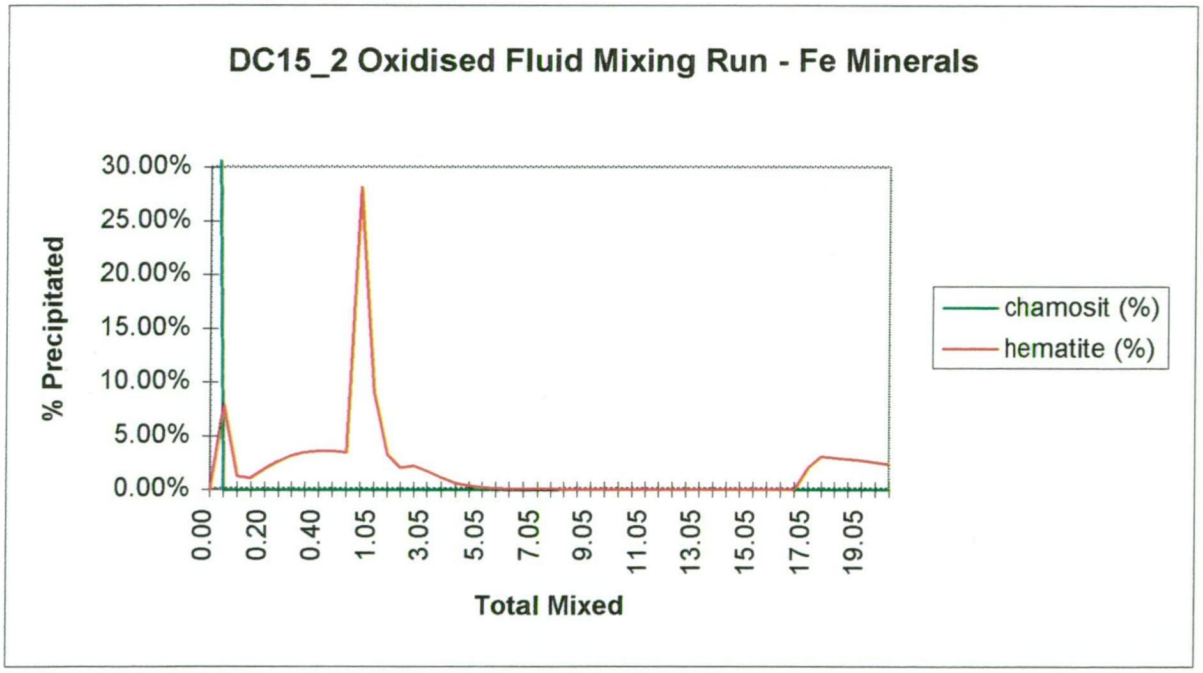
DC15_2 Oxidised Fluid Mixing Run - Fe Minerals
% Precipitated
30.00%
25.00%
20.00%
15.00%
10.00%
5.00%
0.00%
0.00
0.20
0.40
1.05
3.05
5.05
7.05
9.05
11.05
13.05
15.05
17.05
19.05
Total Mixed
chamosit (%)
hematite (%)

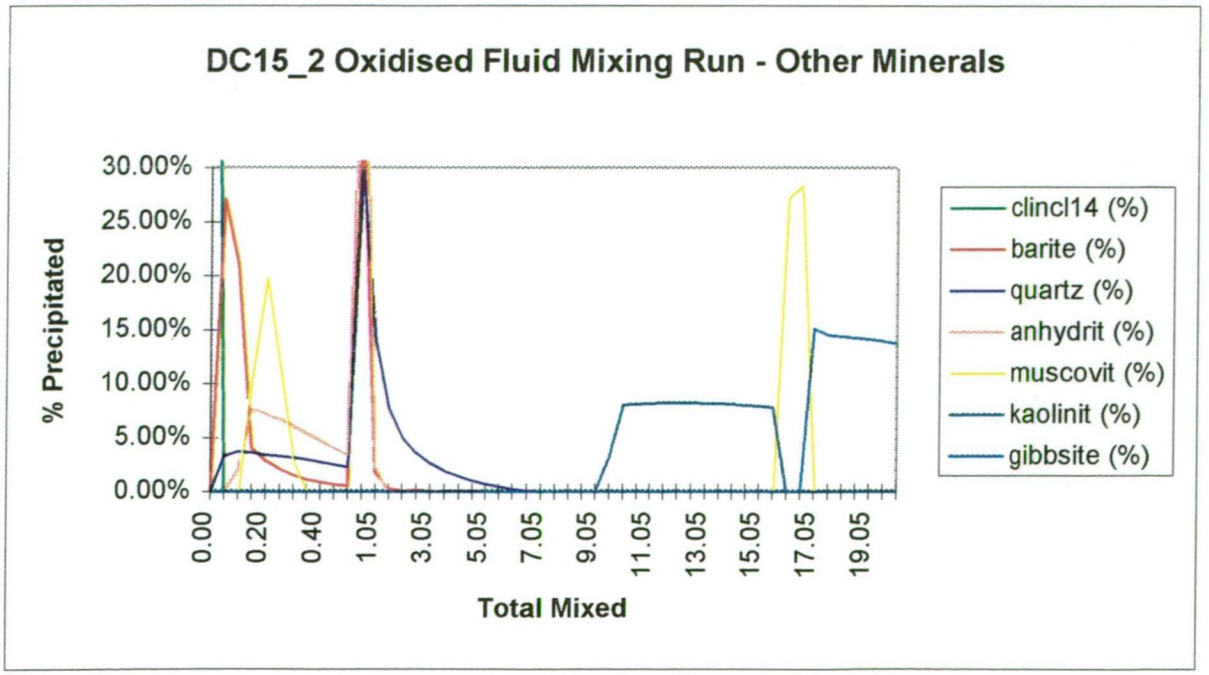
DC15_2 Oxidised Fluid Mixing Run - Other Minerals
% Precipitated
30.00%
25.00%
20.00%
15.00%
10.00%
5.00%
0.00%
0.00
0.20
0.40
1.05
3.05
5.05
7.05
9.05
11.05
13.05
15.05
17.05
19.05
Total Mixed
clincl14 (%)
barite (%)
quartz (%)
anhydrit (%)
muscovit (%)
kaolinit (%)
gibbsite (%)

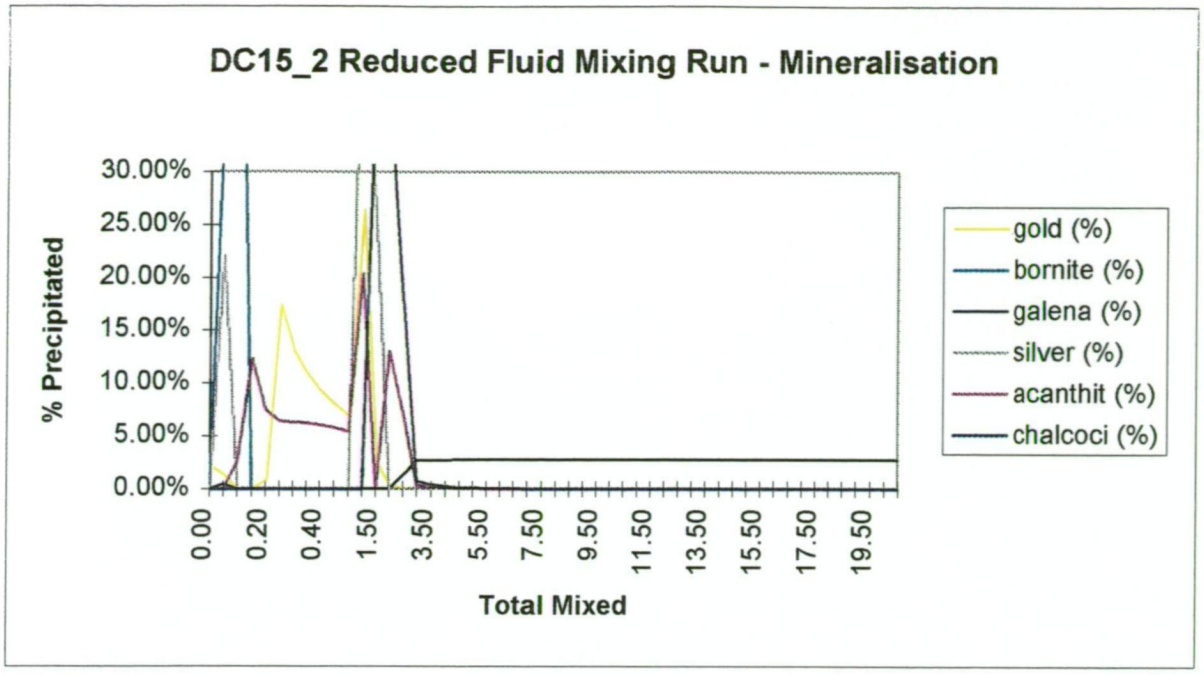
DC15_2 Reduced Fluid Mixing Run - Mineralisation
% Precipitated
30.00%
25.00%
20.00%
15.00%
10.00%
5.00%
0.00%
0.00
0.20
0.40
1.50
3.50
5.50
7.50
9.50
11.50
13.50
15.50
17.50
19.50
Total Mixed
gold (%)
bornite (%)
galena (%)
silver (%)
acanthit (%)
chalcoci (%)

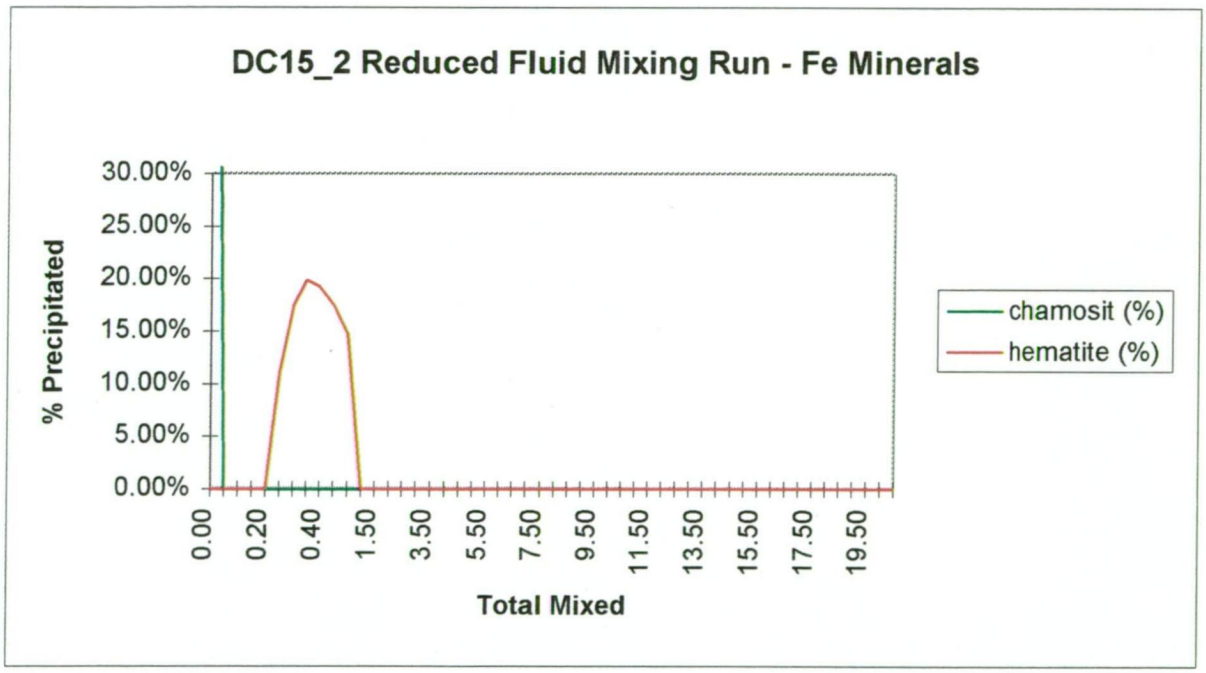
DC15_2 Reduced Fluid Mixing Run - Fe Minerals
% Precipitated
30.00%
25.00%
20.00%
15.00%
10.00%
5.00%
0.00%
0.00
0.20
0.40
1.50
3.50
5.50
7.50
9.50
11.50
13.50
15.50
17.50
19.50
Total Mixed
chamosit (%)
hematite (%)

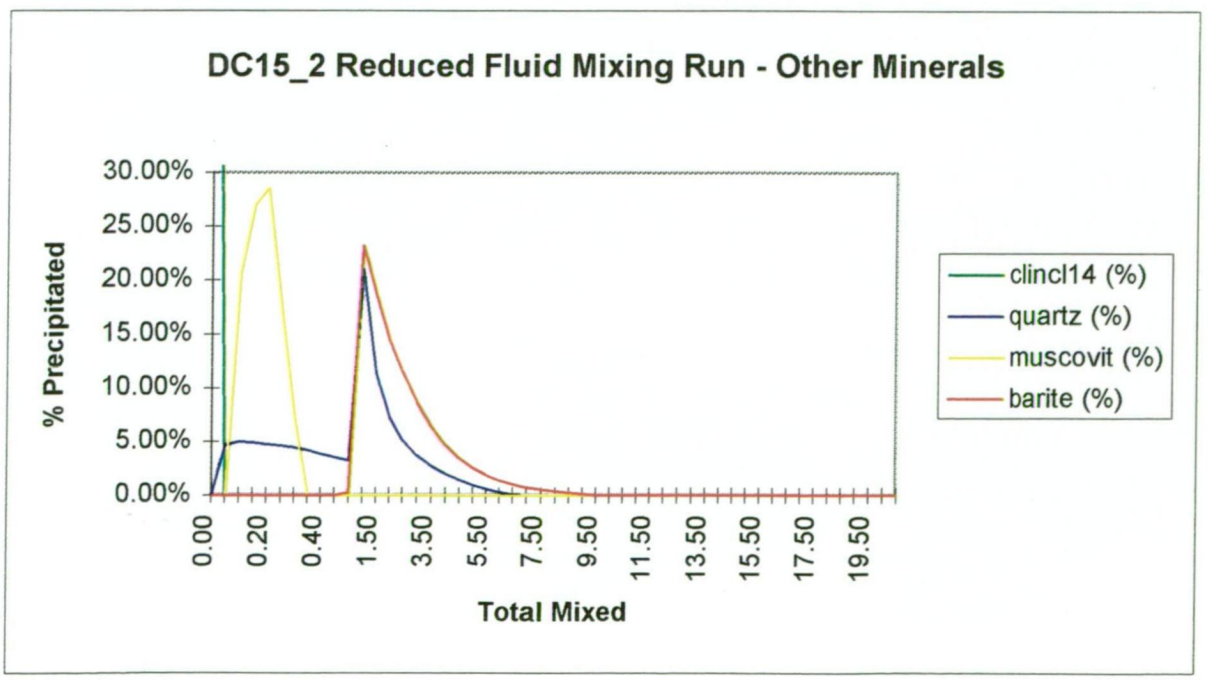
DC15_2 Reduced Fluid Mixing Run - Other Minerals
% Precipitated
30.00%
25.00%
20.00%
15.00%
10.00%
5.00%
0.00%
0.00
0.20
0.40
1.50
3.50
5.50
7.50
9.50
11.50
13.50
15.50
17.50
19.50
Total Mixed
clincl14 (%)
quartz (%)
muscovit (%)
barite (%)

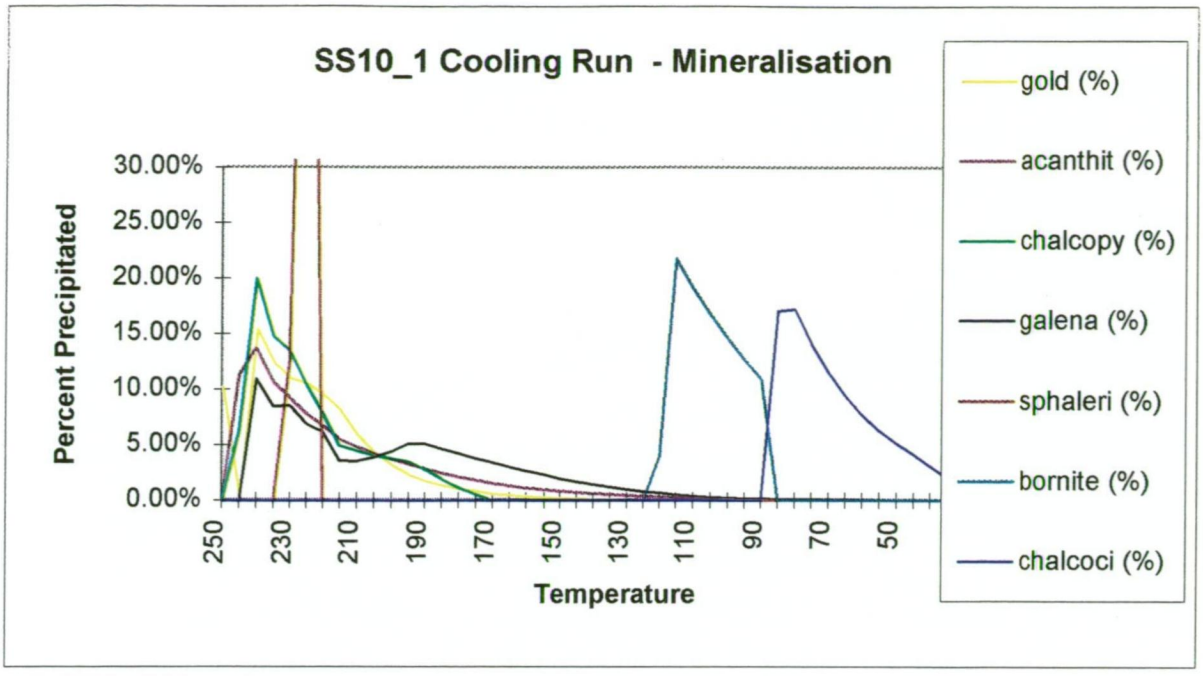
SS10_1 Cooling Run - Mineralisation
Percent Precipitated
30.00%
25.00%
20.00%
15.00%
10.00%
5.00%
0.00%
250
230
210
190
170
150
130
110
90
70
50
Temperature
gold (%)
acanthit (%)
chalcopy (%)
galena (%)
sphaleri (%)
bornite (%)
chalcoci (%)

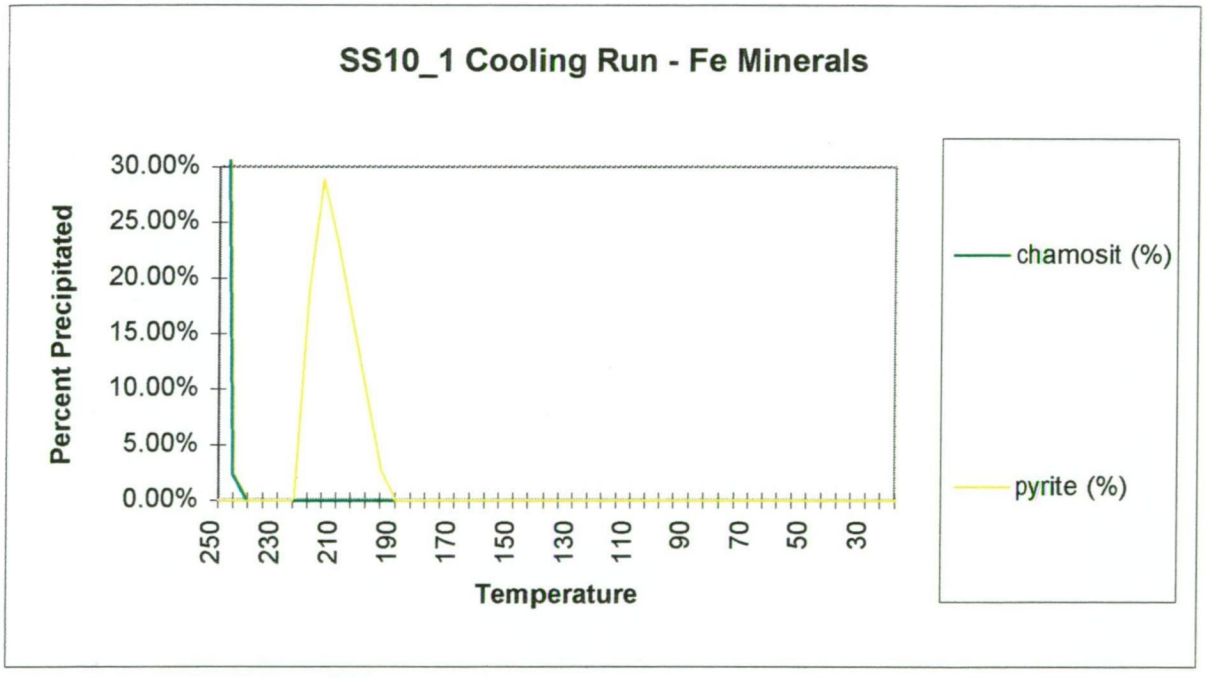
SS10_1 Cooling Run - Fe Minerals
Percent Precipitated
30.00%
25.00%
20.00%
15.00%
10.00%
5.00%
0.00%
250
230
210
190
170
150
130
110
90
70
50
30
Temperature
chamosit (%)
pyrite (%)

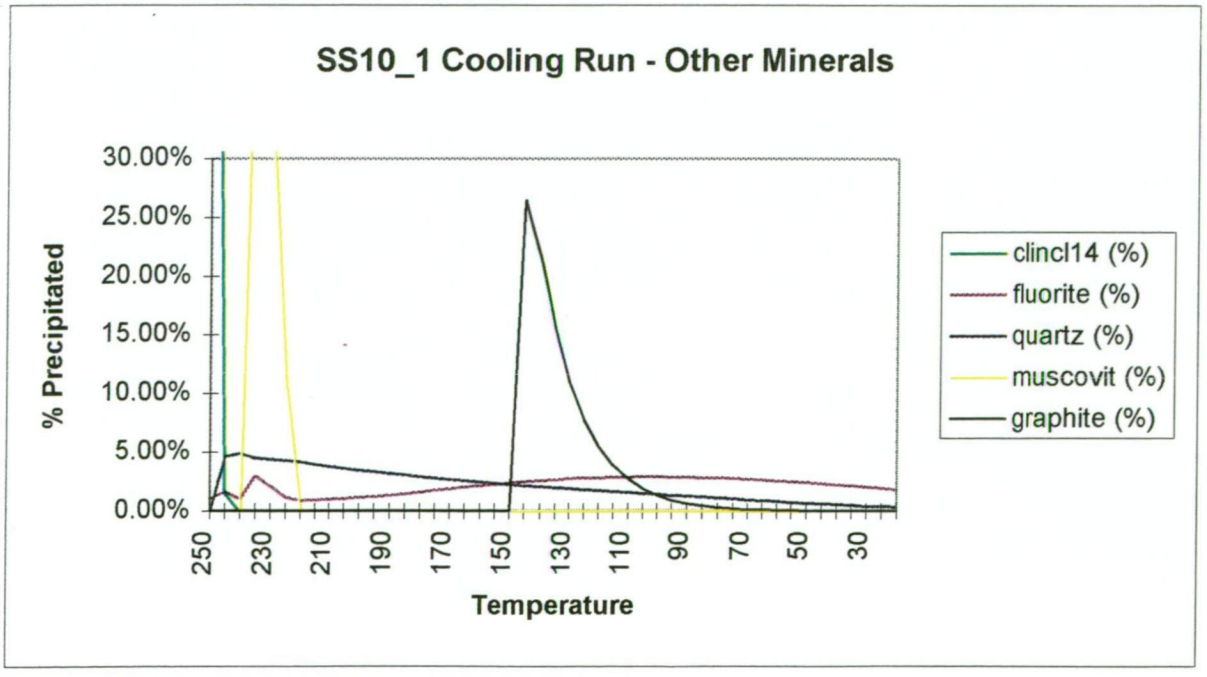
SS10_1 Cooling Run - Other Minerals
% Precipitated
30.00%
25.00%
20.00%
15.00%
10.00%
5.00%
0.00%
250
230
210
190
170
150
130
110
90
70
50
30
Temperature
clincl14 (%)
fluorite (%)
quartz (%)
muscovit (%)
graphite (%)

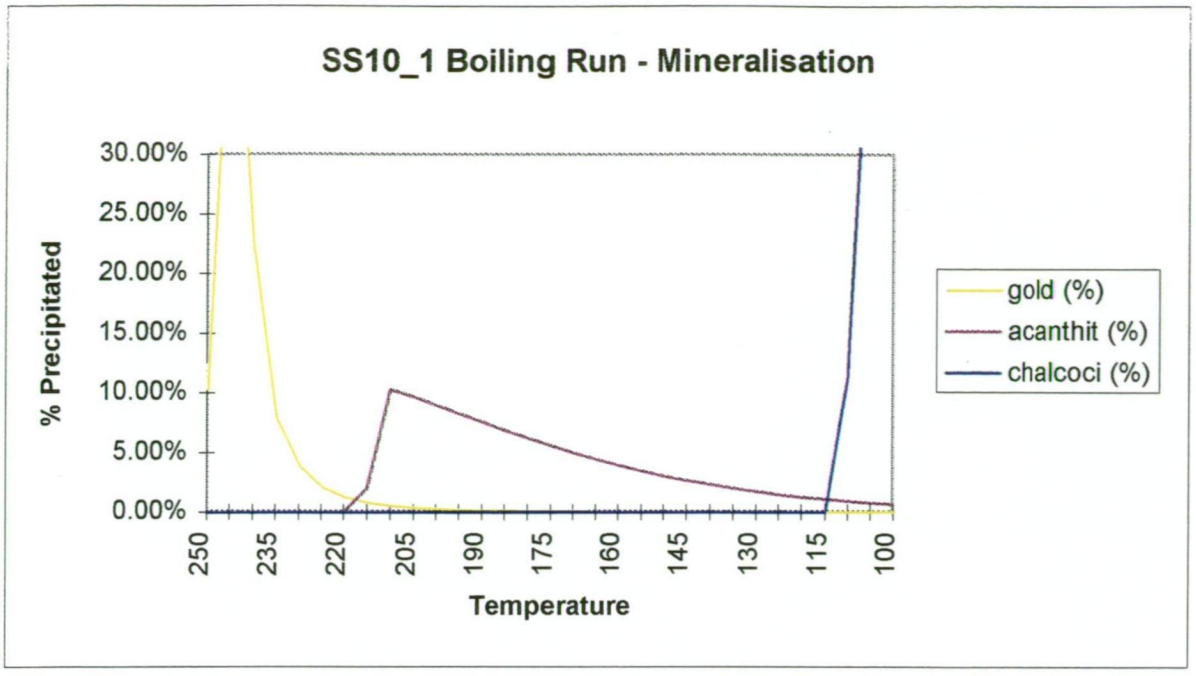
SS10_1 Boiling Run - Mineralisation
% Precipitated
30.00%
25.00%
20.00%
15.00%
10.00%
5.00%
0.00%
250
235
220
205
190
175
160
145
130
115
100
Temperature
gold (%)
acanthit (%)
chalcoci (%)

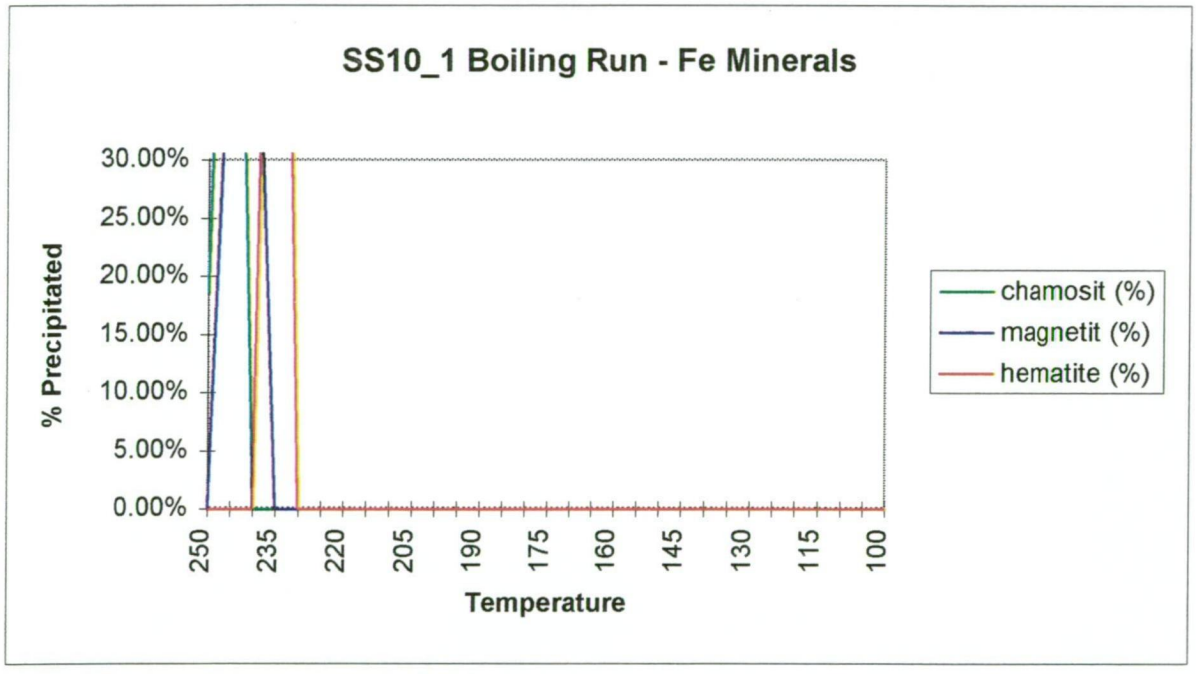
SS10_1 Boiling Run - Fe Minerals
% Precipitated
30.00%
25.00%
20.00%
15.00%
10.00%
5.00%
0.00%
250
235
220
205
190
175
160
145
130
115
100
Temperature
chamosit (%)
magnetit (%)
hematite (%)

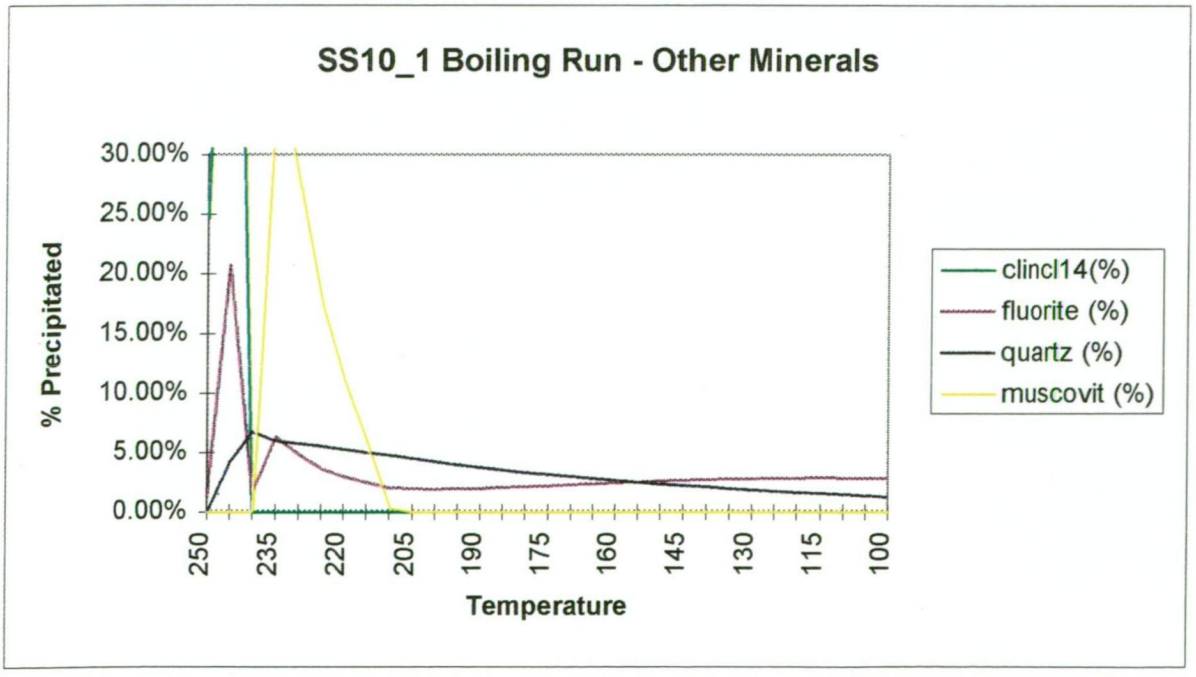
SS10_1 Boiling Run - Other Minerals
% Precipitated
30.00%
25.00%
20.00%
15.00%
10.00%
5.00%
0.00%
250
235
220
205
190
175
160
145
130
115
100
Temperature
clincl14(%)
fluorite (%)
quartz (%)
muscovit (%)

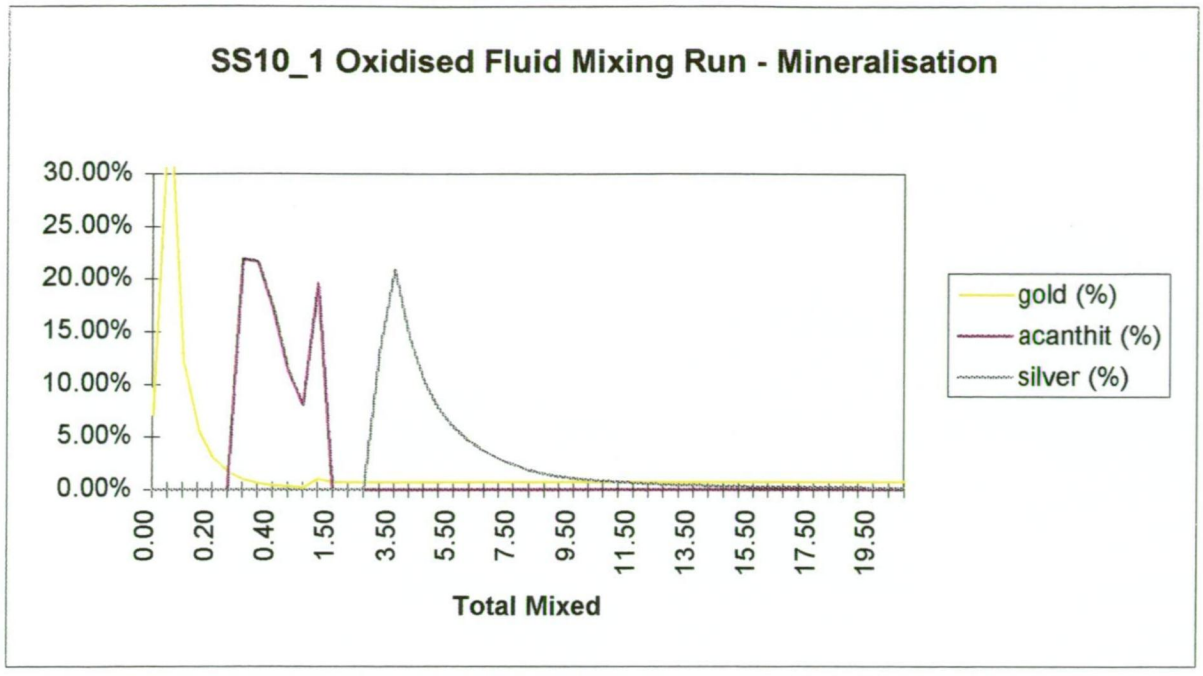
SS10_1 Oxidised Fluid Mixing Run - Mineralisation
30.00%
25.00%
20.00%
15.00%
10.00%
5.00%
0.00%
0.00
0.20
0.40
1.50
3.50
5.50
7.50
9.50
11.50
13.50
15.50
17.50
19.50
Total Mixed
gold (%)
acanthit (%)
silver (%)

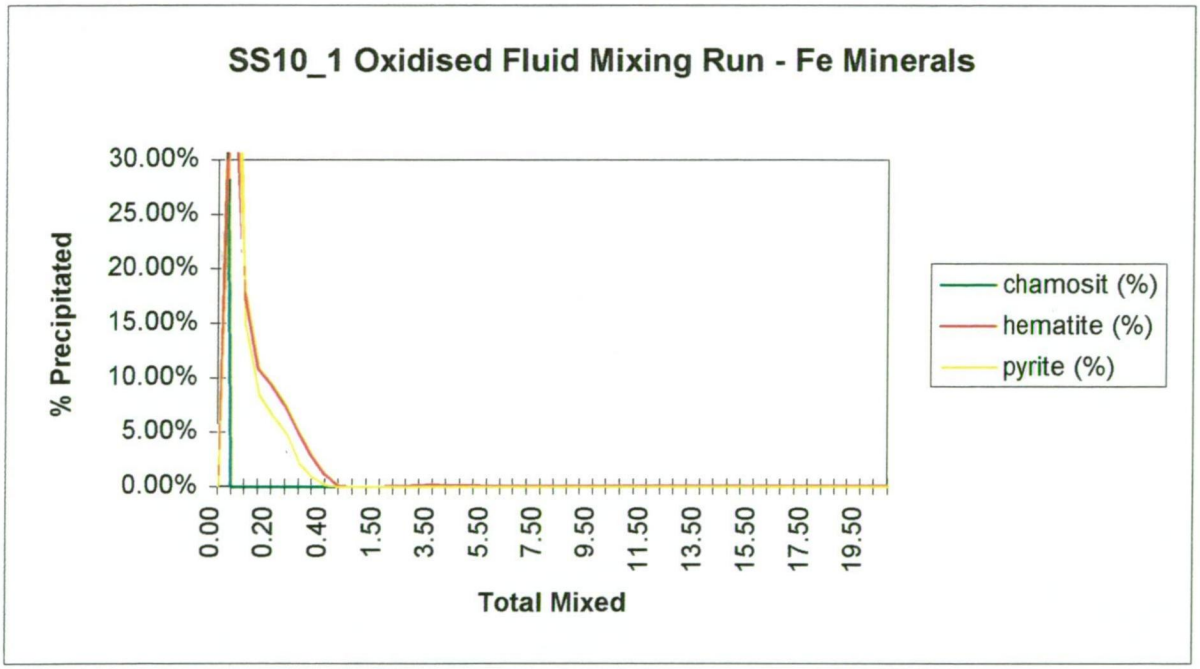
SS10_1 Oxidised Fluid Mixing Run - Fe Minerals
% Precipitated
30.00%
25.00%
20.00%
15.00%
10.00%
5.00%
0.00%
0.00
0.20
0.40
1.50
3.50
5.50
7.50
9.50
11.50
13.50
15.50
17.50
19.50
Total Mixed
chamosit (%)
hematite (%)
pyrite (%)

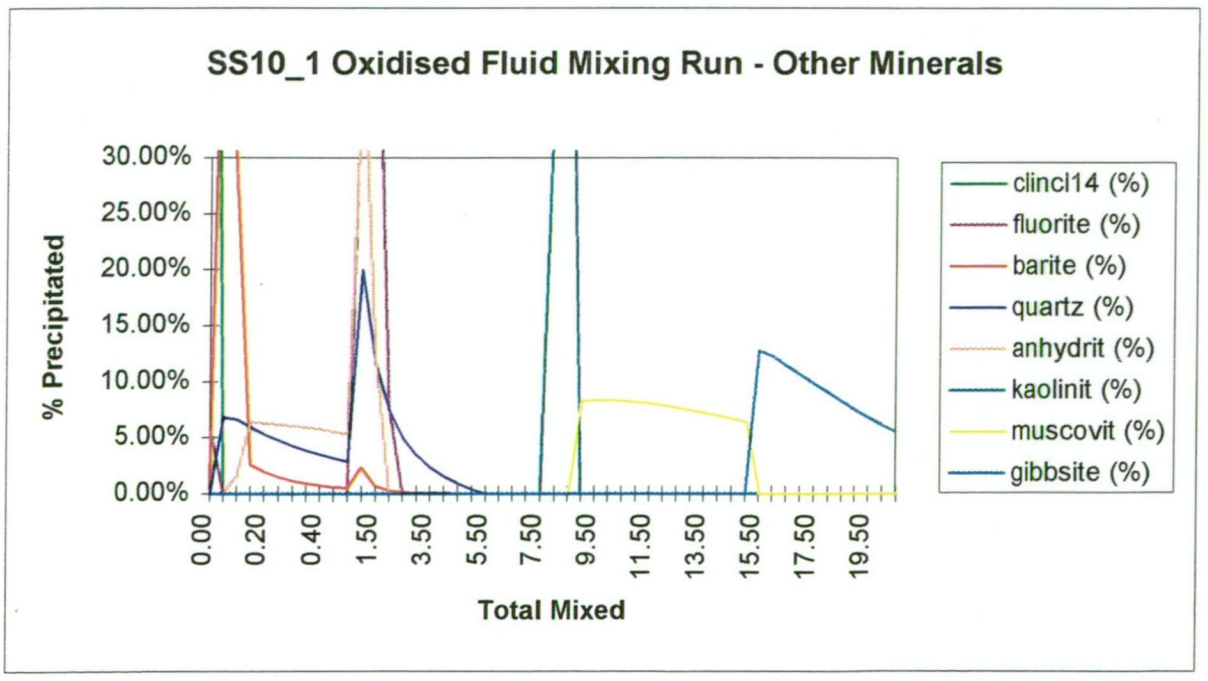
SS10_1 Oxidised Fluid Mixing Run - Other Minerals
% Precipitated
30.00%
25.00%
20.00%
15.00%
10.00%
5.00%
0.00%
0.00
0.20
0.40
1.50
3.50
5.50
7.50
9.50
11.50
13.50
15.50
17.50
19.50
Total Mixed
clincl14 (%)
fluorite (%)
barite (%)
quartz (%)
anhydrit (%)
kaolinit (%)
muscovit (%)
gibbsite (%)

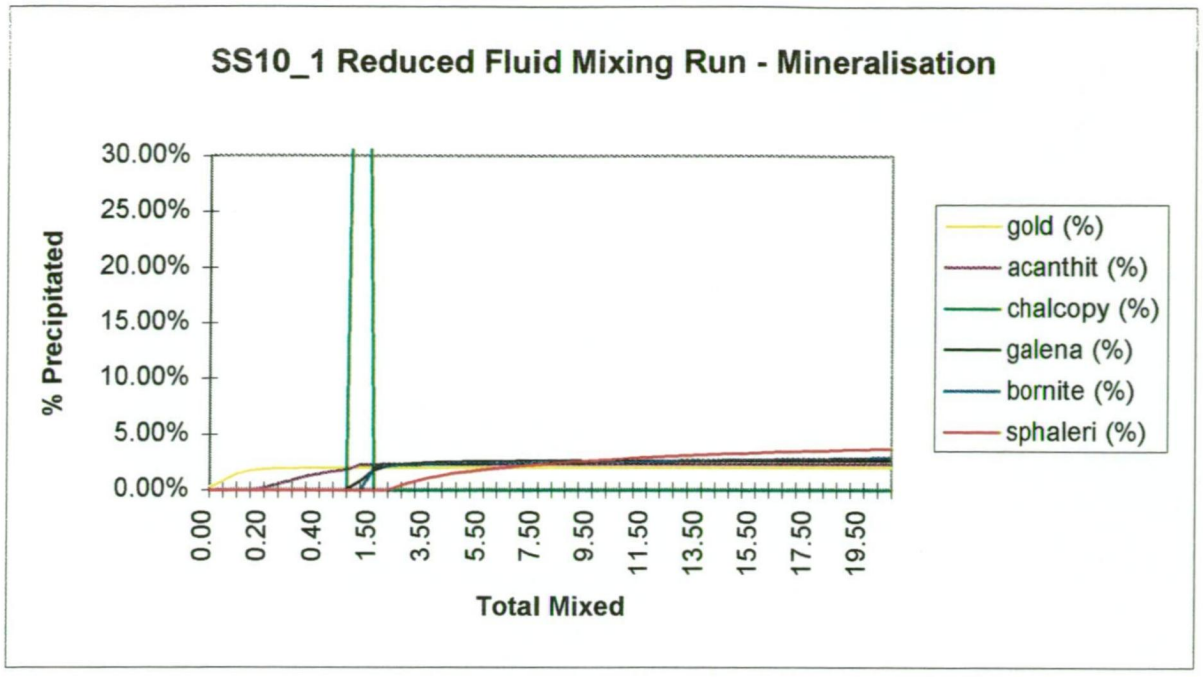
SS10_1 Reduced Fluid Mixing Run - Mineralisation
% Precipitated
30.00%
25.00%
20.00%
15.00%
10.00%
5.00%
0.00%
0.00
0.20
0.40
1.50
3.50
5.50
7.50
9.50
11.50
13.50
15.50
17.50
19.50
Total Mixed
gold (%)
acanthit (%)
chalcopy (%)
galena (%)
bornite (%)
sphaleri (%)

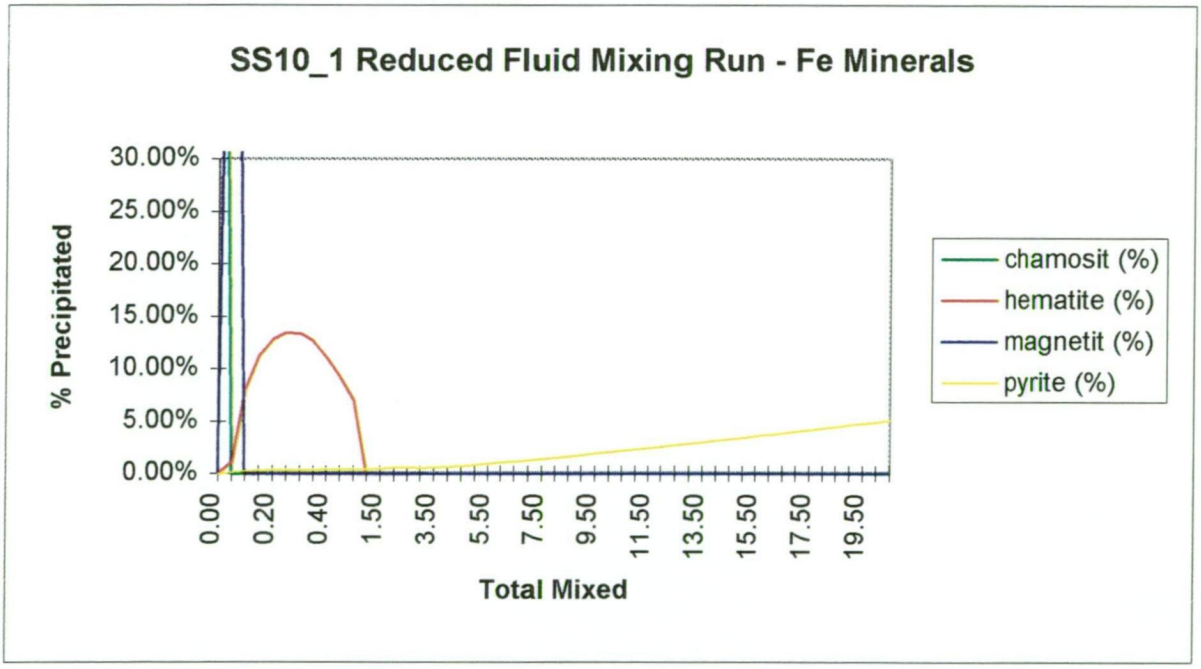
SS10_1 Reduced Fluid Mixing Run - Fe Minerals
% Precipitated
30.00%
25.00%
20.00%
15.00%
10.00%
5.00%
0.00%
0.00
0.20
0.40
1.50
3.50
5.50
7.50
9.50
11.50
13.50
15.50
17.50
19.50
Total Mixed
chamosit (%)
hematite (%)
magnetit (%)
pyrite (%)

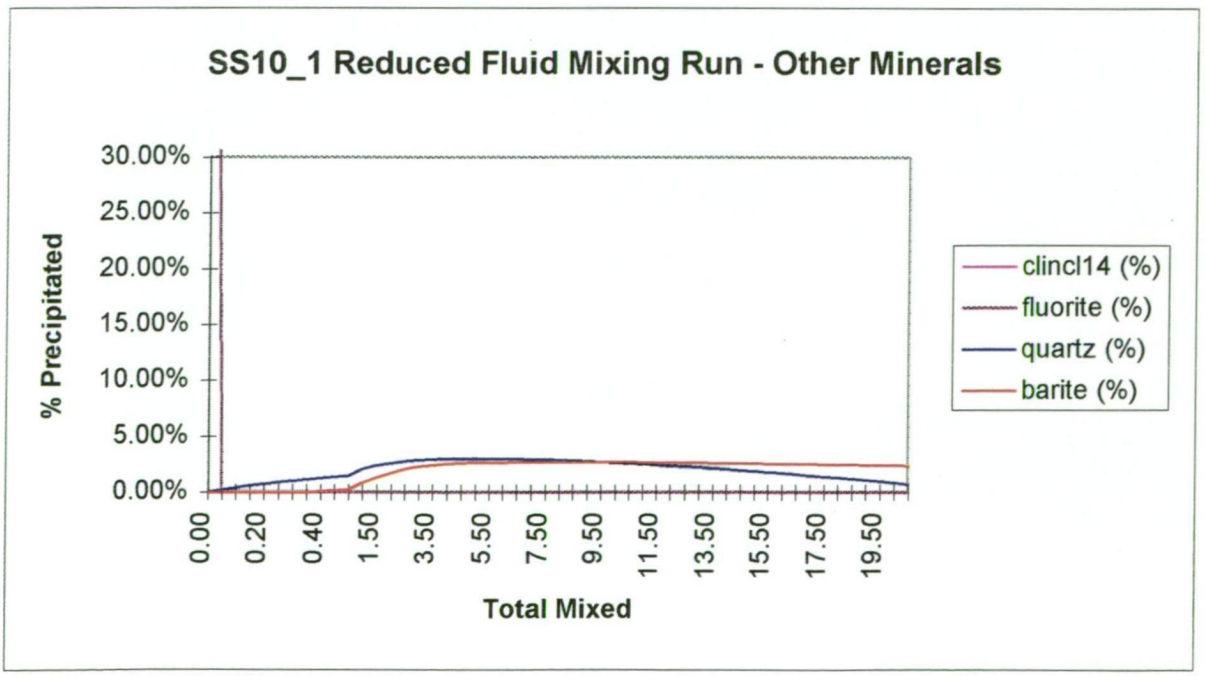
SS10_1 Reduced Fluid Mixing Run - Other Minerals
% Precipitated
30.00%
25.00%
20.00%
15.00%
10.00%
5.00%
0.00%
0.00
0.20
0.40
1.50
3.50
5.50
7.50
9.50
11.50
13.50
15.50
17.50
19.50
Total Mixed
clincl14 (%)
fluorite (%)
quartz (%)
barite (%)

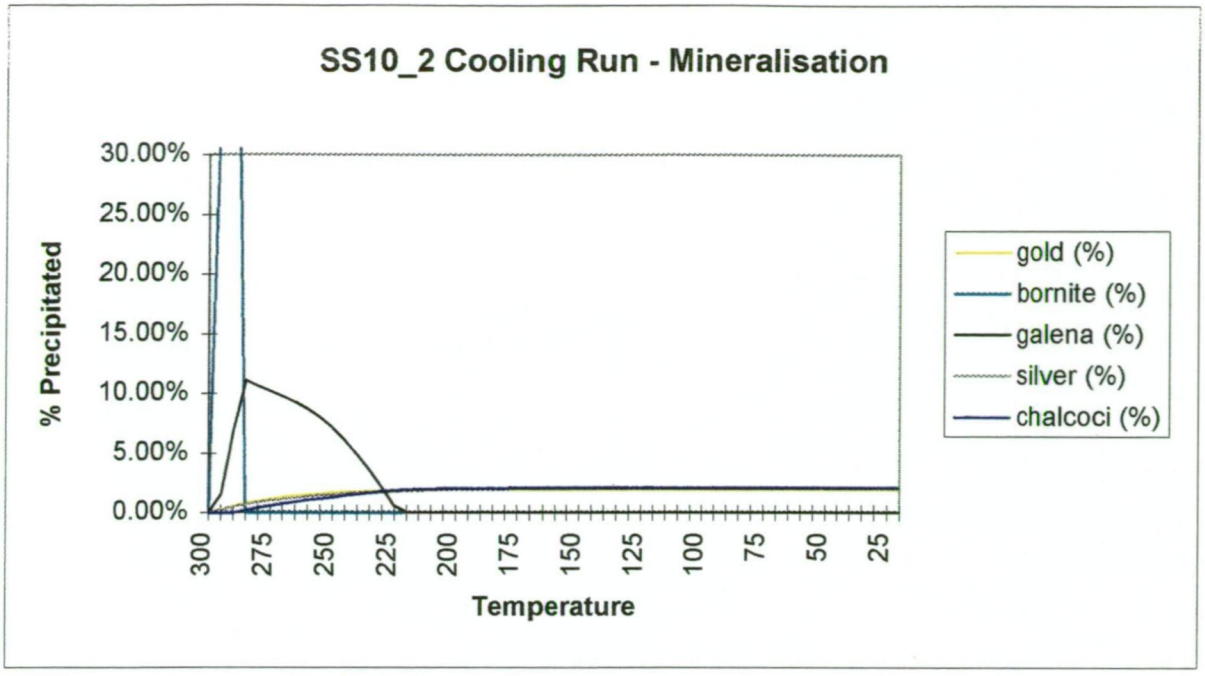
SS10_2 Cooling Run - Mineralisation
% Precipitated
30.00%
25.00%
20.00%
15.00%
10.00%
5.00%
0.00%
300
275
250
225
200
175
150
125
100
75
50
25
Temperature
gold (%)
bornite (%)
galena (%)
silver (%)
chalcoci (%)

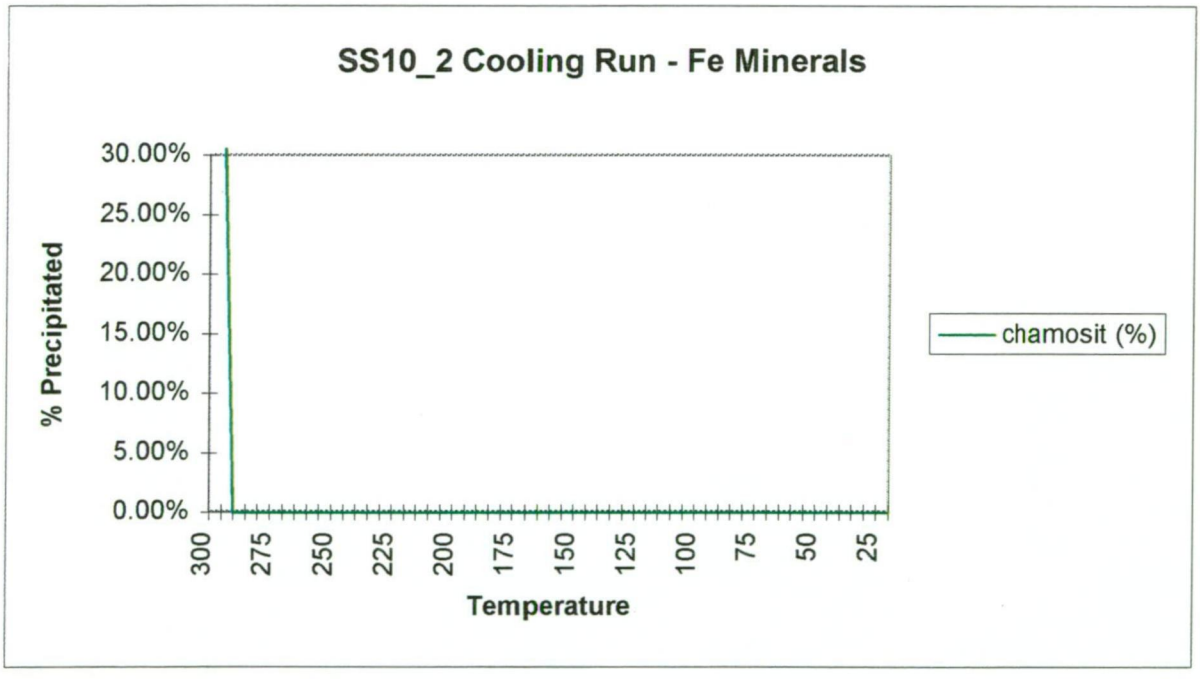
SS10_2 Cooling Run - Fe Minerals
% Precipitated
30.00%
25.00%
20.00%
15.00%
10.00%
5.00%
0.00%
300
275
250
225
200
175
150
125
100
75
50
25
Temperature
chamosit (%)

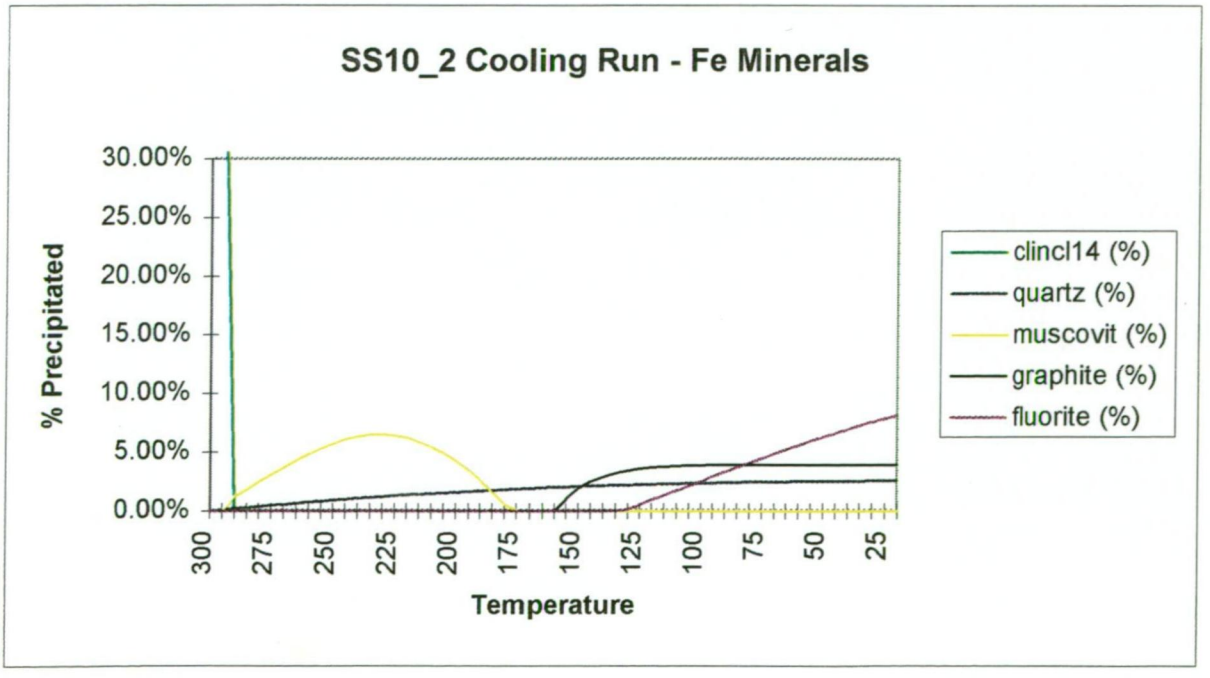
SS10_2 Cooling Run - Fe Minerals
% Precipitated
30.00%
25.00%
20.00%
15.00%
10.00%
5.00%
0.00%
300
275
250
225
200
175
150
125
100
75
50
25
Temperature
clincl14 (%)
quartz (%)
muscovit (%)
graphite (%)
fluorite (%)

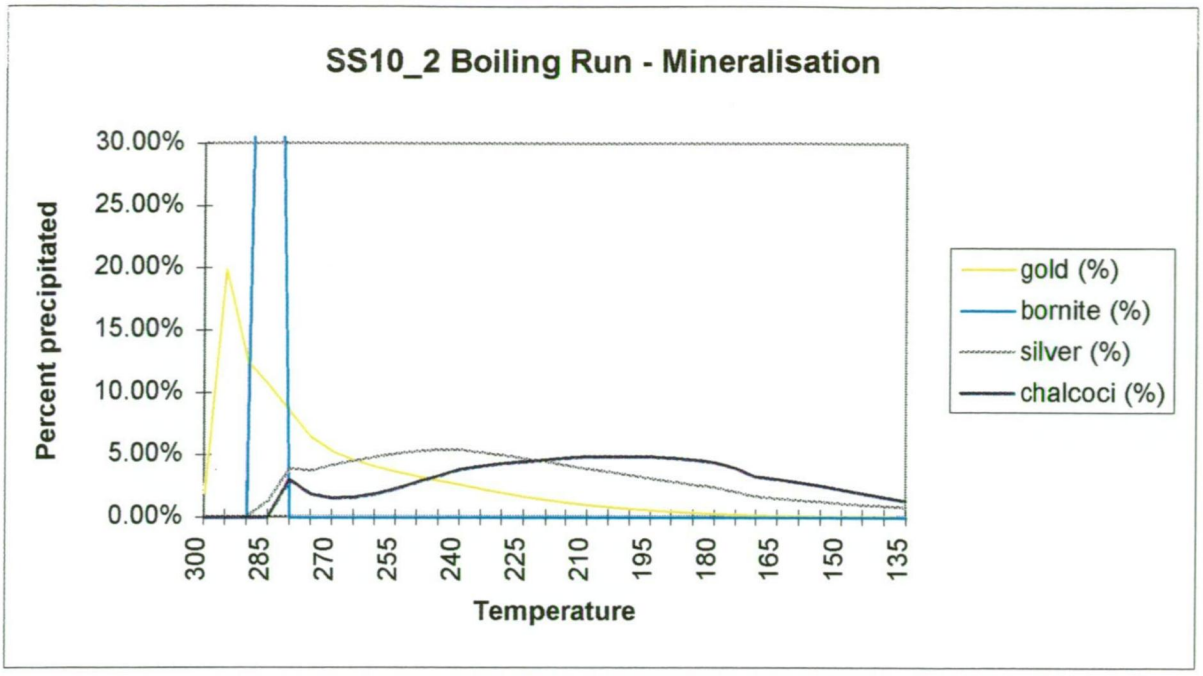
SS10_2 Boiling Run - Mineralisation
Percent precipitated
30.00%
25.00%
20.00%
15.00%
10.00%
5.00%
0.00%
300
285
270
255
240
225
210
195
180
165
150
135
Temperature
gold (%)
bornite (%)
silver (%)
chalcoci (%)

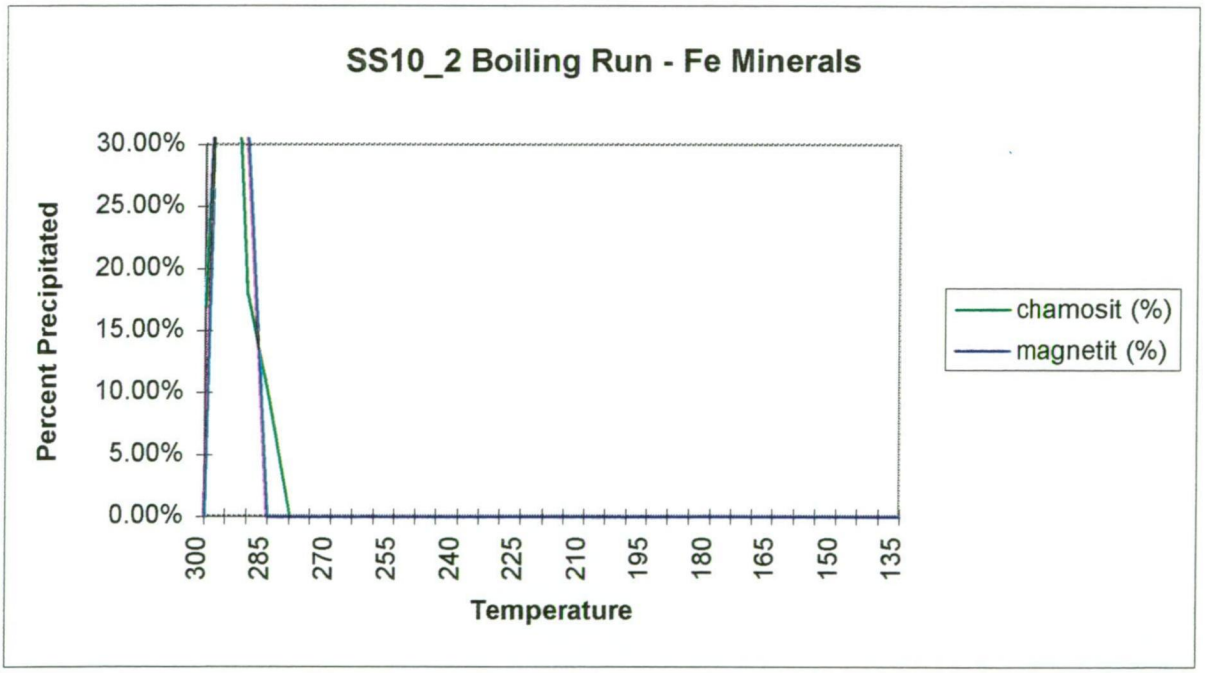
SS10_2 Boiling Run - Fe Minerals
Percent Precipitated
30.00%
25.00%
20.00%
15.00%
10.00%
5.00%
0.00%
300
285
270
255
240
225
210
195
180
165
150
135
Temperature
chamosit (%)
magnetit (%)

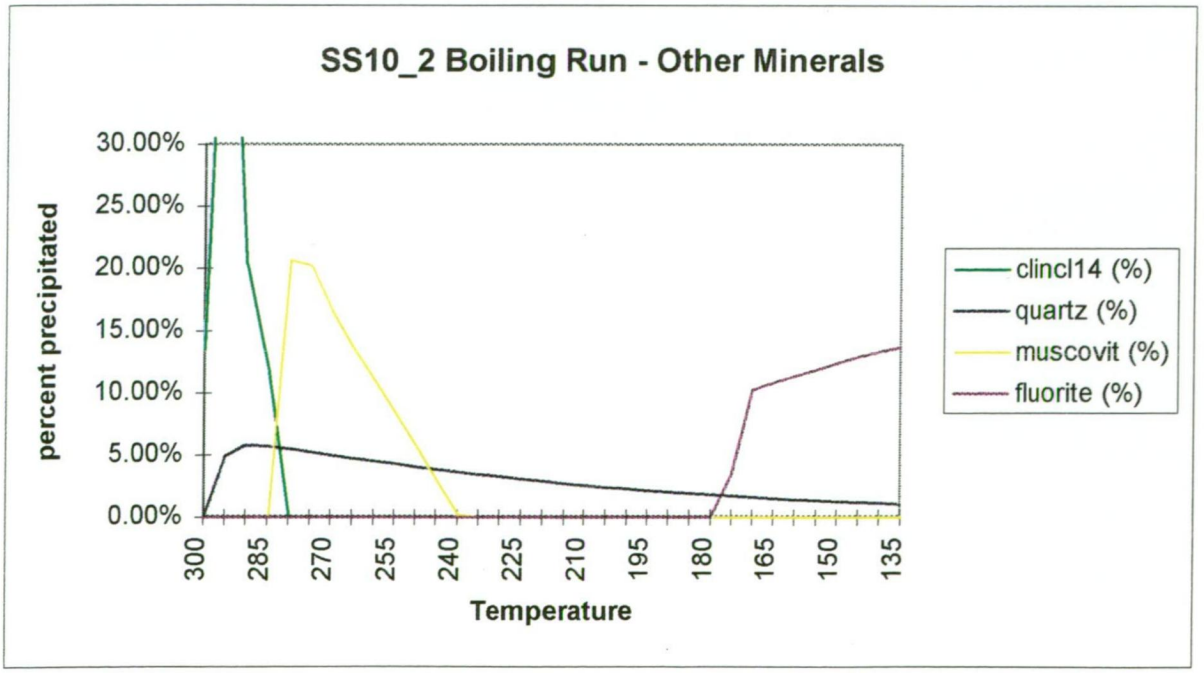
SS10_2 Boiling Run - Other Minerals
percent precipitated
30.00%
25.00%
20.00%
15.00%
10.00%
5.00%
0.00%
300
285
270
255
240
225
210
195
180
165
150
135
Temperature
clincl14 (%)
quartz (%)
muscovit (%)
fluorite (%)

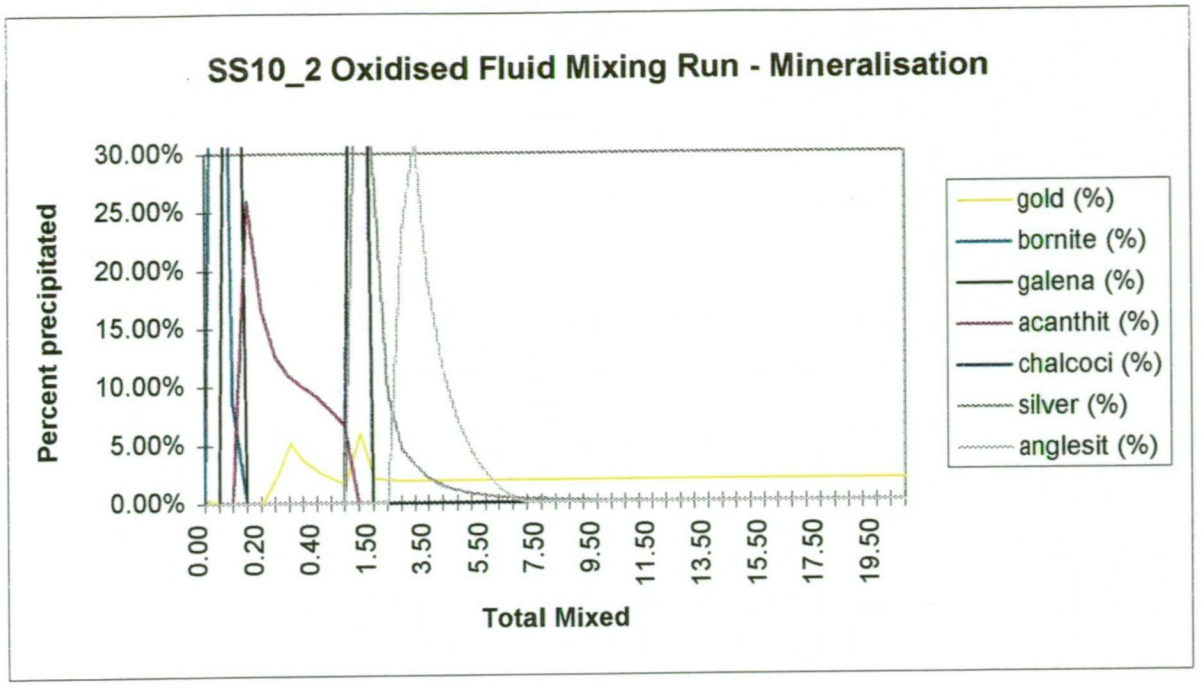
SS10_2 Oxidised Fluid Mixing Run - Mineralisation
Percent precipitated
30.00%
25.00%
20.00%
15.00%
10.00%
5.00%
0.00%
0.00
0.20
0.40
1.50
3.50
5.50
7.50
9.50
11.50
13.50
15.50
17.50
19.50
Total Mixed
gold (%)
bornite (%)
galena (%)
acanthit (%)
chalcoci (%)
silver (%)
anglesit (%)

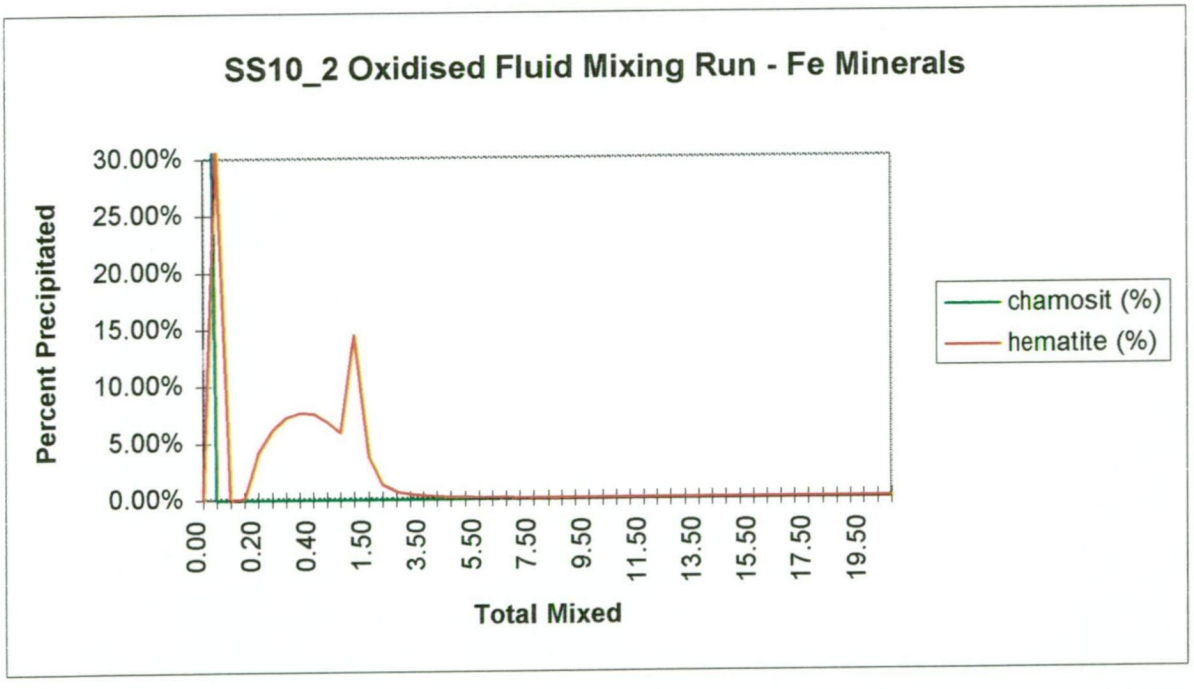
SS10_2 Oxidised Fluid Mixing Run - Fe Minerals
Percent Precipitated
30.00%
25.00%
20.00%
15.00%
10.00%
5.00%
0.00%
0.00
0.20
0.40
1.50
3.50
5.50
7.50
9.50
11.50
13.50
15.50
17.50
19.50
Total Mixed
chamosit (%)
hematite (%)

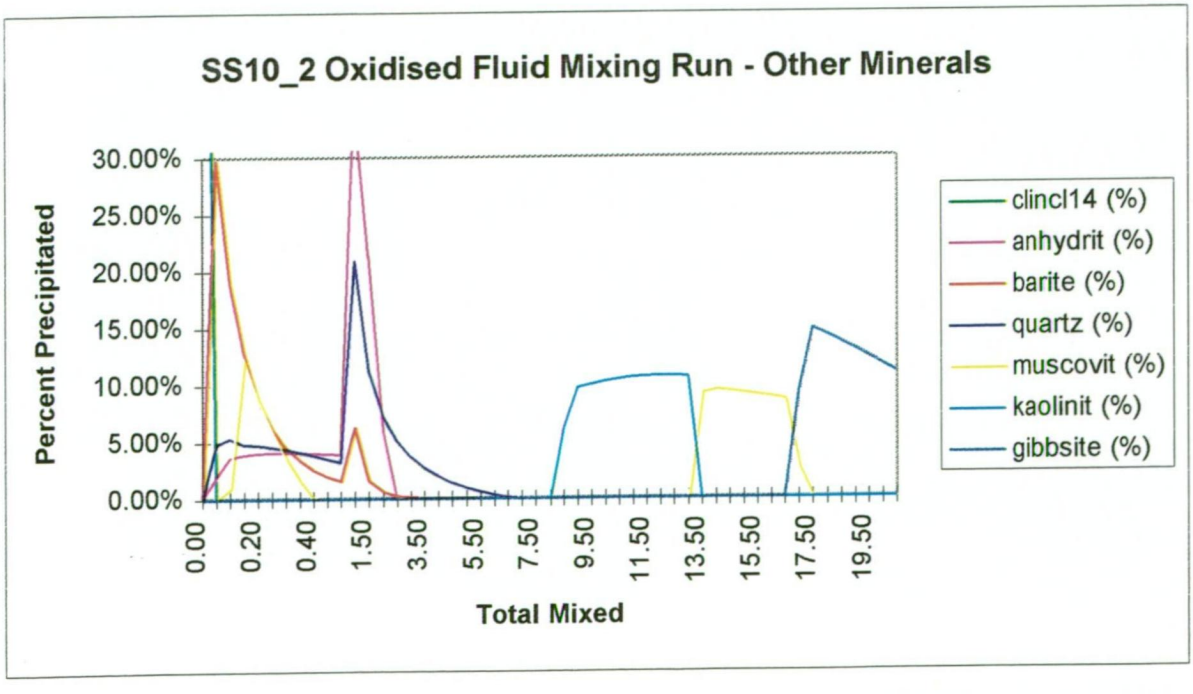
SS10_2 Oxidised Fluid Mixing Run - Other Minerals
Percent Precipitated
30.00%
25.00%
20.00%
15.00%
10.00%
5.00%
0.00%
0.00
0.20
0.40
1.50
3.50
5.50
7.50
9.50
11.50
13.50
15.50
17.50
19.50
Total Mixed
clincl14 (%)
anhydrit (%)
barite (%)
quartz (%)
muscovit (%)
kaolinit (%)
gibbsite (%)

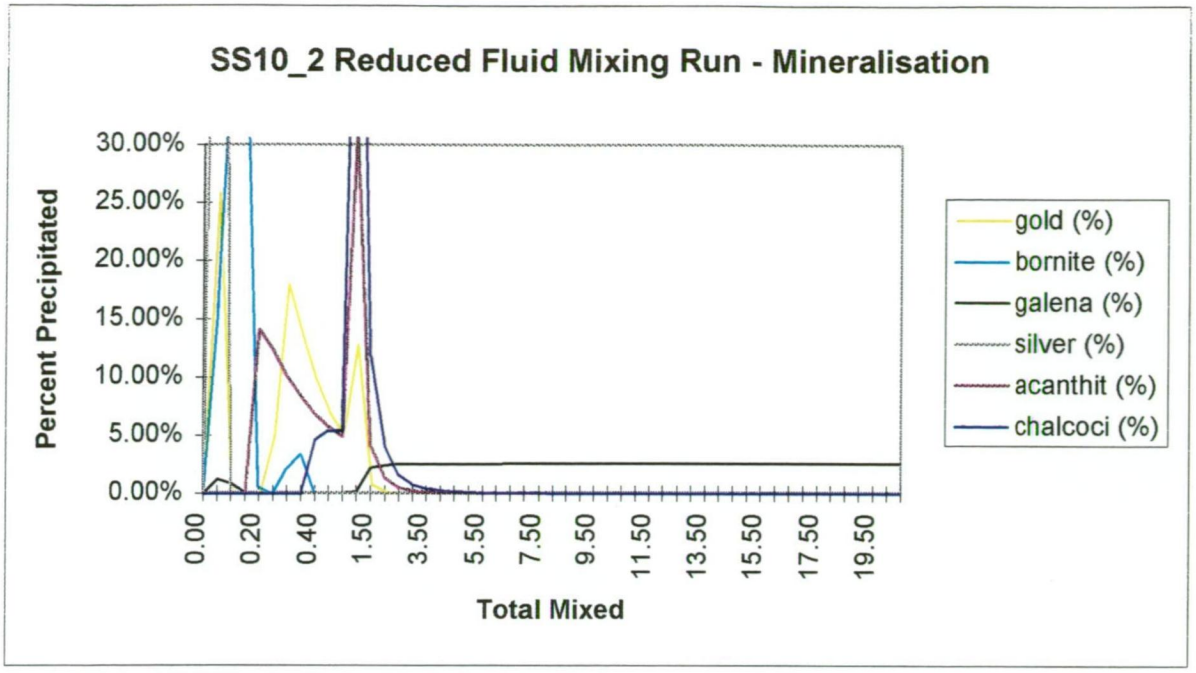
SS10_2 Reduced Fluid Mixing Run - Mineralisation
Percent Precipitated
30.00%
25.00%
20.00%
15.00%
10.00%
5.00%
0.00%
0.00
0.20
0.40
1.50
3.50
5.50
7.50
9.50
11.50
13.50
15.50
17.50
19.50
Total Mixed
gold (%)
bornite (%)
galena (%)
silver (%)
acanthit (%)
chalcoci (%)

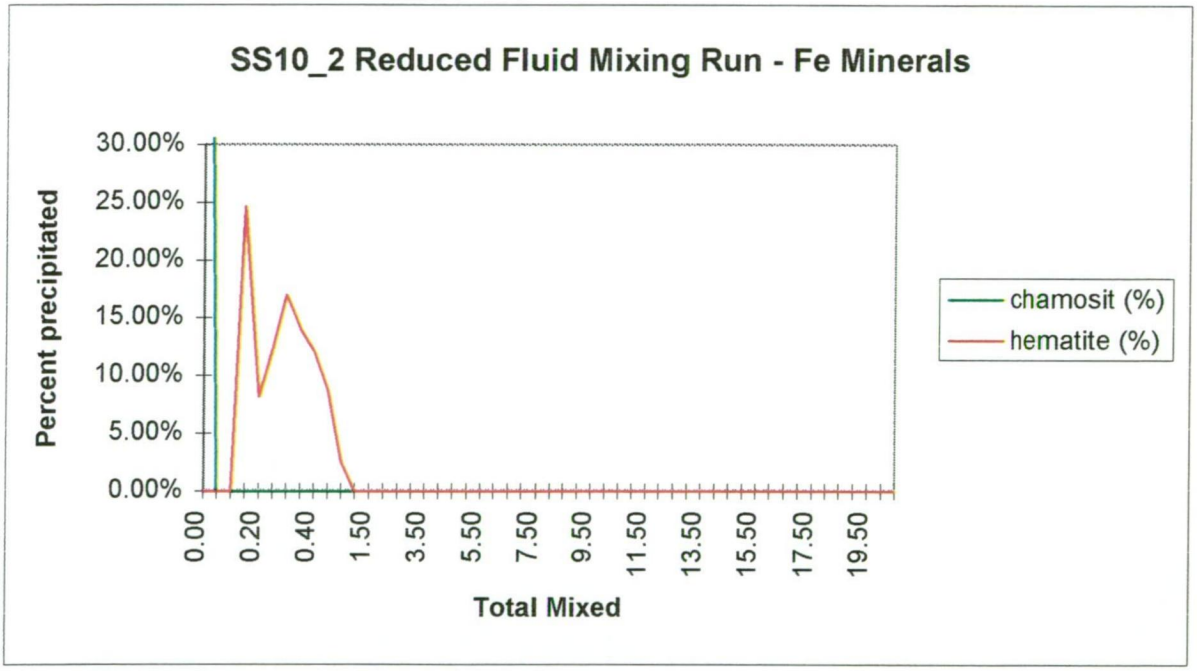
SS10_2 Reduced Fluid Mixing Run - Fe Minerals
Percent precipitated
30.00%
25.00%
20.00%
15.00%
10.00%
5.00%
0.00%
0.00
0.20
0.40
1.50
3.50
5.50
7.50
9.50
11.50
13.50
15.50
17.50
19.50
Total Mixed
chamosit (%)
hematite (%)

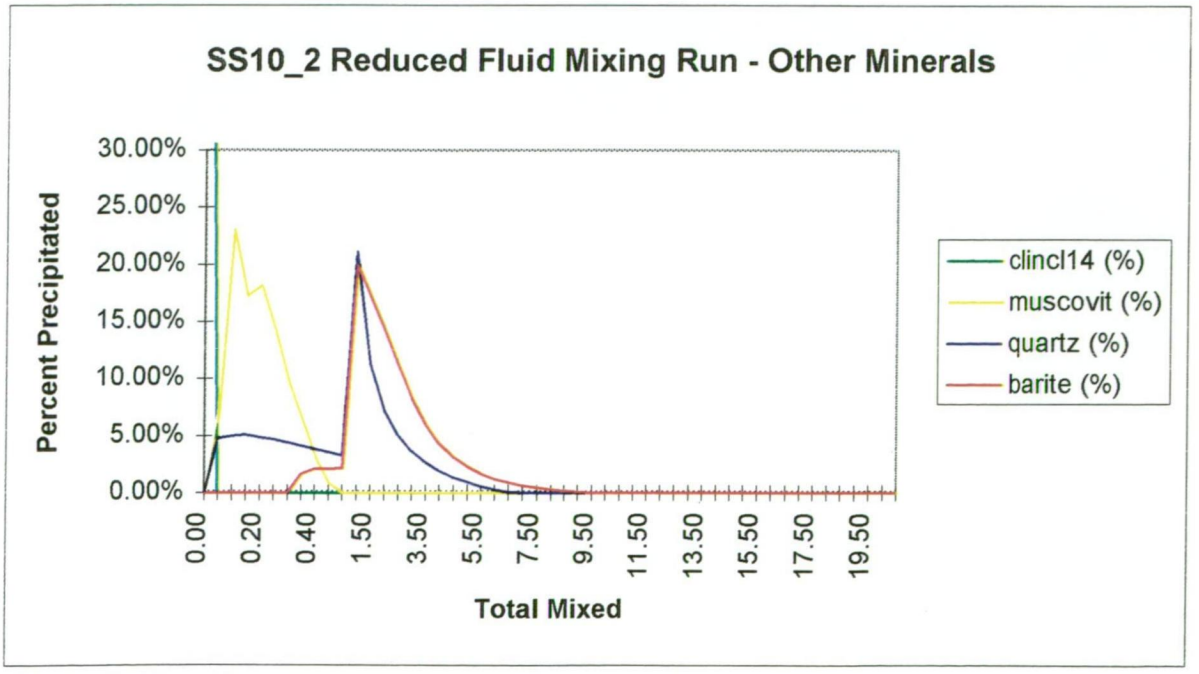
SS10_2 Reduced Fluid Mixing Run - Other Minerals
Percent Precipitated
30.00%
25.00%
20.00%
15.00%
10.00%
5.00%
0.00%
0.00
0.20
0.40
1.50
3.50
5.50
7.50
9.50
11.50
13.50
15.50
17.50
19.50
Total Mixed
clincl14 (%)
muscovit (%)
quartz (%)
barite (%)

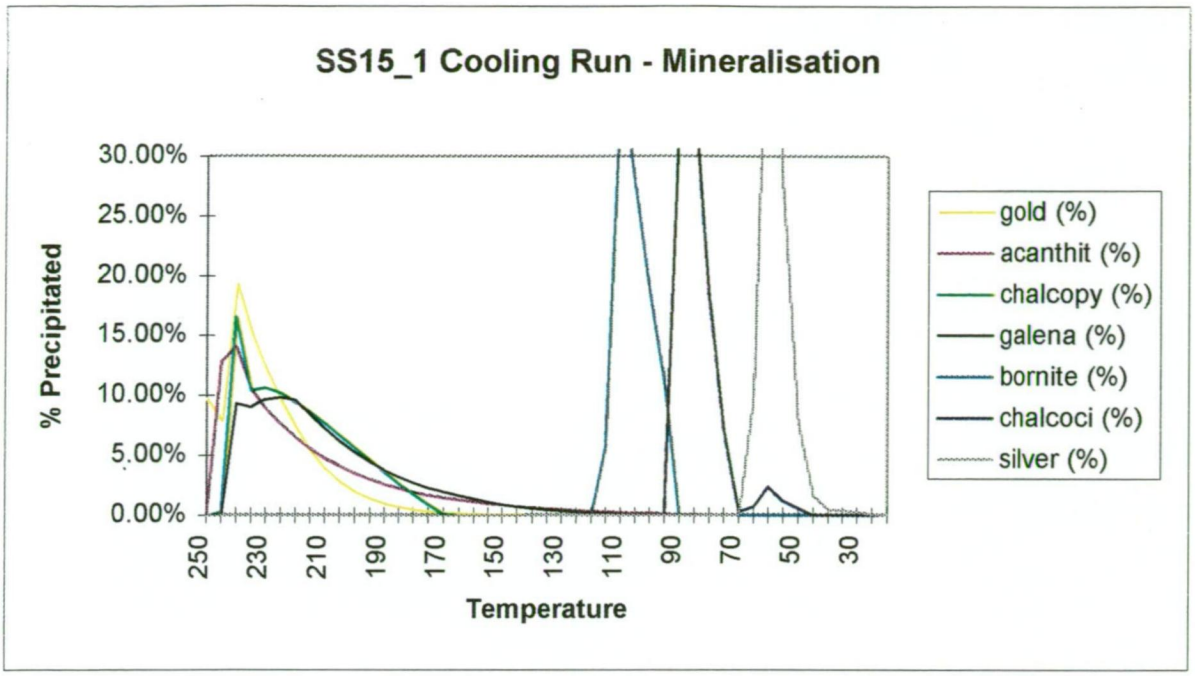
SS15_1 Cooling Run - Mineralisation
% Precipitated
30.00%
25.00%
20.00%
15.00%
10.00%
5.00%
0.00%
250
230
210
190
170
150
130
110
90
70
50
30
Temperature
gold (%)
acanthit (%)
chalcopy (%)
galena (%)
bornite (%)
chalcoci (%)
silver (%)

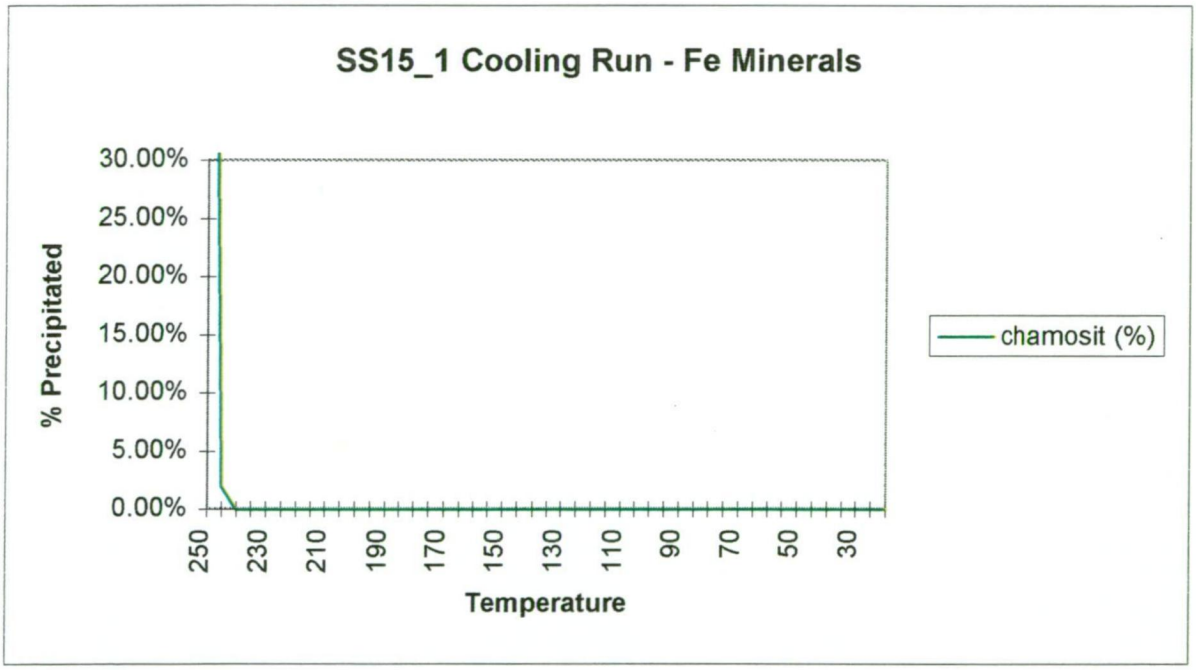
SS15_1 Cooling Run - Fe Minerals
% Precipitated
30.00%
25.00%
20.00%
15.00%
10.00%
5.00%
0.00%
250
230
210
190
170
150
130
110
90
70
50
30
Temperature
chamosit (%)

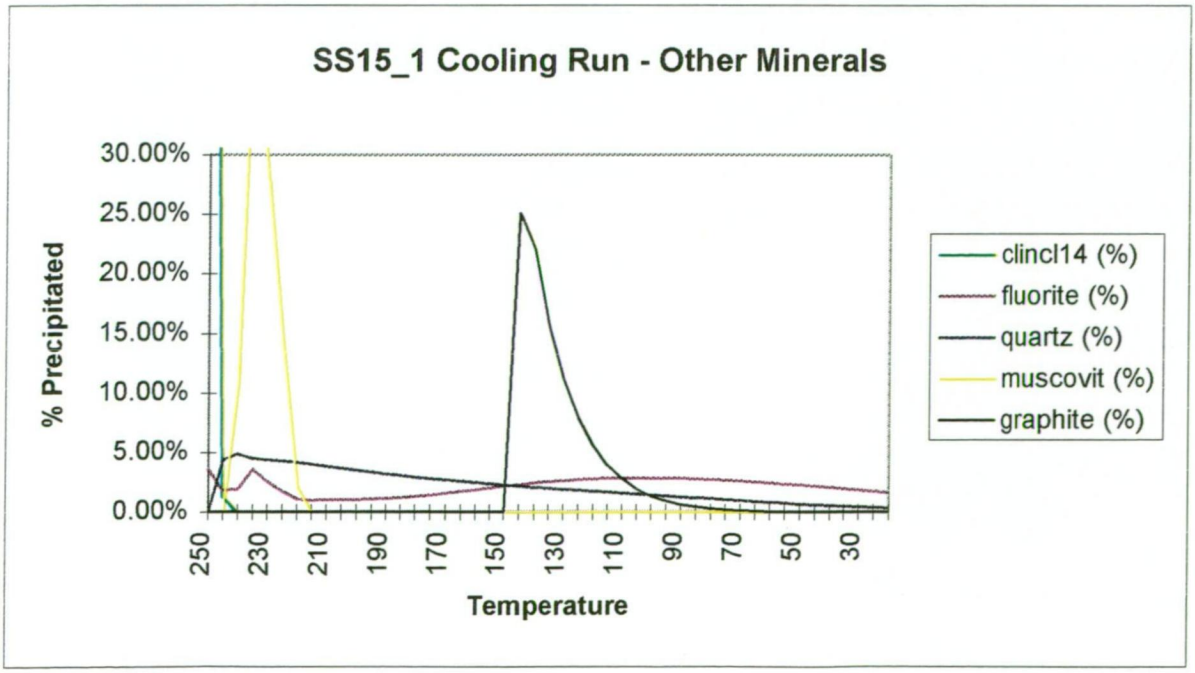
SS15_1 Cooling Run - Other Minerals
% Precipitated
30.00%
25.00%
20.00%
15.00%
10.00%
5.00%
0.00%
250
230
210
190
170
150
130
110
90
70
50
30
Temperature
clincl14 (%)
fluorite (%)
quartz (%)
muscovit (%)
graphite (%)

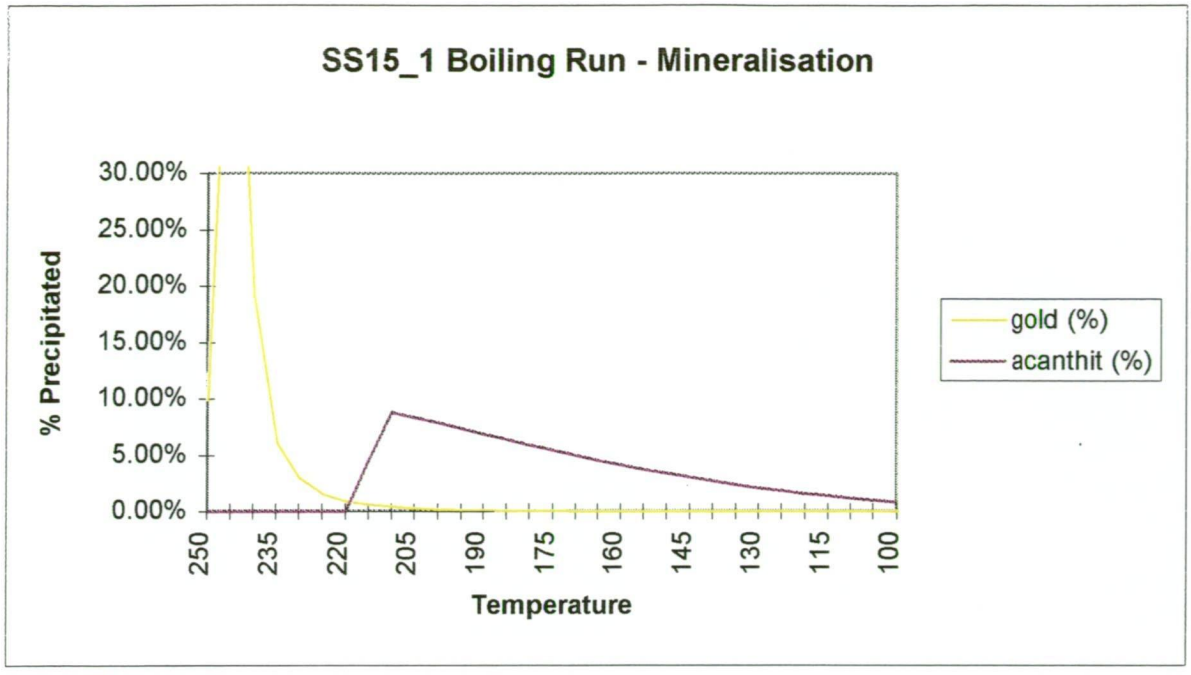
SS15_1 Boiling Run - Mineralisation
% Precipitated
30.00%
25.00%
20.00%
15.00%
10.00%
5.00%
0.00%
250
235
220
205
190
175
160
145
130
115
100
Temperature
gold (%)
acanthit (%)

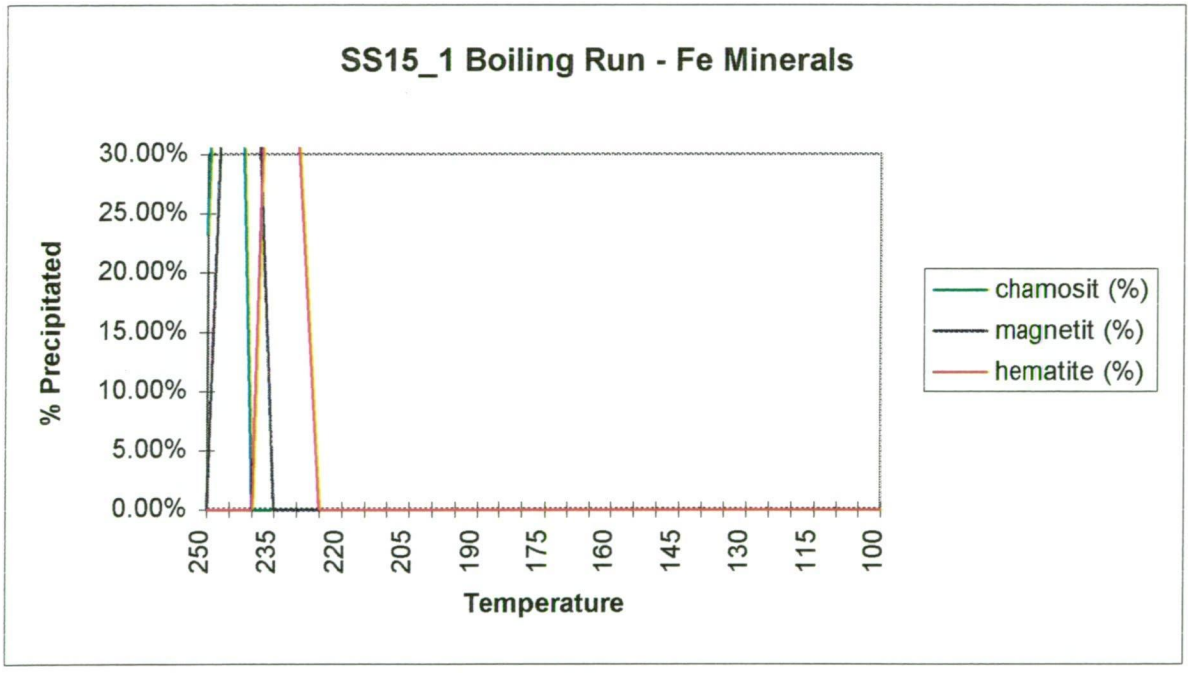
SS15_1 Boiling Run - Fe Minerals
% Precipitated
30.00%
25.00%
20.00%
15.00%
10.00%
5.00%
0.00%
250
235
220
205
190
175
160
145
130
115
100
Temperature
chamosit (%)
magnetit (%)
hematite (%)

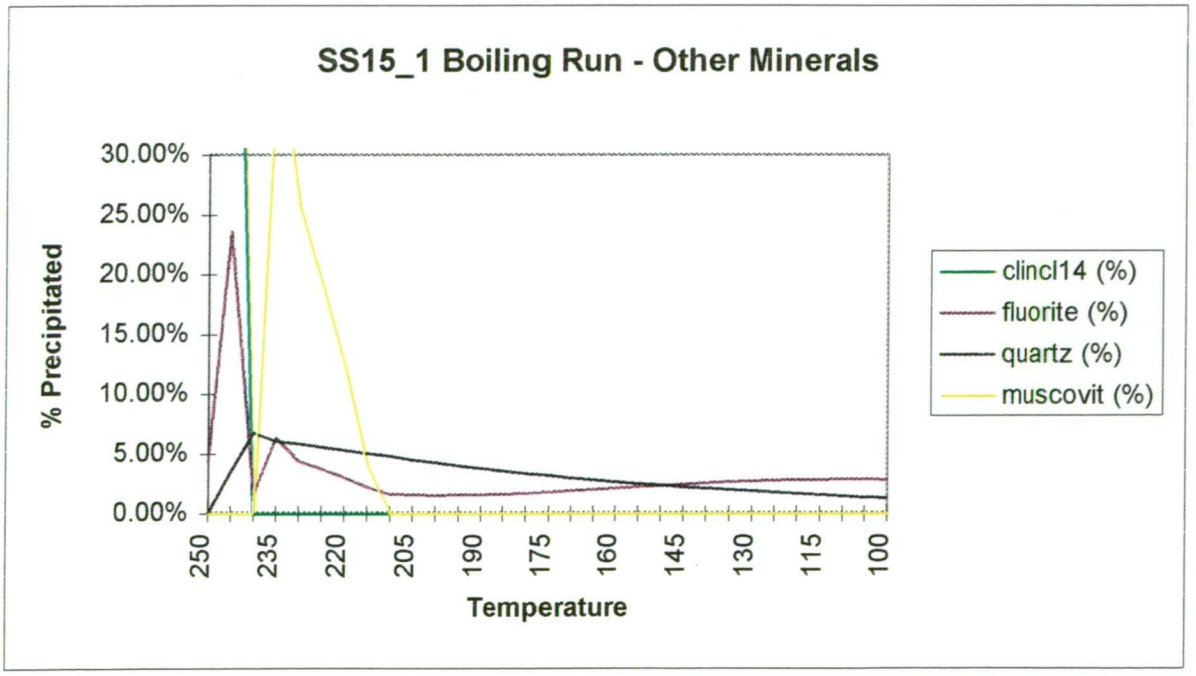
SS15_1 Boiling Run - Other Minerals
% Precipitated
30.00%
25.00%
20.00%
15.00%
10.00%
5.00%
0.00%
250
235
220
205
190
175
160
145
130
115
100
Temperature
clincl14 (%)
fluorite (%)
quartz (%)
muscovit (%)

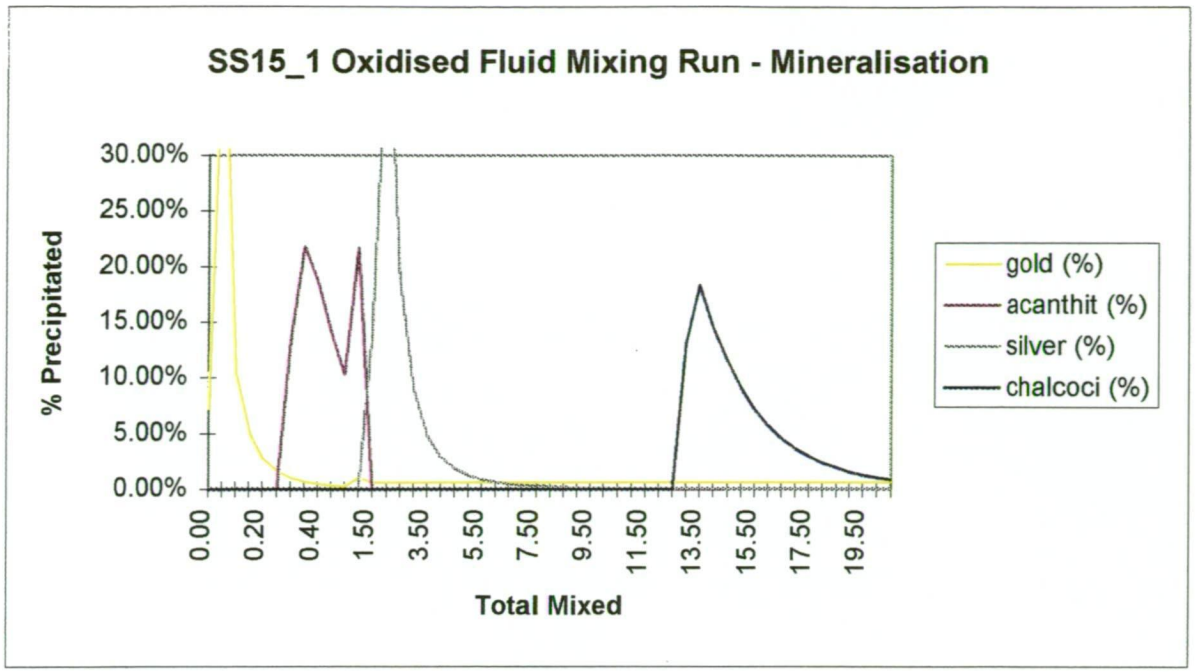
SS15_1 Oxidised Fluid Mixing Run - Mineralisation
% Precipitated
30.00%
25.00%
20.00%
15.00%
10.00%
5.00%
0.00%
0.00
0.20
0.40
1.50
3.50
5.50
7.50
9.50
11.50
13.50
15.50
17.50
19.50
Total Mixed
gold (%)
acanthit (%)
silver (%)
chalcoci (%)

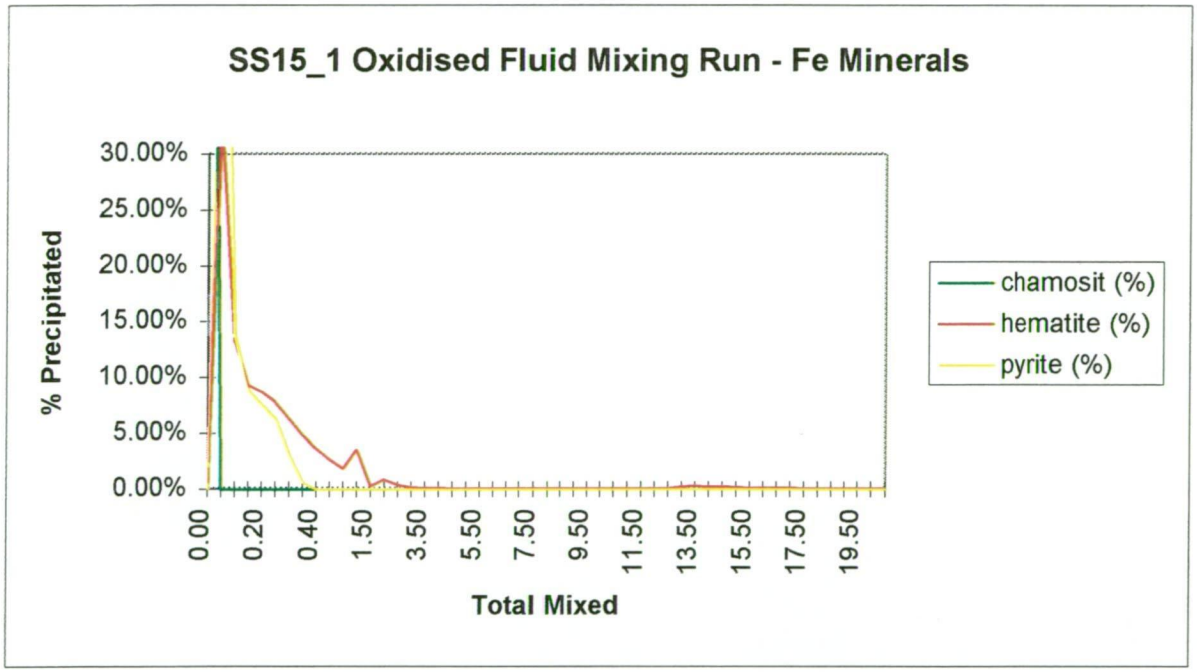
SS15_1 Oxidised Fluid Mixing Run - Fe Minerals
% Precipitated
30.00%
25.00%
20.00%
15.00%
10.00%
5.00%
0.00%
0.00
0.20
0.40
1.50
3.50
5.50
7.50
9.50
11.50
13.50
15.50
17.50
19.50
Total Mixed
chamosit (%)
hematite (%)
pyrite (%)

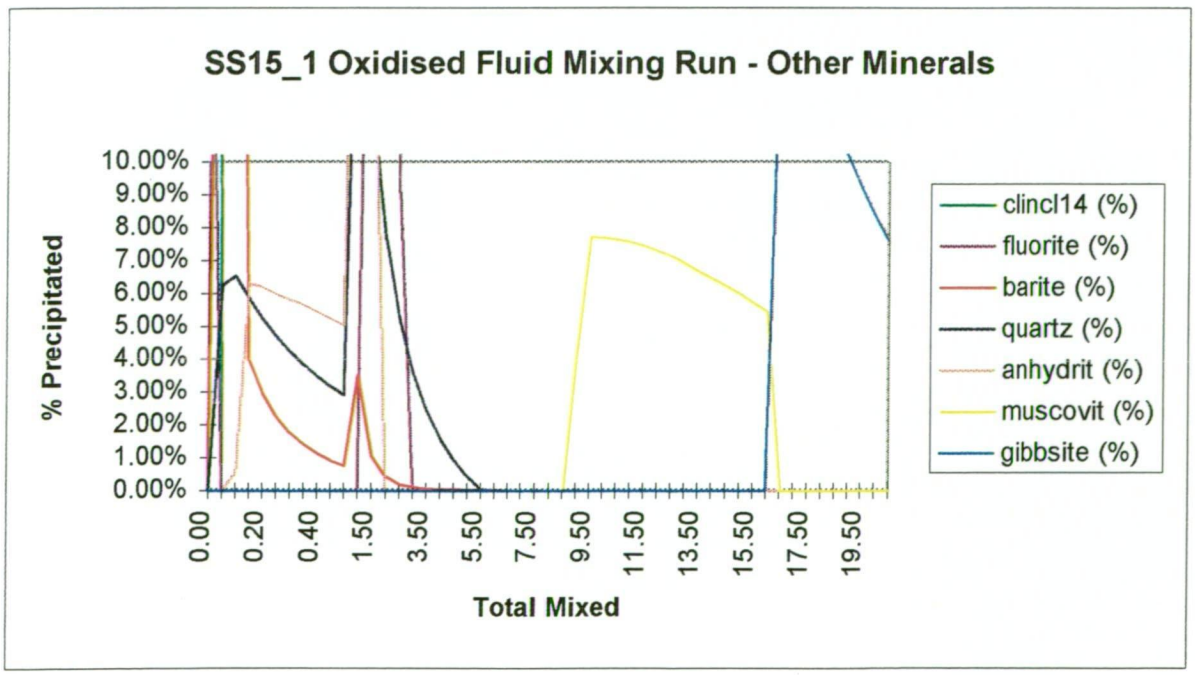
SS15_1 Oxidised Fluid Mixing Run - Other Minerals
% Precipitated
10.00%
9.00%
8.00%
7.00%
6.00%
5.00%
4.00%
3.00%
2.00%
1.00%
0.00%
0.00
0.20
0.40
1.50
3.50
5.50
7.50
9.50
11.50
13.50
15.50
17.50
19.50
Total Mixed
clincl14 (%)
fluorite (%)
barite (%)
quartz (%)
anhydrit (%)
muscovit (%)
gibbsite (%)

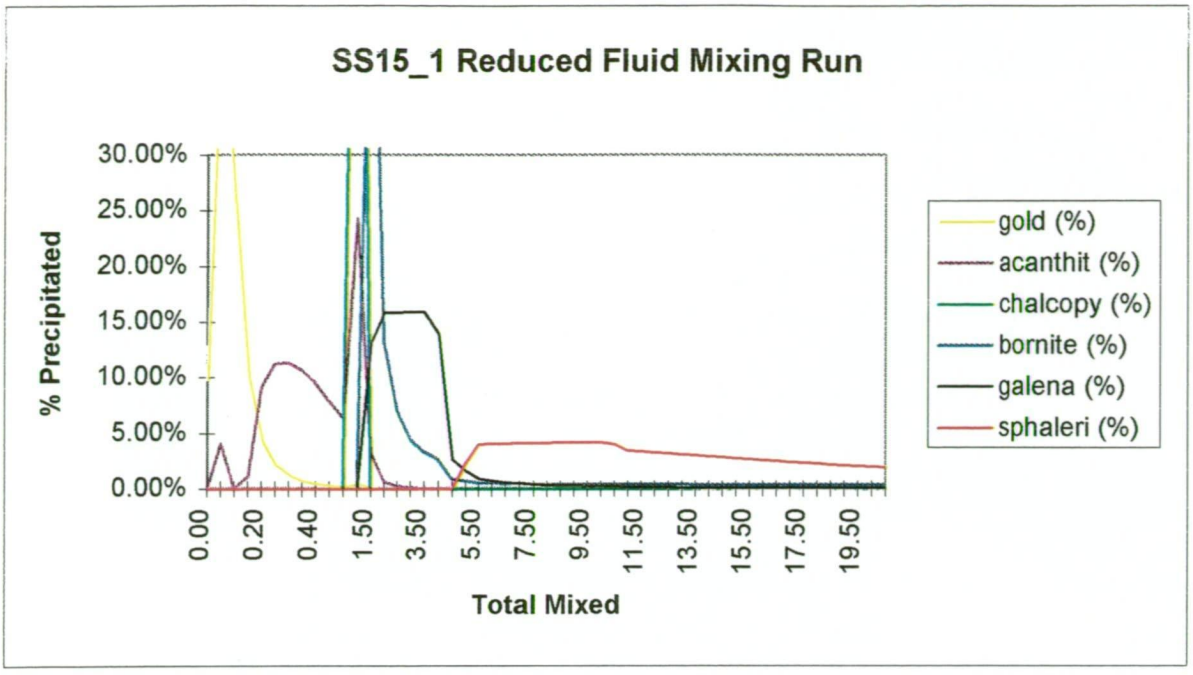
SS15_1 Reduced Fluid Mixing Run
% Precipitated
30.00%
25.00%
20.00%
15.00%
10.00%
5.00%
0.00%
0.00
0.20
0.40
1.50
3.50
5.50
7.50
9.50
11.50
13.50
15.50
17.50
19.50
Total Mixed
gold (%)
acanthit (%)
chalcopy (%)
bornite (%)
galena (%)
sphaleri (%)

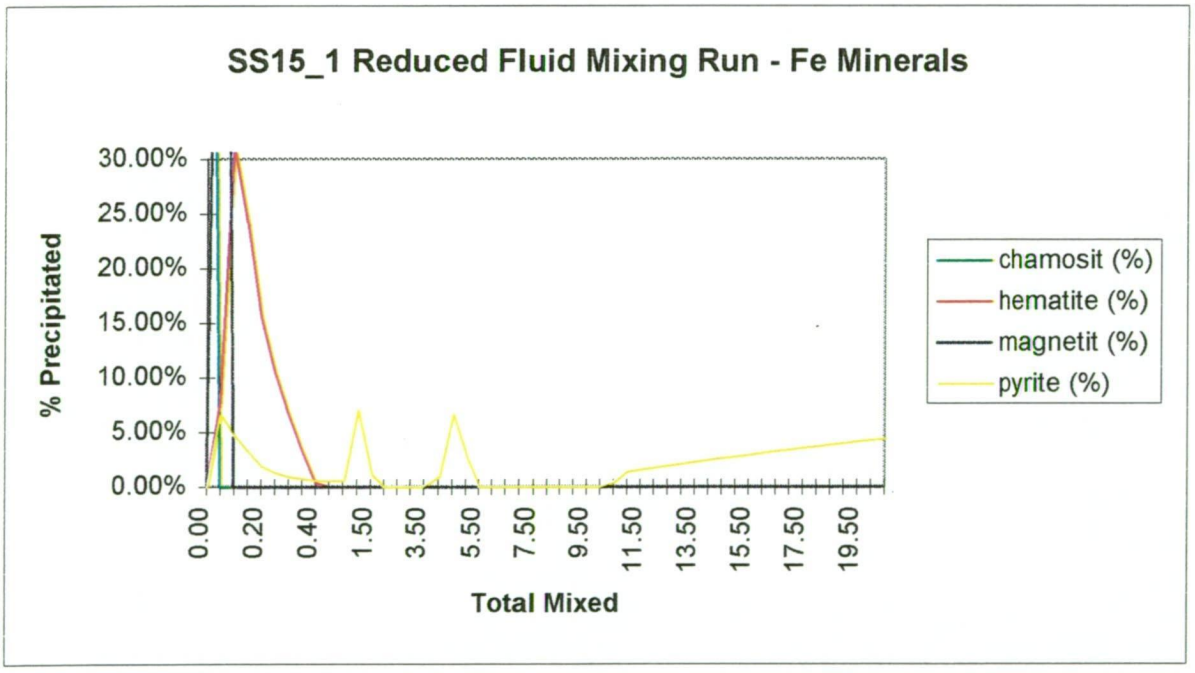
SS15_1 Reduced Fluid Mixing Run - Fe Minerals
% Precipitated
30.00%
25.00%
20.00%
15.00%
10.00%
5.00%
0.00%
0.00
0.20
0.40
1.50
3.50
5.50
7.50
9.50
11.50
13.50
15.50
17.50
19.50
Total Mixed
chamosit (%)
hematite (%)
magnetit (%)
pyrite (%)

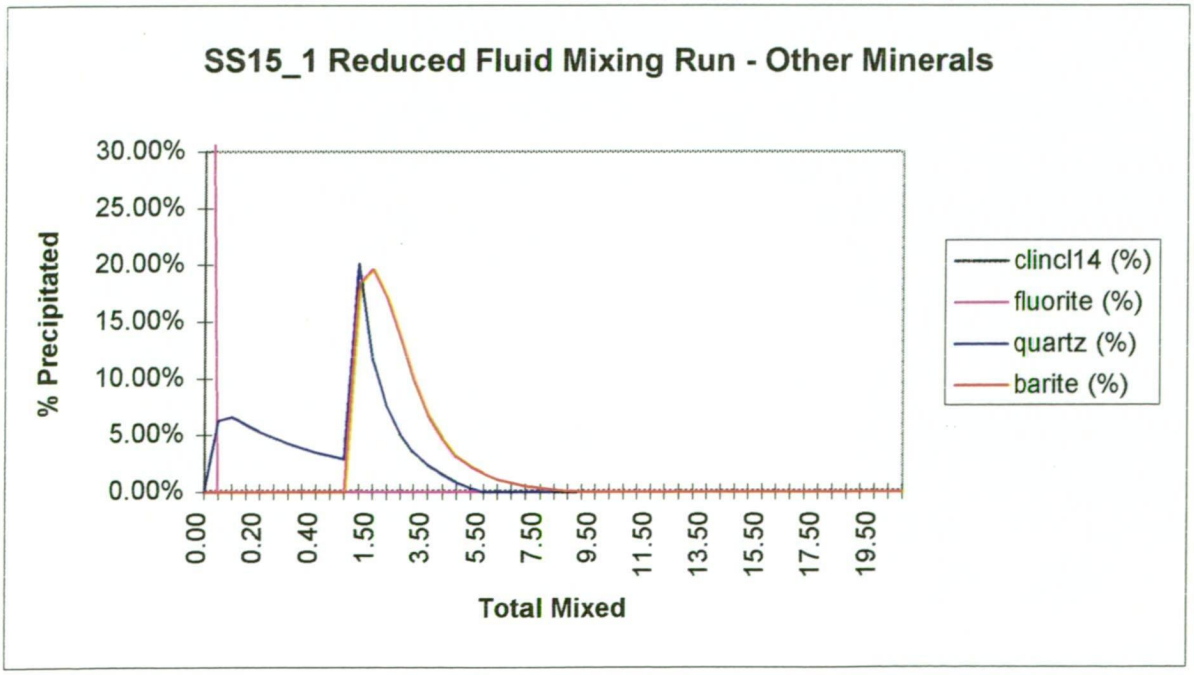
SS15_1 Reduced Fluid Mixing Run - Other Minerals
% Precipitated
30.00%
25.00%
20.00%
15.00%
10.00%
5.00%
0.00%
0.00
0.20
0.40
1.50
3.50
5.50
7.50
9.50
11.50
13.50
15.50
17.50
19.50
Total Mixed
clincl14 (%)
fluorite (%)
quartz (%)
barite (%)

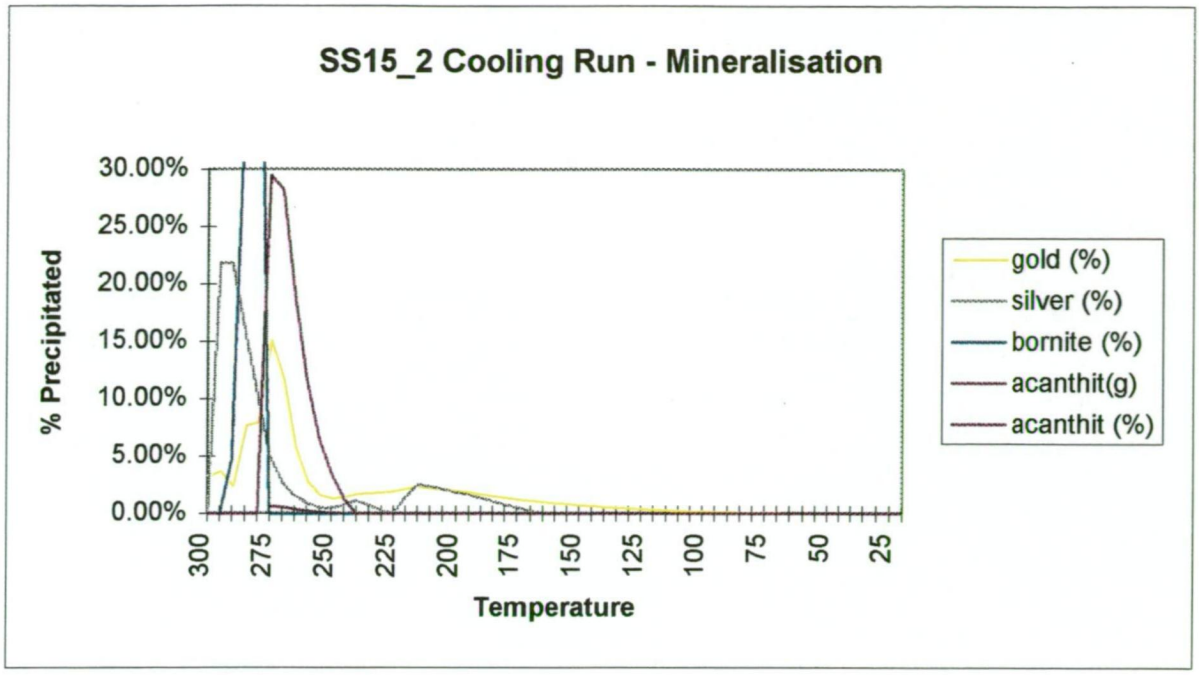
SS15_2 Cooling Run - Mineralisation
% Precipitated
30.00%
25.00%
20.00%
15.00%
10.00%
5.00%
0.00%
300
275
250
225
200
175
150
125
100
75
50
25
Temperature
gold (%)
silver (%)
bornite (%)
acanthit(g)
acanthit (%)

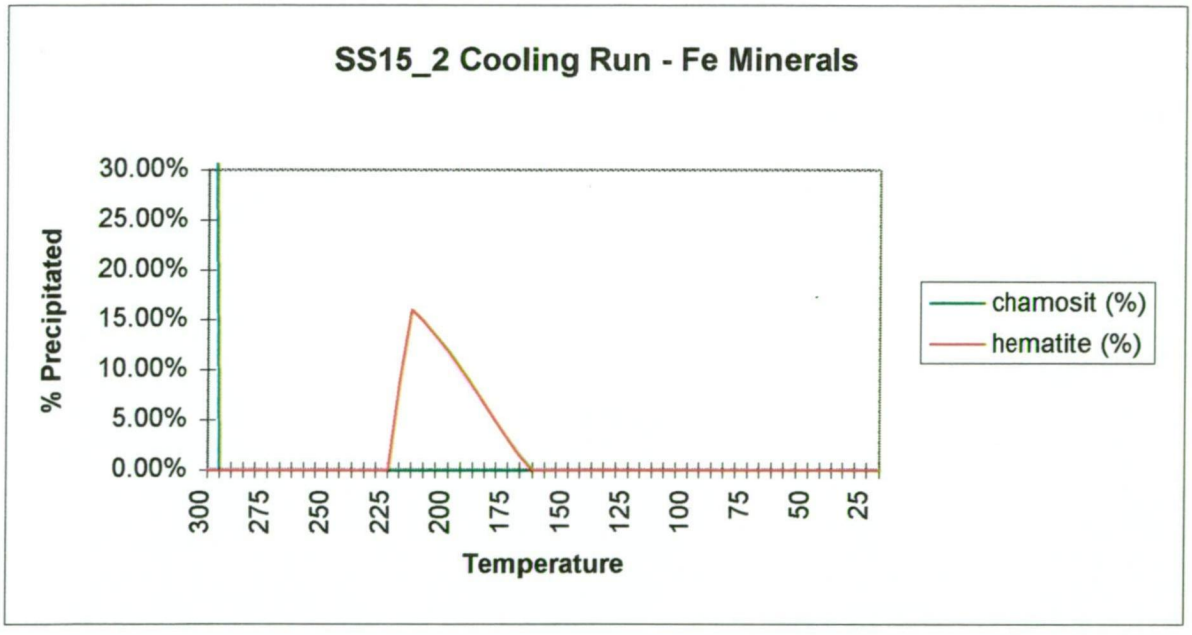
SS15_2 Cooling Run - Fe Minerals
% Precipitated
30.00%
25.00%
20.00%
15.00%
10.00%
5.00%
0.00%
300
275
250
225
200
175
150
125
100
75
50
25
Temperature
chamosit (%)
hematite (%)

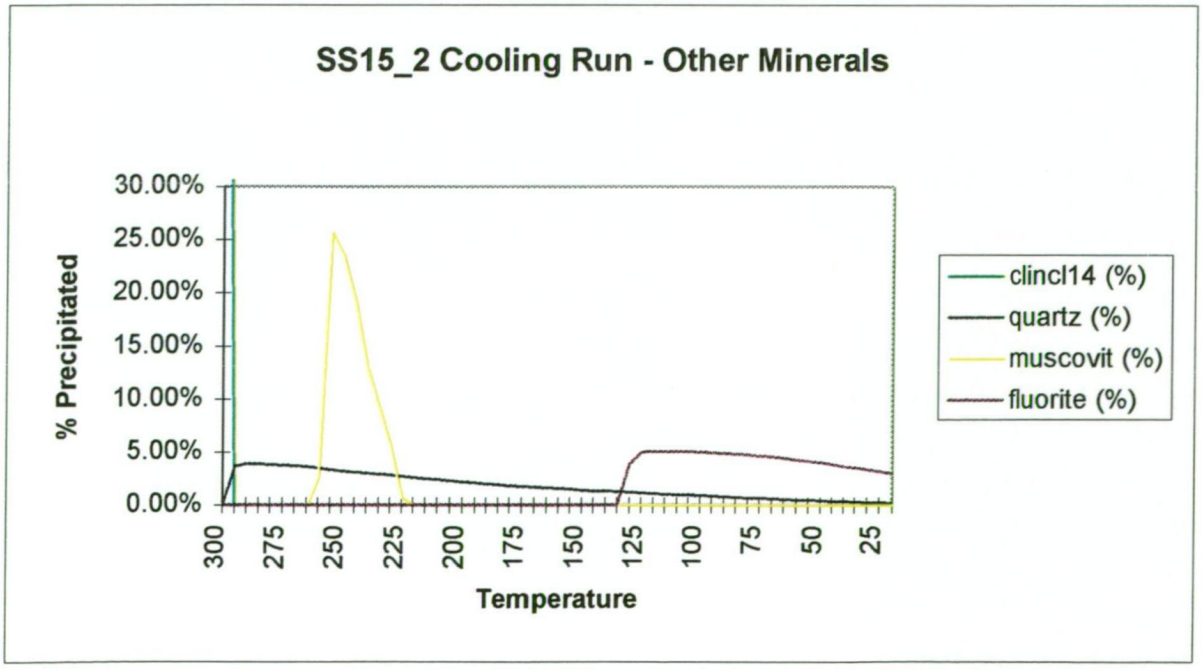
SS15_2 Cooling Run - Other Minerals
% Precipitated
30.00%
25.00%
20.00%
15.00%
10.00%
5.00%
0.00%
300
275
250
225
200
175
150
125
100
75
50
25
Temperature
clincl14 (%)
quartz (%)
muscovit (%)
fluorite (%)

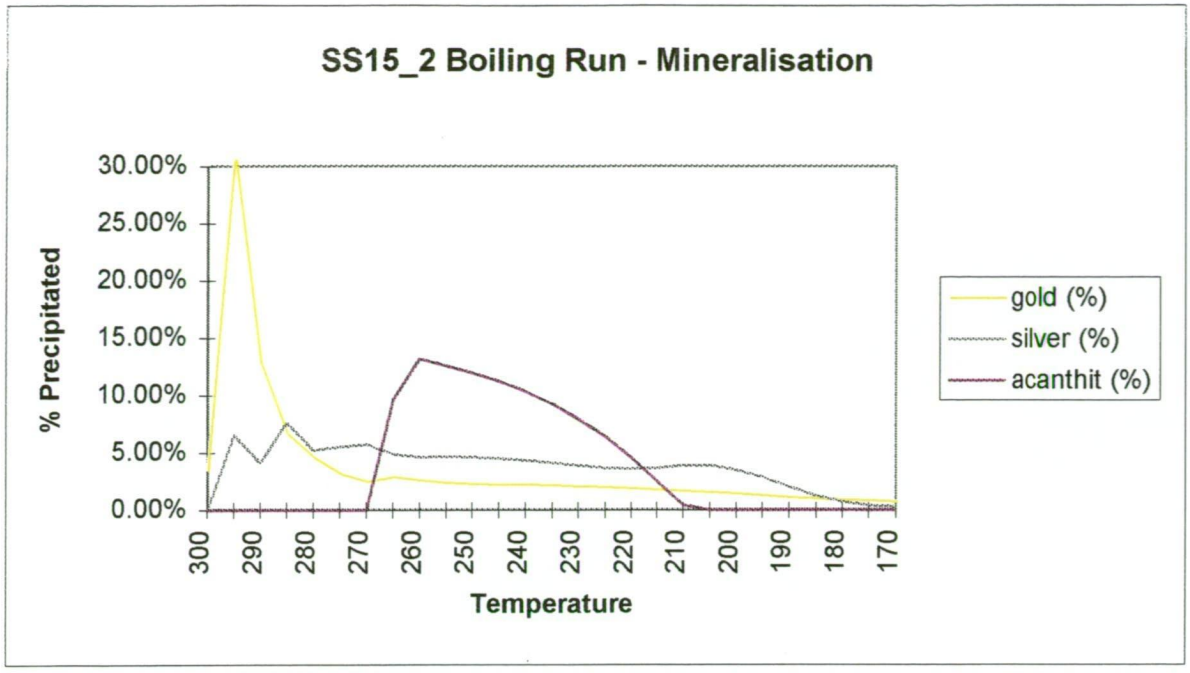
SS15_2 Boiling Run - Mineralisation
% Precipitated
30.00%
25.00%
20.00%
15.00%
10.00%
5.00%
0.00%
300 290 280 270 260 250 240 230 220 210 200 190 180 170
Temperature
gold (%)
silver (%)
acanthit (%)

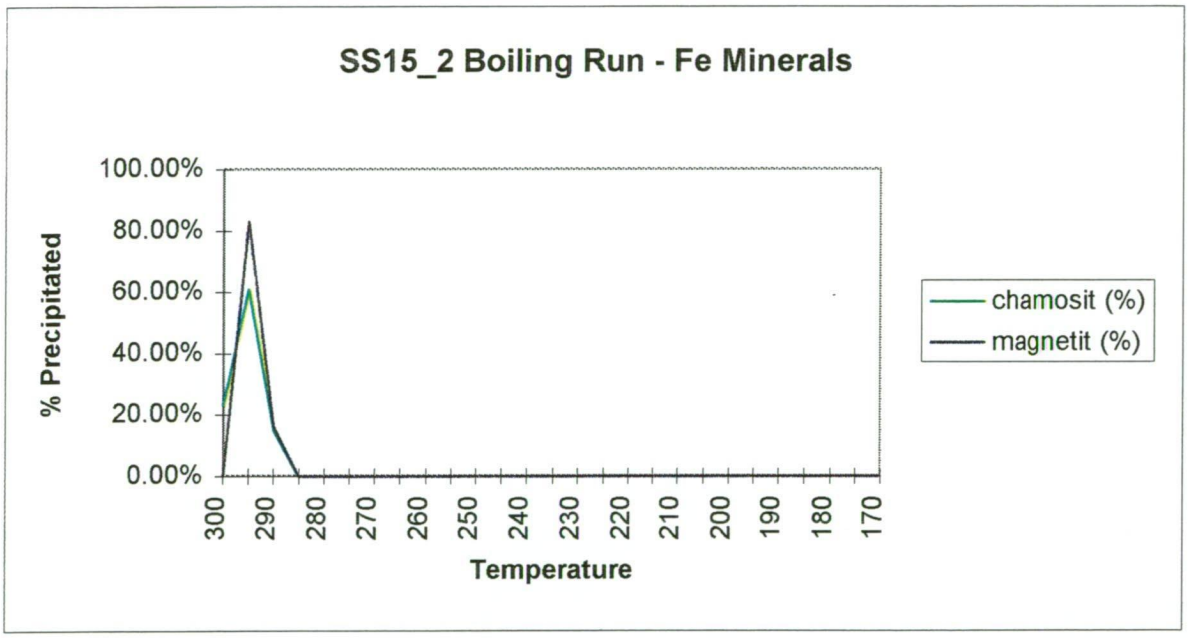
SS15_2 Boiling Run - Fe Minerals
% Precipitated
100.00%
80.00%
60.00%
40.00%
20.00%
0.00%
300 290 280 270 260 250 240 230 220 210 200 190 180 170
Temperature
chamosit (%)
magnetit (%)

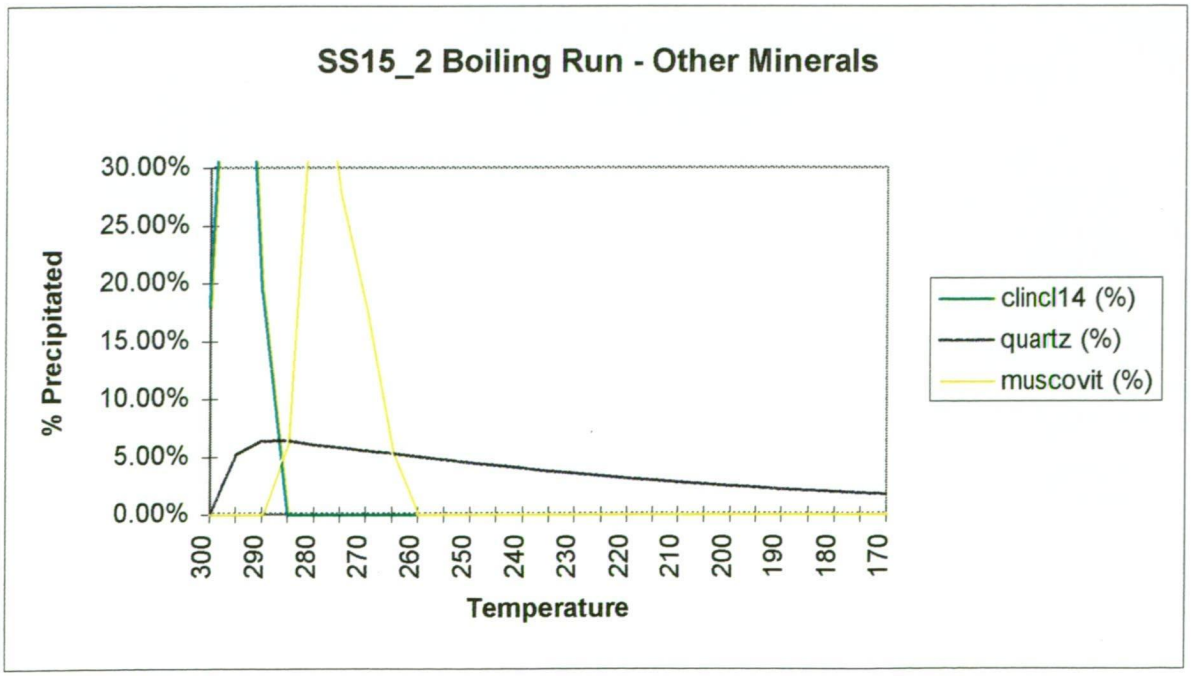
SS15_2 Boiling Run - Other Minerals
% Precipitated
30.00%
25.00%
20.00%
15.00%
10.00%
5.00%
0.00%
300 290 280 270 260 250 240 230 220 210 200 190 180 170
Temperature
clincl14 (%)
quartz (%)
muscovit (%)

SS15_2 Oxidised Fluid Mixing Run - Mineralisation

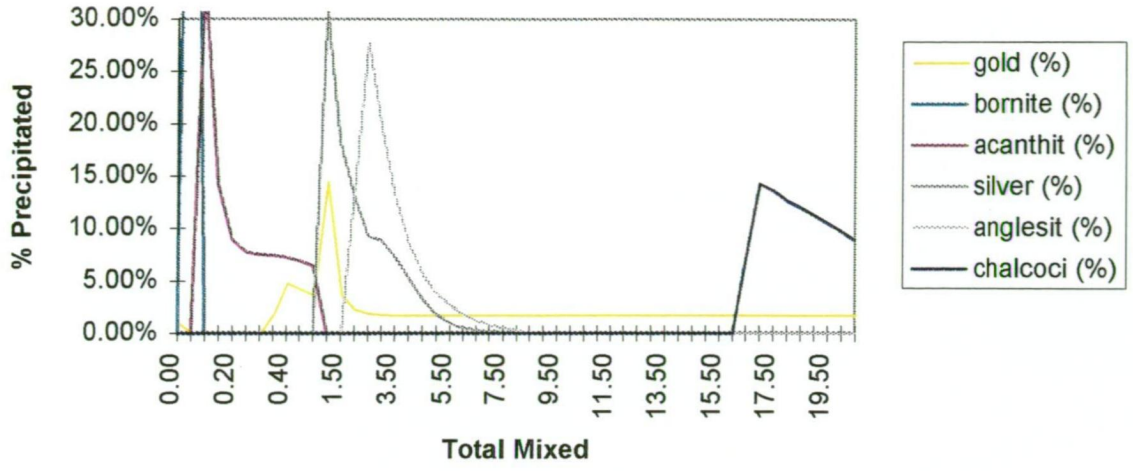

SS15_2 Oxidised Fluid Mixing Run - Fe Minerals

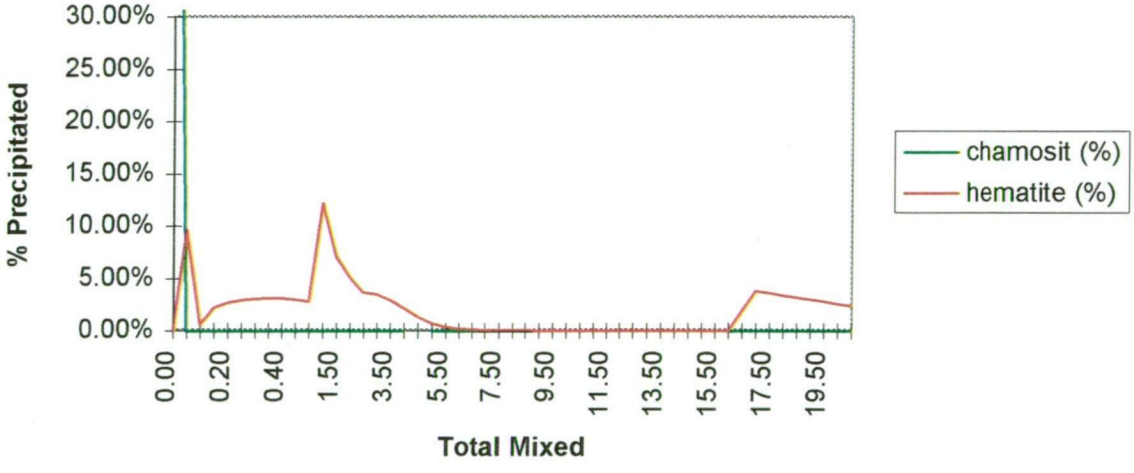

SS15_2 Oxidised Fluid Mixing Run

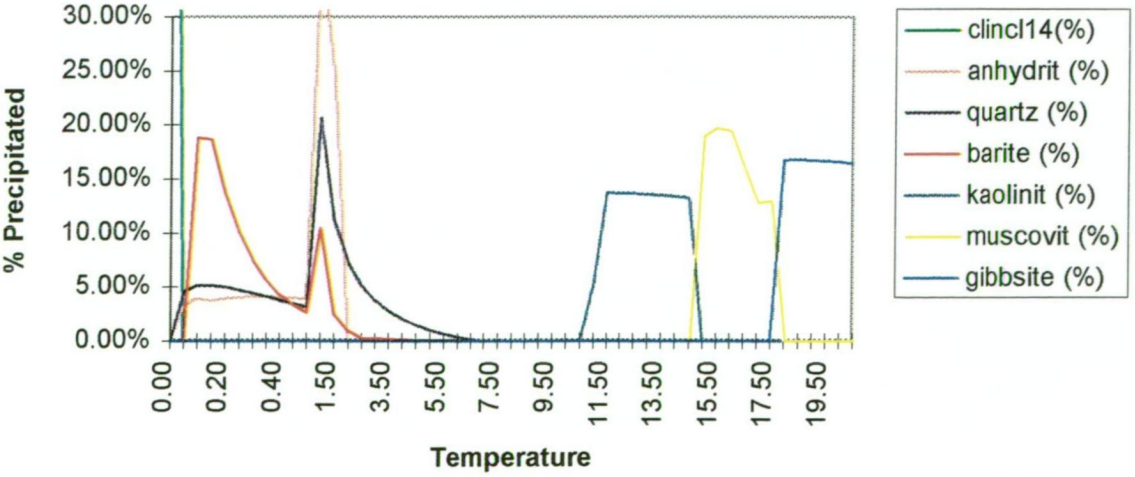

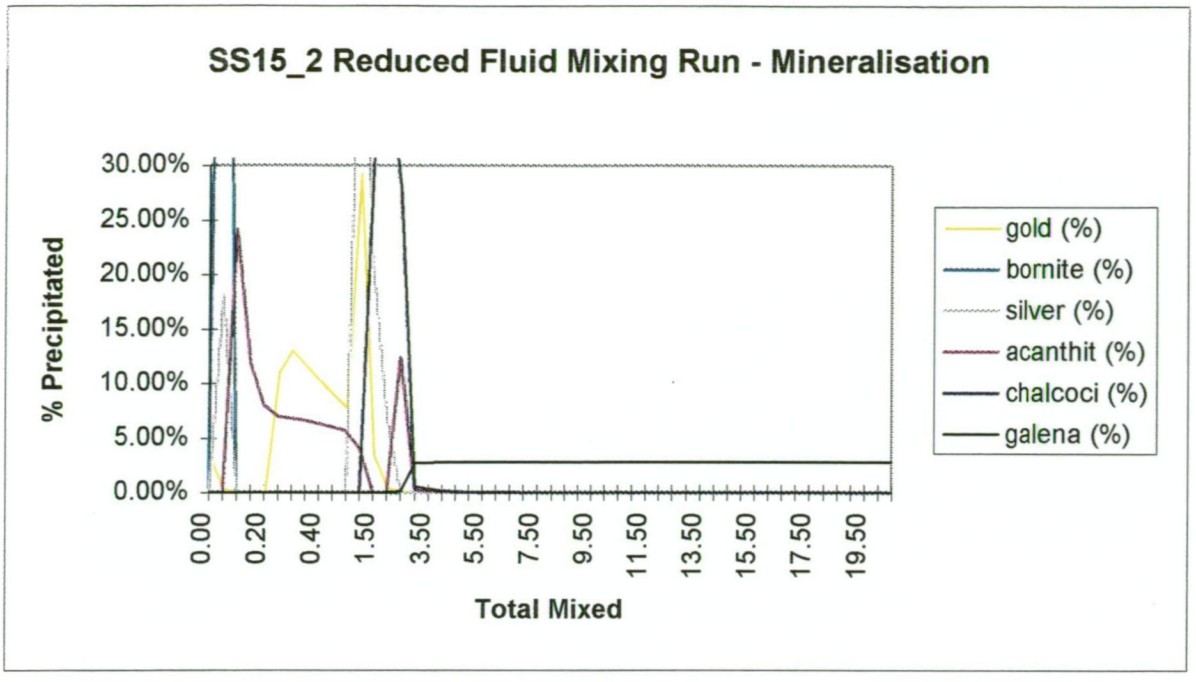
SS15_2 Reduced Fluid Mixing Run - Mineralisation
% Precipitated
30.00%
25.00%
20.00%
15.00%
10.00%
5.00%
0.00%
0.00
0.20
0.40
1.50
3.50
5.50
7.50
9.50
11.50
13.50
15.50
17.50
19.50
Total Mixed
gold (%)
bornite (%)
silver (%)
acanthit (%)
chalcoci (%)
galena (%)

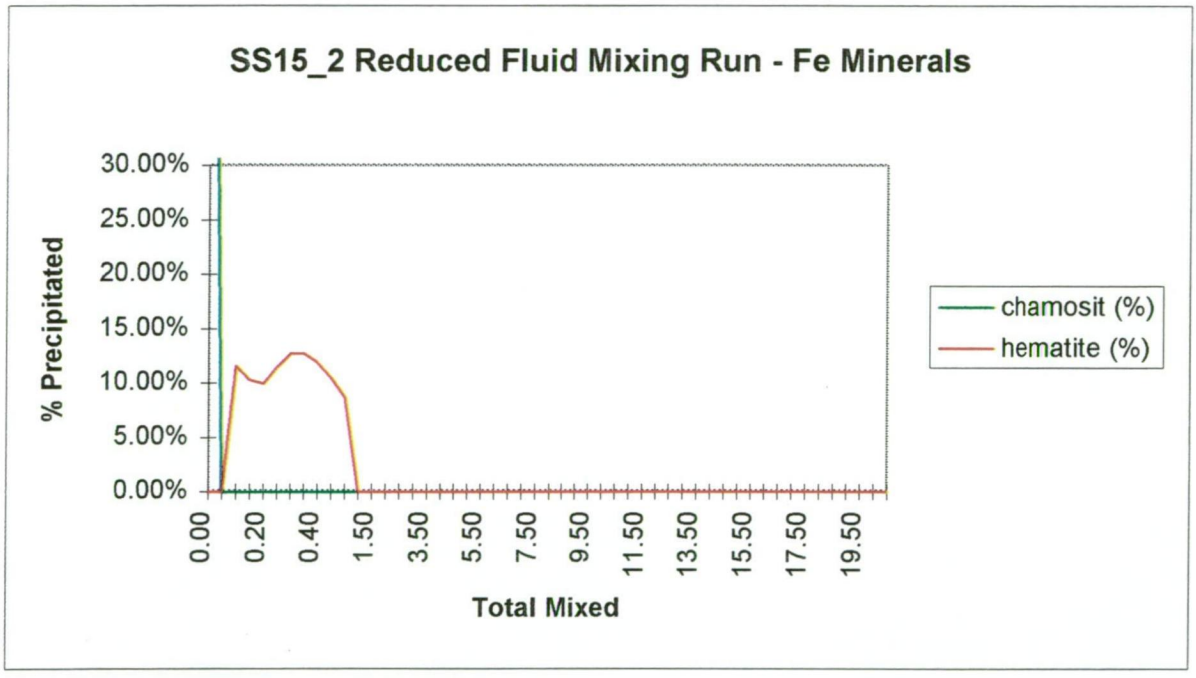
SS15_2 Reduced Fluid Mixing Run - Fe Minerals
% Precipitated
30.00%
25.00%
20.00%
15.00%
10.00%
5.00%
0.00%
0.00
0.20
0.40
1.50
3.50
5.50
7.50
9.50
11.50
13.50
15.50
17.50
19.50
Total Mixed
chamosit (%)
hematite (%)

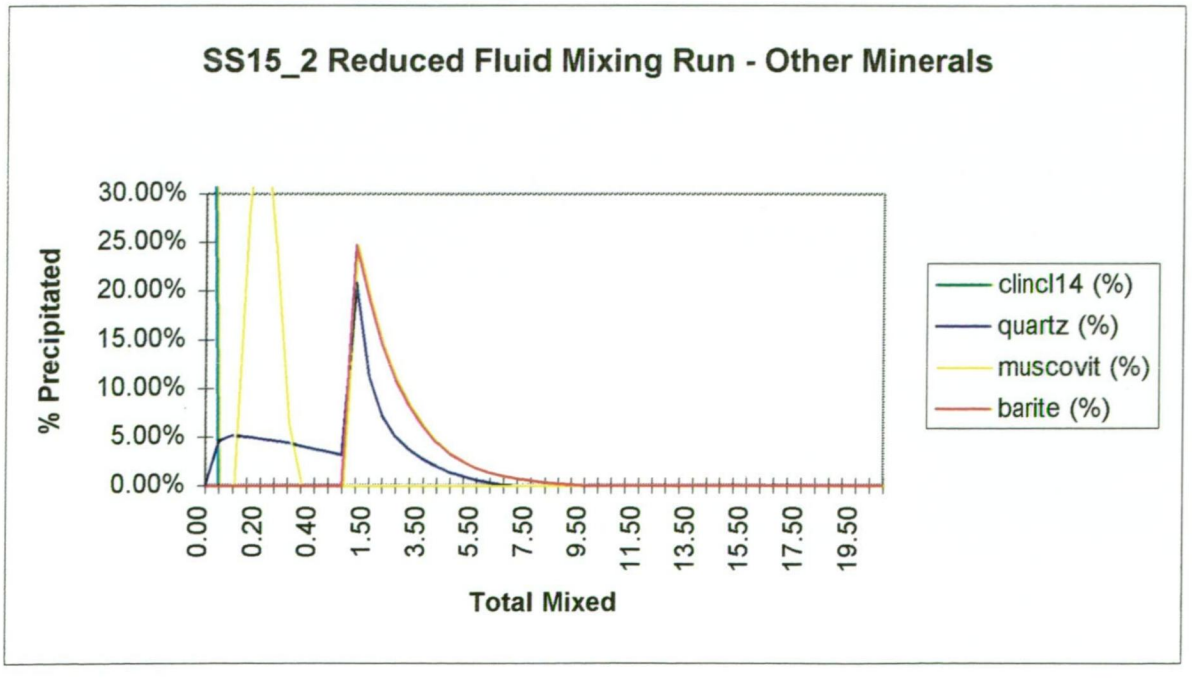
SS15_2 Reduced Fluid Mixing Run - Other Minerals
% Precipitated
30.00%
25.00%
20.00%
15.00%
10.00%
5.00%
0.00%
0.00
0.20
0.40
1.50
3.50
5.50
7.50
9.50
11.50
13.50
15.50
17.50
19.50
Total Mixed
clincl14 (%)
quartz (%)
muscovit (%)
barite (%)

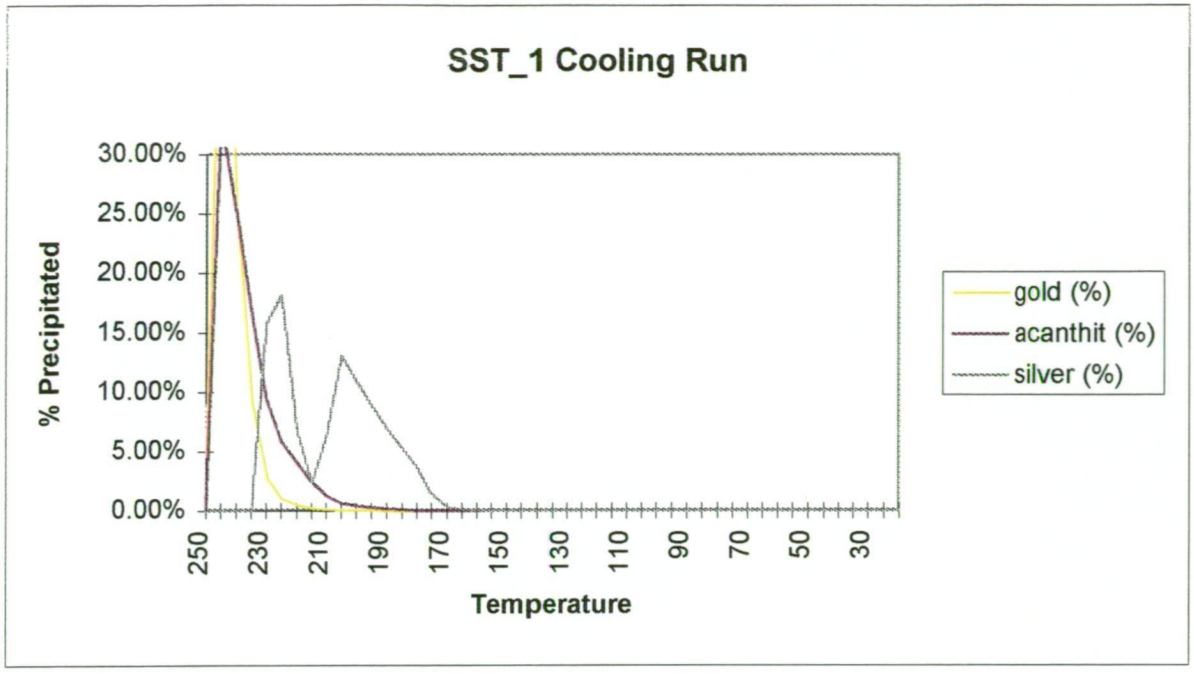
SST_1 Cooling Run
% Precipitated
30.00%
25.00%
20.00%
15.00%
10.00%
5.00%
0.00%
250
230
210
190
170
150
130
110
90
70
50
30
Temperature
gold (%)
acanthit (%)
silver (%)

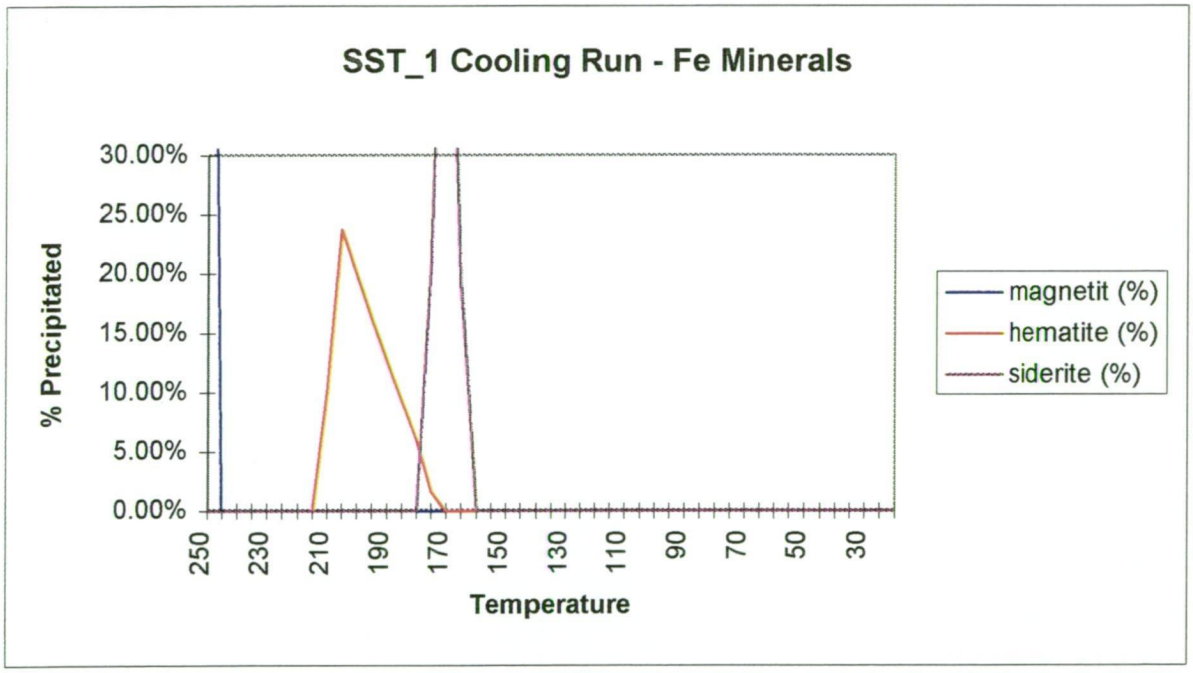
SST_1 Cooling Run - Fe Minerals
% Precipitated
30.00%
25.00%
20.00%
15.00%
10.00%
5.00%
0.00%
250
230
210
190
170
150
130
110
90
70
50
30
Temperature
magnetit (%)
hematite (%)
siderite (%)

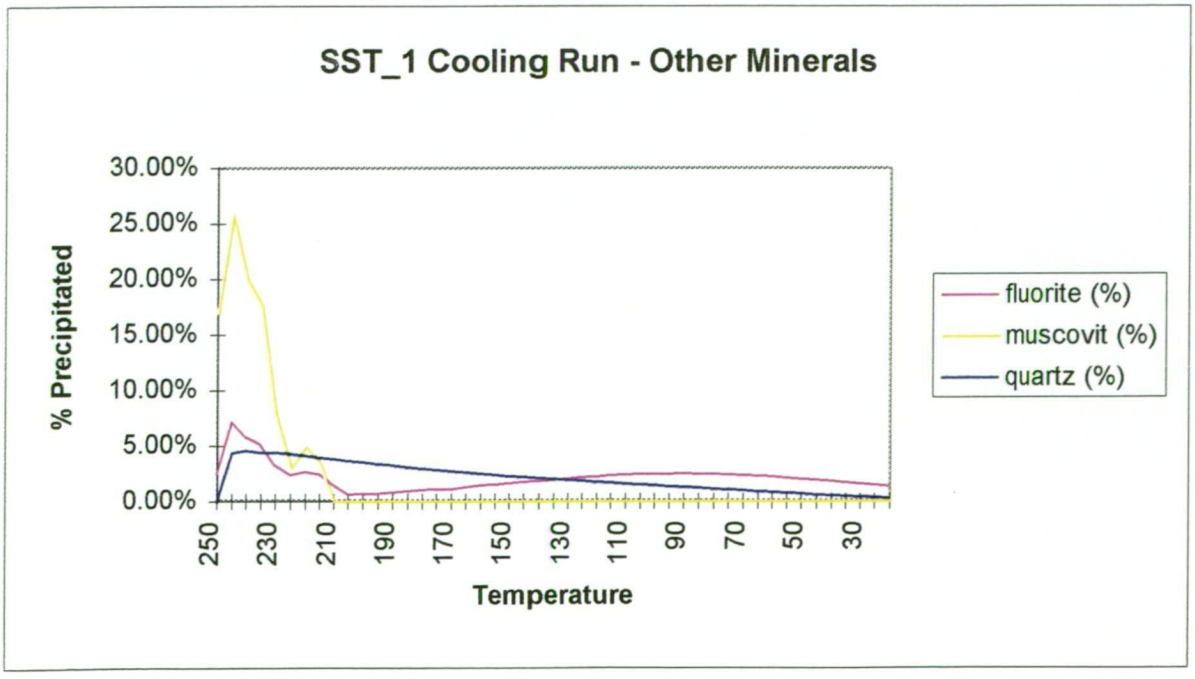
SST_1 Cooling Run - Other Minerals
% Precipitated
30.00%
25.00%
20.00%
15.00%
10.00%
5.00%
0.00%
250
230
210
190
170
150
130
110
90
70
50
30
Temperature
fluorite (%)
muscovit (%)
quartz (%)

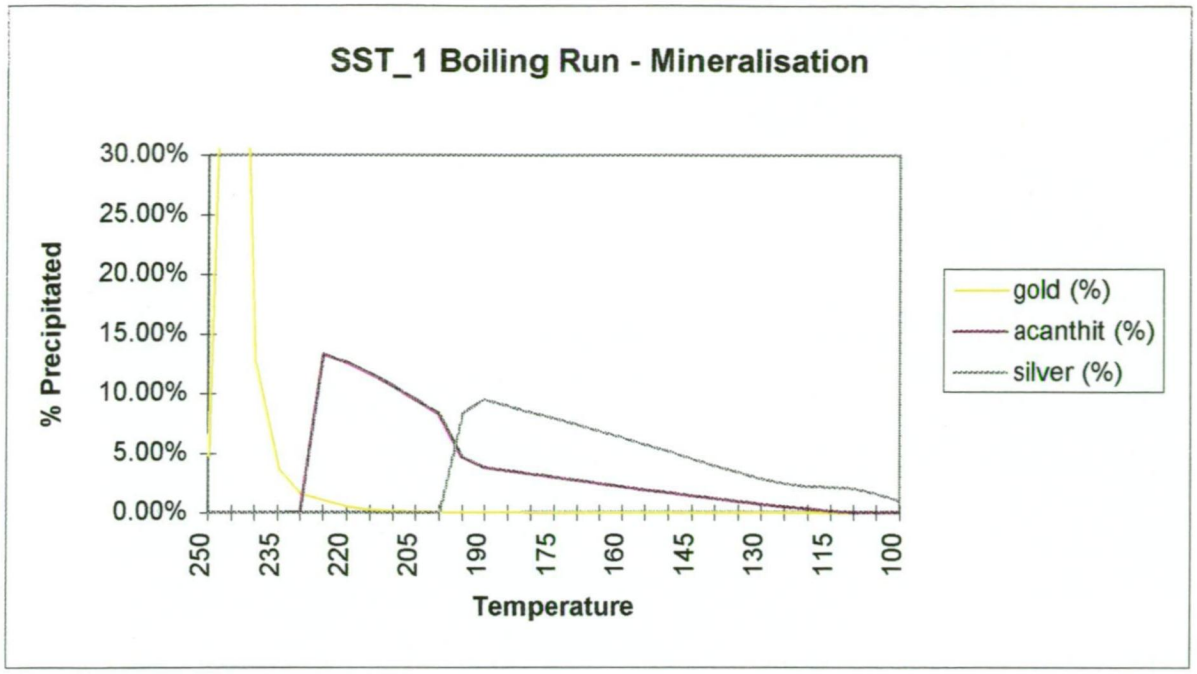
SST_1 Boiling Run - Mineralisation
% Precipitated
30.00%
25.00%
20.00%
15.00%
10.00%
5.00%
0.00%
250
235
220
205
190
175
160
145
130
115
100
Temperature
gold (%)
acanthit (%)
silver (%)

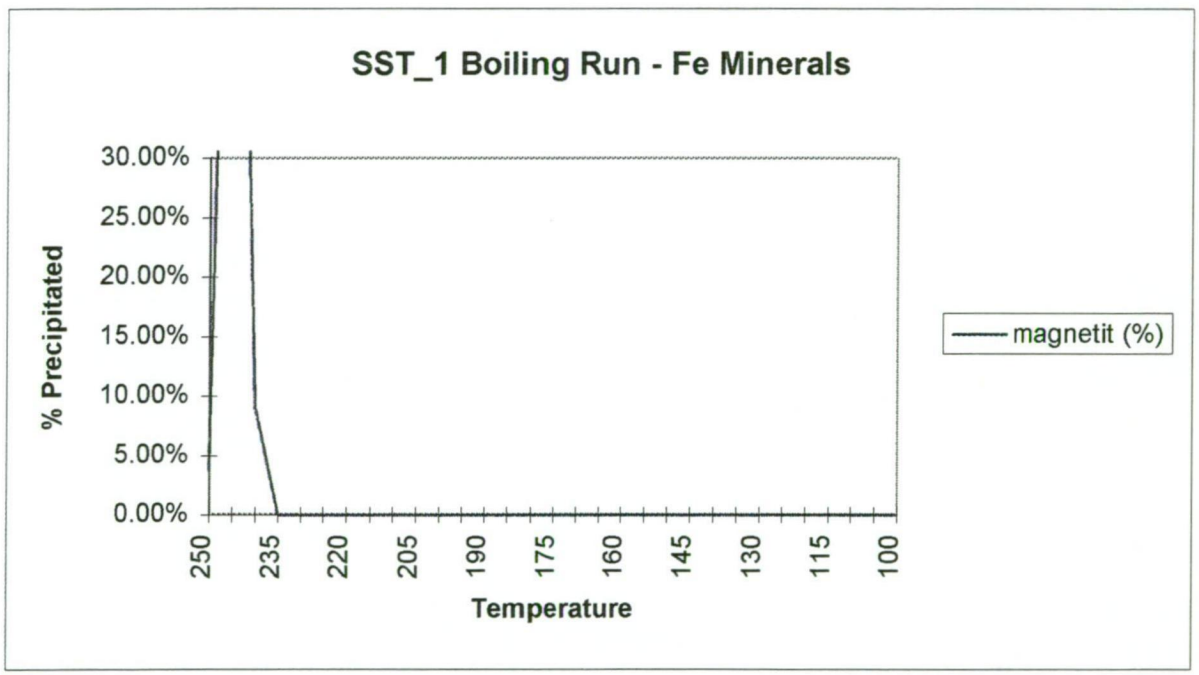
SST_1 Boiling Run - Fe Minerals
% Precipitated
30.00%
25.00%
20.00%
15.00%
10.00%
5.00%
0.00%
250
235
220
205
190
175
160
145
130
115
100
Temperature
magnetit (%)

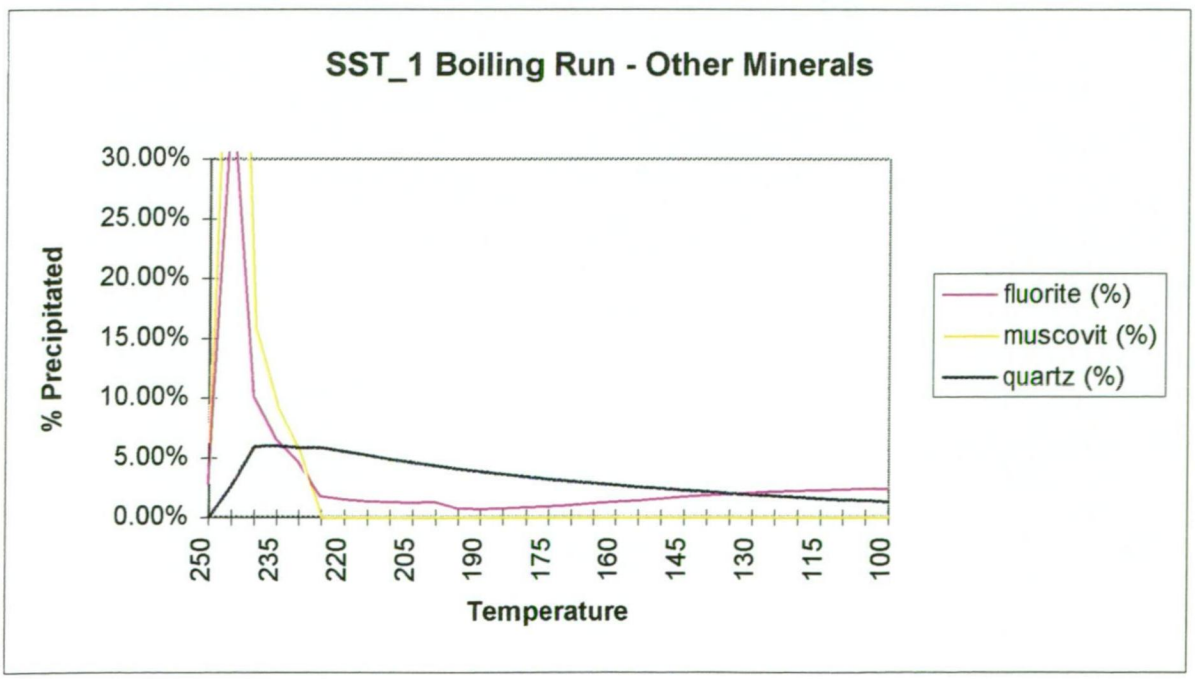
SST_1 Boiling Run - Other Minerals
% Precipitated
30.00%
25.00%
20.00%
15.00%
10.00%
5.00%
0.00%
250
235
220
205
190
175
160
145
130
115
100
Temperature
fluorite (%)
muscovit (%)
quartz (%)

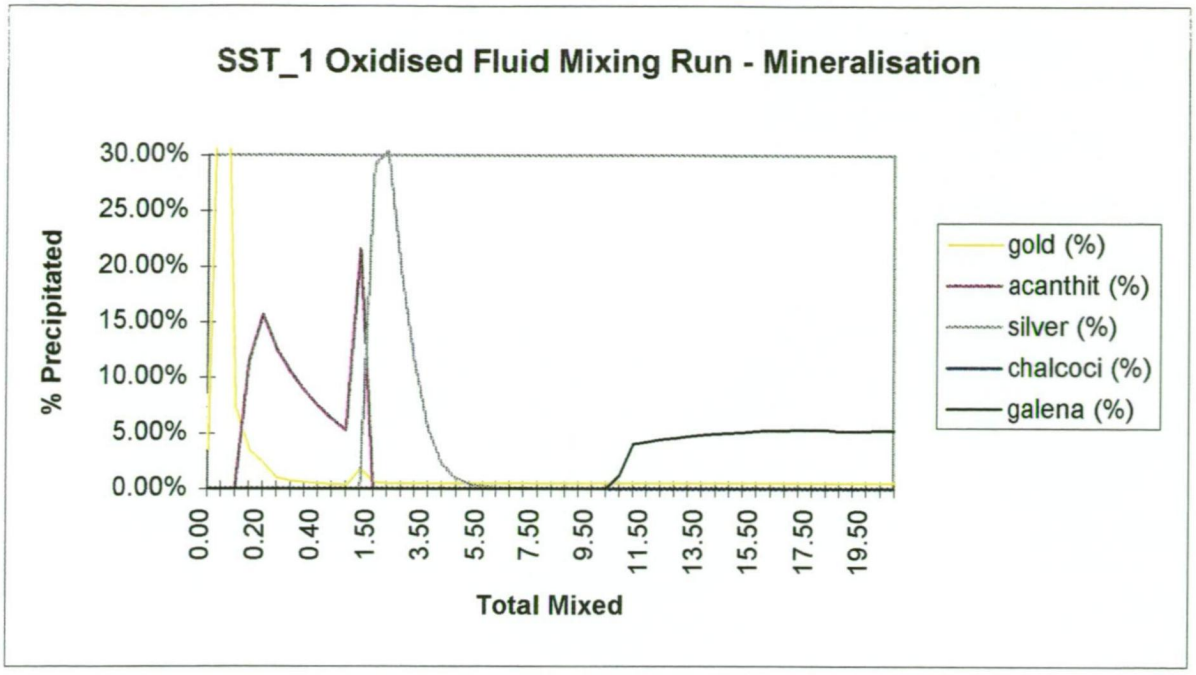
SST_1 Oxidised Fluid Mixing Run - Mineralisation
% Precipitated
30.00%
25.00%
20.00%
15.00%
10.00%
5.00%
0.00%
0.00
0.20
0.40
1.50
3.50
5.50
7.50
9.50
11.50
13.50
15.50
17.50
19.50
Total Mixed
gold (%)
acanthit (%)
silver (%)
chalcoci (%)
galena (%)

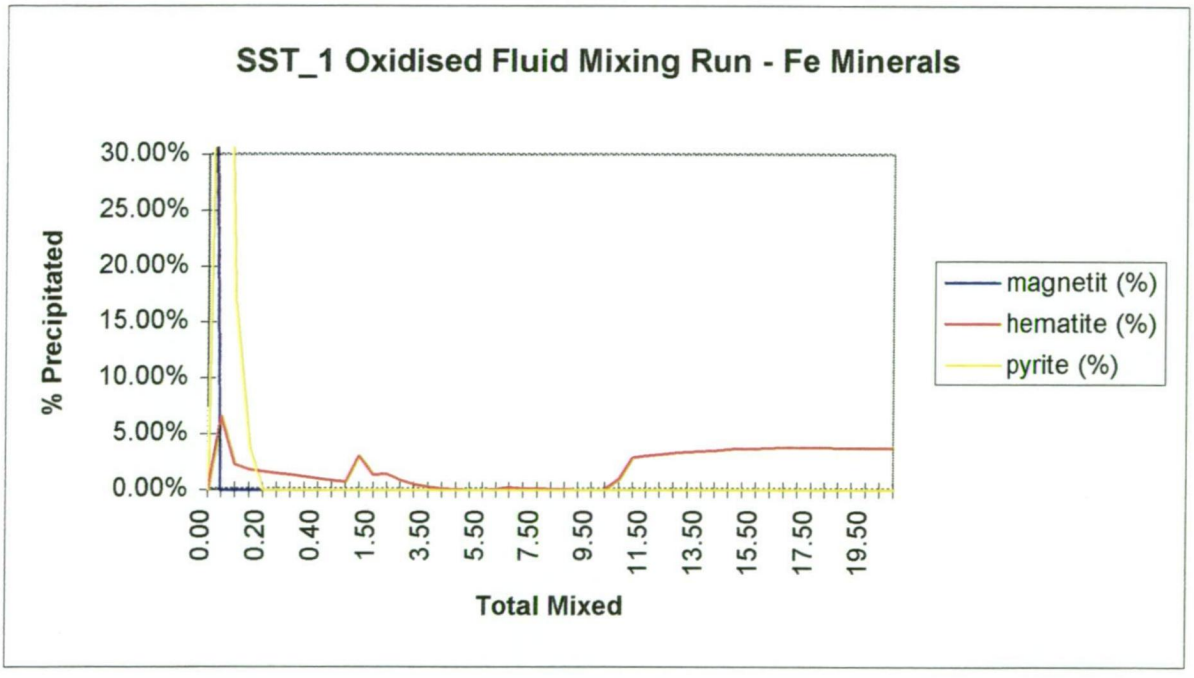
SST_1 Oxidised Fluid Mixing Run - Fe Minerals
% Precipitated
30.00%
25.00%
20.00%
15.00%
10.00%
5.00%
0.00%
0.00
0.20
0.40
1.50
3.50
5.50
7.50
9.50
11.50
13.50
15.50
17.50
19.50
Total Mixed
magnetit (%)
hematite (%)
pyrite (%)

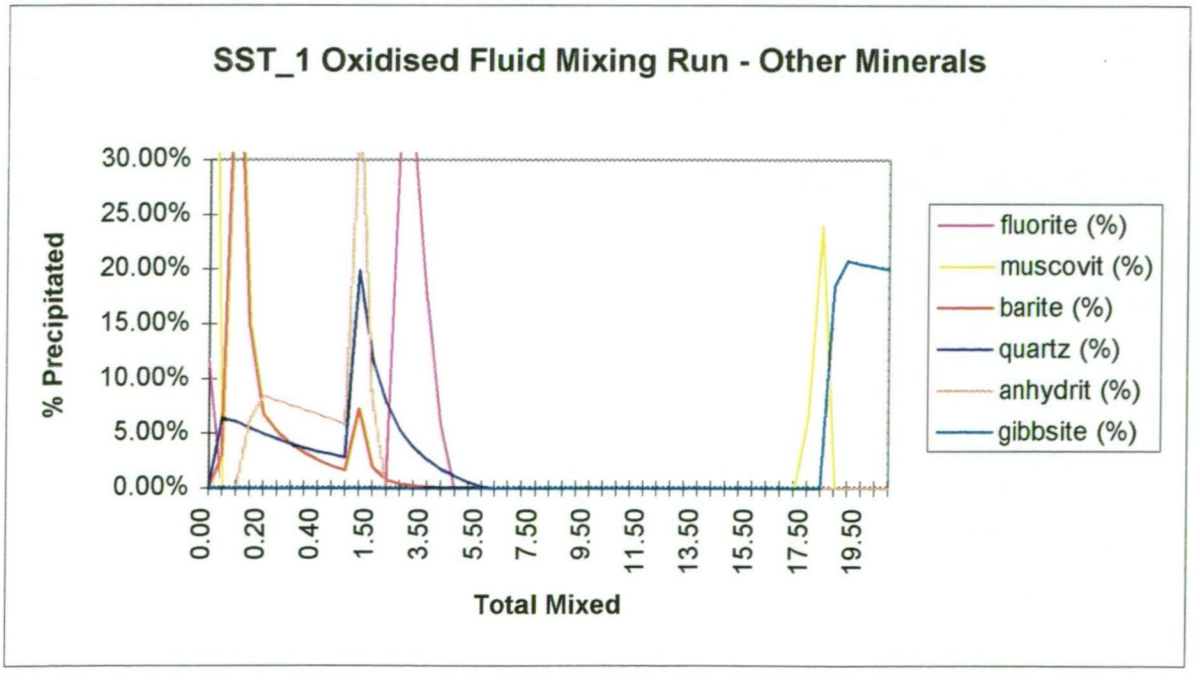
SST_1 Oxidised Fluid Mixing Run - Other Minerals
% Precipitated
30.00%
25.00%
20.00%
15.00%
10.00%
5.00%
0.00%
0.00
0.20
0.40
1.50
3.50
5.50
7.50
9.50
11.50
13.50
15.50
17.50
19.50
Total Mixed
fluorite (%)
muscovit (%)
barite (%)
quartz (%)
anhydrit (%)
gibbsite (%)

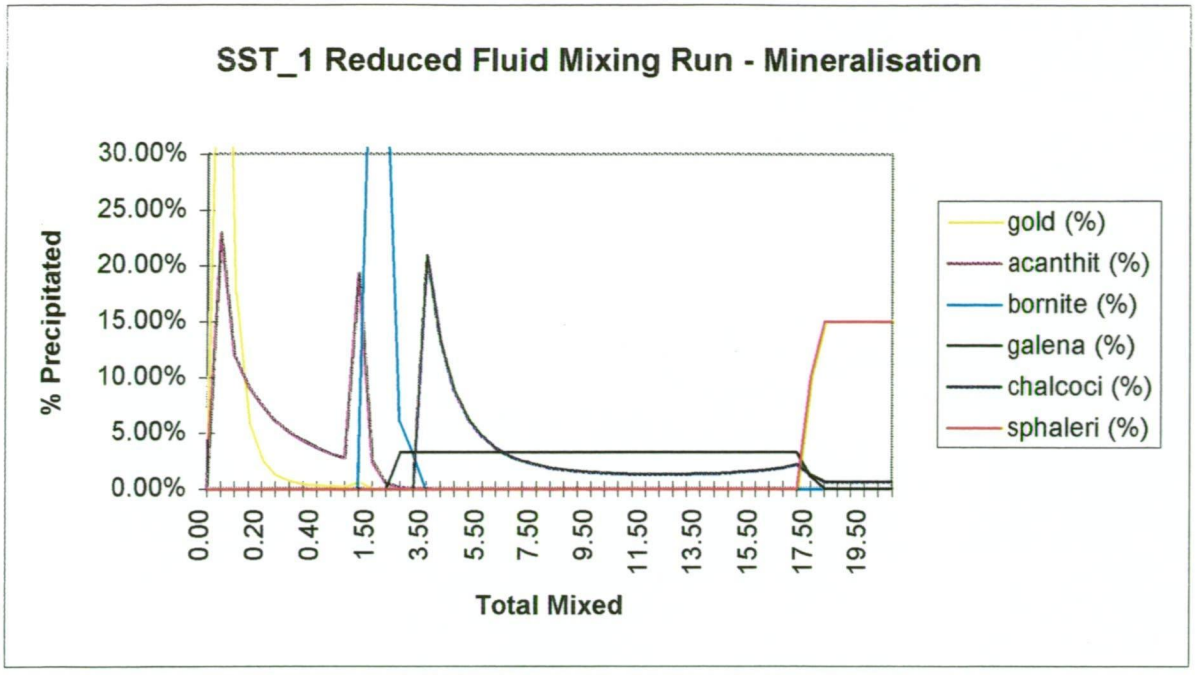
SST_1 Reduced Fluid Mixing Run - Mineralisation
% Precipitated
30.00%
25.00%
20.00%
15.00%
10.00%
5.00%
0.00%
0.00
0.20
0.40
1.50
3.50
5.50
7.50
9.50
11.50
13.50
15.50
17.50
19.50
Total Mixed
gold (%)
acanthit (%)
bornite (%)
galena (%)
chalcoci (%)
sphaleri (%)

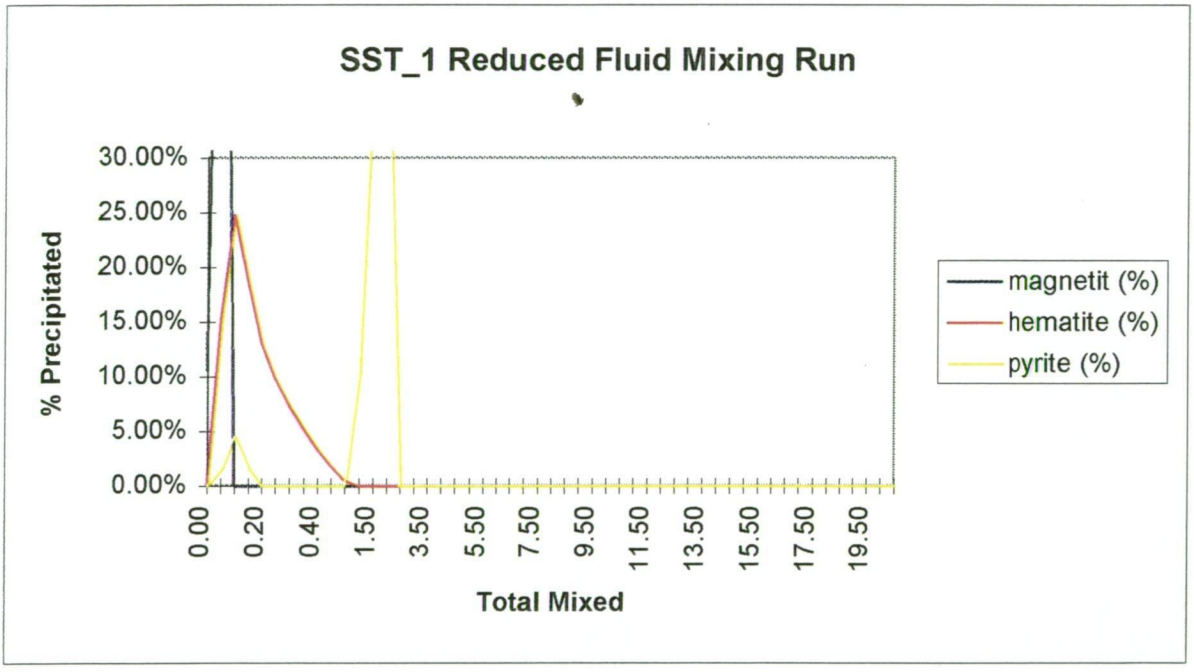
SST_1 Reduced Fluid Mixing Run
% Precipitated
30.00%
25.00%
20.00%
15.00%
10.00%
5.00%
0.00%
0.00
0.20
0.40
1.50
3.50
5.50
7.50
9.50
11.50
13.50
15.50
17.50
19.50
Total Mixed
magnetit (%)
hematite (%)
pyrite (%)

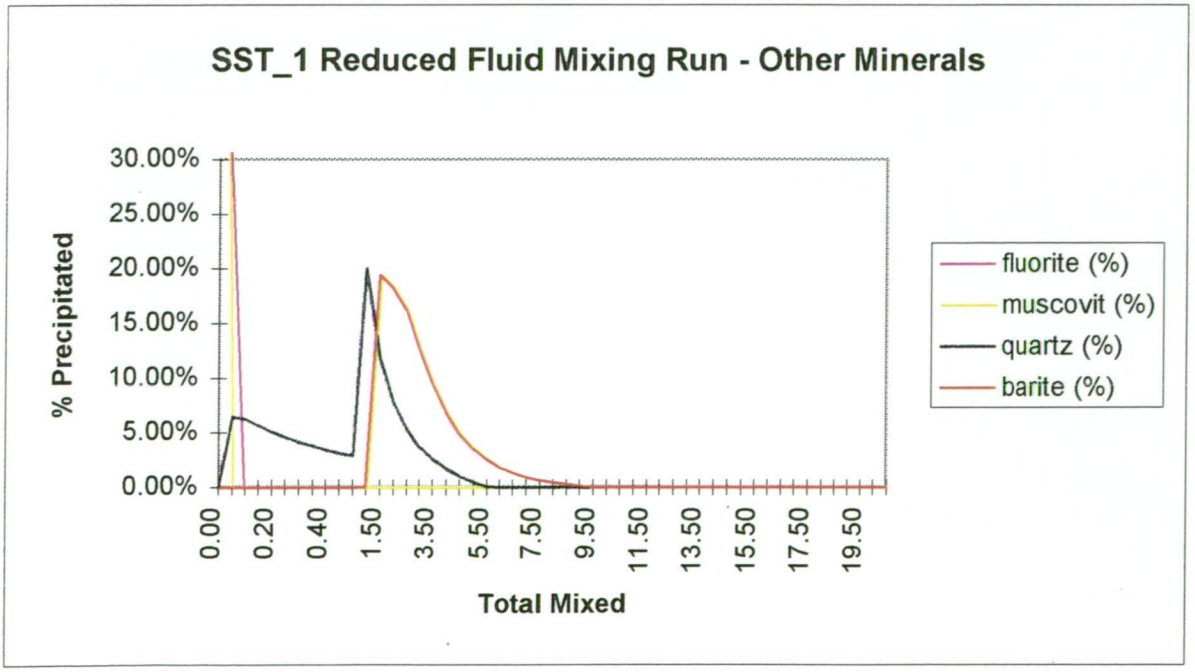
SST_1 Reduced Fluid Mixing Run - Other Minerals
% Precipitated
30.00%
25.00%
20.00%
15.00%
10.00%
5.00%
0.00%
0.00
0.20
0.40
1.50
3.50
5.50
7.50
9.50
11.50
13.50
15.50
17.50
19.50
Total Mixed
fluorite (%)
muscovit (%)
quartz (%)
barite (%)

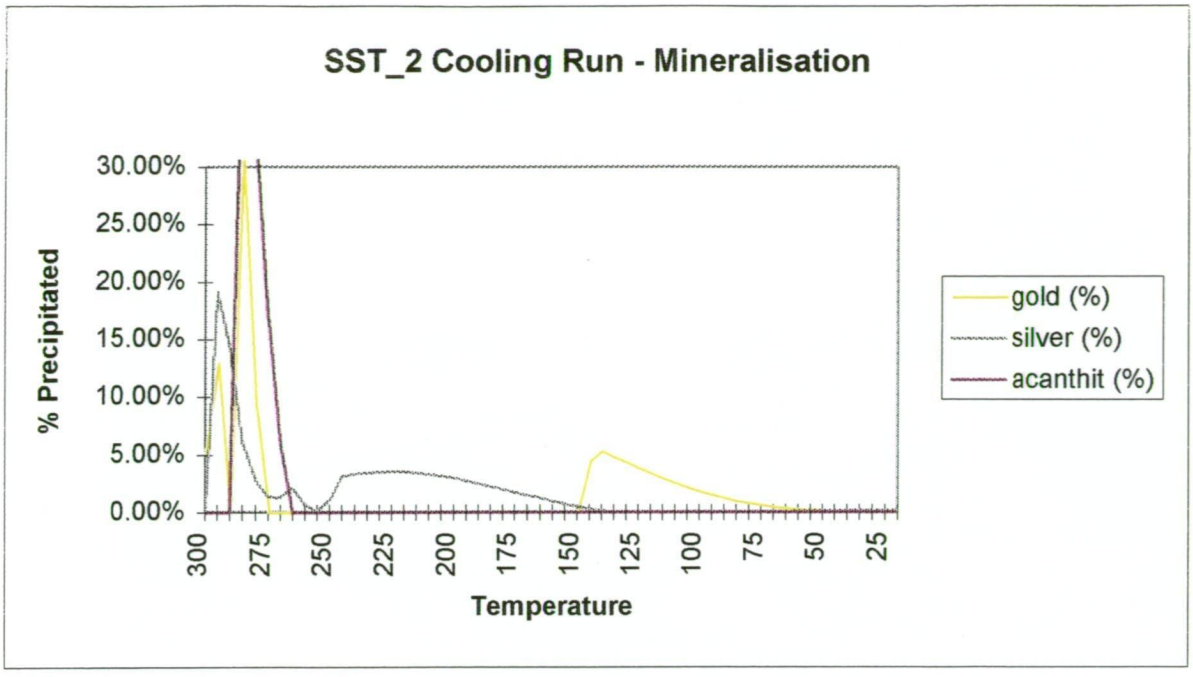
SST_2 Cooling Run - Mineralisation
% Precipitated
30.00%
25.00%
20.00%
15.00%
10.00%
5.00%
0.00%
300
275
250
225
200
175
150
125
100
75
50
25
Temperature
gold (%)
silver (%)
acanthit (%)

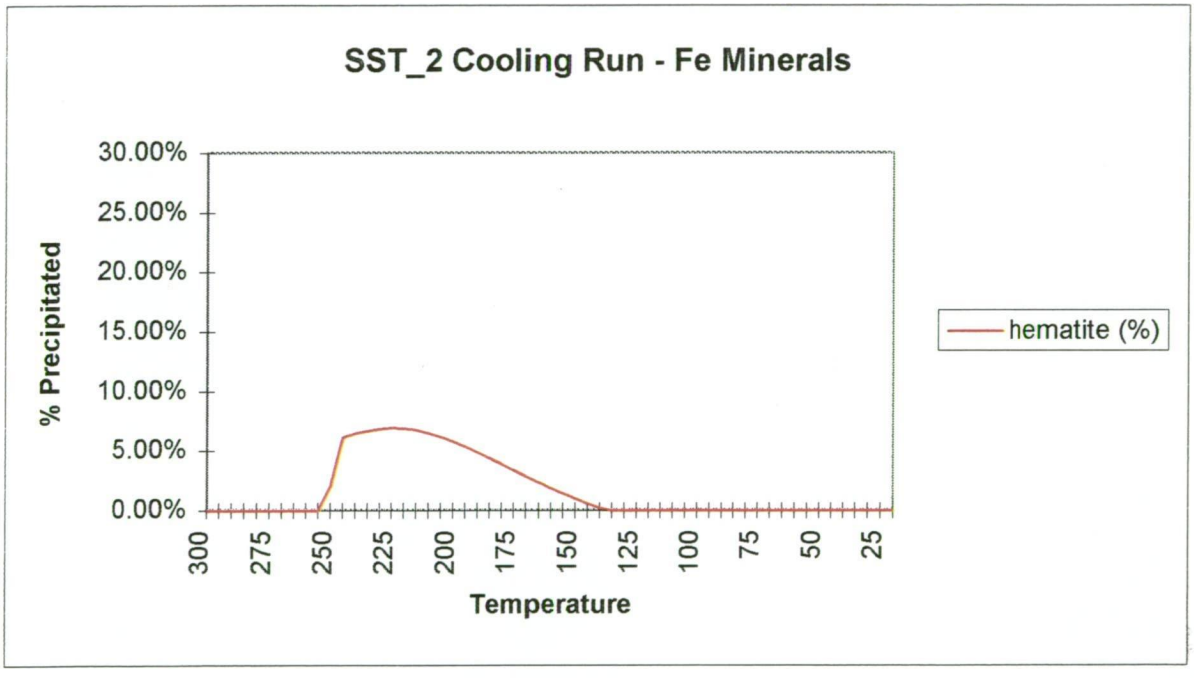
SST_2 Cooling Run - Fe Minerals
% Precipitated
30.00%
25.00%
20.00%
15.00%
10.00%
5.00%
0.00%
300
275
250
225
200
175
150
125
100
75
50
25
Temperature
hematite (%)

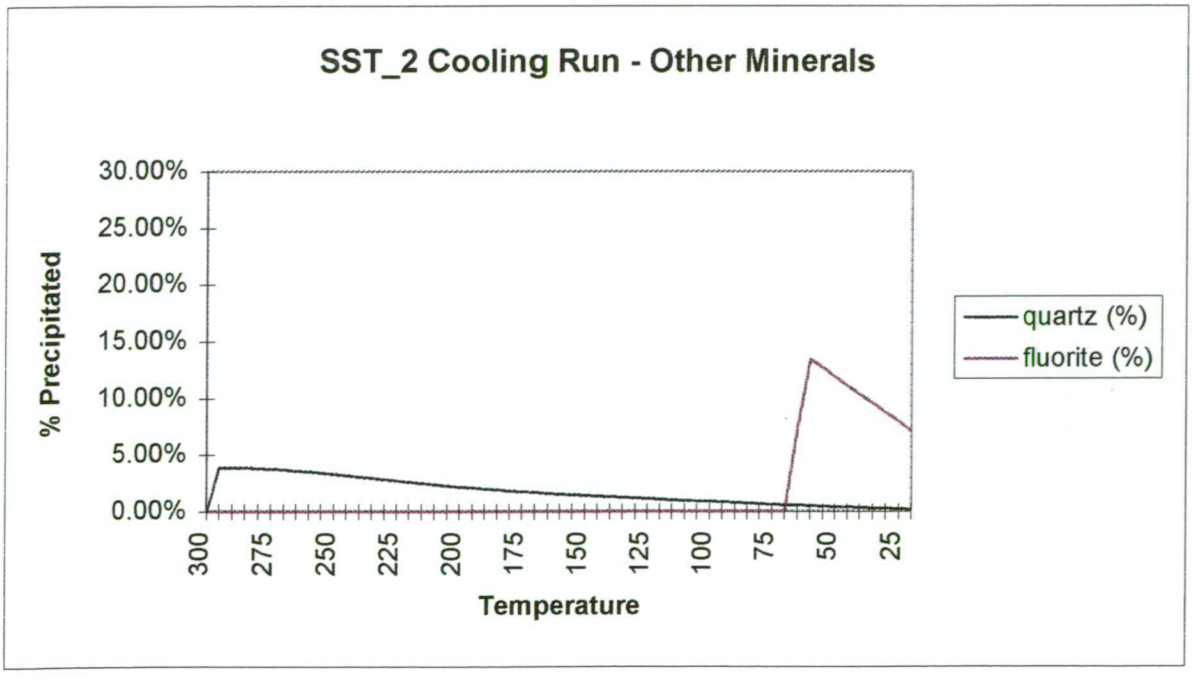
SST_2 Cooling Run - Other Minerals
% Precipitated
30.00%
25.00%
20.00%
15.00%
10.00%
5.00%
0.00%
300
275
250
225
200
175
150
125
100
75
50
25
Temperature
quartz (%)
fluorite (%)

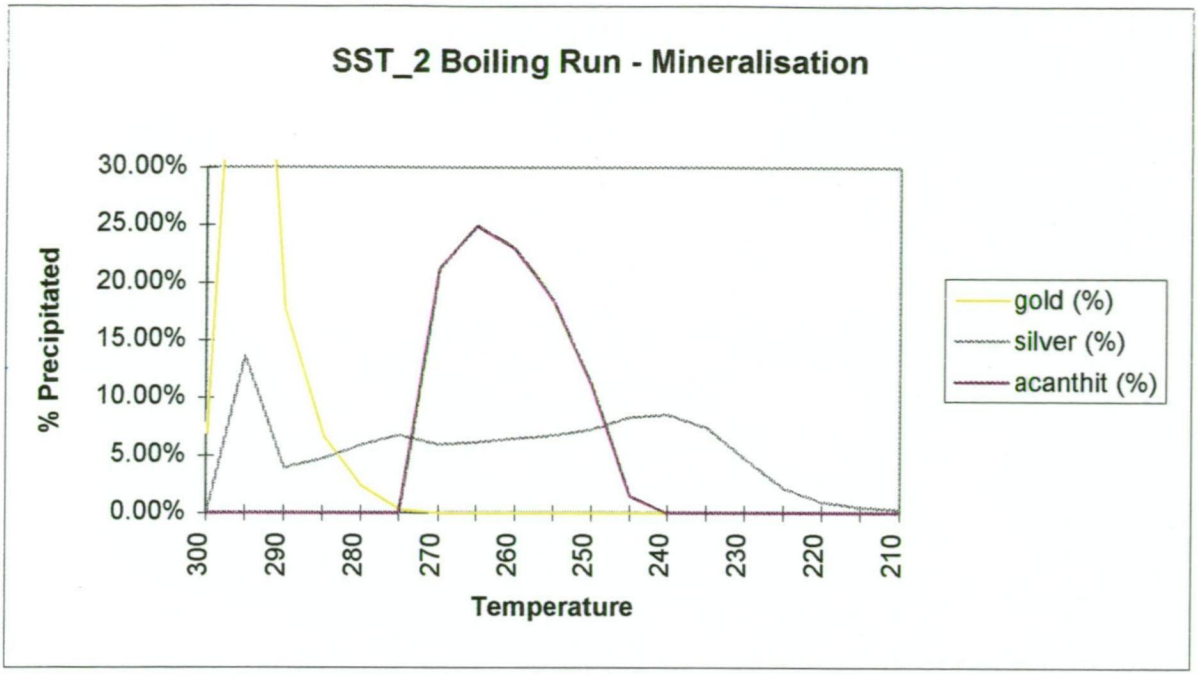
SST_2 Boiling Run - Mineralisation
% Precipitated
30.00%
25.00%
20.00%
15.00%
10.00%
5.00%
0.00%
300
290
280
270
260
250
240
230
220
210
Temperature
gold (%)
silver (%)
acanthit (%)

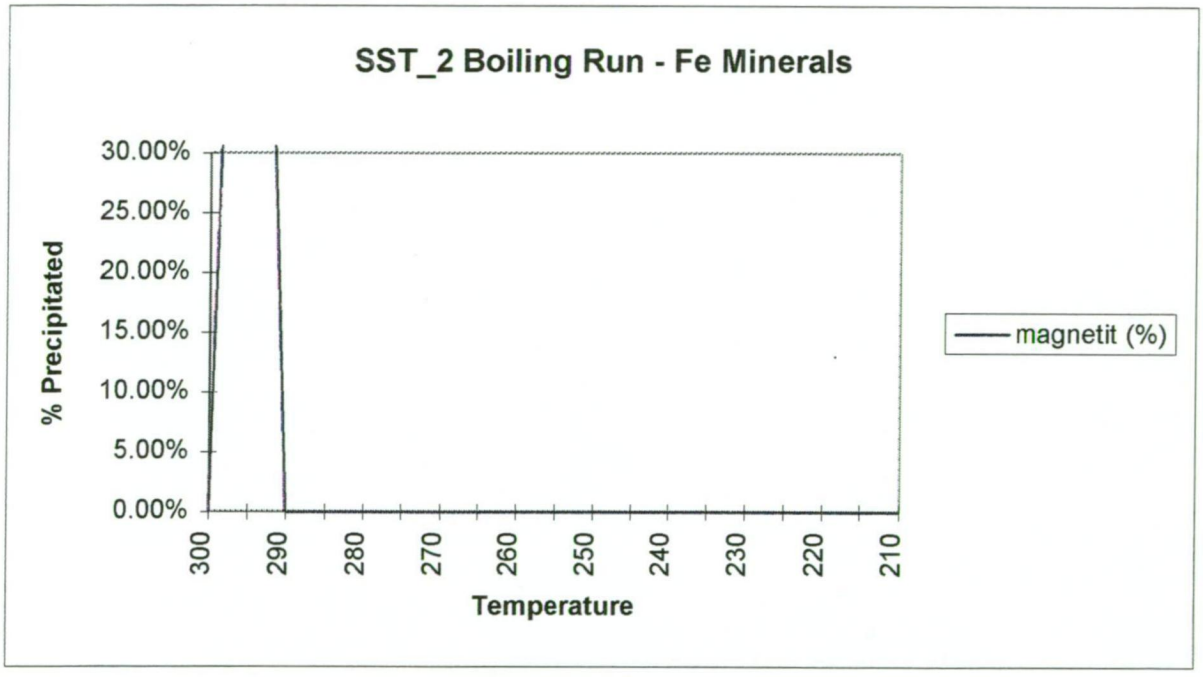
SST_2 Boiling Run - Fe Minerals
% Precipitated
30.00%
25.00%
20.00%
15.00%
10.00%
5.00%
0.00%
300
290
280
270
260
250
240
230
220
210
Temperature
magnetit (%)

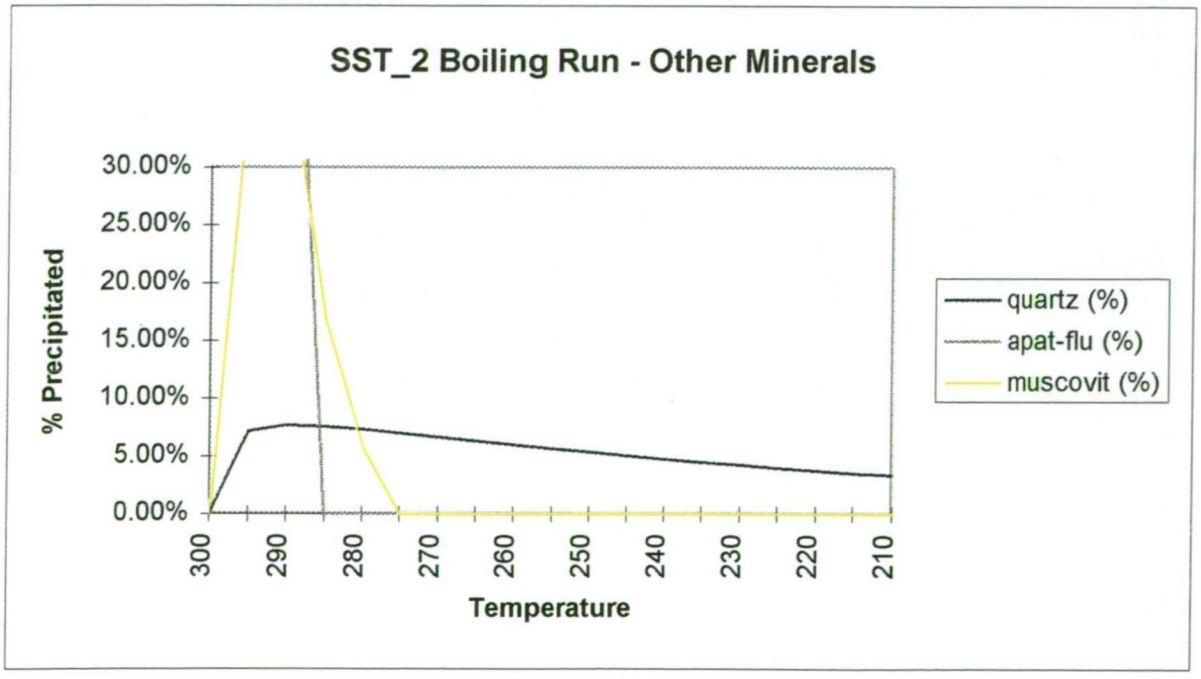
SST_2 Boiling Run - Other Minerals
% Precipitated
30.00%
25.00%
20.00%
15.00%
10.00%
5.00%
0.00%
300
290
280
270
260
250
240
230
220
210
Temperature
quartz (%)
apat-flu (%)
muscovit (%)

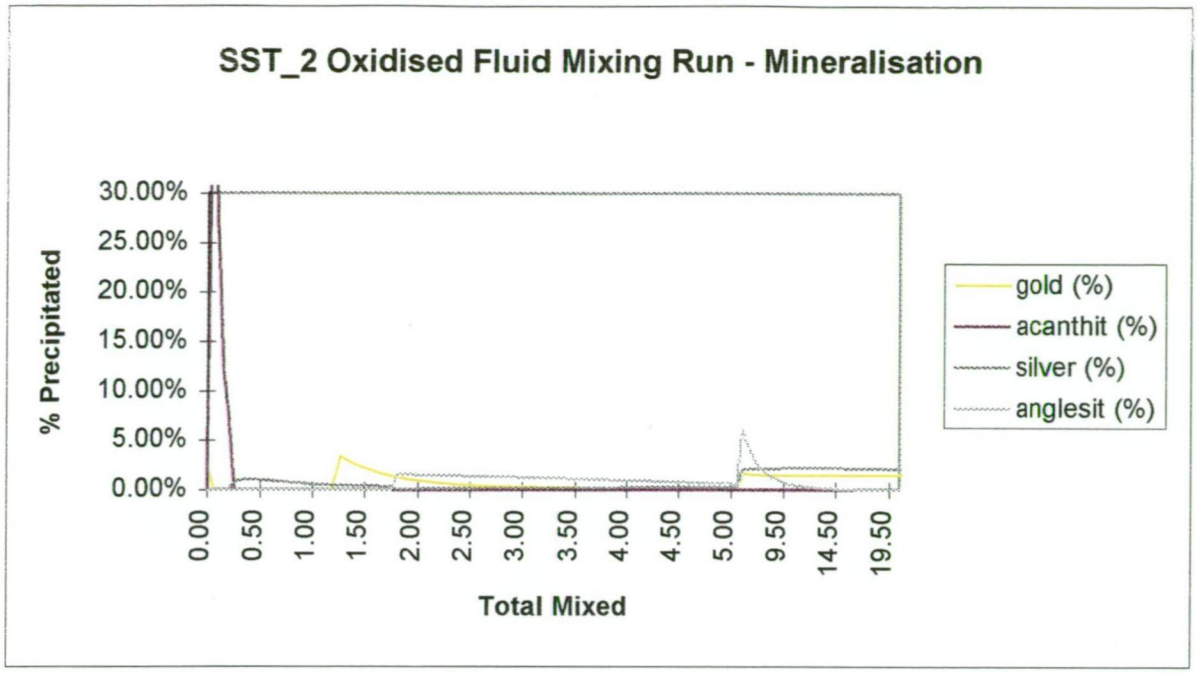
SST_2 Oxidised Fluid Mixing Run - Mineralisation
% Precipitated
30.00%
25.00%
20.00%
15.00%
10.00%
5.00%
0.00%
0.00
0.50
1.00
1.50
2.00
2.50
3.00
3.50
4.00
4.50
5.00
9.50
14.50
19.50
Total Mixed
gold (%)
acanthit (%)
silver (%)
anglesit (%)

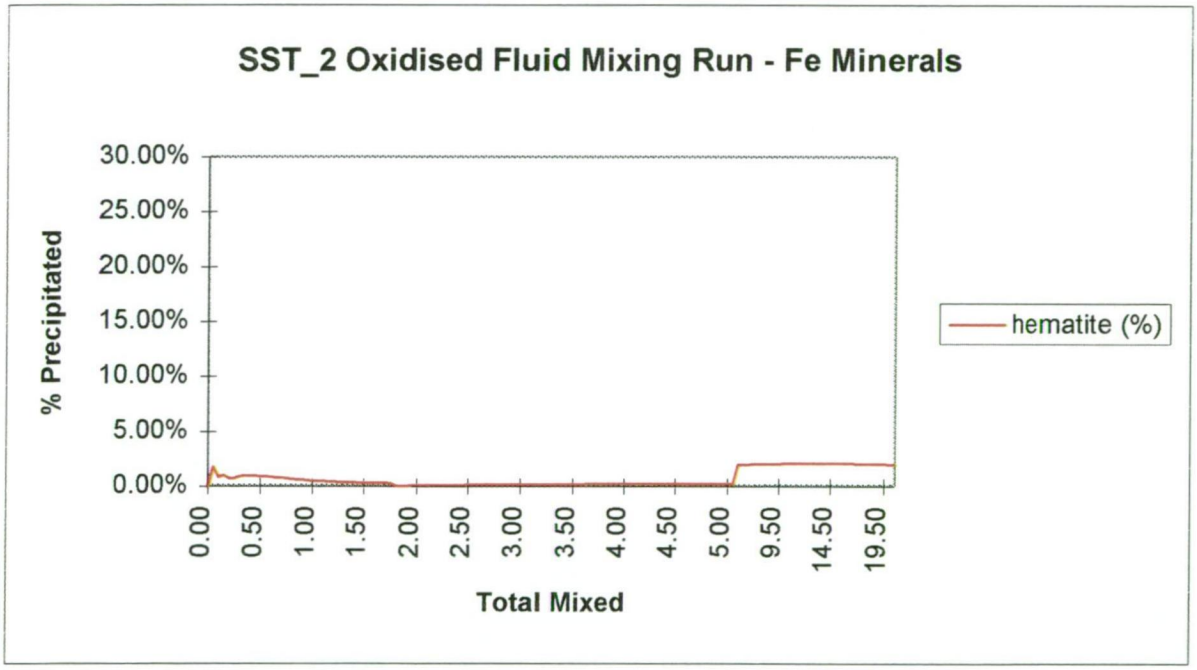
SST_2 Oxidised Fluid Mixing Run - Fe Minerals
% Precipitated
30.00%
25.00%
20.00%
15.00%
10.00%
5.00%
0.00%
0.00
0.50
1.00
1.50
2.00
2.50
3.00
3.50
4.00
4.50
5.00
9.50
14.50
19.50
Total Mixed
hematite (%)

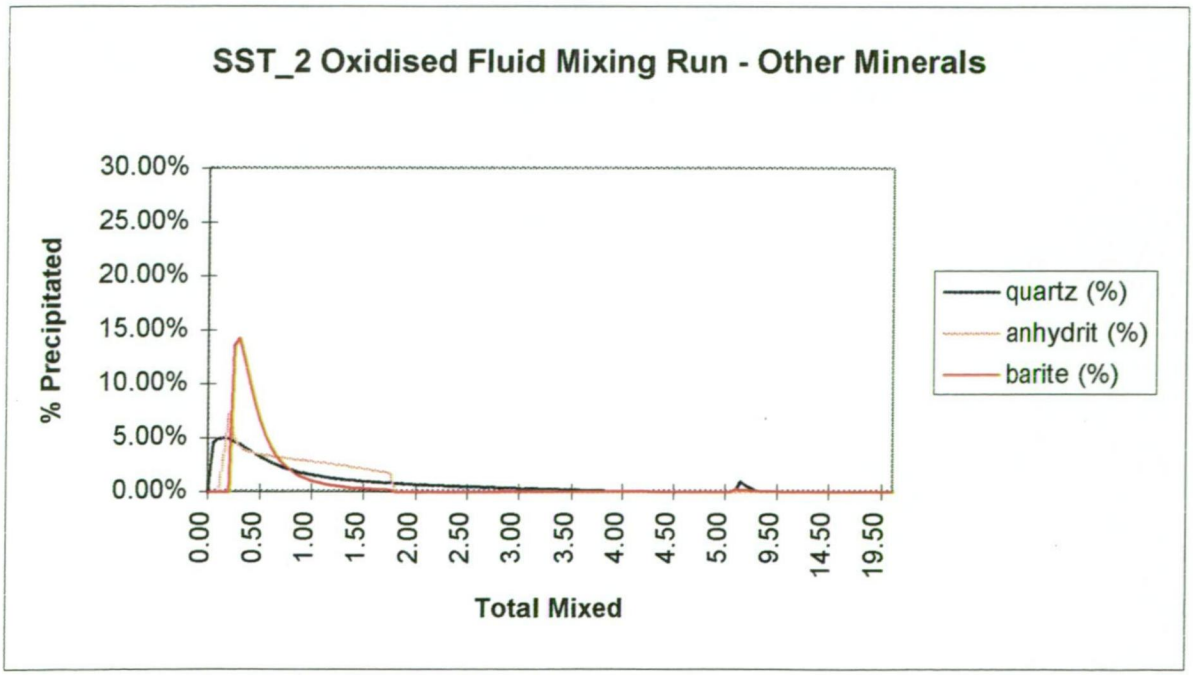
SST_2 Oxidised Fluid Mixing Run - Other Minerals
% Precipitated
30.00%
25.00%
20.00%
15.00%
10.00%
5.00%
0.00%
0.00
0.50
1.00
1.50
2.00
2.50
3.00
3.50
4.00
4.50
5.00
9.50
14.50
19.50
Total Mixed
quartz (%)
anhydrit (%)
barite (%)

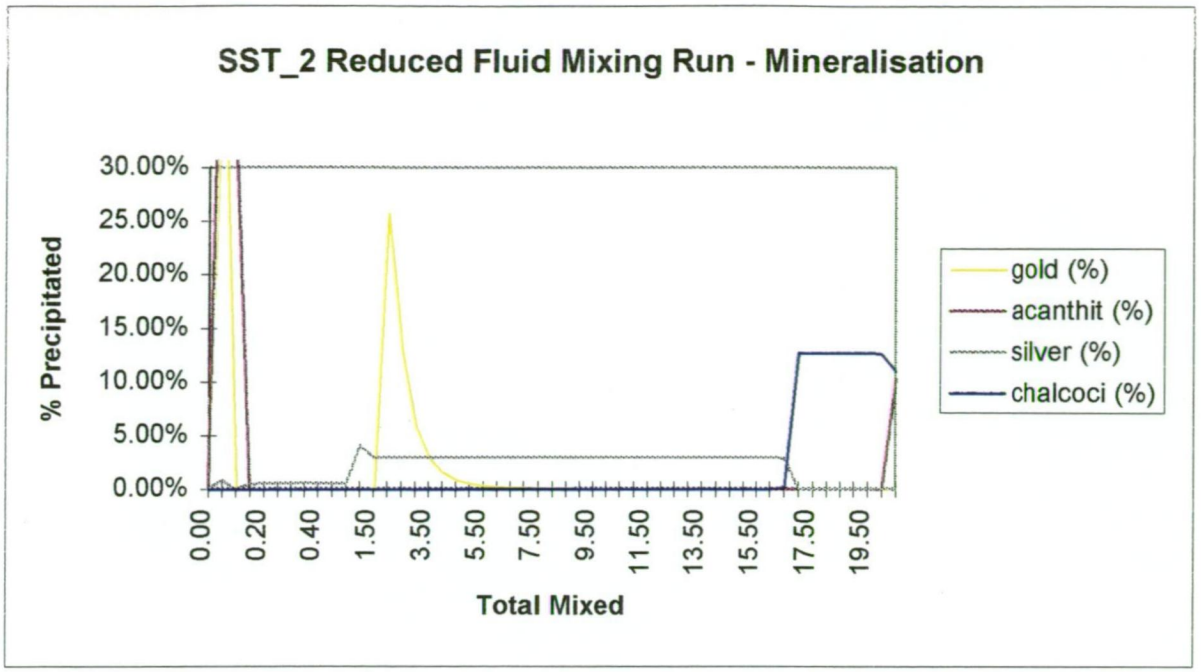
SST_2 Reduced Fluid Mixing Run - Mineralisation
% Precipitated
30.00%
25.00%
20.00%
15.00%
10.00%
5.00%
0.00%
0.00
0.20
0.40
1.50
3.50
5.50
7.50
9.50
11.50
13.50
15.50
17.50
19.50
Total Mixed
gold (%)
acanthit (%)
silver (%)
chalcoci (%)

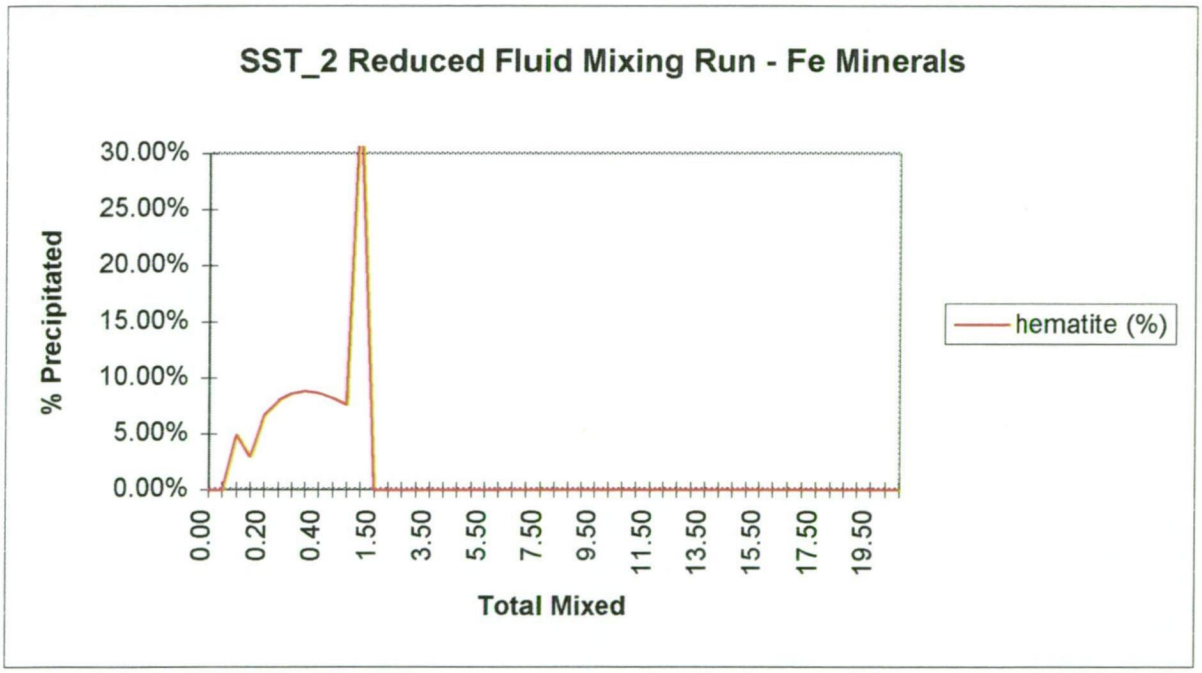
SST_2 Reduced Fluid Mixing Run - Fe Minerals
% Precipitated
30.00%
25.00%
20.00%
15.00%
10.00%
5.00%
0.00%
0.00
0.20
0.40
1.50
3.50
5.50
7.50
9.50
11.50
13.50
15.50
17.50
19.50
Total Mixed
hematite (%)

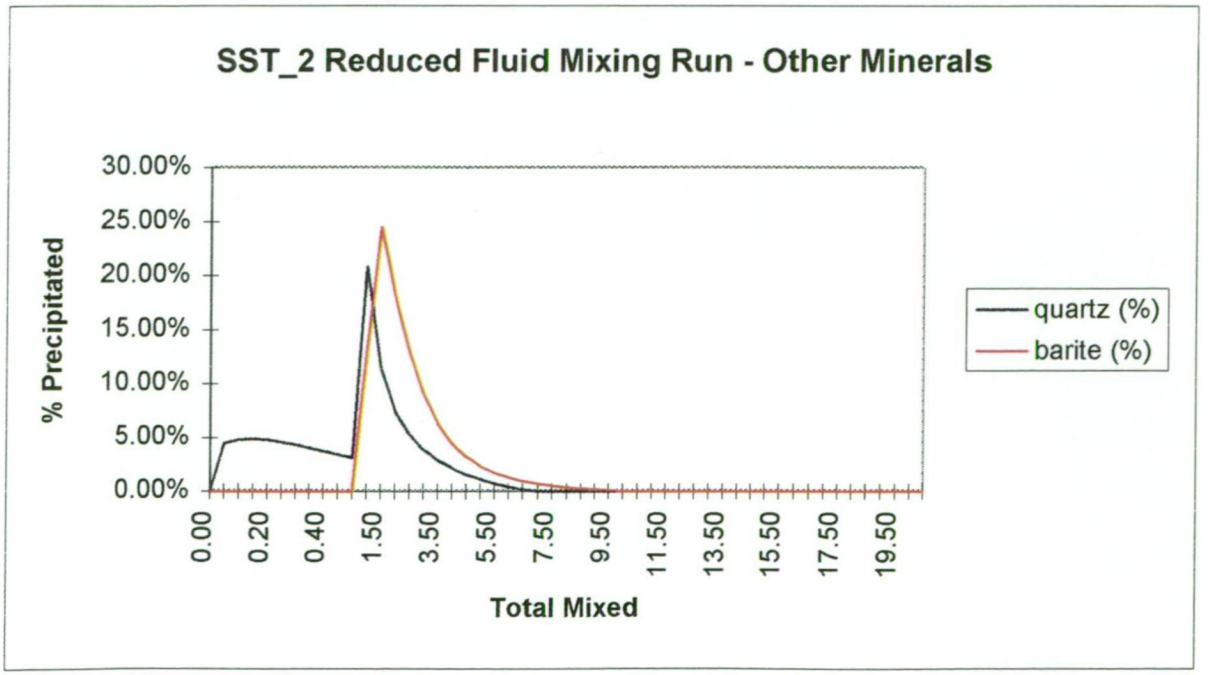
SST_2 Reduced Fluid Mixing Run - Other Minerals
% Precipitated
30.00%
25.00%
20.00%
15.00%
10.00%
5.00%
0.00%
0.00
0.20
0.40
1.50
3.50
5.50
7.50
9.50
11.50
13.50
15.50
17.50
19.50
Total Mixed
quartz (%)
barite (%)